Modelling the impact of *Phytophthora austrocedri* on UK populations of native juniper (*Juniperus communis* s. l.)

Flora Donald

Department of Plant Sciences

University of Cambridge

This thesis is submitted for the degree of *Doctor of Philosophy*

Emmanuel College October 2021

Declaration

This thesis is the result of my own work and includes nothing which is the outcome of work done in collaboration except as declared in the Preface and specified in the text. I further state that no substantial part of my thesis has already been submitted, or, is being concurrently submitted for any such degree, diploma or other qualification at the University of Cambridge or any other University or similar institution except as declared in the Preface and specified in the text. It does not exceed the prescribed word limit of 60,000 words (excluding tables, the bibliography, and appendices) as specified by the Degree Committee of the Faculty of Biology.

Flora Donald October 2021

Abstract

Introductions of non-native plant pests and pathogens are increasing, negatively impacting natural environments. Mitigation requires knowledge of the drivers of pathogen introduction, establishment and spread, rarely available when pathogens first emerge in novel settings. This thesis uses multi-scale ecological modelling to understand environmental and land management factors driving patterns in infection and impact of the newly discovered oomycete pathogen, *Phytophthora austrocedri*, on juniper (*Juniperus communis*).

I first surveyed potential abiotic and biotic drivers of disease severity across three, geographically separate juniper populations with different infection histories. In all populations, disease severity increased with increasing soil moisture. Associated plant species that could be used to locate microsites at higher risk of infection were also identified. Change in infection intensity during a four-year period was then mapped across a single juniper population and related to environmental factors underpinning the presence and density of juniper and driving *P. austrocedri* spread. Colonisations usually occurred within a ~500m radius of previously symptomatic trees, with infrequent dispersal beyond 1km, potentially mediated by livestock and deer. By compiling a novel dataset, I revealed larger, more frequent supplementary juniper planting events increased the likelihood of *P. austrocedri* presence. Stakeholders managing, monitoring, and growing juniper then participated in a survey investigating how practitioners consider disease risks and whether these processes could be better supported by decision tools. Lastly, a machine learning model and risk map was developed that predicted juniper populations in northern England and central Scotland are at highest risk of infection due to acidic soil pH and increased roe deer density.

My research demonstrates how incorporating a wider range of abiotic and biotic drivers, exploring scale dependence, and integrating stakeholder knowledge can improve the predictive accuracy of host-pathogen-environment models. The results are used to recommend strategies (e.g. reductions in grazing pressure, natural juniper regeneration and heightened on-site biosecurity) to mitigate the serious threat posed by the pathogen to UK biodiversity and habitat restoration goals.

Acknowledgements

The work presented in this thesis would not have been possible without an army of friends and colleagues who have enthused, advised, and supported me over the past four years. Firstly, I must thank my exceptional supervisors: Kate Searle, for making sense of that first INLA code and helping me collect temperature loggers in a blizzard; Sarah Green, for sharing her expert knowledge of Paus and improving the structure of every manuscript; Nik Cunniffe, for offering a different perspective, incredible attention to detail and loaning me his office to write-up in; and Beth Purse, for taking a chance on me, giving me the freedom to follow my own path, translating my ideas when I was flailing to articulate them, counselling me when all I could see was failure and reminding me to celebrate the minor successes. Learning from all of you has been a huge privilege and I couldn't have wished for kinder, funnier, or more patient mentors.

Moving so frequently between Wallingford, Cambridge and Edinburgh was made so much easier by all my brilliant friends and family. Thank you so much Barbara and Alistair Wilson for your generosity and sharing your beautiful home with me, and Ben Spencer and Steve Brown for providing a refuge and sage advice whenever I needed it. Thank you: Charlie Outhwaite, for teaching me how to write *for* loops; Melanie Armbruster, for making me a better environmentalist; Ilze Rasnaca and Elmer Swart, for inviting me on adventures and reminding me to eat fruit occasionally; Devanshi Pathak, for making me laugh at myself; Carolyn Riddell, for listening (with and without gin!); Heather Dun, for farm missives and boundless positivity; Michelle Brace, for my little room under the big sky; Anita Spencer, for walks in the Cotswolds; Harriet Downey (and Bryn), for jaunts in the fens; Rachel Murray-Watson, for humouring my advice and teaching me much more in return; Eleni Tente and Lisa Hecker, for laughter and being yourselves, unapologetically; Sally Hames, for lockdown picnics; Engin, for coffee and poking fun at me; and Jordan Chetcuti, for rigging the BAM competition and being an all-round amazing friend. To my oldest pals, Rosie Norman and Charmaine Jones, thank you for pulling me through that first, terrifying lockdown. Thank you, Sandi Aitchison, for keeping me grounded and baking me cookies, and Katie MacCandlish, for reminding me how extraordinary the natural world is. Thank you, Nogs, for picking up my weepy phone calls, calling me out when I was (frequently) ridiculous, and for all the fun road trips with you and Struan. Finally, a whole-hearted thank you to my wonderful Mum and Dad, for inspiring me, offering unwavering support, working from the sofa so I could run an ethernet cable out your office window in midwinter, and telling me it's ok if I just want to come home but never doubting I could do this if I wanted to.

.

Preface

The research chapters (2-6) presented in this thesis were written in the form of manuscripts with the intention to submit the work to peer-reviewed journals. I was responsible for the Conceptualisation, Methodology, Software, Formal analysis, Investigation, Writing - original draft, Visualization, Writing - review and editing of every chapter. However, I received advice on the Conceptualisation, Methodology and Writing – review and editing from the co-authors detailed below and use the pronoun “we” instead of “I” to represent these contributions in the text.

- Chapters 1 and 7 are entirely my own work.
- Chapter 2 is published as Donald, F., Green, S., Searle, K., Cunniffe, N. J., and Purse, B. V. (2020). Small scale variability in soil moisture drives infection of vulnerable juniper populations by invasive forest pathogen. *Forest Ecology and Management*, *473(3)*, 118324. https://doi.org/10.1016/j.foreco.2020.118324
- Chapter 3 is in preparation as Donald, F., Searle, K., Cunniffe, N. J., Wylder, B., Henrys, P. A., Green, S., and Purse, B. V. Informing disease management by disentangling abiotic and biotic determinants of *Phytophthora austrocedri* spread on juniper hosts.
- Chapter 4 is published as Donald, F., Purse, B. V., and Green, S. (2021). Investigating the role of restoration plantings in introducing disease — a case study using *Phytophthora*. *Forests*, *12(6)*, 764. https://doi.org/10.3390/f12060764
- Chapter 5 is in preparation as Donald, F., Hedges, C., Purse, B. V., and Asaaga, F. A. Utility of decision tools for risk assessing plant disease management strategies in natural environments.
- Chapter 6 is in preparation as Donald, F., Green, S., and Purse, B. V. National scale *Phytophthora* presence is better predicted by acidic soils and wildlife densities than soil moisture.

My research was funded in order of contribution by the Scottish Forestry Trust, Scottish Forestry, Forest Research, NatureScot, and the Royal Botanic Garden Edinburgh. Additional funding was received from the UK Centre for Ecology and Hydrology (UKCEH) to cover an extension resulting from a period of Covid-19 related illness and I am especially grateful to all my funders for their flexibility with reporting deadlines following Covid-19 disruption. Extra fieldwork and partnership working undertaken for Chapter 3 was funded by the Frank Smart studentship awarded to me by the University of Cambridge Department of Plant Sciences

and a travel bursary from the Cambridge Philosophical Society enabled me to present a poster at the British Ecological Society conference in 2019. Equipment was provided by UKCEH, Forest Research, NatureScot, and the Theoretical and Computational Epidemiology, and the Epidemiology and Modelling, labs at the University of Cambridge.

The fieldwork undertaken in Chapter 2 was conducted with kind permission from Dalemain Estate, Drummond Estate, Rothiemurchus Estate, the Taylforths, Mr Steele, Piers Voysey and Peter Ferguson. Fieldwork was conducted according to the protocol I devised and executed with additional support from Carolyn Riddell, April Armstrong, Ewan Purser and Sarah Green to collect lesion material and from Fiona Cameron, Deborah Comyn-Platt, Nik Cunniffe, Etienne Duperron, Rory Hodd, Susan Medcalf, Denise Pallett, Beth Purse, Mari Roberts, Kate Searle, and Rosamund Sparks to collect in-situ measurements. I conducted the qPCR analysis under licence in the pathology lab at the Forest Research Northern Research Station in Roslin, Midlothian.

In addition to the work presented here for this thesis I contributed:

- three herbarium specimens and ~140 samples of juniper needles to the genetic resource library held by the Royal Botanic Garden Edinburgh to enable analysis of juniper population genetics.
- to two stakeholder workshops exploring how modelling could better support plant health decision making in Scotland by presenting a similar questionnaire and interactive maps to those presented in Chapter 5 and by facilitating small discussion groups. The data collected are not included in this thesis and are instead used in Barwell, L., White, R. M., Chapman, D., **Donald, F.**, Marzano, M., Green, S., Kleczkowski, A., and Purse, B.V. (2021b). The potential of ecological and epidemiological models to inform assessment and mitigation of biosecurity risks arising from large scale planting. Part of Project Final Report. PHC2019/06 & PHC2019/05. Scotland's Centre of Expertise for Plant Health.
- writing about the need for adaptive woodland management to deliver nature-based solutions to address climate change in Coomes, D., Bowditch, E., Burton, V., Chamberlain, B., **Donald, F.**, Egedusevic, M., Fuentes-Montemayor, E., Hall, J., Jones, A. G., Lines, E., Waring, B., Warner, E., and Weatherall, A. (2021). Section 1: Habitat specific nature-based solutions: a review of the available evidence. Woodlands. In R. Stafford, B. Chamberlain, L. Clavey, P. K. Gillingham, S. McKain, M. D. Morecroft, C. Morrison-Bell, and O. Watts (Eds.), *Nature-based solutions for*

climate change in the UK: a report by the British Ecological Society (pp. 24-37). British Ecological Society. Retrieved from https://www.britishecologicalsociety.org/policy/nature-based-solutions/read-the-report/

- user feedback and imagery to the Scottish Science Advisory Council Future Landscapes: Report on Geospatial Knowledge (2021). Retrieved from https://www.scottishscience.org.uk/sites/default/files/article-attachments/Future%20Landscapes%20Report%20on%20Geospatial%20Knowledge.pdf

Table of contents

List of figures

List of tables

Abbreviations

BCI	Bayesian Credible Intervals
BRT	Boosted Regression Trees
BSBI	Botanical Society of Britain and Ireland
CIR	false colour infrared imagery
DAERA	Northern Ireland Department of Agriculture, Environment and Rural Affairs
DEFRA	UK Government Department for Environment Food and Rural Affairs
DEM	Digital Elevation Model
DIC	Deviance Information Criterion
EPPO	European and Mediterranean Plant Protection Organisation
FAO	Food and Agriculture Organisation
FERA	Food and Environment Research Agency
GB	Great Britain
GLM	Generalised Linear Model
GLMM	Generalised Linear Mixed Model
iid	spatially unstructured random effect
INLA	Integrated Nested Laplace Approximation
IPBES	Intergovernmental Science-Policy Platform on Biodiversity and Ecosystem Services
IUCN	International Union for Conservation of Nature
JNCC	Joint Nature Conservation Committee

ML	Maximum Likelihood
NVC	National Vegetation Classification
PPM	Point Process Model
qPCR	quantitative real-time Polymerase Chain Reaction
RGB	full colour imagery (red, green blue bands)
RF	Random Forest algorithm
RI	Relative Importance
RMSE	Root Mean-Square Error
SAC	Special Areas of Conservation
SDM	Species Distribution Model
SPDE	Stochastic Partial Differential Equations
SSSI	Site of Special Scientific Interest
TWI	Topographic Wetness Index
UK	United Kingdom
UKCEH	UK Centre for Ecology and Hydrology
UKISG	UK and Ireland Sourced and Grown
UN	United Nations
UNESCO	United Nations Economic and Social Council
VWC	Volumetric Water Content

Chapter 1

Introduction

"*The rate of global change in nature during the past 50 years is unprecedented in human history. The direct drivers of change in nature with the largest global impact have been (starting with those with most impact): changes in land and sea use; direct exploitation of organisms; climate change; pollution; and invasion of alien species*." (IPBES, 2019)

1.1 The global importance of plant pathogen invasions

In their global assessment of biodiversity and ecosystem services published in 2019, the Intergovernmental Science-Policy Platform on Biodiversity and Ecosystem Services (IPBES) identified invasions of non-native pests and pathogens as the fifth most important cause of biodiversity loss and changes to ecosystem functioning (IPBES, 2019). Invasions are accelerated, exacerbated, and perpetuated by changes in land and sea use, exploitation of organisms, agricultural intensification, human population expansion, climate breakdown and pollution (IPBES, 2019). All of these drivers are underpinned by societal values and behaviours, and local to global governance (IPBES, 2019). Biological invasions can themselves also manipulate the speed and impact of the aforementioned drivers and frustrate attempts to reverse or mitigate the damage. Global trade networks are the best determinant of novel plant pest and pathogen introductions, with increased invasion risk in import countries with similar climates and in close geographic proximity to the country of export (Brasier, 2008; Chapman et al., 2016; Roy et al., 2014). The impact of such introductions on economies and livelihoods can be disastrous. Hundreds of thousands of people died from starvation in Ireland and continental Europe following the trade facilitated introduction of potato late blight (*Phytophthora infestans* (Mont.) de Bary) in the 1840s (Kamoun et al., 2015). Today, potatoes remain a staple food crop and potato late blight continues to threaten food security causing >1% losses of the global yield (Savary et al., 2019). In Florida, the bacterial citrus huanglongbing disease (*Candidatus liberibacter* spp.) has reduced yields of citrus fruit by 75% and decimated the industry, infecting 100% of orchards over two years old (Milne et al., 2018). In Italy, Spain and Greece, the bacterium *Xyella fastidiosa* Wells et al., now endemic in southern Italy, threatens 75% of global olive oil

production because 99% of olive groves in those countries occupy suitable climatic conditions for pathogen establishment (Schneider et al., 2020). Failure to control the spread of *X. fastidiosa* could cost European consumers 53 billion euros (Schneider et al., 2021). Beyond threats to food and job security, plant pests and pathogens can have serious environmental impacts. Key examples include increased forest fire intensity in California resulting from a build-up of dead wood following disease-induced tree mortality (Metz et al., 2011) or the replacement of biodiverse ecosystems with those of lower value as observed in Australia where woodlands were converted into low-statured heath following infection of important canopy species (Shearer et al., 2007). In the UK, Dutch elm disease (*Ophiostoma novo-ulmi* Brasier) killed 30 million elms (*Ulmus* spp.) following introductions on imported logs. The disease destroyed culturally valued English “elmscapes”, impoverished woodland communities in Scotland and Wales and provided a salutary warning of the dangers posed by non-native plant pests and pathogens crossing over from commercial and garden settings to the wider environment (Potter and Urquhart, 2017). In spite of the policy reforms that followed, including phytosanitary checks on commercial goods at borders, the prioritisation of risks through pest risk analyses and development of molecular tools to rapidly identify pathogens, trade facilitated introductions continue to impact native environments, sometimes across multiple continents (Freer-Smith and Webber, 2017).

Trees are vital to ecosystems and, therefore, to people. Beyond their direct utility in generating products used by people (i.e. provisioning services) or improving wellbeing (i.e. cultural services), trees perform a huge variety of services that regulate their environment (Boyd et al., 2013a). Trees produce oxygen, stabilise soils, modulate temperatures, provide food and habitats for a huge diversity of species spread across taxonomic groups, can reduce flooding and air pollution, and store carbon. Approximately 420 million hectares of forest (equivalent to the area of California) were lost around the world between 1990 and 2020 (FAO and UNEP, 2020), during which time the international community signed up to binding targets to stop biodiversity loss (Secretariat of the Convention on Biological Diversity, 2010; UN, 1992) and limit the climate breakdown by stopping deforestation and restoring forests to reduce greenhouse gas emissions and sequester carbon (UN, 1997). In 2021, goal 15 of the UN Sustainable Development Goals to halt deforestation, restore degraded forests and substantially increase afforestation and reforestation by 2020 (UN, 2015) has not been met. Fewer than ten years remain to deliver the UN Strategic Plan for Forests commitment to establish 120 million hectares of new forest (UNESCO, 2017), and the more ambitious target to restore 350 million hectares of degraded landscapes and forestlands, committed to by signatories of the Bonn Challenge (IUCN, 2020) and the New

York Declaration on Forests (2014). In the UK, the Committee on Climate Change recommended planting at least 30,000 hectares of productive conifers and native broadleaved woodland per year until 2050 (Committee on Climate Change, 2020). The current UK government adopted this target as a manifesto commitment (Conservative Party (UK), 2019) towards which all devolved nations are providing grant assistance. These targets are laudable but are they achievable? Ten percent of the 48 Bonn Challenge pledges were estimated to exceed the biophysical capacity within the pledged country to support forest restoration, based on climatic, edaphic and topographic variables (Bastin et al., 2019). This calculation ignores site histories regarding pest and disease outbreaks that may prohibit new plantings and the possibility for losses to occur because of new pest or pathogen introductions. Arrivals of new tree diseases are highly likely: introductions of invasive forest pathogens have increased exponentially as trade networks expanded across Europe during the past 200 years (Santini et al., 2013). Fifty-seven percent of invasive forest pathogen introductions are directly traceable to the living plants trade while the movement of timber and wood products accounts for a further 10% (Santini et al., 2013). The UK Plant Health Risk Register identified approximately 30% of the 1,000 pest and disease species listed in 2018 as capable of attacking trees and threatening the extent, connectivity, diversity and condition of forests, woodlands and other treescapes (DEFRA, 2018). The Woodland Trust warn that demand for trees raised within the UK and Ireland to limit new pest and pathogen introductions outstrips the supply of UK and Ireland Sourced and Grown (UKISG) certified trees, despite forecasted production of 27 million UKISG trees between 2014 and 2024 (Reid et al., 2021). Coupled with the resultant risk of increased plant pest and disease introductions, climate change is predicted to promote establishment of invasive species, particularly in the northern hemisphere where climates will remain or become more suitable for species introduced from reservoirs in other regions (Bellard et al., 2013).

Pathogen invasions are typically described as following four stages along an invasion pathway: transport, introduction, establishment and spread. Interventions to manage invasions can be implemented at any stage to prevent or minimise invasion progression (Blackburn et al., 2011). Unfortunately, our ability to predict the identity of future invasive species is largely based upon our knowledge of prior invasions (Seebens et al., 2018). A high percentage of plant pathogens are unknown to science at the point of emergence in new areas (Roy et al., 2017). New environments offer new evolutionary opportunities to pathogens that can lead to unpredictable outcomes (e.g. host jumps) (Santini et al., 2013) and knowledge gaps at all stages of the invasion pathway limit our ability to manage threats (Roy et al., 2017). At the transport and introduction stages of invasion, knowledge about

likely source locations or native ranges of pathogenic taxa, potential introductory pathways, and baseline information about pathogen, host, and vector distributions, are most needed. During the establishment and spread phases, predictive understandings of pathogen host specificity, life history traits, transmission dynamics, regulation by competitors and natural enemies, and baseline information about the recipient populations and ecosystem dynamics, are most useful (Roy et al., 2017).

This thesis explores drivers of an emergent, non-native plant pathogen, *Phytophthora austrocedri* Gresl. & E. M. Hansen, most likely introduced to the UK via the live plant trade that then crossed over to infect native tree populations of common juniper (*Juniperus communis* L.) in the wider environment with the potential to cause serious harm to UK ecosystems and biodiversity. Management of the disease is necessary to protect one of the few UK native conifer species, protected by both national and international legislation, already in receipt of significant conservation resources aiming to address serious declines of populations resulting from land use and climate change. Beyond conservation, juniper is subject to some public and commercial interest resulting from the recent proliferation of gin micro-distilling, incentives to restore or create native woodlands, and is recognisable as a garden plant with 76 horticultural varieties catalogued by the Royal Horticultural Society (Ward and Shellswell, 2017). This combination of ecological and commercial interests, in addition to its UK-wide distribution, means juniper populations are managed by many stakeholders with conflicting motivations and priorities. To complicate the issue further, *P. austrocedri* was only described in 2007 (Greslebin et al., 2007) and the UK outbreak is the first invasion of the wider environment known to occur in the northern hemisphere and in juniper as a host species. This limits our understanding of the pathogen biology and how it interacts with the host and environment with which to plan management interventions. Working with stakeholders in plant health and biodiversity, I aimed to improve the targeting of *P. austrocedri* management and containment measures by understanding how environmental factors and land use heterogeneity mediate the introduction, establishment and spread of *P. austrocedri* in juniper from local to national spatial scales using a combination of field and aerial survey data, and a range of statistical modelling techniques (Figure 1).

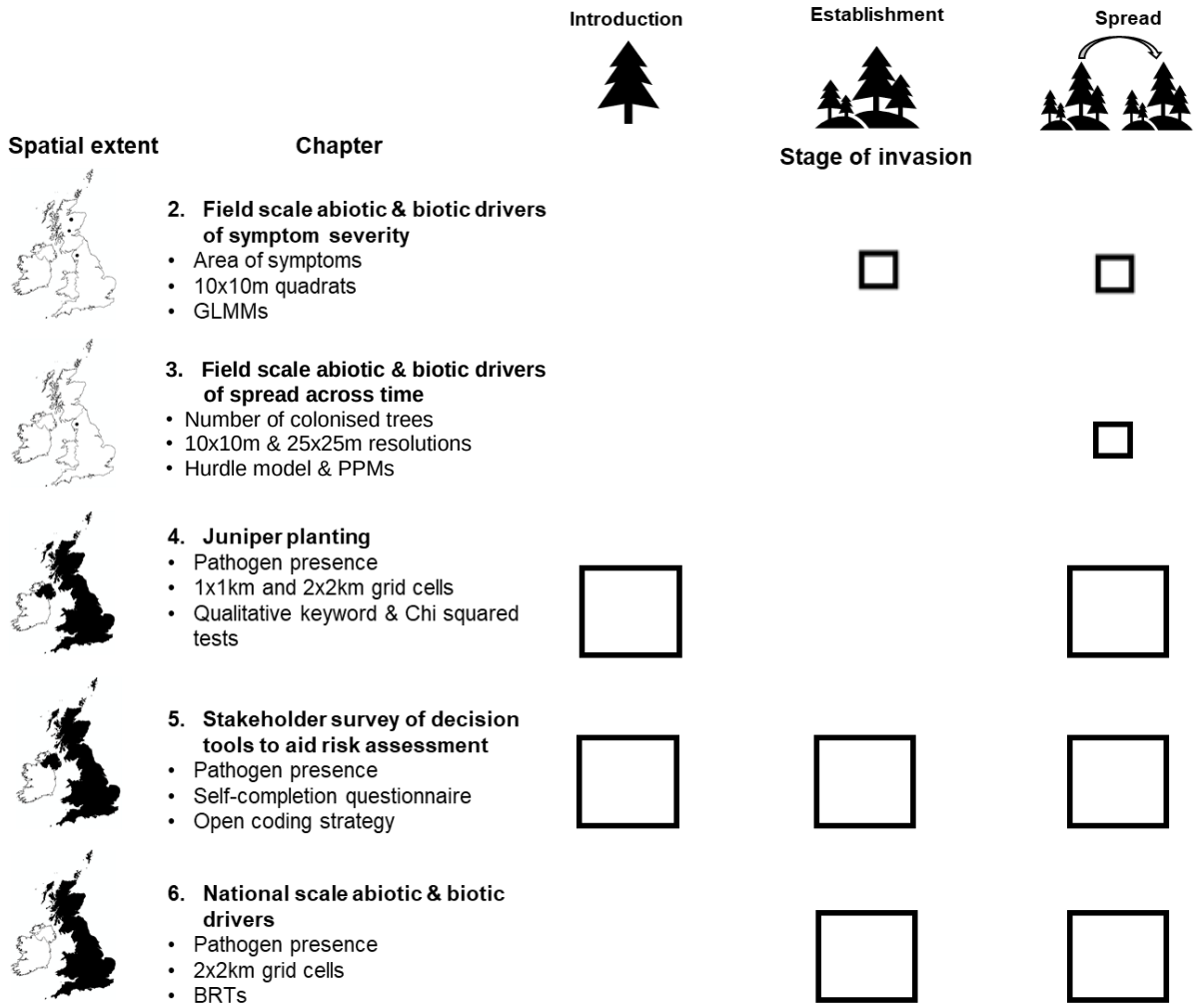

Figure 1. Overview of thesis chapters showing the spatial extent (mapped in black), variable used to describe *P. austrocedri*, the data collection and analysis methods, stage of pathogen invasion (introduction, establishment and/or spread), and spatial scale (field, shown with a small square, or landscape, shown with a large square) explored.

1.2 Biology and distribution of *Phytophthora*

At least 21% of forest disease outbreaks in Europe in the past 200 years resulted from infections with oomycetes (Santini et al., 2013): a class of organisms phenotypically resembling fungi but related instead to diatoms and brown algae. The filamentous oomycete genus *Phytophthora,* translated as “plant-destroyer”, contains many, ecologically diverse pathogenic species complexes with the potential to cause widespread ecological and economic damage. Estimates predict two or three times as many of the ~180 species complexes currently described are likely to exist (Scott et al., 2019), partly because much of

their lifecycle takes place in roots, soil and water making species difficult to detect and control (Erwin and Ribeiro, 1996). In addition to infecting crop plants (e.g. potato late blight), many *Phytophthora* species infect trees with dramatic consequences for host populations, biodiversity and culturally valued species and landscapes. For example, *P. ramorum* Werres, De Cock & Man in't Veld has killed a minimum of 50 million tanoaks (*Notholithocarpus densiflorus* (Hook. & Arn.) Manos, Cannon and S.H. Oh), coast live oak (*Quercus agrifolia* Née) and California black oak (*Quercus kelloggii* Newb.) stems in California and Oregon between 2012 and 2019, risking a further 1.7 billion tanoaks and 68Tg of living biomass carbon (Cobb et al., 2020). In Australia, *P. cinnamomi* Rands can spread 40m per year downslope and along drainage channels, accelerated by road building and translocation of infected soil, irreversibly altering species composition and changing habitat and food resource availability for wildlife, including endemic and endangered species such as the honey possum (*Tarsipes rostratus* Gervais & Verreaux) and driving species in some regions extinct (e.g. *Banksia brownii* Baxter ex R.Br. in SW Australia) (Sena et al., 2018; Shearer et al., 2007). As a final example, *Phytophthora agathidicida* B.S. Weir, Beever, Pennycook & Bellgard is currently causing mortality of kauri trees (*Agathis australis* (D.Don) Lindl.) of immeasurable Māori importance in New Zealand (Bradshaw et al., 2020). A study of *Phytophthora* diversity within Europe found the Atlantic region, in which the UK is located, hosted the highest number of species as a result of the wet and mild climate (Jung et al., 2016). Indeed, five new species have been reported since 2003 causing serious damage to UK tree populations: *P. ramorum*, *P. kernoviae* Brasier, Beales & S.A. Kirk, *P. lateralis* Tucker & Milbrath, *P. pseudosyringae* Jung & Delatour and *P. austrocedri* (Riddell et al., 2019). This climatic suitability for *Phytophthora* species, and the potential for new species to be introduced via global trade pathways, and for hybridisation to occur between species introduced to new geographic locations (Callaghan and Guest, 2015), makes the genus a UK research priority (DEFRA, 2014a).

Recent multigene phylogenies have divided *Phytophthora* into ten (Yang et al., 2017) or 12 (Jung et al., 2017) clades, situating *P. austrocedri* in the same clade (clade eight), but different sub-clade, from *P. ramorum* and *P. lateralis* (Yang et al., 2017). Oomycetes are diploid throughout their lifecycle and can reproduce both sexually and asexually (Erwin and Ribeiro, 1996). Sexual reproduction results in the production of oospores that can persist in soil and infected host tissues for extended periods in harsh conditions (e.g. drought) until the environment becomes suitable for germination and new hyphal production (Erwin and Ribeiro, 1996). By contrast, asexual reproduction occurs when hyphae differentiate into sporangia containing motile, short-lived zoospores that are water-dispersed and attracted to

host tissue to initiate infections (Erwin and Ribeiro, 1996). Mechanisms of zoospore dispersal vary between species: *P. ramorum* and *P. kernoviae* have caducous sporangia (i.e. they break off) to allow wind dispersal, whereas *P. austrocedri* has non-caducous sporangia so disperses via soil water (Greslebin et al., 2007).

First described in 2007 on Chilean cedar (*Austrocedrus chilensis* (D.Don) Pic.Serm. & Bizzarri) in Argentinian Patagonia, *P. austrocedri* was identified as the causal agent of "mal del ciprés", the steady species decline observed since the 1940s (Greslebin et al., 2007; Mundo et al., 2010). Infection generally starts in the roots, spreading into the cambium and phloem and causing necrotic lesions (Figure 2) that can extend for more than one metre above ground (La Manna et al., 2013a). This phloem girdling is thought to lead to the discolouration then desiccation of foliage affecting whole stems or trees and ultimately resulting in tree death (Green et al., 2015) (Figure 2). Infection of juniper with *P. austrocedri* was first detected in the UK in 2011 from a bronzing juniper population (Figure 2) in the Upper Teesdale National Nature Reserve in northern England (Green et al., 2012). Material sampled from this population matched cultured material collected around Glasgow in central Scotland the same year from a Nootka cypress (*Callitropsis nootkatensis* (D.Don) Oerst. ex D.P.Little) growing in a park, and a Port-Orford cedar (*Chamaecyparis lawsoniana* (A.Murray bis) Parl.), known as Lawson cypress in the UK) growing in a private garden (Green et al., 2015). The isolation from juniper in Upper Teesdale satisfied Koch's postulates (Green et al., 2012) but successful isolations have only been obtained from seven locations, despite considerable sampling effort, owing to its slow growth in culture (Green et al., 2015).

Figure 2. Examples of *P. austrocedri* symptoms in common juniper showing a) extensive juniper mortality caused by *P. austrocedri* with arrows highlighting some instances of skeletal dead trees; b) a *P. austrocedri* lesion annotated with arrows indicating necrotic (brown) tissue and the leading infection edge (yellow); c) characteristic progression of *P. austrocedri* foliage symptoms from discoloured (right) to bronzed (centre) compared to healthy foliage (left); d) symptomatic juniper opposite a foot cleaning station at the start of a footpath section traversing a juniper population.

1.3 Discovery and distribution of *Phytophthora austrocedri*

Populations of juniper in the UK (Green et al., 2012) and Chilean cedar in Argentina (Greslebin et al., 2007) are the only tree populations confirmed to be infected with *P. austrocedri* in the wider environment, although symptomatic populations of Chilean cedar have also been observed in Chile (Vélez et al., 2020) (Figure 3). Pathogenicity tests revealed two other native and endangered Patagonian species, *Fitzroya cupressoides* (Molina) I.M.Johnst., and *Pilgerodendron uviferum* (D.Don) Florin, are also susceptible to infection (Taccari et al., 2019). Outside of Argentina, Chile and the UK, the only other

detections of *P. austrocedri* derive from a juniper cultivar, *J. horizontalis* 'Glauca', detected in 2001 upon import to a German nursery (Werres et al., 2014) and an Italian cypress (*Cupressus sempervirens* L.) planted in a park in Qazvin city in Iran detected in 2017 (Mahdikhani et al., 2017) (Figure 3). Symptoms in UK juniper populations were first reported from Glenartney Site of Special Scientific Interest (SSSI) in 2000 as sudden foliage bronzing and a clustered but seemingly random pattern of tree mortality across the site (Broome et al., 2008). In 2003, a report published by NatureScot found 48% of a planted juniper populations exhibited bronze foliage of which the causal agent could not be identified (Sullivan, 2003), echoed in 2004/5 by a Scotland-wide citizen science survey that reported bronzing in 52% of 381 recorded sites (Long and Williams, 2007). Foliage bronzing recorded in this survey could result from a variety of causes including infection with *Phomopsis juniperovora* Hahn or mechanical damage to branches. However, the findings may illustrate that *P. austrocedri* was present in the UK prior to the first confirmed detection in 2011 (Green et al., 2012). Only one genetic lineage of *P. austrocedri* has been detected from these UK isolates, which is distinct from the lineage found in Argentina. Thus the epidemics in each country started from separate introductions of different lineages likely derived from the same source population of currently unknown location (Henricot et al., 2017a). Lack of genetic variation in both UK and Argentinian populations of *P. austrocedri* suggest that the pathogen is spreading asexually, making zoospores the most likely life stage driving pathogen dispersal (Henricot et al., 2017a). Yet the widespread distribution of infected juniper populations throughout Scotland and England is difficult to explain in terms of natural zoospore dispersal through soil water. Alternative spread pathways, such as the translocation of inoculum in infected soil by livestock, wildlife and people (Figure 2), and the distances over which spread may occur, are poorly understood (Henricot et al., 2017a) and were identified as research priorities in the *P. austrocedri* UK pest risk assessment (DEFRA, 2015). Additional priorities also included researching the relative risk of propagating juniper for restoration purposes and understanding the climatic, edaphic and hydrological factors affecting pathogen establishment and spread to aid identification of juniper populations at lower disease risk that could be targeted for conservation (DEFRA, 2015).

Figure 3. Global map of countries where common juniper (*Juniperus communis*) is native (World Checklist of Selected Plant Families, 2017) compared to the current known range of *P. austrocedri*, differentiated as locations where infections are present in native tree populations compared to only nursery or landscaped settings. The distribution shown in Patagonia is derived from a 50km buffer surrounding records of *Austrocedrus chilensis* available from GBIF (2021) 1990-2021.

1.4 Biogeography and conservation importance of common juniper

Common juniper is an evergreen, dioecious, wind-pollinated conifer in the family Cupressaceae, widely found throughout North America, Europe and Asia from 30˚N (Global Biodiversity Information Facility (GBIF), 2016; Green et al., 2015; Ward and Shellswell, 2017) (Figure 3). Only three species of conifer: juniper, Scots pine (*Pinus sylvestris* L.) and yew (*Taxus baccata* Thunb), and two hybrids: Leyland cypress (*Cupressus* x *leylandii* A.B.Jacks. & Dallim.) (Royal Forestry Society, 2011) and Dunkeld larch (*Larix* x *marschlinsii* Coaz) (Nelson, 1980), are thought to be native to the UK. Juniper survived the most recent ice age, rapidly expanding its range across Great Britain as the glaciers retreated and before the succession of birch woodlands (Ince, 1995; Lowe and Walker, 1981). The extent of juniper has always fluctuated in the UK landscape as a result of human activity (Thomas et al., 2007). Historical uses for juniper are described in detail in "*Flora Celtica"* (Milliken and Bridgewater, 2004), including the transport of juniper berries collected in the Scottish Highlands to the Netherlands to make genever (a pre-cursor to gin); ritual burning of juniper in houses at New Year to ward off evil spirits and cleanse the air of pests and diseases (including a strongly held belief on the island of Colonsay that juniper smoke would protect against the Plague), and illicit production of whisky, using juniper wood that burned hot and with little smoke thus concealing the enterprise from the excise man. Following the Highland

clearances and resultant dramatic changes in land use, large juniper populations were seldom maintained and while the species remains relatively widespread across Scotland, large populations in England and Wales are confined to the Lake District, Teesdale, the South Downs and Snowdonia (Ward and Shellswell, 2017) (Figure 5).

Juniper is very morphologically diverse with some trees growing as low, carpet forming mats while others are tall and columnar (Figure 4). Taxonomists identify two subspecies, of which columnar forms are always identified as *J. communis* subsp. *communis* while carpet forms may be identified as *J. communis* subsp. *nana* where more than 40% of the leaves have abruptly pointed tips (Sullivan, 2003). However, many botanists submitting records to the Botanical Society of Britain and Ireland (BSBI) believe the subspecies distinction is poorly characterised and subspecies are more often recorded based on habitat and the recording convention used for any former records than using leaf tip morphology (McIntosh, J., personal communication, 17th August 2017; Stroh, P., personal communication, 5th December 2018). There is genetic support for a third subspecies, *J. communis* subsp. *hemisphaerica*, that is mainly found in mountainous areas of southern Europe and north-west Africa and persists in the UK only on the Lizard peninsula in Cornwall and as a re-introduced population in Pembrokeshire in southwest Wales (Merwe et al., 2000; Preston et al., 2002; Squirrell and Hollingsworth, 2008). With so little available material, *J. communis* subsp. *hemisphaerica* has not been tested for *P. austrocedri* susceptibility but the pathogen has been isolated from material phenotypically identified as *J. communis* subsp. *communis* (Green et al., 2015, 2012) and *nana* (Dun, 2016). Given the uncertainty in subspecies recording, all analyses in this thesis were performed using all subspecies records, i.e., *Juniperus communis* sensu lato.

Figure 4. Examples of common juniper morphology, habitats and pressures showing a) a sprawling form of *J. communis* subsp. *nana* growing in a boulder field in Snowdonia, Wales; b) a tall example of *J. communis* subsp. *communis* growing in improved grassland in the southern uplands, Scotland, with clear browsing damage caused by sheep; c) juniper growing at the edge of birch woodland in the Cairngorms, Scotland; d) a solitary juniper protected from agricultural clearance by growing on an archaeological feature in East Anglia, England, but with few surrounding bushes and little available habitat to permit regeneration.

Juniper is a component of many different national vegetation classification communities including acidic heathlands, calcareous grassland, montane scrub, sand dunes and woodlands, sometimes as a dominant component e.g. W19 *Juniperus communis* subsp. *communis – Oxalis acetosella* national vegetation community or as an occasional species in the understorey of birch (*Betula* spp.) or Scots pine woodlands (JNCC, 2007). As a native species, juniper supports many other taxa including over 100 species of fungi and slime moulds (Ward and Shellswell, 2017), at least 50 species of insects and mites including specialists such as the juniper carpet moth and juniper shield bug, provides nesting habitat for birds such as firecrests and black grouse, produces berries fed upon by fieldfares and

other thrushes which act as the primary agents of seed dispersal (Wilkins and Duckworth, 2011a), and is grazed by small (voles) and large (deer) mammals, particularly during the winter when other food sources are scarce (Thomas et al., 2007). Juniper is a pioneer coloniser of successional habitats, preferring freely drained, open ground (Ward and Shellswell, 2017), can act as a nurse plant protecting saplings of other tree species such as hazel (*Corylus avellana* L.) from grazing (Wilkins and Duckworth, 2011a), and has a variable rooting depth that allows it to grow on and stabilise scree slopes, rock ledges and embankments (Thomas et al., 2007). Consequently, juniper is protected as a component of many nationally designated SSSIs and five Annex 1 habitats listed under the European Economic Community Habitats Directive (1992) protected as features within Special Areas of Conservation that are currently being transcribed into national law following EU exit. Additional protection of all populations is afforded through Schedule 8 of the Wildlife and Countryside Act (1981 as amended) and between 1994 and 2010 juniper received additional conservation resources as a UK Biodiversity Action Plan priority species (JNCC, 2016).

Concerns about loss of juniper extent and lack of regeneration were first raised when English populations surveyed in the 1970s and 1990s were compared (Clifton et al., 1997, 1995; Ward, 1994a). For example, 54% of juniper populations in Northumbria (northern England) declined in extent between 1973 and 1994 with 16% lost completely (Clifton et al., 1995). A decade later, a citizen science survey orchestrated by Plantlife Scotland discovered 40% of the 453 populations surveyed comprised fewer than ten bushes and 67% had no seedlings or young plants (Long and Williams, 2007). Plantlife also reported profound changes in the number of 10x10km grid cells recorded 1987-1999 compared to the period 2000-2016: 44% fewer cells were occupied in England, 44% fewer in Wales, 58% fewer in Northern Ireland and 27% fewer in Scotland (Ward and Shellswell, 2017). In 2017, the BSBI threatened plants projects re-found 17 of 20 juniper populations in southern England last recorded in 1970 but the mean population size was just 26 bushes (Walker et al., 2017). A decline in both population size and quality is also evident from SSSI monitoring, with 66% of 35 English, and 54% of 13 Scottish, juniper features assessed to be in unfavourable condition (Natural England, 2019a; NatureScot, 2017). Hypothesised causes for decline include direct habitat or host tree destruction (e.g. burning or deforestation) or factors that contribute to poor juniper regeneration. These include aging populations leading to reduced reproductive vigour, changes in temperature cycles that trigger germination or diffuse pollution, particularly with a high nitrogen content, hindering fertilisation (Broome et al., 2017; Lavery, 2016; Long and Williams, 2007; Sullivan, 2003; Verheyen et al., 2009). Juniper is a pioneer species so requires high light and moisture levels to germinate successfully

meaning recruitment is affected by undergrazing (where bracken or grasses are allowed to shade out seedlings) as well as overgrazing (where seedlings are eaten) (Figure 4) (Broome et al., 2017; Lavery, 2016; Sullivan, 2003; Ward and Shellswell, 2017; Wilkins and Duckworth, 2011). Juniper population declines have also been recorded in the Netherlands and Belgium with similar explanations (De Frenne et al., 2020; Verheyen et al., 2009). Small percentages of juniper affected by pests or diseases were historically recorded but these were never discussed as major causes of decline until the early 2000s when surveys revealed large areas of foliage browning that was not attributable to known pathogens (Ward and Shellswell, 2017). The extent to which drivers of disease introduction, spread and establishment interlink with these other environmental stressors is a key knowledge gap that could inform future practices for juniper conservation management.

1.5 Plant pathogen host-disease-environment interactions

Understanding how landscape features influence the spatial structuring of hosts and predispose habitat patches to infection is fundamental to sustainable management of forest diseases (Holdenrieder et al., 2004). Diseases emerge from interactions between a pathogen, a susceptible host and suitable environmental conditions that can be thought of as a disease triangle (Francl, 2001). Changes to any of the components can accelerate or curb disease dynamics (Cobb and Metz, 2017). For an introduction to occur, an infectious propagule must be transported from a source to a new receiving environment and infect a susceptible host e.g. via natural phenomena such as wind or water, or the human-mediated movement of infected plants or timber (Brasier, 2008). Host susceptibility can result from intrinsic or extrinsic factors that reduce physiological status, or a combination of both. An example of an intrinsic factor could be poor genetic diversity following a population bottleneck whereas extrinsic factors could be suboptimal abiotic conditions (e.g. waterlogging) and/or detrimental biotic interactions (e.g. competition from other plant species or damage from a plant pest) that predispose the host to infection in response to environmental stress (Cobb and Metz, 2017). For the pathogen to establish and spread it must be able to generate new infectious units, requiring environmental conditions that it can either tolerate or adapt to, a sustained supply of susceptible tissue it can spread to, and a dispersal mechanism e.g. spores spread by rainsplash (Cobb and Metz, 2017; Gilligan and van den Bosch, 2008; Prospero and Cleary, 2017). The abundance and invasiveness of the pathogen is partly regulated by its organismal traits such as sexual vs asexual propagation, thermal and moisture requirements to trigger inoculum production, and the potential of spores to persist in the soil during periods of unsuitable conditions (Prospero and Cleary,

2017). Pathogen abundance can also be affected by the structure of the host population, where denser populations aid the ease of pathogen transmission across landscapes, and the composition of the host community because some species will act as hosts, reservoirs for propagules, or non-hosts that act as barriers to disease dispersal (Meentemeyer et al., 2011; Purse et al., 2013). Host community structure and composition will also be moderated by environmental conditions e.g. the most explanatory variable for oak mortality at the start of the *Phytophthora ramorum* epidemic in California was proximity to the forest edge where the high light conditions supported larger understorey populations of reservoir hosts such as bay laurel (*Umbellularia californica* (Hook. and Arn.) Nutt.) (Holdenrieder et al., 2004). Each of these drivers may vary in time and in space. For example, host susceptibility may fluctuate with changes in environmental conditions throughout the year and ecological processes or land management may change host distributions (Cobb and Metz, 2017). Key factors promoting disease establishment are likely to vary between spatial scales e.g. host species diversity may regulate field scale disease dispersal but might be much less significant at regional scale if pathogen spread is primarily constrained by hydrological features or anthropogenic activities. The failure of the disease to propagate at any one of these spatial scales can prevent further invasion and increased understanding of the scaling of different mechanisms of disease establishment and spread will improve risk assessment and targeting of control measures.

1.6 Modelling the establishment, spread and impact of plant pathogens

Understanding the potential impacts of novel plant pathogen introductions and choosing suitable methods for control depends on knowledge of how each stage in the invasion pathway is mediated by host populations, environmental conditions and spread pathways that determine pathogen dynamics across a range of spatial and temporal scales (Prospero and Cleary, 2017). Models can be used to elucidate these interactions (Haas et al., 2011), predict future spread patterns (Burgess et al., 2017), and even simulate responses to different control measures to help predict impacts and inform containment strategies (Cunniffe et al., 2016). Statistical models are commonly used in ecology to explore correlative relationships between species distributions and gridded spatial datasets of environmental (usually abiotic) variables, to identify the significant factors underpinning spatial patterns of species presence and/or abundance, and predict the suitability of areas outside the sampled range that could support the species (de Rivera et al., 2019; Elith and Leathwick, 2009). Correlative species distribution models can be applied to estimate potential areas of establishment early in pathogen invasion when information about the

pathogen biology and impacts is lacking. A range of potential environmental drivers of pathogen introductions (Chapman et al., 2016) and changes in occupancy during phases of establishment and spread can also be incorporated within such models (Václavík and Meentemeyer, 2012), but the disease-environment relationships quantified are not necessarily robust to novel combinations of conditions.

Similarly, mechanistic models can be used to model the full invasion pathway but tend to explore intrinsic factors that control the shape and speed of an epidemic across a landscape (of any scale, from within the plant (Gomez-Gallego et al., 2019) to across a plant nursery (Bate et al., 2016) to across an entire country or region (Meentemeyer et al., 2011)). These models aid understanding of how the epidemic trajectory may vary depending on the likely locations of initial propagule introduction, dispersal distances, the significance of cryptic infections and asymptomatic hosts, and can predict scenarios where introductions may fail to establish. However, full parameterisation of mechanistic models requires formidable volumes of data, most notably pathogen distributions observed across multiple time intervals. These are often unavailable for emergent pathogens and/or costly and difficult to obtain for invasions that occur across a large area in the wider environment. I aimed to demonstrate ways to obtain early insights into potential drivers of disease introduction, establishment and spread for emergent plant pathogens in novel settings (i.e. non-equilibrium with the new environment) with limited distribution data by improving the range of drivers considered and incorporating proxies for dispersal and infection processes into statistical models that could be used to inform control strategies. While theoretical models of pathogen-environment dynamics have long considered biological drivers of establishment and spread, there are relatively few examples of applied, plant pathogen specific studies that do so. Examples of biotic drivers of pathogen establishment and spread include different grazing regimes (La Manna et al., 2013a) or spread pathways such as roads and wildlife corridors (Jules et al., 2002) or trade pathways (Chapman et al., 2017a). Because social and economic factors are likely to be the most important drivers of pathogen introductions (Santini et al., 2013), I also explore relationships between known disease outbreaks and recreational pressure and the plants-for-planting introductory pathway. Finally, I use the concept of dispersal kernels, widely used in both mechanistic and statistical models (Allouche et al., 2008; Meentemeyer et al., 2008a; White et al., 2017) but rarely at field (<1km) scale, to estimate the likely shape of pathogen dispersal in relation to distance, and estimate force of infection driving pathogen colonisation over time.

The choice of statistical modelling technique with which to explore plant pathogen distributions often depends on the type of data used to characterise the dependent variable. Previous statistical studies generated an understanding of conditions favouring disease establishment using regression based techniques (Haas et al., 2011; Meentemeyer et al., 2008a), such as generalised linear models (GLMs). GLMs are an extension of linear regression which uses a link function to allow for non-linear responses of the dependent variable, and also allows for non-normal error distributions. A common use of GLMs is when the dependent variable is characterised by a binomial distribution because it is measured as a binary form (e.g. presence/absence) or reflects the number of successes out of a certain number of trials (e.g. area of symptoms within a fixed quadrat) (Blangiardo and Cameletti, 2015). Since GLMs are flexible, they allow for hierarchical data and non-normal responses, and as generalised linear mixed models (GLMMs) can incorporate random effects (e.g. to account for unobserved heterogeneity in the data). Implementing GLMMs within a Bayesian statistical framework allows sources of uncertainty in the resulting predictions to be fully accounted for (Blangiardo and Cameletti, 2015). A recently developed method called Integrated Nested Laplace Approximations (INLA) extended the possible uses of Bayesian GLMMs by offering a structurally flexible method to fit regressions in a computationally efficient way that can also explicitly account for spatial autocorrelation (Rue et al., 2009). Spatial autocorrelation occurs where model residuals or errors are more correlated between neighbouring locations than with sites further away so violate the assumption of independence in model residuals (Dormann et al., 2007). A second statistical modelling method used in ecology to predict potential species ranges is point process modelling (PPM) that can be implemented where the dependent variable is only known as a series of presence locations associated with a frequency count. Unlike regressions, PPMs focus on the spatial location of observed presences to identify the relative suitability of other locations with shared environmental characteristics that could be occupied by the species of interest (Renner et al., 2015). As such, this method can be used to understand relationships between observed pathogen abundance (defined, for example, as the number of observed symptomatic trees) and abiotic and biotic disease drivers to predict infection intensity across an area of interest (Cardillo et al., 2021). Machine learning algorithms are also used more widely in ecology than epidemiology to predict the probability of species presences by building regression trees, where predictor space is segmented into regions using a series of splitting rules to identify the relative importance of different predictors in explaining species distributions. These methods can have high predictive accuracy and offer advantages in accommodating different data types and exploring large numbers of alternative trees to find the most parsimonious combination of environmental predictors (Elith et al., 2008). Lastly,

there is a propensity within the current body of statistical plant disease modelling literature to investigate patterns of infection at large (regional or national) spatial scales (e.g. Bebber et al., 2014) where data corresponding to environmental conditions are more readily available but neglect the effect of finer scale detail such as host connectivity and population structure on disease persistence, even though this may be the scale at which control measures are applied (Gilligan and van den Bosch, 2008). Furthermore, despite increasing interest in working with policymakers to translate modelling results from plant pathology studies into action (Cunniffe et al., 2015a), relatively few use participatory approaches to directly involve stakeholders early in the modelling process to frame pertinent questions and inform covariate choices that improve the transferability and understanding of results (Gaydos et al., 2019; Jones and Kleczkowski, 2020).

1.7 Thesis overview

In this thesis I seek to:

1. understand how abiotic and biotic factors interact to favour establishment and spread of *P. austrocedri* infection of common juniper from field to national scales;

2. determine how a) conditions favouring juniper population persistence interface with b) conditions favouring disease establishment;

3. collaborate with stakeholders to develop or improve decision tools used to ascertain which site types may be less vulnerable to *P. austrocedri* infection and identify management actions that could deliver benefits for juniper conservation.

I begin the next chapter (Chapter 2) by reporting the results of a field study conducted at three geographically separate juniper populations with different *P. austrocedri* infection intensities to collect data in 10m quadrats on symptom severity, and abiotic and biotic microsite conditions including topography, soil moisture, juniper density, browsing damage and commonly associated vascular plant species. I use spatially explicit, Bayesian beta-binomial GLMMs to explore population level relationships between juniper symptom severity and microsite conditions and understand if and how these relationships differ between populations to promote pathogen establishment and spread.

Chapter 3 continues with an investigation of field level drivers of *P. austrocedri* infection, this time exploring factors promoting pathogen colonisation of a single juniper population that took place between two aerial surveys conducted four years apart, and to forward predict

infection intensity that could be observed at the end of the following four-year period. Models are developed at 10m and 25m spatial resolutions to better understand the scale over which the colonisation process operates and to find out if the importance of disease drivers varies with spatial scale. Hurdle models are first used to understand how the environmental conditions of interest underpin the presence and density of juniper, followed by point process models that are used to explore the intensity of newly symptomatic trees compared to the initial survey. A range of dispersal kernels with different shapes and scales are incorporated in the models in addition to the environmental conditions tested in the hurdle models to provide the first understanding of how *P. austrocedri* dispersal varies with distance and examine the intersection between conditions occupied by juniper and conditions that facilitate pathogen growth and dispersal.

Disease drivers operating at a national spatial scale were considered in chapter 6, but not before compilation of a 2km resolution dataset documenting the distribution and frequency of supplementary juniper planting conducted across the UK, as a key potential introductory pathway in explaining the national distribution of infected juniper populations. Chapter 4 details the data collection process and evaluates the prevalence of *P. austrocedri* outbreaks in relation to supplementary planting events, analysing if factors including the number of trees, type of source material, propagation location and type of stakeholder overseeing the planting change the likelihood of pathogen introduction. The results are discussed in terms of the diversity of planting practices used and opportunities to reduce the potential for disease transmission via this pathway.

This is followed up in Chapter 5 where stakeholders involved in juniper management, as managers, agents, assessors, or growers participated in an online survey to provide feedback about the utility of decision tools aimed to aid site level risk assessment of juniper management practices. Two decision tools are presented: i) the decision framework provided in the DEFRA juniper management guidelines (DEFRA, 2017) and ii) interactive maps of 1km resolution *P. austrocedri* outbreaks in the wider environment in conjunction with 2km resolution native and planted juniper populations. Stakeholders were additionally asked to identify and prioritise risk factors expected to promote *P. austrocedri* infection of juniper at the national scale, which were subsequently explored in Chapter 6.

The relationship between *P. austrocedri* presence in 2x2km grid cells containing juniper in Great Britain, and abiotic and biotic disease risk factors is investigated using Boosted Regression Trees (BRTs) in Chapter 6 to predict the risk of infection in all juniper grid cells nationwide. Risk factors identified in previous chapters as potential drivers of localised

P. austrocedri introduction, establishment and spread, are included in the analysis with the addition of climatic factors (temperature, rainfall), and supplementary juniper planting conducted across different periods of time since the 1970s. The relative importance of risk factors in predicting the probability of *P. austrocedri* presence is compared to the importance predicted by stakeholders, who were also asked to provide feedback about the utility of the resultant risk map.

To conclude, Chapter 7 draws findings from the preceding chapters across the different model types, stages of invasion, and spatial scales together, and outlines remaining knowledge gaps that would benefit from further research. Recommendations for juniper management identified from the modelling and stakeholder engagement processes are consolidated. Novel findings about *P. austrocedri*-host-environment interactions that will benefit juniper conservation both in the UK and internationally are summarised, alongside the novel contributions made by this thesis to the field of plant health modelling more generally.

Chapter 2

Small scale variability in soil moisture drives infection of vulnerable juniper populations by invasive forest pathogen

Data Availability Statement: The data used in each of the models presented in this chapter are available to download from the Dryad data repository at https://datadryad.org/stash/dataset/doi:10.5061/dryad.3xsj3txc9.

2.1 Abstract

The oomycete plant pathogen, *Phytophthora austrocedri*, is an aggressive killer of cypress trees causing severe mortality of Chilean cedar (*Austrocedrus chilensis*) in Argentina since the 1940s and now of common juniper (*Juniperus communis* s.l.) in the UK. Rapid mortality of key UK juniper populations was first observed in the early 2000s. The causal agent of mortality was confirmed as *P. austrocedri* in 2012 and the pathogen has now been widely detected - but is not ubiquitous - in juniper populations across Scotland and England. Although juniper has a broad distribution across the northern hemisphere, the UK incidence of *P. austrocedri* remains the only confirmed infection of juniper populations globally. Juniper is an important species for biodiversity, so it is imperative to understand the abiotic and biotic drivers of emergent *P. austrocedri* infection to inform detection, containment, and conservation strategies to manage juniper populations across the full extent of its range. As management of UK juniper populations is primarily conducted at a local level, we investigated field scale drivers of disease – in three, geographically separate populations with different infection histories. Variation in the proportion of juniper showing symptoms - discoloured or dead foliage – was measured using stratified sampling across along key environmental gradients within each 100-hectare population. Potential predictors of infection included altitude, slope, distance to nearest watercourse, soil moisture (mean percentage volumetric water content), area of red deer browsing damage and area of commonly associated vascular plant species. We assessed support in the data for alternative models explaining the spatial distribution of *P. austrocedri* symptoms using full subset covariate selection and Deviance Information Criteria (DIC). Despite differences in environmental gradients and infection histories between populations, area of juniper symptomatic for *P. austrocedri* increased with waterlogging, increasing with soil moisture in sites where soils had higher peat or clay contents, and decreasing with proximity to watercourses where sites had shallower, sandier soils. Furthermore, we identified common taxa in the associated plant community that correlated with increased area of symptoms and could be used by land managers as indicators to identify microsites at high risk of infection, enabling site-specific tailoring of disease management strategies. Such strategies could include prioritising detection inspections in microsites with high water tables and high grazing pressure (guided by indicator taxa), limiting soil disturbance in wet microsites and creating sites for natural regeneration in drier microsites, to minimise pathogen spread and maximise the resilience of existing juniper populations.

2.2 Introduction

The frequency of plant pathogen introductions outside their native ranges is increasing as global trade networks expand (Chapman et al., 2017a). Successful establishment of pathogens in these new environments is increasingly being facilitated by degradation of the receiving communities through habitat fragmentation, species turnover and land use change (Chapman et al., 2016; Meentemeyer et al., 2011). Economic losses from plant diseases in the natural environment can result directly from drastic reductions in the extent and viability of host species, increased cost of detection and containment measures, or from indirect losses such as destablisiation of ecosystem functioning from loss of biodiversity or negative visual impacts detering tourists, driving down house prices and increasing local crime rates (Boyd et al., 2013b; Kovacs et al., 2011; Mills et al., 2011; Troy et al., 2012). While it is appealing to act immediately to try to control disease outbreaks, the effectiveness of these actions improves as more information on the processes governing spread becomes available, often relying on information that does not exist prior to pathogen introduction (Thompson et al., 2018). Understanding the subset of abiotic and biotic conditions in the invaded range under which introduced pathogens are likely to infect susceptible host populations can improve targeting of such interventions and highlight risk factors for outbreaks in uninvaded locations (Cunniffe et al., 2015b).

The oomycete genus *Phytophthora* contains many pathogenic species that adversely impact plant health, forestry, and agriculture, necessitating expensive, long-term, landscape scale management. Between 1970 and 1989, 11 *Phytophthora* species were introduced to China, 12 to the UK and 16 to the USA (Barwell et al., 2021a). In the two decades following, the number of additional species introduced at least doubled in China (20) and the UK (29) and increased five-fold in the USA (54). While not all of these species established, some of them have caused serious tree mortality with dramatic landscape and economic consequences. In Western Australia 282 000ha of Jarrah (*Eucalyptus marginata* Donn ex Sm.) have been lost to *P. cinnamomi* (Boyd et al., 2013b), while trade of Port-Orford cedar (*Chamaecyparis lawsoniana*) in the north-western United States was almost eliminated by *P. lateralis* (Hansen, 2015). Meanwhile, millions of coast live oak (*Quercus agrifolia*) and tanoak (*Notholithocarpus densiflorus*) trees in California and Oregon, and 18000ha of Japanese larch (*Larix kaempferi* (Lamb.) Carr.) in the UK and Ireland have been killed by *P. ramorum* (Meentemeyer et al., 2011; O'Hanlon et al., 2018; Peterson et al., 2014).

First described in 2007, *Phytophthora austrocedri* has caused widespread mortality of Chilean cedar (*Austrocedrus chilensis*) in Argentina since the 1940s (Greslebin et al., 2007;

Greslebin and Hansen, 2010). The pathogen is homothallic and is potentially spread by both asexual, motile zoospores dispersed through any form of moving water, and sexually produced, thick-walled oospores that can remain viable for extended periods of time and be translocated in soil (Green et al., 2015; Henricot et al., 2017b). Infection usually starts in the roots before spreading into the cambium and phloem, creating necrotic lesions that can extend to the full width of each layer, starving whole branches, trunks or trees of water and nutrients causing rapid defoliation and mortality (Green et al., 2015). Symptoms were first brought to the attention of UK plant pathologists in the mid-2000s, when significant numbers of symptomatic juniper (*Juniperus communis* s. l.) could be observed in two of the larger populations (Glenartney and Haweswater), but *P. austrocedri* was not confirmed as the causal agent of mortality until 2012 following isolation and confirmation of Koch's postulates (Green et al., 2012). In the UK the pathogen is present as a single genetic lineage exhibiting no diversity in nucleic and mitochondrial loci, suggesting introduction and spread of a single clonal strain (Henricot et al., 2017b). The extent of juniper decline varies, with some populations showing wholesale dieback of bushes compared to others with only localised patches of symptoms, suggesting populations have been infected at different times and/or different site conditions promote different rates of spread.

Although interceptions of infected cypress and juniper trees in Scotland, England and Germany confirm that infected material is being traded (Green et al., 2015; Werres et al., 2014) the outbreak in British juniper populations in the wider environment remains the only detected infection of a natural host population outside Argentina (Green et al., 2012). Globally, juniper has a large, circumboreal distribution extending across the northern hemisphere but as no investigation of environmental drivers of infection has been undertaken, the proportion of juniper vulnerable to *P. austrocedri* infection is unclear. In the UK, juniper has a wide but discontinuous distribution occupying much of Scotland and northern England and remaining as scattered populations in southern England, Wales, and Northern Ireland (Figure 5). Populations are undergoing long term declines in most areas as a result of burning, afforestation, over-grazing, under-grazing, increased levels of diffuse pollution (particularly nitrogen) and poor germination following warmer winter temperatures (Broome and Holl, 2017; Clifton et al., 1997; Long and Williams, 2007; Sullivan, 2003; Verheyen et al., 2009; Walker et al., 2017; Ward and Shellswell, 2017). It is difficult to estimate the area of juniper lost specifically to disease but infected populations are

widespread across Scotland and England, where juniper occupancy of 10x10km cells reportedly declined by 23% and 44% respectively between 2000 and 2016 (Plantlife, 2015).

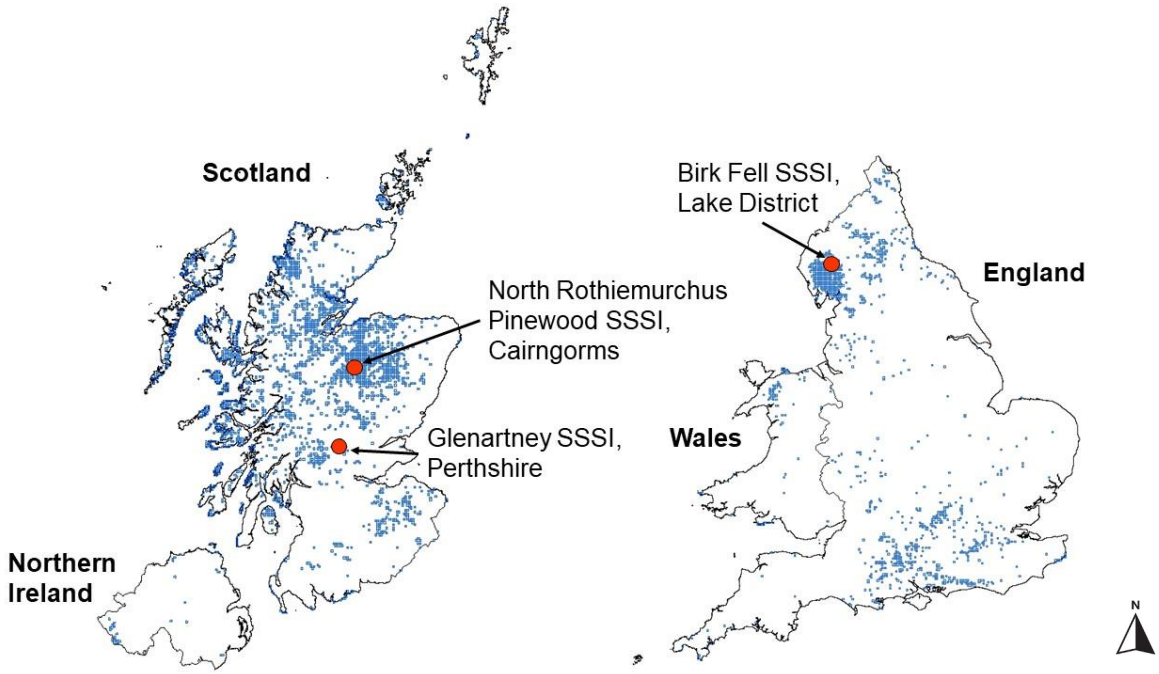

Figure 5. SSSI name and location of the three juniper study populations mapped against the distribution of UK juniper (*Juniperus communis* s. l.) at 2x2 km resolution (shown in blue) recorded during the period 2000 – 2017 (BSBI, 2017).

The societal and environmental value of woodlands was recognised in the 2014 Tree Health Management Plan for England as several times higher than the commercial value of forestry (DEFRA, 2014a) and the Scottish Plant Health strategy identifies plant health in the natural environment as integral to the £1.8 billion rural economy (Scottish Government, 2016). Loss of UK juniper populations to *P. austrocedri* could be significant as the species is highly ecologically important as a dominant component of many habitats including woodland, scrub, heath, dune and calcareous grassland, as a nurse species ameliorating environmental conditions and protecting other seedlings from herbivory, a rare source of winter food and nesting habitat for birds, and a host of many specialist fungi and insects (Thomas et al., 2007; Ward and Shellswell, 2017; Wilkins and Duckworth, 2011). As juniper occupies such a broad variety of habitats, trees are subject to different environmental conditions and land uses that may alter their susceptibility to disease. Epidemics occur across a range of spatial scales, arising first as microscopic infections that can spread to whole plants, populations and landscapes (Gilligan and van den Bosch, 2008). Successful disease control requires matching of the scale of management to the inherent scale of

spread as mediated by host population connectivity and pathogen dispersal distances (Cunniffe et al., 2016). Transmission of soil borne pathogens is likely to occur across short distances resulting in highly aggregated infection prevalence and spatially variable exposure to pathogens within host populations (Penczykowski et al., 2018). However, very few studies of soil borne Phytophthoras investigate spread at field scale and those that do use small (<20) sample sizes (La Manna and Matteucci, 2012; La Manna and Rajchenberg, 2004a; Nagle et al., 2010; Tippett et al., 1989).

We measured juniper symptoms in 147 quadrats across three, geographically separate juniper populations with contrasting infection intensities and analysed the data using Generalised Linear Mixed Models (GLMMs) to compare drivers of spatial variation in symptoms at field scale. Correlative approaches, such as GLMMs, are appropriate tools to perform such exploratory analyses as they can accommodate a broad range of potential covariates as is necessary when drivers of pathogen dispersal and spread in the invaded range are poorly understood (Purse and Rogers, 2009). We expected *P. austrocedri* infection of juniper would exhibit similar responses to environmental covariates as infected Chilean cedar, which occupies a similarly diverse range of ecotypes. Population level studies in Argentina found area of foliage symptoms increased in microsites situated at low altitude with poor soil drainage, flat slopes, close proximity to watercourses and fine soil textures, with greater infection of female cedars because they typically occupy wetter microsites (Baccalá et al., 1998; El Mujtar et al., 2012; La Manna et al., 2008; La Manna and Rajchenberg, 2004a; La Manna and Rajchenberg, 2004b). In addition, we expected that the area of symptoms in juniper would increase with i) increasing host density, as inoculum production is likely to increase with availability of host tissue and dispersal distances between roots will be reduced (Anderson and May, 1986; Dillon et al., 2014); ii) increased ungulate herbivory, and proximity to deer and sheep tracks and lie-ups, as evidence for increased exposure to inoculum transported in soil on herbivore hooves (Jules et al., 2002; La Manna et al., 2013a); and iii) increasing area of individual vascular plant taxa in the associated community that indicate conducive soil conditions for *P. austrocedri*. Given the contrast in abiotic and biotic conditions occupied by each population, we further expected that the relative importance of the investigated covariates would vary between locations and require site specific strategies to manage individual juniper populations.

2.3 Methods

2.3.1 Study Areas

Three infected juniper populations from where *P. austrocedri* had previously been isolated (Henricot et al., 2017) were selected to best represent the diversity of climatic, topographic and edaphic conditions occupied by juniper. Two populations are located in Scotland: one in Perthshire (P) and one in the Cairngorms (C), and one population is situated in the Lake District (LD) in the north of England. In all three locations, the juniper population is a component feature of a Special Area of Conservation designated habitat and a qualifying interest of a Site of Special Scientific Interest (SSSI; Figure 5). Each population contained 100–130 hectares of continuous juniper cover. The greatest area of mortality was observed in the Perthshire population; symptoms were first reported in 2004 and represented a 20% decline in area of live juniper trees compared to a 1983 baseline survey (Tene et al., 2007). The precise duration of infection in the Lake District and Cairngorms populations is unknown, but *P. austrocedri* symptoms were first noted after 2010, and a lower proportion of symptomatic juniper was observed at both sites potentially consistent with a more recent introduction.

2.3.2 Quadrat stratification

Juniper was sampled using 10x10m quadrats from pre-selected locations stratified according to the area and density of juniper, altitude, slope and distance to watercourses. A 2010 distribution map of the Perthshire juniper population derived from 15cm full colour (RGB) and false colour infrared (CIR) imagery was provided by Scottish Natural Heritage (Whittome, 2010) and distribution maps of the remaining two populations were classified from 25 cm RGB imagery supplied for 2010 by NeXTPerspectives™. The classification methods are described in Appendix A. To capture differences in juniper abundance and density, the area of juniper predicted by the image classifications was measured in 10x10m grid cells using landscape class statistical functions in the SDMTools package (Van der Wal et al., 2019) implemented in R v.3.4.2 (R Core Team, 2017). To understand if each 10x10m cell was isolated from other juniper stands or part of a larger stand, the area of juniper in 30x30m including each 10x10m grid cell was also calculated, producing distributions of juniper % cover at each scale for each study population (Figure 6). These distributions were used to devise eight categories to describe juniper abundance that could be easily identified in the field. Each 10x10m cell containing juniper was assigned to one of four categories describing juniper % cover in 10x10m (≤10, 11-25, 26-50, >51 %) and to one of two

categories characterising the area of juniper surrounding the 10x10m cell as isolated from (<20%), or contiguous with (>21%), juniper growing in the wider 30x30m.

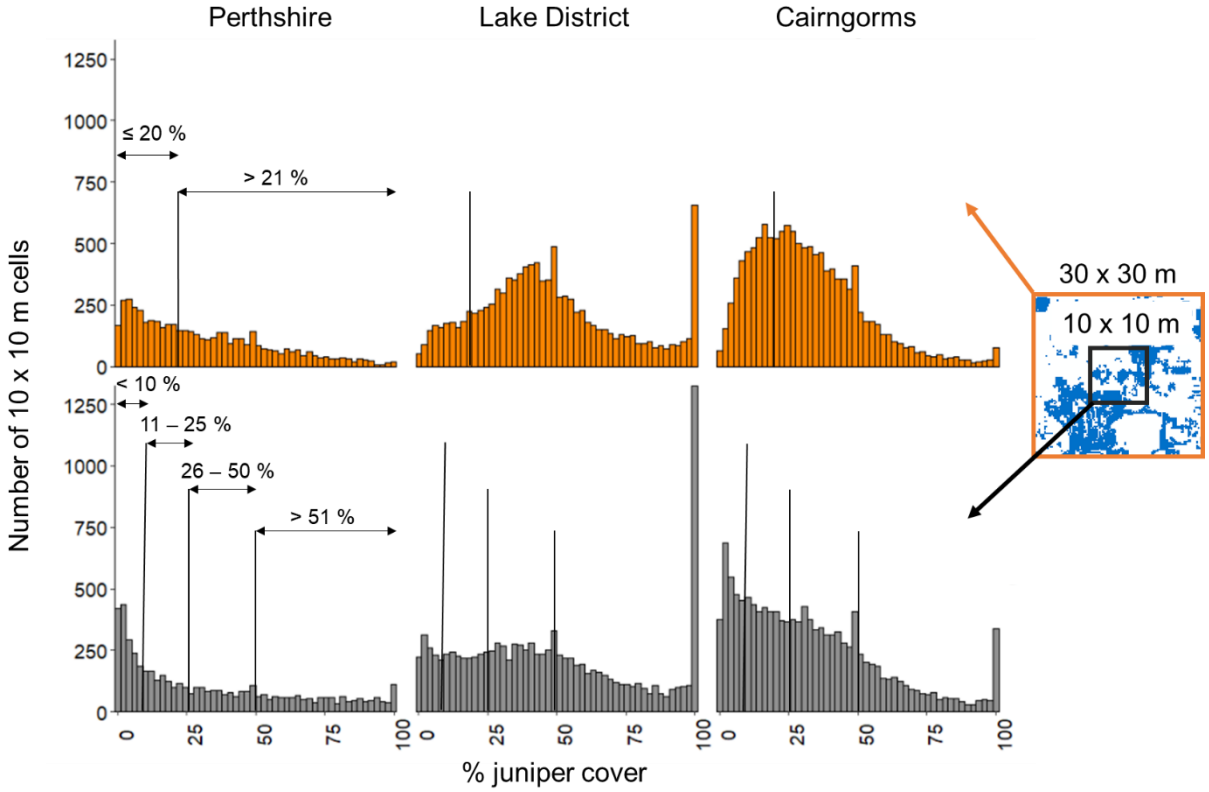

Figure 6. Number of 10x10m cells per study population with estimated % cover of juniper (shown in blue) across 10x10m (grey) cells and the surrounding 30x30m (orange). Thresholds used to divide juniper % cover into categories at each scale are marked with black lines.

Layers of slope and aspect were calculated from the resampled NeXTPerspectives™ 10m digital elevation model (DEM) using the *terrain* function in the raster package (Hijmans, 2020). Slope, aspect, and altitude were then extracted to the centroid of each 10x10m grid cell containing juniper. Euclidean distance (m) from the nearest watercourse to each 10m grid cell centroid was measured from a rasterised version of the 50m digital rivers network (Moore et al., 2000). Survey locations were identified by randomly selecting 10x10m cells out of each category of juniper abundance, in proportion to the total number of cells present in each category, to add up to 50 selected cells per study population. This proportional sampling procedure was repeated five times per population. Each sample of 50 was plotted across the altitudinal, slope and watercourse proximity gradients occupied by juniper at each location. The selection capturing the widest distribution of cells across each of the three gradients was chosen for survey.

2.3.3 Survey of spatial patterns in juniper symptoms

Quadrat sampling was carried out over five days at each location in October 2017. Quadrats were geo-located using ArcPad v.10.2 on a Panasonic FZ-GI tablet with GPS accuracy to three metres. To minimise transference of inoculum across populations, areas of high and low infection were visited on different days and all equipment breaking the soil surface (e.g. marker poles, soil moisture probes) was disinfected between quadrats. All other equipment was thoroughly disinfected between study populations. Juniper quadrats were placed as close to pre-selected locations as was possible to meet the abundance criteria by estimating the area of juniper in 10x10m and scoring abundance in 30x30m as a binary measure of more or less than 20%. The area of symptomatic juniper was measured as a fraction of the total area of juniper present in each quadrat, where symptoms constituted foliage discolouration and dead needles (retained or dropped) that extended to a minimum of a whole branch and did not result from either browsing or mechanical damage. Where a distinctive phloem lesion typical of *P. austrocedri* could be found, a 500mg tissue sample was collected from one representative symptomatic tree per quadrat. The sampled tissue was stored at -20°C until quantitative real-time PCR (qPCR) could be carried out following the protocol described in Mulholland et al. (2013) to verify the consistent presence of *P. austrocedri* across each population.

2.3.4 Abiotic and biotic predictors

We measured a suite of potential abiotic and biotic predictors of spatial patterns in *P. austrocedri* symptoms and included these in statistical models for each population (Table 1). The following predictors were measured in each field quadrat. The binary observation of ≤20% or >21% juniper cover across 30x30m to distinguish between quadrats situated in isolated or contiguous juniper stands was included in the model as juniper “density”. The area of juniper bearing berries was used to estimate the area of female juniper. Area of herbivore damage was measured as the area of bark stripping plus any resulting dead branches / stems (i.e., mechanical breakage from wind or snow damage was excluded). This metric was not included in Cairngorm models as herbivory was only detected in nine quadrats, encompassing an area greater than 10cm^2 in only three quadrats. Soil moisture was measured as % volumetric water content (VWC) using a FieldScout TDR 300 probe. Shallow soil and surface rock only permitted measurements using the 3.8cm depth setting across the Lake District

Table 1. List of covariates included in full subset model selection for each population (P=Perthshire, LD=Lake District, C=Cairngorms). Number of sampled quadrats: P=51, LD=46, C=50.

Measurement category	Specific measurement	Population		
		P	LD	C
Juniper density 30x30m quadrat	≤20% or >21% juniper cover	x	x	x
Juniper metrics 10x10m quadrat	Area of juniper bearing berries (m^2)	x	x	x
	Area of herbivore damage (m^2)	x	x	
Soil moisture	Mean of point samples across quadrat (%VWC)	x	x	x
Vascular plant indicators	Area of individual target taxa (m^2)	x	x	x
Watercourse proximity	Euclidean distance from quadrat centroid to nearest mapped river (m)	x	x	x
Grazing activity	Distance from quadrat centroid to nearest deer or sheep track (m)	x		
Topographic metrics extracted to 10x10m quadrat centroid	Altitude (m)	x	x	x
	Slope (°)	x	x	x
	Aspect (°)			x
Soil type (250m resolution) extracted to 10x10m quadrat centroid	**Perthshire:**			
	Brown forest Balrownie			
	Brown forest Gourdie	x		
	Organic soil, peaty gleys			
	Non-calcareous gleys			
	Peaty gleys Balrownie			
	Cairngorms:			
	Humus-iron podzols; some brown forest soils, noncalcareous gleys and peaty gleys			x
	Humus-iron podzols; some peaty gleys and humic gleys			
Habitat (NVC community)	**Perthshire:**			
	W19 *Juniperus communis* woodland			
	Acid grasslands (U4, U20, U24)	x		
	Mires (M10, M23)			
	Mosaic (U5, M15)			
	Cairngorms:			
	H12 *Calluna vulgaris – Vaccinium myrtillus* heath			
	W18 Scots pine woodland with heather			
	U4 *Festuca ovina - Agrostis capillaris - Galium saxatile* grassland			x
	Coniferous plantation			

population, whereas measurements were collected at 20cm depth in Perthshire and the Cairngorms. Measurements were collected from: i) areas within each quadrat where juniper was absent; ii) under asymptomatic juniper; and iii) under symptomatic juniper. An equal number of measurements (minimum four) were collected from each category present, resulting in eight to twelve point sample measurements from which mean soil moisture was calculated (%VWC). Area of vascular plant taxa present in each quadrat was recorded according to a target list (Appendix B) of taxa likely to co-occur with juniper in the study population habitats, that indicate placement of microsites along soil moisture, nitrogen, and

pH gradients. Use of individual target taxa allowed us to better distinguish between potential drivers of *P. austrocedri* symptom severity and find a small number of common, easily identifiable indicator taxa that land managers could use to predict microsites at higher or lower risk of infection.

Mapping in the field was carried out using the tracking function in ARCpad, to record any watercourses additional to the 50m digital rivers network (Moore et al., 2000). These were merged with the original dataset and used to recalculate the watercourse proximity (m) metric for each quadrat. Clearly visible deer and sheep tracks were also mapped and proximity to sampled quadrat centroids measured as an alternative way to measure the risk of inoculum transference to juniper from herbivores, but stocking density and ground condition only permitted collection of a reliable dataset from Perthshire.

The remaining covariates were obtained from existing GIS datasets. Altitude, slope, and aspect were extracted to each quadrat centroid from the resampled NeXTPerspectives™ 10m layers prepared for the plot stratification. Aspect was not included in the Perthshire or Lake District models as more than 60% of quadrats at each location were clustered in the same octant. The soil type underlying each quadrat centroid was extracted from 250m resolution datasets, obtained from a digitised version of the soil map produced by Forbes (1984), the Soilscapes dataset (Farewell et al., 2011) and the National Soil Map of Scotland (James Hutton Institute, 2011) for the Perthshire, Lake District and Cairngorms populations respectively. Soil type was omitted from model selection for the Lake District population as at 250m resolution all of the quadrats were placed in “freely draining acid loamy soils over rock” (Farewell et al., 2011). To test if a broader description of the vegetative community is a better predictor of *P. austrocedri* symptoms, because it captures more information about edaphic conditions than the presence of individual taxa, National Vegetation Classification (NVC) community data, supplied by Scottish Natural Heritage (2017), was included as a covariate for the Perthshire and Cairngorms populations (Table 1). The eight Perthshire communities were simplified to these four broad types (Table 1), amalgamated as follows: acid grasslands (U4 *Festuca ovina - Agrostis capillaris - Galium saxatile*; U20 *Pteridium aquilinum - Galium saxatile*; U24 *Arrhenatherum elatius - Geranium robertianum*), mires (M10 *Carex dioica – Pinguicula vulgaris*; M23 *Juncus effusus/acutiflorus – Galium palustre*) and mosaic communities suggesting transition from drier to wetter soil (U5 *Nardus stricta – Galium saxatile*; M15 *Trichophorum germanicum - Erica tetralix* wet heath) (Rodwell, 1991). No NVC data was released for the Lake District population.

2.3.5 Model specification

To investigate the relationships between the area of *P. austrocedri* symptoms and environmental covariates, we used a Bayesian beta-binomial GLMM fitted using the Integrated Nested Laplace Approximation (INLA) method with the R-INLA package (Rue et al., 2009) implemented in R v.3.4.2 (R Core Team, 2017). Models were fitted to the number of square metres of symptomatic juniper in each 10x10m quadrat. Using the beta-binomial distribution enabled us to take account of the area of juniper in each cell while allowing the probability of infection to have extra variation associated with spatial clustering of symptoms (overdispersion), thereby accounting for the high frequency of quadrats that contain wholly asymptomatic or symptomatic juniper (Hughes and Madden, 1993).

In particular, our model used the q = 12 environmental covariates for the i^{th} location $\{x_{j,i} | 1 \leq j \leq 16\}$ to estimate the mean probability of infection via a logit link function

$$\text{logit}(\mu_i) = \beta_0 + \beta_1 x_{1,i} + \cdots + \beta_q x_{16,i},$$

in which β_0 is an intercept and β_j is the regression coefficient for the j^{th} predictor. This estimate of the mean probability is then used to predict the area of symptomatic juniper in the i^{th} location (η_i) via

$$\eta_i \sim \text{beta-binomial}(\mu_i, \gamma, N_i),$$

in which N_i is the total area of juniper in the i^{th} cell (m^2) and γ is the overdispersion parameter of the beta-binomial distribution (that was assumed to be constant across all cells at each site). In our Bayesian estimation procedure all regression parameters, including the intercept, were assumed to have minimally informative priors of the form

$$\beta_q \sim \text{Normal}(0, 1/0.001).$$

2.3.6 Model selection

All covariates were centred and standardized prior to model fitting and no pairs of covariates used in any models were correlated with a Pearson r^2 value ≥0.6 (Appendix D). Models were run in two stages. We first performed a full subset selection using all possible combinations of covariates marked against each population (Table 1) except the vascular plant indicators, producing 1023 models for both Perthshire and the Cairngorms, and 127 models for the Lake District, which had seven as opposed to ten covariates. Model fit was compared using

the Deviance Information Criterion (DIC), a Bayesian generalisation of the Akaike Information Criterion (AIC) derived as the mean deviance adjusted for the estimated number of parameters in the model to provide a measure of out-of-sample predictive error (Gelman and Hill, 2006). The model with the lowest DIC is the model with the most support in the data, but the set of models with DICs within two units of the top model DIC are considered to have equivalent support in the data and formed the “top model set”. The area of each vascular plant indicator, present in ten or more quadrats at each population, were then added to the formulae for the top model set per population to assess (using DIC) if the addition of any one indicator improved model fit. Nine additional models were run for Perthshire and the Lake District, and ten for the Cairngorms (Table 3).

To assess the importance of covariate effects, we summarised marginal posterior distributions using 95% (0.025 and 0.975 quantiles of the posterior distribution) Bayesian credible intervals (BCI). The relationship between each covariate and the area of symptoms is considered strongest where BCI do not bridge zero, very strong when ≥0.95, strong when ≥0.90–0.94, and weak when ≥0.80–0.89 of the BCI are above or below zero. Where a strong or very strong relationship was found between the area of symptoms and a covariate, we report the percentage of the posterior predicted data that overlaps zero as calculated in R v.3.5.2 (R Core Team, 2018) using the *rollmean* function in the zoo package (Zeileis and Grothendieck, 2005). The explanatory power (goodness of fit) of each model was evaluated using root mean-square error (RMSE) calculated between the predicted posterior mean values and the corresponding mean sampled area of symptomatic juniper. The residuals of the top models were checked for spatial autocorrelation using Moran’s I statistic implemented using the *correlog* function in R package ncf v1.2.8 (Bjornstad, 2019). Pairs of plots were divided into different distance bins at 100m intervals between 0 and the maximum distance between plot pairs for each site and the Moran’s I value was then calculated for each distance bin. One hundred paired distances were randomly resampled per distance bin to assess Moran’s I correlation significance (Appendix D). As no spatial autocorrelation was found in the residuals, the addition of a spatial component (mesh) to the model formulation was not required.

2.4 Results

2.4.1 Prevalence of symptoms of *P. austrocedri* infection

Fifty-five percent of juniper surveyed in the Perthshire population showed symptoms compared to 28% in the Lake District and 23% in the Cairngorms populations, consistent with a possible earlier pathogen introduction in Perthshire (Figure 7). Though quadrats containing no symptomatic juniper were found in all three populations, the mean area of symptomatic juniper found in Perthshire quadrats was 19 ± 20m^2 out of a mean 34 ± 28m^2 area of juniper, compared to a mean of 7 ± 11m^2 of symptomatic juniper in quadrats from the Cairngorms population where the mean juniper cover found per quadrat was similar (33 ± 22m^2). The mean area of juniper in the Lake District quadrats was higher (44 ± 27m^2) with an intermediate mean area of symptomatic juniper (13 ± 18m^2). Because detection of symptomatic lesions is limited to above-ground live tissue, qPCR results are less reliable indicators of infection than symptoms. However, positive qPCR results were obtained across the full extent of each population giving confidence that site-wide observations of symptoms result from *P. austrocedri* infection (Appendix C).

The mean, standard deviation and range of covariates measured and tested in models across all three populations is shown in Table 2. The Perthshire population is characterised by fragmented juniper stands, only 35% of quadrats contained more than 21% juniper cover across 30x30m compared to c.70% in the Lake District and Cairngorm populations where juniper grows in denser stands (Figure 7, Table 2). Perthshire population quadrats were never further than 174m from a river or drain, compared to 840 and 820m in the Lake District and Cairngorms populations respectively (Figure 7, Table 2). The Lake District population occupied the largest range of altitude (234m compared to 132m in Perthshire and 78m in the Cairngorms) with up to 45° slopes compared to just 20° in both Scottish populations (Figure 7; Table 2). The Cairngorms population had the driest soil conditions across the quadrats (Table 2) with mean soil moisture of 33% VWC, which is 27% and 48% drier than the mean soil moisture found across Lake District and Perthshire quadrats respectively.

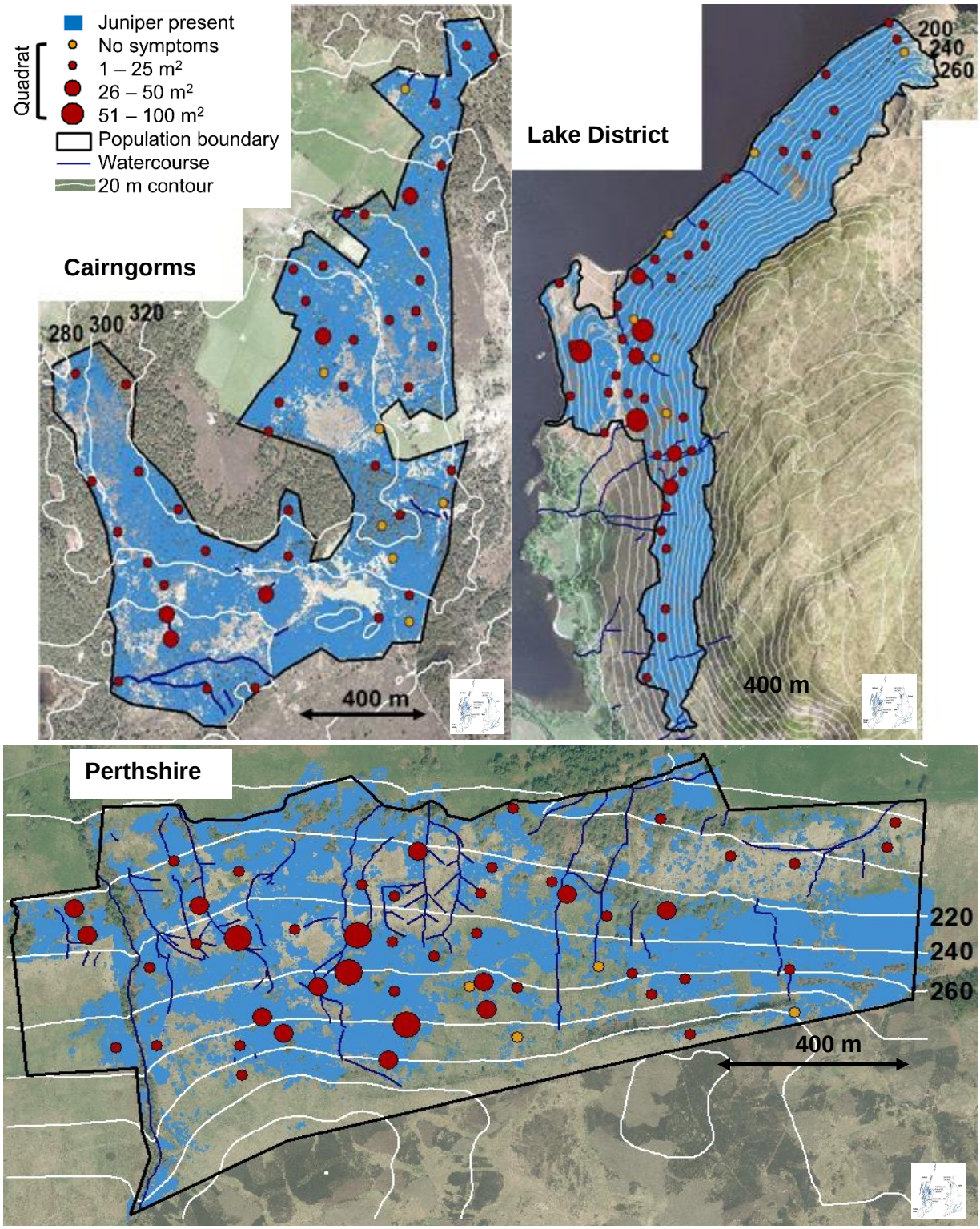

Figure 7. Map of surveyed juniper populations showing the distribution of juniper in relation to the watercourse, altitude and slope covariates used to stratify sampling. The distribution of samples, collected in 10x10m quadrats, is shown with circles coloured orange where no *P. austrocedri* symptoms were found and red where symptoms were present. Circle size corresponds to categories representing the area of symptoms estimated in each quadrat. Imagery licensed to UKCEH for PGA through Next Perspectives™.

Table 2. Comparison of surveyed juniper population covariate means ± 1s.d., and ranges, measured from 10x10m quadrats. P = Perthshire, LD = Lake District and C = Cairngorms study populations. Only numerical / binary coded variables included in the first stage of GLMM modelling (i.e., excluding species indicators) are displayed. Covariates not included in models for specific populations are greyed out.

Covariate	Mean ± s.d.per quadrat			Range per quadrat		
	P	LD	C	P	LD	C
Area of symptomatic juniper (m^2)	19 ± 20	13 ± 18	7 ± 11	0 - 79	0 - 70	0 - 45
Area of juniper (m^2)	34 ± 28	44 ± 27	33 ± 22	2 - 99	1 - 90	1 - 80
Juniper density (% quadrats nested in 30x30m with >21% juniper cover)	35	72	70	NA	NA	NA
Area of juniper bearing berries (m^2)	10 ± 12	9 ± 15	4 ± 9	0 - 49	0 - 66	0 - 49
Area of herbivore damage (m^2)	2 ± 8	0 ± 1	0 ± 1	0 - 50	0 - 3	0 - 7
Mean soil moisture (%VWC)	45 ± 12	63 ± 17	33 ± 9	28 - 84	33 - 108	15 - 52
Watercourse proximity (m)	42 ± 37	144 ± 209	240 ± 193	1 - 174	0 - 840	2 – 820
Grazing activity (m)	16 ± 16	72 ± 68	31 ± 49	0 - 70	1 - 212	1 - 213
Altitude (m)	250 ± 30	248 ± 63	303 ± 21	182 - 314	150 - 384	256 - 334
Slope (°)	11 ± 4	32 ± 7	6 ± 4	5 - 23	15 - 45	1 – 20
Aspect (°)	158 ± 145	276 ± 53	174 ± 99	2 - 357	88 - 342	10 - 348

Nine vascular plant indicators were present in ten or more quadrats in the Perthshire population, nine in the Lake District and ten in the Cairngorms (Table 3). The mix of indicators recorded highlights the difference in microsites occupied by the juniper study populations (Table 3). Of 42 target indicators, only one, V*accinium myrtillus* L., was present at all three study populations while quadrat frequency for the remaining indicators varied from 19–42 quadrats. Indicators of drier, moderately fertile soils were only present in the Lake District quadrats, where no indicators of high soil moisture and three indicators of highly acidic, infertile microsites were also found. In contrast, there were two indicators of high soil moisture in the Cairngorms, six for highly acidic, infertile soils (four present in >40

of 50 quadrats) and no indicators of drier, moderately fertile microsites (Table 3). Quadrats from Perthshire were dominated (both in terms of species composition and prevalence across quadrats) by seven taxa indicating moderate soil moisture (Table 3). However, although only one taxon (*Molinia caerulea* (L.) Moench) indicating high soil moisture was recorded, it was found in 21 of the 51 quadrats, suggesting widespread, continuous waterlogging across the site.

Table 3. Number of 10x10m quadrats containing vascular plant indicators (where present in ≥10 quadrats), out of the total number of quadrats (shown in brackets) surveyed across each population. P = Perthshire, LD = Lake District, C = Cairngorms juniper populations. Taxa were assigned to soil condition categories devised from Ellenberg values given in Hill, Preston, and Roy (2004). Two categories were used to describe reaction (R) and nitrogen (N) soil conditions: highly acidic (R=2) and low nitrogen (N=1-2) or slightly acidic (R=3-5) and moderately fertile (N=3-5). Taxa were then categorized according to soil moisture (F) as high (F=8-9), moderate (F=6-7) or lower (F=5).

Taxon	Soil condition			Population		
	R	N	F	P (51)	LD (46)	C (50)
Vaccinium myrtillus	2	1-2	5	19	27	42
Calluna vulgaris	2	1-2	5		19	46
Pinus sylvestris	2	1-2	5			31
Vaccinium vitis-idaea	2	1-2	6-7			42
Erica cinerea	2	1-2	6-7		13	12
Erica tetralix	2	1-2	8-9			13
Dryopteris affinis	3-5	3-5	5	30	22	
Oreopteris limbosperma	3-5	3-5	5	22	10	
Dryopteris dilatata	3-5	3-5	5	31		
Juncus conglomeratus	3-5	3-5	5	19		10
Juncus effusus	3-5	3-5	5	14		12
Deschampsia cespitosa	3-5	3-5	5	24		
Rubus fruticosus agg.	3-5	3-5	5	12	12	
Pteridium aquilinum	3-5	3-5	6-7		45	
Betula pendula	3-5	3-5	6-7		15	15
Ilex aquifolium	3-5	3-5	6-7		10	
Molinia caerulea	3-5	3-5	8-9	21		15

2.4.2 Abiotic and biotic drivers of spatial variability in disease symptoms of *P. austrocedri*

The full subset selection modelling resulted in one top model each containing abiotic and biotic covariates for the Perthshire and Lake District populations, and two models for the Cairngorms population (Table 4). All models included a strong relationship between increasing area of *P. austrocedri* symptoms and a measure of increasing soil moisture

(Table 5). When the area of different vascular plant indicators was added to these models, this resulted in one top model with improved fit for each population, with strong, positive relationships between increasing symptoms and increasing soil moisture still included but additionally identifying taxa that aid identification of microsites vulnerable to *P. austrocedri* infection in different habitats (Table 4). Across all sites, models with abiotic and biotic covariates vastly outperformed the null model with no covariates.

Table 4. Model results (DIC, RMSE, dispersion and list of covariates present) for each surveyed population, comparing the null model with the top set of models produced before and after addition of vascular plant indicators.

Juniper population	Model	DIC	RMSE	Dispersion	Covariates
Perthshire	Without indicators	167.45	43.89	0.48	Juniper density, berry-bearing, herbivore damage, soil moisture, watercourse proximity, grazing activity, altitude, slope, soil type, habitat
	With indicators	134.96	42.59	0.45	As above with area of *Dryopteris dilatata*
	Null	301.98	37.04	0.55	N/A
Lake District	Without indicators	264.64	32.64	0.44	Juniper density, berry-bearing, soil moisture, watercourse proximity, altitude, slope
	With indicators	208.84	22.99	0.42	As above with area of *Rubus fruticosus* agg.
	Null	301.77	41.54	0.57	N/A
Cairngorms	Without indicators	226.71	21.22	0.33	Juniper density, berry-bearing, soil moisture, aspect, soil type, habitat
		225.40	21.38	0.33	Juniper density, berry-bearing, soil moisture, slope, aspect, soil type, habitat
	With indicators	191.92	21.09	0.30	As above with area of *Erica tetralix*
	Null	293.63	43.92	0.58	N/A

The Cairngorms population models all predicted the distribution of symptoms with reasonable accuracy, as the predicted area of symptoms was within 20% of observed values (Table 4). Addition of a plant indicator improved symptom prediction by 10% in the Lake District to within 20% of the observed values. However, predictive model performance was poorer for the Perthshire population where the predicted area of symptomatic juniper was only within 40% of observed values from both the full subsets and plant indicator models (Table 4). No evidence of overdispersion was found in the residuals of any of the top models (Table 4).

The top model produced for the Perthshire population from the full subset selection included all ten possible covariates (DIC 167.45) with only one strong relationship identified between increasing area of symptomatic juniper and increasing soil moisture (Table 5, BCI = 0.70, 4.08). Model fit improved by 32 units (DIC 134.96) when area of *Dryopteris dilatata* (Hoffm.) A. Gray was included: a species of large fern that prefers moist, moderately acidic and fertile soils (Table 3). In this model, the strongest effect (BCI did not bridge zero) was increasing area of *P. austrocedri* symptoms with increasing area of *D. dilatata* (BCI = 0.70, 4.08). The area of symptoms also increased very strongly with increasing soil moisture (BCI = -0.04, 1.20) and decreasing altitude (BCI = -1.72, 0.05), and strongly with decreasing area of herbivore damage (BCI = -1.41, 0.05).

Six of the seven potential covariates collected across the Lake District population were included in the top model prior to adding indicators (DIC 264.64) with area of *P. austrocedri* symptoms again showing a strong response to soil moisture related covariates, with symptoms strongly increasing with decreasing distance to watercourses (Table 6, BCI = -0.99, 0.08). Including brambles, *Rubus fruticosus* agg., improved the model fit by 56 DIC units (Table 4). The BCI for the relationship between increasing area of symptoms and decreasing distance to watercourses did not bridge zero (BCI = -1.26, -0.14) and the area of symptoms strongly increased with decreasing area of *R. fruticosus* agg. (BCI = -4.19, 0.09), recorded in 12 of 46 quadrats (Table 3).

Two top models were found for the Cairngorms population including six, and seven, of nine possible covariates; including slope marginally improved model fit (DIC decreased from 226.71 to 225.40). In both models the BCI for soil moisture did not bridge zero, showing a very strong relationship between increasing area of *P. austrocedri* symptoms with increasing soil moisture (Table 7). When indicator taxa were added, only one top model (including slope) was found. Of the ten indicator taxa explored, the top model contained area of cross-leaved heath (*Erica tetralix* L.). Model fit was improved by 35 and 33 DIC units compared to the full subset selection models (Table 4). Increasing area of symptoms with increasing area of *E. tetralix* was the only strong relationship present, for which the BCI did not bridge zero (BCI=0.26, 1.28). Recorded in 13 of 50 quadrats (Table 3), *E. tetralix* is the only indicator found out of the target list for highly acidic, infertile microsites with high soil moisture.

In addition to soil moisture directly measured within quadrats, top models for all populations contained weak effects of juniper density and area of juniper bearing berries, and weak effects of slope on symptoms, despite differences in the range of variation sampled across each population (Table 2). Evidence for the direction of correlations between area of

symptoms and juniper density and area of juniper bearing berries varied across the three populations, being consistently positive in the Perthshire population (Table 5), but with less clear directional effects in the other two populations (Tables 6 and 7). Directional effects for slope were also less clear and were generally weaker than those identified for juniper covariates (Tables 5, 6 and 7), Soil and habitat (NVC community) types only included in the Perthshire and Cairngorms models were also always present. However, none of these covariates showed strong relationships with increasing area of symptoms but removing them resulted in poorer model fit (i.e., the DIC increased by more than two units). This suggests these covariates are playing a role in the extent of symptoms in the different populations but the precise nature of these relationships remains unclear.

Table 5. Posterior estimates (mean, standard deviation (SD), 2.5% and 97.5% quantiles, and % that does not bridge zero) for fixed effects included in the top model set for the Perthshire juniper population.

	Covariate	Mean	SD	2.5%	97.5%	% does not bridge zero
	Without indicator species (DIC = 167.45)					
	Soil moisture	0.59	0.31	0.01	1.21	100.00
	Altitude	-0.69	0.43	-1.57	0.13	92.71
	Herbivore damage	-0.39	0.29	-1.01	0.14	90.20
	Juniper density	0.29	0.25	-0.20	0.77	87.70
	Intercept	0.05	21.22	-41.61	41.67	50.17
	Berry-bearing	0.21	0.25	-0.27	0.70	80.19
	Grazing activity	-0.17	0.26	-0.67	0.34	75.21
	Watercourse proximity	-0.03	0.31	-0.66	0.55	53.17
	Slope	-0.08	0.39	-0.84	0.68	57.69
Habitat	Mosaic	-0.70	15.82	-31.76	30.32	51.17
	Mires	-0.03	15.82	-31.09	31.01	50.17
	Juniper wood	0.80	15.83	-30.28	31.86	52.17
	Acidic grassland	-0.08	15.82	-31.14	30.96	50.17
Soil	Peaty gleys	0.22	14.15	-27.57	27.99	50.17
	Organic peaty gleys	0.37	14.15	-27.42	28.13	51.17
	Non-calcareous gleys	-2.65	14.19	-30.52	25.19	55.18
	Brown forest Balrownie	0.66	14.15	-27.13	28.43	51.17
	Brown forest Gourdie	1.40	14.16	-26.40	29.18	53.17
	With indicator species (DIC = 134.96)					
	Dryopteris dilatata	2.36	0.86	0.70	4.08	100.00
	Soil moisture	0.57	0.32	-0.04	1.20	95.21
	Altitude	-0.81	0.45	-1.72	0.05	95.19
	Herbivore damage	-0.65	0.37	-1.41	0.05	95.20
	Juniper density	0.25	0.52	-0.78	1.26	67.69
	Intercept	0.18	21.22	-41.48	41.81	50.17
	Berry-bearing	0.06	0.26	-0.45	0.57	57.68
	Grazing activity	-0.19	0.26	-0.70	0.33	75.21
	Watercourse proximity	-0.18	0.33	-0.85	0.45	67.70
	Slope	0.07	0.41	-0.73	0.87	55.18
Habitat	Mosaic	-0.97	15.82	-32.03	30.06	52.18
	Mires	-0.18	15.82	-31.24	30.86	50.17
	Juniper wood	1.45	15.84	-29.65	32.52	53.17
	Acidic grassland	-0.30	15.82	-31.37	30.73	50.17
Soil	Peaty gleys	-0.14	14.15	-27.93	27.63	50.17
	Organic peaty gleys	0.50	14.15	-27.29	28.26	51.17
	Non-calcareous gleys	-3.05	14.19	-30.91	24.80	57.68
	Brown forest Balrownie	1.06	14.16	-26.73	28.83	52.67
	Brown forest Gourdie	1.62	14.16	-26.18	29.41	54.17

Table 6. Posterior estimates (mean, standard deviation (SD), 2.5% and 97.5% quantiles, and % that does not bridge zero) for fixed effects included in the top model set for the Lake District juniper population.

Covariate	Mean	SD	2.5%	97.5%	% does not bridge zero
Without indicator species (DIC = 264.64)					
Intercept	-1.28	0.45	-2.19	-0.43	100.00
Watercourse proximity	-0.41	0.27	-0.99	0.09	92.70
Soil moisture	0.09	0.25	-0.41	0.58	62.69
Juniper density	0.17	0.50	-0.78	1.17	62.67
Berry-bearing	0.00	0.22	-0.45	0.41	52.18
Altitude	0.22	0.24	-0.24	0.70	80.19
Slope	-0.26	0.28	-0.83	0.29	80.20
With indicator species (DIC = 208.84)					
Intercept	-1.29	0.43	-2.16	-0.47	100.00
Watercourse proximity	-0.66	0.29	-1.26	-0.14	100.00
Rubus fruticosus agg.	-1.81	1.09	-4.19	0.09	95.23
Soil moisture	0.00	0.25	-0.51	0.48	50.17
Juniper density	-0.21	0.55	-1.27	0.88	65.19
Berry-bearing	-0.04	0.22	-0.49	0.36	55.18
Altitude	-0.24	0.30	-0.82	0.35	77.68
Slope	0.06	0.29	-0.53	0.62	57.70

Table 7. Posterior estimates (mean, standard deviation (SD), 2.5% and 97.5% quantiles, and % that does not bridge zero) for fixed effects included in the top model set for the Cairngorms juniper population.

Covariate		Mean	SD	2.5%	97.5%	% does not bridge zero
Without indicator species (DIC = 226.71)						
	Soil moisture	0.54	0.22	0.09	0.98	100.00
	Berry-bearing	0.18	0.18	-0.18	0.53	82.68
	Intercept	-1.15	27.39	-54.93	52.58	51.17
	Juniper density	-0.18	0.44	-1.01	0.70	65.20
	Aspect	-0.02	0.21	-0.45	0.39	54.17
Habitat	Scots pine woodland	0.64	15.82	-30.43	31.67	51.17
	Heath	0.19	15.82	-30.86	31.22	50.17
	Coniferous plantation	-0.73	15.84	-31.83	30.34	51.17
	Acidic grassland	-0.09	15.82	-31.16	30.95	50.17
Soil	Humus-iron podzols; gleys	0.46	22.36	-43.44	44.33	50.17
	Humus-iron podzols; brown forest	-0.46	22.36	-44.37	43.40	50.17
Without indicator species (DIC = 225.40)						
	Soil moisture	0.57	0.23	0.12	1.01	100.00
	Berry-bearing	0.17	0.18	-0.18	0.52	82.68
	Intercept	-1.08	27.39	-54.85	52.66	51.17
	Juniper density	-0.24	0.44	-1.09	0.65	70.19
	Slope	0.13	0.22	-0.31	0.54	72.69
	Aspect	-0.07	0.23	-0.52	0.37	60.17
Habitat	Scots pine woodland	0.67	15.82	-30.39	31.71	51.17
	Heath	0.17	15.82	-30.88	31.20	50.17
	Coniferous plantation	-0.76	15.84	-31.86	30.31	51.17
	Acidic grassland	-0.07	15.82	-31.14	30.97	50.17
Soil	Humus-iron podzols; gleys	0.52	22.36	-43.39	44.38	50.17
	Humus-iron podzols; brown forest	-0.52	22.36	-44.42	43.35	50.17
With indicator species (DIC = 191.92)						
	Erica tetralix	0.73	0.26	0.26	1.28	100.00
	Soil moisture	0.19	0.27	-0.36	0.71	75.21
	Berry-bearing	0.15	0.18	-0.22	0.50	77.72
	Intercept	-1.72	27.39	-55.50	52.02	52.18
	Juniper density	-0.02	0.46	-0.88	0.91	52.68
	Slope	0.04	0.21	-0.39	0.45	57.70
	Aspect	0.05	0.23	-0.42	0.50	57.69
Habitat	Scots pine woodland	1.12	15.82	-29.95	32.16	52.67
	Heath	0.47	15.82	-30.59	31.50	51.17
	Coniferous plantation	-2.26	15.85	-33.39	28.84	55.18
	Acidic grassland	0.69	15.83	-30.39	31.73	51.17
Soil	Humus-iron podzols; gleys	0.30	22.36	-43.60	44.17	50.17
	Humus-iron podzols; brown forest	-0.30	22.36	-44.21	43.56	50.17

2.5 Discussion

Our study provides the first evidence from the northern hemisphere that, out of the wide range of potential abiotic and biotic drivers considered, and despite differences in the range of conditions, geographic location and infection intensity occupied by study populations, soil moisture is the best predictor of *P. austrocedri* symptom distribution in juniper at population scale. This is likely to result from the pathogen's dependence on soil moisture for zoospore dispersal (Green et al., 2015; Greslebin et al., 2007). We further showed that associated plant species with distinctive soil moisture requirements, such as cross-leaved heath, can be used to predict microsites at increased risk of infection. Results from the Lake District and Perthshire populations suggested that the pathogen may also be spread through movement of infected soil on herbivore hooves and tyre treads. Management actions accounting for pathogen transmission in both soil, and soil water are, therefore, needed to prevent or slow spread of *P. austrocedri*.

Introductions of non-native *Phytophthora* taxa have been reported from 176 countries across a wide range of climatic zones (Barwell et al., 2021a). Water availability is commonly identified as an important driver of terrestrial *Phytophthora* distributions at a range of scales. Globally, functional and species diversity increases with precipitation (Redondo et al., 2018a). Landscape scale examples include increased incidence of *P. lateralis* in Port-Orford cedar with increasing creek drainage area (Jules et al., 2008), and increased *P. ramorum* infection of tanoak with increasing stream proximity (Peterson et al., 2014). In individual trees, the length of *P. cinnamomi* lesions increase in Jarrah with increasing precipitation (Bunny et al., 1995) because water is required to stimulate sporangial formation, trigger zoospore release and enable dispersal (Hardham, 2005).

The importance of soil moisture as a driver of *P. austrocedri* infection in juniper populations is likely to vary between sites with different soil types and hydrology. Area of symptoms increased very strongly with point sampled soil moisture in both the Cairngorms and Perthshire populations, which grow on deep soils formed from glacial till, with pockets of gleying, that retain a high volume of soil moisture throughout the year. This is consistent with population level studies of Chilean cedar where *P. austrocedri* infection increases with soil waterlogging caused by high clay content (La Manna and Rajchenberg, 2004a) or features restricting water permeability (La Manna and Rajchenberg, 2004b). Though microsite soil moisture is partly a function of soil type, explicitly including soil type in the Cairngorms and Perthshire models always improved model performance but never strongly predicted the area of symptoms, probably because the available data for soil type were too coarse in

spatial resolution (250m) to capture microsite variation. Spatial variation in area of symptoms was also linked to soil moisture in the Lake District populations but here the strongest association was between symptoms and decreasing proximity to watercourses rather than point sampled soil moisture. Given the steep site topography and freely draining, shallow, sandy soil type, it is likely that juniper in this population is only exposed to long term waterlogging where it grows adjacent to watercourses. Stands of Chilean cedar growing in comparable (freely draining, volcanic) soils also demonstrate increased infection with increasing proximity to watercourses (Calı´, 1996; La Manna and Rajchenberg, 2004a).

A key challenge for investigating field scale drivers of disease is obtaining data at a suitably detailed spatial resolution. Modelling microsite soil moisture patterns was prohibited by the availability of fine scale data on hydrological processes (such as precipitation, potential evaporation, and runoff generation). Topographic wetness index (TWI), calculated from site topography and watercourse networks, is commonly used as a proxy for soil moisture. In the absence of variability in slope and altitude gradients, the calculation tends to overpredict differences (Grabs et al., 2009) and did not yield an informative distribution map for the Cairngorms juniper population (results not shown). It also assumes uniform soil properties and does not account for complex bedrock surfaces, invalidating the data derived for the Lake District population (results not shown) (Kopecký and Čížková, 2010). Measuring soil moisture directly from stratified quadrats as % volumetric water content captured variation in water table heights but only represents conditions at a single point in time and differences between microsites may be exaggerated by rainfall events that occurred during the sampling period. We introduced the area of vascular plant indicators, selected to represent a range of soil moisture preferences, to test whether such indicators capture longer term water table levels than short term soil moisture field observations, or other fine scale soil attributes affecting transmission and disease such as pH and nitrogen content. This was successful in the Cairngorms, where adding area of cross-leaved heath, *Erica tetralix*, resulted in a very strong, positive, relationship with increasing area of symptoms (ΔDIC = 33), corroborating the response with increasing soil moisture as cross-leaved heath grows in constantly wet but not inundated soils (Hill et al., 2004). Managers of juniper populations in heathland habitats could use this result to prioritise detection surveys or identify unsuitable microsites for supplementary planting of juniper seedlings. Moreover, this finding suggests microsites most vulnerable to *P. austrocedri* infection in other habitats could be identified using indicator species with distinctive soil moisture preferences.

Uncoupling relationships between vegetative cover and soil moisture from other factors such as interspecific competition and land management practices proved more difficult for the remaining populations. The best Perthshire model was obtained by adding area of broad-buckler fern, *Dryopteris dilatata,* which increased with increasing area of symptoms (∆DIC = 32, BCI did not bridge zero). This correlation is more likely to result from the fern preferentially colonising dead juniper following *P. austrocedri* induced mortality than suggest a higher percentage of symptoms occurred in the drier soil conditions favoured by the fern (Table 3) (Hill et al., 2004; Rünk et al., 2012). Adding area of brambles (*Rubus fruticosus* agg.) yielded the greatest improvement in Lake District model performance (∆DIC = 56) and showed a strong (BCI 0.90–0.94), negative relationship with area of symptoms. While four other short-listed taxa for the Lake District also indicate lower soil moisture conditions (Hill et al., 2004), brambles are very palatable to both sheep and deer, indicating reduced herbivory where present in quadrats (Harmer et al., 2010; Van Uytvanck and Hoffmann, 2009). Thus increasing symptoms in the absence of brambles might point to herbivore mediated dispersal of inoculum. A cost distance analysis comparing three cattle grazing scenarios (no grazing, roaming with intermittent barriers such as steep slopes and free roaming) found total area and dispersion of *P. austrocedri* was higher in Chilean cedar forests with unrestricted grazing (La Manna et al., 2013a). Similarly, infection of Port-Orford cedar with *P. lateralis* increases along wildlife (including bear) trails that “fill-in” uninfected sites following disease establishment around creek edges (Jules et al., 2008). While our findings also implicate herbivores as potential vectors of inoculum between juniper stands, they clearly indicate that infection does not increase with direct herbivore damage, as this covariate was absent from both the Cairngorms and Lake District models and though present in Perthshire, symptoms decreased with increasing herbivory (BCI 0.90 – 0.94). However, overgrazing has long been implicated in the dramatic decline of UK juniper stands so a reduction in herbivore densities could not only improve the survival rates of existing populations and permit regeneration (Broome et al., 2017; Clifton et al., 1997; Thomas et al., 2007; Ward and Shellswell, 2017) but also reduce the risk of pathogen transmission.

Slope was present in all top models, explaining some of the residual variance with area of symptoms, even in the limited range occupied by the Cairngorms population (Table 2), but the weak evidence for these effects makes it difficult to interpret the precise nature of the relationship between slope and area of symptoms. We also detected weak relationships with area of berry-bearing juniper, evidenced by the presence of this covariate in all top models. However, again the direction of this effect was difficult to ascertain, except for the Cairngorms population where there was weak support for a positive correlation (Table 7).

The weak response could indicate female juniper without berries were missed by the survey. Similarly, juniper density was selected in all top models, and tended to show a weakly positive relationship with symptoms where evidence for the effect was stronger (Perthshire population, Table 5). Other studies of field scale infections, including that of Chilean cedar with *P. austrocedri* and white oak (*Quercus alba* L.) with the similarly soil-borne *P. cinnamomi*, have found symptom intensity to increase with increasing host density. The most likely explanations for the absence of this relationship in our study are i) our characterisation of juniper density as a binary measure of ±20% cover in 30x30m was too simplistic, or ii) juniper density at the 30x30m scale was correlated with the area of juniper in 10x10m, used to define the number of trials in the models. We are currently exploring the role of host connectivity in explaining site-level spread patterns over time, supported by empirical field studies of the dispersal ability of the pathogen (Riddell et al., 2020) to better understand the mechanisms in driving the spread of *P. austrocedri* at different spatial scales.

Models produced for Perthshire had the lowest accuracy (RMSE 42.59) despite containing the largest number of covariates (11) meaning those included poorly account for the spatial distribution of symptoms. The watercourses mapped for Perthshire include herringbone drainage channels opened in 2011 (Taylor, H., personal communication, 1st November 2019) after juniper stands started to decline in the late 1990's (Broome et al., 2008) but before isolation of *P. austrocedri* in 2012 (Green et al., 2015). The drainage work may have inadvertently distributed the pathogen across the site by disturbing watercourses and moving contaminated soil in tyre treads. It is unclear if the very strong increase in area of symptoms with decreasing altitude (BCI >0.95) reflects the location where the pathogen was first introduced or the drainage activity that was concentrated between 220–250m of the 180–310m altitudinal range (Figure 7, Table 2) causing the pathogen to spread further and faster than dispersal through soil moisture alone. This highlights the importance of capturing and integrating the spatial arrangement and intensity of management actions into investigations of drivers of site level variation in plant disease impacts (Fernández-habas et al., 2019).

2.6 Conclusion

Our study provides valuable insights about how conditions favouring newly invading plant diseases can be delineated by collecting and modelling spatially explicit data at field scale. Directly measuring covariates in the field in sites of different disease status, across key environmental gradients using a carefully designed sampling strategy, enabled us to explore a wide range of potential drivers, identify those with the most explanatory power and make

comparisons between populations occupying different ranges along each gradient. Our findings can be used by practitioners to predict areas of increased and decreased infection risk and inform tangible local management inventions to prevent or reduce pathogen spread and aid the restoration or establishment of new juniper populations.

Interventions to manage juniper populations at local level such as drainage, grazing exclosures and seedling propagation require significant resources (Forestry Commission Scotland, 2006). The introduction of *P. austrocedri* to the UK risks this investment and the longevity of these actions if measures to prevent disease introduction and establishment are not undertaken. Our results suggest *P. austrocedri* is most likely to infect juniper where it occupies wet microsites - in the UK and across its global range. Therefore, surveys to detect *P. austrocedri* could initially target stands or populations occupying consistently wet microsites, identified with the aid of plant species indicators. Increased area of symptoms suggests inoculum is present in higher concentrations and that disturbance of soil and soil water in these microsites may pose a higher risk for pathogen translocation and spread. While improved biosecurity measures, such as cleaning all machinery, equipment and footwear before and after accessing juniper sites (irrespective of known disease status), will reduce the risk of pathogen introduction and spread (DEFRA, 2014b), our findings further support recommendations published by the UK Government Department for Environment, Food and Rural Affairs (DEFRA) in the Juniper Management Guidelines to divert footpaths away from waterlogged areas and only plant juniper in drier microsites, giving full consideration to the vulnerability of existing populations, suspected disease status, soil type and the watercourse network (DEFRA, 2017). Continued emphasis on improving the quality and extent of populations in drier soil conditions by regulating grazing levels, curtailing stand removal and creating spaces for natural regeneration (Broome et al., 2017; Wilkins and Duckworth, 2011) will help maximise resilience of native juniper populations to this new disease threat.

Chapter 3

Informing disease management by disentangling abiotic and biotic determinants of *Phytophthora austrocedri* spread on juniper hosts

3.1 Abstract

Understanding drivers of plant pathogen infections at a range of spatial scales is necessary to identify vulnerable host populations and understand and mitigate activities that promote infection. This applies particularly to natural environments where land managers must balance competing land-use, stakeholder, species, and resource priorities. In the UK, native populations of common juniper are undergoing serious mortality from the introduced pathogen *Phytophthora austrocedri* but information on drivers of infection is lacking to support design of management strategies. We used a combination of spatially explicit Bayesian modelling techniques, dispersal kernels and abiotic and biotic disease drivers to understand the speed and patterns of colonisation of a single 1.08km^2 juniper population by the pathogen between 2012 and 2017. Environmental drivers underpinning patterns in occurrence and density of juniper were first identified using hurdle models, then point process models were used to determine conditions promoting *P. austrocedri* colonisation and to predict pathogen distribution and intensity in 2021. All analyses were conducted at 10m and 25m resolutions to find out if drivers varied in importance with spatial scale. Colonisation was better described at 10m resolution with increasing host density and force of infection, resulting in the colonisation of 1.2% new 10x10m cells containing juniper per year. Force of infection was a function of the distance to infected trees that followed a fat-tailed dispersal kernel with most dispersal occurring within ~500m of symptomatic trees observed four years previously but with some, infrequent, dispersal events occurring beyond 1km. The model predicted new juniper infections in 2021 would increase around previously infected disease foci with further low intensity colonisation of almost all stands. This slow intensification of disease poses a severe risk to most UK juniper populations following first introduction by virtue of their small size but also suggests that simple, preventative actions that disrupt both long and short distance disease dispersal, such as limiting movement of potentially infected soil, water, and plants, could reduce risks effectively. Our results will enable land managers to estimate disease vulnerability based on proximity to the nearest infection and could be used to prioritise herbivore control on populations occupying freely draining soils as the most likely to naturally regenerate, to reduce colonisation by *P. austrocedri*.

3.2 Introduction

A key challenge in managing novel pest and disease outbreaks is gathering enough information about dispersal to target interventions that effectively prevent transmission (Cunniffe et al., 2015a). Dispersal is a complex process describing the departure of individuals or propagules from the natal location by active or passive movement to establish in a new location (Bullock et al., 2018). All stages of dispersal are subject to abiotic (e.g. altitude, rainfall) or biotic (e.g. availability of vectors or potential hosts) environmental pressures that can alter the probability and distance of movement from an original source and/or establishment viability in the receiving location. While intervening early is intuitive, control of new outbreaks is more likely to succeed if an understanding of dispersal pathways, environmental interactions and the speed and spatial scales at which they operate can be incorporated into the methods, resulting in a trade-off between intervention speed and specificity (Thompson et al., 2018).

Failure to control pest and disease outbreaks can have disastrous consequences, severely reducing crop production (Savary et al., 2019) (e.g. 75% Florida citrus production lost to citrus huanglongbing disease (Milne et al., 2018)) and timber (e.g. millions of hectares of European spruce killed by bark beetles (Seidl et al., 2016)), altering ecosystem functioning through changes to nutrient cycling and biodiversity (Boyd et al., 2013a), and releasing significant volumes of carbon (Pugh et al., 2019). Managing new introductions of plant diseases can be especially difficult as, unlike invasive pests, the disease front is only evident when symptoms appear, often manifesting in only a small proportion of the infected host population long after first infection (Agrios, 2005). Occurrence and diversity data for even non-cryptic plant pathogens are poorly represented in global and national databases compared to other taxa (Roy et al., 2017). Many pathogen detections are made by plant health inspectors monitoring trade pathways while wider environment locations can go largely un-reported, partly due to uncertainty about where to target inspections for emergent pathogens introduced to heterogeneous landscapes (Parnell et al., 2014). Engagement of citizen scientists to collect disease observations is still restricted to a small number of participants (Observatree, 2018) or covers a small geographical area (Garbelotto et al., 2020). Remote sensing techniques are increasingly being deployed to detect and monitor outbreaks as technological improvements to sensors and image processing capabilities marry the advantages of broad geographical coverage with detection accuracy. Remote surveillance has been used effectively to monitor the progress of diseases causing landscape scale tree mortality (He et al., 2019; Meentemeyer et al., 2011) and even detect

pre-visual symptoms of infection (Wu et al., 2021; Zarco-Tejada et al., 2018). These repeat surveys not only provide information about the spatial distribution of disease but can also permit analysis of disease dispersal through time (Václavík et al., 2010).

First detected killing Chilean cedar in Argentina (Greslebin et al., 2007), *P. austrocedri* was subsequently discovered in 2012 to have infected c.60 disconnected juniper populations across Scotland and England (Green et al., 2015). As one of few UK native conifers, juniper is an important component of many habitats (Ward and Shellswell, 2017) and is widely used to create and restore native woodlands (Donald et al., 2021). The impact of *P. austrocedri* infection varies between populations: some show small numbers of juniper with discoloured (yellowing) foliage, while others exhibit localised mortality (wholly bronzed or skeletal trees) usually situated along watercourses, while the worst affected show widespread, population scale mortality (Green et al., 2015). The pathogen was already widely established in British juniper populations prior to first isolation so the year of introduction is uncertain (Green et al., 2015) and the drivers of *P. austrocedri* colonisation and establishment are unclear. Our first analysis of abiotic and biotic drivers of *P. austrocedri* infection within British juniper populations showed increased disease symptoms in wet microsites and indicated higher grazing pressure may promote infection by vectoring zoospores further than the pathogen could otherwise achieve by passive dispersal in soil moisture (Donald et al., 2020). While this identifies microsites that could be prioritised for disease surveillance, crucial information about *P. austrocedri* dispersal is still required to help land managers assess population level disease vulnerability and prevent or suppress transmission. We aimed to inform site level strategies for juniper management by i) exploring the scaling of dispersal within a single juniper population, namely how colonisation events of *P. austrocedri* depend on proximity to prior known infected hosts; ii) determining the relative influence of environmental factors including juniper host population connectivity, hydrology and topography in promoting pathogen colonisation; iii) investigating the intersection between the site conditions suitable for juniper compared to those suitable for the pathogen; and iv) using all of the preceding information to predict future pathogen spread and inform management across the study population.

We used Bayesian statistical models to relate the change in distribution and density of symptom observations between snapshots four years apart at the same study population, with potential abiotic and biotic disease drivers including juniper stand structure and force of infection estimates derived using dispersal kernels. Conditions promoting juniper presence and density were first related to the potential disease drivers using a hurdle model to

separate conditions promoting juniper persistence from those conducive for the pathogen. A point process model was then used to model the change in *P. austrocedri* symptoms between time periods. Describing the distribution of symptoms observed in 2016/17 relative to those previously observed in 2012/13 allowed us to explore the spatial range over which pathogen infection – identified from foliage symptoms - has spread (both within and between cells, measured by an increase in the number of symptomatic trees per cell) and to investigate the importance of pathogen dispersal from infected trees compared to other environmental factors. Both models were conducted at 10m and 25m spatial resolutions to understand if disease drivers differed with scale and were fitted to data using the Integrated Nested Laplace Approximations (INLA) method via the R-INLA package v.18.7.12 (Lindgren and Rue, 2015). Implementing models within a Bayesian framework allowed for complex model structures and detailed reporting of prediction uncertainty (Blangiardo and Cameletti, 2015) and models were fit with INLA as a computationally efficient method that accounts for spatial dependence in the data (Blangiardo et al., 2013a; Huang et al., 2017; Lindgren and Rue, 2015).

3.3 Data description

3.3.1 Study site

Birk Fell in Cumbria (Figure) was selected as the study location, as one of the few UK juniper populations repeatedly surveyed for *P. austrocedri* symptoms, and from which the pathogen has been successfully isolated (in 2013 at the location “Blowick Fell” detailed in Green *et al.*, 2015). The population is at an early stage of *P. austrocedri* invasion, as although symptoms are distributed across the population, a substantial proportion of the juniper remains asymptomatic and mortality is concentrated in localised clusters. The juniper population extends almost continuously for 3km along the eastern shore of Ullswater making it the largest of 250 juniper populations found in Cumbria (Cumbria Wildlife Trust, 2014), itself the stronghold for juniper in England (Ward and Shellswell, 2017). Designated as part of the Birk Fell Site of Special Scientific Interest (SSSI), juniper occupies predominantly west-facing, steep (to 60°) slopes between 140-484m altitude, where 80% of the population grows on exposed scree slopes in shallow soil and the remaining 20% forms the understorey to ancient oak woodland. The population is intersected by three footpaths that form part of the popular Ullswater Way walking route and is extensively grazed by sheep and red deer (Figure 8).

Figure 8. Location of the Birk Fell juniper population (bottom), in relation to the UK (top left), Cumbria (top right), the Cumbrian lakes (top right, dark grey) and all juniper populations mapped by Cumbria Wildlife Trust (top right, dark blue) (Cumbria Wildlife Trust, 2014). An aerial photograph of the Birk Fell population is annotated with footpaths (dashed lines) and rivers (light blue) intersecting the study area (dark blue) using British National Grid as the projected coordinate system.

3.3.2 Mapping juniper distribution

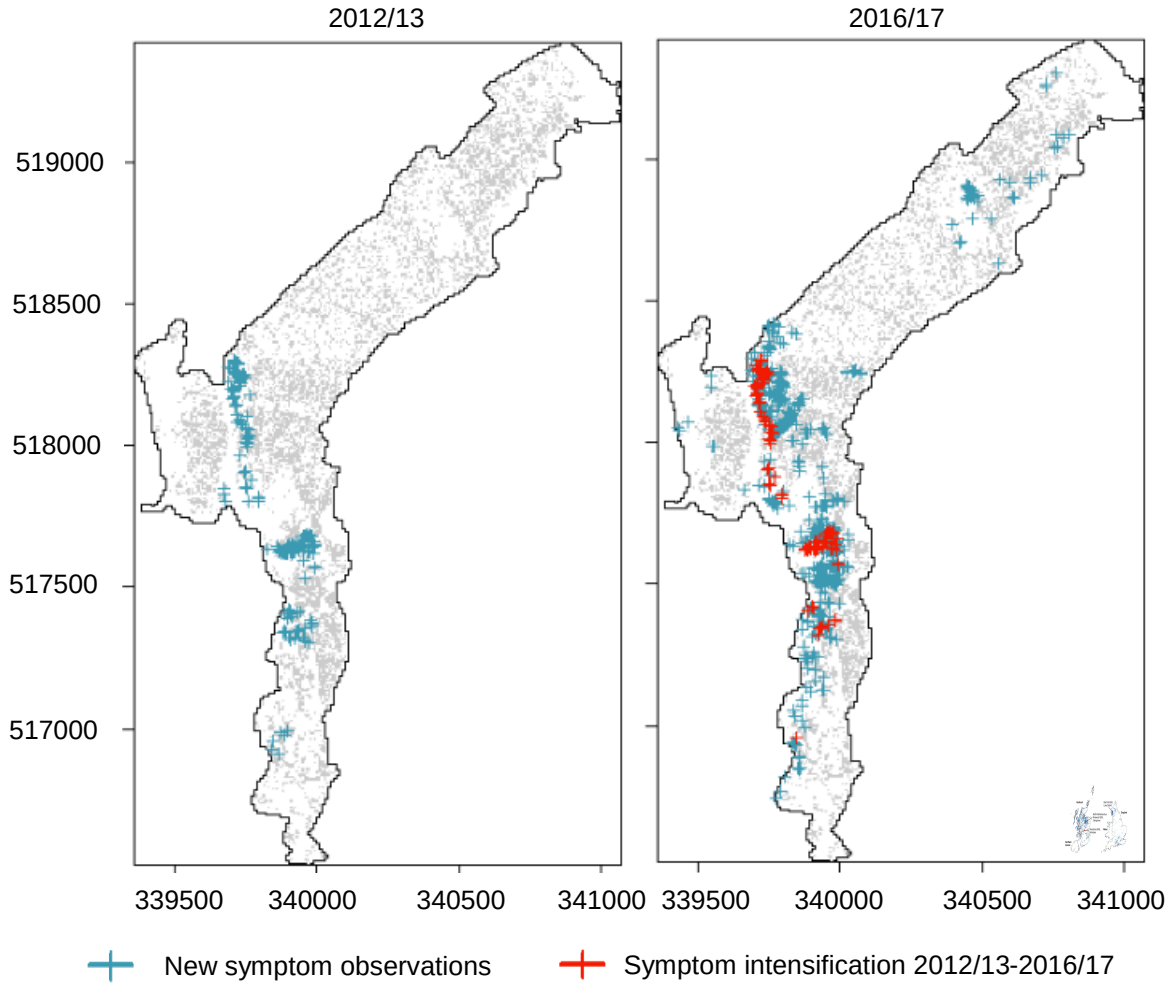

Figure 9. Observations of juniper trees symptomatic for *P. austrocedri* infection identified from helicopter surveys mapped against the distribution of juniper shown in grey. In 2012/13, 176 symptomatic trees were observed (L, shown in blue); in 2016/17 an additional 106 symptomatic trees were recorded in 10x10m grid cells that contained symptoms in 2012/13 (R, shown in red) and 1040 observations were recorded in new 10x10m grid cells (R, shown in blue).

A fine scale distribution map of juniper (Figure 9) was required to explore the area of host available for *P. austrocedri* infection, to relate the presence and density of juniper to abiotic and biotic factors, and to map changes in the spatial distribution of symptomatic trees. We derived a map of the 1.08km^2 of juniper situated within Birk Fell SSSI by performing a supervised, random forest, classification of full colour (RGB), high resolution (25cm), aerial image tiles collected in 2010 by NeXT Perspectives™ (Appendix E). The overall accuracy of the final classification was 83% (percentage of correct predictions) with Cohen's kappa of 0.81 for juniper indicating "substantial" classification accuracy (Landis and Koch, 1977).

Measures of juniper presence and density (% cover) per grid cell, as well as *P. austrocedri* symptom intensity and abiotic and biotic covariates, were estimated across regular 10x10m and 25x25m grids (Appendix E). The landscape class statistical function *ClassStat* in the SDMTools package (van der Wal et al., 2019) was used to calculate juniper density (m^2) in each grid cell. Areas <1m^2 were converted to zero, as both the image classification and symptom observations were estimated to be accurate to 1m.

3.3.3 Calculating *P. austrocedri* symptom intensity

Juniper trees symptomatic for *P. austrocedri* infection were identified from a series of photographs taken from helicopter surveys conducted by Forestry Commission England, following the Tree Heath Aerial Survey Protocol (Jones and Carter, 2018) (Appendix E). Previous research conducted at the study site confirmed, using qPCR analysis of lesion material collected from 49 symptomatic trees distributed across the SSSI, that bronzed or skeletal canopies occurred in juniper trees infected with *P. austrocedri* (Donald et al., 2020; Green et al., 2015). Bronzed or skeletal juniper observed in the aerial photographs were, therefore, inferred to be infected with the pathogen. One partial aerial survey was carried out on 15th May 2012, followed by a second flight across the whole population on 15th July 2013. Individual trees exhibiting bronzed or grey foliage were manually identified from each photograph and mapped to the corresponding location against orthorectified, full colour (RGB), 25cm resolution aerial photographs provided by NeXT Perspectives™. The procedure was repeated following two further flights undertaken on the 8th June 2016 and the 12th September 2017. The data were filtered to remove duplicate 10-figure (accurate to 1m) British National grid references (EPSG Projection 27700) and any observations that fell outside the population boundary, resulting in 176 observations of symptomatic trees in 2012/13 and an additional 980 symptomatic trees in 2016/17 making a combined total of 1160 symptomatic trees for the 2012-2017 period. A small number of symptomatic trees were removed from the dataset where the grid references collected from the helicopter plotted in grid cells where juniper was not identified by the image classification (14 trees at 10m resolution and six at 25m resolution). Change in symptom intensity per grid cell (the dependent variable in the point process model) was then calculated by subtracting the number of symptomatic trees present in grid cells containing juniper in 2012/13 from the number present in 2016/17. This ensured information about the frequency of dispersal events occurring within grid cells could be used to identify the best dispersal kernel, which would otherwise be omitted if only colonisations of new cells were considered. Cells containing the same number of infections in 2016/17 as 2012/13 were removed from the

dataset (55 cells at 10m resolution and 15 at 25m resolution) so as not to bias the selection of the dispersal kernel using cells where no dispersal occurred.

3.3.4 Dispersal kernels for *P. austrocedri*

Dispersal kernels are probability density functions describing the post-dispersal distribution of inoculum or infection relative to the source locations (Nathan and Klein, 2012). Kernels can be defined using many different functions but usually assume the probability of transmission declines uniformly in all directions with distance from the source of inoculum (Fabre et al., 2020). We assumed there were no further introductions of the pathogen from outside the SSSI during the study period, so only sources of inoculum already present within the population drove changes in symptom intensity (the next nearest infected population being 4km away in the same catchment). In the UK, *P. austrocedri* is primarily thought to spread through dissemination of zoospores: short-lived, asexual propagules with bi-flagellate tails produced in sporangia and attracted towards juniper roots (Clark and Green, 2017). Water is required for production of sporangia and as they do not readily detach (i.e. are non-caducous), zoospore dispersal is likely to rely on soil moisture rather than wind, meaning natural spread is hypothesised to occur slowly and over short distances (Greslebin et al., 2011; Riddell et al., 2020). However, *P. austrocedri* DNA was successfully amplified from soil samples scraped off walking boots worn along footpaths and animal trails traversing symptomatic juniper populations (Elliot et al., 2015), and was detected at low frequency in 2m high rain traps (Riddell et al., 2020). This suggests zoospores or hyphal fragments may also be vectored in soil passively transported by people on footwear and vehicles, as well as by animals and birds, which may accelerate dispersal rates and extend the distances over which transmission occurs. Each of these vectors, including soil water, potentially disperse inoculum at different scales and according to different kernel shapes (Bullock et al., 2006). While insufficient data exist to partition the dispersal load and range of distances contributed by each alternative vector, their combined dispersal potential could be explored by comparing dispersal kernels with contrasting shapes fitted to observations of symptom intensity.

We included dispersal kernels in our point process models using the unnormalised form of the exponential power kernel (Nathan and Klein, 2012) chosen for its flexibility to produce alternative kernel shapes (Skelsey et al., 2010), where

$$K(r) = \exp\left(-\left(\frac{r}{\delta}\right)^{h}\right).$$

Each of the 24 dispersal kernels $K(r)$ was characterised by a scale parameter (δ=5, 10, 20, 40, 80, 160, 320 or 640m) that controlled the typical distance range over which dispersal events occurred and a shape parameter (h=0.5, 1, 2) to determine precisely how dispersal probability declines with distance (Table 8). In informal terms, the tail of the distance range is described as “thin” where a low proportion of dispersal events occur there, or “fat” where the shape of the kernel indicates a higher proportion of events occur at longer distances. The exponential (h=1) kernel variant represents the boundary between thin and fat tailed distributions while the Gaussian (h=2) variant has a thin tailed distribution (Fabre et al., 2020). Since both are thin-tailed, the exponential and Gaussian variants predict that most dispersal occurs close to the epidemic front that progresses as a smooth wave travelling at constant speed (Parnell et al., 2010; Shaw, 1995). We compared these kernels to a fat tailed variant (h=0.5) that instead predicts an accelerating epidemic wave with many outbreaks arising far from the source (Figure 10). Although *a priori* based on the pattern of spread we expected the fat tailed kernel to probably be a better fit, we used two standard thin tailed kernels as comparators due to their preeminent position in dispersal studies. Both the exponential and Gaussian kernels have a statistically mechanistic basis with which to compare different movement processes and as such are commonly used to conduct initial explorations of dispersal where detailed knowledge of dispersal patterns is limiting (Bullock et al., 2017; Nathan and Klein, 2012). Though simple, the exponential kernel offered a credible description of plant seed dispersal compared to more complex functions (Bullock et al 2017) and the Gaussian kernel is a useful comparator for fat tailed kernels (Nathan and Klein, 2012). The net force of infection upon every cell containing juniper in 2016/17 was calculated by summing the contributions from cells containing symptomatic juniper in 2012/13, scaled by symptom intensity, according to each dispersal kernel. Given that we also knew the intensity of symptoms found in 2016/17, the same method was used to forward predict pathogen dispersal over the following four-year period to 2020/21 from cells containing symptomatic trees in 2016/17, assuming the abiotic and biotic conditions remain similar to those in 2016/17.

Table 8. Mean dispersal distance (m) according to 24 exponential power kernels characterised by different combinations of values for the shape and scale parameters, calculated as $h\,\Gamma(3/\delta)/\Gamma(2/\delta)$, where $\Gamma(\cdot)$ is the well-known gamma function.

Shape (h)	Scale (δ)							
	5m	10m	20m	40m	80m	160m	320m	640m
Power (h=0.5)	100.00	200.00	400.00	800.00	1600.00	3200.00	6400.00	12800.00
Exponential (h=1)	10.00	20.00	40.00	80.00	160.00	320.00	640.00	1280.00
Gaussian (h=2)	4.43	8.86	17.72	35.45	70.90	141.80	283.59	567.19

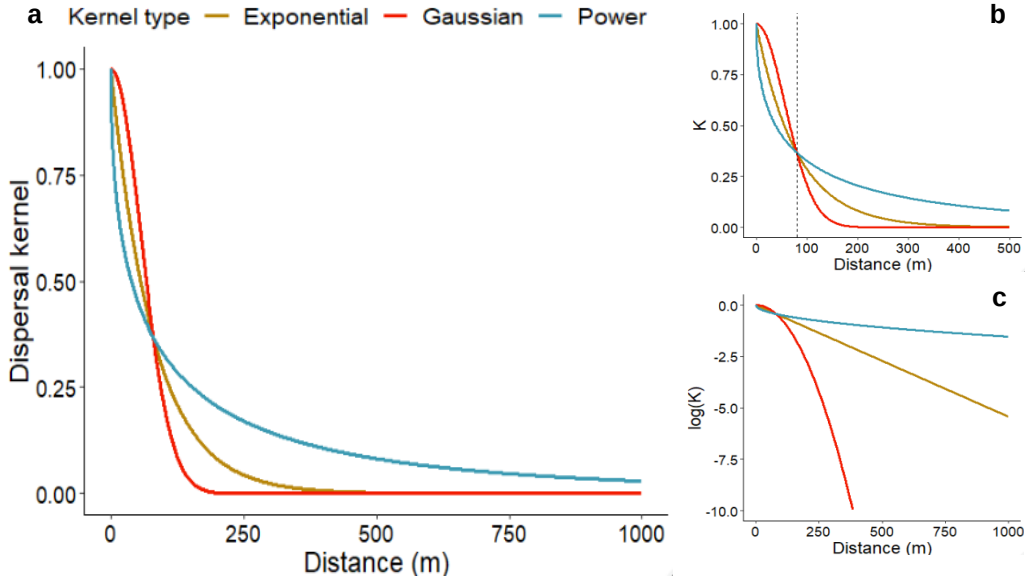

Figure 10. Comparison of dispersal kernels drawn from an exponential power distribution, showing the change in predicted relative dispersal frequencies with distance (m). The exponential (h=1), Gaussian (h=2) and power (h=0.5) kernel variants are arbitrarily set to δ=160m and plotted on a normal (a,b) and log (c) scale to a) compare relative dispersal rates across the full 3km; b) show the behaviour at short distances more precisely (note: kernels cross at δ=80m, marked by the dashed line) and c) compare differences in the behaviour of the tail.

3.3.5 Abiotic and biotic covariates

Potential abiotic and biotic predictors of juniper distribution and density, and *P. austrocedri* symptom intensity in colonised cells, were split into three main categories: juniper connectivity, hydrology, and topography (Table 9). Areas of bracken, rock and trees were included in the connectivity category as covariates that could alter the density and connectivity of juniper stands; all juniper connectivity variables were calculated using the same ClassStat method detailed for juniper density (Chapter 3.3.2 Mapping juniper distribution). Five proxy metrics for soil moisture were used in the hydrology category

because direct measurement in the field was impossible given the shallow soil depth (Donald et al., 2020) and lack of high-resolution hydrological process data (such as precipitation, potential evaporation, and runoff generation) (Table 9) (see Appendix F for detailed methods). Slope and aspect were calculated from the resampled NeXTPerspectives™ digital elevation model (DEM) (Appendix E) using the *terrain* function in the raster package (Hijmans, 2019), and then extracted with altitude to the centroid of each grid cell.

Table 9. Description of abiotic and biotic covariates used in the hurdle models of juniper presence and density, and point process models of *P. austrocedri* symptom intensity. Juniper mean patch area and juniper patch density were excluded from the hurdle models as they were not independent of juniper presence or density.

Category	Covariate name	Covariate description	Juniper density	*P. austrocedri* symptom intensity
Juniper connectivity	Juniper mean patch area (m^2)	Mean area of patches classified as juniper from the aerial image analysis per grid cell		x
	Juniper patch density	Number of juniper patches classified by the aerial image analysis per grid cell, divided by the total area of the grid cells		x
		Area of grid cell classified from aerial image to 1m resolution as:		
	Bracken (m^2)	bracken (*Pteridium aquilinum*)	x	x
	Rock (m^2)	scree or boulders	x	x
	Trees (m^2)	tree species excepting juniper	x	x
Hydrology		*Shortest Euclidean distance between grid cell centroid and the nearest:*		
	Rivers (m)	river pixel	x	x
	Paths (m)	footpath pixel	x	x
	Network (m)	river or footpath pixel	x	x
	Rivers+cost	Shortest “cost distance” between grid cell centroid and the nearest river pixel, accounting for surface distance (altitude), slope angle and curvature (Appendix F)	x	x
	TWI	Topographic Wetness Index	x	x
Topography	Altitude (m)	Mean altitude per grid cell	x	x
	Slope (°)	Mean slope per grid cell	x	x
	Aspect (°)	Mean aspect per grid cell	x	x

Juniper presence and density were expected to increase with:

- decreasing areas of other feature classes (bracken, rock, and trees), partly due to the classification process but also because factors such as greater surface water retention, increased herbivory and canopy cover may further suppress juniper growth in vegetated compared to non-vegetated areas (Ward and Shellswell, 2017).
- decreasing soil moisture because juniper predominantly occurs on thin, nutrient-poor, free-draining soils and is less frequently found where soils are consistently waterlogged (Thomas et al., 2007; Ward and Shellswell, 2017).
- increasing altitude and slope, and no strong correlation with aspect, because juniper stand size in Cumbria peaked at 300-500m and was largely associated with steep slopes where browsing, burning, and harvesting is less common (Cumbria Wildlife Trust, 2014).

Increasing *P. austrocedri* symptom intensity in juniper cells colonised between 2012/13 and 2016/17 was expected to correlate with:

- increasing juniper density, that promotes sporangial production and reduces dispersal distances between hosts;
- decreasing juniper patch density and increasing juniper mean patch area, as both create larger, continuous root systems that may facilitate zoospore dispersal;
- increasing areas of bracken and trees, and decreasing areas of rock, because deeper, damper soils encourage sporangial production (La Manna et al., 2012) and attract herbivores that may passively vector zoospores (Donald et al., 2020);
- increasing soil moisture that promotes sporangial production, release and dissemination of zoospores (Greslebin et al., 2007), characterised as increasing topographic wetness index (TWI), decreasing proximity to rivers and rivers accounting for topography (rivers+cost);
- decreasing proximity to footpaths, as infected soil and water could be transported along paths as runoff or on the footwear of recreational users (Vélez et al., 2020);
- decreasing altitude, slope and northerly aspects also consistent with incidence of *P. austrocedri* symptoms in *A. chilensis* forests (Baccalá et al., 1998a; La Manna et al., 2008a; La Manna and Matteucci, 2012).

3.4 Statistical Methods

The following section describes the workflow undertaken to conduct Bayesian statistical models at both 10m and 25m resolution (Figure 11).

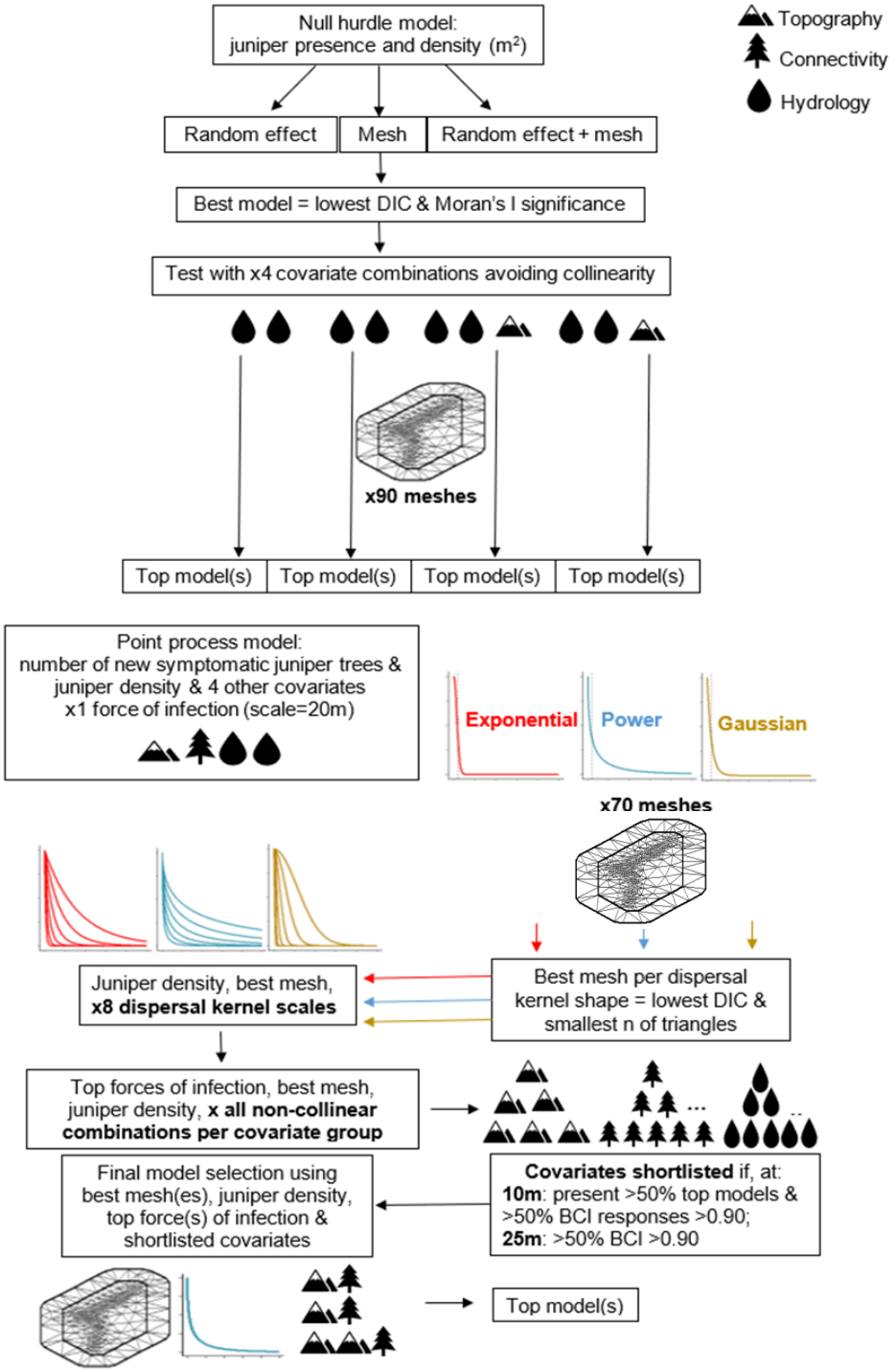

Figure 11. Schematic summarising the major methodological steps employed at 10m and 25m resolution to model juniper presence and density using hurdle models, and *P. austrocedri* colonisation of juniper using point process models.

3.4.1 Hurdle modelling of juniper presence and density

Hurdle models assume that zeros do not result from measurement error, separating the zero and non-zero structures to allow independent inference for each component. Here, we use hurdle models fit with INLA to understand how the abiotic and biotic covariates influence the presence of juniper, and the density of juniper where it is predicted to be present in a grid cell at 10m and 25m spatial resolutions. Because the whole juniper population was mapped and classified, it was appropriate to separate out the zero structure because less than <1m^2 of juniper did not represent missing data, rather the absence of juniper.

For every i^{th} grid cell within the mapped area (M), juniper presence was calculated as a binary measure of juniper density ($y \geq 0$m^2) as either present (1) or absent (0) defined as z_i:

$$z_i = \begin{cases} 1 & \text{if } y_i > 0 \\ 0 & \text{otherwise} \end{cases}$$

modelled with a likelihood drawn from a Bernoulli distribution

$$z_i \sim \text{Bernoulli}(\pi_i, n_i = 1).$$

Juniper density y_i was given as:

$$y_i = \begin{cases} NA & \text{if } y_i = 0 \\ y_i & \text{otherwise} \end{cases},$$

modelled using a likelihood drawn from a Gamma distribution

$$y_i \sim \text{Gamma}(a_i, b_i),$$

characterised by the shape (*a*) and scale (*b)* parameters defined as

$$E(y_i) = \mu_i = a_i/b_i, \text{ and } Var(y_i) = a_i/b_i^2.$$

A gamma distribution was appropriate to use in this instance as juniper density was a continuous, positive variable with a left skew.

The linear predictor for juniper absence (π_i) was specified using a logit link function

$$\text{logit}(\pi_i) = b_0^z + \boldsymbol{q_i \beta^z} + \int_i^z$$

and for juniper density (μ_i) using a log link function

$$\log(\mu_i) = b_0^y + \boldsymbol{q}_i\boldsymbol{\beta}^{\boldsymbol{y}} + f_i^y,$$

where for each model (*z* = Binomial juniper presence/absence model; *y* = Gamma juniper density model), b_0 is the intercept, $\boldsymbol{\beta}$ ($\beta_1, \ldots, \beta_n$) is a vector containing the regression parameters for each of the *n* environmental predictors, $\boldsymbol{q_i}$ is the set of the *n* environmental predictors for each location *i*, and f_i are structured spatial random effects.

The need for a spatial effect was first determined by examining the significance of spatial autocorrelation present in the residuals from the intercept-only (null) model using Moran's I statistic implemented using the *correlog* function in R package ncf v 1.2.9 (Bjornstad, 2020). Pairs of grid cells were divided into distance bins of 100m intervals between 0 and the maximum distance between any two grid cells (3030m at 10m, and 3020m at 25m, spatial resolution). Moran's I values were calculated per distance bin, out of which 100 paired distances were randomly resampled from each bin to assess the significance of the Moran's I correlation.

Where present, spatial autocorrelation can be addressed in models fit using INLA by adding a spatial mesh (f_i). The mesh is specified by the user to subdivide the area of study (i.e. the mapped juniper population) into a series of non-intersecting triangles, providing a structure over which spatial correlation can be approximated using Stochastic Partial Differential Equations (SPDE) (Lindgren and Rue, 2015). The SPDE implement a Matérn covariance function that defines correlation as a function of distance i.e. the closer in space the sample points are, the larger the correlation (Zuur et al., 2017). The values are stored in a covariance matrix to avoid pseudo-replication of the residuals and are fitted jointly with the regression parameters. Detailed descriptions of the Matérn function and how the SPDE approximate the latent continuous spatial random field are given in Lindgren and Rue (2015) and Blangiardo *et al*. (2013b). Models containing only juniper presence and density (i.e., fit with no covariates or spatial effects) were compared with models fit with a combination of different meshes and/or a spatially unstructured random effect (iid) to interrogate the success of each method in reducing spatial autocorrelation in the model residuals. The best performing models were selected using the Deviance Information Criterion (DIC), of which lower values indicate improved support in the data (calculated from the posterior mean of the model deviance) and a parsimonious level of model complexity (the effective number of parameters) (Spiegelhalter et al., 2002). The lowest DIC identifies the "best" model with the

most support in the data but models within two DIC units of the best model are considered to have equivalent support and form the “top model set”. The DIC never improved with the use of an iid but always improved with the addition of a mesh, which successfully eliminated spatial autocorrelation at both 10m and 25m resolution (Appendix H, Tables H1-H2).

Once the need for a structured spatial random effect was assessed, covariates were introduced to the model following screening for collinearity using Pearson’s r^2 correlation. Strong (r^2 ≥0.7) linear relationships between covariates could cause modelling errors such as unstable parameter estimates or biased inference statistics, or hinder interpretation where effects cannot be attributed to one or other covariate (Dormann et al., 2013). Strong correlations were found between paths and altitude, network, and paths, and between rivers and rivers+cost (Appendix H, Figure H1). To prevent including these paired covariates in the same model, four different combinations of covariates were run separately. All four models contained the uncorrelated covariates of areas of bracken, trees, and rock, slope, aspect, and TWI with the addition of a) altitude, rivers, and network; b) altitude, rivers+cost and network; c) rivers and paths; d) rivers+cost and paths. The covariates listed were used in both the presence and density component of each hurdle model. All covariates were centred and standardised prior to model fitting.

The optimal mesh for each covariate model, at each spatial resolution, was selected using DIC (Appendix H); the importance of covariate effects was summarised using 95% (0.025 and 0.975 quantiles) Bayesian credible intervals (BCI) drawn from the marginal posterior distributions. The relationship between each covariate and the presence and density of juniper was considered strongest where the BCI do not bridge zero, very strong when ≥0.95 of the BCI is above or below zero, strong when ≥0.90–0.94 of the BCI is above or below zero, and weak when ≥0.80–0.89 of the BCI are above or below zero. The variance explained by each model was calculated and partitioned to show the percentage explained by the covariates compared to the spatial random field.

3.4.2 Point process modelling of *P. austrocedri* symptomatic host density

The point locations of individual, symptomatic juniper trees showed where the pathogen has thrived sufficiently to cause juniper mortality but do not indicate where the pathogen was absent as this does not equate to absence of foliage symptoms. Point process models (PPMs) were appropriate to use in this context as a method to model predicted intensity of presence-only observations within spatial units (Renner et al., 2015), allowing inference

about relative intensity of symptomatic hosts per unit area across the mapped population (M) in grid cells where juniper was present. The dependent variable was characterised as the intensity of new symptomatic juniper trees per grid cell (x_s), calculated from the number of known presences per cell in 2016/2017 minus observations of symptomatic trees in 2012/13. The models were fit using a Poisson distribution because symptom intensity represented observational counts collected within a fixed unit of space.

Symptom intensity was modelled using a loglinear function:

$$\log(x_s) = b_0 + \boldsymbol{\alpha} F_s + \boldsymbol{\beta q_s} + f_s,$$

where b_0 is the intercept, F_s is the net force of infection upon each location *s* with its corresponding regression coefficient ($\boldsymbol{\alpha}$), $\boldsymbol{\beta}$ ($\beta_1, \ldots, \beta_n$) is a vector containing the regression parameters for each of the *n* biotic and abiotic predictors ($\boldsymbol{q_s}$) , and f_s is a structured spatial random effect that was fit using the same methods in INLA as described for the hurdle model. The net force of infection, F_s, was calculated by summing contributions from every other cell, y, weighted by its density of infection, i.e. $F_s = \sum_y w_y K(r_{s,y})$, in which w_y is the symptom intensity at the previous survey (and is zero for previously uninfected cells), $r_{s,y}$ is the distance between the (centres of) cell s and y, and $K(r)$ is the dispersal kernel at distance r. We subsequently refer to this covariate describing the per cell force of infection as calculated from all hosts detected as symptomatic in the 2012/13 survey as “force of infection”. Further specification of Poisson PPMs with spatial dependence are detailed in Renner *et al.* (2015).

The following workflow was carried out at both 10m and 25m spatial resolutions, to identify PPMs that best predicted symptom intensity in cells newly colonised in 2016/17. The force of infection covariate that best described the spatial distribution of symptoms in 2016/17, given the pattern found in 2012/13, was identified by fitting PPMs with a small number of shortlisted spatial meshes (Appendix I) and covariates consisting only of juniper density and a force of infection covariate created using one of 24 potential dispersal kernels. Models were compared by DIC and only force of infection covariates found in the top model set were carried forward. These models (containing juniper density, a shortlisted force of infection covariate and spatial mesh) were then used to test all possible combinations of covariates (provided Pearson’s $r^2 < 0.7$) within the juniper connectivity, hydrology, and topography categories to identify the most informative covariates and reduce the overall number of models tested. Where collinearity was detected, covariates were not used in the same

model. A thresholding approach was then used as a better alternative to model averaging to ascertain whether the effects of individual covariates were robust to presence or absence of other covariates in the model (Cade, 2015). At 10m resolution, covariates were first shortlisted for final testing if found in ≥50% of the top models and then at both resolutions covariates were shortlisted where ≥50% of responses were strong (BCI ≥ 0.90 above or below zero). Covariates were not selected using the first frequency criterion at 25m resolution because some covariates were only included in a small number of models to avoid collinearity (Appendix I). Thresholding would, therefore only select covariates used in a larger number of models, rather than those with the strongest responses (Appendix I). The final top model set was determined by comparing the DIC of PPMs created using all possible combinations of shortlisted covariates. The posterior distributions of the intercept and covariates in the best models were plotted to check for normality to confirm model convergence (Gelman et al., 2013). The percentage of the posterior predicted data overlapping zero was calculated as a measure of effect significance using the *rollmean* function in the zoo package (Zeileis and Grothendieck, 2005). Lastly, the pattern of symptom intensity likely to be present in 2020/21 was predicted from the best PPM found at each spatial resolution, given the force of infection (this time calculated from symptom locations detected in 2016/17) and assuming the values for any other covariates, and collinearity between them (Dormann et al., 2013), remain static.

Relative predictions of symptom intensity in 2016/17 and 2020/21 were extracted from the best models at each spatial resolution and scaled with observations of symptoms in 2012/13 and 2016/17 to allow comparison. Scaling was carried out by centring column values around the minimum value and re-scaling according to the column range using the base R *scale* function. The spatial patterning of symptom intensity predicted by the models in 2016/17 compared to that observed was visually compared by mapping the re-scaled predictions, converted to rasters using *rasterise* in the raster package (Hijmans, 2020), and plotted using the rasterVis package (Lamigueiro and Hijmans, 2019) in R v.3.6.2 (R Core Team, 2019). The fitted values predicted from the fixed effects without the structured spatial random effect were manually calculated using the model intercept and beta estimates, to perform model validation using Pearson's r^2 correlations between predicted and observed symptom intensity.

3.5 Results

3.5.1 Modelling juniper presence and density

Hurdle models including abiotic and biotic covariates vastly outperformed the null models at 10m resolution, producing one best model (i.e., within 2 DIC units of the model with the lowest DIC) (Appendix H, Table H1). Of the four combinations of covariates pertaining to altitude, distances to footpaths and distances to the nearest river, the model including distances to footpaths and distances to the nearest river accounting for slope (rivers+cost) performed best, yielding the lowest DIC. Juniper presence and density increased with decreasing areas of bracken, rock, and trees (BCI do not bridge zero), decreasing distance to footpaths (BCI do not bridge zero) and increasing slope (BCI do not bridge zero) (Appendix H, Figure H2). The negative correlation between juniper presence and TWI (BCI do not bridge zero) was marginally stronger than that between juniper density and TWI (BCI = -0.01, 0.00). While juniper presence increased with northerly aspects (BCI do not bridge zero), juniper density increased with westerly (W-SW) aspects (BCI = -0.03, 0.02). No relationship was found between juniper presence and density and distances to rivers accounting for slope, even though including this covariate out-performed models with distances to rivers or the amalgamation of rivers and footpaths. The combination of covariates used in the best 10m model accounted for 48% of the explained variance for juniper presence and density identified from the 2010 aerial image.

At 25m resolution the best model contained only a spatially unstructured random effect, returning a much lower DIC than the top model containing covariates (ΔDIC = 321.88) meaning that the covariates included in the model provide a poor explanation of the presence and density of juniper at 25m resolution. The wide confidence intervals spanned by the intercept in the 25m model show a large proportion of the residual variance was not explained by either the covariates or the spatial mesh. Including a spatial mesh in models at both resolutions improved performance compared to the null models and successfully addressed spatial autocorrelation (Appendix H, Figure H4). The spatial random field was much broader at 25m compared to 10m resolution, showing the mesh was invoked to address spatial autocorrelation across the full extent of the population (Appendix H, Figure H5).

3.5.2 *P. austrocedri* symptom patterns

Symptoms were observed in 2012/13 as three discrete outbreaks on the southern scree slope and as a continuous band of symptoms in the centre of the population where a gully containing the central footpath drains into the lake at the base of the slope (Figure 8, Figure 12a). Symptom intensity was highest in the centre of the population, receding further south (Figure 12a). By 2016/17 symptoms had radiated beyond these original foci with symptomatic stands merging and extending across the southern scree slope and expanding uphill from the river basin (Figure 12b). New cells containing symptoms appeared in a small number of disparate cells in the northern part of the SSSI where the deciduous canopy thins and juniper density increases (Figure 12b). The percentage of juniper cells hosting at least one more symptomatic tree in 2016/17 than 2012/13 increased by 3.4% at 10m resolution and 8.7% at 25m resolution and mean symptom intensity of new infections increased from 0.01 to 0.08 symptomatic trees per cell at 10m resolution and from 0.11 to 0.45 at 25m resolution (Table 10).

Table 10. Summary of the colonisation data 2012/13-2016/17 showing the number of host cells available for colonisation, number of cells containing symptomatic trees and mean symptom intensity of newly infected cells detected in 2012/13 and 2016/17 at both 10m and 25m spatial resolutions.

Measurement	Spatial resolution	
	10m	25m
Number of cells containing juniper (compared to the total number of cells) identified from aerial imagery	9679 (11849)	1793 (2035)
Number (and percentage) of juniper cells containing symptomatic trees in 2012/13	126 (1.3%)	76 (4.2%)
Mean number of symptomatic trees per grid cell containing juniper in 2012/13	0.01	0.11
Number of juniper cells containing no additional symptomatic trees in 2016/17	55	15
Number of symptomatic cells in 2012/13 with additional symptoms in 2016/17	70	61
Number of new cells containing symptomatic trees in 2016/17	381	171
Total number (and percentage) of juniper cells containing newly symptomatic trees in 2016/17 i.e. number of symptomatic trees in 2016/17 – number of symptomatic trees in 2012/13	451 (4.7%)	232 (12.9%)
Mean number of newly symptomatic trees per grid cell containing juniper in 2016/17	0.08	0.45

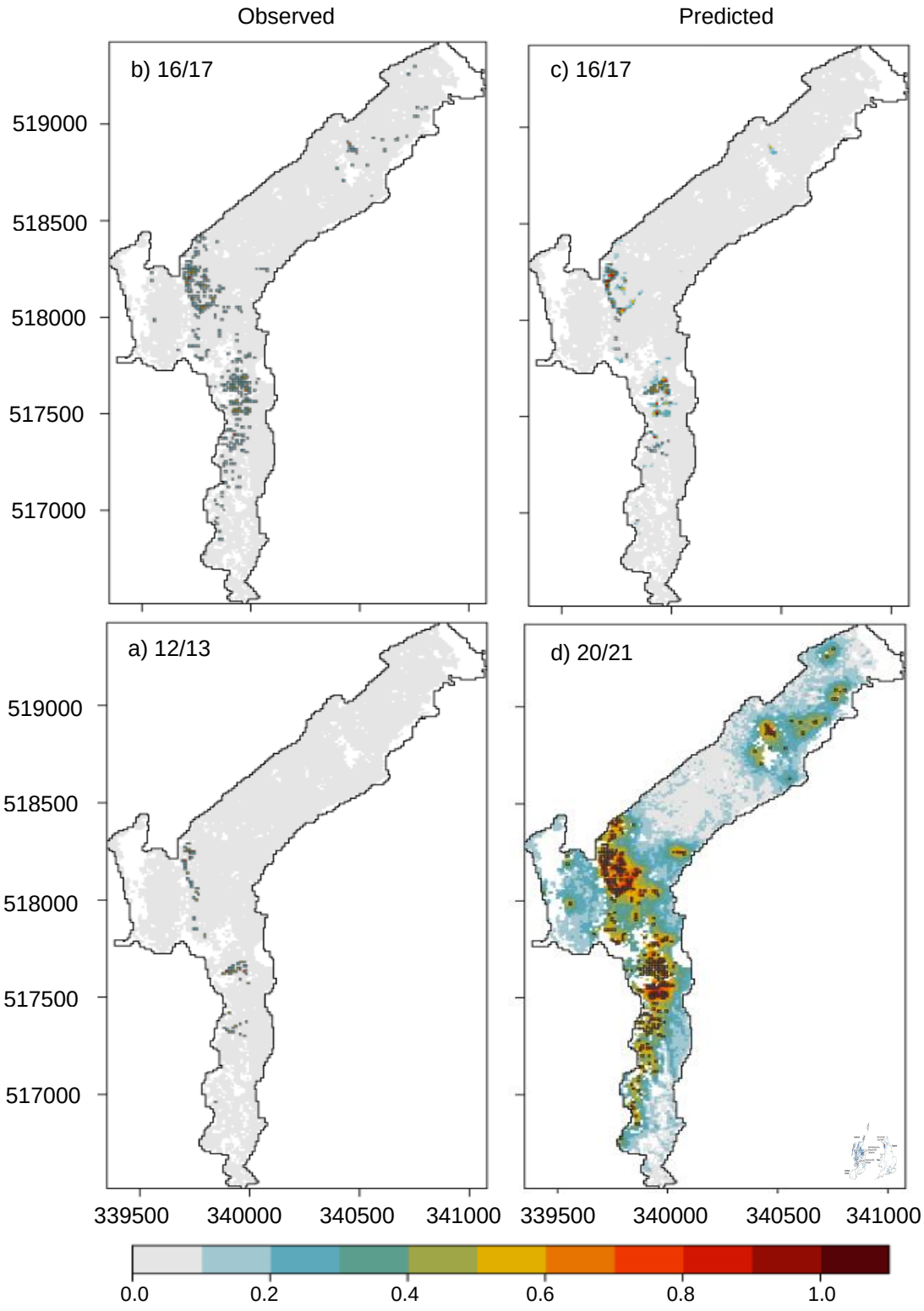

Figure 12. Spatial patterning of symptom intensity observed (a-b) vs predicted by the best PPM (c-d) labelled chronologically with the year of survey/prediction. Cells predicted to contain juniper are shown in grey and black outlines mark cells where symptoms were observed in each survey (a-b) or in the previous survey from which force of infection predictions derive (c-d). Symptom intensity is re-scaled to the colourbar to allow comparison of high and low intensity areas but does not equate to exact numbers of symptomatic trees.

3.5.3 Patterns of *P. austrocedri* colonisation at 10m resolution

The spatial random field accounted for a large proportion of the variance across all models (83.49% in the best model) (Table 11). One force of infection covariate parameterised using a power kernel variant (h=0.5, δ=20m), was clearly identified (∆DIC=4.15 from the next best model using a different force of infection covariate) as the best predictor of colonised cells in 2016/17 according to the pattern of symptoms observed in 2012/13 (Appendix I, Figure I5). Model performance improved when this force of infection covariate was used (∆DIC=22.51 compared to the null model, Table 11) but adding juniper density to the null model resulted in a larger change in DIC (∆DIC=25.78 compared to the null model, Table 11). However, force of infection accounted for a larger percentage (16%) of the explained variation compared to juniper density (9%) (Table 11). When combined, these covariates substantially improved model performance compared to the null model (∆DIC=48.42, Table 11), while adding in covariates had a lesser but nonetheless important impact (∆DIC=5.04 comparing the best overall model to that containing juniper density and force of infection only, Table 11). Four equivalent top models were found containing juniper density, force of infection and different combinations of three environmental covariates (area of bracken, altitude, and aspect) (Appendix I, Table I5).

The best overall model contained juniper density, force of infection and area of bracken (∆DIC = 0.32 to the next top model, Appendix I). Symptom intensity strongly increased (BCI did not bridge zero) with both increasing force of infection (BCI = 1.29, 2.13) and increasing juniper density (BCI = 0.52, 0.84) (Table 11). Area of bracken only accounted for an additional 0.11% of model variance (Table 11). The posterior estimate for area of bracken showed a very strong, positive response (BCI do not bridge zero) but the mean (0.20) was smaller than force of infection from symptomatic hosts present in 2012/13 (mean=1.69) and juniper density (mean=0.68) (Table 11). No hydrological or alternative juniper connectivity covariates were selected as good predictors of symptom intensity at 10m resolution (Appendix I.1.3).

Table 11. Model results obtained from the 10m resolution PPMs comparing the null model with models containing juniper density, force of infection (defined by the dispersal kernel *h*=0.5, δ=20m) and the best model from the subsets selection of additional covariates (Appendix I). The DIC is presented with the posterior estimates (mean, standard deviation (SD), 2.5% and 97.5% quantiles, and % that does not bridge zero) and the percentage of variance attributable to the spatial random field compared to the fixed effects.

Model	DIC	Parameter	Mean	SD	2.5 %	97.5 %	% does not bridge zero	Variance explained by the:	
								spatial random field	fixed effects
Best model including additional covariates	10616.25	Intercept	-10.82	0.38	-11.64	-10.15	100	83.49	16.51
		Juniper density	0.68	0.08	0.52	0.84	100		
		Force of infection	1.69	0.21	1.29	2.13	100		
		Bracken area	0.20	0.10	0.02	0.39	100		
Juniper density and force of infection	10621.29	Intercept	-10.78	0.38	-11.60	-10.10	100	83.60	16.40
		Juniper density	0.55	0.05	0.45	0.66	100		
		Force of infection	1.73	0.21	1.34	2.17	100		
Juniper density	10643.93	Intercept	-11.64	0.70	-13.21	-10.46	100	91.25	8.75
		Juniper density	0.59	0.05	0.48	0.70	100		
Force of infection only	10647.20	Intercept	-10.96	0.39	-11.80	-10.28	100	84.34	15.66
		Force of infection	1.91	0.22	1.51	2.38	100		
Null model	10669.71	Intercept	-12.01	0.71	-13.59	-10.81	100	91.57	8.43

Predicted symptom intensity of newly colonised cells in 2016/17 was highest in cells within a few hundred metres of cells containing symptomatic trees in 2012/13. The best fitting dispersal kernel had a mean effective dispersal distance of 400m (Table 8). Force of infection was predicted to rapidly decline with distance from symptomatic trees (e.g. K=0.5 after only 10m) with most dispersal predicted to occur within a half kilometre radius (K=0.01 at 425m) from cells symptomatic in the previous survey (Appendix I, Figure I6). However, the fat tail of the kernel shows dispersal events could occur at a low frequency beyond this radius, certainly within 1km of a symptomatic host (e.g. K=0.001 at 1km) and even at very

low frequency beyond 3km (the maximum possible within the study area) (Appendix I, Figure I6). The combination of force of infection, juniper density and area of bracken in the best model led to accurate predictions with high symptom intensity predicted around the two larger large scree slope foci and the start of new, low intensity outbreaks in the northern part of SSSI (Figure 12c). Predicted symptom intensity in 2020/21 generated from the best PPM shows a continued trend of local symptom intensification around symptomatic areas observed in 2016/17 and development of low intensity symptoms in the remaining areas of higher juniper density throughout the centre of the SSSI and north of the deciduous woodland (Figure 12d). While the best PPM underestimated the total number of newly symptomatic cells observed in 2016/17 (Figure 12b-c), the prediction of symptom intensity from the fixed effects (force of infection, juniper density and area of bracken) tended to overpredict the observed symptom intensity resulting in a weak correlation between observations and predictions (r^2=0.40) (Appendix I, Figure I11). The dispersal kernel tends to overpredict symptom intensity in all cells except those with very high symptom intensity (>0.75) that it underpredicted (Figure 13).

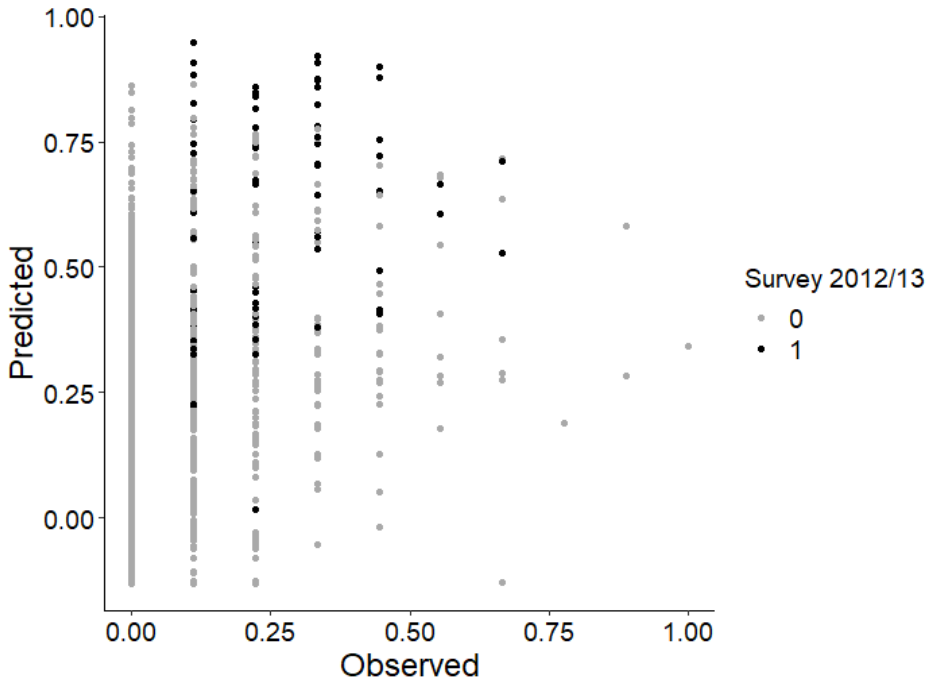

Figure 13. Symptom intensity (number of newly symptomatic trees) observed in each cell containing juniper in 2016/17 compared to symptom intensity predicted by the force of infection covariate defined using a dispersal kernel parameterised as h=0.5, δ=20m. Cells observed to contain symptoms in 2012/13 are coloured black compared to cells with no symptom observations shown in grey. Symptom intensity is rescaled between 0 and 1 to allow comparison and does not equate to exact numbers of symptomatic trees.

3.5.4 *P. austrocedri* colonisation at 25m resolution

The best model found at 25m resolution contained three covariates in addition to juniper density and force of infection but was equivalent to the model containing only the latter two variables (ΔDIC=1.99) (Table 12). Both models showed clear improvement in performance compared to the null model (ΔDIC=14.23, 12.24 respectively) but the fixed effects in the model containing only juniper density and force of infection explained 1.87% more variance than did the fixed effects in the best model (Table 12). This indicated that the fixed effects in the best model, apart from force of infection and juniper density, had a marginal impact on model performance (indeed all Bayesian credible intervals bridged zero, Table 12). The model containing only juniper density and force of infection was, therefore, determined as the best model for forward prediction of *P. austrocedri* colonisation in 2020/21 (Appendix I, Figure I19). Force of infection accounted for 19% of the explained variation compared to 10% explained by juniper density (Table 12). Whenever juniper density and force of infection were present, symptom intensity in newly colonised cells increased with increasing juniper density (BCI do not bridge zero) and increasing force of infection (BCI do not bridge zero). Symptom intensity increased with decreasing distance to the combined network of rivers and footpaths (BCI= -1.17, 0.06), decreasing area of rock (BCI= -0.46, 0.04) and westerly aspects (BCI= -0.34, 0.05) (Table 12). Although only one force of infection covariate was strongly supported at 10m resolution, a range of kernels with different shape and scale parameters were found within 10 DIC units (Appendix I, Table I10).

At 25m resolution, many of these kernels could not be discriminated between using DIC. Eleven equivalent models were present in the top model set, seven of which included force of infection derived from a dispersal kernel with an exponential shape (h=1, δ=80m) while the remaining four used a Gaussian shape (h=2), two with δ=80m and two with δ=160m. The exponential kernel described a mean effective dispersal distance of 160m, a sharp decline in symptom intensity in newly colonised cells with distance from symptomatic cells in 2012/13 (e.g. K=0.01 at 370m) and very low probability of effective dispersal occurring beyond 3km (Figure 10). The larger Gaussian kernel (h=2, δ=160m) predicted a similar range of effective dispersal distances (mean=140m, K=0.01 at 340m) but a shorter overall dispersal range with few infections probable beyond 1km (Appendix I, Figure I17). The smaller kernel predicted still shorter distances for effective dispersal (mean=71m, K=0.01 at 170m, few events beyond 700m) (Figure 10). The prediction of symptom intensity obtained from the best model replicated the spatial distribution of symptoms and symptom intensity found at 10m resolution (Appendix I, Figure I20). Symptom intensity predicted using the fixed

effects included in the best 25m PPM substantially correlated with that observed in 2016/17 (r^2=0.5), tending towards overprediction although at this resolution the best model more accurately predicted cells with the highest observed symptom intensity (Appendix I, Figure I21).

Table 12. Model results obtained from the 25m resolution PPMs comparing the null model with the best model containing covariates and models including only juniper density and/or the force of infection covariate found most frequently in the best model (calculated using a dispersal kernel parameterised with an exponential shape (*h*=1, δ=80m). The columns shown are the same as those described for Table 11.

Model	DIC	Parameter	Mean	SD	2.5 %	97.5 %	% does not bridge zero	Variance explained by the:	
								spatial random field	fixed effects
Best model including additional covariates	11790.30	Intercept	-10.77	0.51	-11.93	-9.91	100	83.34	16.66
		Juniper density	0.47	0.10	0.27	0.67	100		
		Force of infection	1.52	0.31	0.94	2.15	100		
		Network	-0.52	0.31	-1.17	0.06	95		
		Rock area	-0.20	0.13	-0.46	0.04	93		
		Aspect	-0.14	0.10	-0.34	0.05	90		
Juniper density and force of infection	11792.29	Intercept	-10.61	0.43	-11.57	-9.86	100	81.47	18.53
		Juniper density	0.53	0.09	0.36	0.71	100		
		Force of infection	1.64	0.27	1.15	2.21	100		
Juniper density only	11797.19	Intercept	-11.52	0.83	-13.43	-10.16	100	89.96	10.04
		Juniper density	0.58	0.09	0.40	0.76	100		
Force of infection only	11799.94	Intercept	-10.76	0.44	-11.75	-10.00	100	82.00	18.00
		Force of infection	1.78	0.28	1.28	2.38	100		
Null model	11804.53	Intercept	-11.89	0.89	-13.95	-10.46	100	90.02	9.98

3.6. Discussion

3.6.1 Predicted rates of *P. austrocedri* spread

The finding that most dispersal occurred within a short distance of symptomatic trees is expected for a soil borne pathogen dependent on the movement of short-lived zoospores through soil water (Erwin and Ribeiro, 1996; Greslebin et al., 2007). It is consistent with the recovery of *P. austrocedri* DNA from soil samples collected at short distance intervals from a dead juniper in the UK (Riddell et al., 2020) and patterns of *P. austrocedri* infection in both natural and urban populations of *A. chilensis* in Argentina, where spread was observed or predicted to occur <200m from the nearest infected tree (Giordana et al., 2020; La Manna et al., 2012). Over the course of four years, *P. austrocedri* symptom intensity increased in 70 (55%) 10x10m cells that originally showed symptoms and infected a further 381 cells (302% increase), revealing a pattern of both localised symptom intensification and colonisation of new areas >800m away from the nearest prior outbreak. Although only 5.2% of all 10x10m grid cells estimated to contain juniper showed symptomatic mortality in 2016/17, this is an increase of 4.7% in four years filling in gaps between the originally discrete disease foci. Colonisation most frequently occurred within ~500m of previously symptomatic trees but could occur infrequently beyond 1km. The juniper population we studied is the largest in Cumbria (Cumbria Wildlife Trust, 2014) and, therefore, one of the largest in the UK. Cumbrian populations excluding Birk Fell occupy a mean area of 316x316m (Cumbria Wildlife Trust, 2014), while the mean area of Scottish juniper populations is 732x732m (NatureScot/Mountain Woodland Action Group, 2015). A 1.2% annual increase in *P. austrocedri* infection within a 500m radius resulting in 12% mortality over a decade could be highly significant for these small, fragmented populations and the wider biodiversity they support, given the widespread distribution of infections across Scotland and England, the possibility for longer distance transmission events to introduce the pathogen to new locations, the longevity of the species (trees live for >100 years (Ward, 1982)), paucity of regeneration (Broome and Holl, 2017) and ongoing population declines resulting from other environmental pressures (Ward and Shellswell, 2017). Force of infection calculated from all symptomatic hosts in the 2012/13 survey was the most important factor explaining the pattern of *P. austrocedri* colonisation in 2016/17, followed by increasing juniper density. The biggest risk factor for juniper populations is, therefore, the introduction of disease to new locations. Force of infection at both 10m and 25m spatial resolutions always accounted for a larger percentage of model variance (15.66%, 18.00% respectively) than juniper density (8.75%,10.04%), had a bigger impact on model DIC compared to juniper density (ΔDIC 3.27,

2.75), showed the largest mean (1.91, 1.78) and strongest possible response (BCI do not bridge zero) of all covariates tested. The performance of different dispersal kernels describing force of infection was less easy to separate at 25m compared to 10m and mean effective dispersal distances were shorter at 25m than 10m. This suggests that effective dispersal processes are more accurately characterised and predicted at the finer spatial scale, as would befit dispersal of short-lived zoospores primarily through soil and soil water (Ristaino et al., 2000). Increased disease severity in response to increasing host density is consistent with positive relationships also found between *P. ramorum* and area of contiguous forest in California (Condeso and Meentemeyer, 2007), and between *P. cinnamomi* and cover of oak host species Andalusia (Duque-Lazo et al., 2018). The relationship between host density and severity of *P. ramorum* infection was found by Dillon et al. (2014) to be more informative at 15m spatial resolution, diminishing in importance over a threshold of 60m resolution. Because such scale dependence exists, matching the scale of investigation to that of the underlying biological processes aids interpretation of disease drivers and enhances the accuracy of spread predictions (Nathan and Klein, 2012). Our study demonstrates how force of infection can be simply calculated using dispersal kernels to explore scale dependence inherent in pathogen dispersal processes.

3.6.2 Abiotic and biotic drivers of colonisation

The potential for (infrequent) *P. austrocedri* transmission beyond 1km from existing infections has not previously been documented. The probability of infection occurring >1km from the nearest outbreak could be explained by the vectoring of inoculum by people, vehicles, herbivores, or a combination of all three given the land use complexity. Considering these processes further, the terrain prohibits vehicle access to all infected areas apart from the central outbreak; proximity to footpaths was not detected in the models as an important predictor of symptom intensity in colonised cells at either spatial resolution and while one new outbreak in the deciduous woodland occurred within 10m of the main footpath, the others occurred >100m from it in areas poorly accessible to recreational users but where herbivore (deer, sheep) tracks were mapped during fieldwork in 2017 (Donald et al., 2020). Deer and sheep could passively transport infected soil between disease foci as they range across the whole site, providing the most plausible link between outbreaks observed in the centre of the site in 2012/13 and the new locations in the woodland in 2016/17. Other examples of *Phytophthora* vectored by animals include the spread of *P. lateralis* along wildlife trails in the western USA (Jules et al., 2008) and the isolation *of P. cinnamomi* from feral pig trotters in New Zealand (Krull et al., 2013).

Juniper density, the second most important factor driving disease colonisation, may also have been influenced by herbivory. It is unsurprising that colonisation increased with increasing juniper density as increased availability of susceptible host tissue promotes pathogen growth and reduces dispersal distances for zoospores to infect new tissue (Burdon and Chilvers, 1982). Juniper most frequently occurred on steep slopes close to footpaths i.e. areas usually subject to lower grazing pressure. However, these factors may also indicate improved soil drainage, which we found promoted increasing juniper presence and density. This highlights an interesting interaction between the preferred conditions for the host and pathogen, as *P. austrocedri* requires damp soils for growth, sporulation and dispersal; outbreaks tend to arise first in waterlogged microsites and show increasing mortality compared to drier microsites (Donald et al., 2020; Green et al., 2015). Juniper presence and density, meanwhile, increased with decreasing topographic wetness index, corroborating observations that juniper prefers freely drained soils (Thomas et al., 2007; Ward and Shellswell, 2017) and could suggest juniper is more susceptible to infection when occupying soil conditions at the edge of its tolerance. This could have important implications for management and demonstrates the value of separating out environmental conditions that underpin host distributions from those driving pathogen establishment and spread, which is currently rarely conducted for investigations of plant pathogen invasions in the wider environment. At a national scale, juniper exhibits no strong association with aspect (Thomas et al., 2007) but at Birk Fell we found juniper presence increased with northerly aspects while density increased W-SW, suggesting stands were smaller and more fragmented in northerly aspects while larger stands were achieved in the brighter and drier westerly locations.

Additional abiotic and biotic covariates had a small impact in promoting disease colonisation that could only be detected at the finer 10m grid cell resolution. The finding that symptom intensity of colonised cells increased slightly with area of bracken may reflect host stress from increased grazing pressure since sheep were more often observed around bracken stands than under the canopy. Alternatively, symptoms may be easier to detect from aerial photographs of bracken stands compared to woodland canopy, particularly since photographs were specifically collected once the bracken had died down. We tested a variety of metrics aimed at capturing differences in small scale soil moisture, including an extensive methodology to calculate TWI using field sampling data to assess accuracy, incorporating realistic movements of water accounting for topography to calculate cell distances to the nearest river, and combining the river network with footpaths that we observed channelling water in a similar way during periods of heavy rain. While soil moisture

/ proximity to rivers was the best predictor of patterns in symptom severity in field quadrats (Donald et al., 2020), this analysis showed that where conditions are broadly suitable for the pathogen, spread primarily depends on proximity to a source of inoculum and the availability of susceptible hosts. No relationships were found between changes in symptom intensity and increasing juniper patch density or mean patch size suggesting the pathogen can disperse between disconnected stands at microsite level as predicted by the force of infection covariate. Finally, no relationship was determined between colonisation and altitude or slope despite juniper presence and density increasing with slope. Passive movement of inoculum by herbivores may explain the distribution of symptomatic trees across both gradients and the colonisation of stands upslope from the original outbreaks.

3.6.3 Management implications

The predicted distribution and intensity of symptoms in 2020/21 demonstrates the challenge of containing *P. austrocedri* once introduced to a population. Mortality was predicted to radiate from outbreaks observed in 2016/17, expanding the area of mortality in the northern woodland and creating a continuous belt of dead juniper from the population centre along the scree slopes to the southern population edge. Though symptom intensity was predicted to remain low in many areas, few uninfected stands were predicted and these were concentrated in the central woodland where juniper density is low (mean=16m^2, standard deviation=9.5m^2): predictions that could be validated by undertaking new assessments on the ground. The minor relationships found between abiotic and biotic predictors and symptom intensity in colonised cells suggest most cells across a juniper population are likely to become infected and mortality will increase. Yet the collapse of juniper populations is not inevitable and increasing our understanding of how dispersal scales with distance allows identification of management actions that could prevent further introductions and disrupt pathogen spread. We acknowledge the difficulty in extrapolating rates of spread from modelling conducted at one location to populations occupying a different suite of environmental conditions, and that differences in landscape heterogeneity and dispersal vectors may alter the shape of the dispersal kernel underpinning our force of infection estimate. However, the study population occupies similar conditions (upland, acidic heath with deer and sheep grazing and high rainfall) to many other symptomatic populations in northern England and parts of Scotland and our analysis provides a baseline to aid risk assessments and plan preventative action.

Our findings suggest natural spread of the pathogen occurs predominantly within half a kilometre of symptomatic trees and that pathogen invasion could be successfully slowed if new introductory / long distance events are curtailed. Although biosecurity is advocated by tree health plans operating in all parts of the UK, the measures currently adopted to prevent outbreaks of other *Phytophthora* species (*P. ramorum* and *P. kernoviae*) focus on the removal of symptomatic hosts from both natural and commercial environments rather than methods to reduce or disrupt dispersal (DEFRA, 2014a; Welsh Government, 2019; Scottish Forestry, 2021). The actions described below are better tailored to reduce transmission of *P. austrocedri* as a soil-borne pathogen but could also reduce introductions of other plant pests and diseases. Definitive identification of vector(s) may not be possible, so we instead encourage land managers to identify all possible avenues for inoculum introduction and take preventative action accordingly, paying particular attention to routes used by livestock and wildlife. Implementing good biosecurity measures across all populations, irrespective of infection status, such as washing vehicles, machinery and footwear can significantly reduce the spread of soil borne pathogens (e.g. *P. cinnamomi* in bauxite mines in Western Australia (Colquhoun and Kerp, 2007a)) and will additionally reduce the risk of introducing other pathogens and invasive species. Additionally, while zoospores are currently suspected to be the primary infectious agent of *P. austrocedri* spread, abundant oospore production was observed in culture (Henricot et al., 2017). If viable oospores can be produced in natural settings, they would also be transported in soil and could persist in the environment for much longer than zoospores, increasing the distances over which infection would be possible (Henricot et al., 2017). If activities that could disturb infected soil or soil water must be conducted, work could start in uninfected sites and routes could be used that avoid linking uninfected and infected stands to reduce transmission. At Birk Fell there was no evidence of inoculum transmission along footpaths, probably because the majority are surfaced with rock or gravel. Recreational trails with vegetated or bare earth surfaces may still pose a transmission risk, that could be addressed by diverting or surfacing waterlogged or muddy footpaths, or by introducing seasonal closure periods. Repairing or clearing out land drains to improve soil drainage will not only reduce the risk of pathogen transmission but may improve the health of juniper populations if carried out on currently uninfected sites. Restricting the movement of herbivores to reduce transmission is more difficult and requires good liaison between land managers, graziers (if different), deer management groups and regulators to discuss appropriate grazing regimes, stocking densities and opportunities to quarantine livestock before introducing them to uninfected sites and the need/practicality for exclosures.

One further activity that may introduce the pathogen to new populations is the planting of juniper raised in alternative settings to supplement existing stands. We are currently researching how the UK distribution of *P. austrocedri* outbreaks relate to historically planted populations in the wider environment. UK plant nurseries are known to be widely infected with *Phytophthora* species, including *P. austrocedri* (Green et al., 2021a), and introductions of many plant diseases are suspected to have initially occurred via the plant trade (Brasier, 2008). Though steps are being taken to improve nursery biosecurity, encouraging natural juniper regeneration may not only reduce the risk of introducing *P. austrocedri* on planting material but retain or enhance genotypes with putative pathogen resistance, such as those recently discovered in a Scottish juniper population (Green et al., 2021b). Juniper regenerates more successfully on moist but freely draining soils where herbivores (including rabbits and deer as well as livestock) are controlled (Broome and Holl, 2017; Ward and Shellswell, 2017). Sites with these characteristics also have a lower risk of infection (Donald et al., 2020) so could be prioritised for conservation action.

Knowledge of the nearest outbreak may also help land managers assess *P. austrocedri* infection risk. This study was only possible because repeat juniper surveys were carried out in conjunction with ongoing monitoring of another pathogen species (Wylder, B., personal communication, 13th August 2020) and aerial photographs of the site collected prior to the onset of mortality had been archived and could be used as a baseline for juniper extent. Both the UK and Scottish governments have committed to use remote sensing for continued forest monitoring (DEFRA, 2018; Scottish Government, 2019). However, although all data used in our analysis were obtained by remote sensing, prior field surveys were required to confirm pathogen presence and improve the classification accuracy of the juniper map. As image quality and methods separating spectral signatures improve, remote sensing methods may become less labour intensive; this will not negate the need for detailed ground surveys but may allow more frequent collection of snapshots of spatial disease distributions. Should this be undertaken, our study demonstrates methods that could then be used to partition out the contribution of host proximity to prior infections, host density and other environmental covariates to better understand and predict the establishment and spread of novel plant pathogens in wider environment settings.

3.7 Conclusion

Our results show that the introduction of *Phytophthora austrocedri* to UK juniper populations poses a significant risk to the species conservation and continued mortality will be observed in the coming decade. However, we identified that proximity to infected trees was the best predictor of pathogen colonisation at the population level, meaning preventative actions can be taken to reduce transmission. These will not only benefit vulnerable juniper populations but may also reduce the transmission of other pathogens and invasive species and improve the overall condition of a wide variety of habitats occupied by juniper.

Chapter 4

Investigating the role of restoration plantings in introducing disease — a case study using *Phytophthora*

Data Availability Statement: The dataset “Juniper (*Juniperus communis*) planting conducted in the UK wider environment 1960-2020” of planting events analysed in this article is available to download from Zenodo at https://doi.org/10.5281/zenodo.4916250. These data are made available with kind permission from all contributing parties. The *P. austrocedri* distribution records are sensitive and partially derive from information submitted by members of the public via TreeAlert, who request that detailed grid references are not made publicly available. However, infected locations can be viewed from 1km resolution distribution maps available here https://floradonald-juniper-planting-2020.shinyapps.io/Planting2.

4.1 Abstract

Translocating plants to natural habitats is a long-standing conservation practice but is growing in magnitude to deliver international targets to mitigate climate change and reverse biodiversity loss. Concurrently, outbreaks of novel plant pests and pathogens are multiplying with increased global trade network connectivity and larger volumes of imported plants, raising concerns that restoration plantings may act as introductory disease pathways. We used UK common juniper, subject since ~1995 to conservation plantings and now experiencing significant mortality from the non-native pathogen *Phytophthora austrocedri*, as an example species to explore the availability of monitoring data that could be used to assess disease risks posed by planting. We compiled spatial records of juniper planting including qualitative data on sources of planting material, propagation settings and organisation types that managed planting projects. We found that juniper planting activity expanded every decade since 1990 across the UK and while not all planting resulted in outbreaks, 19% of *P. austrocedri* detections were found within 2km of a known planting. We highlight the scale and diversity of organisations raising and planting juniper, as well as the lack of source material traceability, and suggest that cross-sector collaboration and changes in practice are required to reduce the risks of pathogen introduction posed by restoration planting.

4.2 Introduction

The UN General Assembly declared the 2020s as the Decade of Ecosystem Restoration, and recommended scaling up restoration of degraded and deforested ecosystems to enhance food security, safeguard water supplies and address the climate and biodiversity crises (UN, 2020). The aim is to accelerate existing restoration goals such as the Bonn Challenge to restore 350 million hectares of habitat by 2030 (IUCN, 2020). The UN strategic plan for forests aims to reverse worldwide loss of forest cover through protection, restoration, afforestation, and reforestation to increase global forest cover by 3% (120 million hectares) by 2030 (UNESCO, 2017). While a large proportion of degraded forest ecosystems results from active deforestation by people (UNESCO, 2017), losses sustained from invasive forest diseases can be substantial, e.g. 43 million trees killed by *Phytophthora ramorum* in evergreen forests on the western US coast (Cobb et al., 2020) and extensive tree mortality in Europe, North America and Australia induced by infection of multiple genera (including chestnuts, oaks and eucalypts) by the generalist, soilborne pathogen *P. cinnamomi* (Sena et al., 2018). Not only do invasive pest and disease outbreaks destabilise ecosystem processes and decrease biodiversity by killing host species and altering habitat structure

(Roy et al., 2014), they are often impossible to eradicate, thwarting attempts to remediate their impact. Preventing outbreaks will be far more effective at maintaining and enhancing ecosystem functioning than restoration attempts (Jones et al., 2018), but this requires an understanding of infection pathways and effective actions to shut them down. A pathway currently subject to little research is the translocation of planting material from plant nurseries to natural environments for habitat restoration projects. Restoration is defined by the IUCN as the re-establishment of all key ecological processes, functions, and original biodiversity (IUCN, 2003). Planting is a key method used to restore plant populations and their associated ecosystem functions, and governments are signing up to ambitious planting targets, particularly for trees given their carbon capture potential (Committee on Climate Change, 2020). For example, the current UK government has committed to plant 30000 hectares of broadleaf and coniferous woodland every year (Conservative Party (UK), 2019). Though the importance of biosecurity is detailed in national forest strategies (e.g. those produced by the UK devolved nations (DEFRA, 2018; Scottish Government, 2019)), there is good evidence that introductions of pests and diseases are increasing (Freer-Smith and Webber, 2017) as a result of expanding global trade networks (Chapman et al., 2017a), with many historic introductions identified on imported plant nursery stock (Brasier, 2008). The accelerated rate of tree planting may, therefore, risk further introductions of invasive pests and diseases, particularly where nursery stock is replanted in native environments.

One genus causing significant mortality when introduced to habitats outside its native range is *Phytophthora*, which contains many pathogenic species now globally distributed and infecting important native forest species such as Jarrah (*Eucalyptus marginata*) in Western Australia, Kauri (*Agathis australis*) in New Zealand, coast live oak (*Quercus agrifolia*) among many species in the Western USA, Monterey pine (*Pinus radiata* D.Don) in Chile and alder (*Alnus glutinosa* (L.) Gaertn.) in Europe (Hansen, 2015). The genus is also found infesting plant nurseries worldwide; one study of 670 nurseries in 18 European countries found that 91.5% of nurseries tested positive for *Phytophthora* (Jung et al., 2016). A further study of close to 4000 water, soil and root samples collected from 133 British plant nurseries revealed high infestations, with 50% of samples testing positive for Phytophthoras belonging to 63 different species (Green et al., 2021). High levels of *Phytophthora* infestation were also reported from container plant nurseries in Oregon (Redekar et al., 2019) and southern California (Redekar et al., 2020), some of which raise native plant stock to restore ecologically sensitive sites, and indeed disease outbreaks in three such sites in California originated from plants translocated from nurseries (Frankel et al., 2020). This demonstrates the potential for restoration plantings to act as an introductory pathway for disease.

In the UK, one species of particular concern has been detected in British nurseries: *P. austrocedri*, confirmed in 2012 as the agent causing serious mortality of native juniper (Green et al., 2021a; Green et al., 2012). A single genotype has so far been identified in the UK (Henricot et al., 2017c) infecting c.60 geographically separate populations in Scotland and England with varying levels of intensity, accelerating ongoing declines that had already reduced many populations to small numbers of old trees with poor seedling recruitment (Clifton et al., 1997; Hamilton, 2018; Plantlife, 2015; Borders Forest Trust, 1996; Ward, 1994). As one of few UK native conifers and an ecologically important component of many habitats, juniper has been a flagship species for conservation action for >20 years, and supplementary planting was advocated since ~1995 as a mitigating action to reinvigorate moribund populations and create or restore native woodlands (Plantlife International, 2007; Sullivan, 2003; Wilkins and Duckworth, 2011b). In Scotland, specific juniper management guidance was based on Sullivan's (2003) recommendations in 2003 to divide the country into conservation action zones detailing where juniper planting should be prioritised (Forestry Commission Scotland, 2009a). Following identification of the first *P. austrocedri* outbreaks in 2012, the guidance was revised to include further detail about biosecurity measures to prevent inadvertent disease introductions, but planting was still advised in zones where the species was thought to be at greater risk from no natural regeneration (Forestry Commission Scotland, 2013). Juniper management guidance issued for England and Wales by the Department for Environment, Food and Rural Affairs (DEFRA) in 2017 similarly provided a decision tree to assess the vulnerability of populations to *P. austrocedri* but recommended planting where the disease was absent from a catchment and where the population size was declining too rapidly to be sustained by natural regeneration (DEFRA, 2017).

The extent to which juniper planting has been conducted in the wider environment is unknown and we believe requires further scrutiny to investigate any link between planting and *P. austrocedri* outbreaks. The wide geographical coverage of *P. austrocedri* cannot be explained by its slow, natural dispersal through soil and water run-off, and the pathogen has no ability to disperse aerially (Riddell et al., 2020). The findings of *P. austrocedri* infestations in British nurseries and the single pathogen genotype detected across the Great Britain in nurseries and the wider environment alike suggest that outbreaks in native populations may derive from multiple introductions of planted material (Riddell et al., 2020). The focus of this paper, therefore, was to compile the first spatial dataset of juniper planting locations to understand where and when planting has been carried out and by which organisations, to find out where material is sourced from and how frequently *P. austrocedri* outbreaks are associated with planted locations both UK-wide and across the Scottish juniper conservation

zones. In doing so, we hoped to compile a dataset to use as a case study to examine further wider questions about the disease risks posed by supplementary planting, its success as a tool for habitat creation or restoration and to inform the design of future planting schemes.

4.3 Materials and methods

4.3.1 Compilation of UK juniper planting records

The Botanical Society of Britain and Ireland (BSBI) maintains the largest and most comprehensive repository for UK plant species distribution data containing >40 million records (BSBI, 2021). While some records have been digitised from historical accounts, the majority are observations made by volunteers in publicly accessible areas (i.e. not gardens) that are verified by local vice county recorders prior to accession. All records of *Juniperus communis* were downloaded from the BSBI distribution database that spanned from “before 1738” to January 2020 (BSBI, 2020). Records marked as “alien”, “casual”, “deliberate introduction”, “established in wild”, “surviving in wild” or “planted deliberately” in the “locality status” field were first filtered from the data, followed by a keyword search performed in the “comments” field using search terms of “plant*”, “introduc*”, “cultivar”, “garden”, “seed” and “cuttings” to extract further locations of planted populations. Additional localities for planted juniper were then collated from a wider body of literature including survey record cards describing the distribution of juniper sites across England and South Wales 1969–1977 (Ward, 1994a), juniper population surveys commissioned by public bodies (e.g. NatureScot) or conservation charities (e.g. Cumbria Wildlife Trust), records held by Forest and Land Scotland of juniper planting conducted on the National Forest Estate and records maintained by the devolved environmental statutory agencies (NatureScot, Natural England, Natural Resources Wales) detailing supplementary juniper planting conducted on Sites of Special Scientific Interest (SSSIs) or Special Areas of Conservation (SACs). Further sites were identified by searching for references to juniper in archived biodiversity action plans or management notes produced by national parks and checking if these projects were successfully actioned by contacting the relevant county council, national park authority or lead organisation responsible for the action and requesting information about planting locations and any other details relating to the planting year, seed source, information on how and where material was propagated, the number of trees and any subsequent monitoring notes. Organisations that manage woodlands or nature reserves in areas with naturally occurring or declining juniper populations were also identified and contacted directly with requests for the same information. Some organisations held this centrally, while others identified the most likely areas for juniper planting activity and contacted relevant outposted

staff. Some sharing of contacts through plant health inspectors, local knowledge or other professional networks also yielded information about localities not identified by other means. Where locations were supplied as maps, grid references were manually identified at 1km resolution using the Scotland's Bird Club grid reference finder (Scottish Ornithologists' Club, 2020).

Once all records were compiled, filtering operations were conducted in R v.3.6.2 (R Core Team, 2019) using the dplyr R package (Wickham et al., 2020). The planting dataset started with 1306 records. The year of planting was usually supplied with records obtained directly from organisations or survey reports whereas the date recorded in the BSBI database related to the year of observation. Removing these observations would reduce the known spatial distribution of planting which we regarded as more important, so the year of observation was retained as an indication of the most recent year of possible planting, unless it could be substituted with the actual planting year supplied in the "comments" field. Similarly, where the exact year of planting was uncertain but provided as a range of dates, the most recent date was attributed as the planting year. Records supplied with no year of planting or the year of observation were removed from the dataset, as were records where the recorder name, grid reference, record date and associated comment exactly duplicated another record. Planting events may still be duplicated in the dataset if (a) recorded by different individuals, (b) recorded in different years or (c) retrieved from multiple sources. Filtering removed 221 records, before a further 58 with insufficient geographical accuracy (>2km×2km) were removed, leaving 1027 records.

4.3.2 Qualitative analysis of juniper planting records

Qualitative information associated with planting records was explored prior to any further filtering of the dataset. Keywords pertaining to the organisation responsible for planting, the size or purpose of schemes, the source or type of collected material, the type of setting used to propagate material (e.g. nursery, in-situ planting) and any subsequent population monitoring were identified from the information transcribed to the "comments" field. Information for the same planting event could vary with the record source offering further insight. Uncertainty surrounding record duplication prohibited a quantitative keyword analysis but under each theme, the keywords were ordered according to their relative frequency in the dataset.

4.3.3 Spatial analysis of UK juniper planting

The spatial distribution of planting locations was explored at the tetrad (2km×2km) level to reduce spatial bias resulting from duplicate records and to match the resolution of the native juniper distribution map (Chapter 4.3.4 Spatial distribution of native juniper). Grid references supplied at a higher resolution were converted from OS national grid references, latitude/longitude or eastings/northings using the *det_tet_quad*, *gps_latlon2gr* and *gr_num2let* functions in the BRCmap package (Harrower, 2016). As some locations were planted in multiple years, the data were filtered using the combination of tetrad location and planting year and are subsequently referred to as discrete "planting events". The change in the number and spatial distribution of these planting events over time was plotted using the ggplot2 R package (Wickham, 2016) and mapped using ARC GIS v.10.5.1 (ESRI, 2017).

The map of Scottish juniper conservation action zones was digitised from an image in ARC GIS and aligned to county boundaries (GADM, 2017) using the align edge tool under the topology menu. The resulting shapefile was imported to R using the rgdal package (Bivand et al., 2019); the centroids of each planted tetrad were found using the *gr2sp_points* function in the BRCmap package (Harrower, 2016), to which the planting zone was extracted using over from the sp package (Bivand et al., 2013). The frequency and percentages of planting events that took place before and after publication of the revised guidance in each zone were explored in R and mapped in ARC GIS.

4.3.4 Spatial distribution of native juniper

A map of the current UK juniper distribution was compiled to understand planting activity in the context of the species' native range, using the *J. communis* records downloaded from the BSBI database that remained following extraction of all records referencing planting. Additional grid references were added from records of *J. communis* supplied by the Centre for Environmental Data Recording and juniper population surveys provided by Borders Forest Trust (McBride, n.d.; Borders Forest Trust, 1996), Causeway Coast and Heritage Trust (Hamilton, 2018), NatureScot (Lavery, 2016; Sullivan, 2003), Natural Resources Wales (Squirrell and Hollingsworth, 2008) and Plantlife (Dines and Daniels, 2006). Grid references associated with all units within SSSIs and SACs identified by Natural England as hosting juniper features (including habitats and vascular plant assemblages) were copied from the publicly accessible MAGIC database (DEFRA, 2020a), and further records were taken from *P. austrocedri* surveys conducted by the Northern Ireland Department of Agriculture, Environment and Rural Affairs (DAERA), Forestry Commission England and Scottish

Forestry, and from symptomatic juniper samples collected from locations confirmed as "wider environment" (Chapter 4.3.5 Occurrence of *P. austrocedri* in the wider environment) submitted to the Food and Environment Research Agency (FERA) or Forest Research for identification. A point shapefile of the Scottish montane scrub dataset (NatureScot/Mountain Woodland Action Group, 2015) was filtered to retain only records of "Juniperus communis" in the "species" field from which spatial coordinates were extracted using the rgdal R package (Bivand et al., 2019). Polygon shapefiles were supplied by Cumbria Wildlife Trust that mapped the extent of all juniper populations within Cumbria (Cumbria Wildlife Trust, 2014) and by Scottish Forestry for all habitats mapped by the Native Woodland Survey of Scotland (Forestry Commission Scotland, 2009b), filtered to contain locations where the "dominant habitat" was defined as "juniper scrub". A regular 1km grid was created for Scotland and Cumbria using the create fishnet tool in the ARC GIS data management toolbox and overlaid with the corresponding survey polygons so that 1km grid references could be obtained using the intersect tool in the analysis toolbox. Following compilation of all records, grid references were converted to tetrad resolution using the functions described in Chapter 4.3.3 Spatial analysis of UK juniper planting and filtered to retain distinct locations of juniper populations observed between 1990 and 2020.

4.3.5 Occurrence of *P. austrocedri* in the wider environment

To explore the intersection between planting and *P. austrocedri* presence, Forest Research and FERA forwarded all records of *P. austrocedri* symptomatic material submitted to them for testing including samples taken from alternative host species and cultivated settings. The pathogen was first detected in the UK in 2012 (Green et al., 2012) and though the dataset was finalised in 2020, the most recent detection was made in 2016. Detections were based on i) isolation of the pathogen into culture, ii) PCR and sanger sequencing of the ITS region or (most frequently) iii) a pathogen-specific qPCR assay as described in (Mulholland et al., 2013). The absence of *P. austrocedri* from Northern Ireland was confirmed by DAERA (Smith, A., personal communication, 8th May 2019). All samples relating to juniper stands (bark, stem, root, or soil samples) in the "wider environment" were retained if supplied with a grid reference and year of detection, and a result described as "positive", "isolate" or "confirmed". These were mapped against the native juniper distribution map, and any records that did not intersect with an occupied juniper tetrad were queried with plant health inspectors, local foresters, or botanists to confirm the presence of juniper. Seven tetrad locations were discovered by this process to derive from gardens and were discarded from the dataset.

To compare if *P. austrocedri* outbreaks occurred closer to planted locations than populations with no disease incidence, a dataset of apparent “absences” was assembled. It is not possible to prove the absence of a soil pathogen, but we interpreted the absence of foliage symptoms and/or a negative qPCR result as sufficient evidence that a juniper tree was not infected at the time of visit. These locations are henceforth referred to as “absences”. Absence records obtained from Forest Research/FERA that tested “negative” with qPCR were added to records compiled for the Phyto-Threats project (Green, et al., 2021) of all UK *Phytophthora* outbreaks provided by the Animal and Plant Health Agency, Science and Advice for Scottish Agriculture, the Royal Horticultural Society, Forest Research, Scottish Forestry and Natural Resources Wales. This assumes that outbreaks of *P. austrocedri* would be identified if symptomatic juniper was present in the tetrad visited by plant health inspectors (with proof of a visit taken as the presence of a record for another *Phytophthora* species). The data were filtered to retain records from 2012 onwards in environments described as “woodland”, “watercourse”, “heathland”, “WE” or “wider environment”, “plantations”, “mature woodland” or “hedges/screens/riverbanks” that overlapped with the national map of juniper distribution (Chapter 4.3.4 Spatial distribution of native juniper). Additional visits to juniper populations were collected by copying SSSI compartment grid references from MAGIC (DEFRA, 2020a) that matched accessions in site condition monitoring reports made since 2012 by Natural England, populations “refound” as part of the Natural Resources Wales 2014/15 *P. austrocedri* survey and populations with no symptoms visited by the authors between 2012 and 2019. Records occupying the same tetrad as those with positive *P. austrocedri* detections were removed, as were any grid references with >2km resolution. Next, the distance from each absence or infection record to the nearest tetrad centroid planted in the same or previous years to the visit or detection year was calculated using *gDistance* in the rgeos R package (Bivand and Rundel, 2019), and the record with the shortest distance for each monad (1km resolution grid reference) was retained. Records of *P. austrocedri* absences were randomly thinned to match the same number of infected monads using the base R *sample* function (R Core Team, 2019). The minimum distances to the nearest prior planting event were log10 transformed, but the distributions for both infected and absence locations retained non-normal distributions with a strong, left skew. The average minimum distance to the nearest prior planting events was, therefore, compared between the two groups using a Mann-Whitney U test performed using the stats R package (R Core Team, 2019) and the *wilcoxonR* function in the rcompanion package to determine the effect size, r (Mangiafico, 2021).

Lastly, all planting records within a 500m radius of the shortlisted grid references for infected and absence locations were extracted from the planting dataset using the *gBuffer* function from the rgeos R package (Bivand and Rundel, 2019). Because the planting map was produced at 2km resolution, planting records identified within the 500m radius buffer zone could be a maximum distance of 2km from the grid reference. These distances were considered appropriate, following the results from Chapter 3 where *P. austrocedri* colonisation of a single juniper population in northern England occurred frequently within 500m and infrequently beyond 1km of the nearest symptomatic juniper over a four-year period. The number of planting events identified in the buffer zone was compared between infected and absence locations, as was the number of juniper planted per event in categories of <50, 50–499 and >500 trees, as differences in infection might be expected to result from different sizes of planting event. The number and percentage of records distributed in categories describing the organisations conducting planting, the propagation settings, the source and type of propagation material and the country, region (north, south, east, west) and decade during which planting took place were further collated and compared between infected and absence buffer zones using Chi-squared tests. Test results were reported as (degrees of freedom, total number of records with information)=$\chi 2$, p-value.

4.4 Results

4.4.1 Spatial and temporal distribution of juniper planting

Juniper planting has been widely conducted across the UK (Figure 14) with 781 planting events (subject to duplication) conducted in 469 tetrads between 1960 and 2019, of which 149 (32%) were subject to multiple planting events carried out in different years. Planting was recorded in all four nations, in approximately 9% of tetrads occupied by native juniper during the past 30 years (Figure 14). The BSBI contributed the largest number of planted juniper records (41%), augmented with locations submitted by a further 28 organisations.

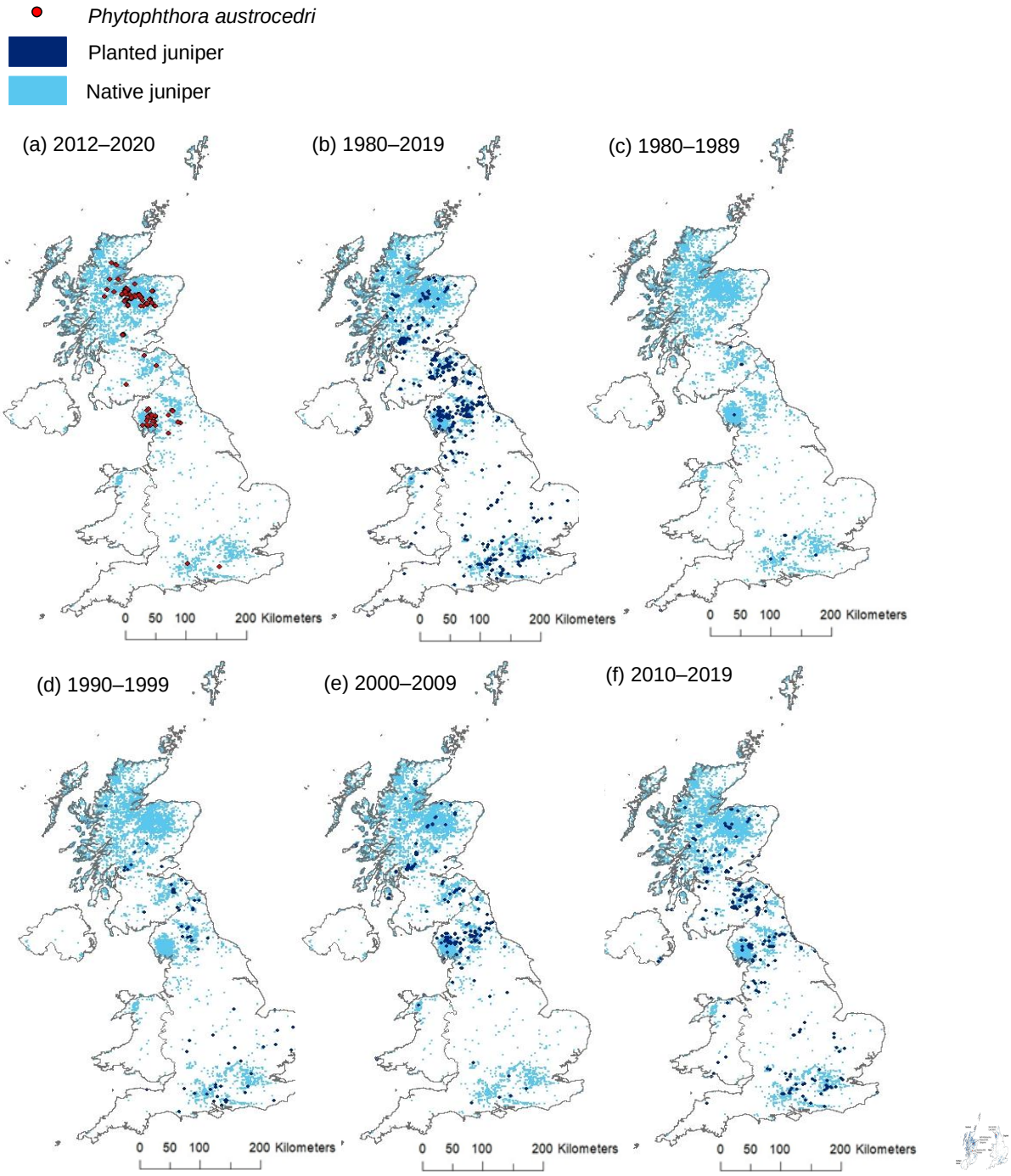

Figure 14. Comparison of the distribution of all *P. austrocedri* detections located in the wider environment (a) with all wider environment juniper planting carried out 1980–2019 (b) and carried out per decade (c–f). Planting locations (dark blue) are mapped against the distribution of native juniper (light blue) recorded since 1990. Maps a and b can be viewed online at https://floradonald-juniper-planting-2020.shinyapps.io/Planting2/ and are reproduced in Appendix J.

Though *P. austrocedri* was first confirmed in the UK in 2012 (Green et al., 2012), symptoms were first reported from one population—now heavily infected—in the 1990s (Tene et al., 2007), suggesting that the pathogen was introduced much earlier. Planting activity markedly increased in both frequency and spatial distribution during the 1990s and is sustained to the present day (Figure 15). The number of planting records and number of planted tetrads show similar trends, but the former shows high peaks concentrated at the start and end of each decade that matches the trend of all juniper record submissions and more likely reflects recording than planting activity, as recorders start to re-visit localities last observed in the previous decade (Figure 15). The number of planted tetrads, therefore, gives a more reliable insight into the distribution of planting activity over time (Figure 15). The mean number of tetrads (36) planted between 2000 and 2009 more than doubled (277%) compared to the 1990s (13 tetrads), which already represented a 750% increase compared to the 1980s (2 tetrads) (Figure 15). Planting from 2010 to 2019 further increased to an average of 53 tetrads per year that were distributed further across the UK than any preceding decade (Figure 14, Figure 15).

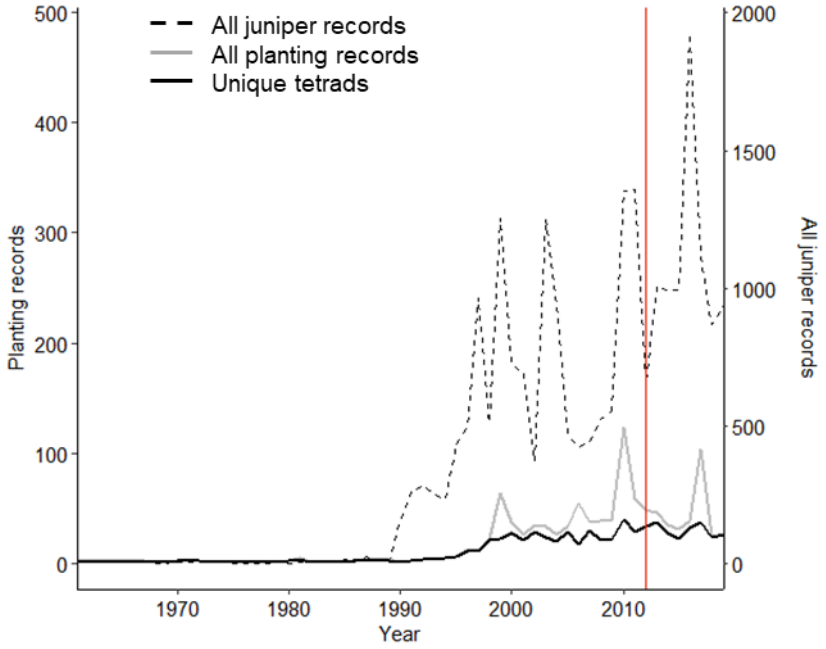

Figure 15. Juniper records 1960 to 2019, comparing all records collected at ≥2km resolution (dotted line) with all planting records (grey line), the number of tetrads (2km×2km grid cells) planted each year (black line) and the first detection of *P. austrocedri* infecting a juniper population in the wider environment (red line).

Planting records associated with publicly funded agri-environment or forestry schemes are missing from the dataset unless recorded ad hoc by BSBI volunteers. Information was requested from Scottish Forestry regarding the extent of funding allocated to subsidise juniper planting in Scotland, but this could not be provided, as species targeted within funding applications have not been recorded (Cummings, 2021). Scottish Forestry was able to advise on the list of “Forestry Grant Scheme” options available 2014–2020 to support juniper management via activities promoting natural regeneration (three options) or planting (four options) (Cummings, 2021). Creation options accounted for the smaller proportion (38%) of the area funded compared to natural regeneration (62%) and formed 33% of the total area (51528ha) funded under all woodland creation options (Cummings, 2021). Scottish Forestry further noted that the area of juniper included in applications for either creation or ongoing management was “extremely small” (Cummings, 2021). It is unclear if these proportions are similar in other parts of the UK and, therefore, the extent to which our planting dataset under-represents juniper planting activity.

4.4.2 Qualitative assessment of organisations, purpose and propagation settings linked to planting, from planting records

The information associated with planting records varied greatly, but 722 of 1059 records contained additional comments that could be used to understand better who is involved in planting schemes and for what reason, as well as the size of schemes and the diversity of locations used to source and propagate material. The organisation responsible for planting could be identified for 44% of records, showing that planting activity is not only associated with the public estate (e.g. National Forest Estate, Ministry of Defence) or conservation areas (e.g. national parks, wildlife trust reserves) but also with commercial enterprises, landscaping for infrastructure projects (dams, motorways), private landowners and community groups (most often managing community woodlands) (Table 13). Scheme size, described by 40% of all records, reflected this diversity with almost equal proportions of tetrads (per year) planted with 50 or fewer juniper plants, or between 50 and 4000 plants (Table 13). Two statutory agencies managing areas of the public estate each planted 10000 junipers, and one conservation charity planted 200 junipers every year for approximately ten years (Table 13). The reasons for planting were only detailed in 12% of records and largely mentioned its use for landscaping around carparks or roads, but some specifically referenced attempts to restore existing moribund or fragmented populations or improve the ratio of male to female plants to encourage natural regeneration (Table 13). A further 45% of

records could be assumed to address conservation aims to restore or create juniper habitats based on the organisation submitting the information.

Table 13. List of responses associated with planting records that address the themes exploring who carries out juniper planting in the UK, their motivations, scheme size and sources of material. Responses are listed in order of frequency.

Theme	Categorized Response
Number of plants	≤50 45% 50–500 35% 500–4000 14% 10,000 2% 200 plants every year for ~10 years 4%
Organisations conducting planting	Conservation charities and wildlife trusts Public estate including county councils and MOD Utility companies National/regional parks Community groups Private individuals Commercial (forestry and landscaping)
Reasons for planting	Landscaping for infrastructure (roads, forest tracks, dams) Amenity (trading estates, hotels, golf courses, churchyards, carparks) Restoration of native woodlands Woodland creation Population conservation with explicit references to loss of extent, lack of natural regeneration, gender imbalance, poor age structure
Source material	Local provenance Native stock Commercial source
Material type	Cuttings Seed
Propagation setting	Central nursery specific to the organization Commercial nursery On-site nursery Research institute (e.g. zoo or botanic garden) Direct in-situ sowing or planting Private garden
Monitoring	Qualitative assessment, e.g. “favourable”, “well established”, “growing well”, “struggling” Assessment of pressures, e.g. poor quality stock; damaged by herbivores including deer, sheep, rabbits, voles; damaged by snow or wind exposure; lost to muirburn; shaded by other trees or smothered by rank grass States that monitoring is taking place but provides no further detail Detailed assessment of planting success, e.g. percentage of surviving plants Observations of subsequent berrying or natural regeneration Presence or absence of *P. austrocedri* symptoms

The source of juniper used for planting and the propagation settings were detailed in 27% and 20% of records, respectively, and yielded important insight about current practices. Where referenced, source material was usually described as native or collected from a specific local source or was infrequently traced back to commercial nurseries of varying size

(Table 13). Cuttings were overwhelmingly used to propagate juniper with only a handful of references to seed collection and four projects that mentioned use of both (Table 13). The locations used to propagate material also varied considerably from nurseries managed "in-house" by a single organisation to commercial nurseries, on-site nurseries, research institute nurseries and, in one instance, an individual's own garden (Table 13). Some organisations emphasised the importance of biosecurity when considering where to propagate material, including one project that chose a nursery because it did not trade with other retailers to reduce any risk. There was some evidence of organisations distributing propagated plants from their central nurseries to other organisations and some movement of plants between countries within the UK. Only one instance of planting stock imported from outside the UK was documented, and the comments noted this was a supply error.

Details of follow-up monitoring conducted to check the success of planting projects represented the smallest subset of comments, associated with 8% of records, and portrayed a mixed picture of the establishment. Some recorders observed that planted populations looked "favourable" or had "80%–90% success", noted that sheep fences or rabbit-proof mesh enclosures were "effective" and noted that plants were berrying or showed no signs of disease. However, comments also reported that some populations were "struggling", often attributed to management pressures including overgrazing, e.g. "50% pulled up by sheep", competition, e.g. "under dense shade of large trees" or the "wrong provenance for site", while others were symptomatic for *P. austrocedri*, e.g. "65% Paus symptoms" or showed high mortality, e.g. "45% dead, 20% poor health".

4.4.3 Associations between spatial patterns in juniper planting and *P. austrocedri*

There were 311 positive *P. austrocedri* detections made from 2012 to 2016 across Scotland and England in the wider environment, distributed across 98 tetrads which represents 2% of UK tetrads occupied by native juniper since 1990. At 1km resolution, *P. austrocedri* occupied 130 monads. The average minimum distances to the nearest prior planting events were significantly different between infected locations and the random sample of visited absence locations according to the Mann-Whitney U test ($U=6531$, $p=0.002$). The small, negative effect size ($r= -0.20$) suggested that absence locations were slightly further from planting events compared to infected locations. However, though the maximum distance between planting events and an infected monad was shorter (33km) compared to absence monads (74km), infected monads occurred at a median distance of 7.7km from the nearest recorded planting compared to absence locations within a median distance of just 3.6km (Figure **16**). A larger proportion of absence monads was situated within 0–5km of a planting event (60%)

compared to infected monads (40%) and double the number of absence locations (30) occupied the same monad as a planting event compared to infected locations (14) (Figure 16).

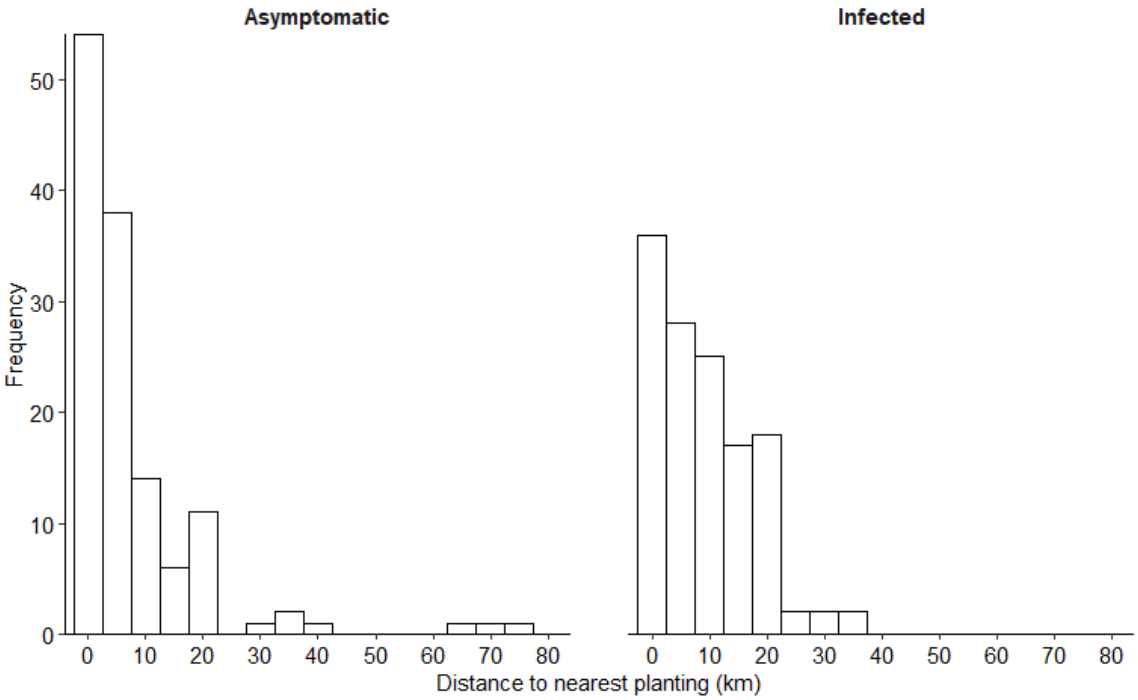

Figure 16. Comparison of distances (km) calculated between 130, 1km resolution grid cells where *P. austrocedri* was apparently absent, and the same number of infected cells, to the nearest 2km resolution planting event conducted before the date visited. Cells treated as "absent" were either visited 2012–2019 and showed no symptoms or sample material tested negative, and were drawn only from 2km tetrads with no disease detections; infected cells contained a positive *P. austrocedri* detection (Chapter 4.3.5 Occurrence of *P. austrocedri* in the wider environment).

This pattern was maintained when events within the 500m radius buffer zone were examined: 41/130 absence locations compared to 25/130 infected locations were associated with planting events conducted in the same or previous year(s) (Table 14). Though a smaller proportion of planting events intersected with buffer zones around infected compared to absence locations, planting nonetheless occurred in buffers surrounding 19% of all *P. austrocedri* detections at 1km resolution. More planting records were collected in the buffer zone around infected locations (115 events) compared to absence locations (89 events) and were associated with higher quality information regarding the scheme size, organisations involved and propagation settings, which constrained the analysis of planting event characteristics (Table 14, Table 15). However, the available information suggested that infected locations were associated with more planting events.

Table 14. Summary of the total number (n) of planting records, total number, and percentage (%) of planting events, numbers, and percentages of planting events and of juniper planted per event found in the 500m radius buffer zone surrounding 130 *P. austrocedri* absence and 130 infected locations, selected as the minimum distance to a planting event per 1km grid cell (monad). Planting events refer to planting carried out at a location in a specific year that could be documented by one or more planting records. *Records were extracted where planting events took place before, or in the same year, as visit or detection.

		Absence locations		Infected locations	
		n	%	n	%
Number of planting records located in buffer zones		89	n/a	115	n/a
Number of previous * planting events located in buffer zones		41	32	25	19
Number of planting events per buffer zone	1	22	54	8	35
	2	9	22	2	9
	3	4	10	3	13
	4	3	7	1	4
	5	1	2	1	4
	7	0	0	1	4
	9	1	2	0	0
	10	0	0	4	17
	11	1	2	0	0
	12	0	0	2	9
	14	0	0	1	4
	records with information	41	46	23	20
Number of juniper planted per event	<50	19	44	16	15
	50–499	11	26	61	56
	>500 (to 3000)	13	30	32	29
	records with information	43	48	109	95

Table 15. Propagation setting of planting material and type of organisation overseeing the planting project according to categories detailed on Table 13. The number (n) and percentage (%) of planting records with associated information per category are shown for planting events occurring in the buffer zone of absence (41 monads, 89 planting events) and infected (25 monads, 115 planting events) locations.

		Absent		Infected	
		n	%	n	%
Propagation setting	Organisation-specific central nursery	17	50	44	57
	Commercial nursery	10	29	33	43
	Research institute	1	3	0	0
	Direct in-situ sowing	6	18	0	0
	records with information	34	38	77	67
Organization	Conservation charities and wildlife trusts	14	35	59	88
	Public estate and statutory agencies	22	53	6	9
	Utility companies	4	10	2	3
	records with information	40	45	67	58

The frequency distributions of planting events conducted per buffer zone surrounding infected and absence locations were significantly different, $\chi 2$ (10, n=204)=18.53, p=0.05, and a higher median number of events was recorded within zones buffering infected (3) compared to absence (1) locations (Table 14). Larger numbers of juniper were also planted per event in infected buffer zones (median 300 trees compared to 100 in absence buffer zones, Table 14), a difference which was highly statistically significant, $\chi 2$ (2, n=152)=17.68, p=0.001, but fewer records identified within absence buffer zones gave details of the size of planting compared to infected zones (Table 14).

A highly significant, greater proportion of planting material was sourced from the central organisation or commercial nurseries in infected compared to absence buffer zones, $\chi 2$ (3, n=111)=18.91, p=0.000, and managed by conservation charities and wildlife trusts compared to a larger percentage of plantings in absence locations conducted by statutory agencies, $\chi 2$ (2, n=107)=32.83, p=0.000 (Table 15). The differences in the distribution of planting events in absence and infected buffers between countries were also highly statistically significant, $\chi 2$ (2, n=204)=33.58, p=0.000. Seventy-eight percent of planting events conducted in the buffer zone of infected locations took place in northern England and 18% in southern Scotland, representing similar percentages in the total number of planting events conducted per country (66% Scottish and 63% English planting events were in infected buffer zones) (Table 16). No locations were infected in Wales, despite planting activity that accounted for 26% of planting events found within absence buffer zones (Table 16). Most of the Welsh planting events related to a project conducted by Natural Resources Wales to restore populations on Anglesey and Ramsey island where local material was propagated at a nursery specifically chosen because it did not trade with other nurseries and only raised juniper collected by the project (Jones, B., personal communication, 5th December 2019). No significant difference was found between the number of planting events conducted each decade between absence and infected buffer zones, $\chi 2$ (4, n=204)=7.95, p=0.094. However, absence locations were associated with similar numbers of planting events conducted between 2000 and 2009 (49%) and from 2010 to 2019 (37%), while 70% of plantings recorded in infected buffer zones were carried out during 2000-2009 followed by 20% between 2010 and 2019, which could illustrate a time lag between *P. austrocedri* introduction and symptom detectability (Table 17).

Table 16. Geographic distribution of planting records in buffer zones associated with absence (41 monads, 89 planting events) and infected (25 monads, 115 planting events) locations shown as the number (n) and percentage (%) of planting records per category.

Country	Region	Absent		Infected	
		n	%	n	%
Scotland	Western	8	9	0	0
	Eastern	3	3	0	0
	Central	1	1	2	2
	Southern	0	0	21	18
	Country total	12	13	23	20
England	Northern	52	58	90	78
	Southern	2	2	2	2
	Country total	54	61	92	80
Wales	North	15	17	0	0
	South	8	9	0	0
	Country total	23	26	0	0

Table 17. Temporal distribution of planting events in buffer zones comparing absence (41 monads, 89 events) and infected (25 monads, 115 events) locations as number (n) and percentage (%) of records per category per decade.

Planting Decade	Absence		Infected	
	n	%	n	%
1970-1979	1	1	0	0
1980-1989	0	0	1	1
1990-1999	11	12	10	9
2000-2009	44	49	81	70
2010-2019	33	37	23	20

4.4.4 Planting in Scottish juniper conservation action zones

Scotland contains 72% of the UK baseline juniper tetrads and 70% of tetrads with *P. austrocedri* positive detections. Records of planting were obtained for 262 events, of which 175 took place between 1983 and 2013 and 87 during 2014–2019 following re-publication of the juniper planting guidance in response to the *P. austrocedri* disease threat that prioritised planting in different zones according to juniper population vulnerability as a function of size (Forestry Commission Scotland, 2013) (Table 18, Figure 17). Thirty-three percent of all planting conducted in Scotland was concentrated in the six-year period following the guidance publication. Indeed, the peak number of tetrad locations (25) planted in one year since 1960 was reached in 2017. The ratio of planting conducted across the three conservation zones during 1983–2013 matched the recommendations that planting was required in zone 3, may be necessary for moribund populations in zone 2 and would rarely be required in zone 1 (Table 18, Figure 17). Following the guidance update, the

proportion of juniper planting conducted during 2014–2019 decreased in zone 3, stayed the same in zone 2 and increased in zone 1: the opposite of the outcome recommended (Table 18, Figure 17). Tetrads infected with *P. austrocedri* were concentrated in zone 1 (84%) followed by small percentages in zones 3 (12%) and 2 (4%) (Table 18, Figure 17). Planting events only occurred in the same tetrad as *P. austrocedri* in three locations, each situated in a different zone and associated with no information about source material. The zone 2 tetrad was subject to planting in five different years while the others were associated with a single event.

Table 18. Number (n) and percentage (%) of juniper tetrads associated with positive *P. austrocedri* detections and planting events during 1983–2013 and 2014–2019 (before and after publication of the most recent planting guidance) in Scottish juniper conservation zones.

		Juniper Conservation Zone		
		1	**2**	**3**
		Planting rarely required	**Some planting for moribund populations only**	**Planting needed to restore minimum breeding population and expand range**
P. austrocedri	n	57	3	8
	%	84	4	12
Planting 1983–2013	n	27	50	98
	%	15	29	56
Planting 2014–2019	n	25	27	35
	%	28	31	40

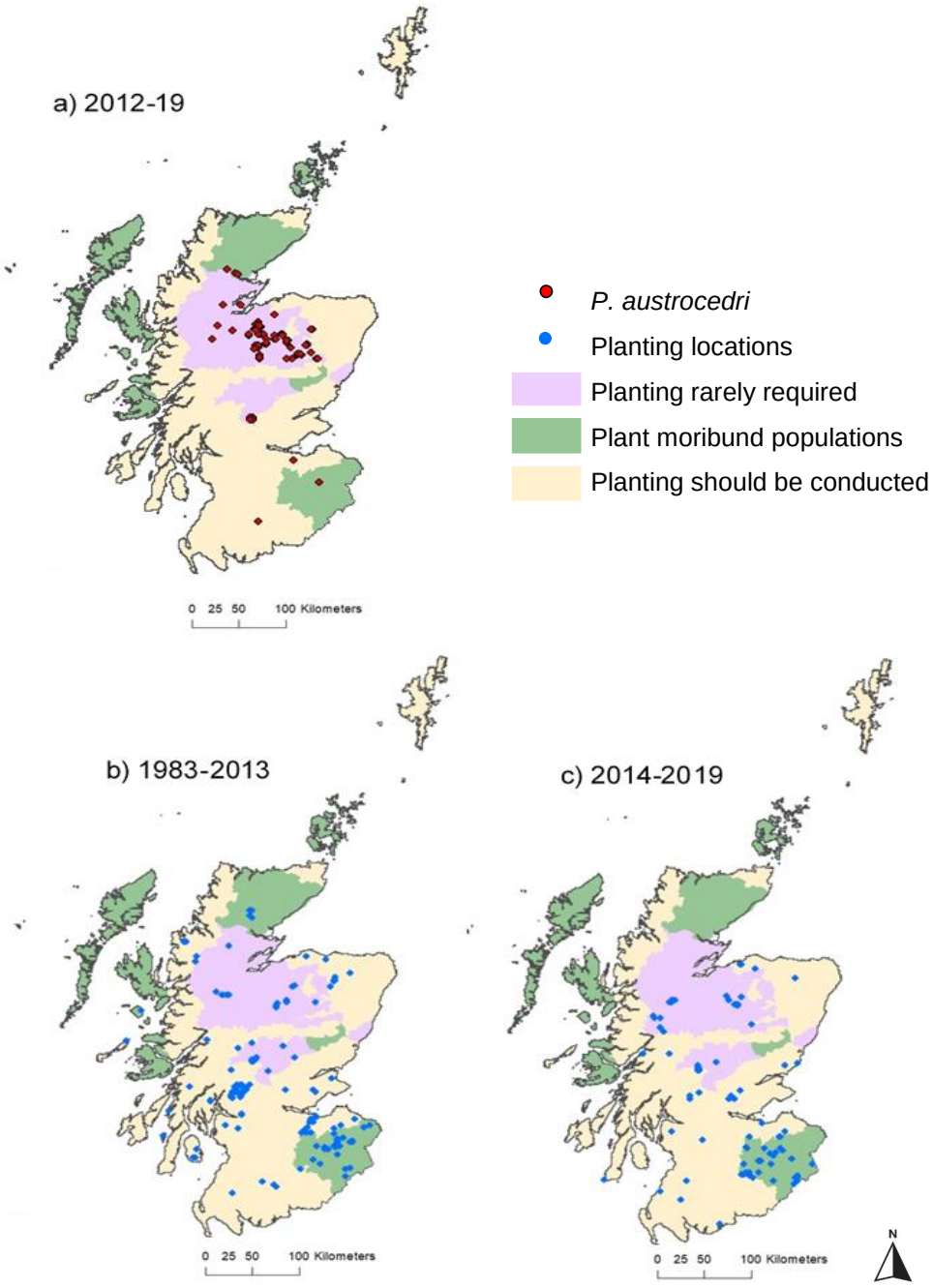

Figure 17. Distribution of tetrads (2x2km cells) across juniper conservation action zones for Scotland (Forestry Commission Scotland, 2013) that specifies different priorities for juniper planting. Maps a–c display tetrads containing (a) positive *P. austrocedri* detections, (b) wider environment juniper planting locations 1983–2013 and (c) planting locations 2014–2019.

4.5 Discussion

Our data show that juniper was introduced by planting to 9% of the species' native range occupied since 1990 at 2km resolution across the UK. We suspect this is an under-estimate as there is currently no requirement to document planting, and projects receiving public funding are not systematically recorded (Cummings, 2021). From the 781 records we could compile from 29 organisations, the number and spatial distribution of juniper planted in the wider environment increased every decade following an initial surge in 1990. Planting was conducted by a range of organisations that accessed different settings to propagate planting material including organisation-specific, commercial, or on-site nurseries, with or without sharing of material between organisations and regions. We discovered that planting occurred close to recorded juniper populations with and without apparent *P. austrocedri* infection, and although there was limited evidence that planting occurred further from absence compared to infected locations, the comparison of median planting distances between the two groups suggested that spatial proximity is not the main risk factor determining the probability that a site is infected. The traceability of planting stock was variable, and too few records were associated with propagation information to allow a nuanced, statistical analysis of settings or procedures that increased the risk of disease introductions. However, 19% of 1km resolution *P. austrocedri* detections occurred within a short distance (500m radius buffer zone) of a previously planted location. Elevated risk factors for infection included increased frequency of planting events and larger planting scheme sizes with highly statistically significant differences detected between countries, managing organisations and stock sources. These findings suggest that supplementary planting bears further scrutiny for all habitat creation or restoration projects because transplanting material is a significant risk pathway for the introduction of disease.

Our results highlight the poor quality and lack of available data as key barriers to assessing the risk of supplementary planting as a pathway for pests and diseases and the overall success of planting schemes as a management tool. In compiling the dataset, we discovered that existing knowledge about the establishment of plantings largely relies on observations made by citizen scientists and the details that individual organisations decide to collect and maintain in relation to their own planting operations. We further illustrated that organisations involved in conservation planting are not limited to small scale projects funded by conservation charities but also include statutory agencies, companies maintaining infrastructure, private landowners, and community groups, and that as many schemes plant hundreds of trees as tens of trees. No disease outbreaks within a 500m radius of planting

carried out by commercial companies, community groups or private individuals were discovered, but these may represent groups least likely to maintain planting records and conduct or report follow-up monitoring. Plantings close to *P. austrocedri* detections included those conducted by statutory agencies and utility companies, but a large number were conducted by conservation charities and wildlife trusts. This highlights the importance of sharing good biosecurity and plant sourcing practices and monitoring with a wide range of organisations, including those in the environmental sector, and analysing further how factors such as sourcing and the size or frequency of planting events are linked to risk. Where specified, most material was sourced from UK native stock and while some projects carefully matched the provenance of source material to the receiving environment, very little juniper was raised in situ, with most material grown up in nurseries of varying size and proximity to the replanting location. While sourcing information was only available for 67% of records found within the 500m buffer zone surrounding *P. austrocedri* outbreaks, a higher percentage of stock used at these locations was recorded as raised in the central organisation or commercial nurseries when compared to absence locations. The association with commercial nurseries is unsurprising given the high incidence and diversity of *Phytophthora* detections in UK nurseries (Hansen, 2015). However, grouping nurseries in these categories is quite artificial, and better insights would be obtained if sufficient information could be collected about nursery practice such as importing plants in the Cupressaceae from international sellers, quarantining material for a year before planting and the irrigation methods used. The absence of *P. austrocedri* detections from Wales, where most of the planting material was sourced from a commercial nursery that only grew juniper collected from Welsh populations and did not trade with any other retailers, may exemplify how good biosecurity can determine the success or failure of restoration projects.

Few studies have investigated the frequency and severity of disease introductions resulting from supplementary planting outside of forestry plantation settings. Accidental *Phytophthora* introductions on planting material used for habitat restoration in three separate locations in California have been documented (Frankel et al., 2020). While the biosecurity measures introduced at donor nurseries to prevent further introductions required significant changes to existing practices, the measures described to remediate sensitive, inaccessible habitats following disease introduction were significantly more onerous, costly, and time-consuming (Frankel et al., 2020). Remediation is also less likely to succeed long term compared to preventing initial introductions (Swiecki and Bernhardt, 2017), which native plant nurseries in California showed can be achieved by implementing biosecurity protocols to maintain *Phytophthora*-free stock (Frankel et al., 2020; Redekar et al., 2019). No method exists to

treat *P. austrocedri* in the wider environment, so, in keeping with many pathogens, management options are limited to actions that can slow spread (Sims et al., 2019; Swiecki and Bernhardt, 2017). The removal of symptomatic trees to reduce pathogen transmission was carried out for six consecutive years at one SSSI designated juniper population, but newly symptomatic trees appeared every year, and work ceased after ~10% of the original population was removed (Furness, M., personal communication, 15th August 2018). The research presented in Chapter 3 found that *P. austrocedri* can disperse several kilometres from its source in fewer than five years, so introducing infected material to new geographical areas risks mortality not only in the receiving but also in any neighbouring populations. However, as Californian case studies demonstrate, the risk associated with supplementary planting depends on the biosecurity practices employed when raising, planting (Redekar et al., 2019; Swiecki and Bernhardt, 2017) and managing populations (Colquhoun and Kerp, 2007b). Hybrid *Phytophthora* species have been detected in nurseries infested with both parents (Leonberger et al., 2012), and introducing material from nurseries where multiple host plants are imported from different origins further increases the likelihood of new strains (Santini et al., 2013). If the disease tolerance detected in two native populations (Green et al., 2021b) is found to be heritable, UK populations may be protected from *P. austrocedri* induced extinction, but this protection could wane with the introduction of new strains or hybrids.

The proliferation of tree and plant health guidance for horticultural (Royal Horticultural Society, 2021), landscaped (Slawson, 2015) and natural environments (Woodland Trust, 2017) in recent years is to be welcomed. However, supplementary juniper planting conducted following publication of the guidance proportionately increased in Scottish zones where it was least recommended (Forestry Commission Scotland, 2013), calling into question if guidance is reaching the intended audiences or aligns with site level priorities of land managers and, in turn, how effectively it is being implemented. In the following chapter, I further explore if and why these publications are not translating to changes in practice by inviting representatives of the user groups identified from the juniper planting dataset to participate in a survey about how risk assessment processes and tools could inform their decision making around planting. Horticultural accreditation schemes, such as the Nursery Industry Accreditation Scheme Australia (2019) and the pilot schemes currently running in California (Frankel et al., 2020) and the UK (Plant Health Alliance Steering Group, 2019), have huge potential to reduce the risk of pest and disease introductions by changing industry practices and allowing customers to make informed choices to source healthy plants, protecting both businesses and natural environments. Sourcing stock from accredited

nurseries could also be used as an eligibility criterion for awards of funding or contracts for projects with a planting component. However, our dataset suggests that a small number of organisations do not routinely access funding or buy in nursery stock, so alternative methods may be required to transfer knowledge and engage these organisations in changing practices to reduce risks. Maintaining uninfected populations with high genetic diversity is likely to be the best recourse against the disease, so reducing risks associated with potential introductory pathways is essential.

Restoration plantings of juniper increased every decade since 1960 but noticeably increased during the 1990s. Planting may have increased during the 1990s following the listing of five Annex 1 habitat types containing juniper under the EEC Habitats Directive (1992) that introduced targets to maintain populations (JNCC, 2007) and early iterations of agri-environment schemes that supported tree planting (Natural England, 2012). Once juniper was listed in all four nations as a priority for biodiversity action (JNCC, 2016), and population surveys showed sharp declines in juniper population extent and condition across the UK (Clifton et al., 1997; Hamilton, 2018; Plantlife, 2015; Borders Forest Trust, 1996; Ward and Shellswell, 2017) planting was actively encouraged via publications (Broome, 2003; Forestry Commission Scotland, 2011; Sullivan, 2003; Wilkins and Duckworth, 2011) and grant support mechanisms (Forestry Commission Scotland, 2009a; Forestry Commission Scotland, 2006). Our dataset suggests that planting projects have had mixed success in addressing restoration aims and that limited follow-up monitoring is being documented. Planting offers a potentially rapid and visible way to re-invigorate moribund populations, particularly where the age or sex distribution of stands is uneven. However, natural regeneration is likely to deliver longer term benefits for population adaptation to climate change as well as novel diseases, and failing populations are often subject to other pressures unlikely to be rectified by planting such as inappropriate grazing regimes, waterlogging, competition with other species and lack of suitable recruitment microsites (Clifton et al., 1997; Cumbria Wildlife Trust, 2014; Ward and Shellswell, 2017). The larger area awarded support payments under the Scottish Forestry Grant Scheme for natural regeneration compared to planting projects suggests this is already being recognised by funding bodies (Cummings, 2021), but expansion of the data collection, monitoring and enforcement capabilities of such schemes are required, as recommended by the Committee on Climate Change (2020). A review of planting schemes could inform thinking about the need for planting as a tool to protect dwindling populations versus its risk as a pathway for the introduction of pests and pathogens. The resulting insights could be used to revise the juniper management guidance (DEFRA, 2017; Forestry Commission Scotland, 2013) with

examples of best practice, appropriate versus inappropriate planting settings and time needed following planting to detect disease symptoms. The finding that the highest percentage of planting events co-occurring with disease outbreaks detected between 2012 and 2016 were conducted in 2000-2009 may indicate a time lag between planting and disease detectability, especially as the initial root infection is difficult to diagnose compared to the foliage discoloration and loss that occurs once the pathogen has migrated into the stem and girdled the phloem with necrotic lesions (Green et al., 2015). If so, the extent of planting conducted 2010-2019 potentially foreshadows many more *P. austrocedri* outbreaks in geographically disparate populations over the coming decade. Though juniper populations planted along coastal fringes of Wales are monitored more routinely than plantings conducted in western Scotland, there is enough active recording to suspect that the lack of pathogen detections in these areas could be limited by shared environmental factors. The collation of this planting dataset will at least enable us to test spatial interactions between planted locations, *P. austrocedri* outbreaks and environmental conditions. However, the traceability of planting material used to restore habitats must be improved to understand better how these environmental relationships interact with planting practices in order to fulfil the UN goals of setting the right incentives and building capacity to ensure sustainable, long term ecosystem restoration (UN, 2020).

Chapter 5

Utility of decision tools for risk assessing plant disease management strategies in natural environments

5.1 Abstract

Increased imports of plants and timber through global trade networks provide frequent opportunities for novel plant pathogen introductions that can cross-over from commercial to natural environments, threatening native species and ecosystem functioning. Prevention or management of such outbreaks relies on a diversity of cross-sectoral stakeholders acting along the invasion pathway. Guidelines relating to specific plant health threats are frequently produced to align biosecurity practices across sectors and spatial scales, but their accessibility and subsequent application is rarely reviewed. We used common juniper (*Juniperus communis*), a UK native species suffering significant mortality from the introduced pathogen *Phytophthora austrocedri*, as a case study to explore how decision tools could be used to assess biosecurity threats. We invited stakeholders who provide advice, grow, manage, or assess juniper to participate in a survey exploring the awareness and utility of host-pathogen distribution maps and a decision framework published within management guidelines produced by a coalition of statutory agencies. Awareness of the decision framework was low across all stakeholder groups. Barriers to the application of decision tools included the inaccessibility of diagnostic and local distribution information. The need to update checklists detailing conditions limiting disease vulnerability and clarify recommendations balancing *P. austrocedri* versus other risks to host populations including lack of regeneration, was clearly articulated. The results demonstrate the need to frame and co-produce decision tools with wide ranging stakeholders, including overlooked groups such as growers and advisory agents, to improve management of plant pathogens.

5.2 Introduction

As the scale and complexity of tree health issues increases, so too does the scope and number of actors involved (Marzano et al., 2016). Almost one fifth of Earth's surface is estimated at risk of plant and animal invasions (IPBES, 2019), with increased numbers of plant pest and pathogen introductions resulting from increased trade in horticultural plants, crops and timber (Brasier, 2008; Chapman et al., 2016). Approximately five new risks are added to the UK plant health risk register every month, of which 30% are identified as capable of infesting or infecting trees (DEFRA, 2018). Many UK tree species are experiencing serious mortality resulting from pathogenic infections. These include ash (*Fraxinus excelsior* L.) killed by the (now endemic) fungus *Hymenoscyphus fraxineus* (T. Kowalski) Baral, Queloz & Hosoya (Forestry Commission, 2020a), larch (*Larix* spp) killed by the oomycete *Phytophthora ramorum* that resulted in the felling of over 18000ha of larch

forests in the UK and Ireland between 2009 and 2016 (O'Hanlon et al., 2018), and elm (*Ulmus* species) more than 30 million of which are estimated to have been killed by the fungus *Ophiostoma novo-ulmi* since its first introduction in the 1960s (Forest Research, 2021a). Collectively, these outbreaks are contributing to serious biodiversity loss (IPBES, 2019) and detrimental changes to ecosystem functioning (Boyd et al., 2013a) with adverse consequences for human health (Maier et al., 2003) and livelihoods (DEFRA, 2018).

Many pests and diseases are introduced and establish as result of anthropogenic behaviours so policy makers rely on the actions of people to prevent or mitigate such invasions, for example through improved biosecurity practices. The success of this depends in some form on the translation of knowledge into practice, which will occur across many different sectors and spatial scales, for example nationwide import restrictions on high-risk host species such as coffee plants as an asymptomatic host for *Xylella fastidiosa* Wells, Raju, Hung, Weisburg, Parl & Beemer or hot-water treating daffodil (*Narcissus* L.) bulbs on a small specialist nursery to prevent the spread of Narcissus eelworm (*Ditylenchus dipsaci* (Kuehn) Filipjev). New information is constantly being compiled by policy makers and researchers about plant health as introductions and distributions of pathogens are tracked, and the risk of newly discovered threats (Spence et al., 2020) or of informative pathogenic traits are assessed (Barwell et al., 2021a). Models are developed to predict areas at increased risk of invasion (Purse, et al., 2013; Václavík, et al., 2010; White, et al., 2017), changes in spread patterns as a result of different management scenarios (Bate et al., 2016; Cunniffe et al., 2016) or changes in climate (Duque-Lazo, et al., 2018; Kleczkowski et al., 2020).

Critical factors determining the translation of research into policy and management actions can be framed in terms of the research credibility, relevance, and legitimacy (CRELE) perceived by stakeholders, of which relevance has the highest importance and can be understood as applicability, comprehensiveness, timing, and accessibility (ACTA) (Dunn and Laing, 2017). Successful tree health management is not solely dependent on growers employing good biosecurity practices but rather relies on a complicated network of cross-sector interactions between suppliers, foresters, landowners and/or land managers, funders, landscape architects, ecologists, contract and project managers, procurement officers, hauliers, machinery contractors, regulators, and inspectors. Individuals or organisations in all these groups can be defined as stakeholders where they can affect and/or are affected by pest or disease outbreaks (after Freeman, 1984). The "stake" they hold will vary depending on their differing abilities to "influence" the introduction, establishment or spread of the

pathogen and their “interest” i.e. capacity to withstand the associated benefits or disbenefits (Dandy et al., 2017). Despite government commitments to engage in cross-sector collaboration with stakeholders (DEFRA, 2018) to solve or mitigate plant health problems, stakeholder involvement is still often only solicited for implementing plant health research or policy (e.g. to institute biosecurity measures or monitor outbreaks) rather than enlisted in earlier stages to frame research questions or policy design (Dandy et al., 2017; Reed, 2008). The diversity of potential pathogen introductory, spread and establishment pathways will vary with the location, scale, and type of landscape being managed, but all are likely subject to some degree of operational constraint relating to time, cost, and expertise (captured as ACTA - timing) that may constitute barriers to the desired implementation if poorly considered during development (Cook et al., 2017). Similarly, if the information is presented in isolation from other considerations valued by stakeholders (e.g. socio-economics) (ACTA – comprehensiveness) or is tailored poorly to the methods stakeholders use to obtain and process it (ACTA – applicability), it is unlikely to reach the intended audience (Dunn and Laing, 2017; Jones and Kleczkowski, 2020). The small number of studies that have explored how plant health research is disseminated to stakeholders (ACTA – accessibility) found academic research is highly trusted but rarely presented in a format accessible to practitioners (Creissen et al., 2019; Marzano et al., 2016) and that stakeholder engagement was more effective when employing interactive or experiential learning (White et al., 2018).

Our prior study of juniper planting events conducted in Scottish juniper conservation zones (Forestry Commission Scotland, 2013) found the guidance was not being followed (Donald et al., 2021), raising questions as to why and how subsequent research outputs on the topic could be more effectively transferred to practitioners. The case study focused on infection of common juniper (*Juniperus communis*) with the introduced pathogen *Phytophthora austrocedri* and found that juniper planting (a potential pathway for disease introduction) was carried out most frequently in the juniper conservation zone where planting was least recommended (Forestry Commission Scotland, 2013). Environmental conditions and management practices supporting growth of native juniper have been the focus of a lot of UK research, disseminated in multiple governmental (DEFRA, 2017; Sullivan, 2003) and charitable reports (Dines and Daniels, 2006; Long and Williams, 2007; Plantlife, 2015; Cumbria Wildlife Trust, 2014; Ward and Shellswell, 2017; Wilkins and Duckworth, 2011). Following discovery of significant population declines (Clifton et al., 1995, 1997; Long and Williams, 2007; McBride, n.d.; Ward, 1994b), considerable effort and expense was exerted over the last thirty years by statutory agencies, conservation charities, utility companies, community groups, national parks and private individuals to conserve juniper populations in

the wider environment (Donald et al., 2021; Plantlife, 2015; Ward and Shellswell, 2017). Despite publications advocating grazing regulation, scrub removal and seed scrapes to stimulate natural regeneration (Broome, 2003; McCartan and Gosling, 2013; Plantlife International, 2007; Forestry Commission Scotland, 2013; Ward and Shellswell, 2017; Wilkins and Duckworth, 2011), new and existing juniper populations in all four nations were planted with cuttings, usually propagated ex-situ in nurseries run by charities, agencies or commercial growers (Donald et al., 2021). Reasons for planting were clearly articulated as attempts to reverse the trend resulting in increasingly small, elderly, and moribund populations and to expand the extent of many native habitats of which juniper is a key component (DEFRA, 2017; Griffiths and McClenaghan, 2010; Forestry Commission Scotland, 2013). Maintaining the extent and quality of juniper populations is also a statutory duty where they are designated as a protected feature of a Site of Special Scientific Interest (SSSI) (see Scottish Natural Heritage (2011) and Natural England (2000) for examples of the associated conservation objectives). As such, some planting projects were funded as part of government assisted woodland (re-)creation schemes, by charities or crowd funding and were carried out within nature reserves, private and publicly owned land (Donald et al., 2021).

However, supplementary planting may increase the risk of introducing *P. austrocedri*, widely detected in UK plant nurseries (Green; et al., 2021; Jung et al., 2016), that could be transported to natural settings in contaminated soil, water or infected host plants (Green et al., 2015; Landa et al., 2021; Riddell et al., 2020). Outbreaks of *P. austrocedri* can lead to severe mortality in juniper populations, as currently observed in northern England and central Scotland (Donald et al., 2020; Green et al., 2015). The pathogen was first identified in the UK in 2011 (Green et al., 2012), was potentially introduced through a trade pathway at least one decade earlier and is yet to be detected in juniper populations in Wales or Northern Ireland (Green et al., 2015). Though historical planting events cannot be directly identified as the source of *P. austrocedri* introductions to the wider environment, the disease was more likely to be present in locations (2x2km grid cells) where planting events were carried out more frequently with larger numbers of trees compared to locations where planting was carried out less frequently (Donald et al., 2021).

Juniper management in the UK is conducted across different sectors including public and private land managers, large and small conservation organisations, independent consultants, commercial growers, gin producers and environmental regulators, all of whom have a vested interest in, and some ability to, maintain disease free populations. Statutory

action is taken to regulate and prevent the movement of *P. austrocedri* between plant nurseries but, in contrast to the related pathogens *P. ramorum* and *P. kernoviae*, no action is taken in the wider environment because land managers currently have no remedial options available to them to eradicate infection (DEFRA, 2017). As a species of conservation importance, removing juniper in anticipation of infection is prohibited and removal following symptom development disturbs potentially infected soil and did not limit pathogen spread within the population where this was trialled (Furness, M., personal communication, 15th August 2018). Infection of Chilean cedar (*Austrocedrus chilensis*) was reduced in adult trees and seedlings with applications of the fungicide fosetyl-Al (Silva et al., 2016) but this remains to be tested on juniper and research into juniper genetic tolerance to the pathogen is only at a preliminary stage (Green et al., 2021b). Actions to limit *P. austrocedri* introductions within and between juniper populations are, therefore, wholly reliant on good biosecurity e.g. use of clean water supplies such as mains or borehole water, or treatment of open water sources to kill pathogens, safe disposal of symptomatic juniper plants in nurseries (requiring burning or composting at high temperatures), washing vehicles to prevent translocation of infected soil between forestry sites, quarantining material before planting out and restricting recreational access in infected areas.

Such measures were first described in guidance issued by Forestry Commission Scotland in 2013 that also presented three zones of differing juniper planting priority based on the extent of the existing populations and their predicted ability to naturally regenerate (Forestry Commission Scotland, 2013). This was followed by juniper management guidelines published by the UK Government Department for Environment, Food and Rural Affairs (DEFRA) in 2017 that aimed to support land managers, conservation organisations and nurseries make sustainable decisions about juniper management and limit the risk of *P. austrocedri* spread (DEFRA, 2017). Instead of planting zones, a decision framework was presented to guide land managers, growers and conservationists through a risk assessment flow chart examining the vulnerability of a particular juniper population to extinction because of its size, structure, site conditions or known presence of *P. austrocedri* (DEFRA, 2017). Only three freely available distribution maps of *P. austrocedri* exist to feed into the risk assessment. Two present a low resolution map of the national distribution in the wider environment, hosted in a Plantlife (2015) report and on the Forest Research website (Forest Research, 2021b), while the third presents the distribution as a freely downloadable shapefile from the UK government website at 10km resolution with limited attribution data and only distinguishing locations as “nursery” or “wider environment” (Forestry Commission, 2020b). We wanted to find out if the DEFRA decision framework is being applied, if parallel

risk assessment processes are employed by different stakeholder types to evaluate risks of juniper management strategies in relation to *P. austrocedri*, and if presenting information via interactive decision tools is useful and/or could be improved to inform dissemination of future modelling results. Using a multi-stakeholder survey and encompassing a range of stakeholder groups across sectors involved in juniper planting, we asked the over-arching question: "*to what extent are decision tools currently used to aid risk assessment of the* P. austrocedri *disease threat in relation to juniper populations and how could they be improved*?"*,* focusing on the DEFRA decision framework and new 1-2km resolution interactive maps showing the current distributions of *P. austrocedri*, native and planted juniper. The survey responses were analysed to recommend updates to both decision tools to improve their applicability.

5.3 Methods

5.3.1 Ethics statement

Participation in the stakeholder survey was entirely voluntary. The first page of the survey described the over-arching aim of the research "*to identify risk factors for* P. austrocedri *infection of UK juniper populations to inform management strategies for juniper conservation*" and the organisations funding the research. Participants were then asked to consent to the ethics statement that outlined the participant's confidentiality, right to withdraw from the survey and request removal of responses. Prior to the thematic analysis, the responses were randomly ordered and all identifying information was removed to ensure themes were analysed without any understanding of the individual, stakeholder type, geographical location, or any other pre-disposing information. Following the thematic analysis, information on the stakeholder type and country was re-introduced to permit analysis within those categories. Illustrative quotes from participants are reported in this study as the random number of the participant in the assigned stakeholder group (e.g. Agent 1).

5.3.2 Conceptual stakeholder categorisation

We restricted survey participation to stakeholders who perform a role connected with juniper management as the target audience for the decision tools. We separated the participants into categories to explore if risk assessments were conducted with a different frequency or if decision tool preferences or barriers to their use differed between stakeholder types (Table 19). Within organisations, stakeholders can take role-specific approaches to risk assessment

that may vary with spatial scale (e.g. local, or national focus) and stage of invasion (e.g. prevention vs adaptive management). As such, we requested that rather than providing answers on behalf of their organisation, participants respond based on their own role, which was used to assign stakeholder type.

Table 19. Description of four stakeholder types involved in risk assessment and decision-making about populations of common juniper in the UK wider environment.

Stakeholder type	Description
Agents	• provide independent (paid) advice • devise management plans • recommend biosecurity practices (e.g. vehicle washing, footpath diversions, sources of disease-free plants) • liaise with stakeholders • are not responsible for implementing management
Assessors	• provide non-commercial management advice e.g. woodland, species, or biodiversity advisers within statutory agencies • perform a regulatory function e.g. comment on planning applications, provide protected area consents for management • conduct monitoring e.g. disease surveillance • evaluate funding applications pertinent to juniper restoration or creation • may advise, recommend, or evaluate biosecurity practices and could make biosecurity conditional for grant or contract awards
Growers	• supply juniper commercially either raising stock themselves or importing plants to sell on • raise and maintain disease-free stock
Managers	• involved in day-to-day management of juniper populations for any purpose e.g. conservation, gin production • could include the landowners themselves, tenants or consultancies who manage land on behalf of the landowner or those who manage ground operations on parts of the public estate • may grow juniper themselves and trade plants but not for a commercial purpose • implement and enforce on-site biosecurity practices e.g. restricting movements between diseased and disease-free zones, quarantining planting stock

Further to this, we were interested if awareness or requirements for decision tools differed between countries in the UK, firstly because the pathogen is only confirmed from the wider environment in Scotland and England, and secondly because the decision framework was published by DEFRA and although they state the guidelines were produced in collaboration with agencies based across the UK (Forest Research), in Scotland (Scottish Government, NatureScot) and Wales (Natural Resources Wales (NRW)) (DEFRA, 2017), DEFRA publications may have limited visibility outside of England.

5.3.3 Survey design

A self-completion questionnaire was designed consisting of 21 open and closed format questions of which 13 were mandatory (Appendix K). The first question asked stakeholders to explain their experience and role to aid identification of the stakeholder type categorisation, followed by two yes/no questions asking if their role involved management of juniper and/or *P. austrocedri* and supplementary juniper planting. The survey was then presented in two main sections: i) six questions pertaining to the awareness and usage of the decision framework found on p.2 of the DEFRA juniper management guidelines (DEFRA, 2017) and ii) nine questions about the sources and utility of spatial information (distribution maps) and three questions about the expected importance of potential infection risk factors. Two, UK-wide, interactive maps were presented in this section. The first map displayed the distributions of native juniper (1990-2020) and positive detections of *P. austrocedri* at 2km and 1km resolution respectively, while the second overlaid this map with 2km resolution juniper planting events conducted 1960-1979, 1980-1999, 2000-2009 or 2010-2020. The maps were created in R v.3.6.2. (R Core Team, 2019) using the datasets compiled in Donald et al. (2021) and presented as an R Shiny app (Chang et al., 2021) using the leaflet package (Cheng et al., 2021) that allowed participants to zoom in on locations of interest against a simple topographic backdrop. The app can be accessed online at https://floradonald-juniper-planting-2020.shinyapps.io/Planting2/ and the maps are reproduced in Appendix J. Stakeholders were asked to pick five of thirteen abiotic, and five of eight biotic, proposed risk factors and to rank them according to importance (w, 5=most important, 1=least important). The perceived importance of potential infection risk factors was then calculated as a weighted mean ($\sum \mathrm{nw} / \sum \mathrm{w}$), where n is the number of times the predictor was selected.

A mixed approach to stakeholder analysis was conducted whereby the authors pooled knowledge of actors associated with juniper in any capacity, from any sector, based in any of the devolved nations. This included actors who retained privileged information and with whom the authors had previously sought advice, data, or access to populations in relation to juniper research, as well as participants present at juniper or tree health group meetings, conferences, or workshops, who had contributed to discussions on juniper management themes, and could, therefore, provide relevant responses to the survey. The survey was distributed by email to named individuals, initially to a pilot sample of 13 stakeholders to ensure the questions elicited responses targeting the areas of interest, which was evident from the three responses received. The survey was then sent to 58 additional recipients who were requested to complete the survey within a two-week period in October 2020.

Recipients were asked to suggest contacts in their network involved in "*managing, growing, advising, surveying or making decisions about juniper populations*" who might be interested in participating. Recipients were asked to provide these details using the survey form to maintain the anonymity of other respondents approached and prevent individuals being bombarded with repeated requests, but seven individuals directly forwarded the survey to their network. Eighteen individuals were identified by recipients as key stakeholders who could be invited to participate in the survey, twelve of which had already been sent requests lending confidence that our stakeholder mapping identified many of the influential actors. In total, we distributed the survey to 109 individuals (not including those forwarded by recipients) and received 41 completed surveys. Despite the small sample size we believe it is defensible to present the results because the stakeholder mapping exercise was thorough and suggests a response rate of 38%, comparable with other studies in forestry with a broader remit (see Marzano et al. (2016) for examples).

A short section at the end of the survey asked participants to provide their job title and a description of their role or specialisation. This information was used to assign their responses to a stakeholder type (agent, assessor, grower, manager) (Table 20). Participants were well distributed across categories, with growers constituting the smallest (15%), and managers the largest (37%), percentage of responses. Participants represented a similar percentage of the number of recipients contacted per stakeholder type (32% assessors, 33% managers and 39% agents) except for growers who were over-represented (60%). Responses were obtained from participants based in all four UK nations, but Scottish participants were under-represented relative to the proportion of the estimated area of juniper and *P. austrocedri* found in the country (Table 20).

Table 20. Number and percentage (in brackets) of stakeholder responses received according to stakeholder type and UK country. The percentage of tetrads (2x2km cells) containing juniper and positive *P. austrocedri* detections are also shown per UK country.

Stakeholder category		Number of respondents (n = 41)
Type	Agents	11 (27%)
	Assessors	9 (22%)
	Growers	6 (15%)
	Managers	15 (37%)
Country	Scotland (69% juniper, 70% *P. austrocedri*	17 (41%)
	England (26% juniper, 30% *P. austrocedri*)	17 (41%)
	Wales (3% juniper, 0% *P. austrocedri*)	6 (15%)
	Northern Ireland (1% juniper, 0% *P. austrocedri*)	1 (2%)

Questions that addressed the main subject areas in the survey were grouped together and the corresponding responses were analysed using an open, line-by-line coding strategy where keywords or important phrases were identified and organised into clusters with shared meaning (Braun and Clarke, 2006). Theme frequencies were explored and presented as the number and percentage of responses in total and/or according to stakeholder type or country. Statistical differences in responses between stakeholder types or countries were assessed using Fisher's exact test and the resulting p-values were adjusted using a Holm-Bonferroni method to control for multiple comparisons. Both tests were implemented using the stats package in R v.3.6.2 (R Core Team, 2019). Finally, these quantitative findings were combined with further distillation of the keyword clusters to identify four main themes and ten sub-themes (Table 21.).

Table 21. Summary of main and sub-themes identified from all the survey responses.

Main theme	Sub-themes
Low awareness of the DEFRA juniper management guidelines	Low awareness across all stakeholder types and those actively involved in juniper planting
Shared desire to assess the risks associated with management actions	Risk assessments were routinely carried out prior to supplementary planting
	Both the decision framework and maps were identified as useful tools to aid risk assessment and decision-making
	Checklists for juniper site-level suitability and vulnerability were highly rated
	Opposing views existed about the utility vs. risk of supplementary planting for juniper conservation but planting was ranked as a highly important disease risk
Decision tools currently lack the detail required for application	Perception that pathogen diagnostic and local distribution data were inaccessible
	Decision framework recommendations were described as ambiguous and complicated
	Disagreement emerged over the intended purpose of the decision framework – planting vs. alternative management

5.4 Results

5.4.1 Low awareness of the DEFRA decision framework

Three years following its publication, stakeholder awareness of the decision framework on p.2 of the DEFRA juniper management guidelines (DEFRA, 2017) was very low, with 71% survey participants reporting that they did not use it (Table 22.). Sixty-five percent of participants explicitly stated they were unaware of the guidelines:

> *"I was unaware of it* [the DEFRA guidelines], *despite having done a reasonable amount of reading on the subject*." (Grower 2).

Awareness was poor across all countries and stakeholder groups. Participants based in England appeared to show higher awareness of the decision framework (47%) compared to respondents based in Scotland, Wales, and Northern Ireland (<20%), as did assessors (56%) compared to managers (40%), agents (9%) and growers (0%) (Table 22.). However, these differences were not statistically significant (Holm Bonferroni corrected p-values = 0.25 between countries and 0.24 between stakeholder types). Twenty-three participants (56%) were involved in planting juniper. Of these, 70% (16/23) did not access the guidelines and presumably conducted planting without reference to the decision framework (Table 22., Figure 18).

Table 22. Number and percentage (%) of participants per stakeholder type, and in total (n=41) who do or do not plant juniper, with or without reference to the DEFRA decision framework (DEFRA, 2017).

Stakeholder type	Planting		No planting		Planting total	DEFRA framework total
	DEFRA framework	No DEFRA framework	DEFRA framework	No DEFRA framework		
Agent	1 (9%)	6 (55%)	0 (0%)	4 (36%)	7 (64%)	1 (9%)
Assessor	3 (33%)	1 (11%)	2 (22%)	3 (33%)	4 (44%)	5 (56%)
Grower	0 (0%)	3 (50%)	0 (0%)	3 (50%)	3 (50%)	0 (0%)
Manager	3 (20%)	6 (40%)	3 (20%)	3 (20%)	9 (60%)	6 (40%)
Totals	7 (17%)	16 (39%)	5 (12%)	13 (32%)	23 (56%)	12 (29%)

Lack of awareness of the decision framework contents could be inferred for the remaining participants who cited lack of involvement in juniper planting (13%) or conducting planting prior to the framework publication (10%) as reasons for not using the framework, suggesting they understood the guidelines to only reference planting decisions. Two participants

involved in planting identified that the decision tree was not user friendly (3%) or did not contain the specific information they needed (3%). Manager 13 stated they did not use the decision framework because:

> "*There were no infected areas known either in collection site or planting areas*",

suggesting they believed the guidelines were only relevant to locations where the disease is present. There was no awareness of the decision framework among participants who stated their role involved collecting or raising stock for planting or habitat restoration, ex-situ conservation, planting advice or outreach, and no awareness in large percentages of those managing (67%) or offering advice (72%) about existing juniper populations or involved in woodland creation (60%) (Figure 18).

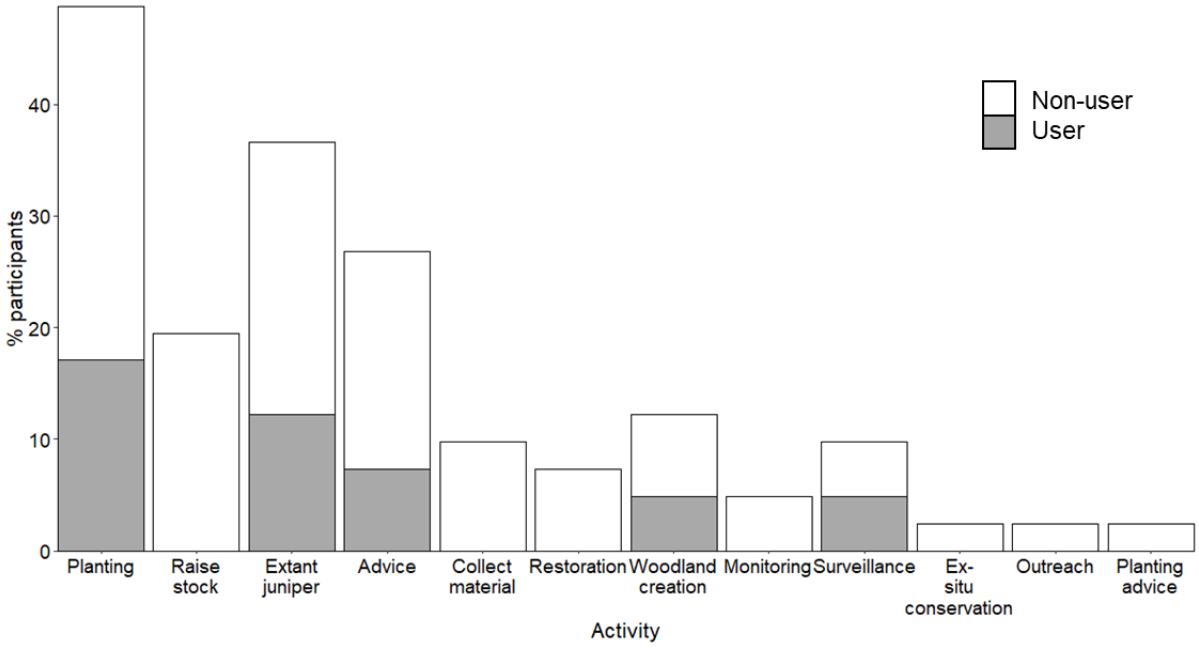

Figure 18. Activities conducted by survey participants when describing their current role showing the percentage of participants who used (grey bars), and did not use (white bars), the decision framework, in order of the % non-users. General "advice" about juniper was categorised separately from responses that detailed specific delivery of "planting advice", "monitoring" existing juniper populations was categorised as distinct from plant pest or pathogen monitoring defined as "surveillance" and management of existing "extant juniper" populations was distinguished from "ex-situ conservation" of juniper.

5.4.2 Utility of the decision tools for risk assessment

Ninety-five percent of participants proposed at least one use for the decision tools applicable to their role in managing juniper, exhibiting a strong preference for provision of both the decision framework and interactive maps (61%) compared to the maps (22%) or decision framework (12%) alone (Appendix L). Both positive and negative feedback was obtained from participants who had not previously encountered the decision framework:

> "*I wouldn't consider planting juniper unless I had gone through a similar process of risk assessment to this decision tree."* (Grower 6), versus

> "*It is an extra layer to management decisions which can make it a diversion. Ignores experience*." (Agent 1).

When asked to identify the most useful sections of the decision framework (irrespective of current use) 22% of participants said all of it was useful but 17% specifically identified the juniper site suitability checklist (Table 23.), writing for example:

> "*Is the site suitable to that species. After this can we control human and environmental impacts on the site."* (Manager 3),

and 12% referred to the checklist that assesses the vulnerability of juniper populations by virtue of their size and potential for natural regeneration (Table 23.):

> "*The levels of vulnerability are useful to consider how best to deal with existing populations, they give cause to stop and think.*" (Grower 2).

Three participants (7%) noted the decision framework was useful to provide an architecture for risk assessment (i.e., the process is intrinsically useful) and three (7%) suggested they would use it to assess the need or potential longevity of planting (Table 23.). Agent 6 noted that the decision framework raised their awareness of biosecurity:

> "*I haven't in the past considered too strongly biosecurity issues but would do so now*."

The scale (national, regional, or local) of map preferred by participants depended on their geographical remit but most requested local maps (39%) or local maps that could be contextualised by national scale maps (27%) (Appendix L). The most popular uses of

interactive maps were to assess the risk of *P. austrocedri* infection (27%), to inform management decisions (15%), assess the site suitability for supplementary planting (12%) or to choose a source of donor material (10%) (Table 23.), as illustrated by Manager 13:

> "*To decide on collection area for juniper that had similar environmental conditions as there were no sites in the same planting zone*.".

The primary reasons to keep maps updated over time as the invasion progresses were to inform management decisions (34%), contain disease (12%) and aid risk assessment (10%) (Table 23.).

Table 23. Themes identified from survey responses (n=41) that addressed the utility of the decision tools examined i.e., the decision framework and the interactive maps of *P. austrocedri*, native and planted juniper distributions showing the number (n) and percentage (in brackets) of survey participants whose responses addressed sub-themes.

Theme	Sub-theme	n
Most useful parts of the decision tree	all of it	9 (22%)
	site suitability checklist	7 (17%)
	site vulnerability checklist	5 (12%)
	as a framework for risk assessment	3 (7%)
	assess need for planting	2 (5%)
	assess longevity of planting	1 (2%)
Uses for interactive maps	assess infection risk	11 (27%)
	inform management decisions	6 (15%)
	assess planting suitability	5 (12%)
	sourcing decisions	4 (10%)
	early disease detection	1 (2%)
	raise awareness of nursery biosecurity	1 (2%)
	monitor losses	1 (2%)
Reasons to keep maps updated	plan management	14 (34%)
	contain disease	5 (12%)
	risk assessments	4 (10%)
	track sources of infection / target monitoring	4 (10%)
	evidence for funding applications	1 (2%)
	save clients money	1 (2%)

Assessor 5 thought the maps would help raise awareness of the need for good biosecurity in plant nurseries (perhaps specifically referring to the visualisation of *P. austrocedri* in locations subject to planting). Manager 1 already used maps to monitor juniper population losses and Agent 3 thought maps would aid earlier disease detection (Table 23.). These

points were reinforced by 10% of participants who cited the ability to track sources of infection and target disease surveillance as reasons to maintain accurate distribution maps (Table 23.), exemplified by Manager 9:

> "*If we knew there was another outbreak in the locality, we would step up the rate of inspections*."

Finally, the financial benefits of accurate distribution maps were discussed by Agent 4 as "good evidence" to support grant applications, and by Manager 14 who identified planting juniper in infected areas would *"result in more expenditure to the client*."

5.3.3 Stakeholder perceptions of *P. austrocedri* risk factors

When participants were asked to rank abiotic and biotic factors most likely to drive outbreaks of *P. austrocedri*, four (10%) highlighted that their responses were based on more limited knowledge of the infection or juniper:

> "*having no first hand experience of the infection or juniper sites, they are more like educated guesses!"* (Agent 7).

Though all the proposed risk factors were selected at least once, a consensus emerged that water availability – characterised as rainfall, soil moisture or surface runoff – would be the most important abiotic risk factor (Figure 19). Juniper planting was the most important biotic risk factor after juniper presence, followed by recreation and livestock density (Figure 19). Additional factors mentioned in responses revealed considerable awareness that land management practices may inadvertently promote pathogen spread, including long distance movements of people, vehicles and livestock, horse-riding, and forestry activities, in addition to asymptomatic host species and climate change.

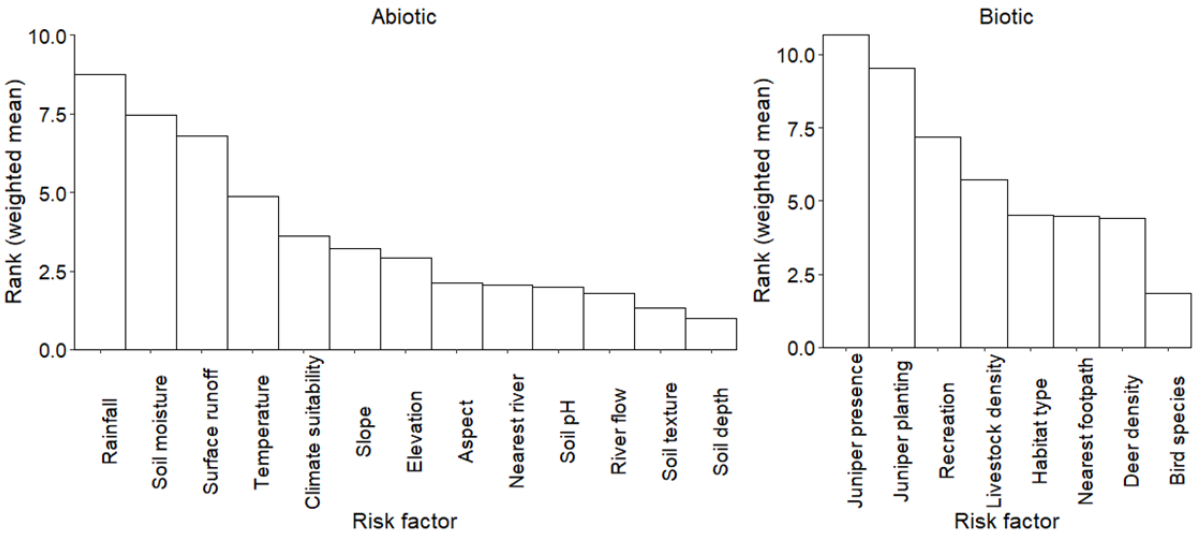

Figure 19. Predicted rank importance of abiotic (L) and biotic (R) risk factors proposed to drive *P. austrocedri* outbreaks in UK juniper populations.

Opposing views emerged concerning the necessity to plant juniper to safeguard populations versus the risk of inadvertently introducing *P. austrocedri* on supplementary material, as illustrated by these two opposite positions:

> *"I believe that most, if not all, tree nurseries are contaminated with* Phytophthora… *A planting scheme close to a juniper site could still spread* P. austrocedri *even if juniper was not planted. Advice on wider planting schemes may be necessary."* (Assessor 5).

> *"It* [the decision framework] *may lead to suitable sites not being planted with juniper due to potential risks and possibly the long term decline in juniper populations across the areas that are most suitable for juniper scrub."* (Manager 11).

The second view was expressed by three participants who wrote that the decision tree could lead to risk averse decisions resulting in worse outcomes for juniper because populations were not naturally regenerating so planting was necessary, or because the guidelines ruled out too large an area as unsuitable for planting, or the complexity of the decision framework resulted in management inaction. It was well acknowledged, however, that planting could pose a significant introductory risk for *P. austrocedri*. A similar percentage (~60%) of participants who did and did not plant juniper ranked "juniper planting" as the first or second most important biotic risk factor for disease. No statistically significant differences were

found between the importance rankings attributed to juniper planting between stakeholder types (Appendix L1) and only weak differences (Holm-Bonferroni corrected p=0.021) were detected between countries with 80% of stakeholders based in England ranking planting as a top two biotic risk factor, followed by 59% of participants based in Scotland and 33% in Wales.

5.4.4 Lack of detail hinders decision tool application

Twelve barriers to using the decision framework were identified from the responses, half of which were described by ≥10% of participants (Table 24.).

Table 24. Number (n=41) and percentage (in brackets) of participants who identified similar themes as barriers to using the decision framework with an example quote summarising the theme.

Barrier	n	Exemplar quote
lack of diagnostic information	5 (12%)	*"I do not know what the signs are of the juniper disease."* (Manager 14)
inappropriate planting scenarios are not made explicit	5 (12%)	*"It's clear in the red boxes that planting is not recommended, but not clear at boxes 4 and 5. Should they have red outlines, or is there ambiguity in advice here?"* (Manager 7)
uncertain where to seek expert advice	5 (12%)	*"Seek expert advice (not sure who to contact)"* (Agent 2)
infection "proximity" is poorly defined	5 (12%)	*"Unfortunately there are no parameters for "proximity of any known juniper infection" … and no guidance about how far from infected juniper is safe to plant."* (Assessor 6)
unclear definition of "water catchment"	4 (10%)	*"at 2 does river catchment area mean the entire catchment? … It's a big area to rule out planting anywhere."* (Manager 10)
insufficient detail to assess site suitability	4 (10%)	*"It would be useful to include a quick reference for suitable ranges for each factor that needs to be assessed for suitability."* (Manager 9)
local disease distribution information is inaccessible	3 (7%)	*"Forest Research map of confirmed locations are insufficiently detailed to confirm whether* P. austrocedri *is in a catchment"* (Agent 2)
ambiguous recommendations	3 (7%)	*"I think I need to be talked through the decision tree to really understand the final recommendations."* (Assessor 3)
biosecurity actions are not clearly articulated	2 (5%)	*"worth pointing people towards what "high-risk biosecurity" measures involve? I don't think this is spelled out in the guidance document itself."* (Assessor 4)
no advice about sourcing of planting material	2 (5%)	*"this document completely misses out a section on verification and disease risk reduction in seed collecting and suitability of potential planting stock."* (Grower 4)
recommendations contradict protected area aims	1 (2%)	*"The decision tree does not quite reflect the position of the SAC designation. Although we have a large population the age structure means we have a high proportion of old juniper with little viable seed germination, therefore planting is undertaken."* (Manager 2)
no emphasis on population sustainability requiring both male and female trees	1 (2%)	*"It might be useful to explain that juniper is dioecious, and therefore it will be important to make sure that both sexes are present, and only look for seeds on female trees."* (Assessor 8)

One manager wrote they were unaware of *P. austrocedri* while two agents conflated risk factors for *P. ramorum* (rhododendron (Purse et al., 2013) and prevailing winds (Rizzo et al., 2005)) with *P. austrocedri*, demonstrating a lack of pathogen specific knowledge. Awareness of the pathogen could otherwise be assumed but a lack of knowledge about the disease identification and distribution, biosecurity measures and sourcing considerations to limit spread, and where to seek advice were described as problems throughout the survey (Table 24.). The lack of detail relating to "safe" distances from the nearest *P. austrocedri* outbreak, microsite conditions preferred by juniper, the need for male and female trees to stimulate natural regeneration and lack of information about biosecurity considerations when sourcing planting material were also identified as omissions limiting framework implementation (Table 24.). Feedback from several participants also suggested recommendations within the framework were not presented in a user-friendly way, were complicated, ambiguous, or too discretionary:

> *"The questions are open to interpretation and professional judgement."* (Assessor 2).

Agent 6 commented that the framework omitted important information about the need for male and female trees and genetic diversity to establish successful juniper populations, remarking:

> *"I know it is meant to cover biosecurity issues mainly but there is a danger that people may use it as the main/only source of decision advice*.".

Not only does this quote harbour concern about the potential negative consequences of applying the recommendations, it also offers insight into the perceived purpose of the guidance. Manager 9 also indicated they thought the purpose of the guidelines was to provide information about biosecurity:

> "*There is a lot of information within the decision tree that does not relate to planting – it is more about an overall management approach for* P. austrocedri",

and presented:

> *"clear guidance that planting should not be undertaken on sites where* P. austrocedri *is present."*,

which Assessor 8 appeared to use the framework to implement:

> *"Mostly I find it useful for helping people through the process of accepting that they might not need to plant, even though they really want to"*.

By contrast, Assessors 5 and 6 suggested planting was not discouraged strongly enough:

> "*The tree … does not explicitly oppose planting. The boxes also mention grant-aid, which suggests that planting is acceptable. If planting risks bringing in* Phytophthora *to a juniper site then perhaps no juniper should be planted in any existing juniper site?*" (Assessor 5).

If the extent to which the decision framework aims to discourage planting was unclear, evidence provided by the 12 current users shows a large proportion of the existing audience used it to assess the risk of planting as a management tool (50%) but a low percentage to actively conduct planting (17%) compared to those using it for knowledge exchange (33%), to raise awareness about biosecurity (25%) and/or find planting alternatives (25%) (Figure 20).

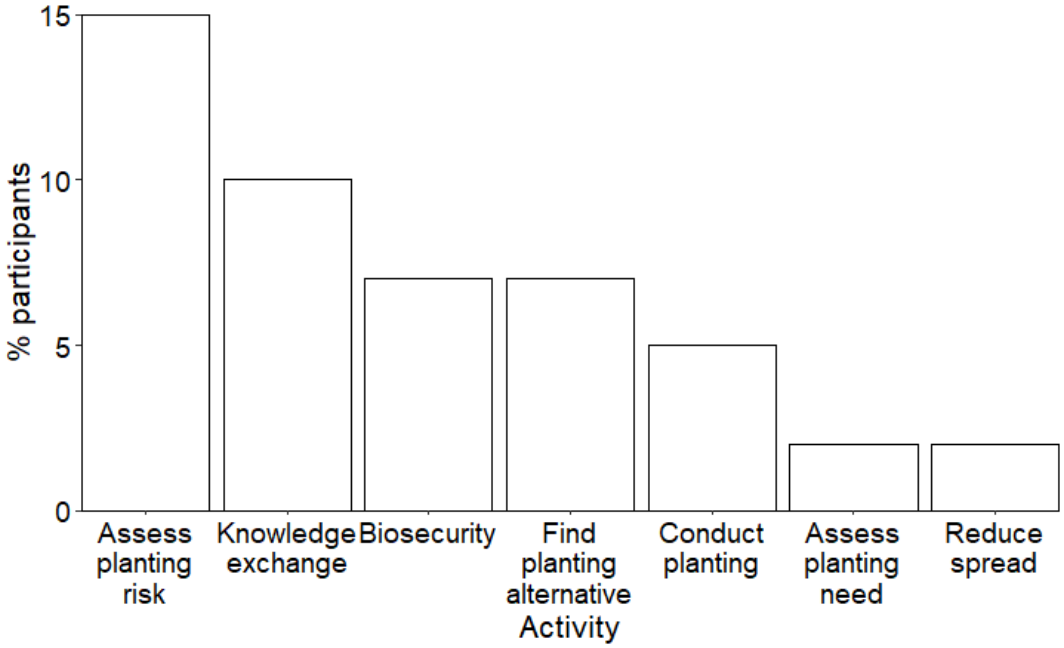

Figure 20. Reasons stated for using the decision framework in the juniper management guidelines (DEFRA, 2017) shown as the percentage of participants (n=41).

Information gaps identified as priorities for decision tool updates can be understood from the list of barriers to their use (Table 24.), and broadly summarised as the need for detailed locations of positive disease detections, clarification of the decision framework

recommendations (including examples of unsuitable planting scenarios, planting alternatives and biosecurity practices), and provision of key advisory contacts. Manager 9 suggested:

> *"Perhaps decisions on management other than whether to plant could be separated into a separate decision tree?"*.

To understand how awareness of the decision tools could be raised, participants were asked to identify sources of juniper management information they currently access. A handful of sources were accessed by small numbers of participants, comprising a combination of private and publicly accessible resources, showing no single repository is used to access information about juniper or *P. austrocedri* (Appendix L). Collating juniper planting records from publicly or charitably funded grants for habitat restoration (17% responses) and citizen science recording initiatives (10%) were the most popular methods cited to collect more information about both planting and disease locations. Ten percent of participants recommended statutory action to enforce planting regulation, either via licensing (5%) or mandatory documentation:

> "*Make it an obligation for all new plantations of juniper to be recorded (as we should be doing with all tree species!) … when management and grant applications are approved by those organisations*." (Assessor 6), and

> "*No planting allowed unless decision tree gone through and location logged*." (Assessor 3).

Preferred locations to host decision tools included websites already used by participants to source information (9%) (Appendix L) or existing governmental land management mapping software (12%) with additional functionality to allow users to directly upload data via a web interface or app (15%). Participants stated map provision would support rather than replace site visits unless *P. austrocedri* presence was shown at the specified location (71%). However, the time-consuming nature and cost-benefit imbalance of maintaining highly accurate distribution maps, potential complacency resulting from outdated or coarse-scale information and the need for funding continuity that is often hard to obtain for ongoing data collection projects, were highlighted as disadvantages to providing interactive maps. Concern was also raised that maps would have limited use unless widespread testing for *P. austrocedri* is undertaken, and multiple organisations work together to contain spread.

5.5 Discussion

This study is among the first investigations of how decision tools are used to implement management to address plant health threats (Marzano et al., 2015) and if they could be used to greater effect to limit outbreaks in wider environment contexts (Figure 21). Juniper is in an interesting case study with which to explore dissemination of plant health management advice because it is grown in the wider environment for a mixture of conservation (native species with high biodiversity value) and commercial (habitat creation and gin production) purposes (Figure 21). Responses to the survey revealed that stakeholders accessing the decision framework in the DEFRA juniper management guidelines (DEFRA, 2017) did so to raise awareness of the pathogen and implement management posing a lower disease risk. Furthermore, 95% of stakeholders proposed ways in which the decision tools would usefully inform risk assessment and decision-making within their role if significant barriers to implementation could be addressed. The results repeatedly highlighted that these barriers could be overcome by co-producing plant health policies and decision tools with stakeholders, as outlined below.

Awareness of the decision framework was overall very low (29% of 41 participants), across all stakeholder types and even among those who plant juniper (30%). This may result from stakeholders lacking time to search for information (Marzano et al., 2016) or a perceived lack of risk (Breukers et al., 2009) but some participants indicated they have searched for biosecurity information and not found the guidelines. There were also strong pre-conceptions that the guidelines were only applicable to juniper populations already subject to disease or supplementary planting. Perceived risks of plant pathogens are lower in areas with no known outbreaks (Pollard et al., 2021), which could explain the lower guideline awareness in Wales and Northern Ireland where *P. austrocedri* is thought to be absent (Green et al., 2015). Yet awareness was also low in Scotland where sizeable juniper populations are already severely infected (Donald et al., 2020). It is more likely that the guidance was overlooked because it was published by DEFRA who only operate within England, even though the guidelines were developed with input from agencies based across the UK, in Scotland and in Wales (DEFRA, 2017).

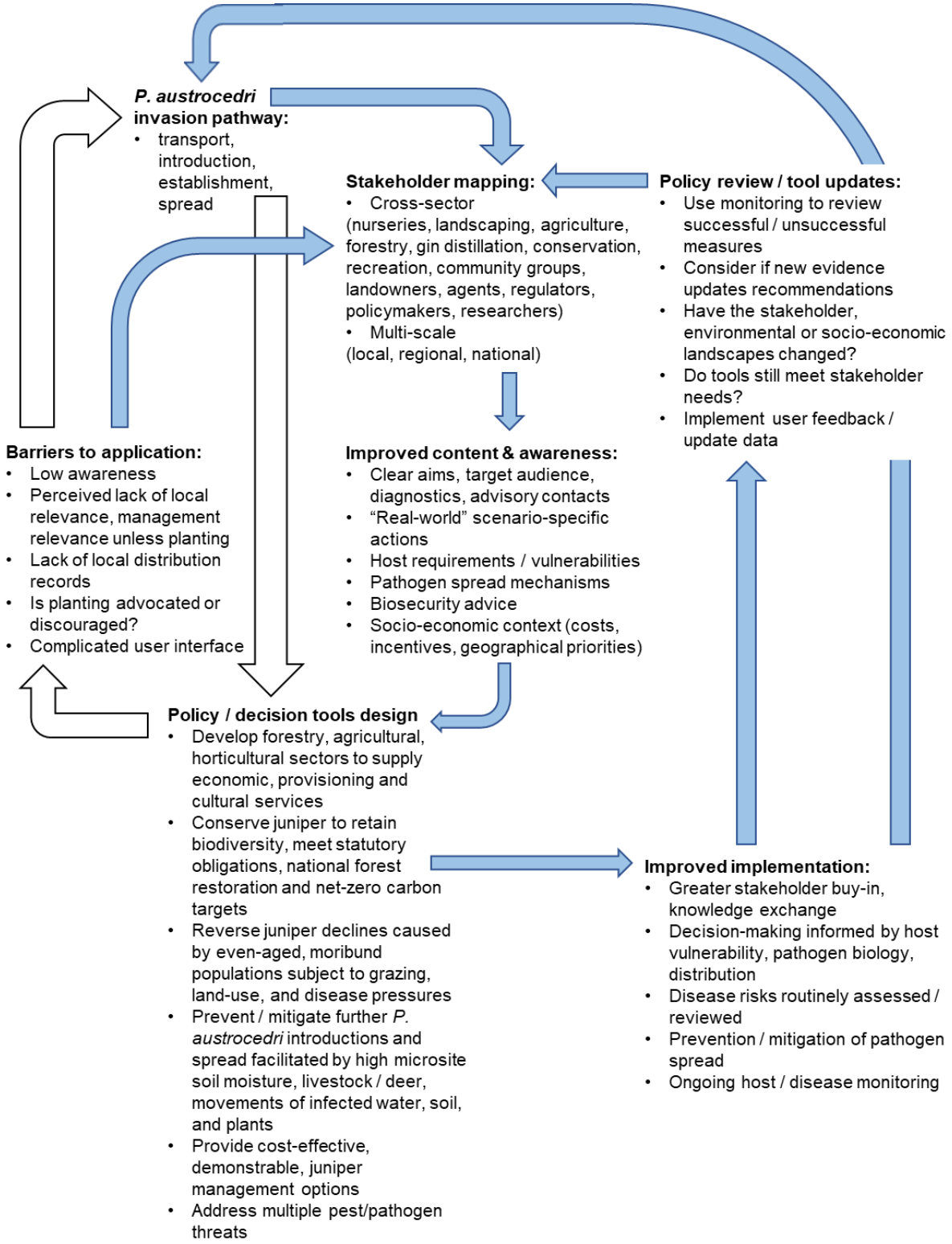

Figure 21. Flow chart created by the authors outlining the potential benefits associated with co-producing policy/decision tools with stakeholders using specific examples from our case study of *P. austrocedri* infection of wider environment juniper populations. Designing policy without stakeholder engagement (white arrows) may lead to application barriers and increase plant pathogen transport, introduction, establishment and spread risks compared to co-producing policies/decision tools (blue arrows) to identify barriers and improve content, awareness, and implementation. Engagement may be iterative, requiring several reviews with or without revised stakeholder mapping and may reduce rates of infection if not prevent new disease outbreaks (Colquhoun and Kerp, 2007a; Creissen et al., 2019).

These findings all highlight the current inaccessibility of the guidelines to stakeholders based in different sectors and geographical areas. Co-producing revised guidelines with stakeholders could address many of these barriers. The first step would be to broaden the existing stakeholder mapping to understand the distribution of stakeholders in different sectors, geographical locations, and stages along the invasion pathway. Inviting representatives from each category to co-produce decision tools allows further exploration and exploitation of their knowledge exchange networks and will inform where the tools could be hosted to aid accessibility as defined by the ACTA framework. In the survey, agents and growers were the least likely to know of and access the juniper guidelines in future, which is concerning given their pivotal role in advising on and implementing good biosecurity. Agents and growers have both been identified as performing key networking roles in plant health, with growers accessing a particularly wide range of information sources (including conferences, workshops, professional magazines, social media and other growers) to facilitate knowledge exchange and agents trusted to disseminate accurate information (e.g. research papers) leading to good plant health decision making (Breukers et al., 2009; Creissen et al., 2019). Milne et al. (2020) modelled control of citrus huanglongbing disease and predicted the probability of successful control would increase with increasing contact between stakeholders and advisers and that informing stakeholders of control effectiveness changed behaviours more than increasing their perception of infection risk. Increasing the representation of agents and growers to co-produce plant health policy and tools could, therefore, improve their accessibility.

Co-producing tools with a diversity of stakeholders will also improve their relevance (CRELE), comprehensiveness and applicability (ACTA), as demonstrated by the survey responses. Participants identified multiple ways to improve the applicability of the decision framework and maps to their work, many of which pertained to juniper planting as a conservation action. Over half (56%) of participants were involved with supplementary planting, which is unsurprising given the large increase in number and geographical distribution of juniper planting events conducted in the UK since the 1990s (Donald et al., 2021). However, supplementary planting is a risk factor for *P. austrocedri* introduction and spread (Donald et al., 2021). The survey identified a lack of shared understanding about the importance of disease between assessors (who were most concerned) and growers (who were least concerned) about juniper planting as a potential disease risk pathway. Further consultation is required to understand if this results from a trade-off between the risk and reward of planting in different sectors, the severity of the observed effects, or lack of information flow back to growers following disease detections at planted locations.

Nevertheless, 63% of participants believed planting was a serious biotic risk factor for introducing disease and 12% identified lack of clarity over scenarios where planting is ill-advised as a barrier to using the decision framework. Stakeholders in favour of planting believed no intervention posed a greater risk to juniper population collapse than *P. austrocedri*. This is highly questionable given the rates of juniper mortality observed within a decade across populations situated in Perthshire and the Lake District (Green et al., 2015) and observable juniper regeneration in populations with lower management intensity (Broome and Holl, 2017). Further triangulation of views between stakeholders is needed to understand why planting is so prevalent compared to management encouraging natural regeneration, and to understand if it is effective, as very few juniper planting records contained information about follow up monitoring (Donald et al., 2021) and the effectiveness of phytosanitary measures is poorly evidenced in general (Marzano 2016). This dialogue is an urgent priority to improve the clarity of planting guidance (ACTA - applicability), counter misleading arguments with evidence-based case studies (ACTA - comprehensiveness) and minimise the risk of planting as a pathway for *P. austrocedri* introduction and spread while uninfected populations remain (ACTA - timing).

A related barrier to decision framework applicability was a perceived lack of clarity about what constitutes good biosecurity: a prevalent view among environmental managers (Dunn et al., 2021). Recommended biosecurity practices to implement when collecting and raising juniper cuttings or seed are given in the main text of the juniper management guidelines that could be better signposted to within the decision framework (DEFRA, 2017). Advice relating to accreditation schemes such as the “Plant Healthy” Certification Scheme (Plant Health Alliance Steering Group, 2019) could also be added. Plant Healthy aims to certify a minimum standard for biosecurity and stakeholders have indicated they may use it to decide where to source planting scheme material, believing that the certification signals a nursery’s commitment to biosecurity (Dunn et al., 2021). Crucially for juniper, however, Plant Healthy does not specify material must be UK-grown and is consequently not endorsed by conservation charities including the Woodland Trust (Woodland Trust, 2017). Juniper is genetically diverse and adapted to local conditions so using material with local provenance is advised (Broome, 2003; DEFRA, 2017; Forestry Commission Scotland, 2013), and very little of the current native juniper planting stock appears to be internationally imported or ex-imported (Donald et al., 2021) so, should planting continue to be advocated, the limitations of certification need to be shared with stakeholders.

Additional barriers to decision framework usage were the lack of *P. austrocedri* diagnostic information and details required to assess key parameters such as distances to the nearest outbreak and the definition of a water catchment. Links to diagnostic information and where to report symptoms are provided in the guidelines (DEFRA, 2017) but in-person training events may improve confidence and disease identification skills more effectively. In chapter two I found *P. austrocedri* infection severity increased in microsites with high soil moisture or close to watercourses, also associated with infection of Chilean cedar (La Manna et al., 2008b), and in chapter three I determined dispersal primarily occurs within 500m of the nearest infected juniper. These details could be used to clarify guidance in the decision framework but a focus on "safe distances" to carry out actions such as planting may reduce risks of pathogen introduction and spread less successfully than emphasising the evaluation and reduction of site-specific risk pathways. Such pathways include the movement of infected water and soil on vehicles or footwear, along livestock or wildlife (deer) trails or via plants for planting (Green et al., 2021a; Riddell et al., 2019). Co-production with stakeholders across environmental, horticultural, and agricultural settings will be required to define how precautionary an approach to disease management is warranted by the evidence and to generate actionable and comprehensive recommendations.

Finally, the survey illustrated that the applicability of both decision tools was hindered by a lack of locally detailed pathogen distribution information. Records of invasive pathogens are scarce across the globe and where distributions are monitored provide powerful information used for horizon-scanning, disease prevention and control (Barwell et al., 2021a; Bebber et al., 2014; Roy et al., 2017). The interactive maps could not be produced at field scale resolution because this was prohibited by some data providers as the locations of outbreaks can be reputationally sensitive to both land/business owners and those who submit observations. A conversation is needed across the plant health, forestry, environmental, landscaping, conservation, and nursery sectors to better understand these sensitivities and the need for gatekeepers of pathogen records, to address the tension between private enterprises who are not obliged to release information about disease detections compared to public and charitable bodies who are. Survey participants stressed the importance of maintaining up-to-date distribution data, which has cost implications when a single species is considered but requirements might be similar for other pathogens (Barwell et al., 2021a). Information for multiple species could be presented using the decision tool frameworks discussed for *P. austrocedri* or new, innovative platforms that provide interactive and experiential knowledge exchange. The value of this will be determined by the number of individuals and organisations who "buy-in" to using the tools and contributing data, which

cross-sector co-production is likely to enhance and lead to longer lasting engagement (Reed, 2008). Furthermore, White et al. (2018) suggest such platforms may effectively engage stakeholders concerned by the additional time and resources required to participate in co-production ventures.

In keeping with findings by Dunn and Laing (2017), survey participants were more pre-occupied with the relevance of the decision tools than their credibility or legitimacy. However, a small group of participants felt the decision framework overrode their own experience and knowledge to make decisions. Involving these practitioners in decision tool co-production may enhance tool legitimacy and ensure they are presented as flexible frameworks that support, rather than prescribe, management decisions to increase implementation (Jones and Kleczkowski, 2020).

Responses were obtained from a wide range of stakeholders involved in juniper management but did under-represent views from landscapers, larger commercial growers for whom juniper is a small component of their overall business, agricultural (compared to forestry) agents and all stakeholders based in Northern Ireland. The responses also represent a single timepoint within a fluid stakeholder landscape where additional sectors may, in future, play a larger role (e.g. agriculture, perhaps influenced by revised agri-environment schemes post EU exit). The survey was disseminated during workplace disruption caused by the COVID 19 pandemic and it is unclear how this impacted participation (e.g. if some sectors were under-represented because of furlough), and while attempts were made to provide the information in accessible formats, it was impossible to enlarge the text in the decision framework sufficiently for one participant to read so their response was discounted. The survey was written from the standpoint that limiting *P. austrocedri* spread is desirable and decision tools are likely to be useful but the decision framework was difficult to use in its current form, and the interactive map was designed by F. Donald who emailed the survey to ~50% of the mailing list. It is possible these factors influenced the feedback obtained from respondents. However, the wording and flow of the questions was carefully considered to maintain neutrality across the survey and open-ended questions were used to afford respondents the space to justify their views (Appendix K) so the qualitative data collected should be largely unaffected.

5.6 Conclusion

The risks posed by *P. austrocedri* to native juniper populations in the UK wider environment are routinely assessed by stakeholders in different sectors. Stakeholders across commercial, land management and regulatory sectors believed tools presented in the form of a decision framework and interactive maps would help them assess, plan, and implement management to maintain disease free populations or limit pathogen spread. The main barriers to decision tool usage were lack of awareness and detailed recommendations, which could be overcome by co-producing tools with a greater diversity of stakeholders – particularly growers and agents – than included for the first iteration. If these barriers are resolved, current uses of the decision framework suggest the tool is effective in raising awareness of the disease and alternative management practices to reduce the risk of pathogen introductions and spread. Inferences for wider plant health management include the need for increased collection of plant pathogen distribution data and a unified approach to make such information available on accessible platforms. The findings also advocate wider use of the ACTA principles and stakeholder co-production to design, evaluate and update plant health policies, guidance, and decision tools to secure better outcomes for biodiversity and habitats going forward.

Chapter 6

National scale *Phytophthora* presence is better predicted by acidic soils and deer densities than soil moisture

6.1 Abstract

Predicting the potential extent and severity of novel plant disease outbreaks can inform strategies that can limit or mitigate impacts on ecosystem functioning (Boyd et al., 2013a). As one of few UK native conifers, common juniper (*Juniperus communis*) is an important component of many habitats, supports large numbers of species, prevents erosion and sequesters carbon (Ward and Shellswell, 2017). Yet British juniper populations are undergoing severe declines, partly because of infection with the aggressive pathogen *Phytophthora austrocedri*. We undertook the first investigation of potential abiotic and biotic drivers of disease patterns at national scale, using machine learning to quantify relationships between the current known distribution of the pathogen and 22 environmental risk factors, producing a map of infection risk in tetrads (2x2km grid cells) containing juniper hosts. The risk factors explored were informed by stakeholders involved in juniper management and included human-mediated spread to new populations through the supplementary planting of hosts to create or restore native habitat. Though 1.8% of British juniper tetrads are currently infected with *P. austrocedri*, the best model predicted that 46% contain suitable conditions for infection (having a 0.5 predicted probability (PP) of presence), of which 11% are highly suitable (>0.75 PP). High roe deer density and pH 4.5-6 were the best predictors of infection, followed by 2.5-3mm daily rainfall and high sheep stocking densities. Supplementary juniper planting was not a strong predictor of infection but models including planting events from the 1970s onwards out-performed those including planting events from the past ten years only. Stakeholders reported the risk map was useful to determine where increased biosecurity measures could be implemented but were uncertain of how the national risk would correspond to factors promoting infection at a local scale. Actions identified to manage national drivers of pathogen spread include limiting human-mediated spread pathways (e.g. supplementary planting) and reducing deer and livestock densities.

6.2 Introduction

Invasions of plant pathogens occur at a range of spatial scales, ordinarily arising as microscopic infections that then propagate to successively larger scales from the plant tissue to whole plants, populations, regions and, in the worst cases, whole continents (Gilligan and van den Bosch, 2008; van den Bosch et al., 1999). Human mediated pathways such as trade and transport networks play important roles in propagating invasions across spatial scales (Brasier, 2008; Roy et al., 2014) but are often poorly captured in models of plant pathogen dynamics (Cunniffe et al., 2015a). Invasions are also facilitated at each scale by interactions with the environment that influence the speed of growth, efficiency of dispersal

and subsequent infection to collectively determine the distribution and persistence of the pathogen (Gilbert, 2002). When a novel pathogen is first detected it is often desirable to explore spatial patterns of infection at a local level while outbreaks pose a lesser risk to host populations and are potentially easier and cheaper to control (Thompson et al., 2018). However, although interactions between the newly arrived pathogen and the receiving environment can be scale-specific, complex feedback loops can also occur between spatial scales (Peters et al., 2004), which if ignored or poorly understood can limit the effectiveness of control (Gilligan and van den Bosch, 2008). Additionally, even if control measures are best targeted at a local level, larger scale predictions of potential spread are useful to contextualise outbreaks, facilitate knowledge exchange and aid risk-based decision-making (Gaydos et al., 2019). There is merit, therefore, in understanding drivers of pathogen infection at regional or national scales, considering how environmental conditions that support natural pathogen infection processes and spread interlink with human-mediated spread pathways such as movements of livestock and wildlife, and understanding how these interact with disease drivers at smaller scales.

Species distribution models (SDMs) are often used to provide such insights. Relationships between abiotic risk factors and the distribution of *Phytophthora* species are frequently modelled (Aguayo et al., 2014; Duque-Lazo et al., 2018; La Manna et al., 2012; Václavík et al., 2010) and modelling studies exploring *Phytophthora* disease patterns in response to land use and anthropogenic activities are also increasingly available (Giordana et al., 2020; Harwood et al., 2009; Hernández-Lambraño et al., 2018; Meentemeyer et al., 2008b). Constructing models at a larger spatial resolution further permits investigation of a wide range of predictors because gridded data are not typically produced at less than 1km resolution. However, SDMs can struggle to produce accurate predictions for newly arrived, actively spreading pathogens where their known distribution is limited by small sample sizes collected from a restricted geographical area (Purse and Golding, 2015; Václavík and Meentemeyer, 2012). This not only leads models to under-predict the potential extent of invasions because suitable conditions are extrapolated from a small subset of locations that may share similar environmental parameters (Václavík and Meentemeyer, 2009) but can also result in over-prediction where a very large area remains from which to draw absence locations (Vaclavik and Meentemeyer, 2012). Attempts to address these limitations include accounting for recording effort when selecting absence locations and using biological information to test out different absence backgrounds e.g. discriminating between areas of pathogen absence outside its environmental tolerance vs constrained by dispersal distances (Chapman et al., 2019; Purse et al., 2013).

First described in 2007 from Argentinian Patagonia as the causal agent of widespread mortality of Chilean cedar (*Austrocedrus chilensis*) (Greslebin et al., 2007), *P. austrocedri* was identified infecting British juniper populations in 2011 (Green et al., 2012). Infection of juniper is of particular concern in GB because the species is one of few native conifers and as such provides extensive biodiversity and habitat benefits (Ward and Shellswell, 2017). A pioneer woodland coloniser, juniper most often occupies nutrient-poor, open grasslands prior to the arrival of larger tree species but can be found as an understorey shrub of native pine or birch woodlands, in montane habitats or as long-established populations around redundant copper or lead mines (Thomas et al., 2007; Ward and Shellswell, 2017). Its tolerance to a wide range of edaphic and climatic conditions means it is widespread across GB (Figure 22). Despite the recent proliferation of micro-distilleries, berry production of native juniper is increasingly declining and only a small handful of companies source local material to produce gin (Craig, P., personal communication, 13th October 2020). This lack of viable seed production (Plantlife, 2015) coupled with a lack of suitable regeneration sites (Plantlife, 2015), milder winters and changes in nutrient cycling (Verheyen et al., 2009) have resulted in steady declines of juniper populations documented since the 1970s (Borders Forest Trust, 1996; Clifton et al., 1997; Hamilton, 2018; Plantlife, 2015; Sullivan, 2003), also experienced in other parts of the species range including Belgium and the Netherlands (De Frenne et al., 2020).

Over 60 geographically separate juniper populations across Scotland and England are now known to be infected with *P. austrocedri* (Figure 22). Large infection foci are present in northern England and north-central Scotland where the disease severity is also highest, with scattered outbreaks in northern and southern Scotland and localised pockets of low intensity infection in southern England (Figure 22). The origin of the pathogen remains unknown, as does the date and source of first introduction to Great Britain (GB), but the wide geographical distribution and extent of long-dead trees in the worst affected populations suggests it has been present for some time (Green et al., 2015). In Patagonia, *P. austrocedri* was widely detected in forest soils spanning the full extent of the natural distribution of Chilean cedar (Vélez et al., 2020) and patterns of spatial spread were strongly related to urbanisation and the insertion of road networks (Giordana et al., 2020) meaning the pathogen is now extremely difficult to control (Vélez et al., 2020). By contrast, the number of infected juniper populations in GB remains relatively small with 97 (1.77%) tetrads (2kmx2km grid cells) infected in the wider environment to date (Donald et al., 2021), suggesting the invasion is at a sufficiently early stage for interventions to potentially limit further spread (Figure 22).

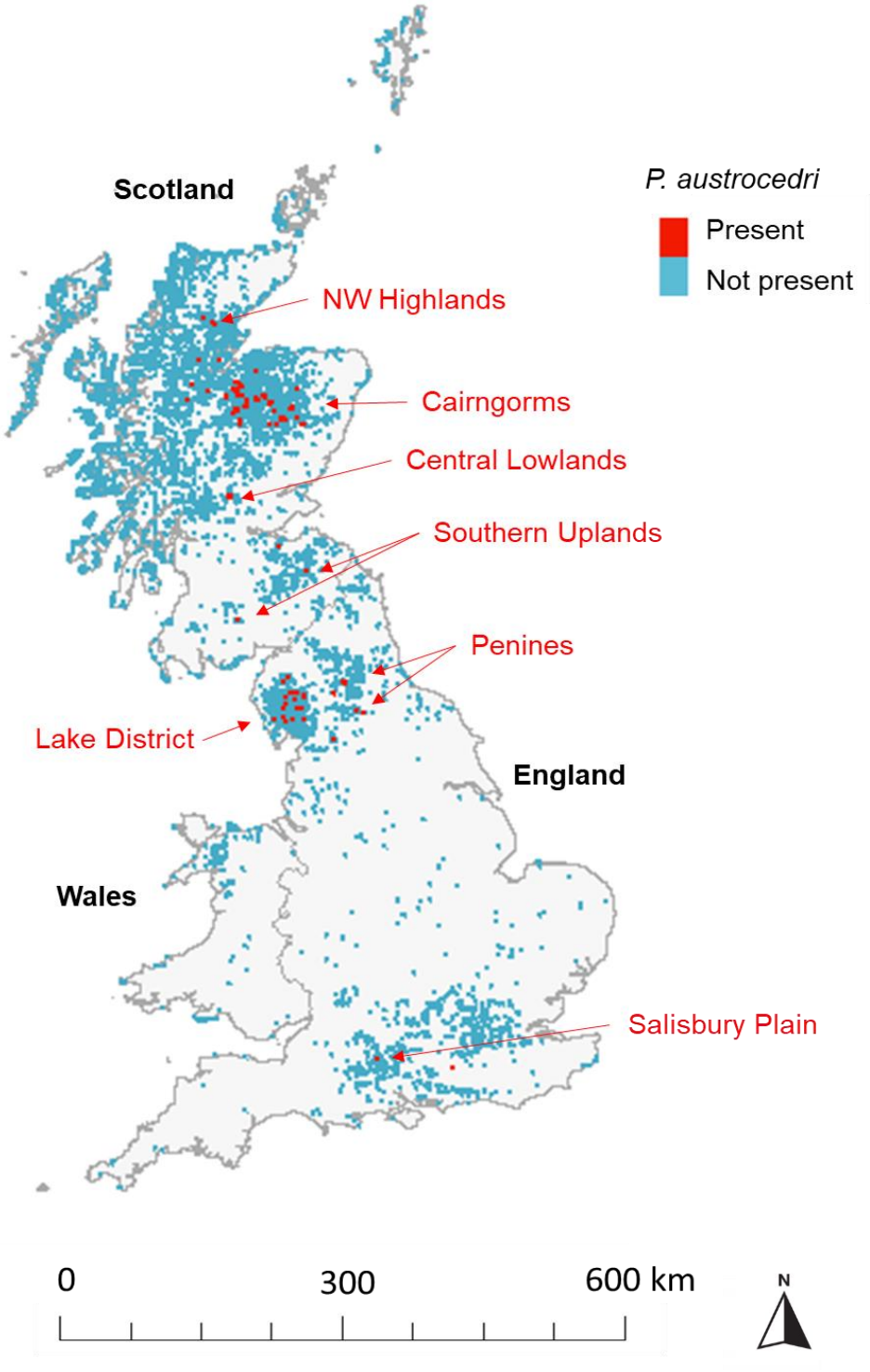

Figure 22. Distribution of 5483 tetrads (2kmx2km grid cells) containing common juniper (*Juniperus communis* s.l.) between 1990 and 2020 in GB (BSBI, 2020). Ninety-seven tetrads are shown in red where *P. austrocedri* has been detected by isolation or a positive qPCR test, labelled with geographical names to highlight infection clusters. The remaining juniper tetrads are shown in blue. Note that tetrads are mapped at greater than 2km resolution to improve visibility.

No new detections have been reported in the wider environment since 2016, indicating that *P. austrocedri* may be slow to establish in new locations. At the field scale, natural spread of the pathogen is thought to be localised and slow (within ~500m of the nearest infected tree in four years) with infrequent longer distance (>1km) dispersal (Chapter 3), and to primarily occur by the release of free swimming zoospores from non-caducous sporangia into soil water and by the passive movement of infected soil on hooves and tyre treads (Riddell et al., 2020). Zoospores then encyst on juniper roots, moving into the stem and creating necrotic lesions that block the phloem to ultimately kill the stem or the whole tree (Green et al., 2015). However, lesions are sometimes observed on aerial branches and suspected to arise from inoculum splashed from soil or transferred by perching birds (Riddell et al., 2020). In the field, infection is recognisable from foliage symptoms that show a progression of yellow to bronzed discolouration (Green et al., 2015) affecting whole branches or stems as photosynthetic capacity is increasingly restricted (Vélez et al., 2012). Symptoms tend to first arise in stands growing in waterlogged soil or adjacent to watercourses (Donald et al., 2020). The slow growth of the pathogen makes it difficult to isolate (Green et al., 2015; Greslebin et al., 2007) with optimal growth determined at 15°C from experimental trials with UK isolates that showed no growth at >20°C (Henricot et al., 2017b).

Considerable efforts to rehabilitate juniper populations have been undertaken since the 1990s across GB, supported by state, charitable or crowd-sourced funding but with little formalised reporting of restoration success (Donald et al., 2021). Introducing cuttings raised ex-situ (i.e. supplementary planting) has been extensively used by stakeholders (including statutory agencies, conservation charities, utility companies and community groups) (Donald et al., 2021) across much of GB despite the frequency of *P. austrocedri* detections made in British nurseries (Green et al., 2021a) and recommendations from published guidance to only plant populations at lower risk of *P. austrocedri* infection that are vulnerable to extinction from other sources (e.g. imbalanced sex or age ratios) (DEFRA, 2017; Forestry Commission Scotland, 2013). A survey of 41 stakeholders connected with juniper management found that 71% were unaware of this guidance and cited lack of clarity about inappropriate planting scenarios and data availability as critical barriers to its use, expressing a preference for a combination of infection maps and decision flow-charts to aid risk assessment of management decisions (Chapter 5). The aim of this study was, therefore, to i) identify and rank important abiotic and biotic drivers of *P. austrocedri* infection of juniper at national scale, ii) determine if proximity to historical supplementary planting increases the likelihood of infection when accounting for these other drivers, and iii) provide a national scale predictive infection risk map that could be used to identify vulnerable juniper populations

across GB. To better tailor the risk map to be used for conservation decision-making for juniper, aligning with recent calls for participatory co-development of risk models for plant health (Jones and Kleczkowski, 2020), stakeholders identified as potential end-users were consulted during model development for their knowledge of locations of historical juniper planting. Stakeholders were also involved in selecting risk factors tested in the model to harness their experience and ensure factors with the highest perceived risk were examined in the study. Feedback was then sought from stakeholders on the resulting risk map to find out how well the relationships identified by the model fit those expected by practitioners and to understand how the map may be used to aid decision-making.

6.3 Methods

6.3.1 Mapping grid cells containing common juniper

The distribution of common juniper in the wider environment that could host *P. austrocedri* was mapped by combining the native and planted juniper datasets at tetrad (2kmx2km resolution) described in Donald et al. (2021). The native juniper dataset comprised of records of *Juniperus communis* s.l. submitted to, and curated by, the Botanical Society of Britain Ireland (BSBI) and survey data collected for specific populations including Site Condition Monitoring of protected areas where juniper was a designated feature and surveys for *P. austrocedri* that detailed juniper as the sampled host. For this analysis, we assumed all cells containing juniper had the potential to host *P. austrocedri*. Two tetrads that contained planted (but not native) juniper were added to the distribution map, resulting in 5483 tetrads occupied by juniper across GB between January 1990 and January 2020 (Figure 22). Records of different juniper subspecies were not differentiated because morphological characteristics separating the subspecies are contested and inconsistently recorded, often with deference to habitat characteristics or historical identifications. Wider environment *P. austrocedri* infections have only been reported from *J. communis* subsp. *communis* but laboratory inoculations showed *J. communis* subsp. *nana* is susceptible to the pathogen (Dun, 2016). While *J. communis* subsp. *hemisphaerica* has never been inoculated it has a very restricted distribution along coastal fringes of Wales and Cornwall (Thomas et al., 2007) and there is no reason to suspect that it differs in susceptibility to *P. austrocedri* compared to the other subspecies.

6.3.2 Mapping the presence of P. austrocedri

Presence of *P. austrocedri* was used as the dependent variable in the model, defined as "present" or "not present" in tetrads containing juniper. A full description of the datasets and methods used to compile the distribution of *P. austrocedri* can be found in Donald et al. (2021). Infection with *P. austrocedri* is confirmed by collecting tissue from the leading edge of the lesion and i) isolating the pathogen into culture (Green et al., 2015), ii) PCR and sanger sequencing of the ITS region (Green et al., 2015) or iii) qPCR using a pathogen-specific assay (Mulholland et al., 2013). As such, *P. austrocedri* presence was defined as successful isolation of the pathogen into culture, or a "positive" or "confirmed" PCR or qPCR result. Ten *P. austrocedri* presence records did not intersect with the juniper distribution map. Discussions with plant health inspectors, local foresters and botanists confirmed three of these locations did contain juniper so the corresponding tetrads were duly added to the juniper distribution map, while the remaining seven detections were mis-identified as wider environment findings that instead derived from gardens. These detections were discarded from the *P. austrocedri* dataset leaving 97 infected juniper tetrads. Since many infected tetrads cluster in particular locations (Figure 22) we checked if the presence records should be thinned to avoid inflating model accuracy and pseudo-replicating specific environmental conditions by inspecting histograms of Euclidean pairwise distances between presence tetrads (Syfert et al., 2013), calculated using rdist::*rdist* (Blaser, 2020) in R. Infected tetrads did not show a strong tendency towards spatial clustering so a post-hoc check for spatial autocorrelation was used instead of data thinning (Appendix M).

BRTs perform best with inputs of presence and absence data in equal proportions (Barbet-Massin et al., 2012). It is impossible to prove the absence of a pathogen, particularly with high levels of inapparent infection in host populations, so "absence" in the context of this study is used as short-hand for "apparent absence". This was defined either as a "random absence" where juniper tetrads that did not contain a confirmed *P. austrocedri* detection were selected at random (5386 tetrads), or as a "visited absence" where the tetrad had been visited since pathogen discovery in 2011 and either no foliage symptoms had been observed or sample material had tested negative for pathogen presence (Figure 23). The "visited absence" locations were selected from the dataset of "apparent absences" compiled in Donald et al. (2021) that intersected with tetrads present in the juniper dataset but not in the *P. austrocedri* dataset (125 tetrads) (Figure 23). BRTs were run with each absence type to compare performance, with the expectation that models with "visited absences" would

outperform models using the “random absences” since the former locations are more likely to represent true pathogen absences.

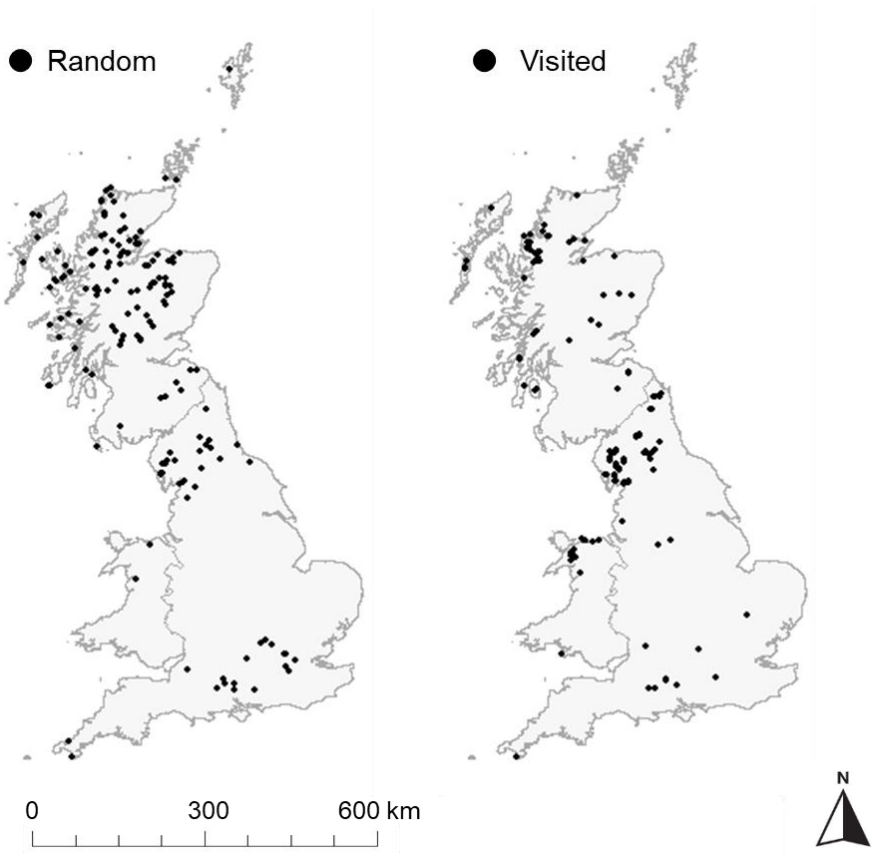

Figure 23. Distribution of absence locations used in BRTs selected as a random sample of (L) juniper tetrads without a positive *P. austrocedri* detection or (R) visited tetrads with no *P. austrocedri* foliage symptoms or a negative PCR or qPCR result. Note that locations are shown at greater than tetrad resolution to improve visibility.

6.3.3 Framing key disease risk factors with stakeholders

For this study, the small number of positive *P. austrocedri* detections increased the risk of model overfitting so our exploration was restricted to a small set of biologically relevant, uncorrelated predictors prioritised by stakeholders, and to investigating simple relationships between the presence of the pathogen and each predictor (Purse et al., 2013). Expectations were formed *a prioiri* around a list of potential abiotic and biotic risk factors for *P. austrocedri* that could promote mycelial or sporangial growth, or the release and transmission of zoospores through the movement of infested water or soil that might predict pathogen presence in tetrads (2kmx2km grid cells) containing juniper (Table 25). The list was compiled

from literature sources and site observations and discussions with pathologists and managers of juniper populations.

Table 25. Expected direction (increasing or decreasing) of response between disease risk factors and presence of *P. austrocedri* in British juniper tetrads resulting from the effect on sporangial growth, zoospore dispersal or inadvertent inoculum transfer.

Disease risk factor	Response direction	Sporangial growth	Zoospore dispersal	Inoculum transfer
Rainfall (duration more important than volume)	↑	x	x	
Soil moisture	↑	x	x	
Snow mass	↑	x	x	
Increasing duration of mean temperatures 10-15°C	↑	x	x	
Increasing numbers of cold triggers of minimum temperatures 0-5°C	↑	x	x	
Slope	↓	x	x	
Altitude	↓	x	x	
pH	↓	x	x	
Nearest river	↓	x	x	x
River lengths	↑	x	x	x
Deep-intermediate soil depths	↓	x	x	
Shallow soils	↑	x	x	
Not sandy soils	↓	x	x	
Sandy soils	↑	x	x	
Presence of more recent juniper planting	↑			x
Population density within recreational distances	↑			x
Sheep and deer densities	↑			x
Road lengths	↑			x
Mycelial growth rate	↑	x	x	

Exploratory temperature trials performed under laboratory conditions using British *P. austrocedri* isolates showed increased sporangial production after five days of constant exposure to 10°C, with lower production at 15°C, very low at 17°C and infrequent at 5°C but only after thirteen days (Frederickson-Matika, D., unpublished data). However, when plates were incubated at 5°C for seven days before the temperature was increased to 10°C, sporangial production was immediately triggered and zoospores started to release within two days, compared to eight when plates were incubated at constant 10°C (Frederickson-Matika, D., unpublished data). In the wider environment, we therefore expected *P. austrocedri* presence would increase with increasing duration of mean temperatures in the optimal 10-15°C range for mycelial growth, and minimum temperatures between 0-5°C that when

intersecting periods of optimal mean temperatures would create the best conditions for sporangial production and zoospore release (Table 25).

Consistent with other *Phytophthora* species, *P. austrocedri* also requires free water for sporangial growth and zoospore dispersal (Greslebin et al., 2007). Conflicting results were obtained from studies exploring infection of Chilean cedar, with one early report of increased annual infection in wet years (Baccalá et al., 1998b) compared to later studies that found mean annual precipitation predicted infection poorly compared to edaphic factors that altered the availability of water once it had percolated into the soil (La Manna et al., 2012, 2008b). Given the pathogen's slow growth rate, we hypothesised that the volume of rain might be less important than the duration of wet conditions, expecting at least five consecutive wet days would be needed for sporangial production as observed for baited colonies of *P. austrocedri* (Clark and Green, 2017). We further expected these five rainy day periods would optimally coincide with five days of consecutive optimal mean temperatures and a cold trigger to release zoospores (Table 25). Soil moisture was the best predictor of juniper symptom intensity at field scale (Donald et al., 2020) and was found to increase with increasing incidence of disease in Chilean cedar (La Manna and Rajchenberg, 2004a) in soils with finer textures (e.g. clay) that retained more water (La Manna and Matteucci, 2012) (Table 25). Soil depth may influence water availability because shallow soils are more likely to quickly saturate, facilitating rapid sporangial growth and dispersal, while deeper soils might be buffered to temperature changes required to trigger zoospore release and impede their movement (Table 25). Lower *P. austrocedri* incidence was found in soils with higher concentrations of sodium fluoride (La Manna et al., 2012) indicating the pathogen prefers acidic soils, again consistent with many *Phytophthora* species that tolerate a broad pH range but show limited expression in alkaline soils (Duque-Lazo et al., 2018; Kong et al., 2009) (Table 25). Topographic interactions with soil moisture were important in describing field scale disease distribution patterns of both juniper and Chilean cedar where a consistently high water table was only maintained on steep, freely draining slopes in proximity to rivers (Donald et al., 2020; La Manna and Matteucci, 2012; La Manna and Rajchenberg, 2004b) (Table 25). No research has been conducted examining the relative importance of river proximity compared to length in predicting *P. austrocedri* presence and discussions with stakeholders revealed a desire to explore how the risk of infection changes with the area of a river catchment (Chapter 5) (Table 25). Interactions between topography and the water table also resulted in increased disease incidence in stands of Chilean cedar growing on flat slopes (La Manna and Matteucci, 2012; La Manna and Rajchenberg, 2004b), which we expected to be replicated in juniper, as well as higher incidence at lower altitude (La Manna

et al., 2012), perhaps as a function of temperature (Table 25). For abiotic interactions, we finally expected that snow too may play an influential role, not only in facilitating zoospore dispersal in meltwater but also by buffering soil temperatures (Hennon et al., 2012), prolonging the duration of suitable sporangial growth conditions (Table 25).

The biotic risk factors we proposed would interact with pathogen presence primarily related to the inadvertent transfer of inoculum between infected populations. Direct analysis of disease presence in response to different grazing pressures is difficult to conduct without detailed field trials but an association between increased symptom intensity and increased deer density was surmised from the composition of vascular plant species found in field quadrats (Donald et al., 2020) and the pattern of disease colonisation of a single juniper population in northern England where symptoms developed >800m from focal outbreaks and >100m distant from footpaths but where deer tracks were observed (Chapter 3). In Patagonia, rates of Chilean cedar infection were highest in areas grazed with freely roaming cattle compared to those with intermittent or no grazing (La Manna et al., 2013b) (Table 25). People are also implicated in transporting infected soils, potentially for long distances along roads and recreational trails on the treads of vehicle tyres or footwear (Cushman and Meentemeyer, 2008; Jules et al., 2002), or in association with plants for planting (Brasier, 2008) (Table 25). The number of supplementary juniper planting events started to increase during the 1960s (only 23 planting records are known from the period 1845-1967) but a marked increase in the number and geographical distribution of events occurred from the 1990s that is sustained to the present day (Donald et al., 2021). We expected pathogen presence would most closely relate to the distribution of more recent juniper planting events given their increasing frequency (Donald et al., 2021) and the higher throughput of imported plants in source nurseries (Spence et al., 2020) (Table 25).

The list of potential abiotic and biotic predictors was then presented in a 21-question survey (Appendix K), sent to over 100 stakeholders connected with juniper management across the UK (Chapter 5), as potential risk factors that may be included in a model exploring the national distribution of *P. austrocedri.* The aim of the survey was to explore the tools used by practitioners to risk assess juniper management activities in relation to *P. austrocedri* and to identify the need for additional tools, including decision trees, maps, and models to aid this process. Stakeholders were asked to complete the survey between 18th and 30th October 2020 and encouraged to reply based on their individual role in juniper management rather than attempting an organisation-wide response, so we could identify differences in needs between those whose role involved day to day management of juniper populations (e.g. land

owners) from those who assessed population condition and/or funding applications (e.g. officers based in the devolved nature agencies), created management plans (e.g. forestry agents) and grew native juniper commercially (e.g. suppliers for habitat restoration schemes). Forty-one practitioners responded from 31 organisations, all of whom answered questions 17-18 that asked participants to select five potential abiotic risk factors, and five potential biotic risk factors from the presented list that they considered most likely to promote infection of juniper, and to rank each of the five factors per group in order of importance (Appendix K). The overall importance attributed to each factor by survey participants was then calculated as a weighted mean to account for the number of times each factor was selected and the assigned rank importance.

6.3.4 Preparation of environmental risk factor layers

Following collation of the survey results, the list of environmental risk factors to include in the model was further refined and layers were prepared. The small number of *P. austrocedri* presence locations limited the number of predictors that could be used in the models so some risk factors included in the survey list were excluded from the analysis. Risk factors were excluded from the models where they were found to i) be data deficient (detailed knowledge of bird species that feed on juniper berries, footpath networks for the whole of GB); ii) contain too many categories with no evidence base in the literature to inform concatenation (habitat type); or iii) offer less insight to the expected biological response compared to other risk factors with higher stakeholder weighted importance (surface runoff compared to soil moisture, river flow speed compared to nearest river). Two additional risk factors not considered in the survey were added to the predictor list - length of roads and average mycelial growth rate (calculated from experimental growth curves fit to diurnal temperature measurements) – while rainfall, temperature, soil moisture, nearest river and juniper planting risk factors were split into more detailed predictors expected to better capture aspects of *P. austrocedri* biology (Table 26). The derivation of all predictors included in the models is described in Appendix M. Model predictions were obtained for 4339 (79%) mapped juniper tetrads. Missing data were most associated with daily temperature and rainfall variables that could not be obtained for Orkney or Shetland, tetrads intersecting coastal boundaries and some mountain peaks.

Table 26. Key characteristics of environmental predictors included in BRTs modelling *P. austrocedri* presence in GB, including how the risk factors included in the stakeholder survey (risk type) and the weighted mean of stakeholder importance scores for abiotic (above the bold line) and biotic (below the bold line) risks relate to predictors subsequently included in the BRTs. The original data resolution, time span, type of transformation (Trnsf) applied and source(s) of data used to create the predictors used in the BRT models are also defined. Risk types/predictors are ordered from highest to lowest stakeholder scores.

Risk type	Survey weight	Predictor name	Risk factor description	Original spatial resolution	Time span	Trnsf	Source
Rainfall	9	Mean rainfall (mm/day)	mean daily rainfall	1km	1990-2016, daily	log10	Robinson et al., 2020
		Rainy days (n)	number of days rainfall > 1mm				
Soil moisture	7	Soil moisture (mm water/m soil)	mean soil moisture calculated from simulated monthly data	1km	1990-2015		Bell et al., 2018
		Snow mass (kg m^2)	mean snow mass calculated from simulated monthly data		1990-2016	log10	Martinez-de la Torre et al., 2018
Temperature	5	Mean temperature (°C)	mean daily temperature	1km	1990-2016, daily		Robinson et al., 2020
		Optimal temperature periods (n)	n periods with 5 consecutive days mean temperature 10-15°C				Robinson et al., 2020
		Minimum temperature (°C)	minimum daily temperature				Met Office et al., 2020
Climate suitability	4	Climate suitability (n)	n periods of 5 consecutive days rain >1mm, mean temperature 10-15°C with a min temperature < 5°C at some point during that window	1km	1990-2016, daily		Robinson et al., 2020 & Met Office et al., 2020
Slope	3	Slope (°)	slope angle	0.03km	2014		NASA, 2014
Altitude	3	Altitude (m)	metres above sea level	0.03km	2014	sqrt	NASA, 2014
Soil pH	2	pH	pH prediction from 2446 samples of top 0-15cm soil	1km	2007	log10	Thomas et al., 2020
Proximity to watercourses	2	Nearest river (m)	distance from tetrad centroid to nearest river	0.05km	1975-2000	log10	Moore et al., 2000
		River length buffer (m)	length of rivers within 2km buffer				
		River length tetrad (m)	… within tetrad				

Soil depth	1	Deep soils (m^2) Intermediate soils (m^2) Shallow soils (m^2)	area of tetrad categorised as "deep" … "intermediate" … "shallow"	1km	up to 2012		Lawley, 2012
Soil texture	1	Sandy soils (m^2)	area of tetrad described as "sandy"	1km	up to 2012		Lawley, 2012
Juniper planting	9	Planting 2007-2016 Planting 1997-2016 Planting 1987-2016 Planting 1977-2016 Planting 1967-2016	presence/absence of planting events within 2km radius (6kmx6km)	2km	2007-2016 1997-2016 1987-2016 1977-2016 1967-2016		Donald et al 2021
Recreation	7	Median population (n) Quartile population (n)	Residential population size within 3.2km radius … within 10.9km radius	1km	2011 census, 2015 landcover	log10 log10	Reis et al., 2017
Livestock density	6	Sheep (n)	Total number of sheep and lambs (i.e. all breeding and non-breeding sheep	2km Scotland & Wales, 5km England	2010	log10	EDINA, 2010
Deer density	4	Roe deer (index of presence) Red deer (index of presence)	Predicted habitat suitability for roe deer … red deer	1km	up to 2012		Alexander et al., 2014 Wint et al., 2014
Not included in questionnaire	NA	Roads (m) Average mycelial growth (mm/day)	Length of roads within tetrad Predicted average daily mycelial growth in response to temperature series fit to minimum, mean, and maximum temperatures	0.015-0.03km 1km	2021 1990-2016, daily	log10	Ordnance Survey, 2021 Henricot et al., 2017; Met Office et al., 2020; Robinson et al., 2020

6.3.5 Modelling the distribution of *P. austrocedri* with Boosted Regression Trees

Pearson's r^2 correlation coefficient was used to check collinearity between risk factors. Very strong correlations (positive or negative r^2 >0.8) were found between average mean daily temperatures/average minimum daily temperatures/cold days, mean rainfall/rainy periods and sandy/not sandy soils (Appendix M). To account for this, BRTs were run including either mean or minimum temperature with otherwise identical combinations of predictors to find the measure of temperature that best explained *P. austrocedri* distribution. One rainfall and one soil texture predictor was chosen for use in all models: mean rainfall as better supported by prior literature, and sandy soil that better characterised soil texture than the amalgamation of non-sandy textures. The following 19 risk factors were present in all models: optimal temperature periods, average mycelial growth, mean rainfall, rainy days, climate suitability, snow mass, soil moisture, nearest river, pH, altitude, slope, deep, intermediate, shallow, and sandy soils, roe and red deer, sheep, and roads (Table 26). Twenty predictor combinations formed from the five different time periods considered for juniper planting activity, each combined with median or quartile population density and river length in tetrads or buffered tetrads (resulting in four model combinations per planting period) were then combined with the constant list of predictors and either mean or minimum temperature to run 40 BRTs with different combinations of 23 predictors. Data transformations were performed using log10 or sqrt functions to nine risk factors identified with very strong positive skews prior to model fitting to allow interpretation of the response curves calculated for the most important predictors (Table 26) (Appendix M).

A BRT modelling framework was chosen to identify environmental risk factors that best predict the current distribution of *P. austrocedri* in juniper tetrads across GB as a flexible modelling approach that generates good predictions for species distributions, allows input of different predictor data types (e.g. binary and numeric), is robust to outliers and only selects informative predictors, which is especially useful for exploratory analyses with a large number of potential predictors (Elith et al., 2008). BRTs generate predictions by combining regression trees, that partition the predictor space into progressively smaller regions with homogeneous responses to the predictors using a set of decision rules, and boosting, that iteratively fits decisions trees to the training data to increasingly focus on the hardest observations to predict and select predictors that best capture the distribution of the input presence-absence data (Elith et al., 2008; Purse et al., 2020).

Prior to modelling, the *P. austrocedri* presence data were split into a set of training and test data with an 80:20 ratio to perform model validation using presence locations withheld from

training the models. As such, 78 of the 97 tetrads with positive *P. austrocedri* detections were used to train the BRTs and 100 samples of 78 tetrads were selected from the "random" and "visited" absence datasets using the R *sample* function. Each of the 20 predictor combinations were fitted with each of the 200 absence selections. Fitting BRTs requires setting the learning rate (*lr*), tree complexity (*tc*) and bag fraction (*bf*). The number of nodes in a tree is controlled by *tc* and influenced by sample size, such that small samples ($n < 250$) are best fit with simple trees (*tc* 2 or 3) (Elith et al., 2008). The speed and accuracy of BRTs can be improved, and the tendency to overfit reduced, by introducing stochasticity by drawing a fraction of the training dataset at random without replacement (Elith et al., 2008). This is specified by *bf* where a value of 0.5 would mean 50% training data are randomly drawn. Finally, the contribution of each tree is shrunk by the *lr* as the tree is added to the model. The smaller the *lr* the more trees are required, which generally improves the predictive power of the model and 1000 trees is recommended as the minimum number required to generate good predictions (Elith et al., 2008). The best combination of settings was identified by running one iteration of presence-absence data with the eighteen environmental risk factors used in every model and 72 possible combinations of *tc* 2 or 3 with *lr* 0.01, 0.05, 0.001, 0.005, 0.0001 or 0.0005 and *bf* 0.50, 0.55, 0.60, 0.65, 0.70 or 0.75 to find the model with the lowest cross-validation mean deviance (Elith et al., 2008). Models set to *tc*=3 and *lr*=0.001 yielded the same cross-validation mean deviance (1.08, 0.2 units better than the worst value) with *bf* > 0.55 so *bf*=0.75 was selected as producing the smallest number of trees (5200) compared to the other *bf* values. The BRTs were fit using dismo::*gbm.step* (Hijmans et al., 2020) in R that automatically identifies the optimum number of trees using ten-fold cross-validation. A simplification step was then performed on each model using dismo::*gbm.simplify* (Hijmans et al., 2020) to remove the lowest contributing predictors and calculate the change in predictive deviance relative to the full predictor complement, thus identifying the sequence of predictors to remove in order of importance (Hijmans et al., 2020). This information was used to re-fit each model with only the top ten most informative predictors. Interactions between all pairs of the ten retained predictors were tested using dismo::*gbm.interactions* (Hijmans et al., 2020) that fits a linear model to the predictions generated by each predictor pair and calculates the mean of the residuals that increases with increasing interaction strength.

Figure 24. Distribution of 19 *P. austrocedri* test presence locations, shown in red, used to calculate the Boyce Index to discriminate the best performing BRTs. The locations represent an 80:20 training:test data split that were randomly selected and withheld from model fitting.

Independent validation of models was performed by calculating the Boyce index as a measure of predicted-to-expected (P/E) ratios. The index is calculated by partitioning BRT predictions into suitability categories and comparing the frequency of presences predicted by the model that fall in each category with the frequency expected from a random distribution (Hirzel et al., 2006). The index is reported as a Spearman rank correlation coefficient between -1 and 1, where a value of 1 indicates model predictions are consistent with the distribution of presences in the test dataset, 0 suggests the model performs no better than random and -1 shows the model predicts unsuitable areas (Hirzel et al., 2006). The Boyce index was calculated using ecospat::*ecospat.boyce* in R (Cola et al., 2017) from predictions averaged across the 100 iterations run for each predictor combination with “random” or “visited” absences using the 19 test locations withheld from the presence dataset (Figure 24). The resulting value was used to find the best model performance in independent validation among the models with different absence selections, mean or minimum

temperature and alternative calculations of planting, river length and population density predictors. The best BRT was assessed for spatial autocorrelation by averaging Moran's I values in residuals and significance across the 100 model iterations within distance bins from 0 to 575km at increments of 25km. The mean and standard deviation of the predicted relative probability of *P. austrocedri* presence in each juniper tetrad was averaged across the 100 iterations of the best model and plotted using the rasterVis R package (Lamigueiro and Hijmans, 2019). For each iteration of the best model, the cross-validation threshold of the relative probability of presence, that maximises discrimination between presence and background cells, was calculated by dismo::*gbm.step* (Hijmans et al., 2020). The cross-validation threshold returned for each iteration was then used to convert the probability of presence predictions for each tetrad to a binary presence/absence value. The number of times a tetrad was predicted to contain *P. austrocedri* could then be summed across all 100 model iterations. The mean, median and standard deviation of the relative importance (RI) of each predictor in the best model was also calculated across the 100 iterations, scaled between 0 and 100 with increasing values indicating increased effect in the model (i.e. increasing use to perform splits in the decision trees and increasing loss of function when dropped from the model).

The number of simplified iterations of the best model each predictor was included in, and the mode of its rank importance across all iterations, was also reported. Finally, response curves for predictors with mean RI in the model over a threshold value of six, and modal rank between one and five, were averaged across the 100 best model iterations by calculating the mean and standard deviation of the marginal predicted probabilities across 40 bins of the predictor values (Purse et al., 2020). This allowed interpretation of the response direction between *P. austrocedri* presence and the most informative environmental risk factors. Finally, the risk map was circulated as an interactive map presented in an RShiny app (Chang et al., 2021) to the 41 stakeholders who participated in ranking model predictors. Stakeholders were requested to provide feedback about their confidence in the map of predicted *P. austrocedri* risk and discuss opportunities and limitations to using the risk map to inform their work (Appendix O).

6.4 Results

The model that best predicted the distribution of *P. austrocedri* across GB used the mean temperature predictor, random absences and yielded a high Boyce index of 0.88 with the validation dataset. Boyce indices varied by 0.54 units between the 40 model combinations tested (Figure 25). Models using mean temperature and random absences showed the greatest variation in Boyce index but produced the top thirteen models with a Boyce index ≥0.70. Two models with a Boyce index >0.70 were also returned using the combination of minimum temperature and random absences (Figure 25). Models drawing absences from the visited locations performed worse with both temperature predictors (Boyce index mean = 0.65, minimum = 0.53) compared to the random absences, and the combination of minimum temperature and visited absences showed the poorest predictive accuracy of all (Figure 25).

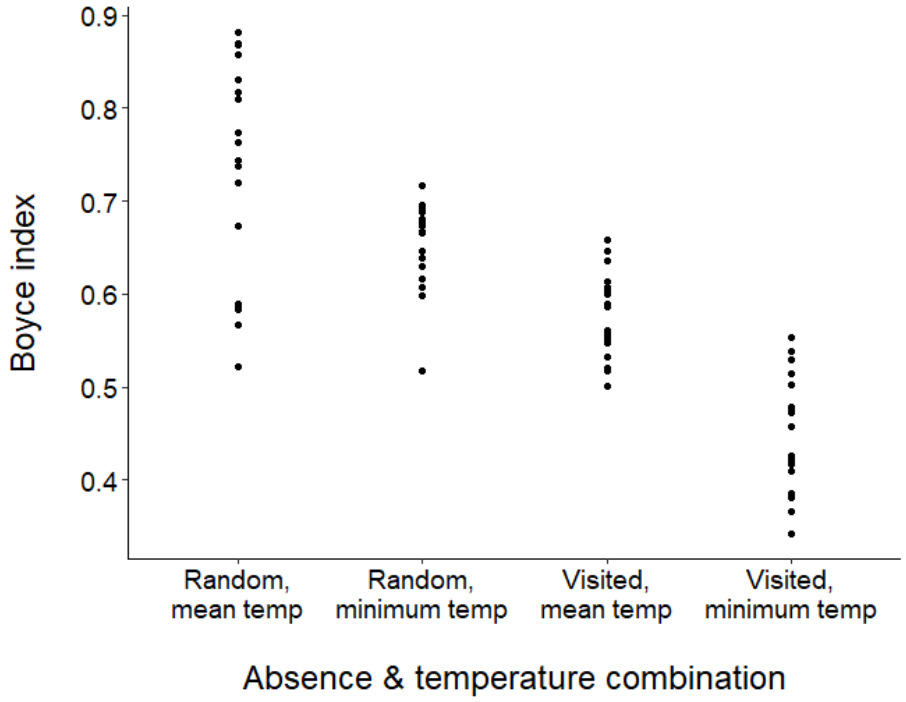

Figure 25. Boyce indices calculated using 19 independent test presence data points to validate BRT model accuracy comparing the predictive accuracy of models using random or visited absences and mean or minimum temperature predictors. Each model combination was tested with all possible combinations of alternative planting, river length and population density predictors.

Significant (p=0.01) spatial autocorrelation in model residuals was only identified up to the first 25km of the distance range for the best model and only at low magnitude (Moran's I = 0.2) that would be unlikely to over-inflate model accuracy or the RI of the environmental

predictors (Appendix N). Boyce indices were used to compare models including mean temperature and random absences to find the best predictors of supplementary planting periods, river lengths and population density (Table 27). Supplementary planting seemed to have marginal importance in driving infection patterns. The planting predictor found in the best model compiled locations of planting events that occurred between 1977 and 2016 but the effect of including alternative planting periods had minimal impact on the Boyce index that ranged from 0.87 to 0.86, with the exception of the most recent period, 2007-2016, where the Boyce index dropped to 0.81 (Table 27). Alternative calculations for river length and population density exerted greater influence on the predictive power of the BRTs; length of rivers measured in the tetrad instead of a wider 6kmx6km buffer improved the Boyce index by 0.05 units and the population density within median (3.2km) radius compared to quartile (10.9km) radius by 0.08 units (Table 27). Additional performance metrics including cross-validation AUC are provided in Appendix N.

Table 27. Comparison of alternative metrics used to describe supplementary planting locations, residential population density (as a proxy for pressure from recreation) and river lengths. For each metric, the Boyce index and number of trees (mean and standard deviation across 100 iterations) returned by the simplified, random absence model with the highest Boyce index is shown.

Metric		Number of trees		Boyce index
		mean	s.d.	
Planting	1977-2016	3975.00	1458.54	0.88
	1987-2016	3982.50	1558.45	0.87
	1997-2016	4095.00	1628.80	0.87
	1967-2016	3984.00	1704.33	0.86
	2007-2016	4007.00	1598.03	0.81
Population density	Median	3975.00	1458.54	0.88
	Quartile	4142.00	1744.22	0.76
River length	Tetrad	3975.00	1458.54	0.88
	Buffer	3915.50	1626.25	0.83

The rank importance of environmental predictors in the best model was generally stable across model iterations (standard deviation ≤5) except for pH which had the highest standard deviation (10) (Table 28). Despite this, soil pH had the highest mean RI (21), was present in 99 model iterations and shared the highest modal rank importance with roe deer density that was included in all 100 iterations (Table 28). Other environmental predictors in the best model with RI >6 were mean rainfall, sheep density, average mycelial growth, and altitude in that order (Table 28). Mean rainfall was present as a top ten predictor in 96 iterations but had a lower modal rank importance of 5 compared to sheep density, average

mycelial growth and altitude that were present in fewer iterations (92, 87 and 79 respectively) but had higher modal rank importance when present in the list of top ten predictors (Table 28). Soil moisture, deep soils, slope, and roads had consistently low rank importance while shallow soil, nearest river, rainy days and climate suitability were not included as a top ten ranked predictor in any of the model iterations (Table 28). While including planting locations 1977-2016, length of rivers within tetrads and median population density marginally improved model performance, none of those predictors had high RI compared to other risk factors (Table 28). Indeed, the planting predictor was only included as a top ten predictor in three iterations of the model while river length and population density were included more often in 64 and 72 iterations respectively (Table 28). The response plots indicate *P. austrocedri* is more likely to infect juniper tetrads with increasing habitat suitability for roe deer (especially with an index of presence > 60), soil pH in the range 4.2-6.0 but peaking at 5.5, mean daily rainfall of 2.5-3mm, increasing stocking density of sheep (particularly >2000 individuals per tetrad), decreasing average daily mycelial growth and increasing altitude up to 400m (Figure 26).

Table 28. Relative importance (RI) of predictors used in the best performing models of *P. austrocedri* distribution. The best simplified model used the random absence selection and had the highest Boyce index (0.88). The predictors shown are those retained as one of the top ten most important predictions in any of the 100 iterations of the model run with different absence selections. The number of times (n) each predictor was present in a model iteration and the mode of its rank importance (Rank) is shown alongside its mean, median and standard deviation RI across all iterations. Predictors are listed in order of mean RI and the rank importance is given as NA where the mode could not be calculated because the predictor was included in a small number of iterations with different importance each time.

Predictor	n	Rank	Mean RI	Median RI	Standard deviation
pH	99	1	21.01	19.88	10.22
Roe deer	100	1	19.36	19.38	5.15
Mean rainfall	96	5	9.69	8.92	4.67
Average mycelial growth	87	3	8.40	8.12	5.05
Sheep	92	3	8.38	8.18	4.57
Altitude	79	4	6.64	7.10	4.51
Median population	72	10	4.52	4.76	3.41
Mean temperature	75	7	4.23	4.58	3.16
River length tetrad	64	8	3.56	3.94	3.32
Red deer	58	8	3.51	3.76	3.58
Soil moisture	58	10	3.48	3.66	3.56
Roads	41	9	2.71	0.00	3.63
Snow mass	28	6	1.91	0.00	3.36
Deep soils	31	10	1.62	0.00	2.79
Sandy soils	8	6	0.38	0.00	1.33
Slope	7	10	0.32	0.00	1.19
Planting 1977-2016	3	NA	0.18	0.00	1.03
Intermediate soils	2	NA	0.10	0.00	0.68

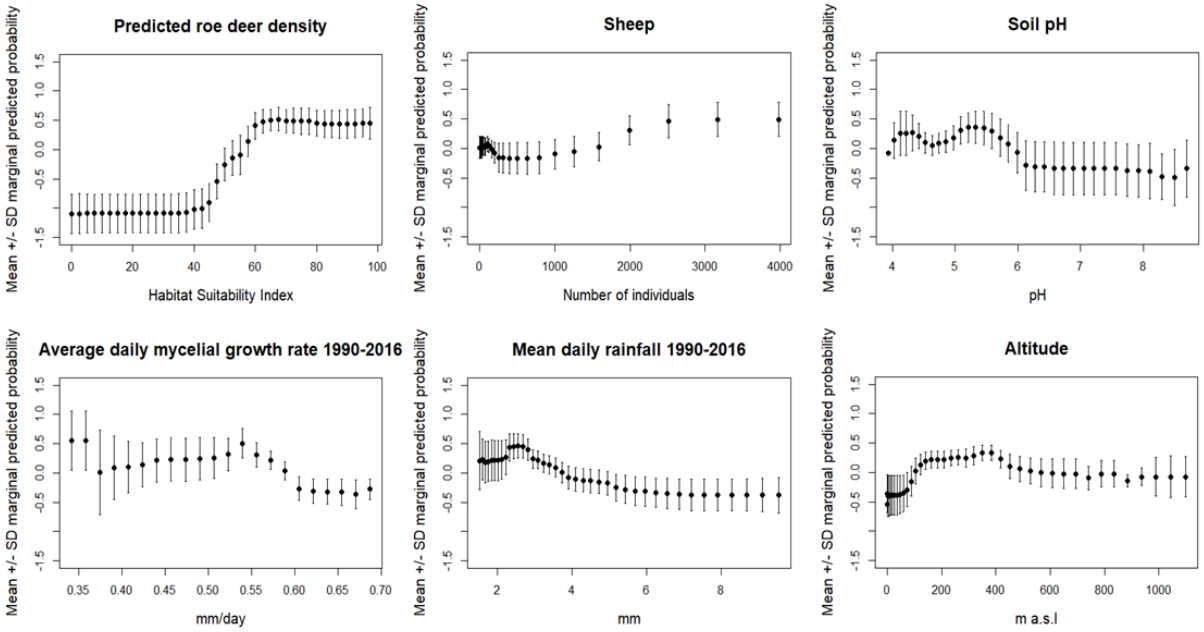

Figure 26. Marginal response plots for key predictors of *P. austrocedri* presence with RI >6 in the BRT with the best Boyce index (0.88) using mean temperature and summarised across 100 iterations of random absence selections.

Pathogen presence corresponded well with areas of high roe deer density and moderately acidic soil pH but this combination of factors was also found in areas where *P. austrocedri* was absent, notably in NW Scotland (Figure 27). NW Scotland is associated with high rainfall but so too are areas in the Lake District where many *P. austrocedri* detections were concentrated (Figure 27). The difference between these two areas may be sheep density that was very high in the Lake District and Pennines, and much lower in juniper tetrads in NW Scotland (Figure 27). Mycelial growth rates were particularly high around mild, coastal fringes of Scotland and Wales where the pathogen was absent, corroborating exploratory lab analyses that some degree of cold shock may be necessary to trigger zoospore release (Frederickson-Matika, D., unpublished data) (Figure 27). Pathogen presence corresponded to areas of higher altitude up to 400m but was absent from higher altitude tetrads where conditions were less suitable for the other predictors, explaining the lower RI of altitude in the best BRT (Figure 27, Table 28).

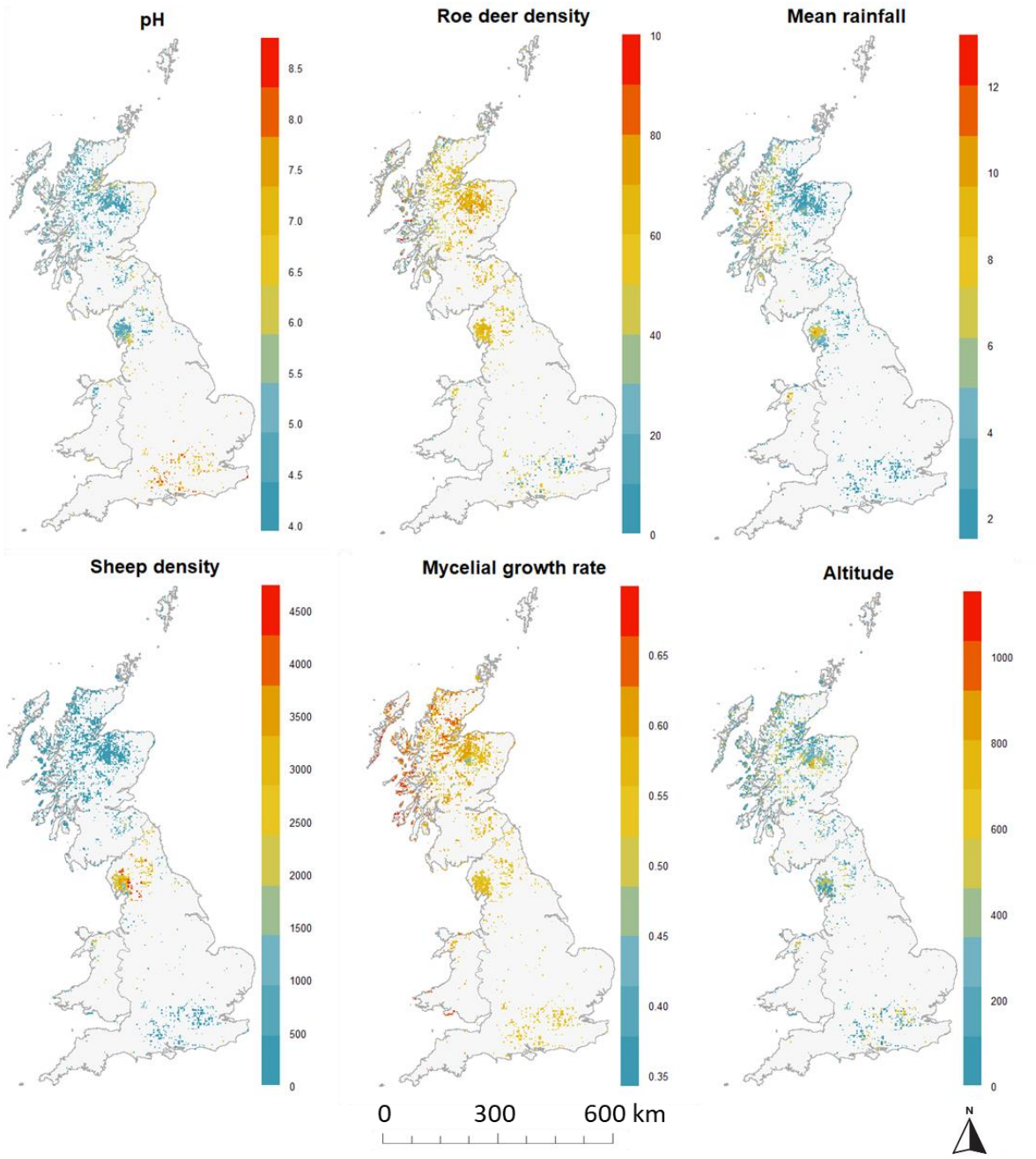

Figure 27. Maps of key predictors of *P. austrocedri* presence with RI >6 in the best BRT as outlined on Table 28. See Figure 22 or Figure 28 for the distribution of *P. austrocedri* presences and Table 26 for data sources of each predictor.

The RI of predictors found in the BRTs was largely different from the responses expected by stakeholders (Table 26, Table 28). Rainfall was given the highest score by stakeholders out of the abiotic predictors suggested and was found to be one of the most important predictors in the best BRT but only with a mode rank importance of 5/10 and mean RI of 9.69 making it considerably less informative than either pH or roe deer density (Table 28). Stakeholders also ranked soil moisture as highly important, likely informed by population level observations where soil moisture has been determined to influence disease severity. However, soil moisture was an unimportant predictor (mean RI 3.48) in the best model and risk factors such as soil pH and altitude with lower stakeholder scores had much higher RI (Table 28). Of the biotic predictors, stakeholders expected juniper planting would best explain *P. austrocedri* presence, followed by the number of recreational users and livestock, then deer, densities (Table 26). Though all four predictors were present in the list of the top ten most important predictors in at least three iterations of the model, their RI in the BRT presented in reverse order. Planting was uninformative and population density had low RI (4.52) while sheep density was more informative than red deer but less so than roe (Table 28).

The predictor combination used in the best model resulted in tetrads with known *P. austrocedri* infection supporting an average of 0.75 mean probability of pathogen presence (PP). Juniper tetrads with highly probable (0.75 PP) and widely predicted (≥80 model iterations) *P. austrocedri* presences were located in the Cairngorms, central lowlands, south-east Scotland, parts of the Lake District and the Pennines where the pathogen has indeed been detected (Figure 28). Presence of *P. austrocedri* was also predicted as highly probable (≥0.75 PP) in juniper tetrads in Northumberland where no positive cases of *P. austrocedri* have yet been identified (Figure 28). Tetrads occupying wider areas around the Cairngorms, central lowlands, Southern Uplands, the Pennines, North York Moors, Peak District, and Snowdonia that are not currently infected were estimated with between 0.50-0.75 PP in >50 model iterations (Figure 28, Appendix N). A few, scattered tetrads in the south of England around uninfected areas in the New Forest and South Downs had slightly elevated PP (~0.50), while the outbreak on Salisbury Plain was predicted with a low PP (~0.40) but the infected tetrads did have higher probability of infection than any in the surrounding area (Figure 28). Overall, the predictions were relatively stable with generally low (~0.15) standard deviation across iterations (Appendix N).

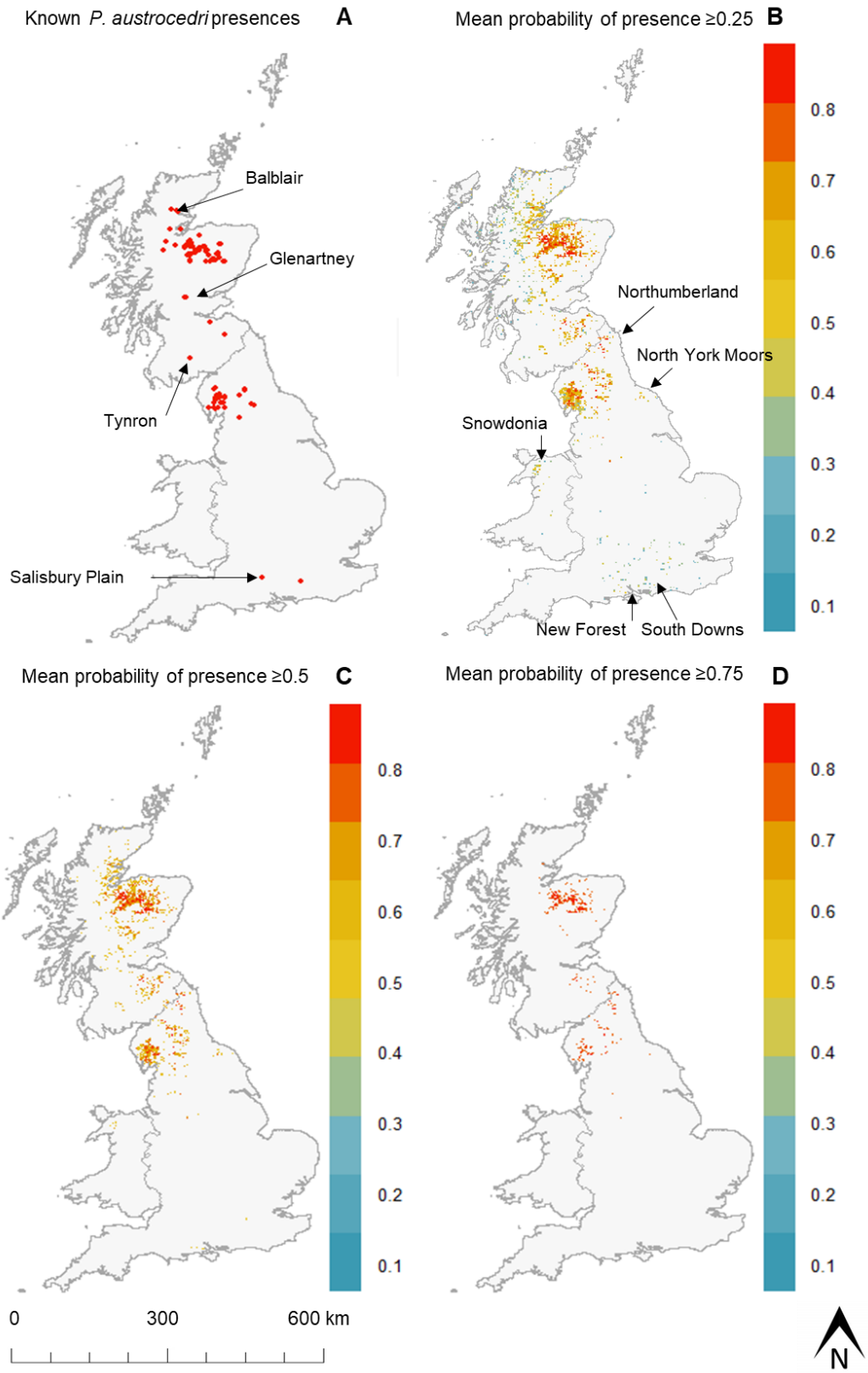

Figure 28. Predictions of *P. austrocedri* presence from the simplified, random absence BRT with the highest Boyce index (0.88). Maps compare the observed presence of *P. austrocedri* per juniper tetrad (2kmx2km grid cell) shown in red (A) with predicted mean probability of presence ≥0.25 (B), ≥0.5 (C) and ≥0.75 (D) calculated across the 100 iterations of the model with different absence selections. Tetrads with highly probable *P. austrocedri* presence are shown in red (B-D).

Eight (19.5%) of the 41 stakeholders contacted submitted feedback about the predictive risk map. One participant had a commercial interest in growing juniper, three participants were employed to advise statutory agencies or environmental charities about juniper regeneration and plant biosecurity, two respondents were employed by statutory agencies to advise about juniper management and assess population fitness, while two participants managed juniper populations on behalf of charitable trusts (Appendix O). Half of the respondents reported confidence in the map, specifically referring to the use of empirical data or the predicted distribution matching their understanding of the known pathogen distribution (Appendix O). The remaining stakeholders expressed their level of confidence in the map as “unsure”. Sources of uncertainty included the lack of accuracy of environmental predictors calculated at a large spatial scale, absence of ground-truthing, uncertainty about the model assumptions, and the modelled importance of roe deer not matching experience at the local level (Appendix O). Seven stakeholders reported uses for the risk map, specified as: i) to raise background understanding of risk, ii) to target surveillance, iii) to inform locations for juniper planting where *P. austrocedri* risk may be lower, and iv) to plan future management and increase associated biosecurity practices, although uncertainty about further specific actions that could be undertaken in high-risk areas was also cited (Appendix O). One stakeholder initially suggested they would recommend deer fencing but when asked how subsequent scrub encroachment would be managed to allow natural regeneration admitted that this required further thought as creating bare ground by hand also has biosecurity implications (Appendix O). Another stakeholder stated they primarily rely on natural juniper regeneration but the risk map would make them “think twice” about supplementary planting given the associated risk of *P. austrocedri* introduction (Appendix O). A third stakeholder requested to overlay the map with recent supplementary planting locations to aid further targeting of surveillance, while a fourth wanted to compare the risk of *P. austrocedri* presence with that of other plant pathogens including different *Phytophthora* species (Appendix O). This stakeholder believed a combined disease map would show much of the country is at high risk of infection with at least one pathogenic species, thus presenting a compelling argument to strengthen biosecurity practices nationwide (Appendix O).

6.5 Discussion

This study offers the first prediction of *P. austrocedri* infection risk for juniper populations across GB and is the first model to examine the impact of supplementary host planting history on the national scale spread of a plant pathogen. The results highlight the difficulty in retrospectively identifying sources of outbreaks associated with historical planting events but demonstrate that spatio-temporal planting metrics could be used more widely in plant pathogen modelling to improve understanding about the likelihood of pathogen introductions and spread. Regarding *P. austrocedri* specifically, the risk map produced by the best model highlights risk factors such as deer and livestock density, and soil pH, may exert greater influence on disease distribution than hitherto considered. It also allows the first comparison of *P. austrocedri* infection of juniper across different spatial scales and suggests predictors driving landscape-scale patterns of infection differ from those acting at the population level. The best model showed high predictive accuracy, correctly identifying some isolated infected tetrads as high risk (including populations in Balblair, Glenartney and Tynron, Figure 28), in addition to locations where outbreaks are widespread (e.g. the Cairngorms and the Lake District, Figure 28). However, the model identified locations with high-moderate infection risk in some areas where *P. austrocedri* is not known to be present and suggests 46% of British juniper tetrads are at considerable risk of infection (≥0.5 mean predicted probability of presence, Figure 28). Relying on a small number of positive locations and their associated underlying conditions could cause over- (or under-) prediction of the infection risk but model validation performed using the Boyce index returned a high predicted-to-expected (P/E) ratio (Boyce index 0.88). The risk map also provides a baseline from which predictions could be improved as further positive cases are detected. The small number of positive locations may indicate that the pathogen is slow to spread at landscape scale so invasion of all tetrads with high predicted risk might be preventable if action is taken to reduce introductions to new populations, including via supplementary planting for conservation purposes. The risk map further identifies areas with low predicted infection risk where it may be especially important to protect populations from other drivers of decline e.g. direct habitat loss and lack of natural regeneration in southern England, and muirburn, inappropriate grazing levels and waterlogging in NW Scotland.

The strongest predictors of *P. austrocedri* presence at national scale were weakly acidic pH and increasing roe deer density. The direction of the pathogen in response to pH aligns with observations of increased infection severity in juniper populations occupying acidic rather than alkaline habitats (Donald et al., 2020). The range and optimum pH at which sporangia

are produced and zoospores encyst differs widely among *Phytophthora* species, some of which can tolerate both extremes of pH 3.0-11.0 (Kong et al., 2009) but fits within the 3.5-6.0 pH ranges tolerated by *Phytophthora* species infecting European oaks, lack of sporangial production at pH <4.0 and optimal sporangial production in *P. syringae* Kleb. and *P. gonapodyides* (Petersen) Buisman at pH 5.0 (Jung et al., 2000). Testing the importance of pH in driving *P. austrocedri* infection of juniper would benefit from the collection of further evidence because the pH map used in the BRTs is itself a prediction generated from a small number of samples (2446 with some nesting within 1kmx1km cells) collected in 2007 (Thomas et al., 2020) (Table 26). The relationship could be further explored by analysing the pH of soil samples collected from underneath infected and uninfected juniper stands and measuring mycelial growth, sporangial formation and zoospore dispersal in cultures grown on media spanning a pH gradient (cf. Kong et al., 2009).

The strong, positive relationship found between *P. austrocedri* presence and roe deer density aligns with the linkage of local pathogen spread across a juniper population in northern England to routes used by deer (and potentially livestock) (Chapter 3) and lower incidence of symptoms in quadrats containing plant species highly palatable to deer that suggested lower grazing pressure (Donald et al., 2020). However, the accuracy of the roe deer density prediction used in this study has not been validated with recent deer counts because these data are largely unavailable (Croft et al., 2019). Predictions of deer density were generated from habitat predictors that may be confounded with *P. austrocedri* presence or other included predictors e.g. temperature and rainfall patterns. Although correlations between roe deer density, mean temperature and mean rainfall were weak (r^2 -0.4, -0.1 respectively) (Appendix M), relatively strong mean interactions were detected in the best model between roe deer density, mean rainfall and sheep density (Appendix N), potentially inflating the relative importance of roe deer density in the BRTs. Directly incorporating dispersal constraints into models of *P. austrocedri* distribution would improve understanding of the potential risk of vectored pathogen spread. However, the relationship is certainly consistent with increased dispersion and area of Chilean cedar infected with *P. austrocedri* in a 30kmx30km area Patagonia under different grazing scenarios (disease prevalence increased with free roaming cattle) (La Manna et al., 2013b). Roe deer are more likely to overlap with juniper tetrads than red deer because they preferentially occupy woodland edges (British Deer Society, n.d.), and during the breeding season, bucks display territorial marking behaviour that includes scraping the ground (Johansson and Liberg, 1996), potentially increasing the likelihood of hooves disturbing, collecting and transporting infested soil. Roe deer typically occupy small territories (<200ha equivalent to a tetrad)

(Linnell and Andersen, 1998; Lovari et al., 2017) although the size varies according to habitat type (territory size decreases in forests) (Lovari et al., 2017) and season (ranges extend outside of the breeding season) (Linnell and Andersen, 1998) so increased pathogen presence is less likely to result from long-distance movements of deer between infected juniper populations. A more credible hypothesis is the transport of inoculum from soil surrounding non-target hosts, from where *P. austrocedri* was frequently amplified in public gardens and amenity woodlands (Riddell et al., 2019), to juniper stands as the deer range between peri-urban habitats, farm- and woodlands (British Deer Society, n.d.). The role of deer and livestock in perpetuating *P. austrocedri* spread poses difficult questions about potential disease control methods but is another facet to add to evolving discussions between land managers and policy makers about deer management practices and stocking densities required to facilitate habitat restoration (Burton et al., 2019; Scottish Government, 2014; Spake et al., 2020).

Though *Phytophthora* rely on water for growth and dispersal, soil moisture was uninformative at this scale, suggesting *P. austrocedri* presence was not limited by soil moisture when modelled and averaged across tetrads but instead modulates infection mechanisms operating at a finer scale (e.g. zoospore release) (Donald et al., 2020). Mean rainfall had only moderate relative importance in the best BRT and pathogen presence declined after a threshold of ~3mm/day. This threshold aligns with rainfall averages reported from infected locations in Argentina (e.g. 15-170mm monthly precipitation in Bariloche (WWIS, 2021a)) and Iran (0-52mm monthly precipitation in Qazvin (WWIS, 2021b)) and could represent optimal rainfall for the pathogen, or suggest there is sufficient rainfall in most parts of GB for sporangial growth and zoospore release but that other factors, such as pH, become limiting. Locations infected with *P. austrocedri* globally also share temperature regimes with significant cold spells (e.g. average monthly minimum temperature is -1.6 in Bariloche (WWIS, 2021a) and -4.7 in Qazvin (WWIS, 2021b)) and mild temperatures, especially in invaded natural areas in Patagonia where the average annual mean temperature is 9.38°C (La Manna et al., 2012). In our study, mean temperature was more informative than minimum temperature but the negative relationship between *P. austrocedri* presence and mycelial growth rate may indicate the requirement for a cold shock to trigger zoospore release as observed in exploratory laboratory analyses (Frederickson-Matika, D., unpublished data). Additional explanations for this inverse relationship could be a lower frequency of inoculum introduction via transport, recreational, livestock or supplementary planting pathways given the remoteness of these largely western, coastal locations and/or predominant distribution of *J. communis* subsp. *nana* that tends to grow at a lower density

than *J. communis* subsp. *communis*. There was no correlation (r^2 <0.8) or interaction between minimum temperatures and mean rainfall in the models (Appendix N) and both climate suitability and periods of optimal temperature performed poorly suggesting that our characterisation of optimal conditions was too limiting. However, greater probability of pathogen presence was predicted in locations that experience colder temperatures (Cairngorms, Southern Uplands, and the Pennines) compared to coastal tetrads across GB and tetrads in southern England where minimum temperatures averaged >5°C (Appendix M).

In response to altitude, *P. austrocedri* incidence was highest in Argentina at the lower end of the examined 350-950m range (La Manna et al., 2008b) and increased in juniper up to 400m. Increasing presence of *P. austrocedri* with increasing altitude may result from an interaction with temperature but in GB could relate to increasing juniper density, shown to accelerate colonisation of stands at field scale (Donald et al., 2020). The altitudinal limit for juniper is 975m in the UK (Preston et al., 2002) but it usually occupies altitudes >500m as a small, scattered component of montane scrub communities (Thomas et al., 2007) with denser stands, particularly of the larger and denser *J. communis* subsp. *communis* form, concentrated between 200 and 400m (Clifton et al., 1997; Lavery, 2016; Thomas et al., 2007; Cumbria Wildlife Trust, 2014). The importance of soil textures in explaining patterns of *P. austrocedri* infection of Chilean cedar was not replicated in British juniper populations, either because these factors relate to soil moisture and processes operating at a finer spatial scale or because our characterisation of soil texture and depth did not capture important edaphic conditions that promote pathogen occurrence.

Supplementary juniper planting was seldom included as a top ten informative predictor of pathogen presence in the BRTs. The map of planting events is known to under-represent the true scale of juniper planting (Donald et al., 2021) and the binary characterisation of planting as present/absent masks important nuances such as the settings used to raise material, and the size and frequency of plantings that alter its risk as an introductory pathway (Donald et al., 2021). DNA of *P. austrocedri* was amplified from root and water samples collected from British plant nurseries between 2016 and 2018 (Green et al., 2021a), mainly associated with juniper and other Cupressaceae hosts. Pathogen DNA was also detected in soil samples collected from thirteen Scottish public gardens, arboreta and amenity woodlands in 2014 and 2015 (Riddell et al., 2019) as well as in soils associated with recent plantings (Landa et al., 2021). In these latter two studies, the soil samples were largely collected from around plant species not known to be *P. austrocedri* hosts, suggesting that the pathogen can survive in

soil in the absence of infected host material, or can associate with a much broader range of plant species than is currently thought (Riddell et al, 2019). Thus, pathogen introductions to juniper populations could be aided by planting of other species, not restricted to juniper or other Cupressaceae. Calculating the presence of planting over different time periods yielded little change in model accuracy, excepting the most recent calculation (2007-2016) that resulted in substantially worse model performance. The largest number of tetrads were planted during this period so improved model performance associated with older planting locations lends weight to assertions that *P. austrocedri* was introduced to the UK at least one decade before first detection (Green et al., 2015; Riddell et al., 2020) and concern that new infections remain undetectable for several years following initial introduction. Improved data collection regarding tree planting conducted outside of the forestry sector could, therefore, have compound benefits for understanding a range of plant pathogen invasions. Such improvements could be achieved by digitising planting maps supplied with applications for planning permission or woodland grants (Donald et al., 2021) and funding the collection and use of high resolution satellite imagery to detect changes in canopy cover and early onset disease symptoms (JNCC, 2020). Despite the lower importance of previous planting events as a disease risk factor, stakeholders noted they would still use the risk map to inform their assessment of new planting proposals.

Neither population density nor river length had high relative importance in the best model but both were present as top ten predictors in more than 50 iterations showing they contributed some predictive information (Table 28). Both measures performed better when calculated over a smaller radius (population density in 3.2km, river length within the tetrad), potentially explained by increased force of infection within short distances (i.e. more recreational visits occur at shorter distances) and the short-lived nature of zoospores. It is also interesting to note that river length was more informative than distance to the nearest river that was never present as a top ten predictor, again illustrating the difference in drivers between microsites and landscape scales (Donald et al., 2020).

Selecting pathogen “absences” randomly from tetrads where *P. austrocedri* was not positively detected yielded higher Boyce indices than visited tetrads with no reports of symptoms or positive qPCR tests. Many of the visited locations were situated in northern England, leading to underprediction of actual pathogen presence in the Lake District where some of the test locations used to calculate the Boyce index were situated (Appendix N). The difference in model accuracy most likely results from the increased number of random tetrads from which to draw different absence selections and the associated range of

conditions available to train the models (Figure 23). However, the selection of visited tetrads may be flawed in that many populations were visited because they occurred close to infected populations so the difference in predictors between infected and uninfected tetrads was negligible at landscape scale and the model is correctly predicting those tetrads that are at higher risk of infection. Furthermore, samples that tested negative with qPCR would only be collected where symptoms were suspected, so juniper may have been infected at the time of visit but the lesion was inactive or difficult to locate. Widening surveillance across a broader geographical area and reporting visited locations without symptoms would likely lead to improved detection rates and predictive capability for infection risk.

The small sample size of stakeholders who provided feedback about the *P. austrocedri* risk map makes it unwise to speculate as to if involving them in describing and ranking input predictors improved their confidence in the results. The stakeholders who responded broadly considered that the risk map was useful to raise awareness of potential pathogen spread and intensity, and to target surveillance in conjunction with other information (e.g. recent plantings). A recent study found optimal disease detection methods differed depending on the sensitivity of the detection method used and generally improved when inspections were conducted across a landscape rather than solely focusing on high risk areas (Mastin et al., 2020). The risk map could, therefore, be used to ensure juniper populations spanning a range of different predicted presence probabilities are monitored to optimise detection likelihood. Both the stakeholder feedback concerned about the applicability of the results at such a large spatial scale, and the difference in ranking between risk factors identified as most important by stakeholders compared to the best model, demonstrate the local focus of many disease management decisions. We expected that the risk map could be used to better co-ordinate juniper conservation actions across the country and find synergies between management strategies that could address pathogen invasion at multiple spatial scales. These uses were not identified by stakeholders, half of whom had strategic or advisory roles at a national level. This could suggest strategic frameworks to manage plant pest and disease outbreaks at larger spatial scales require further development. However, the poor number of stakeholder responses to the interactive map and suggestions regarding its utility also suggest presenting outputs as a standalone risk map is an ineffective means to communicate risk for which additional means of engagement between researchers and decision-makers are required (Barwell, 2021a; Jones and Kleczkowski, 2020).

In summary, our findings show local management is complimentary to management that will address national disease drivers. For example, drier microsites are at lower risk of infection

(Donald et al., 2020) as are tetrads with lower rainfall. Not only will natural juniper regeneration, encouraged by cattle grazing or scarification, benefit the genetic resilience of juniper populations to disease (Broome et al., 2017), it could also reduce the risk of inoculum introductions via supplementary plantings to new areas with or without high risk of infection. Many juniper populations in north/central and southern Scotland, northern England and mid Wales are at high risk of infection (Figure 28) that might be mitigated by reducing livestock and deer densities but while fencing herbviores out may lower the risk of inoculum transport it will hinder regeneration if juniper seedlings are then outcompeted by grasses, so some level of herbivory/scrub control is required (Wilkins and Duckworth, 2011b). If the risk of pathogen spread through human-mediated pathways such as supplementary planting and the movement of infected soil and water can be reduced, a diversity of approaches to manage the other risk factors, as appropriate to local conditions (e.g. drainage, grazing pressure), may afford the best overall outcomes for juniper conservation. Improving biosecurity along planting and livestock pathways could prevent infection increasing from ~1% to the predicted 11% of juniper tetrads with highly suitable (mean predicted probability ≥75%) conditions to host *P. austrocedri*. However, these measures will also have much wider benefit in preventing the spread of existing and emerging infectious diseases: a view independently described by a stakeholder providing feedback about the *P. austrocedri* risk map, and which may become increasingly important as land use change, habitat restoration and tree planting accelerate to meet ambitious biodiversity restoration and carbon sequestration targets (Committee on Climate Change, 2020; IPBES, 2019).

Chapter 7

Discussion

7.1 Summary

To understand how factors promoting disease introduction, establishment and spread vary with spatial scale, I collected, integrated, and modelled the spatial distributions of *P. austrocedri* and its UK host, common juniper, with abiotic and biotic covariates at both local and national scales. Data were collected using detailed field surveys, molecular detection methods, and image analysis, combining existing environmental datasets with newly derived covariates that captured important characteristics of *P. austrocedri* biology and invasion pathways mediated by people and wildlife. I employed a variety of state-of-the-art, spatially explicit, statistical modelling techniques to provide the first insights into environmental and land management processes governing the arrival and spread of the pathogen, and to understand how topography, climate, hydrology, grazing pressure, and host community structure interact to favour disease establishment in common juniper populations across the UK at field to national scales. Using participatory approaches, I actively involved a variety of cross-sectoral stakeholders in identifying risk factors and spread pathways, in collecting and modelling data, and in understanding how research outputs and models could be better disseminated to inform management decisions made by practitioners across different sectors. The following sections interpret the findings in view of prior knowledge and approaches in the field, identify critical remaining knowledge gaps to improve understanding, prediction, and management of *P. austrocedri* and consolidate the juniper management recommendations.

7.2 Supplementary planting as a potential introductory pathway for plant pathogens: the *P. austrocedri* example

The importation of live plants, or the “plants for planting” pathway, is the most common introductory pathway for plant pests and pathogens globally (Brasier, 2008). This pathway was estimated to be responsible for ~70% of 81 economically damaging forest insects and pathogens introduced to the United States between 1860 and 2006 (Liebhold et al., 2012), 57% of 123 invasive forest pathogens introduced to Europe since 1800 (Santini et al., 2013) and 90% of 114 human-assisted introductions of non-native invertebrate plant pests to the UK from 1970 to 2004 (Smith et al., 2007). Yet the volume of live plant imports continues to

increase (Hulme, 2009; Tradingeconomics.com and HM Customs and Excise, 2021), in part driven by ambitious tree planting targets to restore habitats, mitigate flooding, and sequester carbon (IUCN, 2020; Coomes et al., 2021; UN, 2020) that cannot currently be met in the UK without importing trees (Reid et al., 2021). Phytosanitary inspections of plants for planting are failing to prevent new invasions, with US border inspections missing an estimated 72% of infested shipments (Liebhold et al., 2012) and highly variable rates of inspection effectiveness implemented by different European countries (Eschen et al., 2015). However, very little empirical evidence exists documenting the rates of plant pest and pathogen introductions at sub-national spatial scales in relation to the live plant trade, and even then outbreaks are assessed in relation to nursery networks (Harwood et al., 2009; Moslonka-Lefebvre et al., 2011) rather than planting events.

Thus, the investigation of risk factors associated with juniper planting, such as source nurseries and planting frequency, using a newly compiled dataset of juniper planting locations (Chapter 4), is an important contribution to this substantial knowledge gap (Freer-Smith and Webber, 2017; Roy et al., 2014). The dataset also permitted the importance of juniper planting relative to other abiotic and biotic drivers of disease distributions to be investigated (Chapter 6), previously only explored by one study that linked *P. cinnamomi* infection of oaks (*Quercus* spp.) in SW Spain with increasing proximity to areas of subsidised afforestation (Fernández-habas et al., 2019). Juniper planting was a poor predictor of the current GB distribution of *P. austrocedri* but models including historical planting locations outperformed those using only locations from the past ten years (Table 27). This highlights the difficulty in retrospectively linking introductory pathways to established disease outbreaks in complex landscapes where novel pathogens can be sparsely recorded by passive surveillance systems and multiple processes have likely governed pathogen spread.

Improved data collection from standardised monitoring of new plantings, repeated at multiple time intervals, for planting schemes conducted using different source material and numbers of trees across different geographical areas, would permit more detailed analyses of outbreak patterns and potential risk factors, identify biosecurity practices to mitigate such risks, and could explore the cost-benefit trade-offs of implementing such practices to control different organisms (Bate et al., 2016). Such data could be collated in a centralised repository (Barwell et al., 2021b), drawing together records of pest, pathogen and host distributions across sectors to fully capture pathogen behaviour. This could include digitised locations of new planting schemes awarded planning permission or grant support

(Cummings, 2021), monitoring data collected from publicly, privately, and charitably owned land in the wider environment, and data collected from nurseries to audit compliance with new plants for planting biosecurity accreditation schemes (Nursery Industry Accreditation Scheme Australia, 2019; Frankel et al., 2020; Plant Health Alliance Steering Group, 2019). Successful biosecurity strategies could also be shared on this platform or, if favoured by practitioners, on existing websites such as Conservation Evidence (conservationevidence.com) or Collaboration of Environmental Evidence (http://www.environmentalevidence.org/) that aim to synthesise (and translate) accessible summaries of management results in globally available, free, online repositories. Practitioners involved in juniper management identified use cases for such data (Table 23), potential data sources, collection methods and hosting platforms (Appendix L.4, Figure L3) that policymakers, guided by further cross-sector stakeholder engagement, could use to enhance surveillance strategies and information dissemination.

Monitoring for plant pests and pathogens will be critical to understanding and improving the success of habitat creation or restoration projects. Juniper planting was widely used as a conservation measure despite limited evidence that it is delivering the desired outcomes of increased natural regeneration and population age, sex, and genetic diversification (Table 13). Not only does juniper planting risk introducing *P. austrocedri* to new populations (Chapter 4), restoring populations from cuttings limits their genetic diversity (Broome, 2003) with potentially negative consequences for disease resistance (Green et al., 2021b). Interviews with Scottish land managers about the biosecurity risks from large-scale tree plantings conducted for environmental benefits (Dunn et al., 2021), and responses to the juniper management decision support tools survey (Chapter 5), both identified practitioners who believed juniper populations were at greater risk of collapse from lack of regeneration than from *P. austrocedri* and sought to conserve populations by supplementary planting. The longevity of juniper trees means regeneration can occur very infrequently without negative population consequences, so introducing new plants may be less important than managing faster acting, destructive, processes such as disease, muirburn and overgrazing that can cause rapid population-level mortality (Ward and Shellswell, 2017). Unfortunately, my research found *P. austrocedri* is now present in the Scottish juniper conservation zone containing the most viable populations with the lowest requirement for supplementary planting (Figure 17) and is well established in the largest juniper populations in northern England that are at high risk of further pathogen spread (Figure 28). Juniper populations with the lowest prediction of *P. austrocedri* infection risk are situated in NW Scotland and in Wales (Figure 28), where *J. communis* subsp. *nana* predominates (Thomas et al., 2007) and

is rarely subject to planting (Figure 14). Molecular detection methods confirmed *P. austrocedri* infection of some juniper populations in the south of England, but the pathogen could not be isolated into culture and the environmental conditions mean it is unlikely to establish (Figure 28). Use of supplementary planting to reverse population declines in this area may, therefore, be beneficial if implemented with disease-free material of local provenance (Figure 28). In the remaining locations, *P. austrocedri* is likely to spread, causing mortality that land managers may want, or be incentivised, to address by planting juniper. This underlines the need to develop guidance with practitioners to better understand and address motivations for planting and to improve the applicability and adoption of any revised management proposals.

However, though managing risks specifically associated with juniper planting may reduce *P. austrocedri* spread, concurrent research revealed high *Phytophthora* spp. abundance and diversity (including *P. austrocedri*) in soils sampled from Scottish public gardens, arboreta and amenity woodlands subject to ornamental plantings, even in the absence of host species (Landa et al., 2021; Riddell et al., 2019). This is consistent with increasing *Phytophthora* species richness found along a gradient of increased human activity and the matching of species found in infested forests to those found in plant nurseries (Redondo et al., 2018b). The disease risk posed by moving infested soil with non-host species was recognised by a participant in the decision tool survey who raised concern that planting trees other than juniper may still introduce *P. austrocedri* (Assessor 5, Chapter 5). A second participant commented that intersecting the national risk of *P. austrocedri* with risk maps for other species, e.g. *P. ramorum*, would highlight the need for increased biosecurity across the country “as a matter of course, rather than in response to individual diseases.” (Assessor 8, Appendix O). An appetite already exists, therefore, for a wider, cross-sector conversation about biosecurity along the plants for planting pathway that could deliver improved plant health outcomes not only within the horticultural, agricultural and forestry industries but also for the wider environment, as advocated by many other research studies (Chapman et al., 2017; Potter and Urquhart, 2017; Roy et al., 2014, 2017).

7.3 Environmental drivers promoting *P. austrocedri* establishment and spread across spatial scales

Previous modelling studies exploring factors promoting plant pathogen establishment and spread in the wider environment have largely focused on abiotic drivers such as topography and climate, coupled with a small number of key biotic drivers e.g. host abundance measured as the number of host stems (Condeso and Meentemeyer, 2007) or an index of

host habitat suitability (Hernández-Lambraño et al., 2018), proximity to spread pathways including roads (Giordana et al., 2020; Grosdidier et al., 2020; Peterson et al., 2014) and wildlife trails (Jules et al., 2002), or gradients of human population density (Cushman and Meentemeyer, 2008) and international travel volumes (Gottwald et al., 2019). The expanded number and range of potential biotic drivers included in models exploring *P. austrocedri* establishment and spread is, therefore, a key novelty of this thesis. Biotic factors used in my research rarely considered in previous wider environment plant disease models include explicit measures of host connectivity (Chapter 2-Chapter 3), associated vascular plant species (Chapter 2), direct herbivore damage (Chapter 2) and herbivore density (Chapter 6), proximity to footpaths (Chapter 2-Chapter 3), potential numbers of recreational visitors (Chapter 6) and host plantings (Chapter 6). In addition, I explored how the importance of these potential drivers differed with spatial scale (Dillon et al., 2014), particularly those operating within populations where management to alter disease dynamics is most often applied.

7.3.1 Abiotic drivers

At both population and national scales, the strongest relationships were obtained between *P. austrocedri* presence and intensity, and abiotic drivers of establishment and spread. Acidic soil pH was the strongest predictor of *P. austrocedri* presence nationally (Table 28), while at the population level, symptom severity increased with increasing soil moisture directly sampled from deep soils or with decreasing proximity to watercourses on shallow soils (TablesTable **5**-7). This was predicted by stakeholders involved in managing juniper who ranked soil moisture as the highest risk factor for *P. austrocedri* infection (Figure 19, Table 26). Microsite soil moisture also influenced the availability of host trees, with decreasing juniper presence associated with increasingly wet microsites (Figure H2). Further research is needed to understand if disease incidence was higher in waterlogged microsites because of improved *P. austrocedri* dispersal and/or reduced host fitness.

This has wider implications for host-pathogen dynamics under climate change where forests are increasingly stressed by drought and flood events altering host susceptibility to disease (Brown, et al., 2018; Homet et al., 2019). Such analyses are limited, however, by a lack of fine scale hydrological data. Characterisation of soil moisture currently requires extremely labour intensive data collection using soil moisture probes (Chapter 2, La Manna and Rajchenberg, 2004a; Nagle et al., 2010) or proxy measures such as topographic wetness index (TWI) (Anacker et al., 2008; Meentemeyer et al., 2008a). TWI varies in accuracy according to geology and surface to subsurface topography, not to mention the resolution of

the input digital elevation model and algorithms used to calculate the index (Drover et al., 2015; Kopecký and Čížková, 2010) and always performed poorly in models of *P. austrocedri* distribution despite the strong association with soil moisture measured in the field (Chapter 2-Chapter 3). Distributed hydrological models show improved performance compared to TWI but require detailed input parameters about soil type and groundwater flows that generally prohibit their use below 1km resolution (Grabs et al., 2009; Pechlivanidis et al., 2010). An important novelty of my research, therefore, was the discovery that plant species could be successfully used as alternative proxies for soil moisture or other factors influencing disease distributions (Table 4). In the population survey of juniper occupying a heathland habitat, cross-leaved heath (*Erica tetralix)* was the best predictor of *P. austrocedri* symptoms owing to its preference for wet (but not waterlogged) soils (Table 7). This species also prefers very acidic soil pH (Table 3), linking the field scale observations of disease severity to national scale *P. austrocedri* presence (Table 28). Vascular plant associations could, therefore, be used to greater effect by land managers and plant health inspectors to identify microsites at increased risk of infection.

7.3.2 Host connectivity

For soil-borne pathogens, increasing host density enables greater contact between pathogen inoculum and host roots, promoting disease establishment (Jules et al., 2002). Few studies of forest pathogens have, however, investigated how this is mediated by patterns of host connectivity or fragmentation. No strong relationships were detected between juniper connectivity characterised within 10x10m field quadrats and the encompassing 30x30m area (Figure 6) and *P. austrocedri* symptom severity (Table 5-7), or patterns of *P. austrocedri* colonisation in relation to juniper patch density and mean patch area (Table 9) at 10x10m or 25x25m spatial resolutions (Appendix I.1.3 and I.2.3). A subsequent investigation of *P. cinnamomi* infection of holm (*Quercus ilex*) and cork (*Quercus suber*) oak hosts across ~34ha of mixed habitats in Spain similarly found no relationship between infection intensity and host connectivity categorised as either “connected”, where vegetation units were contiguous with other forest stands, or “isolated” if surrounded by crops (Cardillo et al., 2021). Discrete characterisations of host connectivity may poorly encapsulate characteristics modulating disease establishment and spread, so future research could harness the increasing availability of high-resolution satellite, aerial or LiDAR imagery to derive more informative, continuous variables of host connectivity, and to test the importance of connectivity at larger spatial scales. However, the combined findings cited above suggest the spread of soil-borne pathogens is unlikely to be limited by host

connectivity where human, wildlife and livestock vectors can transport infectious propagules within and between populations. This is consistent with the “dispersal scaling hypothesis” that predicts dispersal will be maximised where the scale of spatial heterogeneity (e.g. host patch size) matches the intermediate gap-crossing ability of the dispersing agent (e.g. seeds, zoospores, or insects) (Skelsey et al., 2013). Studies including measures of host population connectivity would, therefore, be best explored in conjunction with covariates capturing these alternative spread pathways.

7.3.3 Vector mediated spread pathways

I attempted to characterise vector mediated pathways in models applied at both population and national spatial scales, accounting for both the natural dispersal of zoospores in soil water and potential pathways for passive inoculum transfer in contaminated soil by livestock, deer and people (Hansen et al., 2000). Hypothesised associations between *Phytophthora* forest disease establishment and these potential spread pathways were previously based on observations of disease distribution patterns (Green et al., 2015; La Manna et al., 2008), surveying symptoms along roads (Jules et al., 2015) or identifying pathogen DNA from soil samples collected from hiking trails (Cushman and Meentemeyer, 2008) or scraped from animal hooves (Krull et al., 2013). Incorporating covariates such as distances to the nearest footpath, lengths of roads, densities of sheep and deer, and potential recreational pressure (Chapter 2, Chapter 3 and Chapter 6) in spatially explicit disease models permitted explicit testing of the spatial relationships across heterogeneous landscapes, separating out responses from human and herbivore mediated spread pathways. While these covariates require further refinement (e.g. by basing deer density predictions on counts rather than habitat suitability or recreational population density calculations on road network distances rather than a radius), they leveraged existing data to allow an understanding of the relative importance of these pathways compared to other disease drivers to inform management decisions.

Livestock and deer were found to aid *P. austrocedri* establishment and spread at both population (Chapter 2-Chapter 3) and national (Chapter 6) scales. No relationship between direct herbivory and symptom severity measured in field quadrats was found (Table 5-7), suggesting the relationships between herbivore density and pathogen presence or intensity did not result from herbivore damage reducing host fitness but instead the passive transport of inoculum. The national scale likelihood of *P. austrocedri* presence increased with both increasing sheep and roe deer (*Capreolus capreolus*) density but the relationship with roe deer was stronger (Table 28, Figure 26). This is perhaps unsurprising as deer can transport

larger volumes of contaminated soil than sheep, and over longer distances where their movements are less constrained by fences. Deer density also more likely accounted for the negative relationship discovered between bramble (*Rubus fruticosus*) abundance and *P. austrocedri* symptoms at population scale (Table 6), with the vascular plant indicator again linking population and national level responses. Population level vectoring of soil-borne *Phytophthora* by wildlife was also suspected in Spain, where both red deer (*Cervus elaphus*) and wild boar (*Sus scrofa* L.) were implicated in the higher incidence of *P. cinnamomi* found in dense oak stands used by ungulates for shelter, and in pathogen transmission >250m from the nearest infected host (Cardillo et al., 2021).

Three stakeholders involved in juniper management expressed scepticism about the impact of livestock and deer in mediating *P. austrocedri* spread, although concern about the latter was more related to the species specificity rather than deer as potential vectors of inoculum (Table O1). More empirical evidence is needed to understand the magnitude of livestock and deer vectored disease spread, potentially by comparing rates of spread in areas with and without ungulates (Velez et al., 2020) or swabbing their hooves (Krull et al., 2013) and correlating the resulting pathogen abundance with patterns of habitat use. Further engagement is also required with stakeholders to understand how management practices could be adapted to mitigate livestock and deer mediated *P. austrocedri* spread, including a review of the onerous livestock quarantine recommendations made in the DEFRA juniper management guidelines (DEFRA, 2017) that would not account for transmission by deer.

7.4 Predicted rates of *P. austrocedri* spread

When *Phytophthora* species were ranked by invasiveness, *P. austrocedri* appeared in the mid-low range, resulting from its limited global distribution and small number of known host species (Scott et al., 2019). Nonetheless, when in contact with susceptible hosts the pathogen can cause extensive tree mortality (Green et al., 2015; Greslebin and Hansen, 2010), and many British juniper populations are predicted to be at risk from future invasion (Figure 28). Using dispersal kernels to predict rates of population scale spread of plant pathogens is not new but has been more often implemented in mechanistic than statistical models of disease spread, commonly in agricultural settings where host plants are not explicitly modelled (Chapman et al., 2017b). Previous studies often had access to large volumes of experimental or field collected spread data e.g. hundreds of *Hymenoscyphus fraxineus* spore traps (Grosdidier et al., 2018), or 890 *P. ramorum* field plots containing two 50x10m transects (Meentemeyer et al., 2008a), collected over many repeat surveys e.g. Asiatic citrus canker of citrus tree hosts in Florida at 30 day intervals between 1997 and

1999 (Neri et al., 2014) or four aerial surveys of *P. cinnamomi* infected oak woodlands collected over a 35 year period (Cardillo et al., 2021). By contrast, my research into patterns of *P. austrocedri* colonisation of juniper demonstrates that dispersal kernels derived from a single repeat survey can be integrated with fine scale measurements of abiotic and biotic drivers and pathways to disentangle factors promoting host colonisation and provide initial predictions as to the likely trajectory and mechanisms of spread (Chapter 3). Local and longer-distance spread processes operating within the same system were not only predicted for *P. austrocedri* infection of juniper, where most dispersal occurred within short (<500m) distances of the nearest infected host alongside evidence for longer distance dispersal (>800m), but also for other soil-borne *Phytophthora* species including *P. lateralis* infection of Port-Orford cedar (*Chamaecyparis lawsoniana*) on the California-Oregon border (Jules et al., 2015) and *P. cinnamomi* spread in Spanish oak woodlands (Cardillo et al., 2021), and also of wind-dispersed *P. ramorum* infection of host trees across California (Meentemeyer et al., 2011). Indeed support for fat-tailed, power-law distributed dispersal kernels was obtained for a variety of plant pathogens including viruses and fungi as well as oomycetes (Fabre et al., 2020). Future studies could concentrate on teasing out the different dispersal kernels associated with natural and vectored spread pathways (Chapman et al., 2017b), to supply land managers with key evidence to support implementation of potentially unpopular biosecurity measures. For example, the impact of vehicle washing or lower stocking densities on the disease dispersal kernels and the resultant patterns of disease spread could be estimated. Conducting such analyses and empirical research using a participatory framework would ensure the research addresses the knowledge gaps required to inform management decisions and increase the accessibility of the results (Barwell et al., 2021b; Petrasova et al., 2020).

7.5 Lessons learned from stakeholder engagement

Different tools have been developed by researchers to aid development of plant health management strategies, primarily using statistical or epidemiological models including:

- horizon-scanning models that identify and rank future plant health threats based on biological traits linked to invasion success at different stages of the invasion pathway (Barwell et al., 2021a) or the phylogenetic relatedness of host plants susceptible to existing invasive species (Gilbert et al., 2015);
- global network models that explore patterns of new detections and international trade connectivity (Chapman et al., 2017a) as well as national or regional network models

that explore links between nursery trade patterns and outbreaks (Harwood et al. 2009);

- ecological niche models that predict the likelihood of pathogen establishment and spread in response to environmental drivers and/or future climate scenarios at global (Bebber et al., 2014; Burgess et al., 2017) or landscape scales (Duque-Lazo et al., 2018; Meentemeyer et al., 2011);
- spread models that simulate pathogen distributions in response to potential detection (Mastin et al., 2020) or control strategies applied at the landscape (Cunniffe et al., 2016; Tonini et al., 2017) or local (Bate et al., 2016) scale.

Additional tools include the collation of information in databases e.g. risk registers (DEFRA, 2015), trait databases (Barwell et al., 2021a) and decision support tools such as the European and Mediterranean Plant Protection Organisation (EPPO) computer assisted pest risk analysis tool (EPPO, 2011) and maps of quarantine or conservation zones (Forestry Commission Scotland, 2013). These tools are currently used most often to inform policy level decision making operating at regional and national scales and focus more frequently on the introduction and establishment compared to future spread and impact phases of the invasion pathway (Barwell et al., 2021b). Yet these tools offer huge potential to incorporate local knowledge and experience, improve engagement and support decision-making with practitioners operating at the site level, who are criticially involved in deploying adaptive management responses to plant health threats (McAllister et al., 2015). While all stages of tool design may not require all, or any, input from stakeholders, and the need for intensive vs extensive participation should always be considered (Voinov et al., 2016), including specific end-users in the framing, knowledge integration and testing of decision tools is likely to improve their utility and longevity of use (Reed, 2008). However, few plant health studies have to date co-designed models with stakeholders (Gaydos et al., 2019). The survey of practitioners involved in managing, growing, advising and assessing UK juniper populations showed the overwhelming importance of co-design to improve the relevance of decision tools to stakeholders, primarily by improving their accessibility, comprehensiveness and applicability (Jones and Kleczkowski, 2020). Where stakeholders had prior knowledge of the guidelines, the DEFRA decision framework was used to implement beneficial juniper management accounting for *P. austrocedri* risk but its wider application was hindered by low awareness of the guidelines. The first step to achieving this would be thorough mapping of the stakeholder landscape with regard to their different roles, geographical remit and needs for decision support. The juniper management guidelines were devised with land managers, conservationists and plant nurseries in mind (DEFRA, 2017), overlooking the important roles

played by advisory agents, landscapers, gin producers and farmers to maintain healthy juniper populations (Chapter 5).

A simulation study of citrus huanglongbing predicted disease control would be more successful where stakeholders were informed of the effectiveness of control measures instead of prematurely increasing perceptions of infection risk (Milne et al., 2020). This was borne out by stakeholder responses to the juniper surveys, where participants were equivocal about the accuracy of the national *P. austrocedri* risk map, despite involving stakeholders in its production (Appendix O). Stakeholders instead preferred information to be presented at the local level alongside the decision framework amended to include a clearer depiction of scenarios where specific management actions (e.g. juniper planting) are appropriate or inappropriate (Chapter 5). Studies of plant pest and pathogen outbreaks in the wider environment generally lack examples where models led to successful interventions (Gottwald et al., 2001). Models of *P. ramorum* spread in Oregon predict management intervention prevented mortality of up to 25 million tanoaks between 2012 and 2019 (Cobb et al., 2020), while eradication of *Phytophthora* species, albeit costly and labour intensive, was achieved in habitat restoration sites in California using solarisation techniques (Frankel et al., 2020).

The latter is an important example because control strategies for many plant pathogens require chemical treatments or the removal of susceptible hosts, sometimes across large control zones e.g. under emergency EU legislation all hosts found within a 100m radius of a positive *Xylella fastidiosa* detection must be destroyed and all business trading host plants within 5km will have restrictions imposed (DEFRA, 2020b). Such methods may be inappropriate for species with high cultural (Almeida, 2018) or conservation value (Roberts et al., 2020), where disease management may instead focus on improved biosecurity practices to limit invasion. In Western Australia, implementation of biosecurity practices in a bauxite mining operation limited the spread of the highly destructive pathogen *P. cinnamomi* by four orders of magnitude (to 0.0006ha yr^{-1}) for every hectare of vegetation cleared (Colquhoun and Kerp, 2007). The success of the operation was attributed to the co-design of the biosecurity procedures involving all levels of personnel within the company, from managers to machine operators, to input ideas, implement, monitor, audit and review the procedures, increasing staff familiarisation and commitment to carry them out (Colquhoun and Kerp, 2007). This provides evidence for the theory that accountability for decision-making and feedback loops that keep people informed of how their knowledge is being used is integral to achieving behavioural change (Bell and Reed, 2021). The predictive *P. austrocedri* risk

maps produced at local (Figure 12) and national (Figure 28) scale are a first attempt to provide stakeholders with a visualisation of the potential extent of spread without management interventions. Effective management of juniper populations, now that *P. austrocedri* is widely distributed across the UK, will require ongoing discussions with a broad range of stakeholders to improve the relevance of the decision tools and translate the management recommendations into action. Future engagement could explore synergies or antagonisms between measures mitigating *P. austrocedri* and other non-native plant pathogens with overlapping distributions, quantify disease impacts stakeholders think are most important and identify metrics to measure the success of interventions, as advocated by Hulme (2020) from experience of preventing invasions of non-native plants in New Zealand. Success targets could in part be developed using plant health accreditation schemes (Plant Health Alliance Steering Group, 2019) or environmental indicators such as the biodiversity intactness indicator (De Palma et al., 2019), to create positive feedback loops between policy design and implementation, and demonstrate causal links between disease management and ecosystem health.

7.6 Recommendations for juniper management in response to disease

Management recommendations to prevent or mitigate *P. austrocedri* introduction, establishment and spread within UK native juniper populations as informed by my analyses were presented at the end of each research chapter and are consolidated below (Table 29), largely focusing on interventions at the population level where most juniper management activity occurs. Preventing infection is almost always easier and more cost-effective than attempts to eradicate or prevent further spread (Frankel et al., 2020; Hulme, 2020; Mack et al., 2000). This requires integrated management across all spatial scales, from improved detections at borders (Eschen et al., 2015), reduced movements of infected plants within countries (Harwood et al., 2009), changes to supply chains (Green, 2020) and potentially to planning legislation and funding criteria to reduce disease introductions (Reid et al., 2021). Infection prevention also requires broad, cross-sector dialogue to understand competing priorities and find compromises on difficult issues such as the economic viability of livestock production vs stocking densities required to avoid environmental degradation. Policymakers could co-ordinate such discussions, set incentives to improve biosecurity practices or deterrents to reduce disease introductions, facilitate data sharing and provide accessible advice (Table 29). Updating the juniper management guidelines (DEFRA, 2017) using stakeholder recommendations could increase adoption of the advocated management practices, especially considering stakeholders who were already aware of the guidelines

used them to raise awareness of biosecurity and consider alternatives to supplementary juniper planting (Chapter 5). Juniper growers of all types will play an important role in maintaining disease free populations by supplying clean planting stock, employing practices used in plant health management standards (Plant Health Alliance Steering Group, 2019) or advocated by horticultural or conservation organisations (RHS, 2021; Slawson, 2015). At both site and landscape levels, biosecurity could also be used as a key criterion with which land managers select contractors or suppliers of plants for planting (Table 29).

Table 29. Summary of *P. austrocedri* management recommendations that could be applied at different spatial scales with the stakeholder types who may be responsible for implementation depending on the infection status of the location(s). Definitions of spatial scale are subjective but 1km^2 could be considered as the boundary between population (≤) and landscape (>) scales. Chapter references are provided where the recommendations derive directly from research conducted in this thesis.

Spatial scale	Stakeholder type	Infection status	Recommendations
Population (≤2km^2) and landscape (>2km^2)	Policymakers	Any	• Provide, consult on, and revise accessible guidance and decision tools using ACTA principles (Jones and Kleczkowski, 2020) (Chapter 5, Figure 21) • Host centralised repositories for pathogen distribution and risk maps, and successful management practices (Chapters 5.4, 6.4, Appendix O.1) • Set biosecurity criteria to assess grants, planning permission, award public sector contracts (Chapters 4.4.3, 5.4.4, Appendix L.4) • Increase resourcing for disease testing (Chapters 4.4.3, 5.4.4). • Explore regulatory options to enforce biosecurity or liability for disease introductions (Chapters 4.5, 5.4.4)
Population and landscape	Juniper growers (commercial or on-site nurseries)	Any	• Supply disease-free planting stock (Chapters 4.4.3, 6.4) • Risk assessment – identify high risk host plants and pathways (Chapters 4.4.3, 6.4) • Mitigation – disease testing, biosecurity accreditation, strict biosecurity focusing on watering and drainage regimes for elimination of *Phytophthora* spp.
Population	Implementation: land managers of natural environments, forestry, and agriculture Advice: advisers and regulators to	Any	Risk assessment • Use the national risk maps to identify probability of infection and nearest outbreak (Chapter 6.4) • Identify potential introductory pathways – most likely plants for planting, movement of people, livestock, and deer (Chapters 3.5.3, 3.5.4, 4.4.3, 6.4) • Use the decision framework to determine i) juniper population vulnerability given its population fitness and age structure; ii) site suitability for *P. austrocedri* (Chapter 2.4.2)

tailor management for specific sites		• Monitoring – diversity of microsites (Chapters 2.4.2, 3.5.3, 3.5.4), plantings (Chapters 4.4.3, 6.4), record absences (Chapter 6.5), report presences (Chapters 5.4.2) Risk mitigation • Training for staff/volunteers – biosecurity practices, symptom identifications and reporting (Chapters 4.4.3, 5.4.4) • Biosecurity – vehicle and footwear washing • Grazing management – review livestock and deer densities (Chapters 2.4.2, 3.5.3, 3.5.4, 6.4) • Explore and prioritise measures to stimulate natural regeneration (Chapters 4.4.3, 6.4) • Use biosecurity criteria to select contractors and source planting material • If planting is necessary, source plants from nurseries with high biosecurity standards, quarantine trees before planting out (Chapters 4.4.3, 6.4)
	Uninfected	• Prioritise preventing disease introductions • Pre-emptive management could include surfacing footpaths, diverting footpaths and carparks from high-risk areas, cleaning, or re-routing drainage channels (Chapter 2.4.2) • Protect existing trees from browsing damage or direct loss (but note some grazing or grass/scrub management is necessary to allow regeneration)
	Infected	• Establishment is most likely in denser juniper stands, subject to grazing, in acidic, wet microsites in poorly drained soils or adjacent to watercourses in free draining areas (Chapter 2.4.2) • Refocus risk assessments to consider spread pathways and prevent the movement of infected water and soils (Chapters 2.4.2, 3.5.3, 3.5.4, 5.5, 6.4) • Limit disturbance to high-risk microsites (Chapters 2.4.2, 3.5.3, 3.5.4) • If work in infected zones is essential, visit clean sites first, plan access routes (Chapter 3.5.3, 3.5.4) • Revise and update biosecurity protocols using staff/volunteer experience and feedback (Chapter 5.5)

Further site level precautions that could be implemented by land managers include recurrent training of staff and volunteers to clean machinery and footwear before and after site visits (Table 29). Such measures have reduced the spread of other soil-borne pathogens including *P. lateralis* (Goheen et al., 2012) and *P. cinnamomi* (Colquhoun and Kerp, 2007). Beyond movements of people and machinery, potential introductory pathways for *P. austrocedri* include plants for planting and movements of livestock and wildlife (especially deer). The

national *P. austrocedri* risk map (Figure 28) shows which populations are at higher risk of infection owing to factors outwith land manager control such as soil pH and rainfall. If the population is currently uninfected and situated in a higher risk area, preventing introductory disease risks from supplementary planting and sheep and deer movements between infected and uninfected sites could be given highest priority, as could protection of the existing juniper trees from browsing damage or habitat loss (Table 29). In areas of lower *P. austrocedri* risk, supplementary juniper planting to bolster moribund populations may be judged to outweigh the risk of disease but siting new plantings on freely draining areas away from watercourses will favour juniper growth (Ward and Shellswell, 2017) and further reduce the risk of *P. austrocedri* infection (Chapter 2). In infected populations, minimising disturbance from people, livestock and wildlife in the highest risk microsites is advisable but note that grazing cessation will require alternative measures such as scrub management or the creation of bare ground to allow juniper regeneration if competitive species are likely to prohibit recruitment of juniper seedlings (Broome, 2003; Wilkins and Duckworth, 2011) (Table 29). Monitoring for disease at repeated time intervals and including records of symptom absences will provide highly valuable data for further research and sharing this information will facilitate adaptive management of neighbouring populations (Chapter 5).

These recommendations may or may not address threats posed by other plant pests and pathogens and were developed in response to the questions this thesis aimed to explore (Chapter 1.7 Thesis overview) so the list is inexhaustive and it will be necessary to integrate other important considerations such as the cultural value of juniper and the financial viability of mitigation measures. Finally, the applicability of the recommendations will depend on the management aims for individual sites and their suitability for both juniper and *P. austrocedri* and will require revision following changes to legislation or new research (e.g. the importance of local juniper provenances for disease resistance) (Table 29). However, the recommendations synthesise the new knowledge obtained throughout this thesis about the drivers promoting *P. austrocedri* introduction, establishment and spread in populations of common juniper, illuminating some practical options that policymakers, land managers, growers and conservationists could take forward to maintain and increase juniper in the UK landscape.

7.7 Conclusion

The major challenge in managing existing and future plant health threats is understanding when, where and how to intervene to minimise or mitigate them. Ultimately, interventions that allow hosts to adapt to emergent pathogens will build longer-lasting disease resilience in

our complex natural environments (Coomes et al., 2021). This thesis provides the first evidence of abiotic and biotic drivers promoting the introduction, establishment and spread of *P. austrocedri* in native tree populations in the northern hemisphere that can be used to inform such management decisions. At the national scale, *P. austrocedri* presence was driven by acidic soil pH, high habitat suitability for roe deer, 2.5-3mm daily rainfall and high sheep stocking density. Juniper populations in northwest Scotland, Wales and southern England have the lowest risk of infection, so conservation attempts could focus here on protecting and increasing population sizes using grazing control and measures to promote natural regeneration, or supplementary planting using clean stock. At the population scale, soil moisture promoted *P. austrocedri* establishment and increasing juniper density and force of infection promoted pathogen spread. Dispersal most frequently occurred within 500m, but infrequently >1km, from the nearest infected tree over a four-year period, meaning spread is slow but not insignificant, especially if infected soil is disturbed and vectored e.g. by drainage works. Management of uninfected juniper populations in central Scotland and northern England at high risk of infection could concentrate on limiting risks associated with introductory pathways such as the movement of people and vehicles, reducing livestock and deer densities and cessation of supplementary planting. Juniper was, and continues to be, widely planted across the UK to re-establish or bolster existing populations, but frequent, large plantings may increase the risk of *P. austrocedri* introduction. Reasons for planting, the genetic implications of doing so, and biosecurity practices that prevent *P. austrocedri* introduction on any planting material, all require urgent review before juniper planting is further promoted as a native species that can be used to restore biodiversity and store carbon. In infected populations, management could focus on limiting spread within and between sites by increasing biosecurity and reducing disturbance to infected microsites. Increasing the availability of disease distribution and risk maps, and co-designing decision tools with stakeholders is likely to prevent or better contain disease outbreaks. This will require cross-sector collaborations, including agents, growers, farmers, and landscapers who are often poorly represented in disease management discussions concerning the wider environment. Juniper populations throughout the northern hemisphere require such actions to be carried out to protect them from mortality caused by *P. austrocedri*.

References

Agrios, G. N. (2005). Plant Pathology. Academic Press. Retrieved from https://ezp.lib.cam.ac.uk/login?url=https://search.ebscohost.com/login.aspx?direct=true&db=nlebk&AN=189453&site=ehost-live&scope=site

Aguayo, J., Elegbede, F., Husson, C., Saintonge, F-X., and Marçais, B. (2014). Modeling climate impact on an emerging disease, the *Phytophthora alni*-induced alder decline. *Global Change Biology*, *20*, 3209–3221. https://doi.org/10.1111/gcb.12601

Alexander, N. S., Morley, D., Medlock, J., Searle, K., and Wint, W. (2014). A first attempt at modelling roe deer (*Capreolus capreolus*) distributions over Europe. *Open Health Data*, *2(1)*, e2. https://doi.org/10.5334/ohd.ah

Allouche, O., Steinitz, O., Rotem, D., Rosenfeld, A., Kadmon, R. (2008). Incorporating distance constraints into species distribution models. *Journal of Applied Ecology, 45*, 599–609. https://doi.org/10.1111/j.1365-2664.2007.01445.x

Allouche, O., Tsoar, A., and Kadmon, R. (2006). Assessing the accuracy of species distribution models: Prevalence, kappa and the true skill statistic (TSS). *Journal of Applied Ecology*, *43(6)*, 1223–1232. https://doi.org/10.1111/j.1365-2664.2006.01214.x

Almeida, R. P. P. (2018) Emerging plant disease epidemics: biological research is key but not enough. *PLoS Biology*, *16(8)*. e2007020. https://doi.org/10.1371/journal.pbio.2007020

Anacker, B.L., Rank, N.E., Hüberli, D., Garbelotto, M., Gordon, S., Harnik, T., Whitkus, R., and Meentemeyer, R. (2008). Susceptibility to *Phytophthora ramorum* in a key infectious host: landscape variation in host genotype, host phenotype, and environmental factors. *New Phytologist*, *177(3)*, 756–766. https://doi.org/10.1111/j.1469-8137.2007.02297.x

Anderson, R. M., and May, R. M. (1986). The invasion, persistence and spread of infectious diseases within animal and plant communities. *Philosophical transactions of the Royal Society of London. Series B, Biological sciences*, *314(1167)*, 533–570. https://doi.org/10.1098/rstb.1986.0072

Attarchi, S., and Gloaguen, R. (2014). Classifying complex mountainous forests with L-Band SAR and landsat data integration: a comparison among different machine learning methods in the Hyrcanian forest. *Remote Sensing*, *6*, 3624–3647. https://doi.org/10.3390/rs6053624

Baccalá, N. B., Rosso, P. H., and Havrylenko, M. (1998). *Austrocedrus chilensis* mortality in the Nahuel Huapi National Park (Argentina). *Forest Ecology and Management*, *109*, 261–269. https://doi.org/10.1016/S0378-1127(98)00250-3

Barbet-Massin, M., Jiguet, F., Albert, C. H., and Thuiller, W. (2012). Selecting pseudo-absences for species distribution models: how, where and how many? *Methods in Ecology and Evolution*, *3(2)*, 327–338. https://doi.org/10.1111/j.2041-210X.2011.00172.x

Barwell, L. J, Perez-Sierra, A., Henricot, B., Harris, A., Burgess, T. I., Hardy, G., Scott, P., Williams, N., Cooke, D., Green, S., Chapman, D. S., Purse, B. V. (2021a). Evolutionary trait-based approaches for predicting future global impacts of plant pathogens in the genus *Phytophthora*. *Journal of Applied Ecology*, *58(4)*, 718-730. https://doi.org/10.1111/1365-2664.13820

Barwell, L., White, R. M., Chapman, D., Donald, F., Marzano, M., Green, S., Kleczkowski, A., and Purse, B.V. (2021b). The potential of ecological and epidemiological models to inform assessment and mitigation of biosecurity risks arising from large scale planting. Part of Project Final Report. PHC2019/06 & PHC2019/05. Scotland's Centre of Expertise for Plant Health.

Bastin, J.-F., Finegold, Y., Garcia, C., Mollicone, D., Rezende, M., Routh, D., Zohner, C. M., & Crowther, T. W. (2019). The global tree restoration potential. *Science, 365(6448)*, 76–79. https://doi.org/10.1126/science.aax0848

Bate, A. M., Jones, G., Kleczkowski, A., MacLeod, A., Naylor, R., Timmis, J., Touza, J., and White, P. C. L. (2016). Modelling the impact and control of an infectious disease in a plant nursery with infected plant material inputs. *Ecological Modelling*, *334*, 27–43. https://doi.org/10.1016/j.ecolmodel.2016.04.013

Bebber, D. P., Holmes, T., and Gurr, S. J. (2014). The global spread of crop pests and pathogens. *Global Ecology and Biogeography*, *23(12)*, 1398–1407. https://doi.org/10.1111/geb.12214

Bell, K., and Reed, M. (2021). The tree of participation: a new model for inclusive decision-making. *Oxford University Press on behalf of Community Development Journal*. 1–20. https://doi.org/10.1093/cdj/bsab018

Bell, V. A., Rudd, A. C., Kay, A. L., and Davies, H. N. (2018). Grid-to-Grid model estimates of monthly mean flow and soil moisture for Great Britain (1891 to 2015): observed driving data [MaRIUS-G2G-Oudin-monthly]. *NERC Environmental Information Data Centre*. https://doi.org/10.5285/f52f012d-9f2e-42cc-b628-9cdea4fa3ba0

Bellard, C., Thuiller, W., Leroy, B., Genovesi, P., Bakkenes, M., & Courchamp, F. (2013). Will climate change promote future invasions? *Global Change Biology, 19(12)*, 3740–3748. https://doi.org/10.1111/gcb.12344

Beven, K. J., and Kirkby, M. J. (1979). A physically based, variable contributing area model of basin hydrology. *Hydrological Sciences Journal, 24(1)*, 43–69. https://doi.org/10.1080/02626667909491834

Bivand, R., Keitt, T., and Rowlingson, B. (2019). rgdal: bindings for the “Geospatial” data abstraction library. R package version 1.4-8. https://CRAN.R-project.org/package=rgdal

Bivand, R., and Rundel, C. (2019). rgeos: interface to geometry engine - open source ('GEOS’). R package version 0.5-5. https://CRAN.R-project.org/package=rgeos

Bivand, R. S., Pebesma, E., and Gomez-Rubio, V. (2013). Applied spatial data analysis with R (2nd ed.). Springer.

Bjornstad, O. N. (2020). ncf: spatial covariance functions. R package version 1.2-9. https://CRAN.R-project.org/package=ncf

Bjornstad, O. N. (2019). ncf: spatial covariance functions. R package version 1.2-8. https://CRAN.R-project.org/package=ncf

Blackburn, T.M., Pyšek, P., Bacher, S., Carlton, J.T., Duncan, R.P., Jarošík, V., Wilson, J.R.U., Richardson, D.M. (2011). A proposed unified framework for biological invasions. *Trends in Ecology and Evolution*, *26(7)*, 333–339. https://doi.org/10.1016/j.tree.2011.03.023

Blangiardo, M., and Cameletti, M. (2015). *Spatial and spatio-temporal Bayesian models with R-INLA*. John Wiley and Sons Ltd.

Blangiardo, M., Cameletti, M., Baio, G., and Rue, H. (2013). Spatial and spatio-temporal models with R-INLA. *Spatial and Spatio-temporal Epidemiology*, *7*, 39–55. https://doi.org/10.1016/j.sste.2013.07.003

Blaser, N. (2020). rdist: calculate pairwise distances. R package version 0.0.5. https://CRAN.R-project.org/package=rdist

Borchers, H. W. (2021). pracma: practical numerical math functions. R package version 2.3.3. https://CRAN.R-project.org/package=pracma

Borders Forest Trust. (1996). Common Juniper (*Juniperus communis* L.): a review of biology and its status in the Scottish Borders. Borders Forest Trust.

Botanical Society of Britain and Ireland (BSBI). (2021). Mapping the flora of the British Isles. Retrieved from https://bsbi.org/maps-and-data

Botanical Society of Britain and Ireland (BSBI). (2020). *Juniperus communis* records from live database. Retrieved from http://bsbi.org/maps?taxonid=2cd4p9h.8r1

Botanical Society of Britain and Ireland (BSBI). (2017). *Juniperus communis* records from live database. Retrieved from http://bsbi.org/maps?taxonid=2cd4p9h.8r1

Boyd, I. L., Freer-Smith, P. H., Gilligan, C. A., and Godfray, H. C. J. (2013). The consequence of tree pests and diseases for ecosystem services. *Science, 342(6160),* 1235773. https://doi.org/10.1126/science.1235773

Bradshaw, R. E., Bellgard, S. E., Black, A., Burns, B. R., Gerth, M. L., McDougal, R. L., Scott, P.M., Waipara, N. W., Weir, B. S., Williams, N. M., Winkworth, R. C., Ashcroft, T., Bradley, E. L., Dijkwel, P. P., Guo, Y., Lacey, R. F., Mesarich, C. H., Panda, P., and Horner, I. J. (2020). *Phytophthora agathidicida*: research progress, cultural perspectives and knowledge gaps in the control and management of kauri dieback in New Zealand. *Plant Pathology, 69(1)*, 3–16. https://doi.org/10.1111/ppa.13104

Brasier, C. M. (2008). The biosecurity threat to the UK and global environment from international trade in plants. *Plant Pathology*, *57(5)*, 792–808. https://doi.org/10.1111/j.1365-3059.2008.01886.x

Braun, V., and Clarke, V. (2006). Using thematic analysis in psychology. *Qualitative Research in Psychology*, *3(2)*, 77–101. https://doi.org/10.1191/1478088706qp063oa

Breukers, A., Bremmer, J., Dijkxhoor, Y., and Janssens, B. (2009). Phytosanitary risk perception and management. Development of a conceptual framework. Report 2009-078. LEI Wageningen. Retrieved from https://edepot.wur.nl/14635

British Deer Society. (n.d.). Wild deer of the UK. Identifying roe deer (*Capreolus capreolus*). Retrieved from https://www.bds.org.uk/wp-content/uploads/pdfs/Deer%20Identification%20sheets-Roe%20Deer.pdf

Broennimann, O., Di Cola, V., and Guisan, A. (2021). ecospat: spatial ecology miscellaneous methods. R package version 3.2. https://CRAN.R-project.org/package=ecospat

Broome, A., and Holl, K. (2017). Can the site conditions required for successful natural regeneration of juniper (*Juniperus communis* L.) be determined from a single species survey? *Plant Ecology & Diversity*, 1–10. https://doi.org/10.1080/17550874.2017.1336186

Broome, A., Long, D., Ward, L. K., and Park, K. J. (2017). Promoting natural regeneration for the restoration of *Juniperus communis*: a synthesis of knowledge and evidence for conservation practitioners. *Applied Vegetation Science, 20(3)*, 1–13. https://doi.org/10.1111/avsc.12303

Broome, A, Hendry, S., Smith, M., Rayner, W., Nichol, B., and Perks, M. (2008). Investigation of the possible causes of dieback of Glenartney Juniper Wood SAC Perthshire. Project No: 18895. Report commissioned by Scottish Natural Heritage. Forest Research.

Broome, A. (2003). Growing juniper: propagation and establishment practices. Forestry Commission Information Note 50. Forestry Commission.

Brown, N., Vanguelova, E., Parnell, S., Broadmeadow, S., and Denman, S. (2018). Predisposition of forests to biotic disturbance: predicting the distribution of Acute Oak Decline using environmental factors. *Forest Ecology and Management*, *407*, 145–154. https://doi.org/10.1016/j.foreco.2017.10.054

Bullock, J. M., Bonte, D., Pufal, G., da Silva Carvalho, C., Chapman, D. S., García, C., García, D., Matthysen, E., and Delgado, M. M. (2018). Human-Mediated Dispersal and the Rewiring of Spatial Networks. *Trends in Ecology and Evolution*, *33(12)*, 958–970. https://doi.org/10.1016/j.tree.2018.09.008

Bullock, J. M., Shea, K. and Skarpaas, O. (2006). Measuring plant dispersal: An introduction to field methods and experimental design. *Plant Ecology*, *186(2)*, 217–234. https://doi.org/10.1007/s11258-006-9124-5

Bunny, F. J., Crombie, D. S., and Williams, M. R. (1995). Growth of lesions of *Phytophthora cinnamomi* in stems and roots of jarrah (*Eucalyptus marginata*) in relation to rainfall and stand density in mediterranean forest of Western Australia. *Canadian Journal of Forest Research*, *25*, 961–969.

Burdon, J. J., and Chilvers, G. A. (1982). Host density as a factor in plant disease ecology. *Annual Review of Phytopathology*, *20(1)*, 143–166. https://doi.org/10.1146/annurev.py.20.090182.001043

Burgess, T. I., Scott, J. K., Mcdougall, K. L., Stukely, M. J. C., Crane, C., Dunstan, W. A., Brigg, F., Andjic, V., White, D., Rudman, T., Arentz, F., Ota, N., and Hardy, G. E. S. J. (2017). Current and projected global distribution of *Phytophthora cinnamomi*, one of the world's worst plant pathogens. *Global Change Biology*, *23(4)*, 1661–1674. https://doi.org/10.1111/gcb.13492

Burton, V., Metzger, M. J., Brown, C., and Moseley, D. (2019). Green gold to wild woodlands: understanding stakeholder visions for woodland expansion in Scotland. *Landscape Ecology*, *34(7)*, 1693–1713. https://doi.org/10.1007/s10980-018-0674-4

Cade, B. S. (2015). Model averaging and muddled multimodel inferences. *Ecology*, *96(9)*, 2370–2382. https://doi.org/10.1890/14-1639.1

Callaghan, S., and Guest, D. (2015). Globalisation, the founder effect, hybrid *Phytophthora* species and rapid evolution: new headaches for biosecurity. *Australasian Plant Pathology, 44(3)*, 255–262. https://doi.org/10.1007/s13313-015-0348-5

Calı´, S. G. (1996). *Austrocedrus chilensis*: estudio de los anillos de crecimiento y su relación con la dinámica del "Mal del Ciprés" en el Parque Nacional Nahuel Huapi, Argentina. Trabajo para optar al grado de Licenciado en Ciencias Biológicas. Universidad Nacional del Comahue.

Cardillo, E., Abad, E., and Meyer, S. (2021). Iberian oak decline caused by *Phytophthora cinnamomi*: a spatiotemporal analysis incorporating the effect of host heterogeneities at landscape scale. *Forest Pathology*, *51(2)*, 1–16. https://doi.org/10.1111/efp.12667

Chang, W., Cheng, J., Allaire, J. J., Sievert, C., Schloerke, B., Xie, Y., Allen, J., McPherson, J., Dipert, A., and Borges, B. (2021). shiny: web application framework for R. Retrieved from https://cran.r-project.org/package=shiny

Chapman, D., Pescott, O. L., Roy, H. E., and Tanner, R. (2019). Improving species distribution models for invasive non-native species with biologically informed pseudo-absence selection. *Journal of Biogeography*, *46(5)*, 1029–1040. https://doi.org/10.1111/jbi.13555

Chapman, D., Purse, B. V., Roy, H. E., and Bullock, J. M. (2017a). Global trade networks determine the distribution of invasive non-native species. *Global Ecology and Biogeography*, *26(8)*, 907–917. https://doi.org/10.1111/geb.12599

Chapman, D. S., White, S. M., Hooftman, D. A. P., and Bullock, J. M. (2017b). Inventory and review of quantitative models for spread of plant pests for use in pest risk assessment for the EU territory. *EFSA Supporting Publications*, *12(4)*, 1-190. https://doi.org/10.2903/sp.efsa.2015.en-795

Chapman, D. S., Makra, L., Albertini, R., Bonini, M., Páldy, A., Rodinkova, V., Šikoparija, B., Weryszko-Chmielewska, E. and Bullock, J. M. (2016). Modelling the introduction and spread of non-native species: international trade and climate change drive ragweed invasion. *Global Change Biology, 22(9)*, 3067–3079. https://doi.org/10.1111/gcb.13220

Cheng, J., Karambelkar, B., and Xie, Y. (2021). leaflet: create interactive web maps with the JavaScript “leaflet” library. Retrieved from https://cran.r-project.org/package=leaflet

Clark, M., and Green, S. (2017.) Investigating the potential waterborne spread of the invasive pathogen, *Phytophthora austrocedri*. Honours degree thesis, University of Edinburgh.

Clifton, S. J., Ranner, D. S., and Ward, L. K. (1995). The conservation of juniper in Northumbria. *English Nature Research Reports, 152*, 1-25.

Clifton, S. J., Ward, L. K., and Ranner, D. S. (1997). The status of juniper *Juniperus communis* L. in north-east England. *Biological Conservation, 79,* 67-77. https://doi.org/10.1016/S0006-3207(96)00101-2

Cobb, R. C., Haas, S. E., Kruskamp, N., Dillon, W. W., Swiecki, T. J., Rizzo, D. M., Frankel, S. J., and Meentemeyer, R. K. (2020). The magnitude of regional-scale tree mortality caused by the invasive pathogen *Phytophthora ramorum*. *Earth's Future*, *8(7)*, 1-15. https://doi.org/10.1029/2020EF001500

Cobb, R., and Metz, M. (2017). Tree diseases as a cause and consequence of interacting forest disturbances. *Forests, 8(147),* 1-13. https://doi.org/10.3390/f8050147

Colquhoun, I. J., and Kerp, N. L. (2007). Minimizing the spread of a soil-borne plant pathogen during a large-scale mining operation. *Restoration Ecology*, *15(4)*, 85–93. https://doi.org/10.1111/j.1526-100X.2007.00296.x

Committee on Climate Change. (2020). Land use: policies for a net zero UK. Retrieved from https://www.theccc.org.uk/publication/land-use-policies-for-a-net-zero-uk/%0Ahttps://www.theccc.org.uk/2020/01/23/major-shift-in-uk-land-use-needed-to-deliver-net-zero-emissions/

Condeso, T. E., and Meentemeyer, R. K. (2007). Effects of landscape heterogeneity on the emerging forest disease sudden oak death. *Journal of Ecology*, *95(2)*, 364–375. https://doi.org/10.1111/j.1365-2745.2006.01206.x

Conservative Party (UK). (2019). The Conservative and Unionist Party Manifesto. Retrieved from https://www.conservatives.com/our-plan

Conrad, O., and Olaya, V. (2004). SAGA-GIS module library documentation (v2.2.1). Library Hydrology. Retrieved from http://www.saga-gis.org/saga_tool_doc/2.2.1/ta_hydrology.html

Cook, D., Fraser, R. W., and Wilby, A. (2017). Plant biosecurity policy evaluation: the economic impacts of pests and diseases. World Scientific Publishing Europe Ltd.

Coomes, D., Bowditch, E., Burton, V., Chamberlain, B., Donald, F., Egedusevic, M., Fuentes-Montemayor, E., Hall, J., Jones, A. G., Lines, E., Waring, B., Warner, E., and Weatherall, A. (2021). Section 1: Habitat specific nature-based solutions: a review of the available evidence. Woodlands. In R. Stafford, B. Chamberlain, L. Clavey, P. K. Gillingham, S. McKain, M. D. Morecroft, C. Morrison-Bell, and O. Watts (Eds.), *Nature-based solutions for climate change in the UK: a report by the British Ecological Society* (pp. 24-37). British Ecological Society. Retrieved from https://www.britishecologicalsociety.org/policy/nature-based-solutions/read-the-report/

Council Directive 92/43/EEC. (1992). Retrieved from http://ec.europa.eu/environment/nature/legislation/habitatsdirective/index_en.htm

Creissen, H., Davis, A., Fitzpatrick, R., Marzano, M., Meador, E., Robinson, J., and White, R. (2019). *Network analysis – where do people get their plant health information? Project final report. PHC2018/10.* Scotland's Centre of Expertise for Plant Health (PHC). Retrieved from https://www.planthealthcentre.scot/publications/phc201810-network-analysis-where-do-people-get-their-plant-health-information

Croft, S., Ward, A. I., Aegerter, J. N., and Smith, G. C. (2019). Modeling current and potential distributions of mammal species using presence-only data: a case study on British deer. *Ecology and Evolution*, *9(15)*, 8724–8735. https://doi.org/10.1002/ece3.5424

Cumbria Wildlife Trust. (2014). Uplands for Juniper survey. Retrieved from http://www.cumbriawildlifetrust.org.uk/what-we-do/conservation-projects/uplands-juniper

Cummings, J. (2021). Request under the Environmental Information (Scotland) Regulations 2004 (EIRs). Reference 2021/00152335. Scottish Forestry.

Cunniffe, N. J., Cobb, R. C., Meentemeyer, R. K., Rizzo, D. M., and Gilligan, C. A. (2016). Modeling when, where, and how to manage a forest epidemic, motivated by sudden oak death in California. *Proceedings of the National Academy of Sciences, 113(20)*, 5640–5645. https://doi.org/10.1073/pnas.1602153113

Cunniffe, N. J., Koskella, B., E. Metcalf, C. J., Parnell, S., Gottwald, T. R., and Gilligan, C. A. (2015a). Thirteen challenges in modelling plant diseases. *Epidemics, 10*, 6–10. https://doi.org/10.1016/j.epidem.2014.06.002

Cunniffe, N. J., Stutt, R. O. J. H., DeSimone, R. E., Gottwald, T. R., and Gilligan, C. A. (2015b). Optimising and communicating options for the control of invasive plant disease when there is epidemiological uncertainty. *PLoS Computational Biology*, *11(4)*, 1–24. https://doi.org/10.1371/journal.pcbi.1004211

Cushman, J., and Meentemeyer, R. (2008). Multi-scale patterns of human activity and the incidence of an exotic forest pathogen. *Journal of Ecology*, *96(4)*, 766-776. https://doi.org/10.1111/j.1365-2745.2008.01376.x

Dandy, N., Marzano, M., Porth, E., Urquhart, J., and Potter, C. (2017). Who has a stake in ash dieback? A conceptual framework for the identification and categorisation of tree health stakeholders. In. R. Vasitis and R. Enderle (Eds.). *Dieback of European ash (*Fraxinus *spp): Consequences and guidelines for sustainable management* (pp. 15–26). Swedish University of Agricultural Sciences. Retrieved from http://www.slu.se/globalassets/ew/org/inst/mykopat/forskning/stenlid/dieback-of-european-ash.pdf

De Frenne, P., Gruwez, R., Hommel, P. W. F. M., De Schrijver, A., Huiskes, R. P. J., De Waal, R. W., Vangansbeke, P., and Verheyen, K. (2020). Effects of heathland management on seedling recruitment of common juniper (*Juniperus communis*). *Plant Ecology and Evolution, 153(2)*, 188–198. https://doi.org/10.5091/plecevo.2020.1656

De Palma, A., Sanchez-Ortiz, K., and Purvis, A. (2019). Calculating the Biodiversity Intactness Index: the PREDICTS implementation (v1.0.0). Zenodo. https://doi.org/10.5281/zenodo.3518067

de Rivera, O. R., Blangiardo, M., López-Quílez, A., and Martín-Sanz, I. (2019). Species distribution modelling through Bayesian hierarchical approach. *Theoretical Ecology*, *12(1)*, 49–59. https://doi.org/10.1007/s12080-018-0387-y

Department for Environment Food and Rural Affairs (DEFRA). (2020a). MagicMap. Retrieved from https://magic.defra.gov.uk/MagicMap.aspx

Department for Environment Food and Rural Affairs (DEFRA). (2020b). Rapid Pest Risk Analysis (PRA) for: *Xylella fastidiosa*. Retrieved from https://planthealthportal.defra.gov.uk/plant-health-api/api/pests/12570/risk-analyses/369/documents/4361/document

Department for Environment Food and Rural Affairs (DEFRA). (2018). Tree health resilience strategy. Retrieved from https://assets.publishing.service.gov.uk/government/uploads/system/uploads/attachment_data/file/710719/tree-health-resilience-strategy.pdf

Department for Environment Food and Rural Affairs (DEFRA). (2017). Juniper: management guidelines. Retrieved from https://www.planthealthcentre.scot/sites/www.planthealthcentre.scot/files/inline-files/JuniperManagementGuidelinesSeptember2017Published.pdf

Department for Environment Food and Rural Affairs (DEFRA). (2015). UK risk register details for *Phytophthora austrocedri*. Retrieved from https://secure.fera.defra.gov.uk/phiw/riskRegister/viewPestRisks.cfm?cslref=27216

Department for Environment, Food and Rural Affairs (DEFRA). (2014a). *Tree Health Management Plan.* Retrieved from https://www.gov.uk/government/uploads/system/uploads/attachment_data/file/307299/pb14167-tree-health-management-plan.pdf

Department for Environment Food and Rural Affairs (DEFRA). (2014b). Protecting plant health. A plant biosecurity strategy for Great Britain. Retrieved from https://assets.publishing.service.gov.uk/government/uploads/system/uploads/attachment_data/file/307355/pb14168-plant-health-strategy.pdf

Dillon, W. W., Haas, S. E., Rizzo, D. M., and Meentemeyer, R. K. (2014). Perspectives of spatial scale in a wildland forest epidemic. *European Journal of Plant Pathology*, *138(3)*, 449–465. https://doi.org/10.1007/s10658-013-0376-3

Dines, T. D., and Daniels, A. (2006). *Wales juniper inventory: an inventory of juniper sites in Wales and an assessment of populations in Snowdonia*. Plantlife, 1-43.

Donald, F., Purse, B. V, and Green, S. (2021). Investigating the role of restoration plantings in introducing disease - a case study using *Phytophthora. Forests, 12(6),* 764. https://doi.org/10.3390/f12060764

Donald, F., Green, S., Searle, K., Cunniffe, N. J., and Purse, B. V. (2020). Small scale variability in soil moisture drives infection of vulnerable juniper populations by invasive forest pathogen. *Forest Ecology and Management, 473(*3*)*, 118324. https://doi.org/10.1016/j.foreco.2020.118324

Dormann, C. F., Elith, J., Bacher, S., Buchmann, C., Carl, G., Carré, G., Marquéz, J. R. G., Gruber, B., Lafourcade, B., Leitão, P. J., Münkemüller, T., Mcclean, C., Osborne, P. E., Reineking, B., Schröder, B., Skidmore, A. K., Zurell, D., and Lautenbach, S. (2013). Collinearity: a review of methods to deal with it and a simulation study evaluating their performance. *Ecography*, *36(1)*, 27–46. https://doi.org/10.1111/j.1600-0587.2012.07348.x

Dormann, C., McPherson, J. M., Araújo, M. B., Bivand, R., Bolliger, J., Carl, G., Davies, R. G., Hirzel, A., Jetz, W., Kissling, W. D., Kühn, I., Ohlemüller, R., Peres-Neto, P. R.,

Reineking, B., Schröder, B., Schurr, F. M., and Wilson, R. (2007) Methods to account for spatial autocorrelation in the analysis of species distributional data: a review. *Ecography*, *30(5)*, 609–628. https://doi.org/10.1111/j.2007.0906-7590.05171.x

Drover, D. R., Jackson, C. R., Bitew, M., and Du, E. (2015). Effects of DEM scale on the spatial distribution of the TOPMODEL topographic wetness index and its correlations to watershed characteristics. *Hydrology and Earth System Sciences Discussions*, *12(11)*, 11817–11846. https://doi.org/10.5194/hessd-12-11817-2015

Dun, H. (2016). Investigating the infectious capacity of *Phytophthora austrocedri*. Honours degree thesis, University of Edinburgh.

Dunn, G., and Laing, M. (2017). Policy-makers perspectives on credibility, relevance and legitimacy (CRELE). *Environmental Science and Policy*, *76*, 146–152. https://doi.org/10.1016/j.envsci.2017.07.005

Dunn, M., Marzano, M., and Finger, A. (2021). Assessment of large-scale plant biosecurity risks to Scotland from large-scale tree plantings for environmental benefits project. Project Final Report. PHC2019/06. Scotland's Centre of Expertise for Plant Health. Retrieved 22nd June 2021 from https://www.planthealthcentre.scot/projects/assessment-large-scale-plant-biosecurity-risks-scotland-large-scale-tree-plantings

Duque-Lazo, J., Navarro-Cerrillo, R. M., van Gils, H., and Groen, T. A. (2018). Forecasting oak decline caused by *Phytophthora cinnamomi* in Andalusia: identification of priority areas for intervention. *Forest Ecology and Management*, *417(5)*, 122–136. https://doi.org/10.1016/j.foreco.2018.02.045

EDINA. (2010). AgCensus. Grid square agricultural census data for England, Scotland and Wales. *EDINA at Edinburgh University Data Library and DEFRA for England, The Welsh Assembly Government and The Scottish Government (formerly SEERAD).* http://agcensus.edina.ac.uk/

El Mujtar, V. A., Perdomo, M. H., Gallo, L. A. and Grau, O. (2012). Sex-related difference in susceptibility to cypress mortality in *Austrocedrus chilensis* from Northwestern Patagonia (Argentina). *Bosque*, *33(2)*, 23–24. https://doi.org/10.4067/S0717-92002012000200012

Elith, J., and Leathwick, J. R. (2009). Species Distribution Models: ecological explanation and prediction across space and time. *Annual Review of Ecology, Evolution, and Systematics*, *40(1)*, 677–697. https://doi.org/10.1146/annurev.ecolsys.110308.120159

Elith, J., Leathwick, J. R., and Hastie, T. (2008). A working guide to boosted regression trees. *Journal of Animal Ecology, 77(4)*, 802–813. https://doi.org/10.1111/j.1365-2656.2008.01390.x

Elliot, M., Schlenzig, A., Harris, C. M., Meagher, T. R., and Green, S. (2015). An improved method for qPCR detection of three *Phytophthora* spp. in forest and woodland soils in northern Britain. *Forest Pathology*, *45*, 537–539. https://doi.org/10.1111/efp.12224

Environmental Systems Research Institute (ESRI). (2017). ArcGIS Desktop: Release 10.5.1

Environmental Systems Research Institute (ESRI). 2016. How maximum likelihood classification works. Retrieved from http://desktop.arcgis.com/en/arcmap/10.3/tools/spatial-analyst-toolbox/how-maximum-likelihood-classification-works.htm

Erwin, D. C., and Ribeiro, O. K. (1996). *Phytophthora Diseases Worldwide.* pp. 1-592. APS Press, St Paul.

Eschen, R., Rigaux, L., Sukovata, L., Vettraino, A. M., Marzano, M., and Grégoire, J. C. (2015). Phytosanitary inspection of woody plants for planting at European Union entry points: a practical enquiry. *Biological Invasions*, *17(8)*, 2403–2413. https://doi.org/10.1007/s10530-015-0883-6

Evans, J. S., Murphy, M. A., Holden, Z. A., and Cushman, S. A. (2011). Modelling species distribution and change using Random Forests. In C. A. Drew, Y. F. Wiersma and F. Huettmann (Eds.), *Predictive species and habitat modeling in landscape ecology: concepts and applications* (pp. 139–159). Springer.

European and Mediterranean Plant Protection Organization (EPPO). (2011). CAPRA - Computer Assisted Pest Risk Analysis. User's Manual. 1–25. https://doi.org/10.1002/9783527678679.dg02267

Fabre, F., Coville, J., and Cunniffe, N. J. (2020). Optimising reactive disease management using spatially explicit models at the landscape scale. In P. Scott, R. Strange, L. Korsten

and L. Gullino (Eds.), *Plant Diseases and Food Security in the 21st Century* (pp.1-284). Springer International. https://doi.org/10.1007/978-3-030-57899-2

Farewell, T. S., Truckell, I. G., Keay, C. A., and Hallett, S. (2011). Use and applications of the Soilscapes datasets. http://www.landis.org.uk/downloads/downloads/Soilscapes_Brochure.pdf

Fernández-Habas, J., Fernández-Rebollo, P., Rivas Casado, M., García Moreno, A. M., and Abellanas, B. (2019). Spatio-temporal analysis of oak decline process in open woodlands: a case study in SW Spain. *Journal of Environmental Management*, *248(8)*, 109308. https://doi.org/10.1016/j.jenvman.2019.109308

Food and Agriculture Organisation (FAO) and United Nations Environment Programme (UNEP). (2020). The state of the world's forests. https://doi.org/10.4060/ca8642en

Forbes, A. R. D. (1984). Glen Artney juniper wood: an ecological study. Honours degree thesis, Stirling University.

Forestry Commission. (2021). Map Browser. Retrieved from https://www.forestergis.com/Apps/MapBrowser/

Forestry Commission (2020a). Chalara (*Hymenoscyphus fraxineus*) - infections confirmed in the wider environment as at 6th November 2020. Retrieved from http://chalaramap.fera.defra.gov.uk/

Forestry Commission (2020b). *Phytophthora austrocedri* - confirmed infection sites GB 10K grid. data.gov.uk. Retrieved from https://data.gov.uk/dataset/766d2f7c-f678-475d-a40f-5e59866e3b11/phytophthora-austrocedri-confirmed-infection-sites-gb-10k-grid

Forestry Commission Scotland. (2013). Guidance planting juniper in Scotland: reducing the risk from *Phytophthora austrocedrae*. Retrieved from https://forestry.gov.scot/images/corporate/pdf/juniper-planting-guidance.pdf

Forestry Commission Scotland. (2011). Landowners urged to stop juniper disappearing off the map in Scotland. News release no: 15192, 19th December 2011. Retrieved from https://webarchive.nationalarchives.gov.uk/ukgwa/20120214195119/http://www.forestry.gov.uk/newsrele.nsf/WebNewsReleases/F339E0C1077D45B18025796B004C6417

Forestry Commission Scotland. (2009a). Action for juniper. Retrieved from https://scotland.forestry.gov.uk/images/corporate/pdf/fcs-species-juniper.pdf

Forestry Commission Scotland. (2009b). Native Woodland Survey of Scotland (NWSS). Retrieved from https://data.gov.uk/dataset/da3f8548-a130-4a0d-8ddd-45019adcf1f3/native-woodland-survey-of-scotland-nwss

Forestry Commission Scotland. (2006). Technical note: support for juniper conservation under the Scottish Rural Development Programme (SRDP). Retrieved from https://scotland.forestry.gov.uk/images/corporate/pdf/junipersrdptechnicalnote.pdf

Forest Research. (2021a). Dutch elm disease (*Ophiostoma novo-ulmi*). Retrieved from https://www.forestresearch.gov.uk/tools-and-resources/fthr/pest-and-disease-resources/dutch-elm-disease/

Forest Research. (2021b). Ecological Site Classification Decision Support System. Retrieved from http://www.forestdss.org.uk/geoforestdss/

Forest Research. (2021c). *Phytophthora austrocedri* disease of juniper and cypress. Retrieved 19th June 2021 from https://www.forestresearch.gov.uk/tools-and-resources/fthr/pest-and-disease-resources/phythopthora-austrocedri/

Francl, L. J. (2001). The disease triangle: a plant pathological paradigm revisited. The Plant Health Instructor. https://doi.org/https://doi.org/10.1094/PHI-T-2001-0517-01

Frankel, S. J., Conforti, C., Hillman, J., Ingolia, M., Shor, A., Benner, D., Alexander, J. M., Bernhardt, E., and Swiecki, T. J. (2020). *Phytophthora* introductions in restoration areas: responding to protect California native flora from human-assisted pathogen spread. *Forests*, *11(12)*, 1291. https://doi.org/10.3390/f11121291

Freeman, R. E. (1984). *Strategic management: a stakeholder approach*. Basic Books.

Freer-Smith, P. H., and Webber, J. F. (2017). Tree pests and diseases: the threat to biodiversity and the delivery of ecosystem services. *Biodiversity and Conservation, 26(13)*, 3167–3181. https://doi.org/10.1007/s10531-015-1019-0

GADM. (2017). Download data by country. Version 1.0. Retrieved from https://www.diva-gis.org/gData

Garbelotto, M., Popenuck, T., Hall, B., Schweigkofler, W., Dovana, F., Goldstein de Salazar, R., Schmidt, D., and Sims, L. L. (2020). Citizen science uncovers *Phytophthora ramorum* as a threat to several rare or endangered California Manzanita species. *Plant Disease, 104*, 3173–3182. https://doi.org/10.1094/pdis-03-20-0619-re

Gaydos, D. A., Petrasova, A., Cobb, R. C., and Meentemeyer, R. K. (2019). Forecasting and control of emerging infectious forest disease through participatory modelling. *Philosophical Transactions of the Royal Society B: Biological Sciences*, *374(1776)*, 20180283. https://doi.org/10.1098/rstb.2018.0283

Gelman, A., Carlin, J. B., Stern, H. S., Dunson, D. B., Vehtari, A., and Rubin, D. B. (2013). Bayesian data analysis (3rd Edition). Taylor & Francis.

Gelman, A., and Hill, J. (2006). Data analysis using regression and multilevel/hierarchical models. Cambridge University Press.

Gilbert, G. S., Briggs, H. M., and Magarey, R. (2015). The impact of plant enemies shows a phylogenetic signal. *PLoS One*, *10(4)*, 1–11. https://doi.org/10.1371/journal.pone.0123758

Gilbert, G. S. (2002). Evolutionary ecology of plant diseases in natural ecosystems. *Annual Review of Phytopathology*, *40(1)*, 13–43. https://doi.org/10.1146/annurev.phyto.40.021202.110417

Gilligan, C. A., and van den Bosch, F. (2008). Epidemiological models for invasion and persistence of pathogens. *Annual Review of Phytopathology, 46*, 385–418. https://doi.org/10.1146/annurev.phyto.45.062806.094357

Giordana, G., Kitzberger, T., and La Manna, L. (2020). Anthropogenic factors control the distribution of a southern conifer *Phytophthora* disease in a peri-urban area of Northern Patagonia, Argentina. *Forests*, *11(11)*, 1–17. https://doi.org/10.3390/f11111183

Global Biodiversity Information Facility (GBIF). (2021). Occurrence data *Austrocedrus chilensis* (D.Don) Pic.Serm. & Bizzarri. https://doi.org/10.15468/dl.99vh6a

Global Biodiversity Information Facility (GBIF). (2016). GBIF backbone taxonomy. https://doi.org/10.15468/39OMEI

Goheen, D. J., Mallams, K., Betlejewski, F., and Hansen, E. (2012). Effectiveness of vehicle washing and roadside sanitation in decreasing spread potential of Port-Orford cedar root disease. *Western Journal of Applied Forestry*, *27(4)*, 170–175. https://doi.org/10.5849/wjaf.11-011

Gomez-Gallego, M., Gommers, R., Bader, M. K. F., and Williams, N. M. (2019). Modelling the key drivers of an aerial Phytophthora foliar disease epidemic, from the needles to the whole plant. *PLoS ONE*, *14(5)*, 1–23. https://doi.org/10.1371/journal.pone.0216161

Gottwald, T., Luo, W., Posny, D., Riley, T., and Louws, F. (2019). A probabilistic census-travel model to predict introduction sites of exotic plant, animal and human pathogens. *Philosophical Transactions of the Royal Society B: Biological Sciences*, *374(1776)*, 20180260. https://doi.org/10.1098/rstb.2018.0260

Gottwald, T. R., Hughes, G., Graham, J. H., Sun, X., and Riley, T. (2001). The citrus canker epidemic in Florida: the scientific basis of regulatory eradication policy for an invasive species. *Phytopathology*, *91(1)*, 30-34. https://doi/10.1094/PHYTO.2001.91.1.30

Grabs, T., Seibert, J., Bishop, K., and Laudon, H. (2009). Modeling spatial patterns of saturated areas: a comparison of the topographic wetness index and a dynamic distributed model. *Journal of Hydrology*, *373(1)*, 15–23. https://doi.org/10.1016/j.jhydrol.2009.03.031

Green, S., Cooke, D. E. L., Dunn, M., Barwell, L., Purse, B. V., Chapman, D., Valatin, G., Schlenzig, A., Barbrook, J., Pettitt, T., Price, C., Pérez-Sierra, A., Frederickson-Matika, D., Pritchard, L., Thorpe, P., Cock, P., Randall, E., Keillor, B., and Marzano, M. (2021a). PHYTO-THREATS: addressing threats to UK forests and woodlands from *Phytophthora*; identifying risks of spread in trade and methods for mitigation. *Forests*, *12(12)*, 1617. https://doi.org/10.3390/f12121617

Green, S., James, E. R., Clark, D., Clarke, T.-K., and Riddell, C. E. (2021b). Evidence for natural resistance in *Juniperus communis* to *Phytophthora austrocedri*. *Journal of Plant Pathology*, *103(1)*, 55–59. https://doi.org/10.1007/s42161-020-00693-1

Green, S., Elliot, M., Armstrong, A., and Hendry, S. J. (2015). *Phytophthora austrocedrae* emerges as a serious threat to juniper (*Juniperus communis*) in Britain. *Plant Pathology*, *64(2)*, 456–466. https://doi.org/10.1111/ppa.12253

Green, S., Hendry, S. J., MacAskill, G. A., Laue, B. E., and Steele, H. (2012). Dieback and mortality of *Juniperus communis* in Britain associated with *Phytophthora austrocedrae*. *New Disease Reports, 26(1)*, 2–2. https://doi.org/10.5197/j.2044-0588.2012.026.002

Greslebin, A., Hansen, E. M., and La Manna, L. (2011). *Phytophthora austrocedrae*. *Forest Phytophthoras, 1(1)*. https://doi.org/10.5399/osu/fp.1.1.1806

Greslebin, A. G., and Hansen, E. M. (2010). Pathogenicity of *Phytophthora austrocedrae* on *Austrocedrus chilensis* and its relationship with mal del ciprés in Patagonia. *Plant Pathology*, *59(4)*, 604–612. https://doi.org/10.1111/j.1365-3059.2010.02258.x

Greslebin, A. G., Hansen, E. M., and Sutton, W. (2007). *Phytophthora austrocedrae* sp. nov., a new species associated with *Austrocedrus chilensis* mortality in Patagonia (Argentina). *Mycological Research, 111(3)*, 308–316. https://doi.org/10.1016/j.mycres.2007.01.008

Griffiths, A., and McClenaghan, R. (2010). *Survey, conservation, and propagation* of Juniperus communis *susbp.* hemisphaerica *on the Lizard, Cornwall*. Eden Project.

Grosdidier, M., Scordia, T., Ioos, R., and Marçais, B. (2020). Landscape epidemiology of ash dieback. *Journal of Ecology*, *108(5)*, 1789-1799. https://doi.org/10.1111/1365-2745.13383

Grosdidier, M., Ioos, R., Husson, C., Cael, O., Scordia, T., and Marçais, B. (2018). Tracking the invasion: dispersal of *Hymenoscyphus fraxineus* airborne inoculum at different scales. *FEMS Microbiology Ecology*, *94(5)*, 1–11. https://doi.org/10.1093/femsec/fiy049

Gruber, S., and Peckham, S. (2009). Chapter 7 Land-Surface Parameters and Objects in Hydrology, in: Hengl, T., Reuter, H. I. (Eds.), *Geomorphometry: Concepts, Software, Applications* (pp. 171–194). Elsevier Science. https://doi.org/10.1016/S0166-2481(08)00007-X

Haas, S. E., Hooten, M. B., Rizzo, D. M., and Meentemeyer, R. K. (2011). Forest species diversity reduces disease risk in a generalist plant pathogen invasion. *Ecology Letters*, *14(11)*, 1108–1116. https://doi.org/10.1111/j.1461-0248.2011.01679.x

Hamilton, K. (2018). *Juniper* Juniperus communis *and Yew* Taxus baccata *survey in the Binevenagh area, Co. Londonderry*. Mantella Environmental.

Hansen, E. M. (2015). Phytophthora species emerging as pathogens of forest trees. *Current Forestry Reports*, *1(1)*, 16–24. https://doi.org/10.1007/s40725-015-0007-7

Hansen, E. M., Goheen, D. J., Jules, E. S., and Ullian, B. (2000). Managing Port-Orford cedar and the introduced pathogen *Phytophthora lateralis*. *Plant Disease*, *84(1)*, 4-14.

Hardham, A. R. (2005). *Phytophthora cinnamomi*. *Molecular Plant Pathology*, *6(6)*, 589–604. https://doi.org/10.1111/j.1364-3703.2005.00308.x

Harmer, R., Kiewitt, A., Morgan, G., and Gill, R. (2010). Does the development of bramble (*Rubus fruticosus* L. agg.) facilitate the growth and establishment of tree seedlings in woodlands by reducing deer browsing damage? *Forestry*, *83(1)*, 93–102. https://doi.org/10.1093/forestry/cpp032

Harrower, C. (2016). BRCmap: Biological Records Centre Atlas Mapping. R package version 0.10.3.1. UK Centre for Ecology and Hydrology.

Harwood, T. D., Xu, X., Pautasso, M., Jeger, M. J., and Shaw, M. W. (2009). Epidemiological risk assessment using linked network and grid based modelling: *Phytophthora ramorum* and *Phytophthora kernoviae* in the UK. *Ecological Modelling*, *220(23)*, 3353–3361. https://doi.org/10.1016/j.ecolmodel.2009.08.014

He, Y., Chen, G., Potter, C., and Meentemeyer, R. K. (2019). Integrating multi-sensor remote sensing and species distribution modelling to map the spread of emerging forest disease and tree mortality. *Remote Sensing of Environment, 231*, 111238. https://doi.org/10.1016/j.rse.2019.111238

Hennon, P. E., Amore, D. V. D., Schaberg, P. G., Wittwer, D. T., and Shanley, C. S. (2012). Shifting climate, altered niche, and a dynamic conservation strategy for yellow-cedar in the north Pacific coastal rainforest. *Bioscience*, *62*, 147–158. https://doi.org/10.1525/bio.2012.62.2.8

Henricot, B., Pérez-Sierra, A., Armstrong, A. C., Sharp, P. M., and Green, S. (2017). Morphological and genetic analyses of the invasive forest pathogen phytophthora austrocedri reveal that two clonal lineages colonized britain and argentina from a common ancestral population. *Phytopathology, 107(12)*, 1532–1540. https://doi.org/10.1094/PHYTO-03-17-0126-R

Hernández-Lambraño, R. E., González-Moreno, P., and Sánchez-Agudo, J. Á. (2018). Environmental factors associated with the spatial distribution of invasive plant pathogens in the Iberian Peninsula: the case of *Phytophthora cinnamomi* Rands. *Forest Ecology and Management, 419–420(3)*, 101–109. https://doi.org/10.1016/j.foreco.2018.03.026

Hijmans, R. J. (2020). raster: geographic data analysis and modeling. R package version 3.0-12. https://CRAN.R-project.org/package=raster

Hijmans, R. J., Phillips, S., Leathwick, J., and Elith, J. (2020). dismo: Species Distribution Modeling. R package version 1.3-3. https://CRAN.R-project.org/package=dismo

Hijmans, R. J. (2019). raster: Geographic Data Analysis and Modeling. R package version 2.8-19. https://CRAN.R-project.org/package=raster

Hijmans, R. J. (2016). raster: geographic data analysis and modeling. R package version 3.0-2. https://CRAN.R-project.org/package=raster

Hill, M. O., Preston, C. D., and Roy, D. B. (2004). PLANTATT Attributes of British and Irish plants: status, size, life history, geography and habitats. UK Centre for Ecology and Hydrology.

Hill, P. W., Handley, L. L., and Raven, J. A. (1996). *Juniperus communis* L. ssp*. communis* at Balnaguard, Scotland: foliar carbon discrimination ($\delta^{13}C$) and 15-N natural abundance ($\delta^{15}N$) suggest gender-linked differences in water and N use. *Botanical Journal of Scotland, 48(2),* 209–224. https://doi.org/10.1080/03746609608684842

Hirzel, A. H., Le Lay, G., Helfer, V., Randin, C., and Guisan, A. (2006). Evaluating the ability of habitat suitability models to predict species presences. *Ecological Modelling*, *199(2)*, 142–152. https://doi.org/10.1016/j.ecolmodel.2006.05.017

Holdenrieder, O., Pautasso, M., Weisberg, P. J., and Lonsdale, D. (2004). Tree diseases and landscape processes: the challenge of landscape pathology. *Trends in Ecology and Evolution*, *19(8)*, 446–452. https://doi.org/10.1016/j.tree.2004.06.003

Homet, P., González, M., Matías, L., Godoy, O., Pérez-Ramos, I. M., García, L. V., and Gómez-Aparicio, L. (2019). Exploring interactive effects of climate change and exotic pathogens on *Quercus suber* performance: damage caused by *Phytophthora cinnamomi*

varies across contrasting scenarios of soil moisture. *Agricultural and Forest Meteorology*, *276–277(5)*, 107605. https://doi.org/10.1016/j.agrformet.2019.06.004

Horner, I. J. (2020). *Phytophthora agathidicida*: research progress, cultural perspectives and knowledge gaps in the control and management of kauri dieback in New Zealand. *Plant Pathology*, *69(1)*, 3–16. https://doi.org/10.1111/ppa.13104

Huang, J., Malone, B. P., Minasny, B., McBratney, A. B., and Triantafilis, J. (2017). Evaluating a Bayesian modelling approach (INLA-SPDE) for environmental mapping. *Science of the Total Environment, 609*, 621–632. https://doi.org/10.1016/j.scitotenv.2017.07.201

Hughes, G., and Madden, L. V. (1993). Using the beta-binomial distribution to describe aggregated patterns of disease incidence. *Phytopathology*, *83*, 759–763.

Hulme, P. E. (2020). Plant invasions in New Zealand: global lessons in prevention, eradication and control. *Biological Invasions*, *22(5)*, 1539–1562. https://doi.org/10.1007/s10530-020-02224-6

Hulme, P. E. (2009). Trade, transport and trouble: managing invasive species pathways in an era of globalization. *Journal of Applied Ecology*, *46(1)*, 10–18. https://doi.org/10.1111/j.1365-2664.2008.01600.x

Ince, B. Y. J. (1995). Late-glacial and early Holocene vegetation of Snowdonia. *New Phytologist*, *132(2)*, 343–353.

Intergovernmental Science-Policy Platform on Biodiversity and Ecosystem Services (IPBES). (2019). *Summary for policymakers of the global assessment report on biodiversity and ecosystem services of the Intergovernmental Science-Policy Platform on Biodiversity and Ecosystem Services.* https://doi.org/https://doi.org/10.5281/zenodo.3553579

International Union for Conservation of Nature (IUCN). (2020). The Bonn Challenge. Retrieved from https://www.bonnchallenge.org/about

International Union for Conservation of Nature (IUCN). (2003). IUCN Definitions ─ English. 1-79. Retrieved from https://www.iucn.org/downloads/en_iucn__glossary_definitions.pdf

James Hutton Institute. (2011). 1:250,000 Soil map (National soil map of Scotland). https://www.hutton.ac.uk/learning/natural-resource-datasets/soilshutton/soils-maps-scotland/download#soilmapdata

Johansson, A., and Liberg, O. (1996). Functional aspects of marking behavior by male roe deer (*Capreolus capreolus*). *Journal of Mammalogy*, *77(2)*, 558–567. https://doi.org/10.2307/1382829

Joint Nature Conservation Committee (JNCC). (2020). The Copernicus Project. Retrieved from https://jncc.gov.uk/our-work/copernicus-project/#applications-using-copernicus-data-using-eo-in-scanning-for-emerging-infectious-diseases

Joint Nature Conservation Committee (JNCC). (2016). UK BAP priority vascular plant species. Retrieved from http://jncc.defra.gov.uk/page-5171

Joint Nature Conservation Committee (JNCC). (2007). Second report by the United Kingdom under Article 17 on the implementation of the Habitats Directive from January 2001 to December 2006. Retrieved from www.jncc.gov.uk/article17

Jones, G., and Kleczkowski, A. (2020). Modelling plant health for policy. *Emerging Topics in Life Sciences*, *4(5)*, 473–483. https://doi.org/10.1042/ETLS20200069

Jones, B., and Carter, H. (2018). *Tree health aerial survey protocol summary of how helicopter-based aerial survey is undertaken by the FCE Tree Health Team*. pp. 1-28. Forestry Commission England.

Jones, H. P., Jones, P. C., Barbier, E. B., Blackburn, R. C., Rey Benayas, J. M., Holl, K. D., McCrackin, M., Meli, P., Montoya, D., and Mateos, D. M. (2018). Restoration and repair of Earth's damaged ecosystems. *Proceedings of the Royal Society B: Biological Sciences*, *285(1873)*, 20172577. https://doi.org/10.1098/rspb.2017.2577

Jules, E. S., Kauffman, M. J., Ritts, W. D., and Carroll, A. L. (2002). Spread of an invasive pathogen over a variable landscape: a non-native root rot on Port Orford cedar. *Ecology*, *83(11)*, 3167–3181. https://doi.org/10.1890/0012-9658(2002)083[3167:SOAIPO]2.0.CO;2

Jules, E. S., Steenbock, C. M., and Carroll, A. L. (2015). Update on the 35-year expansion of the invasive root pathogen, *Phytophthora lateralis*, across a landscape of Port Orford cedar

(*Chamaecyparis lawsoniana*). *Forest Pathology*, *45(2)*, 165–168. https://doi.org/10.1111/efp.12158

Jung, T., Jung, M. H., Cacciola, S. O., Cech, T., Bakonyi, J., Seress, D., Mosca, S., Schena, L., Seddaiu, S., Pane, A., Magnano di San Lio, G., Maia, C., Cravador, A., Franceschini, A., and Scanu, B. (2017). Multiple new cryptic pathogenic *Phytophthora* species from Fagaceae forests in Austria, Italy, and Portugal. *IMA Fungus*, *8(2)*, 219–244. https://doi.org/10.5598/imafungus.2017.08.02.02

Jung, T., Orlikowski, L., Henricot, B., Abad-Campos, P., Aday, A. G., Aguín Casal, O., Bakonyi, J., Cacciola, S. O., Cech, T., Chavarriaga, D., Corcobado, T., Cravador, A., Decourcelle, T., Denton, G., Diamandis, S., Doğmuş-Lehtijärvi, H. T., Franceschini, A., Ginetti, B., Green, S., … Peréz-Sierra, A. (2016). Widespread *Phytophthora* infestations in European nurseries put forest, semi-natural and horticultural ecosystems at high risk of *Phytophthora* diseases. Forest Pathology, 46(2), 134–163. https://doi.org/10.1111/efp.12239

Jung, T., Blaschke, H., and Osswald, W. (2000). Involvement of soilborne *Phytophthora* species in Central European oak decline and the effect of site factors on the disease. *Plant Pathology*, *49(6)*, 706–718. https://doi.org/10.1046/j.1365-3059.2000.00521.x

Kamoun, S., Furzer, O., Jones, J. D. G., Judelson, H. S., Ali, G. S., Dalio, R. J. D., Roy, S. G., Schena, L., Zambounis, A., Panabières, F., Cahill, D., Ruocco, M., Figueiredo, A., Chen, X., Hulvey, J., Stam, R., Lamour, K., Gijzen, M., Tyler, B. M., … Govers, F. (2015). The top 10 oomycete pathogens in molecular plant pathology. *Molecular Plant Pathology*, *16(4)*, 413–434. https://doi.org/10.1111/mpp.12190

Khatami, R., Mountrakis, G., and Stehman, S. V. (2016). A meta-analysis of remote sensing research on supervised pixel-based land-cover image classification processes: general guidelines for practitioners and future research. *Remote Sensing of Environment*, *177*, 89–100. https://doi.org/10.1016/j.rse.2016.02.028

Kleczkowski, A., Castle, M., Jones, G., Keenan, V., Revie, C., and Sheremet, O. (2020). *Impact of climate change on the spread of pests and diseases in Scotland. Project final report. PHC2018/14.* Scotland's Centre of Expertise for Plant Health (PHC). Retrieved from https://doi.org/10.5281/zenodo.3906052

Kong, P., Moorman, G. W., Lea-Cox, J. D., Ross, D. S., Richardson, P. A., and Hong, C. (2009). Zoosporic tolerance to pH stress and its implications for *Phytophthora* species in

aquatic ecosystems. *Applied and Environmental Microbiology*, *75(13)*, 4307–4314. https://doi.org/10.1128/AEM.00119-09

Kopecký, M., and Čížková, Š. (2010). Using topographic wetness index in vegetation ecology: does the algorithm matter? *Applied Vegetation Science*, *13(4)*, 450–459. https://doi.org/10.1111/j.1654-109X.2010.01083.x

Kovacs, K., Václavík, T., Haight, R. G., Pang, A., Cunniffe, N. J., Gilligan, C. A., and Meentemeyer, R. K. (2011). Predicting the economic costs and property value losses attributed to sudden oak death damage in California (2010-2020). *Journal of Environmental Management*, *92(4)*, 1292–1302. https://doi.org/10.1016/j.jenvman.2010.12.018

Krull, C. R., Waipara, N. W., Choquenot, D., Burns, B. R., Gormley, A. M., and Stanley, M. C. (2013). Absence of evidence is not evidence of absence: feral pigs as vectors of soil-borne pathogens. *Austral Ecology*, *38(5)*, 534–542. https://doi.org/10.1111/j.1442-9993.2012.02444.x

La Manna, L., Greslebin, A. G., and Matteucci, S. D. (2013). Applying cost-distance analysis for forest disease risk mapping: *Phytophthora austrocedrae* as an example. *European Journal of Forest Research, 132(5–6)*, 877–885. https://doi.org/10.1007/s10342-013-0720-3

La Manna, L., Matteucci, S. D., and Kitzberger, T. (2012). Modelling *Phytophthora* disease risk in *Austrocedrus chilensis* forests of Patagonia. *European Journal of Forest Research*, *131(2)*, 323–337. https://doi.org/10.1007/s10342-011-0503-7

La Manna, L., and Matteucci, S. D. (2012). Spatial and temporal patterns at small scale in *Austrocedrus chilensis* diseased forests and their effect on disease progression. *European Journal of Forest Research*, *131(5)*, 1487–1499. https://doi.org/10.1007/s10342-012-0617-6

La Manna, L., Matteucci, S. D., and Kitzberger, T. (2008). Abiotic factors related to the incidence of the *Austrocedrus chilensis* disease syndrome at a landscape scale. *Forest Ecology and Management*, *256(5)*, 1087–1095. https://doi.org/10.1016/j.foreco.2008.06.023

La Manna, L., and Rajchenberg, M. (2004a). Soil properties and *Austrocedrus chilensis* forest decline in Central Patagonia, Argentina. *Plant and Soil*, *263(1-2)*, 29–41. https://doi.org/10.1023/B:PLSO.0000047723.86797.13

La Manna, L., and Rajchenberg, M. (2004b). Soil properties and *Austrocedrus chilensis* forest decline in Central Patagonia, Argentina. *Plant and Soil*, *263*, 29–41. https://doi.org/10.1023/B:PLSO.0000047723.86797.13

Lamigueiro, O. P., and Hijmans, R. J. (2019). rasterVis. R package version 0.47. https://rdocumentation.org/packages/rasterVis/versions/0.47

Landa, B. B., Arias-Giraldo, L. F., Henricot, B., Montes-Borrego, M., Shuttleworth, L. A., and Pérez-Sierra, A. (2021). Diversity of Phytophthora species detected in disturbed and undisturbed British soils using high-throughput sequencing targeting ITS rRNA and COI mtDNA regions. *Forests*, *12(2)*, 229. https://doi.org/10.3390/f12020229

Landis, J. R., and Koch, G. G. (1977). The measurement of observer agreement for categorical data. *Biometrics, 33(1),* 159–174.

Lavery, L. (2016). *Juniper survey of Perth and Kinross, 2010*. Scottish Natural Heritage Commissioned Report Vol. 920. Retrieved from http://www.snh.org.uk/pdfs/publications/commissioned_reports/920.pdf

Lawley, R. (2012). *User guide: soil parent material 1km dataset*. British Geological Survey Internal Report.

Leonberger, A. J., Speers, C., Ruhl, G., Creswell, T., and Beckerman, J. L. (2012). A survey of *Phytophthora* spp. in Midwest nurseries, greenhouses, and landscapes. *Plant Disease*, *97(5)*, 635–640. https://doi.org/10.1094/PDIS-07-12-0689-RE

Liebhold, A. M., Brockerhoff, E. G., Garrett, L. J., Parke, J. L., and Britton, K. O. (2012). Live plant imports: the major pathway for forest insect and pathogen invasions of the US. *Frontiers in Ecology and the Environment*, *10(3)*, 135–143. https://doi.org/10.1890/110198

Lindgren, F., and Rue, H. (2015). Bayesian spatial modelling with R-INLA. *Journal of Statistical Software, 63(19),* 1–25. https://doi.org/10.18637/jss.v063.i19

Linnell, J. D. C., and Andersen, R. (1998). Territorial fidelity and tenure in roe deer bucks. *Acta Theriologica*, *43(1)*, 67–75.

Long, D., and Williams, J. (2007). Juniper in the British uplands: the Plantlife juniper survey results. Plantlife. Retrieved from https://www.plantlife.org.uk/application/files/6514/8233/2671/Juniper-report-2007.pdf

Lovari, S., Serrao, G., and Mori, E. (2017). Woodland features determining home range size of roe deer. *Behavioural Processes*, *140(4)*, 115–120. https://doi.org/10.1016/j.beproc.2017.04.012

Lowe, J. J., and Walker, M. J. C. (1981). The early Postglacial environment of Scotland: evidence from a site near Tyndrum, Perthshire. *Boreas*, *10(3)*, 281–294. https://doi.org/10.1111/j.1502-3885.1981.tb00489.x

Mack, R. N., Simberloff, D., Lonsdale, W. M., Evans, H., Clout, M., and Bazzaz, F. A. (2000). Biotic invasions: causes, epidemiology, global consequences and control. *Ecological Applications*, *10(3)*, 689–710. https://doi.org/10.1890/1051-0761

Magarey, R. D., Sutton, T. B., and Thayer, C. L. (2005). A simple generic infection model for foliar fungal plant pathogens. *Phytopathology*, *95*, 92–100. https://doi.org/10.1094/PHYTO-95-0092

Mahdikhani, M., Matinfar, M., and Aghaalikhani, A. (2017). First report of *Phytophthora austrocedri* causing phloem lesions and bronzing on *Cupressus sempervirens* in northern Iran. *New Disease Reports*, *36*, 10. https://doi.org/10.5197/j.2044-0588.2017.036.010

Maier, H., Spiegel, W., Kinaciyan, T., Krehan, H., Cabaj, A., Schopf, A., and Honigsmann, H. (2003). The oak processionary caterpillar as the cause of an epidemic airborne disease: survey and analysis. *British Journal of Dermatology, 149(5)*, 990–997. https://doi.org/10.1111/j.1365-2133.2003.05673.x

Mangiafico, S. (2021). rcompanion: functions to support extension education program evaluation. R package version 2.4.0. https://CRAN.R-project.org/package=rcompanion

Martinez-de la Torre, A., Blyth, E. M., and Robinson, E. L. (2018). Water, carbon, and energy fluxes simulation for Great Britain using the JULES Land Surface Model and the Climate Hydrology and Ecology research Support System meteorology dataset (1961-2015) [CHESS-land]. *NERC Environmental Information Data Centre*. https://doi.org/10.5285/c76096d6-45d4-4a69-a310-4c67f8dcf096

Marzano, M., Dandy, N., Bayliss, H. R., Porth, E., and Potter, C. (2015). Part of the solution? Stakeholder awareness, information, and engagement in tree health issues. *Biological Invasions, 17(7)*, 1961–1977. https://doi.org/10.1007/s10530-015-0850-2

Marzano, M., Dandy, N., Papazova-Anakieva, I., Avtzis, D., Connolly, T., Eschen, R., Glavendekić, M., Hurley, B., Lindelöw, Å., Matošević, D., Tomov, R., and Vettraino, A. M. (2016). Assessing awareness of tree pests and pathogens amongst tree professionals: a pan-European perspective*. Forest Policy and Economics, 70*, 164–171. https://doi.org/10.1016/j.forpol.2016.06.030

Mastin, A. J., Gottwald, T. R., van den Bosch, F., Cunniffe, N. J., and Parnell, S. (2020). Optimising risk-based surveillance for early detection of invasive plant pathogens. *PLoS Biology*, *18(10)*, 1–25. https://doi.org/10.1371/journal.pbio.3000863

McAllister, R. R. J., Robinson, C. J., Maclean, K., Guerrero, A. M., Collins, K., Taylor, B. M., and De Barro, P. J. (2015). From local to central: a network analysis of who manages plant pest and disease outbreaks across scales. *Ecology and Society*, *20(1)*, art67. https://doi.org/10.5751/ES-07469-200167

McBride, A. D. (n.d.). *Implementation plan for Borders Forest Trust juniper project*. Borders Forest Trust, 1-24.

McCartan, S. A., and Gosling, P. G. (2013). Guidelines for seed collection and stratification of common juniper (*Juniperus communis* L.). *Tree Planters' Notes, 56,* 24–29.

Meentemeyer, R. K., Cunniffe, N. J., Cook, A. R., Filipe, J. A. N., Hunter, R. D., Rizzo, D. M., and Gilligan, C. A. (2011). Epidemiological modeling of invasion in heterogeneous landscapes: spread of sudden oak death in California (1990–2030). *Ecosphere*, *2(2)*, 1-24. https://doi.org/10.1890/ES10-00192.1

Meentemeyer, R. K., Anacker, B. L., Mark, W., and Rizzo, D. M. (2008a). Early detection of emerging forest disease using dispersal estimation and ecological niche modeling. *Ecological Applications*, *18(2)*, 377–390. https://doi.org/10.1890/07-1150.1

Meentemeyer, R. K., Rank, N. E., Anacker, B. L., Rizzo, D. M., and Cushman, J. H. (2008b). Influence of land-cover change on the spread of an invasive forest pathogen. *Ecological Applications*, *18(1)*, 159–171. https://doi.org/10.1890/07-0232.1

Met Office. (2021). Met Office numerical weather prediction (NWP) system. Centre for Environmental Data Analysis. https://catalogue.ceda.ac.uk/uuid/f46cfa4784fb454e105f336981f1a82b

Met Office, Hollis, D., McCarthy, M., Kendon, M., Legg, T., and Simpson, I. (2020). HadUK-Grid Gridded Climate Observations on a 1km grid over the UK, v1.0.2.1 (1862-2019). Centre for Environmental Data Analysis. https://doi.org/10.5285/89908dfcb97b4a28976df806b4818639

Met Office. (2011). UKCP09: time series of annual values of rainfall intensity on days of rain ≥1 mm (mm/day). *data.gov.uk.* https://data.gov.uk/dataset/05306277-040b-4e6a-a2a4-2aef81e32697/ukcp09-time-series-of-annual-values-of-rainfall-intensity-on-days-of-rain-1-mm-mm-day

Metz, M. R., Frangioso, K. M., Meentemeyer, R. K., and Rizzo, D. M. (2011). Interacting disturbances: wildfire severity affected by stage of forest disease invasion. *Ecological Applications*, *21(2)*, 313–320. https://doi.org/10.1890/10-0419.1

Milliken, W., and Bridgewater, S. (2004). Flora Celtica. Birlinn Limited.

Mills, P., Dehnen-Schmutz, K., Ilbery, B., Jeger, M., Jones, G., Little, R., MacLeod, A., Parker, S., Pautasso, M., Pietravalle, S., and Maye, D. (2011). Integrating natural and social science perspectives on plant disease risk, management and policy formulation. *Philosophical Transactions of the Royal Society B: Biological Sciences*, *366(1573)*, 2035–2044. https://doi.org/10.1098/rstb.2010.0411

Milne, A. E., Gottwald, T., Parnell, S. R., Alonso Chavez, V., and van den Bosch, F. (2020). What makes or breaks a campaign to stop an invading plant pathogen? *PLOS Computational Biology*, 16(2), e1007570. https://doi.org/10.1371/journal.pcbi.1007570

Milne, A. E., Teiken, C., Deledalle, F., van den Bosch, F., Gottwald, T., and McRoberts, N. (2018). Growers' risk perception and trust in control options for huanglongbing citrus-disease in Florida and California. *Crop Protection, 114,* 177–186. https://doi.org/10.1016/j.cropro.2018.08.028

Moore, R. V., Morris, D. G., and Flavin, R. W. (2000). CEH digital river network of Great Britain (1:50,000). NERC Environmental Information Data Centre. https://catalogue.ceh.ac.uk/documents/7d5e42b6-7729-46c8-99e9-f9e4efddde1d

Moslonka-Lefebvre, M., Finley, A., Dorigatti, I., Dehnen-Schmutz, K., Harwood, T., Jeger, M. J., Xu, X., Holdenrieder, O., and Pautasso, M. (2011). Networks in plant epidemiology. *Phytopathology*, *101(4)*, 392-403. https://doi.org/10.1094 /PHYTO-07-10-0192

Mulholland, V., Schlenzig, A., MacAskill, G. A., and Green, S. (2013). Development of a quantitative real-time PCR assay for the detection of *Phytophthora austrocedrae*, an emerging pathogen in Britain. *Forest Pathology*, *43*, 513–517. https://doi.org/10.1111/efp.12058

Mundo, I. A., El Mujtar, V. A., Perdomo, M. H., Gallo, L. A., Villalba, R., and Barrera, M. D. (2010). *Austrocedrus chilensis* growth decline in relation to drought events in northern Patagonia, Argentina. *Trees - Structure and Function*, *24(3)*, 561–570. https://doi.org/10.1007/s00468-010-0427-8

Nagle, A. M., Long, R. P., Madden, L. V., and Bonello, P. (2010). Association of *Phytophthora cinnamomi* with white oak decline in southern Ohio. *Plant Disease*, *94(8)*, 1026–1034. https://doi.org/10.1094/PDIS-94-8-1026

Nathan, R., Klein, E. K., Robledo-Arnuncio, J. J., and Revilla, E. (2012). Chapter 15: Dispersal kernels: review. In J. Clobert, M. Baguette, T. G. Benton, and J. M. Bullock (Eds.), *Dispersal Ecology and Evolution* (pp. 210). Oxford University Press. https://doi.org/10.1093/acprof:oso/9780199608898.001.0001

National Aeronautics and Space Administration (NASA). (2014). Shuttle Radar Topography Mission 1 arc-second global elevation data in raster format. *Earth Resources Observation and Science (EROS) Center.* https://doi.org/10.5066/F7PR7TFT

National Biodiversity Network. (2021). NBN Atlas. Retrieved from https://nbn.org.uk/

Natural England (2019a). Access to information request RFI 4662 Juniper features, received 13th June 2019.

Natural England. (2019b). Monitor of Engagement with the Natural Environment: adult respondent and visit data (DATA006) Year 1 to 10. *Natural England Access to Evidence.* http://publications.naturalengland.org.uk/publication/4897139222380544

Natural England. (2019c). Monitor of Engagement with the Natural Environment: the national survey on people and the natural environment. Technical Report to the 2009 - 2019 surveys.

Retrieved from https://assets.publishing.service.gov.uk/government/uploads/system/uploads/attachment_data/file/875153/MENE_Technical_Report_Years_1_to_10v2.pdf

Natural England. (2012). Evolution of agri-environment schemes in England. Retrieved from http://publications.naturalengland.org.uk/publication/3567470

Natural England. (2000). Naddle Forest SSSI: views about management. Retrieved from http://www.sssi.naturalengland.org.uk/Special/sssi/vam/VAM 1005932.pdf

NatureScot. (2017). Site condition monitoring for protected areas (SSSI/SACs) with reportable juniper features, received 3rd August 2017.

NatureScot/Mountain Woodland Action Group (2015). *Montane scrub database*. NatureScot.

Nelson, E. (1980). What is the correct name for the Dunkeld hybrid larch (*Larix decidua* x *L. leptolepis*)? *Irish Forestry*, *37(2)*, 112–118.

Neri, F. M., Cook, A. R., Gibson, G. J., Gottwald, T. R., and Gilligan, C. A. (2014). Bayesian analysis for inference of an emerging epidemic: citrus canker in urban landscapes. *PLoS Computational Biology*,*10(4)*, e1003587. https://doi.org/10.1371/journal.pcbi.1003587

New York Declaration on Forests (2014). Retrieved from https://forestdeclaration.org/images/uploads/resource/NYDF_Declaration.pdf

Nursery Industry Accreditation Scheme Australia. (2019). Best management practice guidelines. 8th edition. Greenlife Industry Australia. Retrieved from https://nurseryproductionfms.com.au/wp-content/uploads/2020/04/NIASA-Guidelines-8th-Edition-2019_Preview.pdf

O'Hanlon, R., Choiseul, J., Brennan, J. M., and Grogan, H. (2018). Assessment of the eradication measures applied to *Phytophthora ramorum* in Irish *Larix kaempferi* forests. *Forest Pathology, 48(1)*, 2003–2010. https://doi.org/10.1111/efp.12389

Observatree. (2018). Observatree monitoring tree health. Retrieved from https://www.observatree.org.uk/

OpenDoorLogistics. (2015). UK postcode boundary polygons. OpenDoorLogistics. https://www.opendoorlogistics.com/downloads/

Ordnance Survey. (2021). OS Open Roads. Ordnance Survey. https://www.ordnancesurvey.co.uk/business-government/products/open-map-roads

Parnell, S., Gottwald, T. R., Riley, T., and van den Bosch, F. (2014). A generic risk-based surveying method for invading plant pathogens. *Ecological Applications*, *24(4)*, 779–790. https://doi.org/10.1890/13-0704.1

Parnell, S., Gottwald, T. R., Gilligan, C. A., Cunniffe, N. J., and van den Bosch, F. (2010). The effect of landscape pattern on the optimal eradication zone of an invading epidemic. *Phytopathology, 100(7),* 638–644. https://doi.org/10.1094/PHYTO-100-7-0638

PCI Geomatics. (2010). Geomatica version 9.1.7-R5.

Pechlivanidis, I. G., McIntyre, N. R., and Wheater, H. S. (2010). Calibration of the semi-distributed PDM rainfall-runoff model in the Upper Lee catchment, UK. *Journal of Hydrology, 386(1-4)*, 198–209. https://doi.org/10.1016/j.jhydrol.2010.03.022

Penczykowski, R. M., Parratt, S. R., Barrès, B., Sallinen, S. K., and Laine, A. L. (2018). Manipulating host resistance structure reveals impact of pathogen dispersal and environmental heterogeneity on epidemics. *Ecology*, *99(12)*, 2853–2863. https://doi.org/10.1002/ecy.2526

Peters, D. P. C., Pielke, R. A., Bestelmeyer, B. T., Allen, C. D., Munson-mcgee, S., and Havstad, K. M. (2004). Cross-scale interactions, nonlinearities, and forecasting catastrophic events. *Proceedings of the National Academy of Sciences*, *101(42)*, 15130–15135.

Peterson, E., Hansen, E., and Kanaskie, A. (2014). Spatial relationship between *Phytophthora ramorum* and roads or streams in Oregon tanoak forests. *Forest Ecology and Management*, *312*, 216–224. https://doi.org/10.1016/j.foreco.2013.10.002

Petrasova, A., Gaydos, D. A., Petras, V., Jones, C. M., Mitasova, H., and Meentemeyer, R. K. (2020). Geospatial simulation steering for adaptive management. *Environmental Modelling and Software*,*133(8)*, 104801. https://doi.org/10.1016/j.envsoft.2020.104801

Pierce, D. (2019). ncdf4: interface to Unidata netCDF (Version 4 or Earlier) Format Data Files. R package version 1.17. https://CRAN.R-project.org/package=ncdf4

Planchon, O., and Darboux, F. (2001). A fast, simple and versatile algorithm to fill the depressions of digital elevation models. *Catena, 46(2-3),* 159–176. https://doi.org/10.1016/S0341-8162(01)00164-3

Plant Health Alliance Steering Group. (2019). Plant health management standard general requirements for plant growers and suppliers. Finalised version 1.0. 1-8. Retrieved from https://planthealthy.org.uk/assets/downloads/3_Plant-health-management-standard-v1.0-published-240119.pdf

Plantlife. (2015). The state of Scotland's juniper in 2015. Retrieved from http://www.plantlife.org.uk/application/files/6514/8241/0951/ScotsJuniper_report_2015.pdf

Plantlife International. (2007). *Juniperus communis* L. UK Biodiversity Action Plan (BAP). Retrieved from http://adlib.everysite.co.uk/resources/000/091/214/Jun1_dossier.pdf

Pollard, C. R. J., Marzano, M., and Paterson, A. (2021). *Assessment of large-scale plant biosecurity risks to Scotland from non-specialist and online horticultural sales. Project final report PHC2019/04.* Scotland's Centre of Expertise for Plant Health (PHC).

Potter, C., and Urquhart, J. (2017). Tree disease and pest epidemics in the Anthropocene: a review of the drivers, impacts and policy responses in the UK. *Forest Policy and Economics*, *79*, 61–68. https://doi.org/10.1016/j.forpol.2016.06.024

Preston, C. D., Pearman, D. A., and Dines, T. D. (2002). *New Atlas of the British and Irish Flora*. Oxford University Press.

Prospero, S., and Cleary, M. (2017). Effects of host variability on the spread of invasive forest diseases. *Forests*, *8*, 1–21. https://doi.org/10.3390/f8030080

Pugh, T. A. M., Arneth, A., Kautz, M., Poulter, B., and Smith, B. (2019). Important role of forest disturbances in the global biomass turnover and carbon sinks. *Nature Geoscience, 12,* 730–735. https://doi.org/10.1038/s41561-019-0427-2

Purse, B. V., Darshan, N., Kasabi, G. S., Gerard, F., Samrat, A., George, C., Vanak, A. T., Oommen, M., Rahman, M., Burthe, S. J., Young, J. C., Srinivas, P. N., Schäfer, S. M., Henrys, P. A., Sandhya, V. K., Chandaid, M. M., Murhekarid, M. V., Hoti, S. L., and Kiran, S. K. (2020). Predicting disease risk areas through co-production of spatial models: the

example of Kyasanur Forest Disease in India's forest landscapes. PLoS Neglected Tropical Diseases, 14(4), 1–20. https://doi.org/10.1371/journal.pntd.0008179

Purse, B. V., and Golding, N. (2015). Tracking the distribution and impacts of diseases with biological records and distribution modelling. *Biological Journal of the Linnean Society*, *115(3)*, 664–677. https://doi.org/10.1111/bij.12567

Purse, B. V., Graeser, P., Searle, K., Edwards, C., and Harris, C. (2013). Challenges in predicting invasive reservoir hosts of emerging pathogens: mapping *Rhododendron ponticum* as a foliar host for *Phytophthora ramorum* and *Phytophthora kernoviae* in the UK. *Biological Invasions, 15(3),* 529–545. https://doi.org/10.1007/s10530-012-0305-y

Purse, B. V., and Rogers, D. J. (2008). Chapter 16. Bluetongue virus and climate change. In P. S. Mellor, M. Baylis, and P. P. C. Mertens (Eds.), *Bluetongue* (pp. 343–364). Elsevier Ltd.

R Core Team. (2019). R: A language and environment for statistical computing. R Foundation for Statistical Computing. https://www.R-project.org/

R Core Team. (2018). R: A language and environment for statistical computing. R Foundation for Statistical Computing. https://www.R-project.org/

R Core Team. (2017). R: a language and environment for statistical computing. R Foundation for Statistical Computing. https://www.R-project.org/.

Redding, D. W., Lucas, T. C. D., Blackburn, T. M., and Jones, K. E. (2017). Evaluating Bayesian spatial methods for modelling species distributions with clumped and restricted occurrence data. *PLoS One, 12,* e0187602. https://doi.org/10.1371/journal.pone.0187602

Redekar, N. R., Bourret, T. B., Eberhart, J. L., Johnson, G. E., Pitton, B. J. L., Haver, D. L., Oki, L. R., and Parke, J. L. (2020). The population of oomycetes in a recycled irrigation water system at a horticultural nursery in southern California. *Water Research*, *183*, 116050. https://doi.org/10.1016/j.watres.2020.116050

Redekar, N. R., Eberhart, J. L., and Parke, J. L. (2019). Diversity of *Phytophthora*, *Pythium*, and *Phytopythium* species in recycled irrigation water in a container nursery. *Phytobiomes Journal*, *3(1)*, 31–45. https://doi.org/10.1094/PBIOMES-10-18-0043-R

Redondo, M. A., Boberg, J., Stenlid, J., and Oliva, J. (2018a). Contrasting distribution patterns between aquatic and terrestrial *Phytophthora* species along a climatic gradient are linked to functional traits. *The ISME Journal*, *12(12)*, 2967–2980. https://doi.org/10.1038/s41396-018-0229-3

Redondo, M. A., Boberg, J., Stenlid, J., and Oliva, J. (2018b). Functional traits associated with the establishment of introduced *Phytophthora* spp. in Swedish forests. *Journal of Applied Ecology*, *55(3)*, 1538–1552. https://doi.org/10.1111/1365-2664.13068

Reed, M. S. (2008). Stakeholder participation for environmental management: a literature review. *Biological Conservation*, *141(10)*, 2417–2431. https://doi.org/10.1016/j.biocon.2008.07.014

Reid, C., Hornigold, K., McHenry, E., Nichols, C., Townsend, M., Lewthwaite, K., Elliot, M., Pullinger, R., Hotchkiss, A., Gilmartin, E., White, I., Chesshire, H., Whittle, L., Garforth, J., Gosling, R., Reed, T., and Hugi, M. (2021). State of the UK's woods and trees. Woodland Trust. Retrieved from https://www.woodlandtrust.org.uk/state-of-uk-woods-and-trees/

Reis, S., Liska, T., Steinle, S., Carnell, E., Leaver, D., Roberts, E., Vieno, M., Beck, R., and Dragosits, U. (2017). UK gridded population 2011 based on census 2011 and Land Cover Map 2015. NERC Environmental Information Data Centre. https://doi.org/10.5285/0995e94d-6d42-40c1-8ed4-5090d82471e1

Renner, I. W., Elith, J., Baddeley, A., Fithian, W., Hastie, T., Phillips, S. J., Popovic, G., and Warton, D. I. (2015). Point process models for presence-only analysis. *Methods in Ecology and Evolution, 6(4),* 366–379. https://doi.org/10.1111/2041-210X.12352

Reuter, H. I., Hengl, T., Gessler, P., and Soille, P. (2009). Chapter 4: Preparation of DEMs for Geomorphometric Analysis. In T. Hengl and H. I. Reuter (Eds.), *Geomorphometry: Concepts, Software, Applications* (pp. 87–120). Elsevier Science. https://doi.org/10.1016/S0166-2481(08)00004-4

Richards, J. A. (1999). Remote sensing and digital image analysis: an introduction (2nd ed.). Springer.

Riddell, C. E., Dun, H. F., Elliot, M., Armstrong, A. C., Clark, M., Forster, J., Hedley, P. E., and Green, S. (2020). Detection and spread of *Phytophthora austrocedri* within infected

Juniperus communis woodland and diversity of co-associated Phytophthoras as revealed by metabarcoding. *Forest Pathology, 50(3)*, e12602. https://doi.org/10.1111/efp.12602

Riddell, C. E., Frederickson-Matika, D., Armstrong, A. C., Elliot, M., Forster, J., Hedley, P. E., Morris, J., Thorpe, P., Cooke, D. E. L., Pritchard, L., Sharp, P. M., and Green, S. (2019). Metabarcoding reveals a high diversity of woody host-associated *Phytophthora* spp. in soils at public gardens and amenity woodlands in Britain. *PeerJ*, *7*, 2-31. https://doi.org/10.7717/peerj.6931

Righetto, A. J., Faes, C., Vandendijck, Y., and Ribeiro Jr, P. J. (2018). On the choice of the mesh for the analysis of geostatistical data using R-INLA. *Communications in Statistics – Theory and Methods*, *49(1)*, 203-220. https://doi.org/10.1080/03610926.2018.1536209

Ristaino, J. B., and Gumpertz, M. L. (2000). New frontiers in the study of dispersal and spatial analysis of epidemics caused by species in the genus *Phytophthora*. *Annual Review of Phytopathology*, *38(1)*, 541-576. https://doi.org/10.1146/annurev.phyto.38.1.541

Rizzo, D. M., Garbelotto, M., and Hansen, E. M. (2005). *Phytophthora ramorum*: integrative research and management of an emerging pathogen in California and Oregon forests. *Annual Review of Phytopathology, 43(1)*, 309–335. https://doi.org/10.1146/annurev.phyto.42.040803.140418

Roberts, M., Gilligan, C. A., Kleczkowski, A., Hanley, N., Whalley, A. E., and Healey, J. R. (2020). The effect of forest management options on forest resilience to pathogens. *Frontiers in Forests and Global Change*, *3(3)*, Article 7. https://doi.org/10.3389/ffgc.2020.00007

Robinson, E. L., Blyth, E., Clark, D. B., Comyn-Platt, E., Finch, J., and Rudd, A. C. (2020). Climate hydrology and ecology research support system meteorology dataset (1961-2017) [CHESS-met]. NERC Environmental Information Data Centre. https://doi.org/https://doi.org/10.5285/2ab15bf0-ad08-415c-ba64-831168be7293

Rodríguez de Rivera, O., Blangiardo, M., López-Quílez, A., and Martín-Sanz, I. (2018). Species distribution modelling through Bayesian hierarchical approach. *Theoretical Ecology*, *12(1)*, 49-59. https://doi.org/10.1007/s12080-018-0387-y

Rodwell, J.S. (1991). British plant communities. Volumes 1:5. Cambridge University Press.

Roy, B. A., Alexander, H. M., Davidson, J., Campbell, F. T., Burdon, J. J., Sniezko, R., and Brasier, C. (2014). Increasing forest loss worldwide from invasive pests requires new trade regulations. *Frontiers in Ecology and the Environment*, *12(8)*, 457–465. https://doi.org/10.1890/130240

Roy, H. E., Hesketh, H., Purse, B. V., Eilenberg, J., Santini, A., Scalera, R., Stentiford, G. D., Adriaens, T., Bacela-Spychalska, K., Bass, D., Beckmann, K. M., Bessell, P., Bojko, J., Booy, O., Cardoso, A. C., Essl, F., Groom, Q., Harrower, C., Kleespies, R., … Dunn, A. M. (2017). Alien pathogens on the horizon: opportunities for predicting their threat to wildlife. *Conservation Letters, 10(4)*, 476–483. https://doi.org/10.1111/conl.12297

Royal Forestry Society (2011). Leyland cypress. Retrieved from https://web.archive.org/web/20110215115929/http://www.rfs.org.uk/learning/leyland-cypress

Royal Horticultural Society (RHS). (2021). RHS plant health principles. Retrieved from https://www.rhs.org.uk/about-the-rhs/policies/plant-health-principles

Rue, H., Martino, S., and Chopin, N. (2009). Approximate Bayesian inference for latent Gaussian models by using integrated nested Laplace approximations. *Journal of the Royal Statistical Society. Series B: Statistical Methodology*, *71(2)*, 319–392. https://doi.org/10.1111/j.1467-9868.2008.00700.x

Rünk, K., Zobel, M., and Zobel, K. (2012). Biological Flora of the British Isles: *Dryopteris carthusiana*, *D. dilatata* and *D. expansa*. *Journal of Ecology*, *100(4)*, 1039–1063. https://doi.org/10.1111/j.1365-2745.2012.01985.x

Santini, A., Ghelardini, L., De Pace, C., Desprez-Loustau, M. L., Capretti, P., Chandelier, A., Cech, T., Chira, D., Diamandis, S., Gaitniekis, T., Hantula, J., Holdenrieder, O., Jankovsky, L., Jung, T., Jurc, D., Kirisits, T., Kunca, A., Lygis, V., Malecka, M., … Stenlid, J. (2013). Biogeographical patterns and determinants of invasion by forest pathogens in Europe. *New Phytologist*, *197(1)*, 238–250. https://doi.org/10.1111/j.1469-8137.2012.04364.x

Savary, S., Willocquet, L., Pethybridge, S. J., Esker, P., McRoberts, N., and Nelson, A. (2019). The global burden of pathogens and pests on major food crops. *Nature Ecology and Evolution*, *3(3)*, 430–439. https://doi.org/10.1038/s41559-018-0793-y

Schneider, K., Mourits, M., van der Werf, W., and Lansink, A. O. (2021). On consumer impact from *Xylella fastidiosa* subspecies *pauca*. *Ecological Economics*, *185(8),* 107024 https://doi.org/10.1016/j.ecolecon.2021.107024

Schneider, K., van der Werf, W., Cendoya, M., Mourits, M., Vicent, A., and Lansink, A. O. (2020). Impact of *Xylella fastidiosa* subspecies *pauca* in European olives. *Proceedings of the National Academy of Sciences*, *117(7)*, 9250-9259. https://doi.org/10.1073/pnas.1912206117

Scott, P., Bader, M. K. F., Burgess, T., Hardy, G., and Williams, N. (2019). Global biogeography and invasion risk of the plant pathogen genus *Phytophthora*. *Environmental Science and Policy*, *101(9)*, 175–182. https://doi.org/10.1016/j.envsci.2019.08.020

Scottish Forestry. (2021). *Phytophthora ramorum* on larch: action plan. Retrieved from https://forestry.gov.scot/publications/1024-scottish-forestry-p-ramorum-action-plan-june-2021/download

Scottish Government (2019). Scotland's Forestry Strategy 2019-2029. Retrieved from https://www.gov.scot/publications/scotlands-forestry-strategy-20192029/

Scottish Government. (2016). The Scottish plant health strategy 2016-2021. Retrieved from https://www.gov.scot/publications/scottish-plant-health-strategy/

Scottish Government. (2014). *Scotland's wild deer a national approach including 2015-2020 priorities.* Retrieved from https://www.nature.scot/sites/default/files/2020-01/Scotland%27s%20Wild%20Deer_%20A%20National%20Approach%202015-2020%20Priorities.pdf

Scottish Natural Heritage. (2017). National Vegetation Classification. Natural Spaces. https://gateway.snh.gov.uk/natural-spaces/dataset.jsp?dsid=NVC

Scottish Natural Heritage. (2011). Glenartney juniper wood Site of Special Scientific Interest Site management statement. Retrieved from https://sitelink.nature.scot/site/730

Scottish Ornithologists' Club. (2020). Our interactive site. Retrieved from https://www.the-soc.org.uk/bird-recording/grid-reference-finder

Secretariat of the Convention on Biological Diversity. (2010). Strategic plan for biodiversity and the Aichi Targets. Retrieved from https://www.cbd.int/doc/strategic-plan/2011-2020/Aichi-Targets-EN.pdf

Seebens, H., Blackburn, T. M., Dyer, E. E., Genovesi, P., Hulme, P. E., Jeschke, J. M.,Pagad, S., Pyšek, P., van Kleunen, M., Winter, M., Ansong, M., Arianoutsou, M., Bacher, S., Blasius, B., Brockerhoff, E. G., Brundu, G., Capinha, C., Causton, C. E., Celesti-Grapow, L., … Essl, F. (2018). Global rise in emerging alien species results from increased accessibility of new source pools. *Proceedings of the National Academy of Sciences of the United States of America*, *115(10)*, E2264–E2273. https://doi.org/10.1073/pnas.1719429115

Seidl, R., Müller, J., Hothorn, T., Bässler, C., Heurich, M., and Kautz, M. (2016). Small beetle, large-scale drivers: how regional and landscape factors affect outbreaks of the European spruce bark beetle. *Journal of Applied Ecology, 53(2),* 530–540. https://doi.org/10.1111/1365-2664.12540

Sena, K., Crocker, E., Vincelli, P., and Barton, C. (2018). *Phytophthora cinnamomi* as a driver of forest change: implications for conservation and management. *Forest Ecology and Management*, *409(12)*, 799–807. https://doi.org/10.1016/j.foreco.2017.12.022

Shaw, M. W. (1995). Simulation of population expansion and spatial pattern when individual dispersal distributions do not decline exponentially with distance. *Proceedings of the Royal Society B Biological Sciences, 259(1356)*, 243–248. https://doi.org/10.1098/rspb.1995.0036

Shearer, B. L., Crane, C. E., Barrett, S., and Cochrane, A. (2007). *Phytophthora cinnamomi* invasion, a major threatening process to conservation of flora diversity in the south-west botanical province of Western Australia. *Australian Journal of Botany*, *55(3)*, 225–238. https://doi.org/10.1071/BT06019

Silva, P. V., Vélez, M. L., Hernández Otaño, D., Nuñez, C., and Greslebin, A. G. (2016). Action of fosetyl-al and metalaxyl against *Phytophthora austrocedri*. *Forest Pathology, 46(1)*, 54–66. https://doi.org/10.1111/efp.12216

Sims, L., Tjosvold, S., Chambers, D., and Garbelotto, M. (2019.) Control of *Phytophthora* species in plant stock for habitat restoration through best management practices. *Plant Pathology*, *68*, 196–204. https://doi.org/10.1111/ppa.12933

Skelsey, P., With, K. A., and Garrett, K. A. (2013). Why dispersal should be maximized at intermediate scales of heterogeneity. *Theoretical Ecology*, *6(2)*, 203–211. https://doi.org/10.1007/s12080-012-0171-3

Skelsey, P., Rossing, W. A. H., Kessel, G. J. T., and van der Werf, W. (2010). Invasion of *Phytophthora infestans* at the landscape level: how do spatial scale and weather modulate the consequences of spatial heterogeneity in host resistance? *Phytopathology 100(11),* 1146–1161. https://doi.org/10.1094/PHYTO-06-09-0148

Slawson, D. (2015). Guidance plant biosecurity number 1 – sourcing plants. Recommended practice. National Trust. Retrieved from https://plantnetwork.org/wordpress/wp-content/uploads/3376/24082015-plant-biosecuritynote1sourcing-final.pdf

Smith, R. M., Baker, R. H. A., Malumphy, C. P., Hockland, S., Hammon, R. P., Ostojá-Starzewski, J. C., and Collins, D. W. (2007). Recent non-native invertebrate plant pest establishments in Great Britain: origins, pathways, and trends. *Agricultural and Forest Entomology*, *9(4)*, 307–326. https://doi.org/10.1111/j.1461-9563.2007.00349.x

Spake, R., Bellamy, C., Gill, R., Watts, K., Wilson, T., and Ditchburn, B. (2020). Forest damage by deer depends on cross-scale interactions between climate, deer density and landscape structure. *Journal of Applied Ecology*, *57(7)*, 1–161. https://doi.org/10.1111/1365-2664.13622

Spence, N., Hill, L., and Morris, J. (2020). How the global threat of pests and diseases impacts plants, people, and the planet. *Plants, People, Planet, 2(1)*, 5–13. https://doi.org/10.1002/ppp3.10088

Spiegelhalter, D. J., Best, N. G., Carlin, B. P., and van der Linde, A. (2002). Bayesian measures of model complexity and fit. *Journal of the Royal Statistical Society Series B: Statistical Methodology, 64, Part 4,* 583–639. https://doi.org/10.1111/1467-9868.00353

Squirrell, J., and Hollingsworth, P. M. (2008). An assessment of *Juniperus communis* ssp. *hemisphaerica* in Britain using molecular markers. CCW Contract Science Report No. 848. Countryside Council for Wales.

Sullivan, G. (2003). Extent and condition of juniper scrub in Scotland. Scottish Natural Heritage Archive Report (026). NatureScot. Retrieved from https://media.nature.scot/record/~8e94e99258

Swiecki, T. J., and Bernhardt, E. A. (2017.) Testing and implementing methods for managing Phytophthora root diseases in California native habitats and restoration sites. *Proceedings of the Sudden Oak Death Sixth Science Symposium*, *General Technical Report PSW-GTR-255*, 53-55. Retrieved from https://www.fs.fed.us/psw/publications/documents/psw_gtr255/psw_gtr255_053.pdf

Syfert, M. M., Smith, M. J. and Coomes, D. A. (2013). The effects of sampling bias and model complexity on the predictive performance of MaxEnt Species Distribution Models. *Plos One*, *8(2)*, e55158. https://doi.org/10.1371/journal.pone.0055158

Taccari, L. E., Greslebin, A. G., Salgado Salomón, M. E., and Vélez, M. L. (2019). Two conifer species native to Patagonia threatened by *Phytophthora austrocedri*. *Forest Pathology*, *49(2)*, 1–4. https://doi.org/10.1111/efp.12496

Tene, A., Broome, A., and Connolly, T. (2007). Investigation of possible causes of die-back of Glenartney Juniper Wood SAC, Perthshire 2006/07-2007/08-Part1: age structure analysis. Report commissioned by Scottish Natural Heritage. Forest Research.

Thomas, A. R. C., Cosby, B. J., Henrys, P. A., and Emmett, B. A. (2020). Topsoil pH estimates from the Countryside Survey of Great Britain, 2007 using a generalized additive model. NERC Environmental Information Data Centre. Retrieved from https://doi.org/10.5285/4b0e364d-61e6-48fb-8973-5eb18fb454cd

Thomas, P. A., El-Barghathi, M., and Polwart, A. (2007). Biological flora of the British Isles: *Juniperus communis* L. *Journal of Ecology*, *95(6)*, 1404–1440. https://doi.org/10.1111/j.1365-2745.2007.01308.x

Thompson, R. N., Gilligan, C. A., and Cunniffe, N. J. (2018). Control fast or control smart: when should invading pathogens be controlled? *PLoS Computational Biology*, *14(2)*, 1–21. https://doi.org/10.1371/journal.pcbi.1006014

Tippett, J. T., McGrath, J. F., Hill, T. C. (1989). Site and seasonal effects on susceptibility of *Eucalyptus marginata* to *Phytophthora cinnamomi*. *Australian Journal of Botany*, *37(6)*, 481–490. https://doi.org/10.1071/BT9890481

Tonini, F., Shoemaker, D., Petrasova, A., Harmon, B., Petras, V., Cobb, R. C., Mitasova, H., and Meentemeyer, R. K. (2017). Tangible geospatial modeling for collaborative solutions to

invasive species management. *Environmental Modelling and Software*, *92*, 176–188. https://doi.org/10.1016/j.envsoft.2017.02.020

Tradingeconomics.com and HM Customs and Excise. (2021). United Kingdom imports of live trees and plants, graphical summary 2000 - 2021. Retrieved from https://tradingeconomics.com/united-kingdom/imports-of-live-trees-plants

Troy, A., Morgan Grove, J., and O'Neil-Dunne, J. (2012). The relationship between tree canopy and crime rates across an urban–rural gradient in the greater Baltimore region. *Landscape and Urban Planning*, *106(3)*, 262–270. https://doi.org/10.1016/J.LANDURBPLAN.2012.03.010

United Nations (UN). (2020). The United Nations decade on ecosystem restoration strategy executive summary 2030. Retrieved from https://wedocs.unep.org/bitstream/handle/20.500.11822/31813/ERDStrat.pdf?sequence=1&isAllowed=y

United Nations (UN). (2015). Transforming our world: the 2030 agenda for sustainable development A/Res/70/1. Retrieved from https://sdgs.un.org/2030agenda

United Nations (UN). (1997). Kyoto protocol to the United Nations framework convention on climate change. Retrieved from https://unfccc.int/sites/default/files/resource/docs/cop3/l07a01.pdf

United Nations (UN). (1992). Convention on Biological Diversity. Retrieved from http://www.cbd.int/doc/legal/cbd-en.pdf

United Nations Economic and Social Council (UNESCO). (2017). United Nations strategic plan for forests 2017-2030 and quadrennial programme of work of the United Nations forum on forests for the period 2017-2020. E/RES/2017. Retrieved from https://www.un.org/esa/forests/documents/un-strategic-plan-for-forests-2030/index.html

Václavík, T., and Meentemeyer, R. K. (2009). Invasive species distribution modeling (iSDM): are absence data and dispersal constraints needed to predict actual distributions? *Ecological Modelling*, *220(23)*, 3248–3258. https://doi.org/10.1016/j.ecolmodel.2009.08.013

Václavík, T., Kanaskie, A., Hansen, E. M., Ohmann, J. L., and Meentemeyer, R. K. (2010). Predicting potential and actual distribution of sudden oak death in Oregon: prioritizing

landscape contexts for early detection and eradication of disease outbreaks. *Forest Ecology and Management*, *260(6)*, 1026–1035. https://doi.org/10.1016/j.foreco.2010.06.026

Václavík, T., and Meentemeyer, R.K. (2012). Equilibrium or not? Modelling potential distribution of invasive species in different stages of invasion. *Diversity and Distributions*, *18(1)*, 73–83. https://doi.org/10.1111/j.1472-4642.2011.00854.x

van den Bosch, F., Metz, J. A. J., and Zadoks, J. C. (1999). Pandemics of focal plant disease, a model. *Phytopathology*, *89(6)*, 495–505. https://doi.org/10.1094/PHYTO.1999.89.6.495

van der Merwe, M., Winfield, M. O., Arnold, G. M., and Parker, J. S. (2000). Spatial and temporal aspects of the genetic structure of *Juniperus communis* populations. *Molecular Ecology*, *9(4)*, 379–386. https://doi.org/10.1046/j.1365-294X.2000.00868.x

van der Wal, J., Falconi, L., Januchowski, S., Shoo, L., and Storlie, C. (2019). SDMTools: species distribution modelling tools: tools for processing data associated with species distribution modelling exercises. R package version 1.1-221. https://cran.r-project.org/package=SDMTools

van Uytvanck, J., and Hoffmann, M. (2009). Impact of grazing management with large herbivores on forest ground flora and bramble understorey. *Acta Oecologica*, *35*, 523–532. https://doi.org/10.1016/j.actao.2009.04.001

Vélez, M. L., La Manna, L., Tarabini, M., Gomez, F., Elliott, M., Hedley, P. E., Cock, P., and Greslebin, A. (2020). *Phytophthora austrocedri* in Argentina and co-inhabiting Phytophthoras: roles of anthropogenic and abiotic factors in species distribution and diversity. *Forests*, *11*, 1–24. https://doi.org/10.3390/f11111223

Vélez, M. L., Silva, P. V., Troncoso, O. A., and Greslebin, A. G. (2012). Alteration of physiological parameters of *Austrocedrus chilensis* by the pathogen *Phytophthora austrocedrae*. *Plant Pathology*, *61(5)*, 877–888. https://doi.org/10.1111/j.1365-3059.2011.02585.x

Verheyen, K., Adriaenssens, S., Gruwez, R., Michalczyk, I. M., Ward, L. K., Rosseel, Y., van den Broeck, A., and García, D. (2009). *Juniperus communis*: victim of the combined action of climate warming and nitrogen deposition? *Plant Biology, 11(Suppl.1)*, 49–59. https://doi.org/10.1111/j.1438-8677.2009.00214.x

Voinov, A., Kolagani, N., McCall, M. K., Glynn, P. D., Kragt, M. E., Ostermann, F. O., Pierce, S. A., and Ramu, P. (2016). Modelling with stakeholders - next generation. *Environmental Modelling and Software, 77*, 196–220. https://doi.org/10.1016/j.envsoft.2015.11.016

Walker, K. J., Stroh, P. A., and Ellis, R. W. (2017). *Threatened plants in Britain and Ireland*. Botanical Society of Britain and Ireland.

Wang, L., and Liu, H. (2006). An efficient method for identifying and filling surface depressions in digital elevation models for hydrologic analysis and modelling. *International Journal of Geographical Information Science, 20(2)*, 193–213. https://doi.org/10.1080/13658810500433453

Ward, L. K., and Shellswell, C. H. (2017). Looking after juniper: ecology, conservation and folklore. Plantlife. Retrieved from https://www.plantlife.org.uk/application/files/7614/8958/6210/JUNIPER_DOSSIER_13_2_17_CS.pdf

Ward, L. K. (1994). Evaluation of juniper sites in England and South Wales: the EC Species and Habitat Directive 1992. Project report TO8079M1. Institute of Terrestrial Ecology (Natural Environment Research Council).

Ward, L. K. (1982). The conservation of juniper: longevity and old age. *Journal of Applied Ecology*, *19(19)*, 917–928. Retrieved from http://www.jstor.org/stable/2403293

Waske, B., and Braun, M. (2009). Classifier ensembles for land cover mapping using multitemporal SAR imagery. *ISPRS Journal of Photogrammetry and Remote Sensing*, *64(5)*, 450–457. https://doi.org/10.1016/j.isprsjprs.2009.01.003

Welsh Government. (2019). *Phytophthora ramorum* strategy for Wales. Retrieved from https://gov.wales/sites/default/files/publications/2019-05/phytophthora-ramorum-management-strategy.pdf

Werres, S., Elliot, M., and Greslebin, A. G. (2014). Plant diseases and diagnosis JKI Data Sheets. 1–13. https://doi.org/10.5073/jkidspdd.2014.001

White, R. M., Young, J., Marzano, M., and Leahy, S. (2018). Prioritising stakeholder engagement for forest health, across spatial, temporal and governance scales, in an era of

austerity. *Forest Ecology and Management, 417(1)*, 313–322. https://doi.org/10.1016/j.foreco.2018.01.050

White, S. M., Bullock, J. M., Hooftman, D. A. P., and Chapman, D. S. (2017). Modelling the spread and control of *Xylella fastidiosa* in the early stages of invasion in Apulia, Italy. *Biological Invasions, 19(6)*, 1–13. https://doi.org/10.1007/s10530-017-1393-5

Whittome, T. (2010). Report No CASL-0909-129-1a Glenartney juniper wood aerial photography. Report commissioned by Scottish Natural Heritage.

Wickham, H. (2016). ggplot2: elegant graphics for data analysis. Springer-Verlag.

Wickham, H., François, R., Henry, L., and Muller, K. (2020). dplyr: a grammar of data manipulation. R package version 0.8.4. https://CRAN.R-project.org/package=dplyr

Wildlife and Countryside Act. (1981). Retrieved from https://www.legislation.gov.uk/ukpga/1981/69

Wilkins, T. C., and Duckworth, J. C. (2011). Breaking new ground for juniper - a management handbook for lowland England. Plantlife. Retrieved from https://www.plantlife.org.uk/application/files/4814/8155/5952/Breaking_new_ground_20_5_11.pdf

Wint, W., Morley, D., Medlock, J., and Alexander, N. S. (2014). A first attempt at modelling red deer (*Cervus elaphus*) distributions over Europe. *Open Health Data*, *2(1)*, e1. https://doi.org/10.5334/ohd.ag

Woodland Trust. (2017). Position statement. Tree health. UK Biosecurity and plant imports. Retrieved from https://www.woodlandtrust.org.uk/publications/2017/07/biosecurity-and-plant-imports-position-statement/

World Checklist of Selected Plant Families. (2017). The International plant names index and world checklist of selected plant families. Retrieved from http://www.plantsoftheworldonline.org/taxon/urn:lsid:ipni.org:names:30088655-2#distribution-map

World Weather Information Service (WWIS). (2021a). Bariloche Argentina-Servicio Meteorologico Nacional. World Meteorological Organisation. Retrieved from https://worldweather.wmo.int/en/city.html?cityId=858

World Weather Information Service (WWIS). (2021b). Ghazvin Islamic Republic of Iran Meteorological Organisation. World Meteorological Organisation. Retrieved from https://worldweather.wmo.int/en/city.html?cityId=1447

Wu, B., Liang, A., Zhang, H., Zhu, T., Zou, Z., Yang, D., Tang, W., Li, J., and Su, J. (2021). Application of conventional UAV-based high-throughput object detection to the early diagnosis of pine wilt disease by deep learning. *Forest Ecology and Management, 486*, 118986. https://doi.org/10.1016/j.foreco.2021.118986

Yang, X., Tyler, B. M., and Hong, C. (2017). An expanded phylogeny for the genus *Phytophthora*. *IMA Fungus*, *8(2)*, 355–384. https://doi.org/10.5598/imafungus.2017.08.02.09

Zarco-Tejada, P. J., Camino, C., Beck, P. S. A., Calderon, R., Hornero, A., Hernández-Clemente, R., Kattenborn, T., Montes-Borrego, M., Susca, L., Morelli, M., Gonzalez-Dugo, V., North, P. R. J., Landa, B. B., Boscia, D., Saponari, M., and Navas-Cortes, J. A. (2018). Previsual symptoms of *Xylella fastidiosa* infection revealed in spectral plant-trait alterations. *Nature Plants, 4*, 432–439. https://doi.org/10.1038/s41477-018-0189-7

Zeileis, A., and Grothendieck, G. (2005). zoo: S3 infrastructure for regular and irregular time series. *Journal of Statistical Software*, *14(6)*, 1–27. https://doi.org/10.18637/jss.v014.i06

Zuur, A. F., Ieno, E. N., and Saveliev, A. A. (2017). Spatial, temporal and spatial-temporal ecological data analysis with R-INLA. Volume I: using GLM and GLMM. Highland Statistics Ltd.

Appendix A. Mapping juniper field study populations

To identify sampling locations along a gradient of juniper density, juniper distribution maps were first required for each population.

A.1 Distribution mapping of the Perthshire juniper population

A map of the Perthshire population was created from a classification of imagery collected and processed by Caledonian Air Surveys Ltd (Whittome, 2010) under contract to NatureScot. Full colour (RGB) and false colour infrared (CIR) imagery was collected in August 2010 at 15cm resolution from a light aircraft using a 50-megapixel Hasselblad H4D-50 digital camera (Whittome, 2010). Maximum likelihood (ML) classification of the resulting imagery was implemented in the Focus program included in Geomatica version 9.1.7-R5 (PCI Geomatics, 2010). The classification used five object classes: asymptomatic juniper, dead juniper, trees, bracken and other. The spectral signature space occupied by each object class is assigned a multivariate Gaussian distribution, with a mean and covariance matrix fit for each class from sets of training pixels (Richards, 1999). Each pixel in the image is then assigned by the ML classifier to the object class with the highest likelihood (ESRI, 2016). No information about the number of training pixels used for classification or the resulting classification accuracy was supplied (Whittome, 2010). Two shapefiles of juniper, classified as asymptomatic or dead, were produced and made available to the authors by NatureScot. We joined the shapefiles in R v.3.4.0 (R Core Team, 2017) and converted it to a raster, resampled to 1m resolution (i.e. the minimum unit of juniper increased from 0.15m^2 to 1m^2) using the *rasterize* function in the raster package (Hijmans, 2016) implemented with a mean function. The raster was then overlain with a 10x10m grid created from 5m digital elevation models (DEM) supplied by NeXTPerspectives™ (updated February 2014), averaged to 10m using the *aggregate* function in the raster package (Hijmans, 2016).

A.2 Distribution mapping of the Lake District and Cairngorms juniper populations

No pre-existing spatial information was available for the Lake District or Cairngorms juniper populations, so we used ARC GIS v.10.5 (ESRI, 2017) to carry out a supervised ML classification of RGB, 25cm imagery collected in 2010 and supplied by NeXTPerspectives™. One image was provided for each location, which was aligned and clipped to the boundary of the corresponding juniper population then classified using the ML method described above. A dataset of pixels representing different observable object classes was created for each image and partitioned into a training set and a test set at a ratio of 80:20 pixels (Table

A1). As few *P. austrocedri* symptoms were visible across either population in 2010, separation of asymptomatic and symptomatic juniper object classes was not required for classification.

Table A1. List of object classes, number of training and test pixels used to classify 25cm RGB images of the Lake District and Cairngorms juniper populations.

Population	Object classes	Training	Test
Lake District	Juniper	54000	10800
	Trees	47271	9454
	Tree shadow	496	99
	Rock	1514	303
	Other	156124	31225
Cairngorms	Juniper	35057	7011
	Trees	121016	24203
	Tree shadow	6643	1329
	Rock	6060	1212
	Bracken	5881	1176
	Grass	56072	11214
	Heath	62335	12467

Classification was performed using the *create signatures* and *maximum likelihood classification* tools in the spatial analyst toolbox. The value of each pixel in the test dataset was extracted from the classified image using *extract* in the raster package (Hijmans, 2016) implemented in R v.3.4.0 (R Core Team, 2017). Confusion matrices were used to summarise the probability of correctly assigning test pixels to object classes (Table A2). Commission is the number of pixels incorrectly included in an object class whereas omission is the number of pixels incorrectly missed out; user's accuracy is 1-commission error and producer's accuracy is 1-omission error. Cohen's kappa statistic was calculated using the *accuracy* function in the rfUtilities package (Evans et al., 2011) as a commonly used metric to interpret test pixel classification accuracy, accounting for both commission and omission errors and correcting overall prediction accuracy by the accuracy expected to occur by chance (Allouche et al., 2006). The following indicative kappa thresholds were suggested by Landis and Koch (1977): 0.41–0.6 moderate, 0.61–0.8 substantial and >0.81 almost perfect. As the kappa statistics for juniper classification met the threshold for "moderate" and "substantial" classification accuracy in the Cairngorms and Lake District populations respectively, the analysis was considered sufficiently accurate at the time to identify potential sampling locations described in the quadrat stratification section in the methods. The resulting rasters of juniper distribution were then resampled to 1m resolution and overlain with a 10x10m grid using the same methods described for the Perthshire population.

Table A2. Confusion matrix presenting rates of omission and commission, user's and producer's accuracies per object class obtained from the ML classification of the 25cm RGB imagery supplied by Next Perspectives™ of a) the Lake District b) the Cairngorms juniper study populations.

a)

		Reference					Total	User's	Commission	Kappa
		Juniper	Trees	Tree shadow	Rock	Other				
Predicted	Juniper	7655	441	35	70	2969	11170	0.69	0.31	0.62
	Trees	758	8388	14	0	847	10007	0.84	0.16	0.83
	Tree shadow	260	219	49	3	244	775	0.06	0.94	0.11
	Rock	543	1	1	190	6198	6933	0.03	0.97	0.04
	Other	1584	405	0	40	20967	22996	0.91	0.09	0.54
	Total	10800	9454	99	303	31225				
	Producer's	0.71	0.89	0.49	0.63	0.67				
	Omission	0.29	0.11	0.51	0.37	0.33				

b)

		Reference							Total	User's	Commission	Kappa
		Juniper	Trees	Tree shadow	Rock	Bracken	Grass	Heath				
Predicted	Juniper	4483	2489	0	2	0	469	2712	10155	0.44	0.56	0.44
	Trees	2210	20981	11	0	0	785	0	23987	0.87	0.13	0.80
	Tree shadow	0	604	1311	0	0	0	0	1915	0.68	0.32	0.99
	Rock	0	0	0	1197	7	0	10	1214	0.99	0.01	0.81
	Bracken	0	0	0	1	1149	0	0	1150	1.00	0.00	0.99
	Grass	17	120	0	3	11	9601	1	9753	0.98	0.02	0.90
	Heath	301	9	7	9	9	359	9744	10438	0.93	0.07	0.44
	Total	7011	24203	1329	1212	1176	11214	12467				
	Producer's	0.64	0.87	0.99	0.99	0.98	0.86	0.78				
	Omission	0.36	0.13	0.01	0.01	0.02	0.14	0.22				

A.3 Revised distribution mapping of the Lake District juniper population

Concerned that inaccuracy in the image classification may lead to errors in proportional sampling of the eight juniper density categories, we wanted to compare the density distribution of sampled quadrats to those derived from the original, and an improved, image classification. The quality of the Cairngorms image was insufficient to make re-analysis practicable but the opportunity arose to re-classify the Lake District image using ARC GIS v.10.5 after fieldwork was completed. We addressed the uneven illumination by separating the image, by eye, into five different sections with different depths of shadow and developing sets of 70 training to 30 test pixels unique to each section (Table A3). Multiple studies have shown maximum likelihood classification of land cover is outperformed by using the random forest (RF) algorithm (Attarchi and Gloaguen, 2014; Khatami et al., 2016; Waske and Braun, 2009). We implemented the algorithm using the *random trees* tool in the spatial analyst toolbox. Maximum number of trees was set to 200, maximum tree depth to 50 and maximum number of samples per class to 1000. The resulting ESRI classification definition file was then loaded in the *classify raster* tool in the spatial analyst toolbox to produce classified rasters of each image section, assessed using confusion matrices and kappa as outlined in Appendix A.2. Once the best classification of juniper according to the accuracy statistics (minimum kappa of 0.7) was obtained for each section, the classified image sections were mosaiced back together for the remaining processing. Predicted juniper pixels isolated from any other juniper pixels in eight neighbouring directions were identified and deleted using the *freq* function in the raster package (Hijmans, 2019) implemented in R v.3.5.2 (R Core Team, 2018). Juniper pixels visible in the centre of deciduous tree crowns were then manually deleted. These operations deleted 0.05% juniper pixels identified by the classifier.

Table A3. List of object classes and total number of pixels used to train the RF algorithm and test the result of the classification of 25cm RGB image of the Lake District juniper population.

Class	Training	Test
Juniper	17747	7606
Trees	36782	15764
Tree shadow	9369	4041
Rock	15231	6528
Bracken	49218	21092
Grass	9541	4158
Heath	1828	784

Compared to the original Lake District image analysis, the revised classification of juniper improved by 0.13 kappa units keeping it within the range for substantial classification accuracy (Table A4). Where the original classification predicted 29% more juniper pixels than the number observed, the revised classification predicted 15% fewer juniper pixels (Table A2a, Table A4). User's accuracy improved to 82% reducing the number of pixels incorrectly classified as juniper by 13% and producer's accuracy improved to 74% increasing the number of pixels correctly classified as juniper by 3% (Table A2a, Table A4). The largest proportion of pixels mistakenly identified as juniper were donated from the "tree shadow" category (10%) and the greatest percentage of misidentified juniper pixels were predicted to be grass (9%).

Pixels classified as juniper in the revised image were subset to a new raster, then resampled to 1m using *rasterize* in the raster package (Hijmans, 2016) implemented with a mean function. The same method outlined in the quadrat stratification section was used to calculate the area of juniper at 10x10 and 30x30m scales for each cell and then assign it to one of the eight juniper density categories (Table A5). The ML analysis identified 10795 10x10m cells containing juniper, compared to 8399 in RF classification. The proportion of cells distributed across density categories were comparable between the original and revised classifications (Figure A1, Table A5). Few cells were found in categories with dense 10x10m but sparse 30x30m cover (categories 3-4), or sparse 10x10m and dense 30x30m cover (category 5). The greatest proportion of cells were allocated to categories 7-8 with high % cover at both scales but the category with the highest proportion of cells differed by method. The sum of the area of juniper calculated at 10x10m and 30x30m for each juniper cell is highly correlated (Pearson $r^2 = 0.69$) between the two classifications. Comparing the sample distribution to that of the revised image classification suggests too many quadrats were sampled at high juniper density (category 8) but this may arise from the slight under-prediction of juniper occurrence in the revised image classification (Table A4). The sample distribution does match the revised classification well in the lower density categories (Figure A1), so we are satisfied that juniper sampling based on the original image classification was roughly proportional to the juniper density actually present across the site.

Table A4. Confusion matrix presenting rates of omission and commission, user's and producer's accuracies per object class obtained from the RF revised classification of the 25 cm RGB image supplied by Next Perspectives™ of the Lake District juniper population.

		Reference							Total	User's	Commission	Kappa
		Juniper	Trees	Tree shadow	Rock	Bracken	Grass	Heath				
Predicted	Juniper	5626	396	668	80	61	42	17	6890	0.82	0.18	0.75
	Trees	503	13474	100	4	987	344	0	15412	0.87	0.13	0.82
	Tree shadow	275	116	3187	12	12	0	14	3616	0.88	0.12	0.82
	Rock	57	43	50	5641	1183	34	6	7014	0.8	0.2	0.82
	Bracken	303	52	5	605	17537	478	5	18985	0.92	0.08	0.81
	Grass	667	1660	19	34	1305	3251	0	6936	0.47	0.53	0.55
	Heath	175	23	17	12	8	0	742	977	0.76	0.24	0.84
	Total	7606	15764	4046	6388	21093	4149	784				
	Producer's	0.74	0.85	0.79	0.88	0.83	0.78	0.95				
	Omission	0.26	0.15	0.21	0.12	0.17	0.22	0.05				

Table A5. Description of the eight juniper density categories based on % juniper cover in 10x10m quadrats and the 30x30m including each quadrat, the percentage of cells allocated to each category following classification of 1m resolution RGB imagery supplied by Next Perspectives™ using ML (original) and RF (revised) algorithms and the percentage of cells sampled by the field survey in each category.

Density category	% juniper cover		%10x10 m cells per category		
	30x30m	10x10m	Original	Revised	Sample
1	0 - 20	1 – 10	9	14	11
2		11 – 25	5	13	11
3		26 – 50	1	2	0
4		50 - 100	0	0	0
5	21 - 100	1 – 10	3	4	0
6		11 – 25	12	15	13
7		26 – 50	28	29	26
8		50 - 100	42	23	39

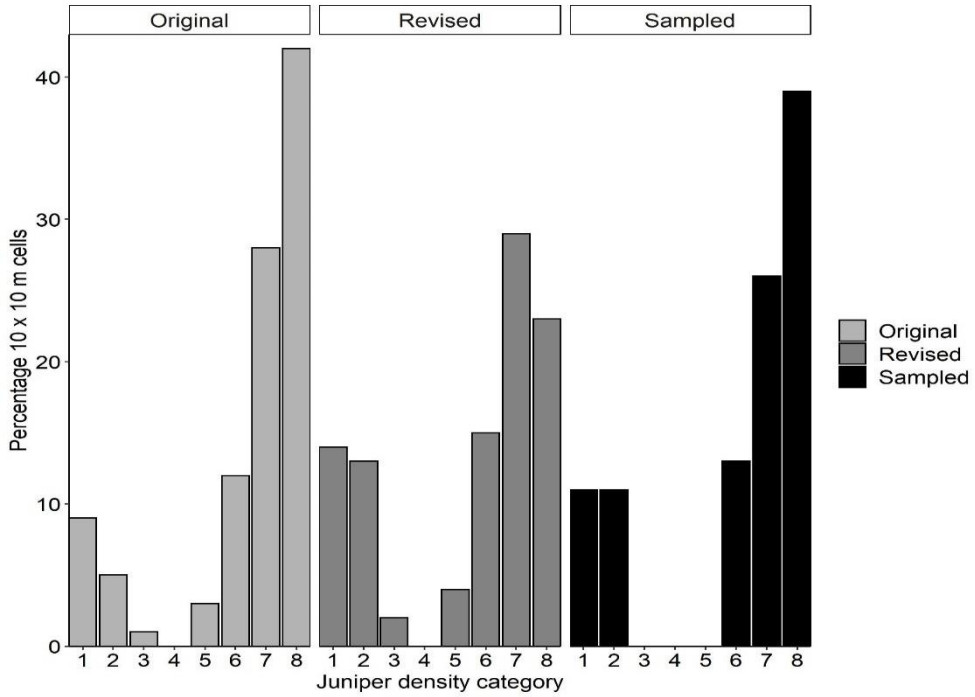

Figure A1. Distribution of 10x10m cells in the Lake District study area across eight juniper density categories (Table A5) comparing the classification of 1m resolution RGB imagery supplied by Next Perspectives™ using the original (ML) and revised (RF) methods and the percentage of cells sampled by the field survey. The number of 10x10m cells containing juniper compared is 10795 (original), 8399 (revised), 46 (sampled).

Appendix B. Associate species target list recorded in survey quadrats

Table B1. List of 42 target vascular plant species to record in 10x10m quadrats categorised using Ellenberg moisture (F), reaction (R) and nitrogen (N) values given in Hill, Preston, and Roy (2004).

Vascular plant taxon	Soil pH and fertility			Soil moisture		
	Highly acidic (R = 2), nutrient poor (N = 1-2)	Slightly acidic (R = 3-5), moderately fertile (N = 3-5)	Neutral (R = 6-7), fertile (N = 6)	High moisture (F = 8-9)	Moderate moisture (F = 6-7)	Lower moisture (F = 5)
Erica tetralix	x			x		
Calluna vulgaris	x				x	
Empetrum nigrum	x				x	
Pinus sylvestris	x				x	
Vaccinium myrtillus	x				x	
Arctostaphylos uva-ursi	x					x
Erica cinerea	x					x
Vaccinium vitis-idaea	x					x
Betula pendula		x				x
Fagus sylvatica		x				x
Ilex aquifolium		x				x
Luzula sylvatica		x				x
Pteridium aquilinum		x				x
Quercus robur		x				x
Rubus fruticosus agg.		x				x
Taxus baccata		x				x
Ulex europaeus		x				x
Alnus glutinosa			x	x		
Iris pseudacorus			x	x		
Fraxinus excelsior			x		x	
Acer pseudoplatanus			x			x
Coryllus avellana			x			x
Crataegus monogyna			x			x
Hedera helix			x			x
Ulmus glabra			x			x
Molinia caerulea				x		
Myrica gale				x		
Salix cinerea				x		
Athyrium filix-femina					x	
Betula pubescens					x	
Deschampsia cespitosa					x	
Dryopteris affinis					x	
Dryopteris dilitata					x	
Dryopteris filix-mas					x	
Juncus conglomeratus					x	
Juncus effusus					x	
Lonicera periclymenum					x	
Oreopteris limbosperma					x	
Quercus petraea					x	
Sorbus aucuparia					x	

Appendix C. Distribution of *P. austrocedri* qPCR results in survey quadrats

Tissue from lesions symptomatic for *P. austrocedri* was collected from juniper with foliage symptoms within field quadrats and tested for *P. austrocedri* DNA using qPCR. Positive results were obtained for 49% of quadrats in Perthshire, 58% in the Lake District and 60% in the Cairngorms (Table C1), distributed across the full extent of each juniper population (Figure C1). Symptomatic lesions were not found in the remaining quadrats, with the exception of three quadrats (5%) in Perthshire and three (6%) in the Lake District, where the presence of DNA was not positively confirmed by qPCR (Table C1, Figure C1). Inability to detect lesions on dead trees explains the inverse relationship between the percentage of quadrats with positive qPCR results and the area of symptoms detected across each study population (Figure 3, Table 2).

Table C1. Comparison of the numbers of quadrats, lesion samples, positive and "not detected" qPCR results for *P. austrocedri* DNA for each study population. No detection of *P. austrocedri* occurs where symptomatic lesions could not be found within quadrats or where qPCR did not confirm DNA presence.

Measurement	Perthshire	Lake District	Cairngorms
Number of 10 x 10 m quadrats surveyed	51	48	50
Number of lesion samples collected	28	31	30
Number of quadrats where *P. austrocedri* present	25	28	30
Number of quadrats where *P. austrocedri* not detected	26 (3)	20 (3)	20 (0)

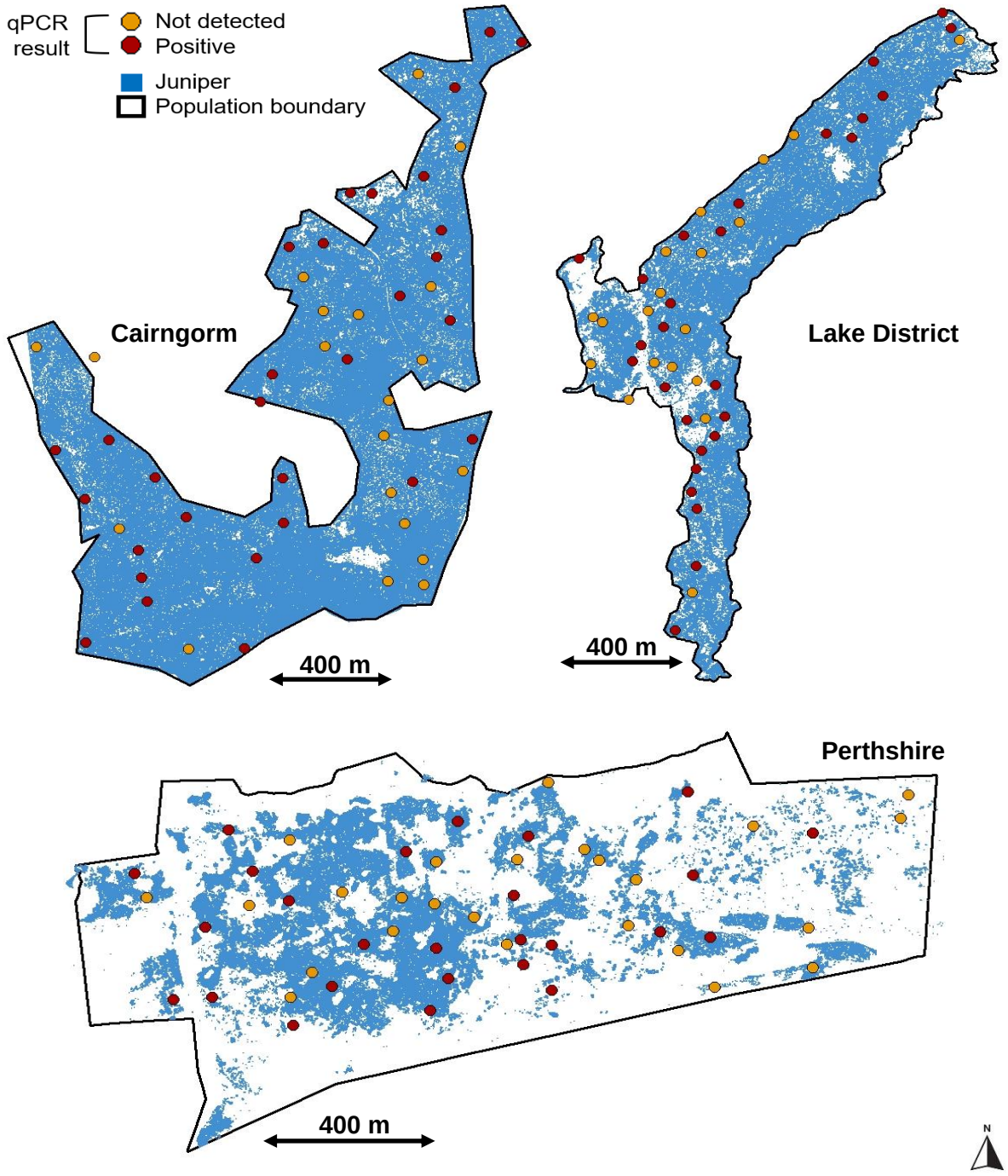

Figure C1. Spatial distribution of qPCR results obtained from lesions symptomatic for *P. austrocedri* collected from 10x10m quadrats at each study population.

Appendix D. Additional information for GLMM model selection

D.1 Correlations between environmental covariates

Correlations between all covariates investigated in the Perthshire, Lake District and Cairngorms juniper populations were investigated (Figure D1). The dependent variable “Symptoms” (area of symptomatic juniper in 10x10m) and the independent variable “Area” (area of juniper in 10x10m) were included in the analysis but collinearity was only examined between the covariates (Figure D1). No covariates were correlated with a Pearson r^2 value ≥0.6.

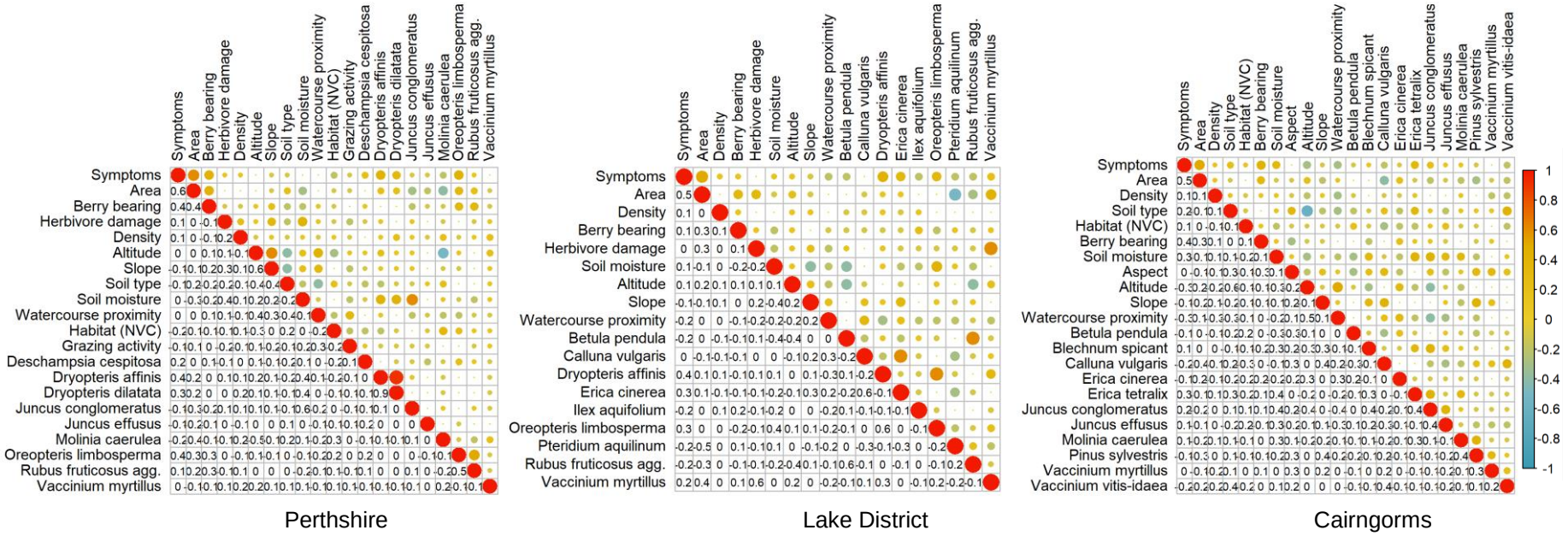

Figure D1. Correlation plot between all investigated metrics for the Perthshire, Lake District and Cairngorms juniper populations. Pearson r^2 values are shown using colour scale and text to 1 decimal place. Covariate descriptions and units of measurement are given on Table 1.

D.2 Accounting for spatial autocorrelation in model residuals

Correlations in the residuals generated from beta-binomial GLMMs were calculated using Moran's I statistic. Positive spatial autocorrelation of the residuals was rarely significant in any of the top models for any of the populations up to the first 1000m of inter-quadrat distance (Figure D2).

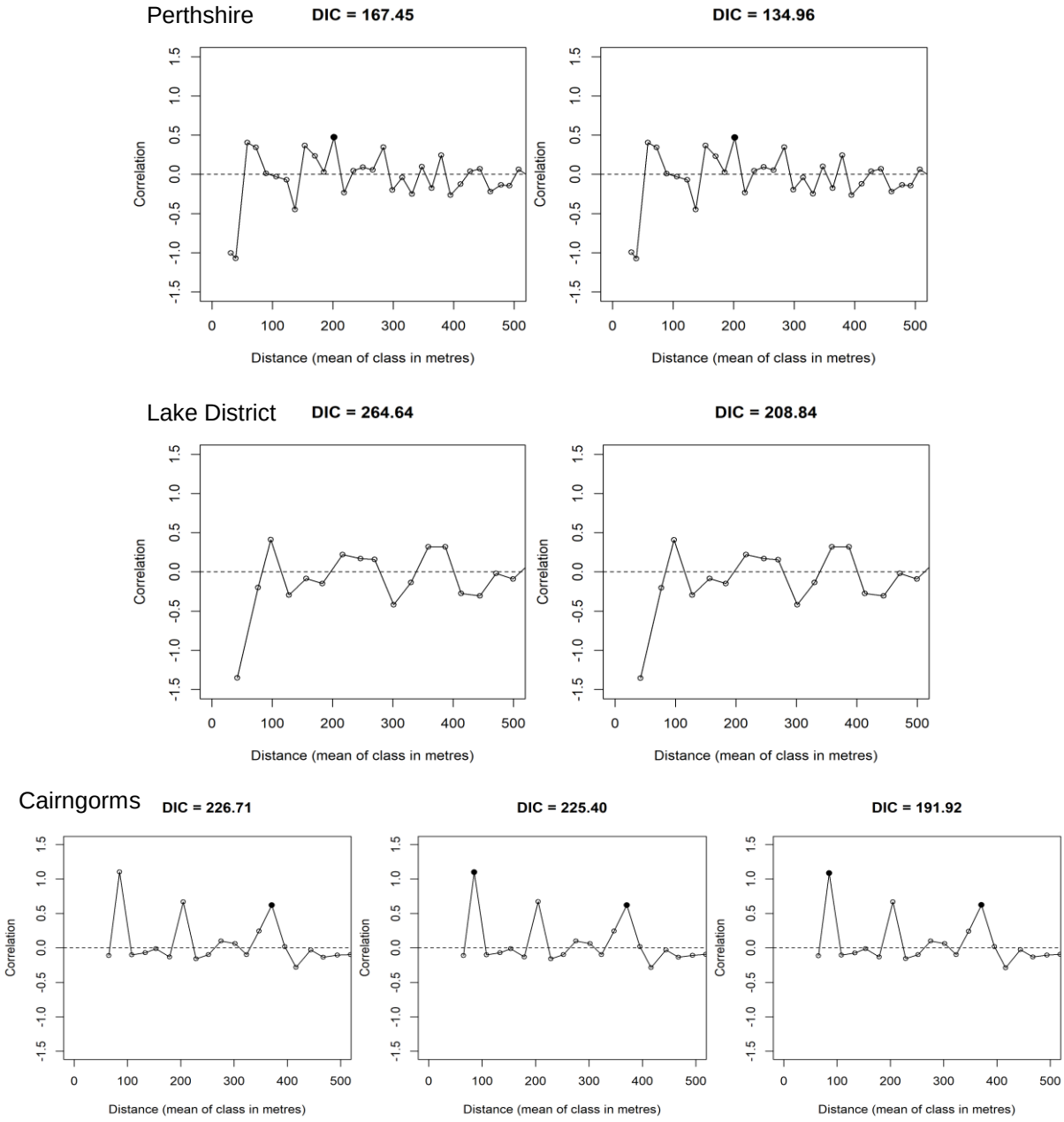

Figure D2. Moran's I p-values calculated from the residuals of the top set of beta-binomial GLMMs plotted against the inter-cell distance (m). Significant p-values (95% confidence interval) are shown in black.

Appendix E. Preparing juniper and *P. austrocedri* distribution maps for colonisation modelling of Birk Fell SSSI

E.1 Aerial image feature classification

An analysis of high-resolution aerial imagery was performed to produce a detailed distribution map of juniper from which to derive the area and connectivity of juniper stands available for *P. austrocedri* colonisation. Full colour (RGB) aerial imagery collected in 2010 at 25cm resolution was obtained from NeXT Perspectives™ for the Ullswater catchment. A 1.14km^2 polygon capturing the extent of the juniper population within Birk Fell SSSI was mapped in 2011 and provided by Cumbria Wildlife Trust (Cumbria Wildlife Trust, 2014). The survey notes state the population was "huge… with dense, mostly healthy juniper" and identified herbivory as the primary cause of juniper death (Cumbria Wildlife Trust, 2014). Deriving the distribution and connectivity of juniper from the 2010 imagery was, therefore, likely to be an accurate representation of the population structure prior to infection. The survey polygon was aligned to the aerial image in ARC GIS v.10.5.1 and refined to 1.10km^2, excluding areas of high light exposure at the northern tip of the boundary and along the eastern ridge that would be difficult to classify and contained little or no juniper (Figure E1). To minimise the impact of uneven illumination, imagery within the survey polygon was divided into sections: section one had deep shadow caused by cliffs, sections two and four had very high exposure and sections three and five had moderate exposure (Figure E1). Prior to classification, the contrast of each image section was increased to 10, and gamma to 1.5, using the ARC GIS image analysis toolbox.

The image sections were classified separately using a dataset of 25x25cm training pixels developed for seven feature classes: juniper, bracken, grass, heath, rock, shadow, and trees (Table E1). ARC GIS was used to draw polygons around groups of pixels clearly representing one of the feature classes. The shapefiles were then read into R version 3.5.2 (R Core Team, 2018) where 30% of the pixels per feature class per section were randomly selected using the *sample* function and removed from the dataset to withhold them from the classification as test data. The remaining pixels were uploaded to the training sample manager in the ARC GIS image classification toolbox to create training feature classes. These feature classes were then used by the random forest (RF) algorithm in the Random Trees tool (spatial analyst toolbox) to create an ESRI classification definition file. The maximum number of trees was set to 200, maximum tree depth to 50 and maximum number of samples per class to 1000, chosen as setting that adequately traded off classification

accuracy with processing time. The resulting definition file was then loaded in the classify raster tool in the spatial analyst toolbox to produce the classified output raster.

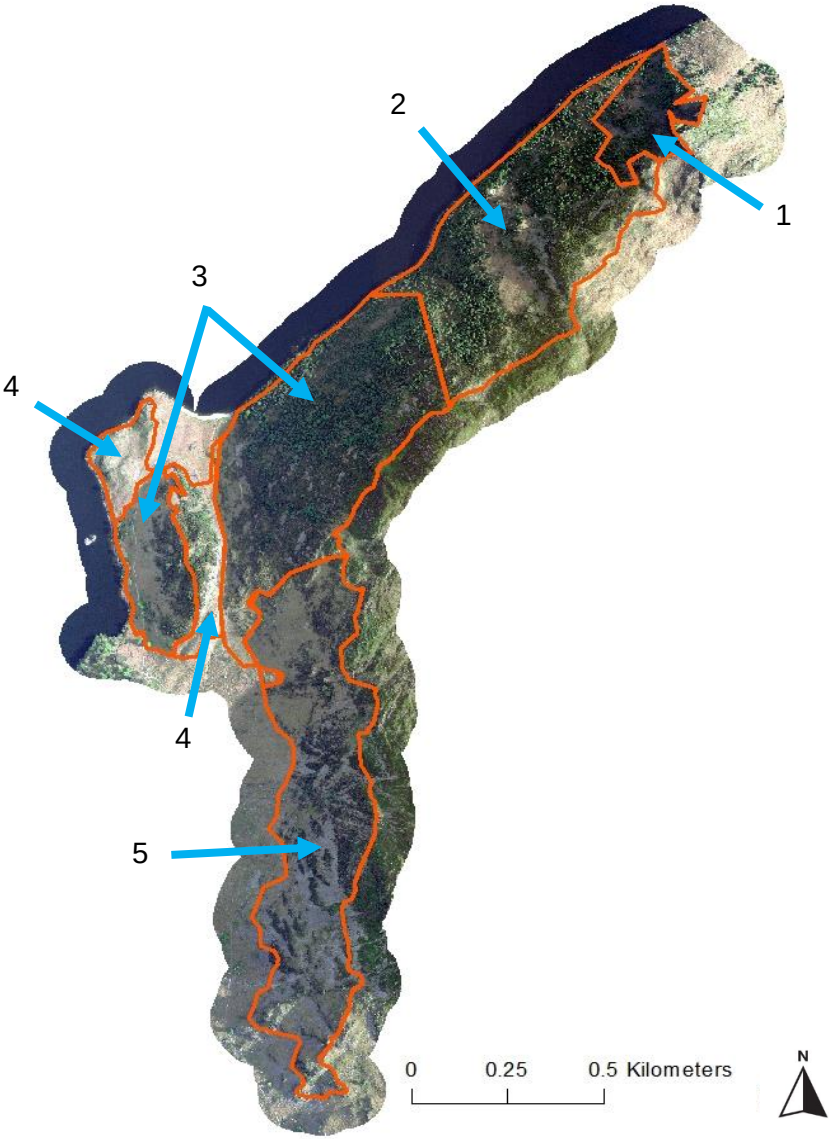

Imagery licensed to: NERC Centre for Ecology & Hydrology for PGA, through NeXT Perspectives™

Figure E1. Aerial image of Birk Fell from 2010 supplied at 25cm resolution by NeXT Perspectives™ clipped to the extent of the Cumbria Wildlife Trust Birk Fell SSSI juniper population survey polygon plus a 100m buffer. The image sections (1-5) used to perform the supervised classification are marked in orange.

The number of pixels observed in the test dataset and classified by the RF algorithm was compared by calculating producer (1-commission) and user (1-omission) accuracies, Cohen's kappa and True Skill Statistic (TSS) using the *accuracy* function in the rfUtilities R package (Evans, Murphy, Holden, & Cushman, 2011). Commission is the number of pixels incorrectly included in each feature class whereas omission is the number of pixels

incorrectly missed out. Cohen's kappa is commonly used to assess accuracy because it accounts for both commission and omission errors in one metric and corrects overall prediction accuracy by the accuracy expected to occur by chance (Allouche, Tsoar, & Kadmon, 2006). Kappa is most useful as a relative value to indicate change in probability of classification accuracy rather than as an absolute measure of accuracy. However, Landis and Koch (1977) suggested the following indicative thresholds to interpret classification accuracy using kappa: 0.41 – 0.6 moderate, 0.61 – 0.8 substantial and > 0.81 almost perfect. We decided values of kappa ≥ 0.7 would indicate sufficient accuracy for the use of the juniper classification in modelling analyses (Table E1). Sections with lower values were re-analysed by creating additional training and test pixels maintained as a 70:30 training:test ratio. This level of accuracy could not be achieved for image sections two and four; the final classifications were accepted following six and ten re-analyses respectively, that improved kappa from 0.47 to 0.65 in section two and 0.40 to only 0.54 in section four (Table E1).

Table E1. Cohen's kappa and True Skill Statistic (TSS) returned for each feature class present in the final classification iteration for each image section. Kappa is sensitive to the prevalence of pixels in different feature classes so TSS is also reported as a prevalence independent metric derived from kappa (Allouche et al., 2006).

Image section	Statistic	Feature Class						
		Juniper	Bracken	Grass	Heath	Rock	Shadow	Trees
1	Kappa	0.75	0.71			0.88	0.83	0.85
	TSS	0.76	0.72			0.94	0.79	0.84
2	Kappa	0.65	0.69	0.48		0.56		0.83
	TSS	0.66	0.74	0.38		0.44		0.87
3	Kappa	0.90	0.87	0.53		0.96		0.65
	TSS	0.91	0.86	0.46		0.96		0.61
4	Kappa	0.54	0.96	0.84		0.94	0.74	0.95
	TSS	0.44	0.96	0.85		0.93	0.86	0.94
5	Kappa	0.70	0.73	0.32	0.86	0.74	0.89	0.72
	TSS	0.75	0.70	0.27	0.81	0.75	0.84	0.78

Confusion matrices produced from the final classifications show overall classification accuracy of each image section ranged from 0.75 to 0.88 (Table E2). User and producer accuracies returned for the juniper class from sections one, three and five were greater than 70% showing substantial classification accuracy, despite areas of deep shadow and dense tree cover in sections one and three (Figure E1). The classification of juniper in section two was almost substantial (users accuracy 0.70, producers accuracy 0.69) and was acceptable

for section four (users accuracy 0.46, producers accuracy 0.80) where over-exposure resulted in the inaccurate classification of many juniper pixels as shadow (Table E2).

Table E2. Confusion matrices produced from the final accepted classification of image sections 1-5 (Figure E1) showing the users accuracy, commission, producers accuracy and omission rates for each feature class found in each section. The area of each image section is shown next to the section number in hectares. The number of test pixels for each feature class is given in comparison to the number of training pixels used (shown in brackets). The overall accuracy (OA) of the section classification was calculated by dividing the total number of correctly classified pixels by the total number of test pixels.

Section 1: 56062m^2		**Classified pixels**							
		Juniper	Bracken	Rock	Shadow	Trees	Total	Users	Commission
Reference pixels	Juniper	1325	41	92	66	125	1649	0.80	0.20
	Bracken	172	1354	183	0	40	1749	0.77	0.23
	Rock	12	34	1518	0	3	1567	0.97	0.03
	Shadow	123	3	8	841	82	1057	0.80	0.20
	Trees	65	388	4	18	3608	4083	0.88	0.12
	Total test	1697	1820	1805	925	3858	8646 10105		
	(training)	(3959)	(4246)	(4211)	(2100)	(9002)	OA = 0.86		
	Producers	0.78	0.74	0.84	0.91	0.94			
	Omission	0.22	0.26	0.16	0.09	0.06			

Section 2: 289382m^2		**Classified pixels**							
		Juniper	Bracken	Grass	Rock	Trees	Total	Users	Commission
Reference pixels	Juniper	1346	219	37	29	284	1915	0.70	0.30
	Bracken	45	5586	112	50	4	5797	0.96	0.04
	Grass	345	1202	1273	19	385	3224	0.39	0.61
	Rock	8	794	5	678	37	1522	0.45	0.55
	Trees	208	2	41	0	3209	3460	0.93	0.07
	Total test	1952	7803	1468	776	3919	12092 15918		
	(training)	(4554)	(18210)	(3425)	(1810)	(9144)	OA = 0.76		
	Producers	0.69	0.72	0.87	0.87	0.82			
	Omission	0.31	0.28	0.13	0.13	0.18			

Section 3: 371305m²		Classified pixels									
		Juniper	Bracken	Grass	Heath	Rock	Shadow	Trees	Total	Users	Commission
Reference pixels	Juniper	1604	45	0	20	0	2	298	1969	0.81	0.19
	Bracken	39	1890	329	4	317	0	0	2579	0.73	0.27
	Grass	198	28	451	0	0	0	789	1466	0.31	0.69
	Heath	148	0	0	742	0	21	3	914	0.81	0.19
	Rock	28	271	0	0	1047	0	3	1349	0.78	0.22
	Shadow	84	0	0	18	0	617	11	730	0.85	0.15
	Trees	170	0	115	0	0	0	2710	2995	0.90	0.10
	Total test (training)	2271 (5300)	2234 (5212)	895 (1927)	784 (1828)	1364 (3183)	640 (1492)	3814 (8899)	9061 / 12002 OA = 0.75		
	Producers	0.71	0.85	0.50	0.95	0.77	0.96	0.71			
	Omission	0.29	0.15	0.50	0.05	0.23	0.04	0.29			

Section 4: 75043m²		Classified pixels								
		Juniper	Bracken	Grass	Rock	Shadow	Trees	Total	Users	Commission
Reference pixels	Juniper	710	0	139	0	673	12	1534	0.46	0.54
	Bracken	1	1804	14	44	0	0	1863	0.97	0.03
	Grass	90	7	1040	12	10	30	1189	0.87	0.13
	Rock	0	59	5	1320	32	0	1416	0.93	0.07
	Shadow	71	0	0	3	1678	0	1752	0.96	0.04
	Trees	13	0	34	0	83	2239	2369	0.95	0.05
	Total test (training)	885 (2064)	1870 (4364)	1232 (2875)	1379 (3217)	2476 (5777)	2281 (5323)	8791 / 10123 OA = 0.87		
	Producers	0.80	0.96	0.84	0.96	0.68	0.98			
	Omission	0.20	0.04	0.16	0.04	0.32	0.02			

Section 5: 308819m^2		Classified pixels							
		Juniper	Bracken	Grass	Rock	Trees	Total	Users	Commission
Reference pixels	Juniper	721	25	6	1	29	782	0.92	0.08
	Bracken	35	6726	14	50	6	6831	0.98	0.02
	Grass	26	0	366	0	372	764	0.48	0.52
	Rock	1	27	6	1153	2	1189	0.97	0.03
	Trees	18	587	171	0	1483	2259	0.66	0.34
	Total test (training)	801 (1870)	7365 (17186)	563 (1314)	1204 (2810)	1892 (4414)	10449 11825 OA = 0.88		
	Producers	0.90	0.91	0.65	0.96	0.78			
	Omission	0.10	0.09	0.35	0.04	0.22			

To calculate classification accuracies for each feature class across the whole image, the five classified sections were joined into a single raster using the *mosaic* function in the raster R package (Hijmans, 2019) and the test pixels were compiled into a single reference dataset to produce a confusion matrix for the image as a whole (Table E3). Overall accuracy was 82% with excellent kappa and TSS statistics reported for the bracken, heath, rock, shadow, and trees feature classes (Table E3). The classification of juniper was substantial, with good kappa (0.70) and TSS (0.69) statistics and similar user (73%) and producer (75%) accuracies (Table E3). Commission error was largely attributable to the inclusion of shadow (9%) and tree (10%) pixels as juniper, while omitted juniper pixels were more evenly distributed across other feature classes with the highest percentage (9%) misidentified as grass (Table E3). Of all the feature classes, classification of grass was poorest with poor kappa (0.54) and TSS (0.45) values and low user accuracy (47%) resulting from rates of ~20% confusion with the bracken and trees classes (Table E3).

Table E3. Accuracy metrics for the classification of a 25 cm resolution aerial image of Birk Fell SSSI, collected in 2010 and supplied by NeXT Perspectives™. A) Confusion matrix showing users and producers accuracies, and rates of commission and omission for each of the seven feature classes, alongside the number of test and training (in brackets) pixels used and the calculation of overall classification accuracy (OA). B) Cohen's kappa and True skill statistic (TSS) calculated per feature class.

A

		Classified pixels									
		Juniper	Bracken	Grass	Heath	Rock	Shadow	Trees	Total	Users	Commission
Reference pixels	Juniper	5706	330	182	20	122	741	748	7849	0.73	0.27
	Bracken	292	17360	469	4	644	0	50	18819	0.92	0.08
	Grass	659	1237	3130	0	31	10	1576	6643	0.47	0.53
	Heath	148	0	0	742	0	21	3	914	0.81	0.19
	Rock	49	1185	16	0	5716	32	45	7043	0.81	0.19
	Shadow	278	3	0	18	11	3136	93	3539	0.89	0.11
	Trees	474	977	361	0	4	101	13249	15166	0.87	0.13
	Total test (training)	7606 (17747)	21092 (49218)	4158 (9541)	784 (1828)	6528 (15231)	4041 (9369)	15764 (36782)	4903 59973 OA = 0.82		
	Producers	0.75	0.82	0.75	0.95	0.88	0.78	0.84			
	Omission	0.25	0.18	0.25	0.05	0.12	0.22	0.16			

B

Statistic	**Feature Class**						
	Juniper	Bracken	Grass	Heath	Rock	Shadow	Trees
Kappa	0.70	0.81	0.54	0.87	0.82	0.82	0.81
TSS	0.69	0.83	0.45	0.81	0.80	0.87	0.82

E.2 Mapping juniper distribution and density

It was important to further refine the classification of juniper as the results would be used to interpret the relationship between the area and connectivity of juniper with intensity of *P. austrocedri* symptoms. Pixels classified as juniper were first subset to a new raster in R. Scattered pixels were removed using the *freq* function in the raster package (Hijmans, 2019). Deleting clumps of up to two neighbouring pixels in any of the adjacent eight directions was optimal compared to removing clumps of 1, 3 or 4 pixels, identified using juniper vs not juniper test pixels to calculate kappa, that varied by 0.12 units between all iterations. The raster was then converted to a spatial polygons layer, imported to ARC GIS and overlain on the original high resolution image to allow groups of obviously mis-classified pixels (e.g. pixels hanging in the centre of deciduous tree crowns, Figure E2) to be identified by eye and deleted manually.

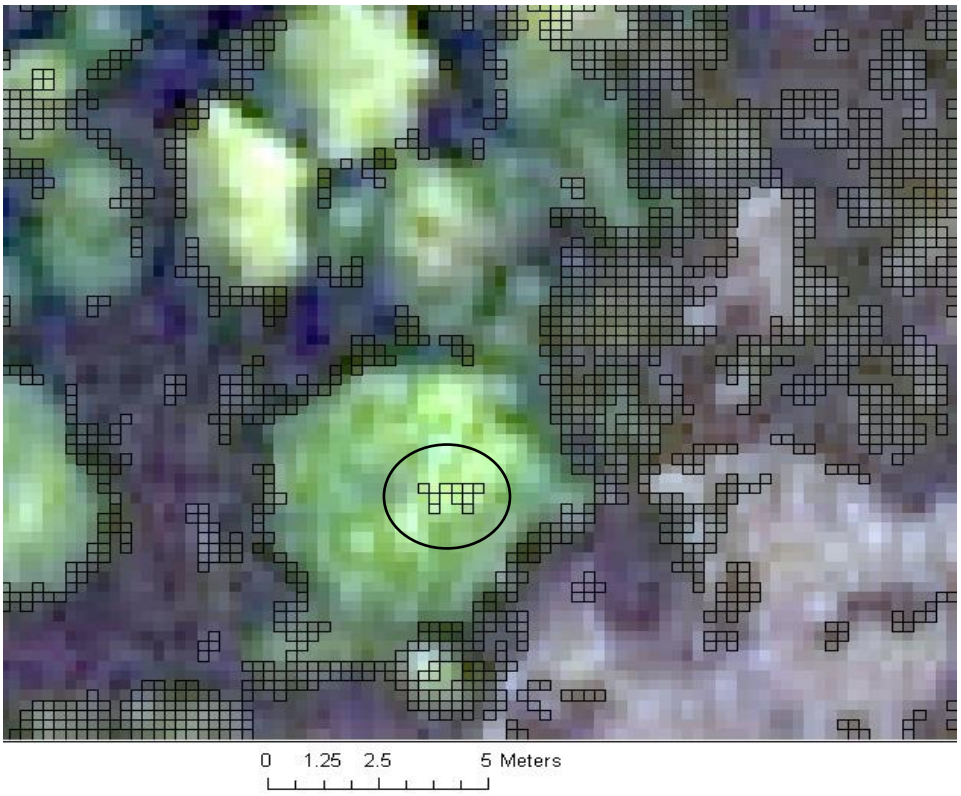

Figure E2. Illustration of the manual correction of juniper pixels classified by the random forest algorithm. Juniper pixels (black squares) that were conspicuously mis-classified when overlain on the 25cm aerial photograph, such as those circled in the centre of a deciduous tree crown, were deleted from the dataset.

Following these corrections, the revised layer of juniper polygons was converted back to a raster in R and stacked on top of the original raster containing the seven classified feature classes (Figure E3). Where pixels in the revised classification had been removed, the value of the corresponding pixel in the original raster was changed to zero using the *overlay* function in the raster package (Hijmans, 2019), to allow revision of the accuracy statistics. The overall accuracy of the corrected classification only improved by 1% but the kappa and TSS statistics for the juniper feature class improved from 0.70 to 0.81, and 0.69 to 0.84 respectively, improving the classification from substantial to near perfect (Table E4). Producers accuracy decreased slightly from 75% to 74% but users accuracy improved from 73% to 82% (Table E4). There was no change in the percentage of shadow pixels commissioned as juniper (9%) but large reductions in commission from the tree (5%), bracken (<1%) and grass (<1%) feature classes (Table E3, Table E4).

The steps above classified the juniper population up to the boundary of the modified survey polygon (Figure E1). However, data were extracted for modelling to two regular grids with cell sizes of 10x10m and 25x25m. The polygon grids were created using the *create fishnet* tool in the data management toolbox in ARC GIS v.10.6.1 from centroids derived from a 5m digital elevation model (DEM, supplied by NeXTPerspectives™, updated February 2014) resampled to 10m and 25m resolutions using the *aggregate* function in the raster package (Hijmans, 2019) implemented in R v.3.5.2 (R Core Team, 2018). The resulting polygon grids were clipped to the juniper population boundary. All grid cells intersecting the boundary were retained to their full extent - either 100m^2 or 625m^2 – meaning some cells were only partially populated by the image classification. To rectify this, an additional 100m buffer was extended beyond the mapped juniper population (Figure E1, Figure E3). The original imagery was cropped to this revised extent and the classification was repeated using the same methods and training pixels, minus the juniper feature class as the buffer zone lies outwith the juniper survey polygon. The lake feature class was added following the classification by manually setting the raster values within the clearly defined lake area. The resulting raster was laid underneath the juniper population raster to ensure the total area of all boundary cells at both spatial resolutions was fully classified (Figure E3). The final step in preparing the distribution data for modelling was to remove an area of 18088m^2 from the classification where juniper coverage was over-predicted according to knowledge on the ground (Figure E3).

Table E4. Accuracy metrics for the final image classification used to map the distribution and area of juniper present within Birk Fell SSSI. A) Confusion matrix showing users and producers accuracies, rates of commission and omission, numbers of test and training (in brackets) pixels for each feature class and the overall classification accuracy (OA). B) Cohen's kappa and True skill statistic (TSS) calculated per feature class.

A

		Classified pixels									
		Juniper	Bracken	Grass	Heath	Rock	Shadow	Trees	Total	Users	Commission
Reference pixels	Juniper	5626	61	42	17	80	668	396	6890	0.82	0.18
	Bracken	303	17537	478	5	605	5	52	18985	0.92	0.08
	Grass	667	1305	3251	0	34	19	1660	6936	0.47	0.53
	Heath	175	8	0	742	12	17	23	977	0.76	0.24
	Rock	57	1183	34	6	5641	50	43	7014	0.8	0.2
	Shadow	275	12	0	14	12	3187	116	3616	0.88	0.12
	Trees	503	987	344	0	4	100	13474	15412	0.87	0.13
	Total test (training)	7606 (17747)	21093 (49218)	4149 (9541)	784 (1828)	6528 (14899)	4046 (9369)	15764 (36782)	49458 59830 OA = 0.83		
	Producers	0.74	0.83	0.78	0.95	0.88	0.79	0.85			
	Omission	0.26	0.17	0.22	0.05	0.12	0.21	0.15			

B

Statistic	**Feature Class**						
	Juniper	Bracken	Grass	Heath	Rock	Shadow	Trees
Kappa	0.81	0.55	0.84	0.75	0.82	0.82	0.82
TSS	0.84	0.45	0.76	0.78	0.79	0.87	0.82

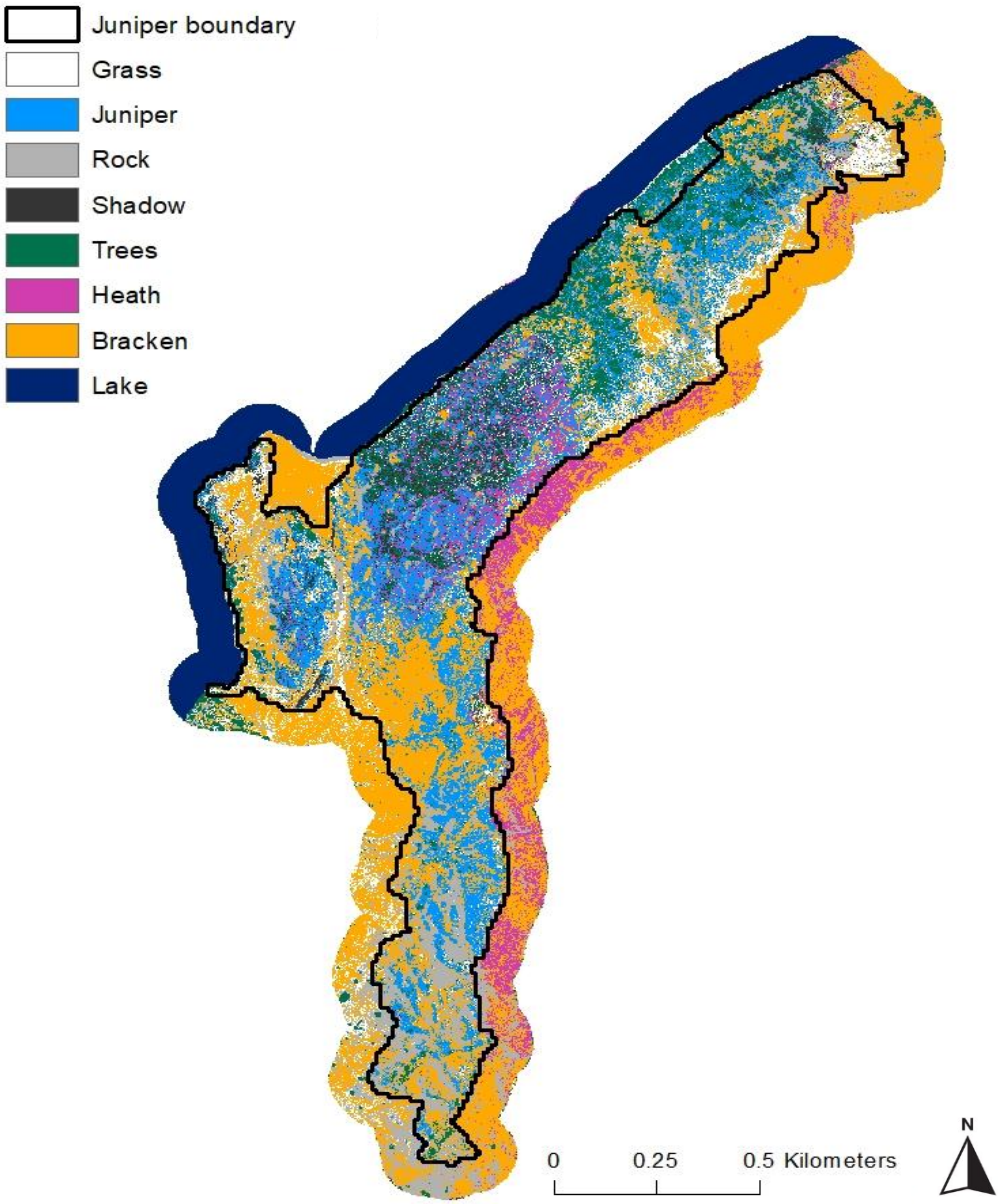

Figure E3. Final supervised image classification of the Birk Fell SSSI juniper population produced at 1m resolution. Feature classes are shown according to the colour key. The black outline delineates the area of the juniper population used in the modelling analyses (see Table E4 for the corresponding accuracy metrics) surrounded by the additional 100m classified buffer.

E.3 Mapping *P. austrocedri* colonisation of juniper through time

Flights were undertaken in summer when the vegetation was mostly green, allowing easier identification of symptomatic (bronzed or grey) juniper. Photographs were taken from 150-300m above ground using Nikon D5300 cameras with an attached GPS, by two photographers, facing opposite directions, who directed the pilot's flight path to ensure good coverage of the SSSI. All photographs were geo-referenced using the flight track collected using a handheld Garmin GPSmap 62S GPS unit and the geo-tags extracted from each photograph using GPSBabel v.1.5.4. Symptom observations were mapped against NeXT Perspectives™ imagery provided from 2010 (for the 2012/13 survey) and 2014 (for the 2016/17 survey). The total number of symptomatic trees observed for the 2016/17 survey was 1288, 256 of which were removed as duplicates or observations made outside the boundary of the mapped juniper population.

Appendix F. Derivation and mapping of hydrological covariates across Birk Fell SSSI

The distribution of soil moisture across the juniper population was expected to be a key factor explaining both the distribution and density of juniper - that prefers freely drained microsites (Ward et al., 2017; Thomas et al., 2007) - and *P. austrocedri* symptom intensity, as water is required to produce and transport zoospores (Greslebin et al., 2007; Riddell et al., 2020). This appendix gives further detail as to the derivation of the alternative approximations of soil moisture used in the models: topographic wetness index, distances to rivers, footpaths, network, and rivers+cost.

F.1 Topographic Wetness Index

F.1.1 Workflow

Topographic wetness index is commonly used in ecological studies as a proxy for long-term soil moisture patterns derived from the underlying landscape topography (Kopecký and Čížková, 2010) and was calculated to approximate the distribution of soil moisture across the Birk Fell juniper population. The standard index is defined as TWI = ln(As/tanβ), where As = specific catchment area / contour length and β is the local slope (Beven and Kirkby, 1979). The specific catchment area is calculated from the cumulative upslope area draining through a cell, divided by the contour width (Gruber and Peckham, 2009) but the exact method of calculation depends on the choice of flow routing algorithm that can lead to substantial differences in the TWI values calculated (Kopecký and Čížková, 2010). Numerous methods to pre-prepare the input digital elevation model (DEM), such as removing sinks and burning stream networks, can also be used before running the flow routing algorithm. To find the TWI calculation method that best captured patterns of soil moisture across Birk Fell SSSI, we tested fifteen different flow routing algorithms, two “fill sinks” and three “burn streams” DEM pre-processing methods and correlated values extracted from each resulting TWI layer with soil moisture values collected in field quadrats. Following a pilot study carried out using field data and TWI layers created for the juniper population within North Rothiemurchus Pinewood SSSI in the Cairngorms (results not shown), the best workflow for TWI calculation was determined as:

1) find flow routing algorithms implementing a range of methods (single and multi-neighbour, trace, top-down and recursive flow routing) that best correlate with field collected data points, as the choice of algorithm will have the largest impact on the accuracy of TWI prediction;

2) compare “fill sinks” DEM pre-processing methods using the best flow routing algorithms identified at step 1;

3) use the best performing DEM from step 2 to compare the performance of “burn stream” methods.

F.1.2 Preparation of input variables

Point samples of soil moisture used to evaluate the TWI layers were collected in October 2017 during investigation of 46, 10x10m quadrats at Birk Fell SSSI. Quadrats were placed in locations pre-selected to ensure sampling across the range of juniper area, altitude, slope and distance to watercourse gradients present on site (Donald et al., 2020). Soil moisture was measured in each quadrat as % volumetric water content (VWC) at 3.8cm depth using a FieldScout TDR 300 probe. Measurements were collected from: 1) areas within each quadrat where juniper was absent; 2) under asymptomatic juniper; and 3) under symptomatic juniper. An equal number of measurements (minimum four) were collected from each category present, resulting in eight to twelve point samples per quadrat. Mean and maximum %VWC was calculated across all samples (categories 1-3, labelled as “soil moisture”) and only samples collected underneath juniper stands (categories 2-3, labelled as “juniper moisture”) for each quadrat.

Calculation of TWI requires rasters of flow accumulation and slope for the full catchment extent, in this instance the 145km^2 Eamont at Pooley Bridge river catchment downloaded from the National River Flow Archive (Hydrology, 2018). Flow accumulation is calculated from a DEM and, optionally, a raster of the stream network. The following input layers were prepared in R v.3.5.2 (R Core Team, 2018) using the raster package (Hijmans, 2019). A 5m DEM supplied by NeXTPerspectives™ (updated February 2014) was clipped to the catchment boundary, from which a 5m raster of slope was created using the *terrain* function. The 50m CEH digital river network of Great Britain (Moore et al., 2000), clipped to the catchment boundary and corrected to 1m accuracy on site within Birk Fell SSSI, was converted to a 5m resolution raster using *rasterize* specifying a “length” function. Finally, each raster was resampled to 10m using *aggregate* to match the scale of the field data. Following the creation of TWI layers, values were extracted to each field quadrat centroid using *extract* and correlated with the field collected values using *cor* from the base-R stats package. All remaining calculations were performed in SAGA GIS v.2.3.2 (Conrad et al., 2015) as it offered a wide choice of DEM processing tools and flow routing algorithms.

F.1.3 Types of flow routing algorithm

Flow routing algorithms determine how water moves across each cell in the DEM, allowing differences in water accumulation to be calculated. Single neighbour algorithms constrain flow out of a cell so water can only move into one adjacent cell (Table F1), whereas multiple neighbour algorithms allow water to flow into (a set number of) multiple neighbouring cells (Table F2). Both types of algorithm calculate convergent flow but only multiple neighbour algorithms accommodate divergent flow paths, which can either improve the accuracy of flow tracing across the catchment or reduce it if flow is dispersed too widely compared to actual distribution patterns (Gruber and Peckham, 2009). Flow is most commonly directed through cells in the DEM using one of the three following methods: i) trace – flow is traced separately through each individual cell ii) top-down – flow is processed downwards through the highest to lowest cells iii) recursive – flow is processed upwards through connected cells. Some algorithms are restricted to a particular method while others allow the user to choose different implementations (Table F1,Table F2).

Table F1. List of single neighbour algorithms, and the flow routing types they can implement, available to calculate flow accumulation in SAGA GIS v.2.3.2. Algorithm citations were copied from the SAGA GIS website (Conrad and Olaya, 2004) and a description of how each algorithm works was taken from Gruber & Peckham, 2009.

Algorithm name	Citation	Description	Flow routing type		
			Trace: traces flow from each cell separately until it leaves the DEM / ends in a sink	Top down: processes flow downwards from highest to lowest cell	Recursive: processes flow through all upwards connected cells
D8 (Deterministic eight neighbours)	O'Callaghan, J.F. / Mark, D.M. (1984): 'The extraction of drainage networks from digital elevation data', Computer Vision, Graphics and Image Processing, 28:323-344	Apportions flow from each grid cell to a single adjacent cell through the steepest downslope gradient, resulting in eight possible drainage directions. Any ambiguous flow directions are resolved by an arbitrary assignment.		x	x
Rho8 (randomised single flow direction)	Fairfield, J. / Leymarie, P. (1991): 'Drainage networks from grid digital elevation models', Water Resources Research, 27:709-717	A stochastic extension of Deterministic 8 that randomly runs the flow to an adjacent cell with a probability proportional to the slope gradient. The randomness reduces the grid bias but produces different results every time it is implemented.	x	x	x
KRA (kinematic routing algorithm)	Lea, N.L. (1992): 'An aspect driven kinematic routing algorithm', in: Parsons, A.J., Abrahams, A.D. (Eds.), 'Overland Flow: hydraulics and erosion mechanics', London, 147-175	Directs flow into the cell corner with the lowest value; value is calculated by averaging the elevations of adjoining cells. Creates a continuous flow direction with less bias than D8.	x		

Table F2. List of multiple neighbour algorithms, the number of adjacent cells flow can be diverted to and the flow routing types they can implement, available in SAGA GIS v.2.3.2. Algorithm citations were copied from the SAGA GIS website (Conrad and Olaya, 2004) and a description of how each algorithm works was taken from Gruber and Peckham (2009*)*.

Algorithm name	Citation	N of cells	Description	Flow routing type		
				Trace	Top down	Recursive
DEMON (Digital elevation model network)	Costa-Cabral, M. / Burges, S.J. (1994): 'Digital Elevation Model Networks (DEMON): a model of flow over hillslopes for computation of contributing and dispersal areas', Water Resources Research, 30:1681-1692	2	Constructs four flow tubes through each corner of a cell and assigns the flow to the best matching plane. Method used to determine aspect angle can lead to inconsistent flow geometry and does not address flow direction ambiguity on peaks and ridges.	x		
D∞ (Deterministic Infinity)	Tarboton, D.G. (1997): 'A new method for the determination of flow directions and upslope areas in grid digital elevation models', Water Resources Research, Vol.33, No.2, p.309-319	2	Apportions flow based on the function of eight triangular planes determined by the steepest slope gradient.		x	x
Multiple Flow Direction	Freeman, G.T. (1991): 'Calculating catchment area with divergent flow based on a regular grid', Computers and Geosciences, 17:413-22 Quinn, P.F., Beven, K.J., Chevallier, P. & Planchon, O. (1991): 'The prediction of hillslope flow paths for distributed hydrological modelling using digital terrain models', Hydrological Processes, 5:59-79	8	Drives the flow down to all downslope neighbours through a flow partition exponent		x	x

Braunschweiger Reliefmodell	Bauer, J. / Rohdenburg, H. / Bork, H.-R. (1985): 'Ein Digitales Reliefmodell als Vorraussetzung fuer ein deterministisches Modell der Wasser- und Stoff-Fluesse', Landschaftsgenese und Landschaftsoekologie, H.10, Parameteraufbereitung fuer deterministische Gebiets-Wassermodelle, Grundlagenarbeiten zu Analyse von Agrar-Oekosystemen, (Eds.: Bork, H.-R. / Rohdenburg, H.), p.1-15	3	Chooses the cell nearest to the aspect of the source cell and its two neighbouring cells according to downslope gradient		x	
Multiple Flow Direction based on Maximum Downslope Gradient	Qin, C. Z. / Zhu, A. X. / Pei, T. / Li, B. L. / Scholten, T. / Behrens, T. / & Zhou, C. H. (2011): 'An approach to computing topographic wetness index based on maximum downslope gradient', Precision Agriculture, 12(1), 32-43	8	Drives the flow up to all downslope neighbours based on the linear function of the maximum downslope gradient		x	
Mass Flux Method	Gruber, S., Peckham, S. (2008): Land-Surface Parameters and Objects in Hydrology. In: Hengl, T. and Reuter, H.I. [Eds.]: Geomorphometry: Concepts, Software, Applications. Developments in Soil Science, Elsevier, Bd.33, S.293-308.	4	Divides each cell into four quarter-pixels, the plane of which is determined by elevations of whole pixels and two neighbouring cells. The flow is routed to the neighbouring cells at the quarter-pixel scale. Removes the ambiguity of plane fitting and ambiguity of flow direction for grid cells that correspond to peaks or ridges as it allows flow from these grid cells to be routed in different directions.			

F.1.4 TWI method selection

As the accuracy of TWI prediction depends on the suitability of the flow routing algorithm used, it was important to test a range of single and multiple neighbour algorithms, and flow routing methods, through all stages of the workflow. Each TWI layer was created using the Topographic Wetness Index tool found under the Terrain Analysis > Hydrology > Topographic Indices menu with rasters of flow accumulation and slope as inputs and the default settings “method = standard” and “area conversion = no conversion”.

F.1.4.1 Flow routing

Fifteen rasters of flow accumulation were calculated using the algorithms and flow routing types available under the Terrain Analysis > Hydrology > Flow Accumulation menu and the 10m DEM (Table F1, Table F2, Figure F1). All of the resulting TWI layers poorly correlated with mean and maximum soil moisture values obtained from quadrats, with r^2 ranging from 0.13 to 0.32 (Table F3). This could be because factors not captured by TWI (such as soil type or vegetation cover) significantly influence the distribution of soil moisture at Birk Fell or because rainfall events occurred during the course of the data collection, exaggerating short-term differences in point sampled soil moisture between locations (Donald et al., 2020). Although little difference was found between flow routing implementations of the same algorithm, and between the best performing single and multiple neighbour algorithms there were small differences in the strength of correlations that we could use to select four flow routing methods to test at the next step of the workflow. There was one best algorithm overall (D8) that produced the highest correlation with two different flow routing types (top-down and recursive). As D8 was a single neighbour algorithm further testing would also require a multiple neighbour algorithm, of which maximum downslope gradient (top-down) produced the strongest correlation across all metrics, and an algorithm implementing the flow tracing method, of which Rho8 (trace) was the best performing (Table F3).

Table F3. Pearson r^2 correlations between TWI values and mean or maximum soil moisture measured across the whole 10x10m quadrat (soil moisture) or only underneath juniper (juniper moisture). Fifteen methods of calculating flow accumulation, using different algorithms and flow routing type implementations, are compared. The highest correlation (to 2 decimal places) with each field measure is highlighted in bold.

	Flow routing algorithm	Routing type	Soil moisture		Juniper moisture	
			Mean	Maximum	Mean	Maximum
Single neighbour	D8	top-down	**0.23**	**0.25**	0.25	**0.32**
	D8	recursive	**0.23**	**0.25**	0.25	**0.32**
	Rho8	trace	**0.23**	0.23	0.25	0.30
	Rho8	top-down	0.21	0.22	0.21	0.25
	Rho8	recursive	0.13	0.16	0.16	0.24
	KRA	trace	0.22	0.21	0.25	0.30
Multiple neighbour	DEMON	trace	0.22	0.22	0.25	0.29
	D∞	top-down	**0.23**	0.23	0.25	0.30
	D∞	recursive	**0.23**	0.23	0.25	0.30
	Multiple Flow Direction	top-down	**0.23**	0.23	**0.26**	0.29
	Multiple Flow Direction	recursive	**0.23**	0.23	**0.26**	0.29
	Braunschweiger Reliefmodell	top-down	**0.23**	0.23	0.25	0.30
	Triangular Multiple Flow Direction	top-down	**0.23**	0.22	0.25	0.30
	Maximum Downslope Gradient	top-down	**0.23**	0.23	**0.26**	0.31
	Mass Flux Method	See Table F2	0.18	0.19	0.22	0.25

F.1.4.2 Sinks

Sinks are cells with local elevation minima that occur as an artefact of DEM generation and do not relate to terrain features but cause premature flow termination because all neighbouring cells have higher elevations (Reuter et al., 2009). We compared two of the four algorithms available in SAGA GIS (Terrain Analysis > Preprocessing) to remove sinks from the DEM, choosing the methods that differed most significantly. The “Fill sinks XXL (Wang/Liu)” algorithm progressively increases the elevation values of sinks until the lowest value is found from which the water can “spill” out into the rest of the DEM (Wang and Liu, 2006). This is combined with a least cost algorithm to seek the most likely flow path of water out of each cell. The algorithm “Fill sinks (Planchon/Darboux)” instead inundates the DEM surface with a layer of water and then removes the excess to leave the sinks topped up (Planchon and Darboux, 2001). The 10m DEM was input to each tool, run with the default minimum slope value of 0.1 and 0.01 for XXL and Planchon/Darboux respectively. The resulting DEMs were then used to generate rasters of flow accumulation and TWI. Compared to the original DEM (Table F3) all correlations between TWI and quadrat data were worse using the Planchon/Darboux correction and improved using the XXL correction (Table F4). The D8 flow routing algorithm coupled with the XXL DEM correction yielded the

highest correlations found so far (mean soil moisture $r^2 = 0.28$, mean juniper moisture $r^2 = 0.30$), producing the same result with both top-down and recursive flow routing (Table F4).

Table F4. Comparison of "Fill sinks XXL (Wang/Liu)" (XXL) and "Fill sinks (Planchon/Darboux)" (PD) algorithms used to pre-process the DEM before generating flow accumulation rasters using four different flow routing methods. The highest Pearson r^2 values (to 2 decimal places) between TWI and each field measurement are highlighted in bold.

Flow routing algorithm	Routing type	Sinks	Soil moisture		Juniper moisture	
			Mean	Maximum	Mean	Maximum
D8	top-down	PD	0.17	0.21	0.20	0.28
D8	recursive	PD	0.24	0.27	0.26	0.34
Rho8	trace	PD	0.19	0.19	0.22	0.29
Maximum Downslope Gradient	top-down	PD	0.24	0.24	0.27	0.31
D8	top-down	XXL	**0.28**	**0.31**	**0.30**	**0.38**
D8	recursive	XXL	**0.28**	**0.31**	**0.30**	**0.38**
Rho8	trace	XXL	0.26	0.26	**0.30**	0.35
Maximum Downslope Gradient	top-down	XXL	0.25	0.26	0.29	0.34

F.1.4.3 Stream network

A further difficulty that can occur from generalising gridded data to produce a DEM is the loss of drainage lines or creating lines where none exist in reality (Gruber and Peckham, 2009). Integrating a known stream network into the DEM can correct for this, for which SAGA GIS offers three methods using the "Burn stream network to DEM" tool in the Preprocessing menu. The channel is created by decreasing the value of each DEM cell interfacing with a watercourse pixel by a) epsilon - a value you can specify (default = 1), b) the minimum elevation in a neighbouring cell minus epsilon, or c) tracing the stream network downstream. This final option ensures a steady downstream gradient and requires a flow direction raster (in addition to the watercourse raster) to be generated from the DEM using the "sink drainage route detection" tool. Three versions of both the original and XXL sink corrected DEMs were created using the three alternative "burn stream" methods, which were then input to flow accumulation tools using the four shortlisted flow routing methods (Table F5). Burning the stream network improved the correlation between TWI and the quadrat measurements in two instances: Rho8 (trace type) flow routing with watercourse pixel values either decreased by the neighbouring cell minimum -1, or by flow tracing, and Maximum Downslope Gradient (top-down type) with stream pixels decreased by -1 (Table F5). With all other DEM preparations and flow routing methods, burning streams always resulted in weaker r^2 values (Table F5).

Table F5. Comparison of three stream network integration methods that decreased pixel values by: -1, minimum neighbouring value -1 (min-1) or flow tracing (trace). Each method was used to burn the stream network into the original (sink = NA) and sink corrected (sink = XXL) DEMs before flow accumulation was calculated using four alternative flow routing methods to calculate TWI. The highest Pearson r^2 values (to 2 decimal places) between TWI and each field measurement are highlighted in bold.

Flow routing algorithm	Routing type	Burn streams	Sinks	Soil moisture		Juniper moisture	
				Mean	Maximum	Mean	Maximum
D8	top-down	-1	NA	0.19	0.21	0.22	0.27
		min-1	NA	0.19	0.21	0.22	0.27
		trace	NA	0.22	0.22	0.26	0.29
		-1	XXL	0.23	0.25	0.26	0.32
		min-1	XXL	0.23	0.25	0.26	0.32
		trace	XXL	0.23	0.25	0.27	0.32
D8	recursive	-1	NA	0.19	0.21	0.22	0.27
		min-1	NA	0.19	0.21	0.22	0.27
		trace	NA	0.22	0.22	0.26	0.29
		-1	XXL	0.23	0.25	0.26	0.32
		min-1	XXL	0.23	0.25	0.26	0.32
		trace	XXL	**0.26**	**0.26**	0.28	0.33
Rho8	trace	-1	NA	0.22	0.23	0.26	0.31
		min-1	NA	0.25	0.23	**0.29**	0.31
		trace	NA	0.25	0.24	**0.29**	0.31
		-1	XXL	0.25	0.24	0.28	0.32
		min-1	XXL	0.24	0.22	0.27	0.29
		trace	XXL	0.25	0.22	0.27	0.29
Maximum Downslope Gradient	top-down	-1	NA	**0.26**	**0.26**	**0.29**	**0.34**
		min-1	NA	0.22	0.22	0.26	0.28
		trace	NA	0.20	0.18	0.24	0.25
		-1	XXL	0.24	0.24	0.27	0.30
		min-1	XXL	0.20	0.19	0.23	0.25
		trace	XXL	0.18	0.15	0.21	0.21

Using D8 flow routing calculated from an XXL corrected DEM with no stream burning (Figure F1) remained the best method for calculating TWI, yielding the strongest correlations with soil moisture measurements collected on site (Table F4). This layer was, therefore, used as TWI in the models by resampling the resulting 10m raster in R to 25m using the *aggregate* function in the raster package (Hijmans, 2019) and extracting values to the centroid of each grid cell at both spatial resolutions.

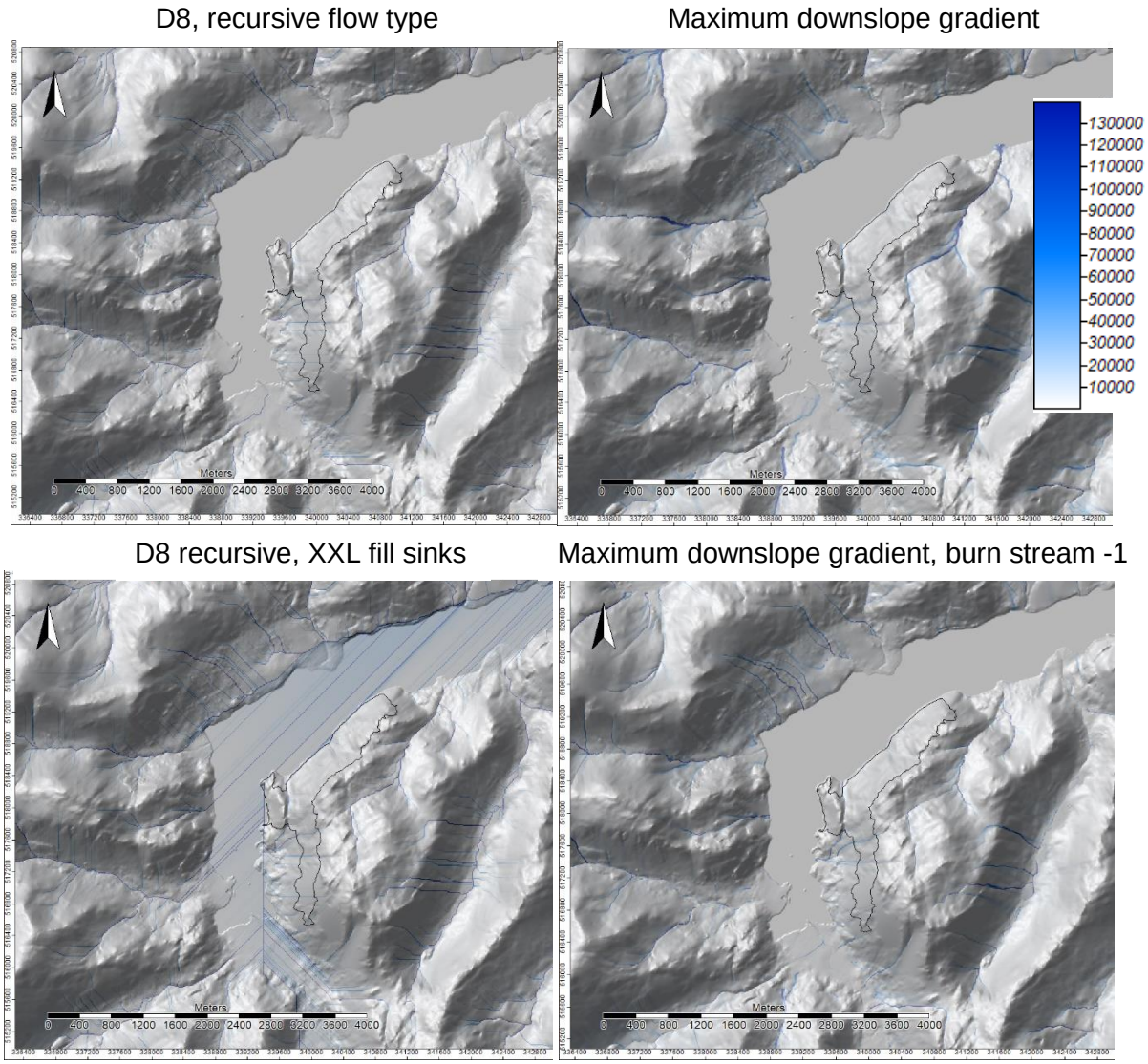

Figure F1. Examples of flow accumulation (mapped in blue) generated using two different flow routing algorithms. The D8 recursive flow routing algorithm (L) traces flow upslope through single neighbouring cells while the maximum downslope gradient algorithm (R) uses top-down flow routing and partitions flow into up to eight neighbouring cells. Top panels show flow accumulation calculated without any DEM pre-processing compared to the bottom panels implementing the fill sinks XXL (L) method and decreasing stream network pixel values by -1.

F.2 Hydrological distance metrics

Soil moisture levels were expected to increase with decreasing distance from a river, footpath or the combined network. The river and footpath networks intersecting Birk Fell SSSI were mapped on site during fieldwork undertaken in October 2017. Prior to fieldwork, the 50m CEH digital river network of Great Britain (Moore et al., 2000) was clipped to the catchment boundary while the footpath network intersecting the study population was traced in ARC GIS from the Ordnance Survey 1:25000 scale colour raster (© Crown copyright and database rights OS 2017 100017572). Both shapefiles were exported to ArcPad v.10.2 loaded on a Panasonic FZ-GI tablet and manually corrected in the field against the 2010 NeXT Perspectives™ 25cm aerial image using the ArcPad tracking function (accurate to 3m). To understand if the combined network of rivers and paths better explained *P. austrocedri* colonisation compared to the individual layers, the two corrected shapefiles were merged into a single "network" layer. The shortest, straight-line (Euclidean) distance (m) from the centroid of each grid cell to the nearest pixel in each river, footpath and network layer was then calculated as a straight line using the *gDistance* function in the rgeos R package (Bivand, Roger; Rundel, 2019). However, the actual distance between two points will be impeded by altitude, as water cannot flow uphill, and by the curvature (convex or concave shape) of the intervening slope, which could accelerate or decelerate the speed and direction of flow. This cost of movement from one cell to the next can be measured by combining movement constraints (altitude) with a calculation of surface resistance (slope or curvature) and the shortest distance can then be identified as the path with the lowest cost of movement. Using slope, or slope and curvature, as surface resistance layers, we created three alternative metrics incorporating movement costs to measure distances between each grid cell centroid and the nearest river or network.

The first step was to calculate a raster of curvature from the 5m slope raster using the *curvature* function in the ARC GIS v.10.5.1 spatial analyst toolbox, implemented with the 'standard' curvature type that accounts for both flow speed (profile curvature) and flow convergence or divergence (plan curvature). The resulting raster was re-scaled to the slope raster and then the two were added together (without weighting) using the ARC GIS raster calculator creating the final curvature raster. The path distance tool in the ARC GIS spatial analyst toolbox was used to create three, 5m resolution, cost distance layers to the full extent of the catchment, using the DEM as the raster of surface distance, either rivers or network as the input feature, and either slope or curvature as the cost raster. The three layers created were rivers+slope, rivers+curvature and network+curvature. Each layer was

subsequently resampled to 10m and 25m using the raster package function *aggregate* (Hijmans, 2019) and extracted to the requisite grid cell centroids in R v.3.5.2 (R Core Team, 2018). Correlations between the cost distance rasters and the topographic and hydrological covariates used to create them was tested at each spatial resolution using Pearson's r^2. At both resolutions, the cost rasters were highly correlated with each other, so rivers+curvature was selected for use in the models - labelled as "rivers+cost" in the main text - as the layer showing the least collinearity with the other topographic and hydrological covariates (all r^2 values <0.7 with the exception of network) (Figure F2).

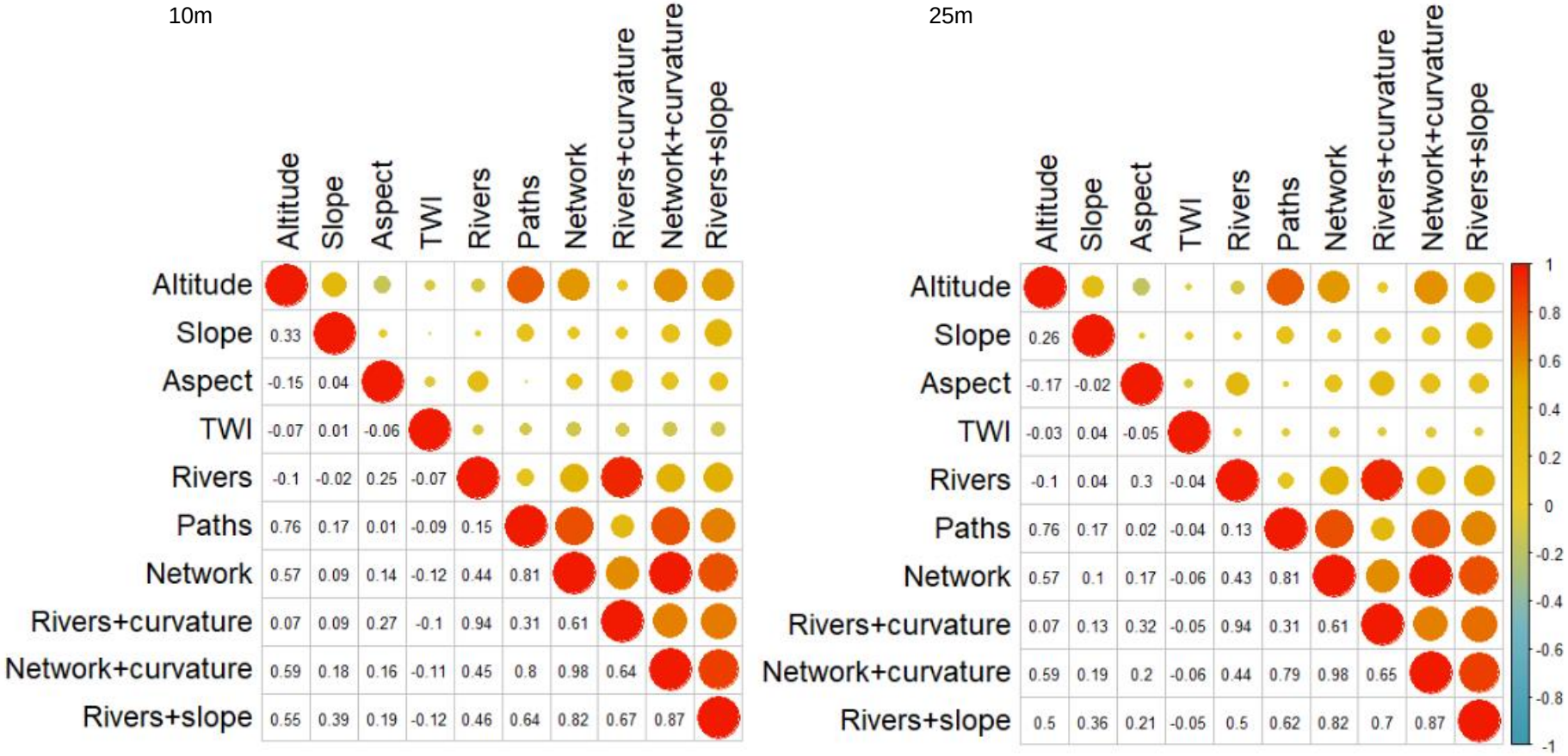

Figure F2. Pearson's r^2 correlation plots between topographic and hydrological covariates at 10m (L) and 25m (R) spatial resolutions shown using a colour scale and text to 1 decimal place. The shortest Euclidean distance to each watercourse type is labelled as river, paths and network while covariates incorporating a cost surface are labelled with the input feature (rivers or network) and the cost surface (curvature or slope).

Appendix G. Methods used to identify the best spatial mesh for Birk Fell SSSI hurdle and point process models

G.1 Identifying the best mesh to address spatial autocorrelation in the hurdle model

Spatial autocorrelation occurs where values sampled from neighbouring locations are more similar to each other than values sampled further away, commonly arising as a result of biological factors (e.g. dispersal limitations), non-linear responses to environmental gradients or responses to spatially structured environmental factors that are missing from the model (Dormann et al., 2007). The assumption of independence in the model residuals is violated where they retain spatial patterning, leading to increased bias in parameter estimates and potential for false rejection of null hypotheses (Dormann et al., 2007).

The INLA fitting method addresses spatial autocorrelation by implementing a spatial mesh, parameterised by the user. The accuracy of the spatial random field predictions depends on the size of the mesh triangles in relation to the density of input locations (Redding et al., 2017). Smaller triangles generally improve results where locations are densely clustered but risk over-prediction and reduced computational efficiency in regions with sparser input (Righetto et al., 2018). As such, we expected the mesh used in the 25m resolution model would require fewer, larger triangles compared to the 10m model. Meshes were created to the extent of the 10m and 25m grids with the input locations defined as the centroid of each grid cell. Triangle size was constrained by supplying different value combinations to three parameters: i) cut-off – the shortest permitted distance between input locations, limiting the generation of triangles around clustered data; ii) maximum edge in the inner domain, altering the density of triangles across the mapped area; iii) maximum edge in the outer domain, used to avoid border effects (Table G1). Ninety different meshes were derived from all possible combinations of the parameters values listed (Table G1). Each of the four covariate hurdle models was run at both spatial resolutions with each mesh to check the robustness of covariate responses to different parameterisations.

Table G1. List of values used to create spatial meshes for hurdle models at 10m and 25m resolution. Ninety different meshes were tested, created from all possible combinations of cut-off and inner domain values, and all outer domain values larger than that specified for the inner domain (e.g. an inner domain of 500m could only be combined with an outer domain length of 800m).

Mesh parameter	Values (m)
Cut-off (minimum distance allowed between points)	2, 5, 10, 25, 50, 100
Maximum triangle edge lengths – inner domain	50, 100, 150, 200, 250, 500
Maximum triangle edge lengths – outer domain	100, 200, 400, 800

G.2 Selecting the best mesh for point process modelling

Prior to shortlisting the dispersal kernel with the most explanatory power, the first step in fitting the PPMs was to choose appropriate values for the cut-off, maximum inner and outer domain mesh parameters (Table G2). Seventy meshes were tested at both spatial resolutions using three models that all included juniper density, juniper patch density, slope, rivers and paths plus one of three force of infection covariates parameterised using different dispersal kernel shapes (h=0.5,1 or 2) set with scale=20m. Different cut-off values were used at 10m and 25m resolution to account for the differences in grid cell size but the same maximum triangle edge length values were tested at both spatial scales (Table G2). Meshes resulting in the lowest DIC for models containing each dispersal kernel variant were shortlisted for further testing. Where multiple meshes produced the same DIC (to 2dp), the mesh with the smaller number of triangles (hence faster computation) was selected. The strength and direction of covariate responses to meshes with different cut-off values was visually inspected to check robustness of covariate effects.

Table G2. List of values used to create seventy different meshes to test with different dispersal kernels (δ=20) in PPMs at 10m and 25m spatial resolution. Meshes were created from all possible combinations of cut-off and inner domain values, and all outer domain values larger than that specified for the inner domain.

Mesh parameter	Spatial resolution	Values (m)
Cut-off (minimum distance allowed between points)	10m	2, 5, 10, 50, 75
	25m	10, 25, 50, 75, 100
Maximum triangle edge lengths – inner domain	10 and 25m	50, 75, 150, 200, 500
Maximum triangle edge lengths – outer domain	10 and 25m	100, 200, 400, 800

Appendix H. Supplementary results from the hurdle models

H.1 Correlations between environmental covariates

Correlations between all covariates used in the hurdle models of juniper presence (including all grid cells within the site boundary) and density (grid cells containing juniper) at 10m and 25m spatial resolution were explored using Pearson r^2 values (Figure H1). Covariates correlated r^2 >0.7 were not included in the same model to avoid collinearity.

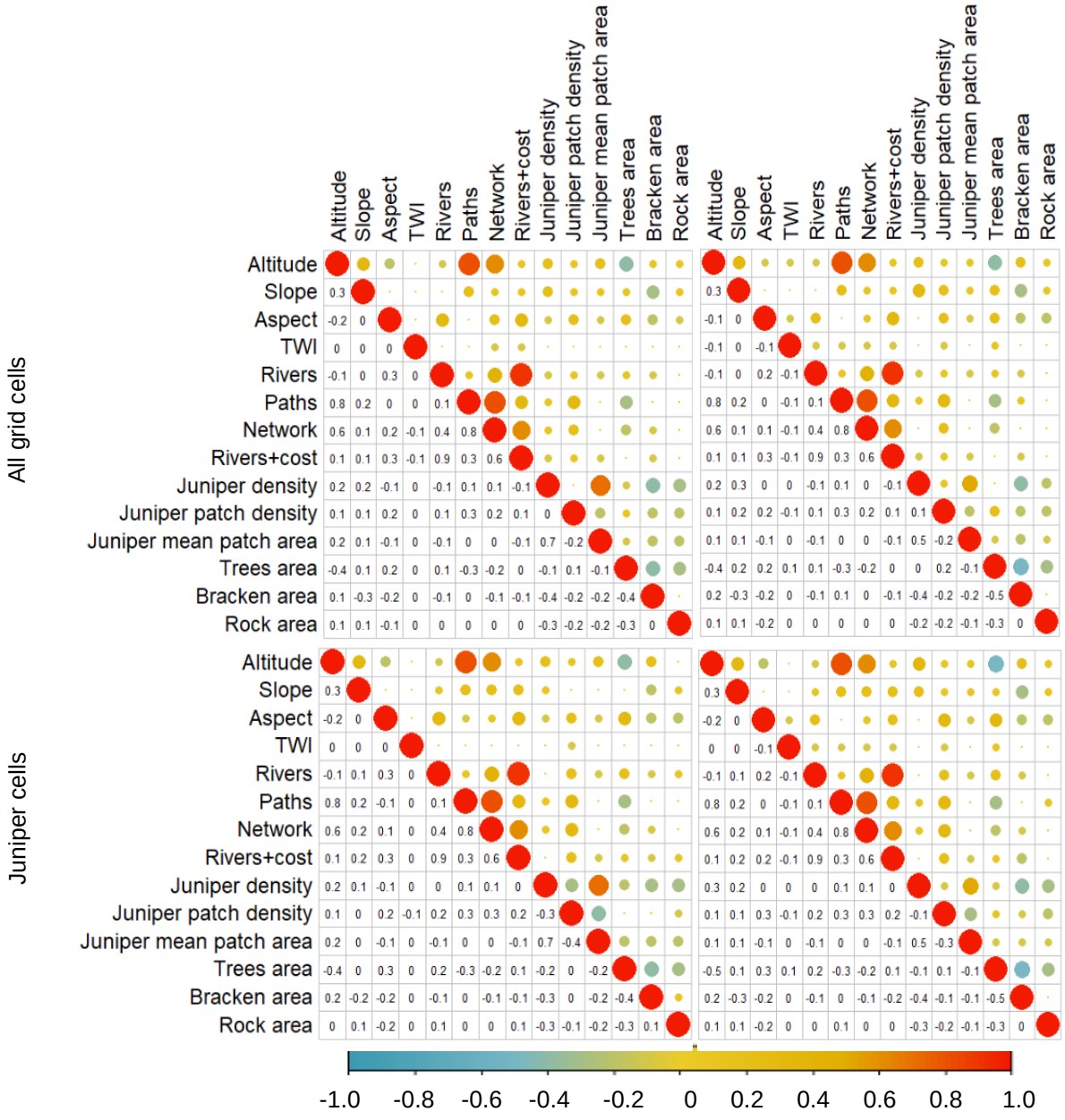

Figure H1. Correlation plot between all covariates used in the hurdle model measured across all grid cells within the site boundary (top) and only grid cells containing ≥1m^2 juniper (bottom) at 10m (L) and 25m (R) spatial resolution. Pearson r2 values are shown using a colour scale and text to 1 decimal place. Covariate descriptions and units of measurement are given on Table 9.

H.2 Comparison of covariate responses across top model sets

At both spatial resolutions, hurdle models of juniper presence and density were run as intercept only (null) models and compared to models including different combinations of spatial meshes and/or spatially unstructured random effects, as well as four different sets of covariates devised to avoid collinearity between combinations of altitude, distances to paths and rivers. Here we tabulate the results to evidence the findings described in the main text that the best model obtained at 10m resolution included a spatial mesh and covariates (Table H1) while the best model at 25m resolution included only the intercept, a spatial mesh and a spatially unstructured random effect (Table H2). Where present, the same covariate set was used in both the juniper presence and density components of the hurdle model. Each covariate set was tested with 90 different meshes (see Table H1). Of the 90 models tested per covariate set, the top models are identified as those with DIC values within 2 DIC units of the best performing model with the lowest DIC.

Table H1. Hurdle model results (DIC) for juniper presence and density at 10m resolution comparing the null models with and without spatial meshes, unstructured spatial random effects (iid) and four covariate sets (labelled with the combination of covariates unique to each set). Models are ordered from best (low DIC) to worst performing (high DIC). Mesh parameters are given as the maximum allowed triangle edge lengths in the inner and outer domains, and the cut-off value (minimum allowed distance between points). The mesh yielding the top model set (within 2 DIC units of the best model) is shown for each covariate set and the parameters used to obtain the best overall model were also used to parameterise the mesh tested with the null model to aid comparison.

Model	Mesh parameters	DIC
Rivers+cost, paths	50, 800, 5	75886.61
Rivers+cost, network, altitude	50, 800, 2	75915.82
Rivers, paths	100, 800, 5	75961.39
Rivers, network, altitude	250, 800, 5	75993.10
Null, mesh	50, 800, 5	80803.90
Null, mesh, iid	50, 800, 5	81271.93
Null	NA	96364.77
Null, iid	NA	96365.27

Table H2. Hurdle model results (DIC) for juniper presence and density at 25m resolution comparing the null models with and without spatial meshes, unstructured spatial random effects (iid) and four covariate sets (labelled with the combination of covariates unique to each set). Models and mesh parameters are described in the same way as for *At both spatial resolutions, hurdle models of juniper presence* and *density* were run as intercept only (null) models and compared to models including different combinations of spatial meshes and/or spatially unstructured random effects, as well as four different sets of covariates devised to avoid collinearity between combinations of altitude, distances to paths and rivers. Here we tabulate the results to evidence the findings described in the main text that the best model obtained at 10m resolution included a spatial mesh and covariates (Table H1) while the best model at 25m resolution included only the intercept, a spatial mesh and a spatially unstructured random effect (Table H2). Where present, the same covariate set was used in both the juniper presence and density components of the hurdle model. Each covariate set was tested with 90 different meshes (see Table H1). Of the 90 models tested per covariate set, the top models are identified as those with DIC values within 2 DIC units of the best performing model with the lowest DIC.

.

Model	Mesh parameters	DIC
Null, mesh, iid	250, 800, 10	20130.77
Rivers+cost, paths	250, 800, 10	20452.65
Rivers+cost, network, altitude	100, 200, 100	20771.67
	100, 400, 100	20772.32
	100, 800, 100	20772.65
	150, 200, 100	20773.62
Rivers, paths	100, 800, 100	20794.18
	100, 400, 100	20794.68
	100, 200, 100	20795.28
Rivers, network, altitude	500, 800, 100	20799.91
Null	NA	23379.11
Null, iid	NA	23379.29
Null, mesh	250, 800, 10	INF

The comparison of hurdle model DICs showed that the presence and density of juniper across Birk Fell SSSI was adequately explained by the examined covariates at 10m, but not 25m, resolution. However, the top model containing covariates at 25m used the same covariate set as the best 10m model and the relationships found between juniper presence and density and these covariates were consistent at both resolutions despite differences in mesh parameter values (Figure H2).

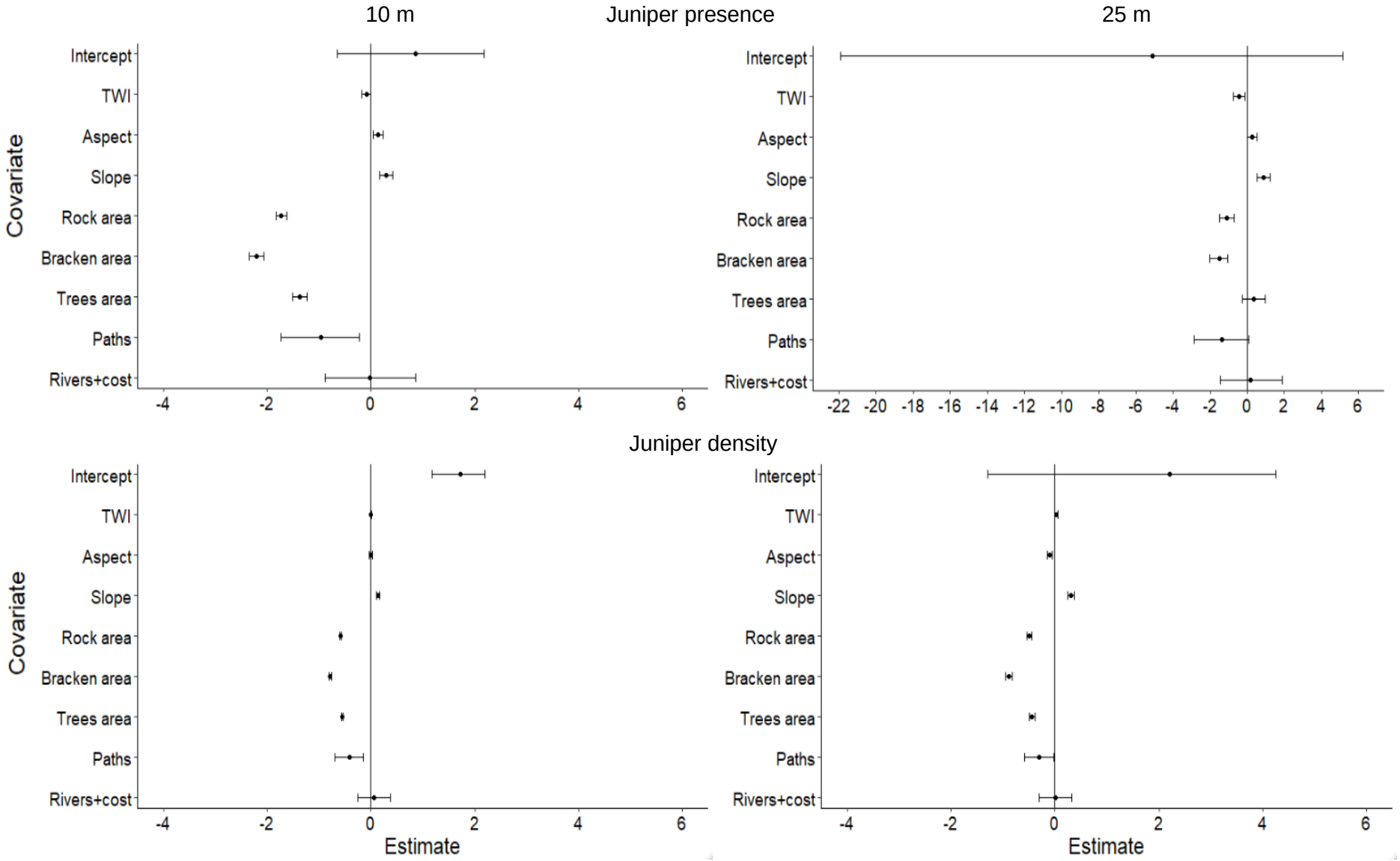

Figure H2. Posterior estimates (mean, 2.5% and 97.5% quantiles) for covariates included in the best models obtained at 10m (L) and for the corresponding covariate model at 25m (R) resolution, showing separate responses to juniper presence (top) and density (bottom) in grid cells.

One best model was produced from each of the four covariate sets at 10m resolution that all outperformed models without covariates (Table H1). Here we describe the consistency of covariate effects in the top model sets for juniper presence and density at 10m, to augment results detailed in the main text. The strength of relationships was broadly consistent across all four models and responses were always strongest in the presence part of the model compared to the density part (Figure H3). The direction of each correlation was also the same across all four models (Figure H3). Models containing footpaths produced lower DICs and elicited very strong, negative responses in both juniper presence and density (Figure H3). Very strong responses were also found between presence of juniper and decreasing distance to rivers, included on its own or amalgamated with footpaths in the network covariate. However, when rivers, network and altitude were included together the DIC increased further and the strength of the relationships was diminished. In all models, juniper presence and density increased with decreasing (drier) topographic wetness index (TWI). The model including rivers+cost and paths in the covariate set was the top model overall (ΔDIC = 29.21 units from the next top model).

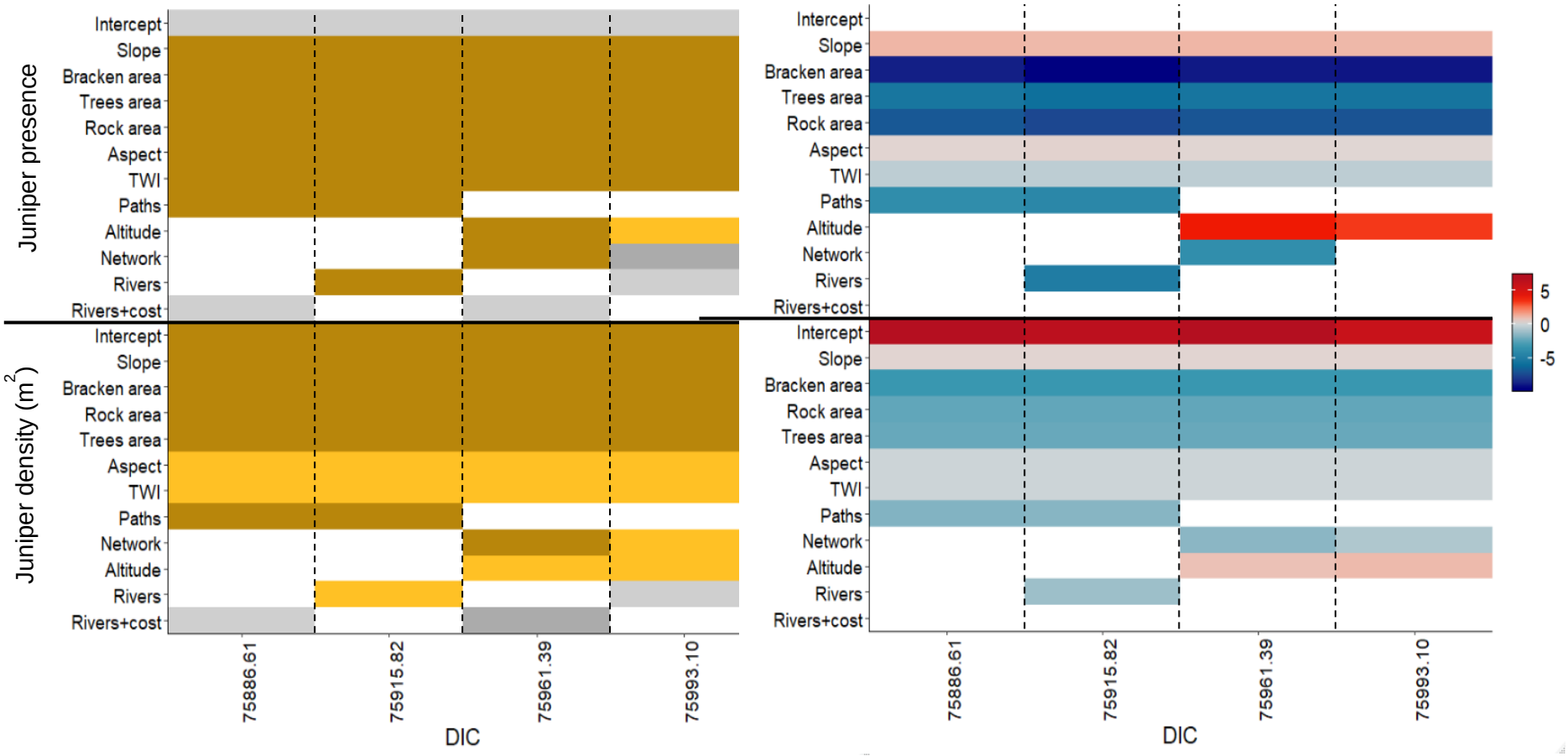

Figure H3. Presence, significance, and coefficient values for fixed effects present in both parts of the top hurdle model produced from each set of covariates at 10m resolution. Covariates were absent (white), weakly present (grey) or strongly present (yellow) in each top model (L). Coefficient values for covariates (where present) are shown as positive (red) or negative (blue) (R). Top models are ranked on the x-axis from lowest (best performing) to highest (worst performing) DIC and covariates are ordered according to the number of times they are present in the top models. See Table H1 for details of the mesh parameter values used in each top model.

H.3 Accounting for spatial autocorrelation in model residuals

Spatial autocorrelation of the residuals was calculated using Moran's I statistic to compare hurdle models at both spatial resolutions with no covariates (null model) (Tables H1-H2). Significant, positive, spatial autocorrelation was present up to 75m in the null model at both spatial scales. This was not improved by including an unstructured spatial random effect (iid) but was addressed by using a spatial mesh (Figure H4). No significant spatial autocorrelation was present in the best models determined at 10 and 25m resolution (Figure H4).

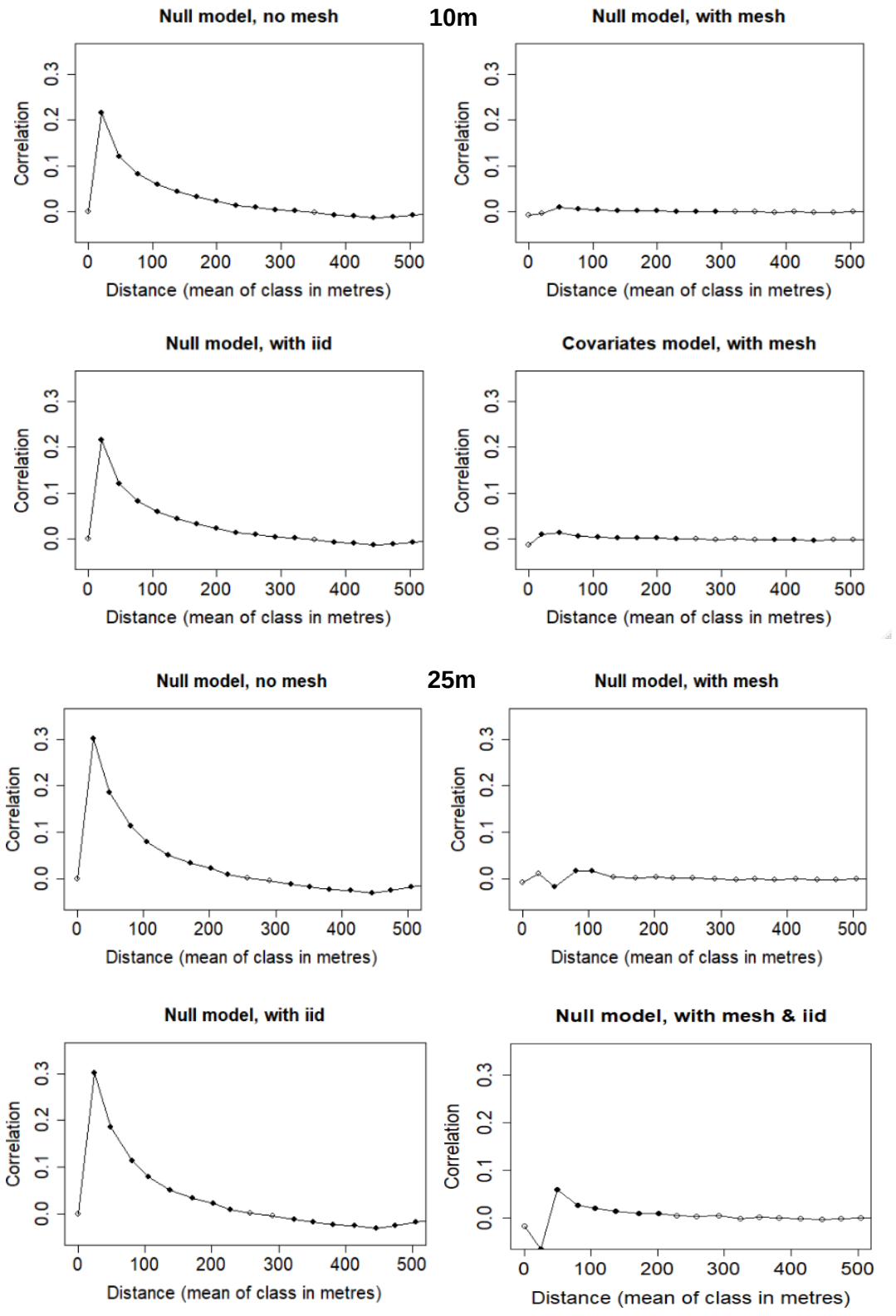

Figure H4. Moran's I p-values calculated from the residuals of hurdle models at 10m (top) and 25m (bottom) spatial resolutions plotted against the inter-cell distance up to the first 500m. Significant p-values (95 % confidence interval) are shown in black. Values used to parameterise the mesh are shown on Tables H1-H2.

H.4 The posterior mean spatial random field

The posterior means of the spatial random field calculated for each mesh triangle were mapped for the best hurdle model identified at each resolution (Figure H5). The spatial random fields from both best models were largely smooth and both showed improved performance (values closer to zero) in the juniper density compared to juniper presence model components (Figure H5). This is unsurprising as 81% of 10m grid cells and 88% of 25m grid cells contained juniper. The range of values found in the presence component of both models were very similar, and though the range of values was slightly broader in the 10m model (-9.9 to 7.6 compared to -7.40 to 7.26 at 25m), a smaller number of cells contained values tending away from zero (Figure H5). Higher values in both model components seemed to correspond to areas of higher juniper density but most cells containing juniper in the 25m presence model component showed high positive values in the spatial random field (Figure H5). This demonstrates that the spatial random field was unable to adequately account for the spatial patterns in the data at this resolution.

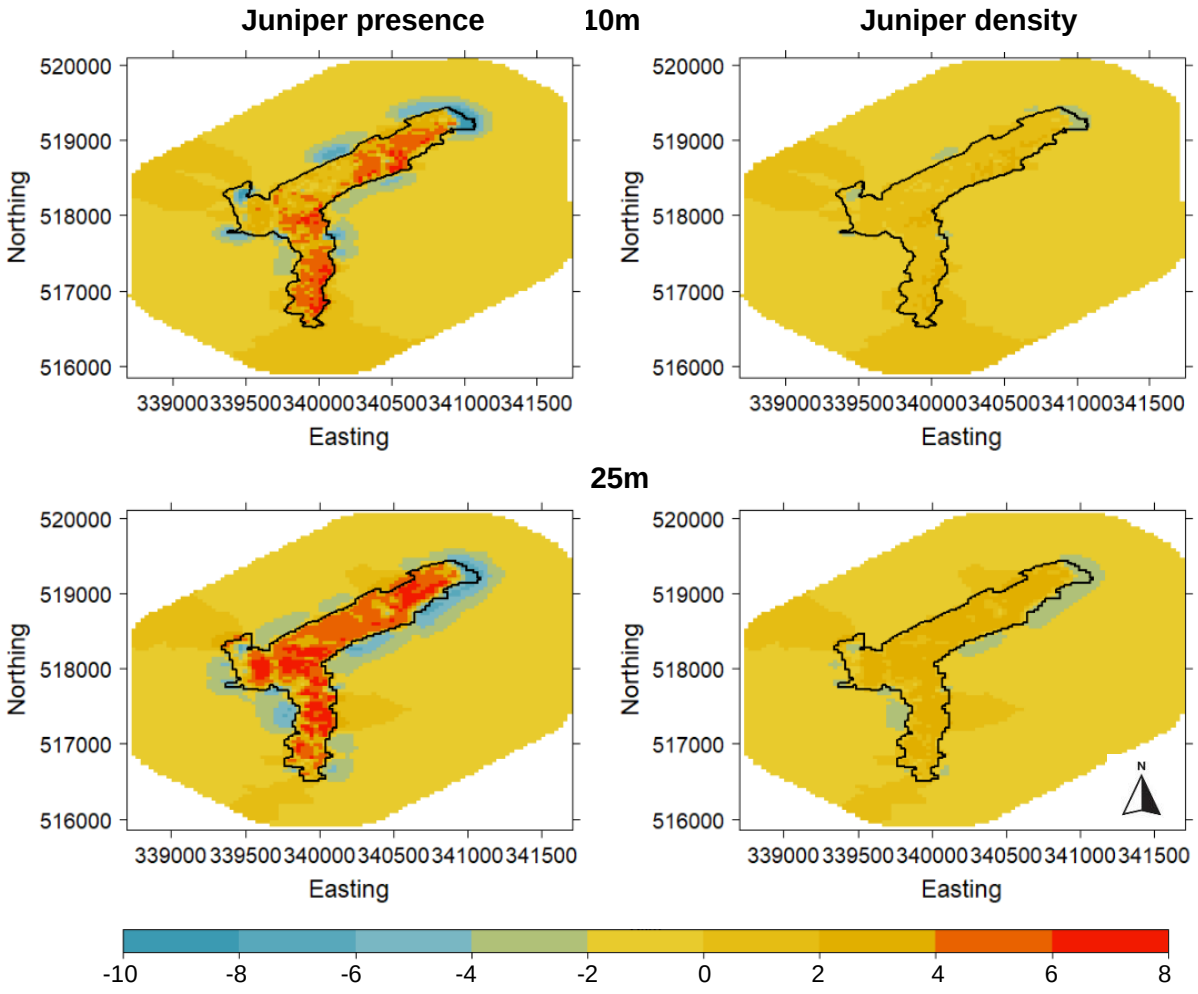

Figure H5. Spatial random fields for the juniper presence (L) and density (R) components of the best hurdle model obtained at 10m (top) and 25m (bottom) spatial resolutions, plotted to the extent of the mesh used in each analysis (n = 16045 triangles at 10m, 2428 at 25m; see Tables H1-H2 for parameter values). Data were supplied to the model within the black outline of Birk Fell SSSI.

Appendix I. Supplementary results from the Point Process Models

I.1 Point Process Modelling of 10m resolution symptomatic host density

I.1.1 Calibration of the spatial mesh

Different top models were produced from the saturated PPMs at the first mesh selection step (see Appendix G) depending on the dispersal kernel (δ=20m, h=0.5, 1 or 2) used to create the force of infection covariate (Table I1). The power (h=0.5) kernel produced the best models overall (DIC=10618.57), followed by the exponential (h=1, DIC=10623.69) and then the Gaussian (h=2, DIC=10633.84) (Table I1). The same meshes were present in the top model set with 28 equivalent meshes for each force of infection covariate. Models produced using cut-off values of two and five yielded the same DIC, so only results obtained with a cut-off of five were retained as these meshes had a smaller number of triangles making them computationally more efficient. Meshes with a cut-off value of five were present in the top model set for each dispersal kernel, in combination with all possible inner and outer domain values (Table G1,Table I1). The three meshes selected used similar values, with cut-off set to 5m, inner domains of 75m or 150m and outer domains of 400m or 800m, meaning each mesh contained similar numbers of triangles ranging from 10721 to 11817 (Table I1, Figure I1).

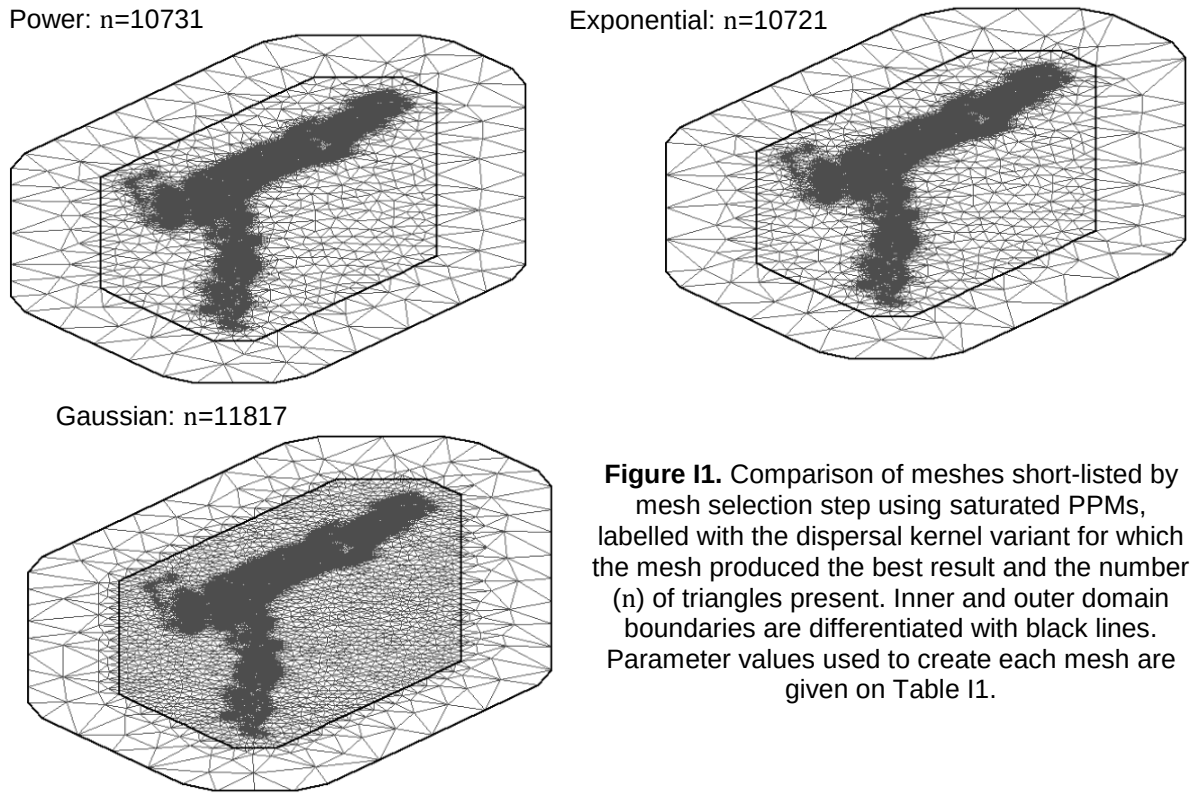

Figure I1. Comparison of meshes short-listed by mesh selection step using saturated PPMs, labelled with the dispersal kernel variant for which the mesh produced the best result and the number (n) of triangles present. Inner and outer domain boundaries are differentiated with black lines. Parameter values used to create each mesh are given on Table I1.

Table I1. Mesh parameter values (m) returning the top model set per force of infection covariate created using a dispersal kernel parameterised as δ=20m and a power (h=0.5), exponential (h=1) or Gaussian (h=2) shape. Model DICs are given where the combination of mesh cut-off values and maximum triangle edge lengths in the inner and outer domains resulted in a top model for each kernel; the best DIC for each is highlighted in bold.

Cut-off (m)	Maximum inner edge length (m)	Maximum outer edge length (m)	Dispersal kernel (δ=20m)		
			Power	Exponential	Gaussian
5	50	100	10619.16	10624.21	10634.30
5	50	200	10619.17	10624.22	10634.40
5	50	400	10619.16	10624.72	10634.30
5	50	800	10619.16	10624.58	10634.42
5	75	100	10618.87	10623.78	10633.94
5	75	200	10618.87	10623.87	10633.94
5	75	400	10618.73	10623.83	10633.94
5	75	800	10618.70	10624.20	**10633.84**
5	150	200	10618.83	10624.24	10633.94
5	150	400	**10618.57**	10625.02	10633.95
5	150	800	10618.75	**10623.69**	10633.94
5	200	400	10618.73	10623.79	10634.03
5	200	800	10618.63	10623.90	10634.02
5	500	800	10618.70	10623.80	10634.03

The cut-off value precipitated the largest change in DIC across all models (F. Donald, data not shown). To check that using the force of infection covariate used to select optimal mesh values would not bias inferences for the additional abiotic and biotic covariates, the saturated PPMs including alternative force of infection covariates were re-run using meshes parameterised using each cut-off value listed on Table G1. The maximum inner and outer triangle edge length values were kept the same as the best performing mesh with each alternative force of infection (Table I1). Covariate responses differed depending on the dispersal kernel used in the model but the impact of changing the mesh cut-off value was replicated across all models irrespective of the force of infection parameterisation (Figures I2-I4). The posterior estimates remained stable across all covariates with cut-off values of 2-10m, while cut-off values of 50-75m altered the mean and confidence intervals of all covariates but never changed the strength or direction of the response in a way that would lead to a different interpretation of the relationship (Figures I2-I4).

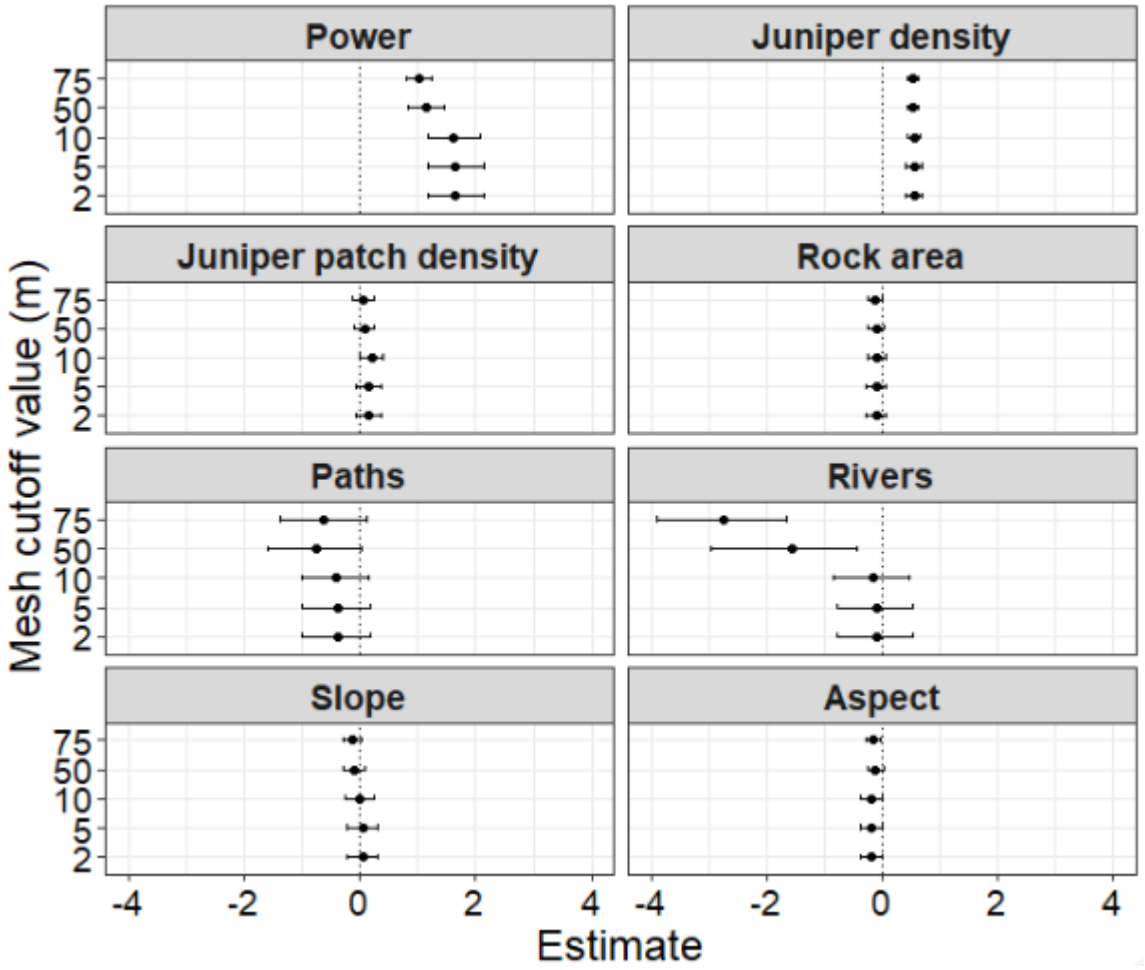

Figure I2. Comparison of posterior estimates (mean, 2.5 % and 97.5 % quantiles) obtained for each covariate used in a PPM including a spatial mesh parameterised with different cut-off values (m). The PPM included force of infection defined using a power dispersal kernel (δ=20m, h=0.5); the maximum triangle edge lengths were set as inner=150m and outer=400m.

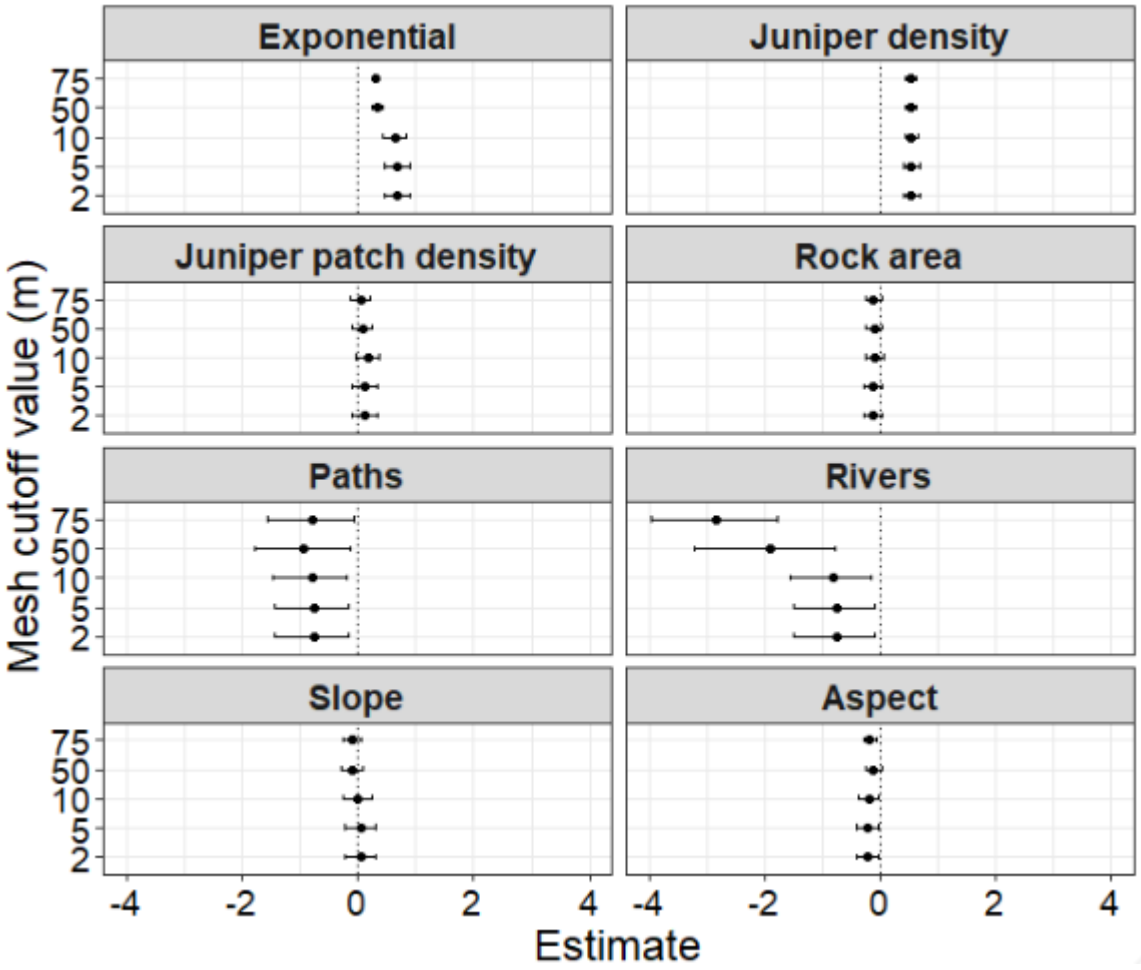

Figure I3. Comparison of posterior estimates (mean, 2.5% and 97.5% quantiles) obtained for each covariate used in a PPM including a spatial mesh parameterised with different cut-off values (m). The PPM included force of infection derived using an exponential dispersal kernel (δ=20m, h=1); the maximum triangle edge lengths were set as inner=150m and outer=800m.

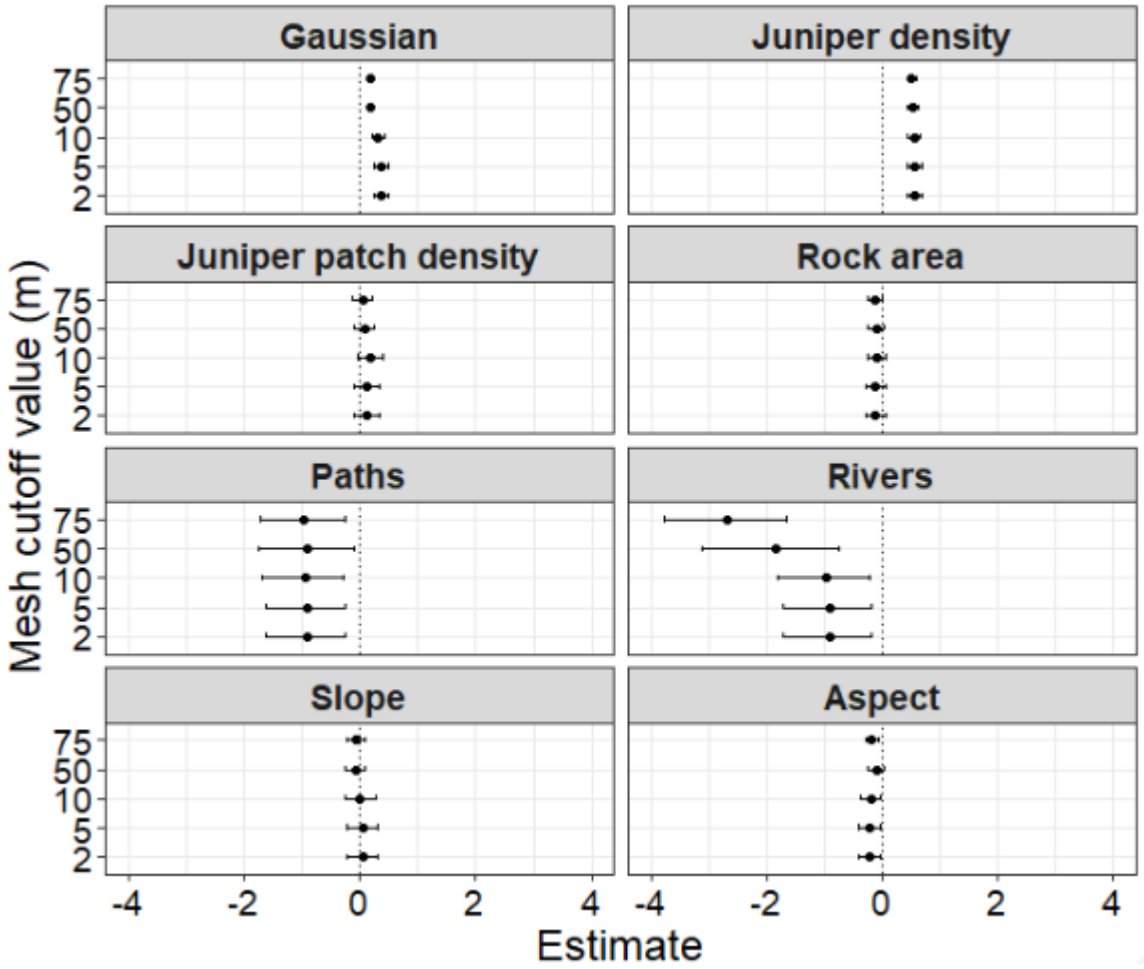

Figure I4. Comparison of posterior estimates (mean, 2.5 % and 97.5 % quantiles) obtained for each covariate used in a PPM including a spatial mesh parameterised with different cut-off values (m). The PPM included force of infection derived using a Gaussian dispersal kernel (δ=20m, h=2); the maximum triangle edge lengths were set as inner=75m and outer=800m.

I.1.2 Selecting optimal parameters to calculate force of infection

The choice of dispersal kernel used to calculate force of infection was critical to model performance as DICs ranged considerably with the 21 kernels tested, from 10621.09 (the best model) to 10640.92. At all values of h, DICs converged on a best scale (δ) value and subsequently decreased, confirming an appropriate value range was tested (Figure I5).

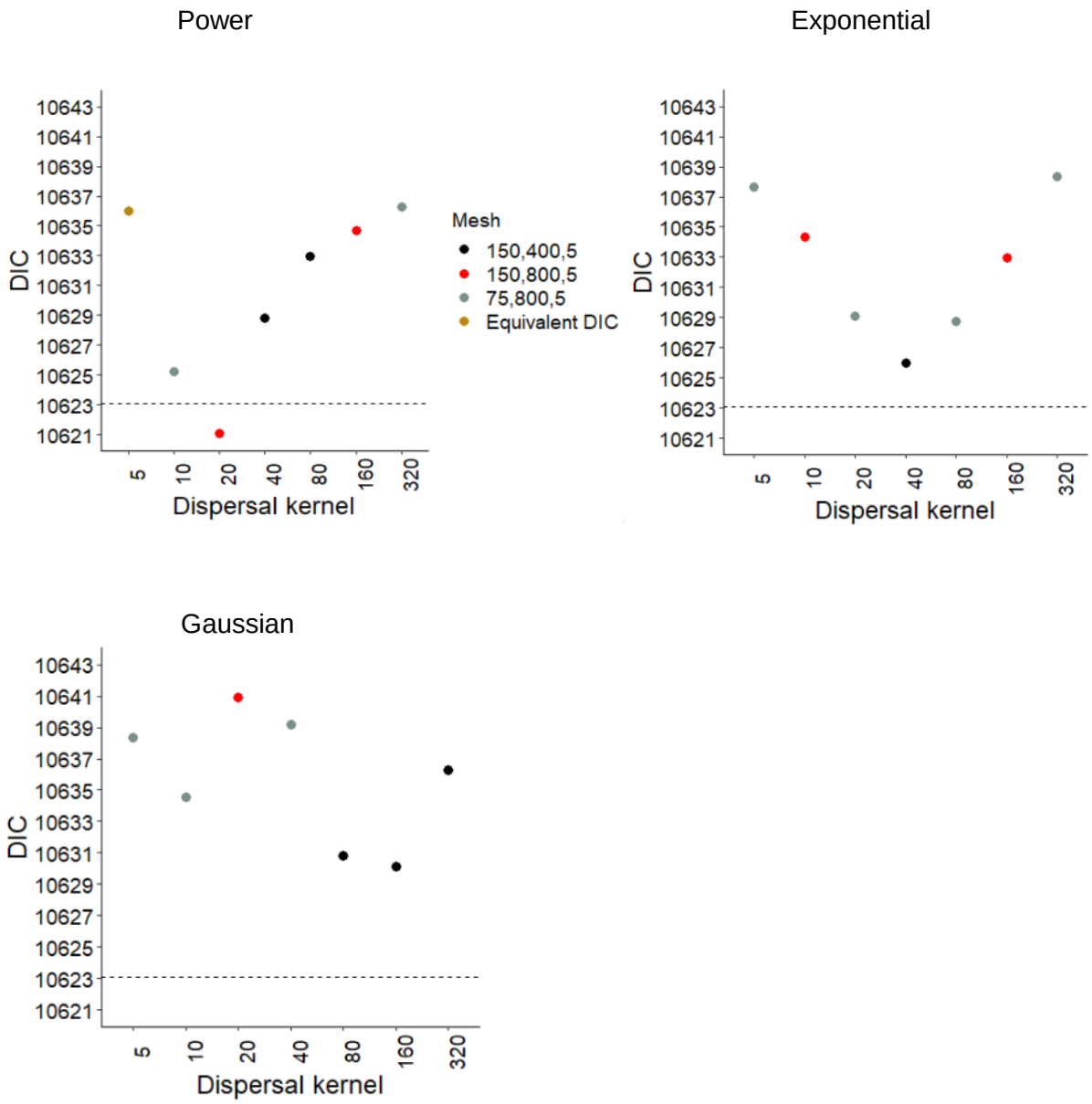

Figure I5. PPM DICs returned for force of infection covariates, each derived using a dispersal kernel variant grouped by the shape parameter (h): power (h=0.5), exponential (h=1) or Gaussian (h=2), and arranged in order of increasing scale (δ, m). All kernels were tested with each of the three short-listed spatial meshes. The mesh yielding the best model is shown using the colour legend labelled according to the maximum triangle edge lengths (m) in the inner and outer domains, and the cut-off value (m). The dashed line marks the upper threshold for the top model set (DIC within two units of the best DIC).

One best model was found, fit with force of infection parameterised using a power kernel (h=0.5, δ=20m) and a mesh created using cut-off=5m, inner domain=150m and outer domain=800m (Figure I6). As there were no equivalent models within 2 DIC units of the best model, this mesh and force of infection covariate were used in all following 10m model selection steps.

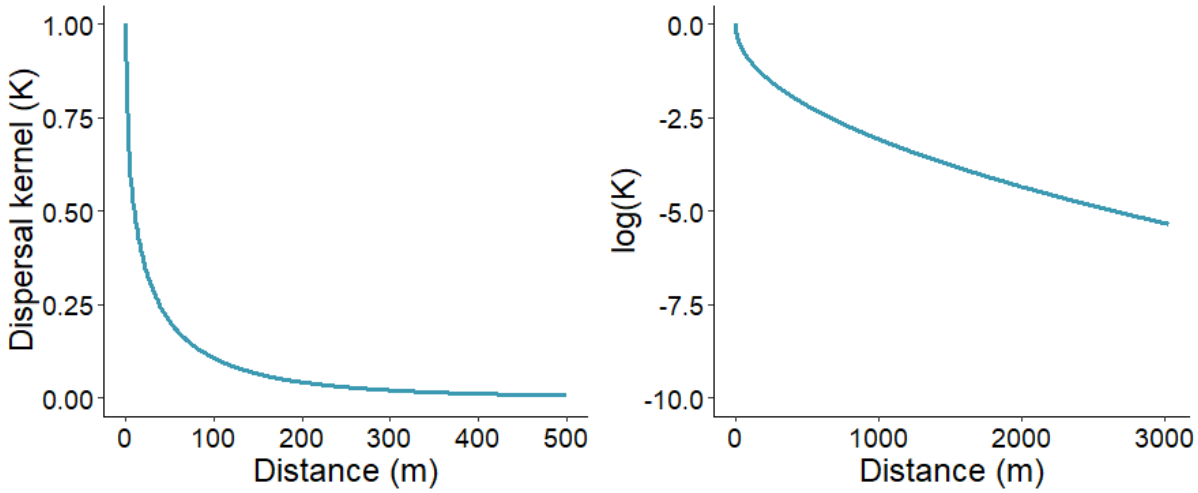

Figure I6. The exponential power dispersal kernel (h=0.5, δ=20m) identified as the best predictor of *P. austrocedri* effective dispersal from 2012/13 to 2016/17. The change in predicted dispersal frequencies with distance (m) is plotted to the first 500m on a normal scale (L) and on a log scale (R) to show the behaviour in the tail.

I.1.3 Covariate selection

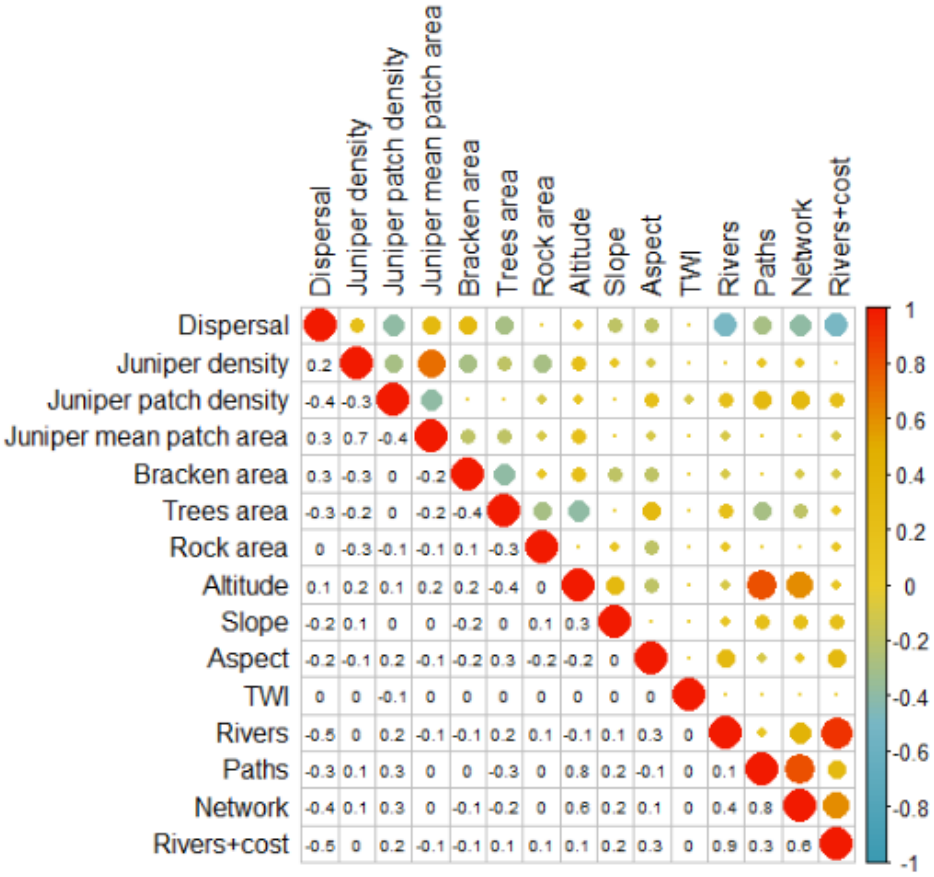

Figure I7. Correlation plot between all covariates measured across 10x10m grid cells containing ≥1m2 juniper. Pearson r^2 values are shown using a colour scale and text to 1 decimal place. "Dispersal" refers to the dispersal kernel (h=0.5, δ=20m) shortlisted in I.1.2. Descriptions and units of measurement for the remaining covariates are given on Table 9 in the main text.

Correlations between all covariates used in the 10m resolution PPM models were explored using Pearson r^2 values (Figure I7). Collinearity (r^2 >0.7) was detected between paths and altitude, paths and network, rivers, and rivers+cost so these covariate pairs were not included in the same models (Figure I7). To reduce the number of models run overall, covariates were first shortlisted by determining the strongest predictors within the juniper connectivity, hydrology and topography categories, the results of which are detailed below. Seventeen of sixty-two models run with juniper connectivity covariates comprised the top model set (Table I2). Force of infection was present and showed the strongest response (BCI do not bridge zero) in all top models (Table I2). Of the juniper connectivity covariates, only juniper mean patch area occurred in fewer than 50% of the top models but of the

remaining covariates (juniper patch density, areas of bracken, rock and trees) only area of bracken had >50% strong (BCI ≥ 0.90) responses with symptom intensity of cells colonised in 2016/17 (Table I2).

Table I2. Importance of juniper connectivity covariates in predicting *P. austrocedri* symptom intensity in cells colonised in 2016/17. The top model set contained 17, of a possible 62, models. The % column details the % of top models containing each covariate; the remaining columns contain % covariate relationships found in BCI strength categories ranging from <0.8 (interpreted as showing no relationship) to 1.00 i.e., the BCI do not bridge zero (strongest relationship). Covariates are ordered from the largest % present in the top model set followed by the % of strongest relationships.

Covariate	%	<0.8	0.80–0.89	0.90–0.94	0.95–0.99	1.00
Force of infection	100	0	0	0	0	100
Bracken area (m^2)	76	15	15	0	39	31
Rock area (m^2)	65	0	64	0	36	0
Trees area (m^2)	59	60	0	0	40	0
Juniper patch density	59	0	60	40	0	0
Juniper mean patch area (m^2)	47	0	0	0	100	0

Force of infection was again present in all top models run with hydrological covariates, showing the strongest responses (BCI do not bridge zero) (Table I3). The hydrological covariates, however, showed very weak relationships with all five covariates present in fewer than 50% of the 15 top models out of a possible 34 (Table I3).

Table I3. Importance of hydrological covariates in predicting *P. austrocedri* symptom intensity in cells colonised in 2016/17. Of 34 models with different covariate combinations, 15 were present in the top set.

Covariate	%	<0.8	0.80–0.89	0.90–0.94	0.95–0.99	1.00
Force of infection	100	0	0	0	0	100
TWI	47	0	0	100	0	0
Rivers (m)	40	100	0	0	0	0
Network (m)	33	20	80	0	0	0
Paths (m)	33	100	0	0	0	0
Rivers+cost	27	100	0	0	0	0

By contrast, all three topographic covariates were present in at least two of four top models (of a possible 15 models) with aspect showing very strong (BCI 0.95-0.99) relationships and 75% of models containing altitude showing the strongest possible response (BCI do not bridge zero) (Table I4). Force of infection was again present in all top models and the BCI do not bridge zero in all instances (Table I4).

Table I4. Importance of topographic covariates in predicting *P. austrocedri* symptom intensity in cells colonised in 2016/17. Four of a possible 15 models were present in the top model set.

Covariate	%	<0.8	0.80–0.89	0.90–0.94	0.95–0.99	1.00
Force of infection	100	0	0	0	0	100
Altitude (m)	57	0	0	0	25	75
Aspect (°)	57	0	0	50	50	0
Slope (°)	57	100	0	0	0	0

The shortlist of covariates for the final model selection, therefore, contained only area of bracken, aspect, altitude, and force of infection. A full subsets selection was carried out and of the 15 possible models, four were found in the top set (Figure I8). All four top models contained force of infection and area of bracken, all of which showed the strongest possible response (BCI do not bridge zero) (Table I5, Figure I8). In addition, two top models contained altitude and two contained aspect, with either very strong (BCI 0.95-0.99) or the strongest possible (BCI do not bridge zero) responses (Table I5, Figure I8).

Table I5. Importance of covariates shortlisted for the final model selection in predicting *P. austrocedri* symptom intensity in colonised cells in 2016/17. The top model set contained four of a possible 15 models and all models contained the spatial mesh and juniper density. The % column details the % of top models containing each covariate; the remaining columns contain % covariate relationships found in BCI strength categories ranging from <0.8 (interpreted as showing no relationship) to 1.00 i.e., the BCI do not bridge zero (strongest relationship). Covariates are ordered from the largest % present in the top model set followed by the % of strongest relationships.

Covariate	%	<0.8	0.80–0.89	0.90–0.94	0.95–0.99	1.00
Force of infection	100	0	0	0	0	100
Bracken area (m^2)	100	0	0	0	0	100
Altitude (m)	50	0	0	0	50	50
Aspect (°)	50	0	0	0	50	50

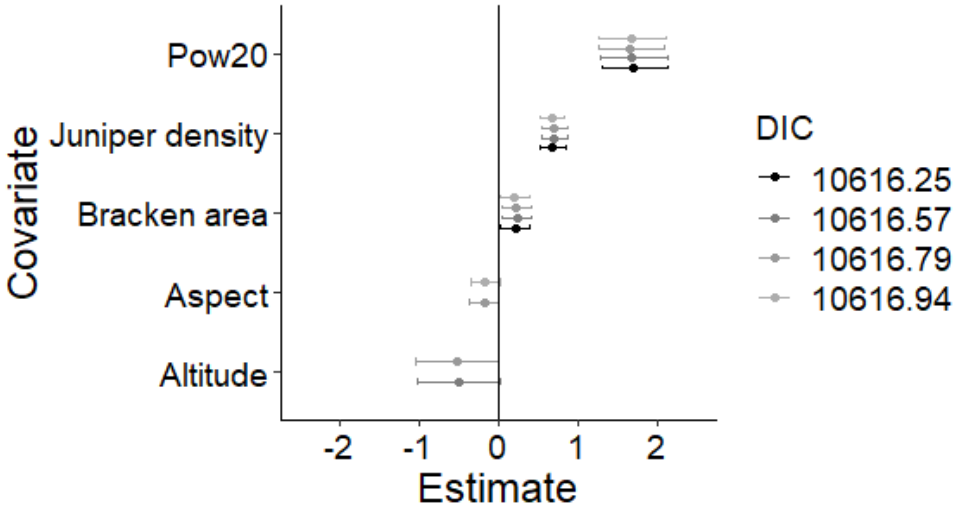

Figure I8. Top model set obtained at 10m resolution showing 95% Bayesian credible intervals (0.025 and 0.975 quantiles of the posterior distribution) for covariate responses found in the best model (DIC=10616.25, shown in black) and three equivalent models shown in grey. All models contained force of infection derived using the power kernel variant h=0.5, δ=20m ("Pow20"). The remaining covariates are ordered according to the number of times they were present in the top models. Model intercepts are not shown but, in each model, the intercept had a mean value of -10.8 (to 1 decimal place) and a standard deviation of 0.38.

I.1.4 Spatial random field of the 10m PPM

The spatial random field of the best model was largely smooth and showed good differentiation between grid cells showing the spatial mesh was invoked to address spatial autocorrelation in discrete areas within the mapped population. Higher values appeared to correspond with areas of higher symptom intensity in 2016/17 and lower values corresponded to areas of lower symptom intensity but high juniper density (Figure I9).

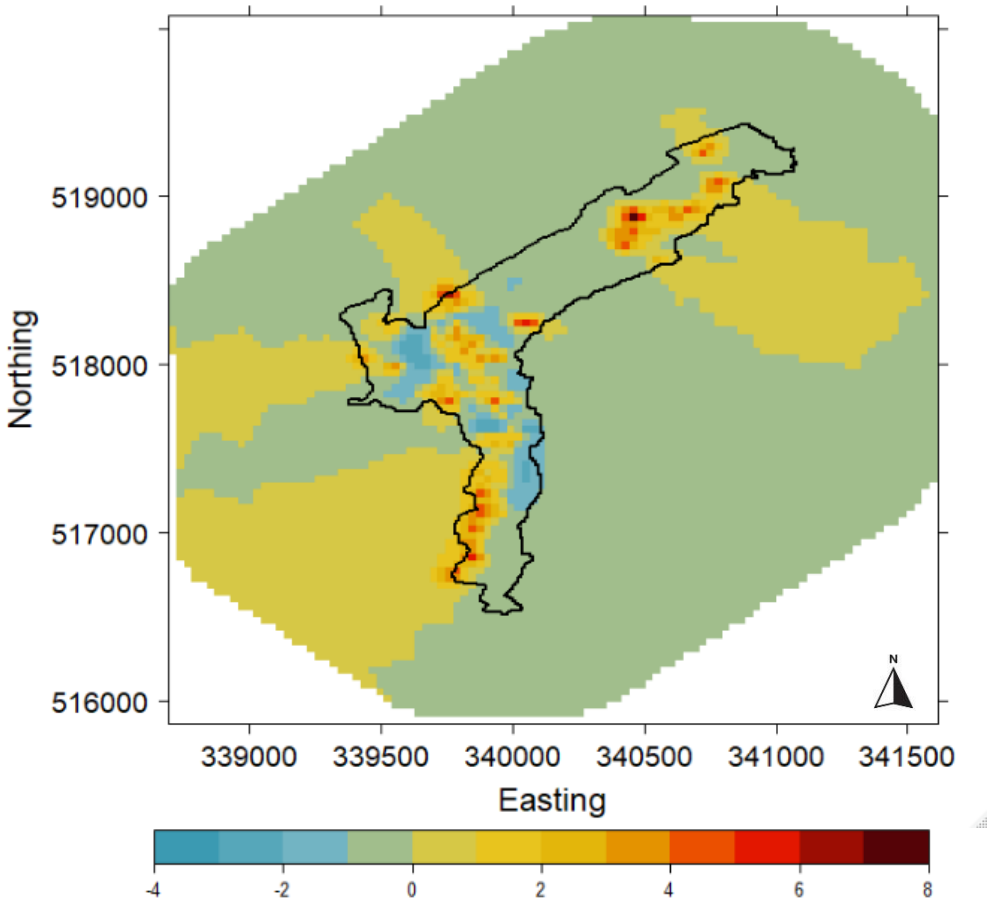

Figure I9. Spatial random field of the best model mapped to the extent of the spatial mesh with values mapped according to the colour scale, ranging from –2.6 to 7.2. The boundary of the 10x10m grid cells used in the model is outlined in black.

I.1.5 Posterior distributions derived from the best PPM

The posterior distributions obtained from the best model for the intercept, juniper density, force of infection and area of bracken were all normal, demonstrating model convergence and acceptable parameter estimations (Figure I10).

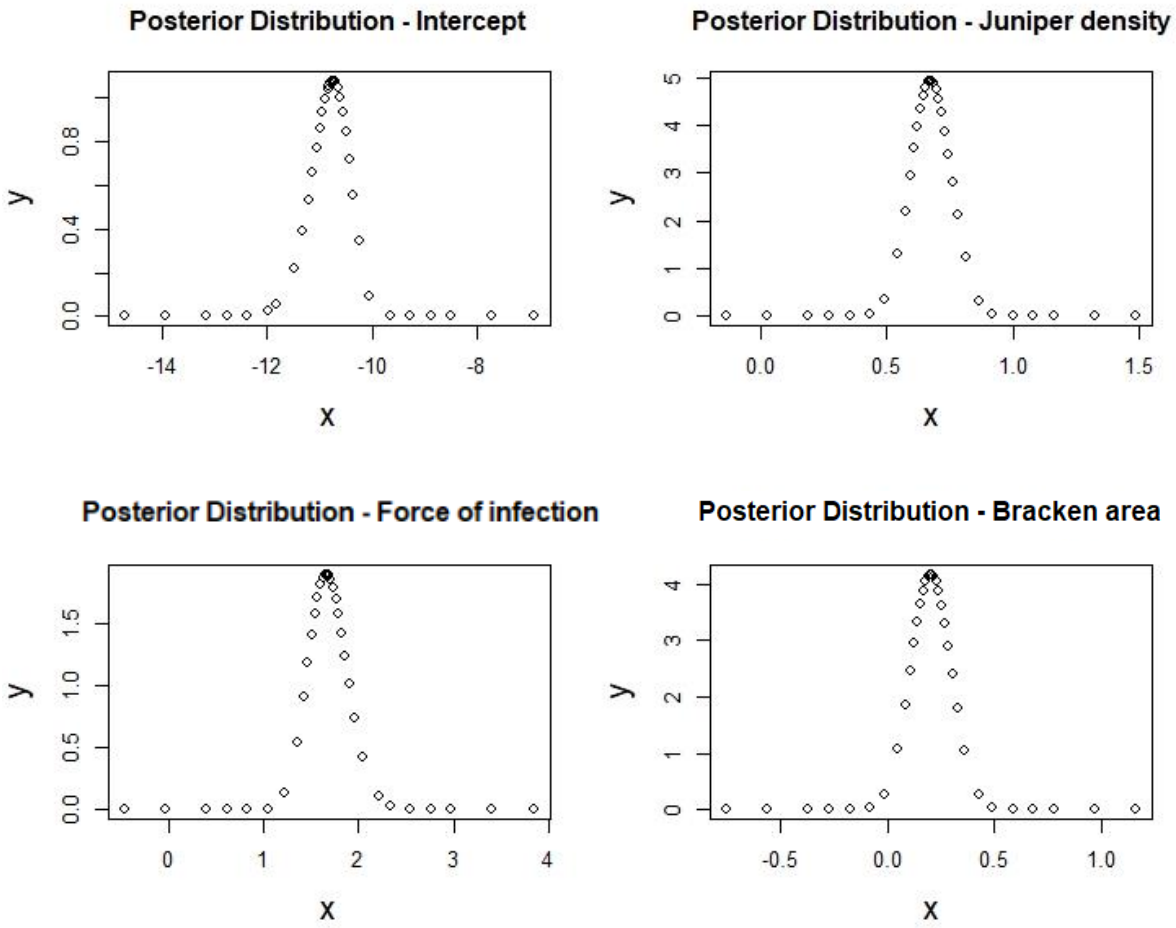

Figure I10. Posterior distributions returned by the best 10m PPM for the intercept, juniper density, area of bracken and force of infection characterised using the dispersal kernel h=0.5, δ=20m.

I.1.6 Validation of the best 10m PPM

The predictions of symptom intensity manually calculated from estimates returned by the best model for the intercept and fixed effects tended towards overprediction compared to the observed values of symptom intensity (Figure I11).

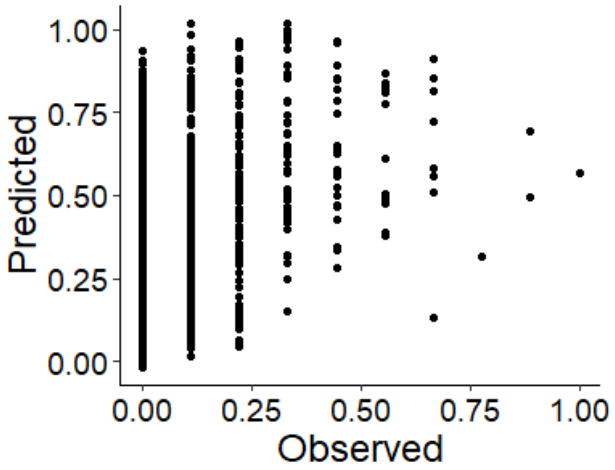

Figure I11. Comparison of observed and re-scaled predicted symptom intensity calculated using estimates of beta returned in the best 10m PPM for the intercept, juniper density, area of bracken and force of infection characterised using the dispersal kernel h=0.5, δ=20m.

I.2 Point Process Modelling of 25m resolution symptomatic host density

I.2.1 Calibration of the spatial mesh

At 25m resolution, the top model set for each force of infection covariate derived using a dispersal kernel (δ=20m, h=0.5, 1 or 2) contained the same 14 meshes that used all possible combinations of maximum triangle edge lengths with cut-off=10m (Table I6). There was little variation in DIC between alternative force of infection covariates; the best model using the power dispersal kernel (h=0.5) was 11796.85 compared to 11798.43 with the exponential (h=1), and 11799.27 with the Gaussian (h=2) kernel (Table I6). All models fit with a spatial mesh parameterised as cut-off=10m and inner maximum triangle edge length=50m returned the same DIC irrespective of the outer maximum triangle edge length and force of infection (Table I6). One best mesh, using 800m as the maximum triangle edge length in the outer domain, was therefore identified as the best performing mesh with the smallest number of triangles (5483) for computational efficiency (Figure I12).

Table I6. Mesh parameter values (m) returning the top model set per force of infection covariate. Each covariate was created using a dispersal kernel (δ=20m, h=0.5, 1 or 2) and is labelled as power, exponential and Gaussian respectively. Model DICs are given where the combination of mesh cut-off values and maximum triangle edge lengths in the inner and outer domains resulted in a top model for each alternative force of infection covariate used and the best DIC for each is highlighted in bold.

Cut-off (m)	Maximum inner edge length (m)	Maximum outer edge length (m)	Dispersal kernel (δ=20m)		
			Power	Exponential	Gaussian
10	50	100	**11796.85**	**11798.43**	**11799.27**
10	50	200	**11796.85**	**11798.43**	**11799.27**
10	50	400	**11796.85**	**11798.43**	**11799.27**
10	50	800	**11796.85**	**11798.43**	**11799.27**
10	75	100	11797.31	11799.04	11799.83
10	75	200	11797.32	11799.03	11799.83
10	75	400	11797.31	11799.04	11799.83
10	75	800	11797.31	11799.04	11799.83
10	150	200	11797.19	11798.82	11799.61
10	150	400	11797.19	11798.83	11799.61
10	150	800	11797.19	11798.83	11799.61
10	200	400	11797.16	11798.75	11799.54
10	200	800	11797.16	11798.75	11799.54
10	500	800	11797.16	11798.74	11799.51

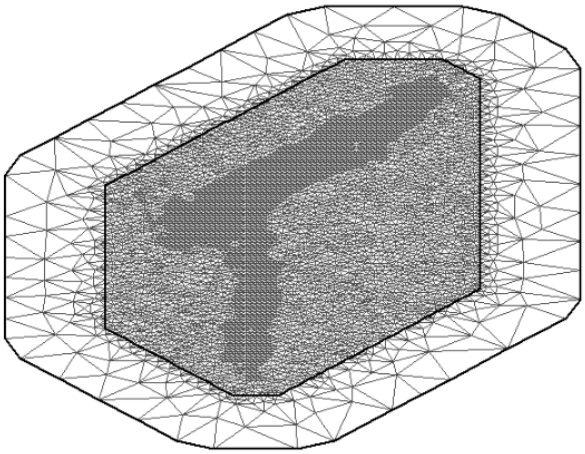

Figure I12. Mesh yielding the best 25m PPMs fit with force of infection covariates created using a power (h=0.5), exponential (h=1) or Gaussian (h=2) dispersal kernel variant (δ=20m), parameterised using the values given on Table I6. Inner and outer domain boundaries are differentiated with black lines.

Covariate responses were robust to different cut-off values when meshes were created using the best identified inner and outer domain maximum triangle edge length values found for each force of infection covariate (Figures I13-I15). The posterior estimates obtained from models containing the same force of infection covariate and meshes using cut-off values of 10-25m were largely the same, while cut-off values of 50m or 75m and 100m changed the mean and confidence intervals of covariate responses but never the direction of the relationship. The shortlisted mesh (Figure I12) was used in all following 25m model selection steps.

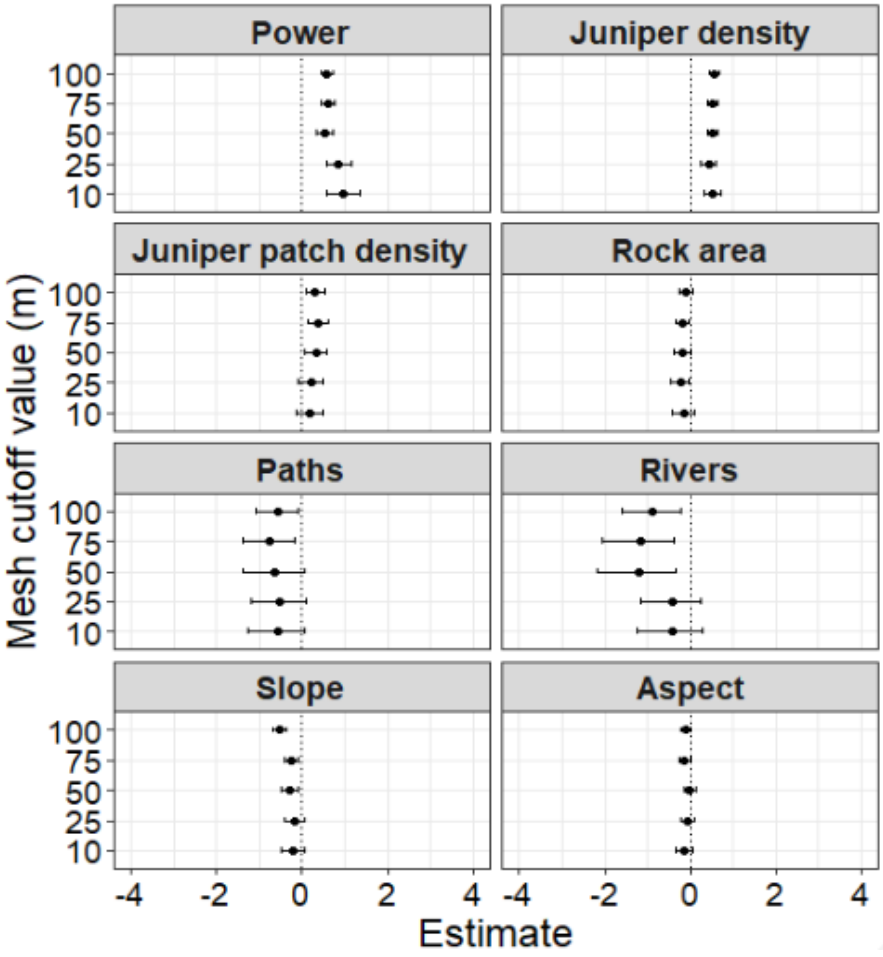

Figure I13. Comparison of posterior estimates (mean, 2.5 % and 97.5 % quantiles) obtained for each covariate used in a PPM including a spatial mesh parameterised with different cut-off values (m). The PPM included force of infection derived using a power dispersal kernel (δ=20m, h=0.5); the maximum triangle edge lengths were set as inner=50m and outer=800m.

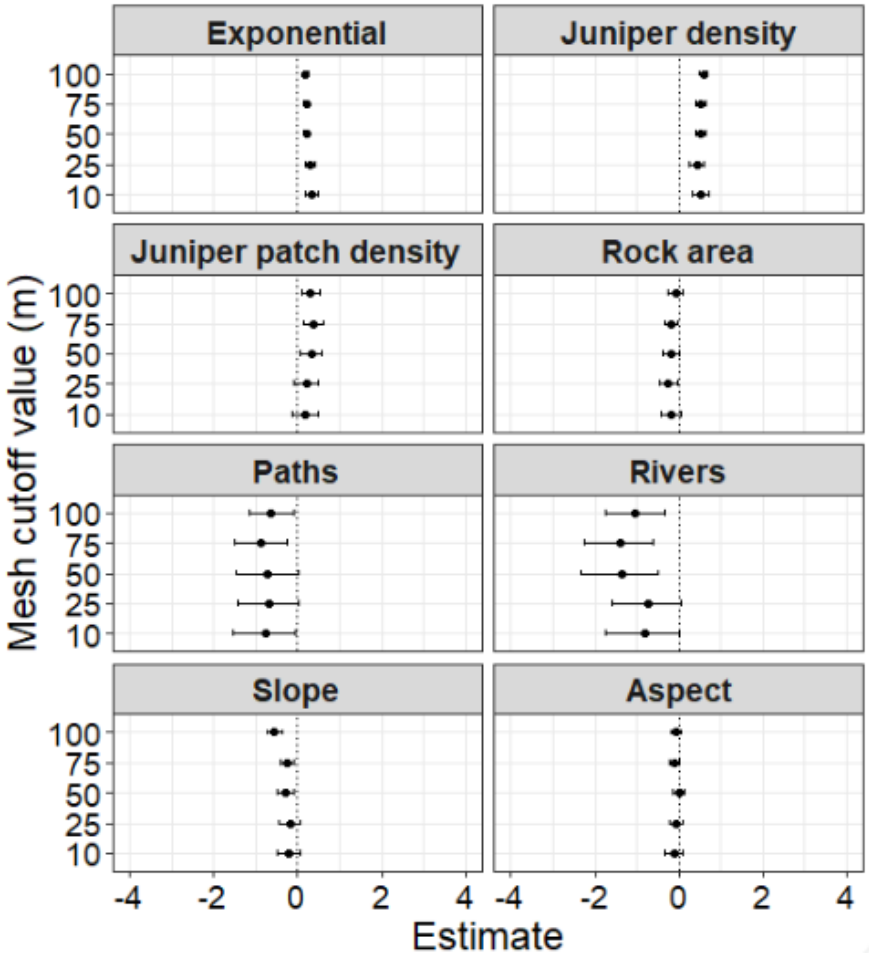

Figure I14. Comparison of posterior estimates (mean, 2.5% and 97.5% quantiles) obtained for each covariate used in a PPM including a spatial mesh parameterised with different cut-off values (m). The PPM included force of infection derived using an exponential dispersal kernel (δ=20m, h=1); the maximum triangle edge lengths were set as inner=50m and outer=800m.

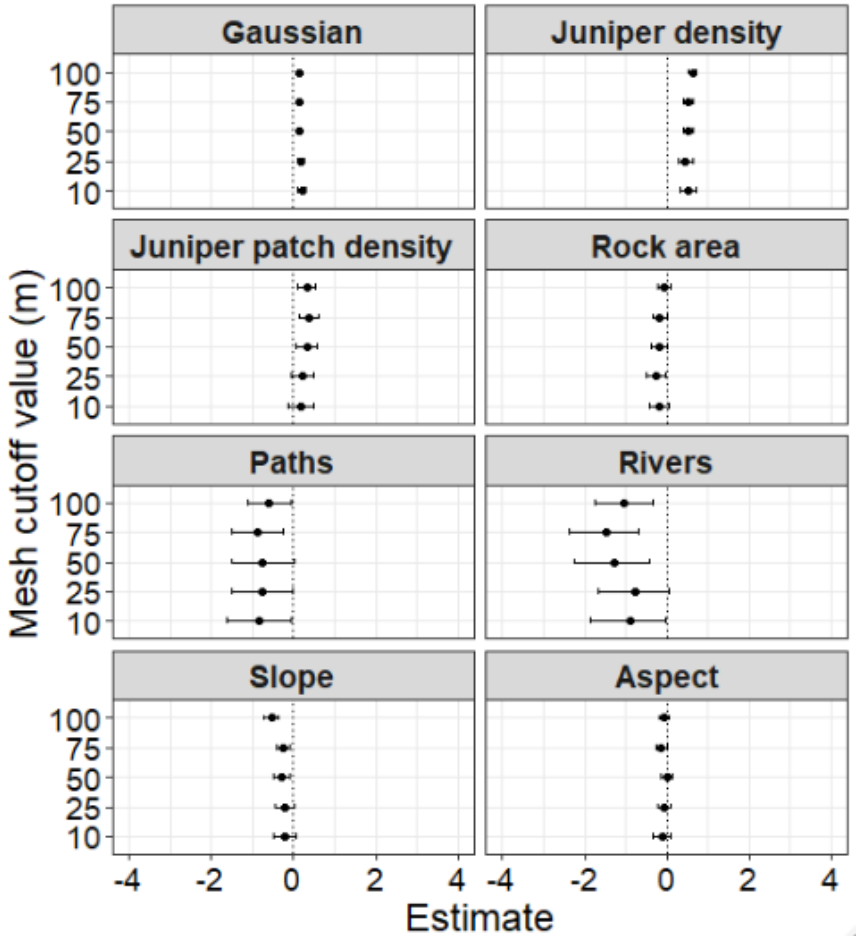

Figure I15. Comparison of posterior estimates (mean, 2.5% and 97.5% quantiles) obtained for each covariate used in a PPM including a spatial mesh parameterised with different cut-off values (m). The PPM included force of infection derived using a Gaussian dispersal kernel (δ=20m, h=2); the maximum triangle edge lengths were set as inner=50m and outer=800m.

I.2.2 Selection of the best fitting dispersal kernel variant

The DICs obtained from PPMs using 24 dispersal kernels paired with each short-listed mesh showed a short range from 11792.29 (the best model) to 11799.24. The DICs of all force of infection covariates for each dispersal kernel shape (power: h=0.5, exponential: h=1, or Gaussian: h=2) converged, showing an adequate range of scale values was tested (Figure I16). Eight force of infection covariates were present in the top model set, two derived from power and three from both Gaussian and exponential dispersal kernels (Figure I16). The best model was found using an exponential kernel with δ=80m; the top model using force of infection calculated with a Gaussian kernel was 11793.35 with δ=160m and the top model including force of infection calculated with a power kernel was 1193.98 with δ=40m (Figure I16).

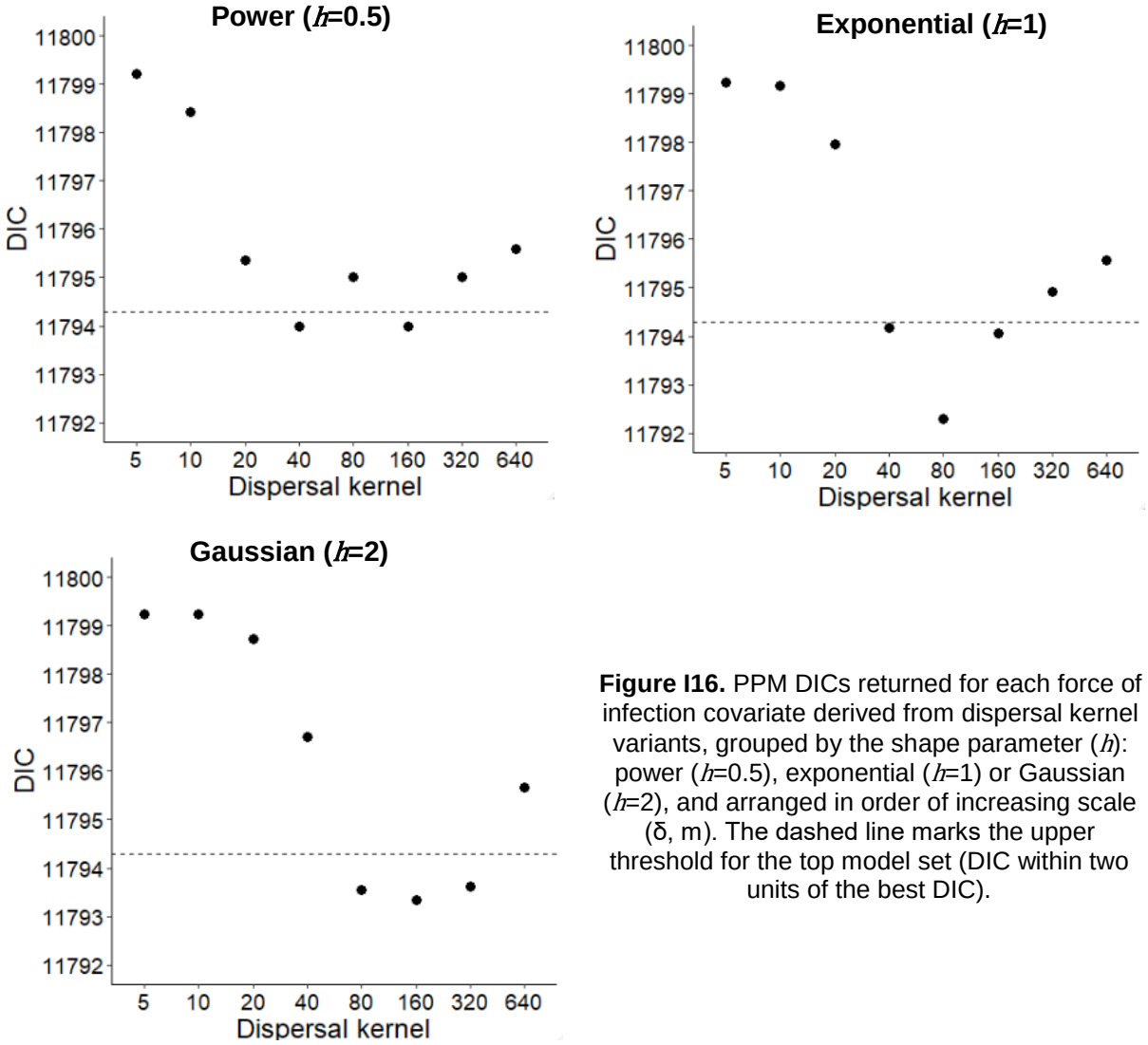

Figure I16. PPM DICs returned for each force of infection covariate derived from dispersal kernel variants, grouped by the shape parameter (h): power (h=0.5), exponential (h=1) or Gaussian (h=2), and arranged in order of increasing scale (δ, m). The dashed line marks the upper threshold for the top model set (DIC within two units of the best DIC).

The eight shortlisted kernel variants describe quite different dispersal probabilities that tend towards zero after only ~200m with the smallest exponential (h=1, δ=40m) and Gaussian kernels (h=2, δ=80m) to more than 3000m with the largest exponential kernel (h=0.5, δ=160m) and varying frequencies of long-distance dispersal events (Figure I17).

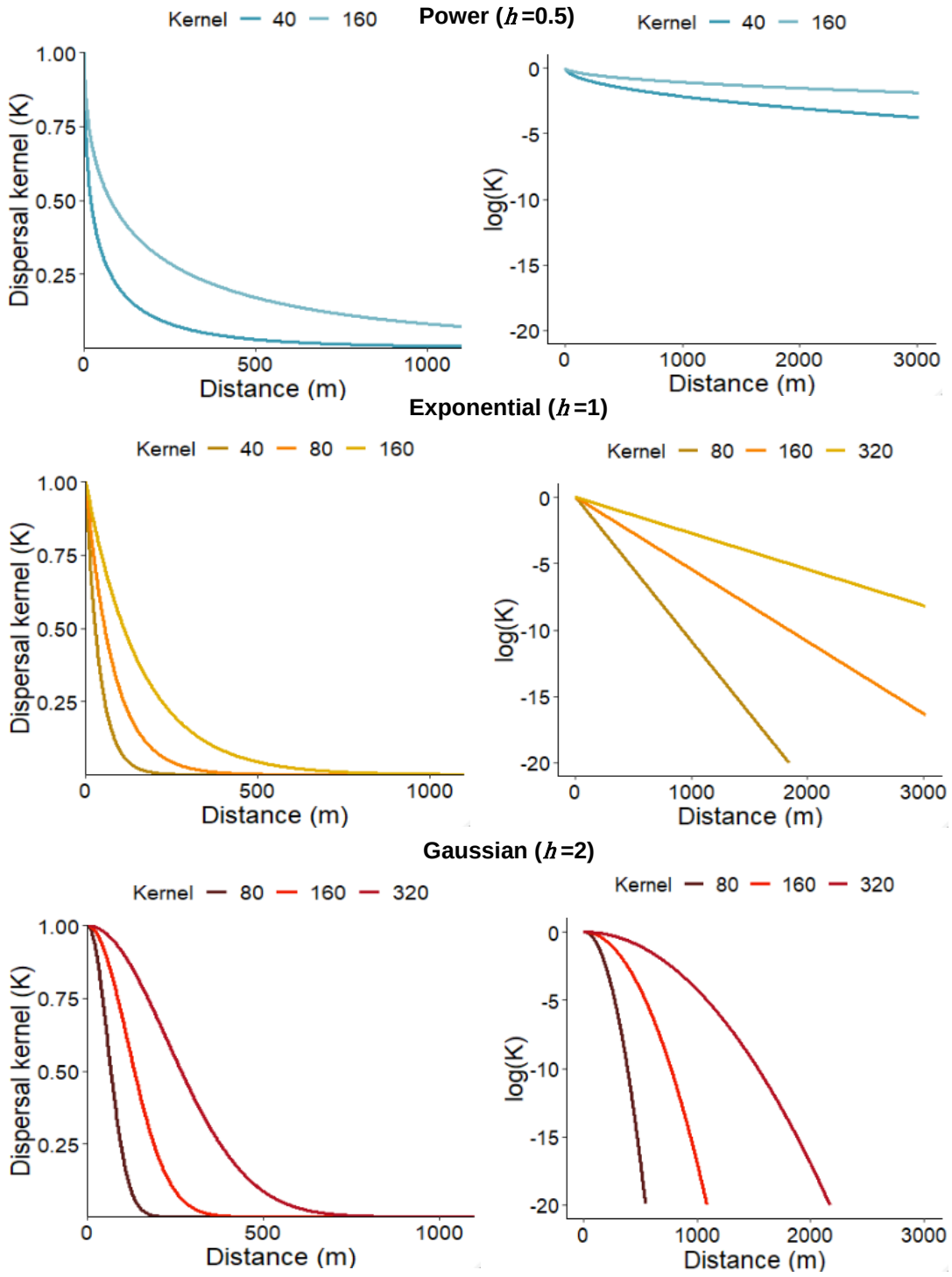

Figure I17. Comparison of the eight equivalent dispersal kernels identified using model selection, showing the change in predicted dispersal frequencies with distance (m) grouped according to the shape parameter (h) and plotted on a normal (L) and log (R) scale to i) compare relative dispersal rates within the first 1000m and ii) compare differences in the behaviour of the tail.

I.2.3 Covariate selection

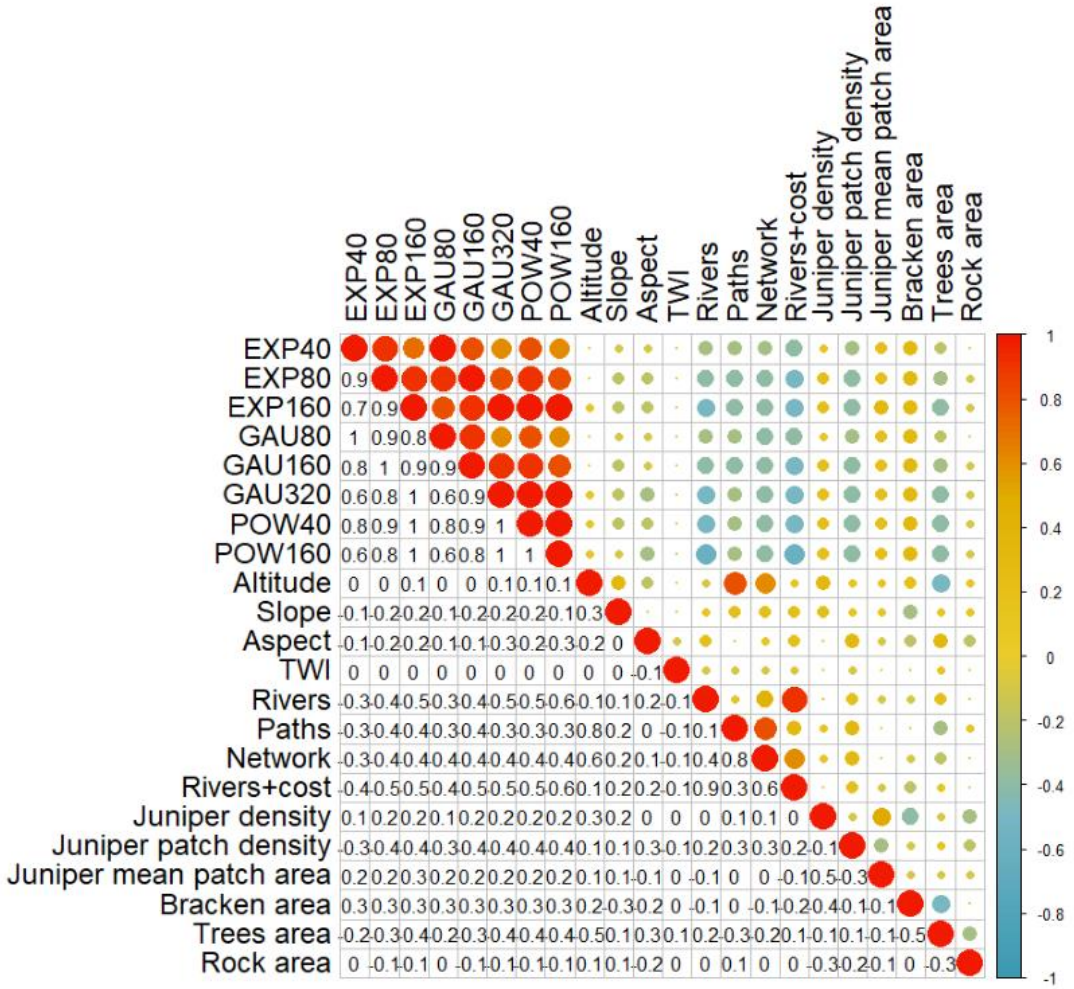

Figure I18. Correlation plot between all covariates measured across 25x25m grid cells containing ≥1m^2 juniper. Pearson r^2 values are shown using a colour scale and text to 1 decimal place. The shortlisted dispersal kernels are labelled with "POW" (h=0.5), "EXP" (h=1) or "GAU" (h=2) and the scale value (m). Outstanding covariate descriptions and units of measurement are given on Table 9.

Collinearity was explored using Pearson r^2 values between all covariates used in the 25m resolution PPM models (Figure I18). Values of r^2 ≥0.7 were only detected between three covariate pairs, namely rivers and rivers+cost, network and paths, and paths and altitude, which were prevented from occurring in the same models (Figure I18). All eight force of infection covariates were included in the model selection within each covariate group and were selected using the same criteria (present in ≥50% of top models and ≥50% of responses BCI ≥ 0.90 above or below zero) but because only one force of infection covariate was included per model, the number of times it could appear in the top model set differed from the remaining covariates resulting in different threshold values (detailed in captions for Tables I7-I9).

Combinations of juniper connectivity and force of infection covariates were tested in 279 models, of which 46 were found in the top model set (Table I7). Juniper mean patch area and juniper patch density were only found in 26% of top models and while the three covariates describing alternative feature classes to juniper (areas of bracken, rock and trees) were all present in more than 50% of the top models, only area of rock showed very strong responses (79% BC ≥ 0.90) (Table I7). All force of infection covariates calculated using shortlisted exponential (h=1, δ=40, 80 or 160m) or Gaussian (h=2, δ=80,160 or 320m) kernels were present in the top model set, and where present showed the strongest response (BCI do not bridge zero) but only one force of infection covariate, calculated using an exponential kernel (h=1, δ=80m), was found in ≥50% top models (Table I7).

Table I7. Importance of juniper connectivity covariates in predicting *P. austrocedri* symptom intensity in cells colonised in 2016/17 found in the top model set (46/279) with and without shortlisted force of infection covariates (labelled as shape parameter "POW" h=0.5, "EXP" h=1, or "GAU" h=2 and the scale parameter δ in m). All models included the spatial mesh and juniper density. The percentage (%) of top models containing each covariate is detailed alongside the % model responses in BCI strength categories. Force of infection covariates are grouped together above connectivity covariates; covariates are ordered within groups as largest % present in the top model set followed by response strength. The maximum % of top models containing any force of infection covariate was 67% so ≥34% must be present in top models for forward selection.

Covariate	%	<0.8	0.80–0.89	0.90–0.94	0.95–0.99	1.00
EXP80	50	0	0	0	0	100
GAU160	22	0	0	0	0	100
GAU80	17	0	0	0	0	100
GAU320	4	0	0	0	0	100
EXP160	4	0	0	0	0	100
EXP40	2	0	0	0	0	100
Rock area (m^2)	72	0	21	67	12	0
Trees area (m^2)	57	100	0	0	0	0
Bracken area (m^2)	52	92	8	0	0	0
Juniper patch density	26	33	67	0	0	0
Juniper mean patch area (m^2)	26	0	0	0	100	0

Combinations of hydrological covariates resulted in 40 of 153 top models. Only network and force of infection calculated using the same exponential kernel as shortlisted in the juniper connectivity selection (h=1, δ=80m) were present in ≥50% top models (Table I8). All of the force of infection responses were very strong (BCI do not bridge zero), as were 40% of the network responses while a further 40% were strong (BCI 0.90-0.99) (Table I8). None of the remaining covariates were present in a sufficient number of top models for further testing (Table I8).

Table I8. Top model set (40/153) of hydrological covariate combinations with and without eight shortlisted force of infection covariates. The percentage (%) of top models containing each covariate is detailed alongside the % of those models with responses in BCI strength categories. The maximum % of top models containing any force of infection covariate is 42% so ≥21% must be present in top models for forward selection.

Covariate	%	<0.8	0.80–0.89	0.90–0.94	0.95–0.99	1.00
EXP80	28	0	0	0	0	100
GAU80	15	0	0	0	0	100
GAU160	15	0	0	0	0	100
GAU320	12	0	0	0	0	100
EXP40	10	0	0	0	0	100
EXP160	10	0	0	0	0	100
POW40	8	0	0	0	0	100
POW160	3	0	0	0	0	100
Network (m)	88	0	20	11	29	40
Rivers (m)	40	100	0	0	0	100
Rivers+cost	33	100	0	0	0	100
TWI	33	0	46	54	0	0
Paths (m)	8	100	0	0	0	0

Aspect and altitude were found in 62% and 57% of the 21 top models returned by the topographic covariate selection from a possible 63 models (Table I9). However, only aspect showed sufficiently strong responses for the covariate shortlist with 100% responses present in BCI 0.90-0.99 categories (Table I9). Four of eight force of infection covariates were present in the top model set of which three were present in ≥50% top models and all responses were very strong (BCI do not bridge zero) (Table I9).

Table I9. Top model set (21/63) of topographic covariate combinations with and without shortlisted force of infection covariates. The percentage (%) of top models containing each covariate is detailed with the % of those models with responses in BCI strength categories. The maximum % of top models containing any force of infection covariate is 33% so ≥16.5% must be present in top models for forward selection.

Covariate	%	<0.8	0.80–0.89	0.90–0.94	0.95–0.99	1.00
EXP80	33	0	0	0	0	100
GAU160	33	0	0	0	0	100
GAU80	19	0	0	0	0	100
EXP160	14	0	0	0	0	100
Aspect (°)	62	0	0	54	46	0
Altitude (m)	57	8	50	17	25	0
Slope (°)	43	0	0	11	56	33

The final covariate selection tested all possible combinations of area of rock, aspect, and network with and without force of infection created using the 80m exponential kernel (h=1, δ=80m). Combinations of the above covariates that contained aspect were additionally run with force of infection covariates derived using Gaussian kernels (h=2, δ=80 or 160m). Of the 22 models tested, 11 were present in the top model set; aspect and network were present in 73% of those and rock area in 45% (Table I10, Figure I19). All three force of infection covariates were present in the top model set but the covariate derived using the exponential kernel was present in 64% of top models while the Gaussian derived covariates were each only present in 18% (Table I10). All force of infection covariates showed the strongest possible responses (BCI do not bridge zero) (Table I10, Figure I19). Of the remaining covariates, 100% responses were strong (BCI ≥0.9); network had the largest proportion of very strong responses as 25% of BCI responses do not bridge zero and 50% were categorised in BCI 0.95-0.99 (Table I10, Figure I19). Sixty percent of the area of rock covariate responses were very strong (BCI 0.95-0.99) as were 25% of the aspect responses (Table I10, Figure I19).

Table I10. Importance of covariates shortlisted for the final model selection in predicting *P. austrocedri* symptom intensity in cells colonised in 2016/17 found in the top model set (11/22). Force of infection covariates are labelled with the shape parameter "EXP" h=1, or "GAU" h=2 and the scale parameter (m). All models included the spatial mesh and juniper density. The percentage (%) of top models containing each covariate is detailed alongside the % of those model responses in BCI strength categories. Force of infection covariates are grouped together above abiotic covariates; covariates are ordered within groups as largest % present in the top model set followed by response strength.

Covariate	%	<0.8	0.80–0.89	0.90–0.94	0.95–0.99	1.00
EXP80	64	0	0	0	0	100
GAU80	18	0	0	0	0	100
GAU160	18	0	0	0	0	100
Aspect (°)	73	0	0	75	25	0
Network (m)	73	0	0	25	50	25
Rock area (m^2)	45	0	0	40	60	0

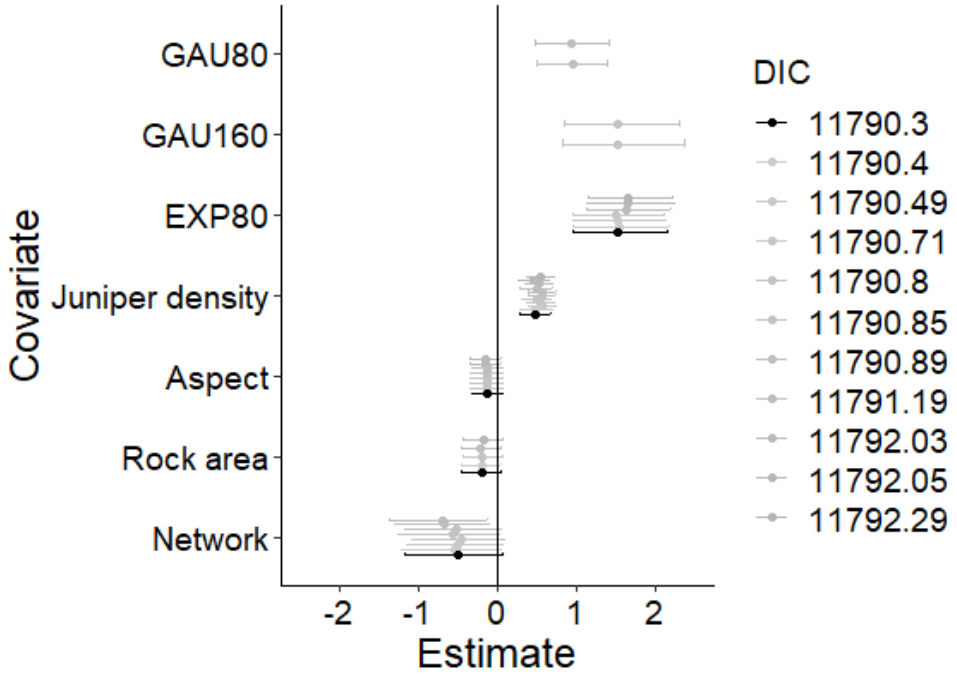

Figure I19. 95 % Bayesian credible intervals (0.025 and 0.975 quantiles of the posterior distribution) for covariates present in the top model set obtained from the 25m resolution PPMs. Responses found in the best model are highlighted in black (DIC=11790.30) compared to responses from the remaining 15 equivalent models shown in grey, ranked in order of DIC to the poorest equivalent model (DIC=11792.29 units. Force of infection (derived using an exponential "EXP": h=1, δ=80m, or Gaussian "GAU": h=2, δ=80 or 160m dispersal kernel variants) responses are shown first, followed by the remaining covariates ordered according to the number of times they were present in the top models. Model intercepts are not shown; mean intercept values ranged from -10.59 to -10.88 with standard deviations ranging from of 0.42 to 0.56.

I.2.4 Prediction of symptom intensity at 25m resolution

The equivalent performing PPM at 25m resolution (DIC=11792.29, Table 12) correctly predicted the spread of low intensity symptoms around the main clusters observed on the scree slope and gully, and the emergence of low intensity symptoms in the northern part of the SSSI replicating the pattern observed in 2016/17 (Figure I20). The prediction for 2020/21 shows the same pattern of symptom spread and intensification as the 10m resolution model suggesting gradual infection of juniper stands surrounding existing foci (Figure I20).

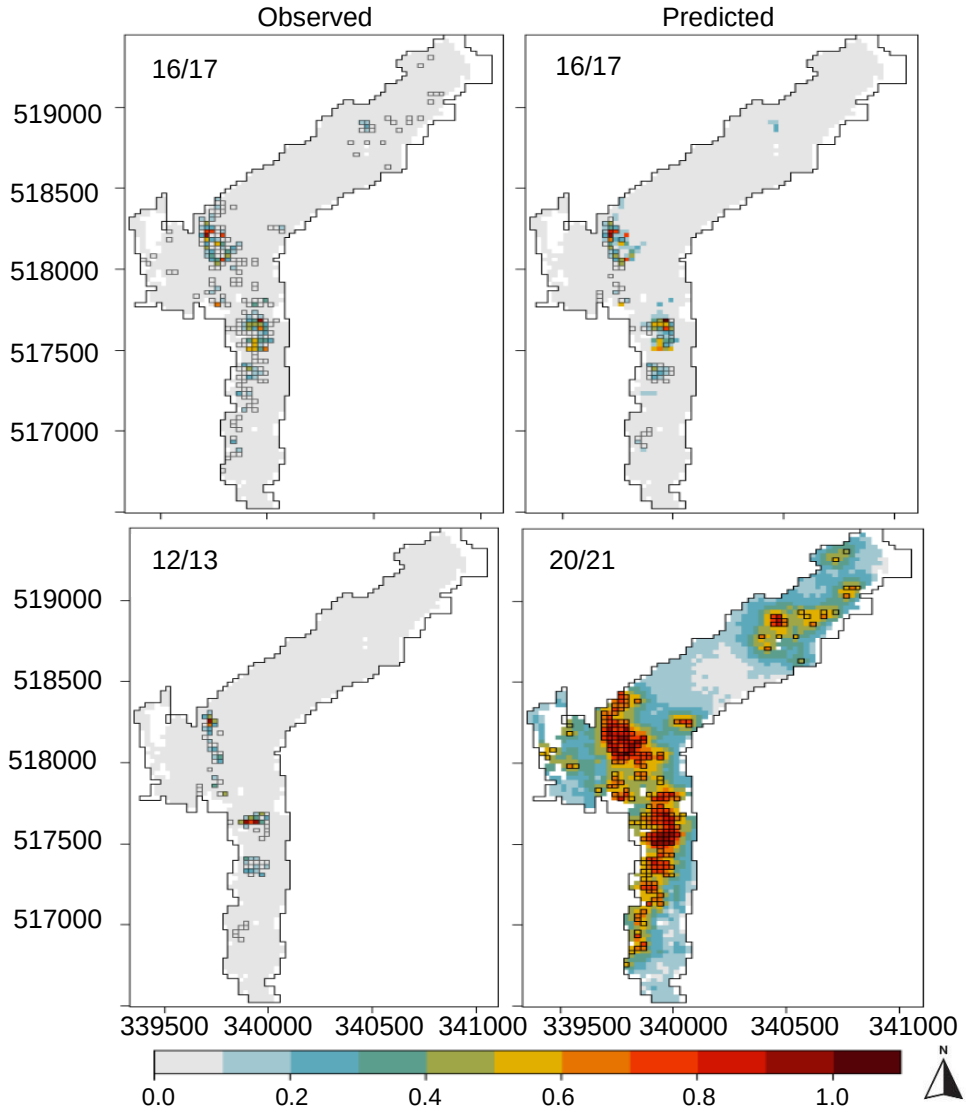

Figure I20. Spatial patterning of symptom intensity observed (L) vs predicted by the 25m PPM including juniper density and force of infection (R) labelled with the surveyed or predicted period. Cells estimated to contain juniper form aerial image analysis are shown in grey; black outlines mark cells where symptoms were observed in (L) each survey or (R) in the previous survey from which dispersal predictions derive. Symptom intensity is re-scaled to the colourbar to allow comparison of high and low intensity areas but does not equate to exact numbers of symptomatic trees.

While the best dispersal kernel did predict infections would occur in new cells in 2016/17 compared to 2012/13, it tended to overpredict symptom intensity compared to that observed (Figure I21).

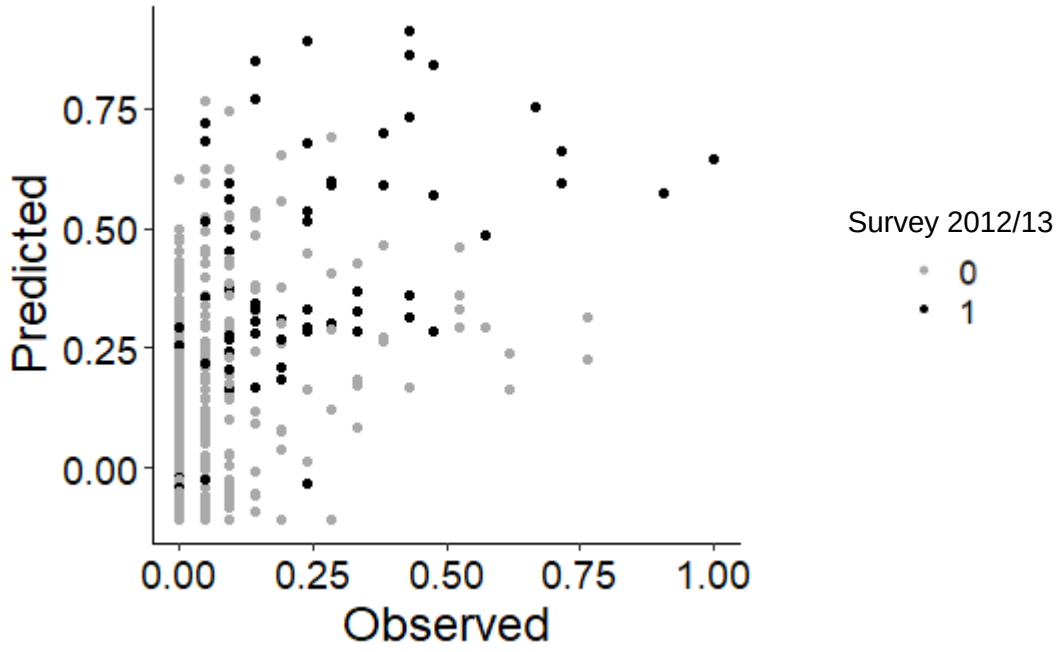

Figure I21. Symptom intensity observed in each cell containing juniper in 2016/17 compared to symptom intensity predicted by the force of infection covariate defined using a dispersal kernel parameterised as h=0.1, δ=80m. Cells observed to contain symptoms in 2012/13 are coloured black compared to cells with no symptom observations shown in grey. Symptom intensity is rescaled between 0 and 1 to allow comparison and does not equate to exact numbers of symptomatic trees.

I.2.5 Spatial random field of the 25m PPM

The spatial random field of the equivalent model (DIC=11792.29) at 25m also showed good differentiation between grid cells, with higher values corresponding to cells with high juniper density and predicted infection intensity in 2016/17, and the lowest values to cells containing low symptom intensity but high juniper density (Figure I22).

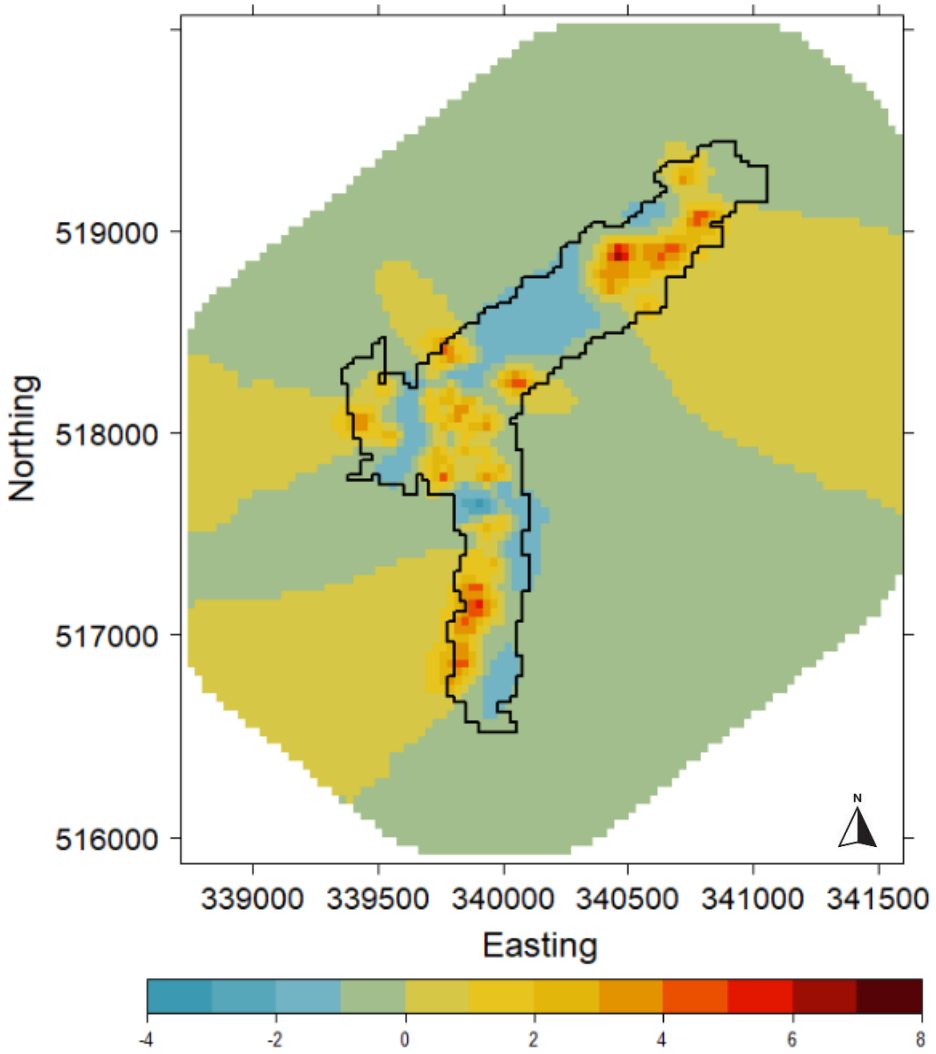

Figure I22. Spatial random field of the 25m PPM containing juniper density and force of infection mapped to the extent of the spatial mesh. Values are mapped according to the colour scale ranging from –3.1 to 6.5. The boundary of the 25x25m grid cells used in the model is outlined in black.

I.2.6 Posterior distributions derived from the best PPM

The posterior distribution for the intercept and all covariates included in the best PPM at 25m resolution were all normally distributed showing that the model converged (Figure I23).

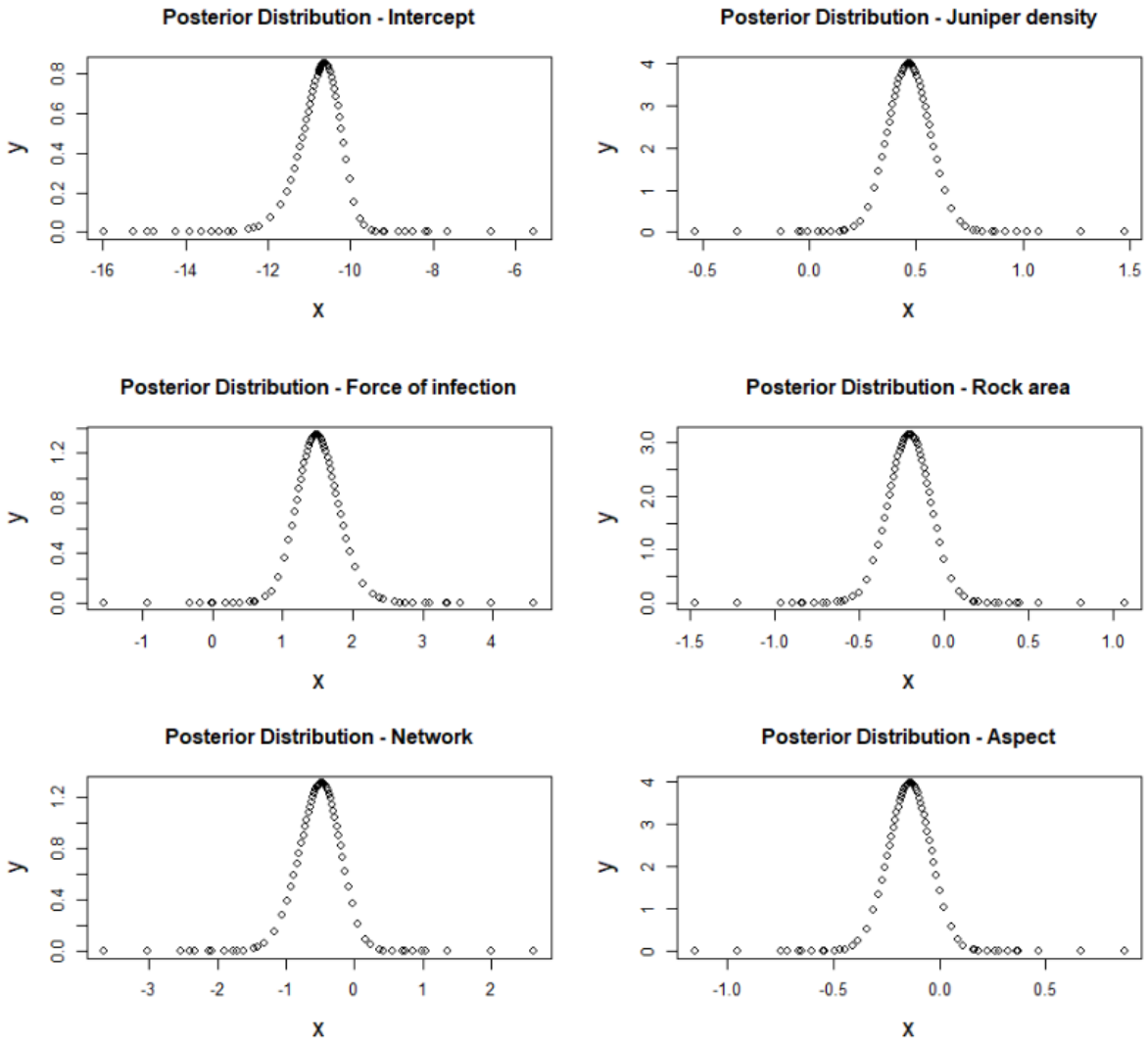

Figure I23. Posterior distributions returned by the best 25m PPM for the intercept, juniper density, force of infection (derived from an exponential dispersal kernel characterised as h=1, δ=80m), area of rock, network, and aspect.

I.2.7 Validation of the best 25m PPM

As observed at 10m resolution, symptom intensity predicted by the fixed effects in the best model at 25, resolution tended to overpredict the symptom intensity observed in 2016/17 (Figure I24).

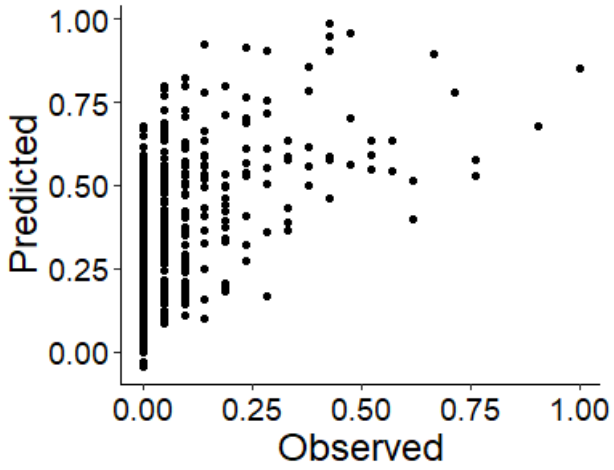

Figure I24. Comparison of observed symptom intensity in 2016/17 compared to symptom intensity predicted from the fixed effects included in the best 25m PPM (juniper density, aspect, network, area of rock and force of infection characterised using the dispersal kernel h=1, δ=80m.

Appendix J. Reproduction of the Shiny App hosting interactive maps of *P. austrocedri*, native and planted juniper distributions

UK incidence of *Phytophthora austrocedri* infecting native juniper

Records of *P. austrocedri* are positive qPCR results collated by Forest Research, Forestry Commission and FERA displayed at 1km resolution, labelled with the year of first detection. Blue squares show 2x2km records of *Juniperus communis* s.l. observed 1990-2020 by the Botanical Society of Britain and Ireland filtered to exclude records notated as alien or planted.

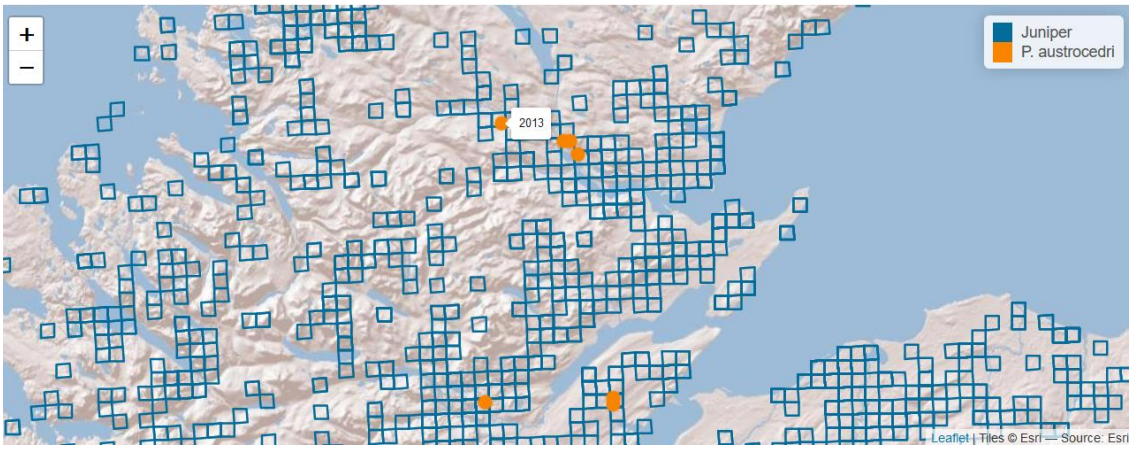

Juniper planting in the wider environment

Records of planted juniper compiled with kind permission from individual land managers. Juniper planting locations are shown according to year of planting (colour categories) and displayed at 2x2km resolution. We are uncertain how long foliage symptoms take to develop following infection with *Phytophthora austrocedri* but expect populations planted after 2009 may still be asymptomatic.

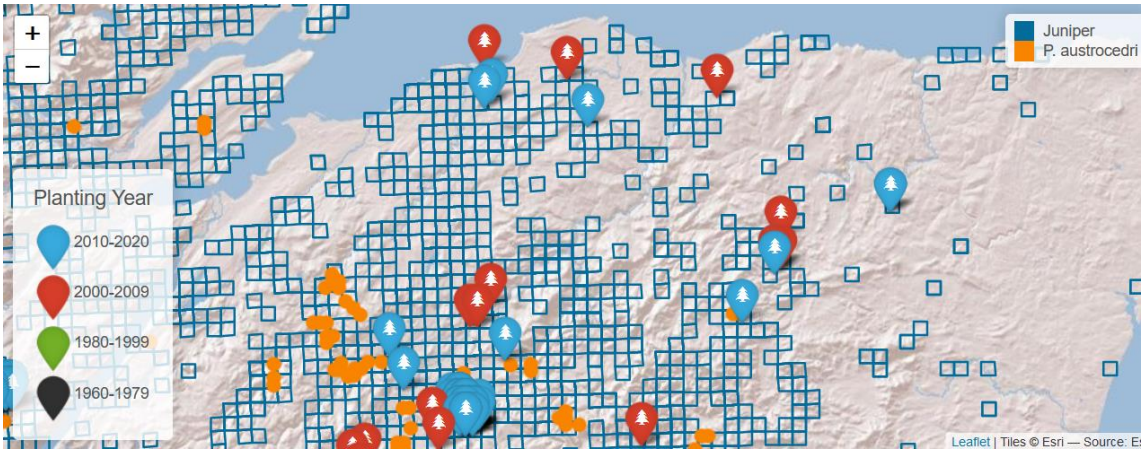

Appendix K. Stakeholder questionnaire

This appendix reproduces the self-completion survey emailed to stakeholders involved in juniper management

Risk assessing supplementary juniper planting

Thank you for taking time to complete this questionnaire. The purpose of this questionnaire is to understand the extent to which the decision tree in the juniper management guidance is currently used and identify the need for additional tools to aid risk assessment of juniper populations in relation to the plant pathogen *Phytophthora austrocedri*. The overarching aim of our research is to identify risk factors for *P. austrocedri* infection of UK juniper populations to inform management strategies for juniper conservation.

This research will be used as part of Flora's PhD project "Mapping the impact of Phytophthora austrocedri infection of UK native juniper" supported by

Before proceeding to the complete this survey, please take time to read the following information carefully:

a. Your participation in this research is entirely voluntary and you are free to withdraw at any time.
b. Should you decide to withdraw from the survey, you have the right to request that information already provided be removed and excluded from the research and not used for any other purposes. You can exercise this right at any time and for any reason.
c. Your personal information and other information collected will not be passed onto any person and/ or organisation. Your information is confidential and will be treated with utmost privacy.
d. You are free to contact Flora Donald at the UK Centre for Ecology and Hydrology in the event that you have any queries or concerns. Her contact email is flodon@ceh.ac.uk

Are you willing to proceed with this survey? Tick here to confirm consent: ☐ Yes ☐ No

1. Could you tell us about your experience and role?

2. Does your role include management of juniper or *P. austrocedri*? ☐ Yes ☐ No

3. Are you involved in juniper planting? ☐ Yes ☐ No

Juniper management guidance accessibility

Juniper has widely been planted for conservation purposes to re-invigorate dwindling, native populations. However, the introduced plant pathogen, *Phytophthora austrocedri*, is now causing widespread mortality in juniper populations across the UK. Supplementary juniper planting is a potential pathway by which the pathogen could be introduced or spread. Management guidance for juniper was issued by DEFRA in 2017, including a decision tree to help assess the need and site suitability for supplementary planting. We aim to find out how the decision tree could be made more accessible to inform juniper conservation strategies.

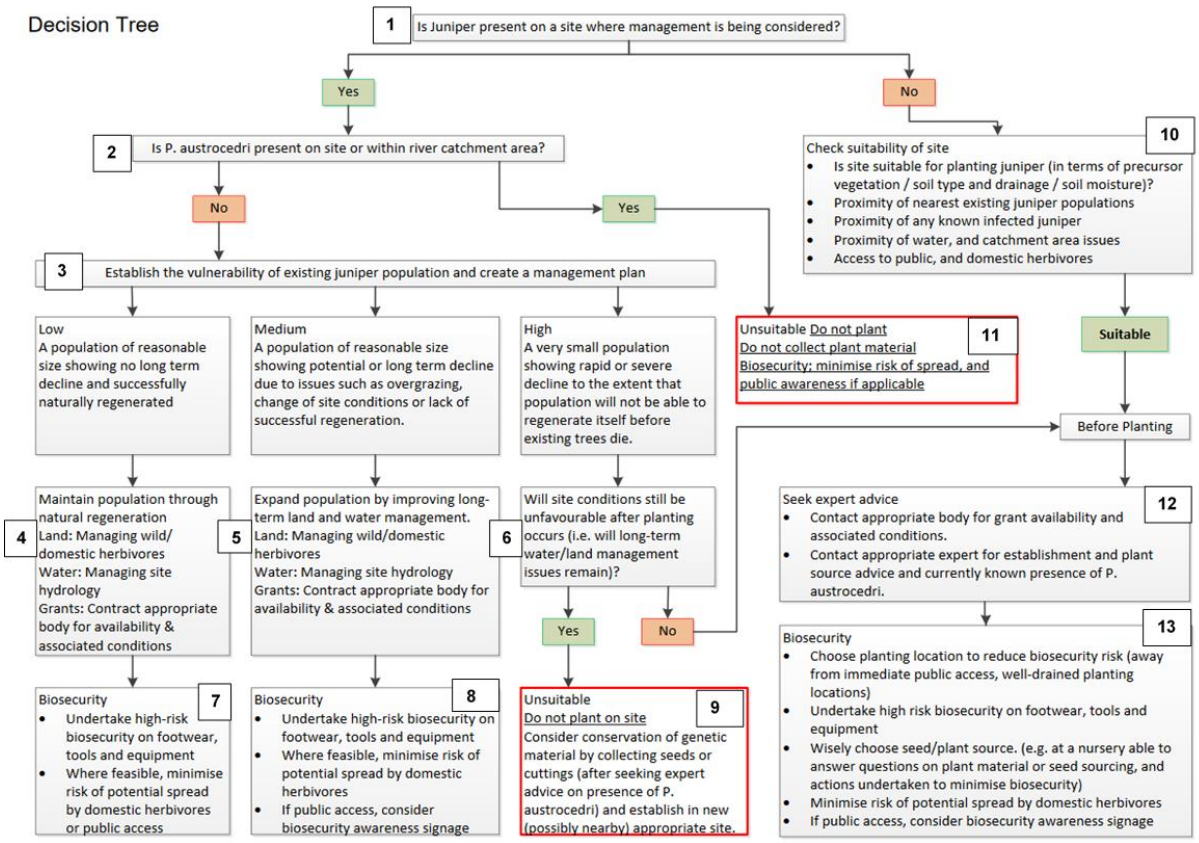

4. Do you already use the decision tree in your work? ☐ Yes ☐ No

5. If Yes to Q.4, tell us how you have used it?

6. If No to Q.4, please explain why.

7. How likely are you to use the decision tree to assess the suitability of planting juniper at a proposed location?

☐ Very likely ☐ Likely ☐ Unsure ☐ Unlikely ☐ Not at all likely

8. In its current presentation, which parts of the decision tree:

a) are additional to any planting decision process or risk assessment you currently use?

b) are most useful for determining the suitability of planting? Why do you say that?

c) would you find difficult to assess and why?

9. Do you have any additional comments about the decision tree?

Maps of *P. austrocedri*, native juniper and planted juniper

We are developing a range of national level and sub-national level maps (a) showing where *P. austrocedri* has already been recorded in relation to native juniper and planted juniper and (b) predicting where else in the UK landscape conditions are suitable for *P. austrocedri* to establish and spread.

Access example maps here: https://floradonald-juniper-planting-2020.shinyapps.io/Planting2/

10. Do you already use maps of juniper and/or *P. austrocedri* for management decision-making? ☐ Yes ☐ No

11. If yes, how do you use them?

12. If yes, where are these maps sourced from?

13. If a map of *P. austrocedri* were made available, would you be more or less likely to conduct a site visit to check for the pathogen?

☐ Very likely ☐ Likely ☐ Unsure ☐ Unlikely ☐ Not at all likely

14. Please may you explain your response?

15. Which scale of geographical information would be most useful to you? (Tick as appropriate)

☐ National ☐ Sub-national ☐ Other (please specify)

16. Why do you say this?

To understand the national distribution of *P. austrocedri*, our model may include some of the following risk factors:

Category	Risk factor	Detailed description (units in brackets)
Abiotic risk factors	Rainfall	annual mean precipitation 1980-2015 (kg m^{-2} s^{-1})
	Soil moisture	annual mean 1980-2015 (mm)
	Surface runoff	annual mean 1980-2015
	River flow speed	annual mean 1980-2015 (m^{-3} s^{-1})
	Nearest river	Euclidean distance (m)
	Elevation	(m)
	Slope	(°)
	Aspect	(°)
	Temperature	annual mean air temperature (K)
	Climate suitability index	derived from lab based temperature growth curves and relative humidity
	Soil texture	categories from the British Geological Survey
	Soil depth	(mm)
	Soil pH	mean
Biotic risk factors	Juniper presence	volunteer records at 2x2km or predicted using model of juniper habitat suitability
	Wider environment juniper planting	Euclidean distance to nearest juniper planting in the following year groups < 1980, 1980-89, 1990-99, 2000-09, > 2010 (m)
	Deer density estimates	($LUha^{-1}$)
	Livestock density	($LUha^{-1}$)
	Habitat type	21 categories taken from the 2017 landcover map
	Bird species estimates	species richness and/or abundance of species known to feed on juniper berries
	Recreational habitat use	human population density fitted to the distance distributions of travel distances for activity types in the Monitor of Engagement with Natural Environment (MENE) and Nature Scot People & Nature Survey
	Nearest footpath	Euclidean distance (m)

17. Which of the abiotic risk factors do you think are most likely to promote infection of juniper? Please pick your top five risks where 1 is most important. (Please mark one column per row)

	Rainfall	Soil moisture	Surface runoff	River flow	Nearest river	Elevation	Slope	Aspect	Temperature	Climate suitability	Soil texture	Soil depth	Soil pH
1													
2													
3													
4													
5													

18. Which of the biotic risk factors do you think are most likely to promote infection of juniper? Please pick your top five risks where 1 is most important. (Please mark one column per row)

	Juniper presence	Juniper planting	Deer density	Livestock density	Habitat type	Bird species	Recreation	Nearest footpath
1								
2								
3								
4								
5								

19. Are there any additional factors you think may be driving the spread of the pathogen that we should explore?

20. In your view, how could we keep the juniper planting map (see https://floradonald-juniper-planting-2020.shinyapps.io/Planting2/) up to date?

21. What do you see as the benefits of keeping the planting map up to date, if any, to your management?

Personal information

Please tell us a little more about your work with juniper.

Your name:

Job title:

Organisation:

Role description or specialisation:

Geographical area (e.g. UK wide, national, county):

Email address:

Would you be interested in participating in a follow-up workshop to discuss the tools we develop? ☐ Yes ☐ No

Many thanks for participating in our research.

We expect to share the model results with you by March 2021.

Appendix L. Supplementary results from the stakeholder questionnaire

This appendix presents additional information obtained from the stakeholder survey to supplement results described in the main text.

L.1 Participant decision tool preferences

Responses to questions asking survey participants to identify uses for the decision framework in the DEFRA juniper management guidelines (DEFRA, 2017) and the new distribution maps were collated to understand if the utility of the decision tools varied with stakeholder type. Two of 41 participants did not identify a use for either the decision framework or the interactive maps. Most of the other participants (61%) detailed uses for both decision tools (Table L1). Although the differences in decision tool preference were not statistically significant, all but one assessor specified uses within their role for both the decision framework and maps (89%), while there was less consensus among growers who described uses for either the decision framework or the maps (Table L1).

Table L1. Number and percentage (in brackets) of participants per stakeholder type who described uses for the decision framework and/or distribution maps in relation to their work. Column totals report the total number (n=41) and percentage of all participants using each decision tool category.

Stakeholder type	Decision framework & maps	Maps only	Decision framework only
Agent	6 (55%)	4 (36%)	0 (0%)
Assessor	8 (89%)	0 (0%)	1 (11%)
Grower	1 (17%)	2 (33%)	2 (33%)
Manager	10 (67%)	3 (20%)	2 (13%)
Total	25 (61%)	9 (22%)	5 (12%)

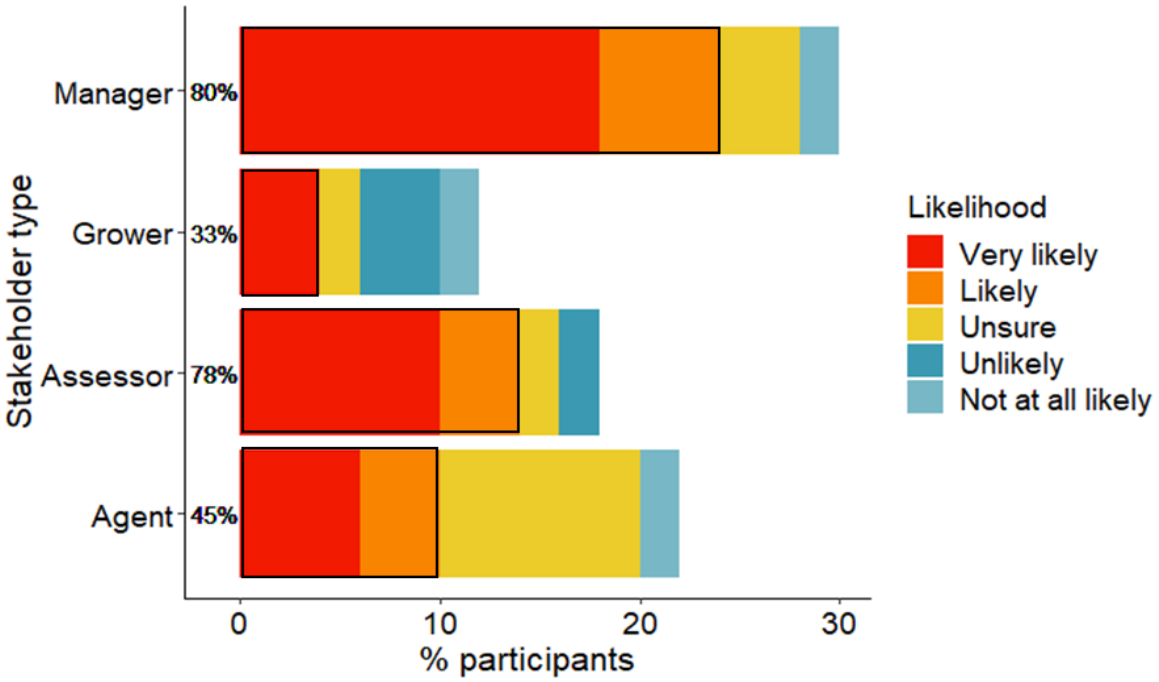

Figure L1. Likelihood attributed to use of the decision framework to assess suitability of future juniper planting projects. The percentage of participants (n=41) that selected each likelihood category are shown according to stakeholder type, and the percentage within each type likely or very likely to use framework (shown in red/orange) are reported right of the y-axis.

L.2 Perceived risks of juniper planting

Question 18 in the survey (Appendix K) asked participants to pick five out of a possible eight biotic risk factors they perceived as most likely to drive *P. austrocedri* infection of juniper and to rank them in order of importance (Figure L2). Assessors appeared most, and growers least, concerned about planting (89% and 30% ranked planting 4 or 5 respectively) (Figure L2) but the differences were not statistically significant between stakeholder types (Holm-Bonferroni corrected p=0.25).

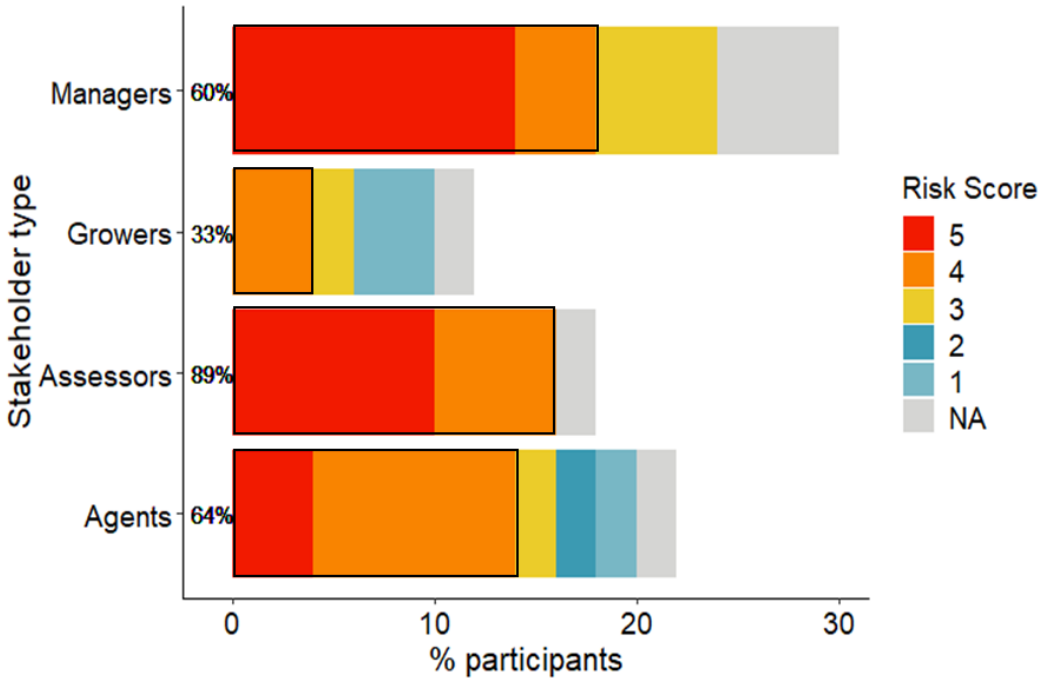

Figure L2. Percentage of participants (n=41) attributing each risk score to juniper planting according to stakeholder type. The percentage of participants per stakeholder type who ranked planting as a highly important risk factor for *P. austrocedri* (risk score 4 or 5) is written at the right of the y-axis.

L.3 Spatial scale preferences for host/pathogen maps

Survey questions 15 and 16 asked participants to specify the spatial scales at which maps of *P. austrocedri*, juniper and juniper planting would deliver maximum benefit to their role connected with juniper management. Local maps were most popular with requests for detailed (6-8 figure) grid references and the ability to zoom in further than allowed on the 1-2km resolution interactive map provided with the survey (Table L2). Twelve percent of participants who worked across the UK requested national (UK-wide) distribution maps but a further 27% requested national maps to contextualise local maps (Table L2). Maps displaying pathogen and juniper distributions within single counties or countries within the

UK were requested by 20% of participants and only one participant identified the need to contextualise their region within the wider UK distribution (Table L2).

Table L2. Number (n) and percentage (in brackets) of participants who chose each spatial scale as the most useful for distribution maps to aid decision-making. An example quote representing the most frequent justification for using maps at each scale is provided.

Spatial scale	n	Exemplar quote
Local (sub-county)	16 (39%)	"*I'd want site grid refs or a zoomable map to work out exact locations. Your maps need place names and roads or some way of working out where the squares actually are e.g. national grid."* (Manager 6)
Regional (country / county)	8 (20%)	*"we operate on a regional and countywide basis."* (Assessor 7)
National (UK)	5 (12%)	*"We could be asked to propagate from other areas in the future."* (Grower 3) *"I have various clients around the country and the more information the better."* (Manager 3)
Local & national	11 (27%)	*"A national overview is important so that regional/local decisions can be put into the wider context."* (Agent 6)
Regional & national	1 (2%)	*"I work on a regional scale but it is good to understand the national picture too."* (Manager 11)

L.4 Participant recommendations to improve decision tool accessibility

Survey question 12 asked participants to detail where they sourced information if they already use maps of juniper and/or *P. austrocedri* for management decision-making (Appendix K). Private sources of information including organisation specific or participant's own knowledge were reported most frequently (24% participants) (Figure 3a). Publicly accessible sources were cited by 15% of participants; the Forest Research website was used most often (7%) followed by individual participants (2% each) who cited using the National Biodiversity Network (NBN) gateway (The National Biodiversity Network, 2021), the Ecological Site Classification Decision Support System (ESC) hosted on the Forest Research website that matches site factors with ecological requirements of different tree species and woodland communities to aid site-based choices about suitable plantings (Forest Research, 2021c), and "FC Tools" more generally which could correspond to ESC or another platform (for example the Forestry Commission Land Information Search (FC LIS) (Forestry Commission, 2021)) (Figure 3a). Both the ESC and NBN currently only host records of juniper, and not *P. austrocedri*, as is the case for records accessed by a further 9% of participants from maps hosted by the Botanical Society of Britain and Ireland (BSBI) or published by Plantlife (Ward and Shellswell, 2017) (Figure 3a).

Participants suggested a variety of information sources that could be used to improve the distribution maps and maintain up to date records but the question posed was insufficiently specific to always pinpoint if answers related specifically to juniper planting locations, those infected with *P. austrocedri*, or both (Figure L3c). Thirteen percent of participants suggested actively writing to public bodies (7%), nurseries (2%) or individual stakeholders (2%) to request records or obtain information from management plans (2%):

“Regular updates from FLS/FE [Forest and Land Scotland / Forestry England] sub-compartment database, updates from forestry grant scheme payment every 6 months. Not sure this would capture all the charity sector planting or enrichment planting schemes though. Agreements for updates could be made with main players though.” (Manager 11),

while a further 4% suggested liaison with pathologists or forest reproductive material officers (FRMOs) who:

“must be notified of any marketing of juniper including all seed collecting and plant supply” (Grower 4).

Unsurprisingly, when asked where the decision tools could be hosted to improve awareness and accessibility, many of the suggestions included the platforms already cited as current sources of information, such as the Forest Research website (5%), NBN (2%) and Plantlife (2%). Additional suggestions included the popular citizen science platform iNaturalist (2%), a bespoke central repository specifically for juniper (2%), an online juniper management forum (2%) or incorporation into existing governmental land management mapping software including FC LIS (7%) and the DEFRA MAGIC viewer (5%) (Figure L3b). Except for the NBN and iNaturalist, however, these platforms only permit data entry or modification by internal staff members. A large proportion of survey participants suggested data entry should be performed by the data handlers themselves, ideally entering information directly via a web interface or app (15%), compared to making public agencies (2%), action groups (2%) or a dedicated operative (2%) responsible to update the distribution maps (Figure L3d). Further collaboration between these platforms and stakeholders is required, therefore, to add functionality for data entry to the existing platforms or explore further options.

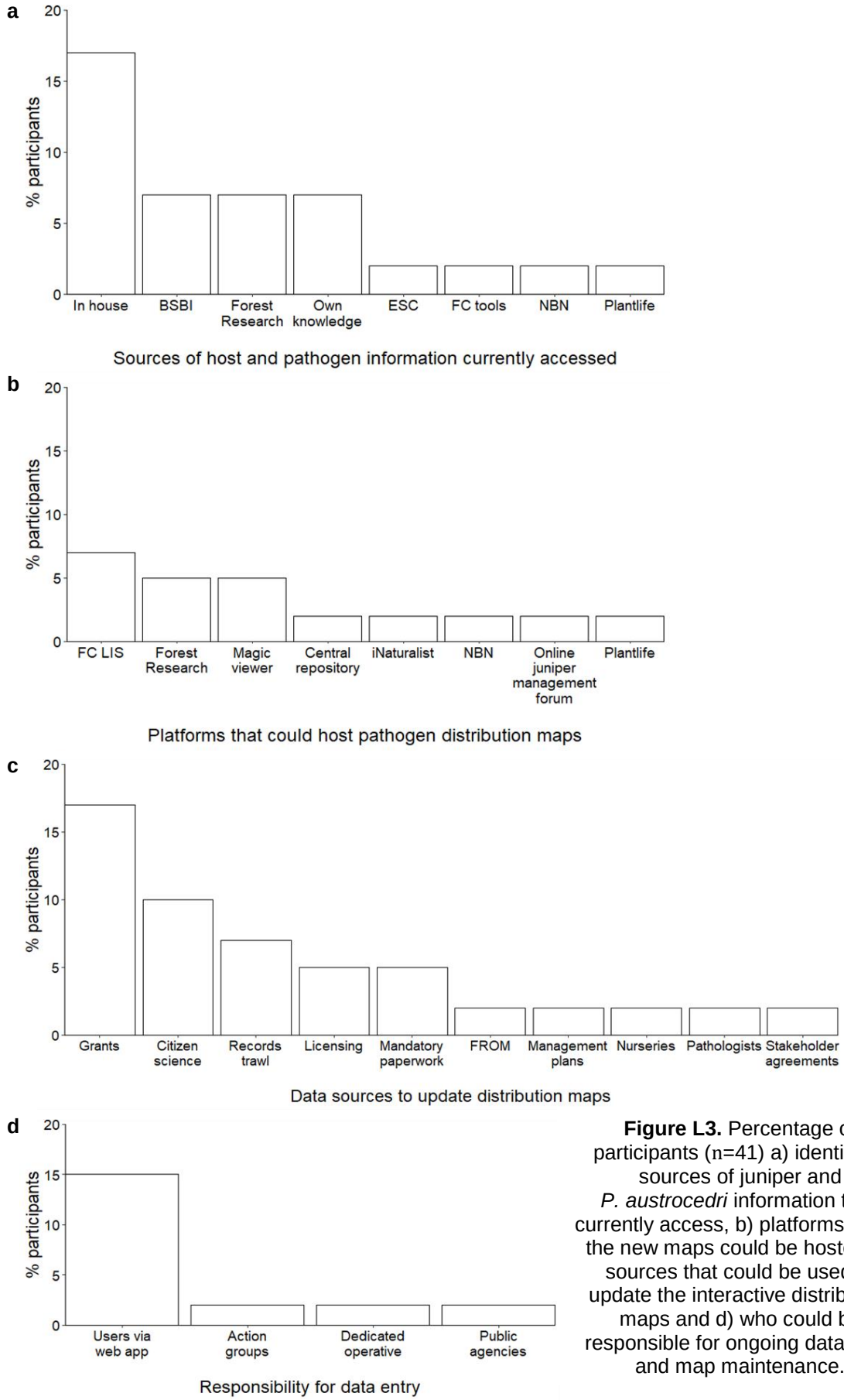

Figure L3. Percentage of participants (n=41) a) identifying sources of juniper and *P. austrocedri* information they currently access, b) platforms where the new maps could be hosted, c) sources that could be used to update the interactive distribution maps and d) who could be responsible for ongoing data input and map maintenance.

Appendix M. Preparation of national scale abiotic and biotic covariates

M.1 Distribution and clustering of *P. austrocedri* presence locations

The number of positive *P. austrocedri* detections made in each GB juniper tetrad (5483) ranged from 1 (26% tetrads) to 23 (1% tetrads) and reflected sampling effort related to i) date of first detection and ii) year of survey. For example, Haweswater reservoir and High Force in Upper Teesdale were the first symptomatic populations and had the largest number of detections (23 and 16 respectively) (Green et al., 2015). Moreover, 63% detections were made in 2013 when the Forestry Commission, Scottish Forestry and Natural Resources Wales all conducted large-scale surveys to detect *P. austrocedri* following confirmation of Koch's postulates in 2012 (Green et al., 2012) (Figure M1).

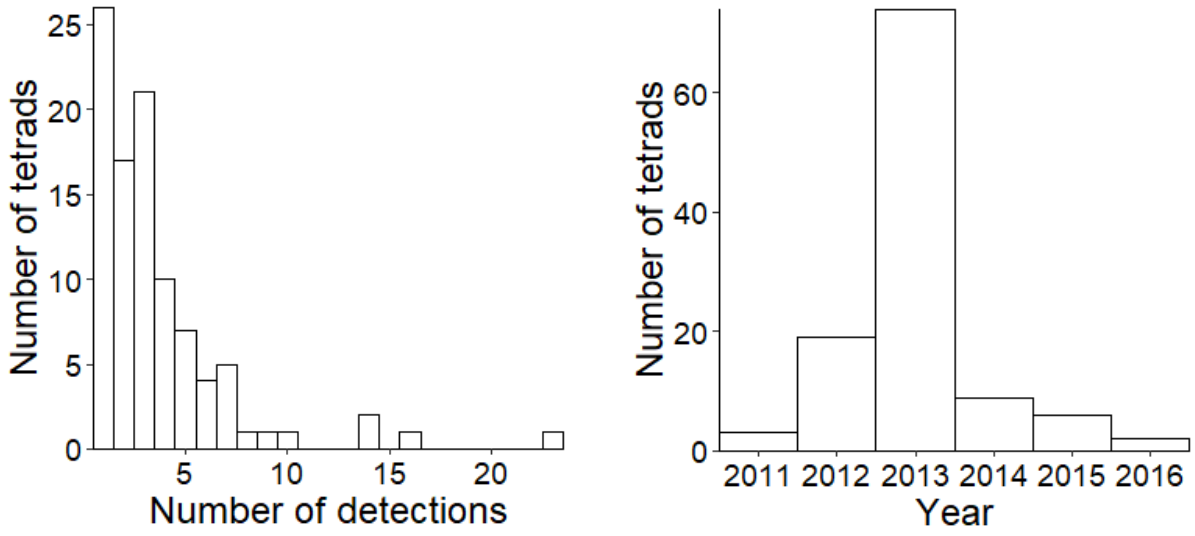

Figure M1. Distribution of *P. austrocedri* found in British tetrads containing juniper, comparing the number of positive detections found per tetrad (L) and the year of detection (R).

Despite some geographical clustering, distances between pairs of infected tetrads were sufficiently well distributed across distance bins to use all locations in the BRTs without the need for data thinning (Syfert et al., 2013) (Figure M2).

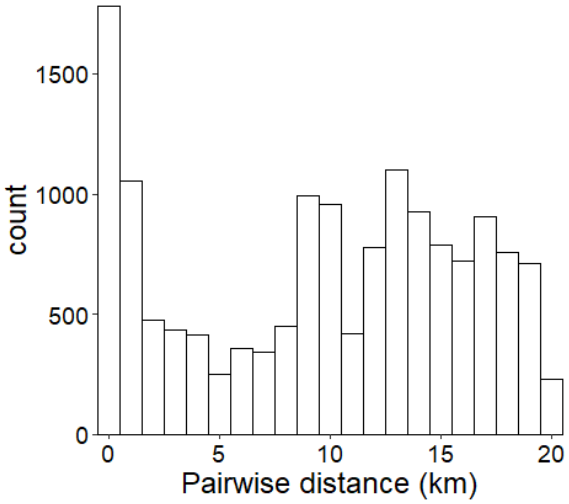

Figure M2. Frequency of Euclidean pairwise distances measured between centroids of juniper tetrads with positive *P. austrocedri* detections, shown for the first 20km of the full 800km distance range.

M.2 Preparation of potential abiotic and biotic predictors of *P. austrocedri* presence

Data were prepared using a combination of R version 3.6.2. (R Core Team, 2019) and ARC GIS version 10.5.1 (ESRI, 2017). The 5483 tetrads containing juniper were converted to 2kmx2km polygons using BRCmap::*gr2sp_poly* (Harrower, 2016) in R and used to delimit values extracted from the following datasets of environmental risk factors. Risk factors with a temporal element (e.g. rainfall and temperature, sources detailed below) were obtained for the period 1st January 1990 to 31st December 2016 to correspond with the starting period for the juniper baseline and the most recent *P. austrocedri* detection. The exception was soil moisture that could not be obtained for 2016 at the time of modelling so was extracted from 1st January 1990 to 31st December 2015. Monthly means of daily (09:00 to 09:00) soil moisture (mm water/ m soil) were obtained from the Grid-to-Grid soil moisture estimates at 1km resolution (Bell et al., 2018) using the *ncdf4* R package (Pierce, 2019) and extracted to the juniper tetrads using raster::*extract* (Hijmans, 2019). Monthly soil moisture was converted to tetrad resolution by taking the mean of the four 1kmx1km values returned per tetrad. Mean soil moisture (mm water/m soil) was then calculated across all months from 1990 to 2015 for each tetrad. The same method was used to calculate tetrad values for predictors with 1km resolution data for the period 1990-2016: mean monthly snow mass (kg m^2) from the CHESS-Land dataset (Martinez-de la Torre et al., 2018), mean daily rainfall (mm/day, converted from kg m^2 s^2) using daily precipitation estimates extracted from the CHESS-MET dataset (Robinson et al., 2020), mean daily temperature (°C, converted from K) extracted from the CHESS-MET daily air temperature dataset (Robinson et al., 2020) and

mean daily minimum and maximum temperatures (°C) extracted from the HadUK-Grid daily (09:00 to 09:00) minimum and maximum air temperature datasets respectively (Met Office et al., 2020). The use of two different datasets to derive daily mean, maximum, and minimum temperatures resulted in a small percentage of daily records with minimum temperatures exceeding (0.7% records), or maximum temperatures below (0.6% records), the mean. These errors only occurred where the daily values were very similar and there is an implicit assumption in all temperature calculations that minimum < mean < maximum temperature. Therefore, where the mean temperature was below the minimum temperature, the mean value was adjusted by adding 0.1°C and conversely by subtracting 0.1°C where the mean value exceeded the maximum temperature. The number of rainy days (days with mean rainfall ≥1mm according to the Met Office definition (Met Office, 2011)) and the number of periods of optimal mean temperature (five consecutive days of mean daily temperature between 10°C and 15°C) were calculated per tetrad from the corresponding parameter extractions detailed above. Average daily mean temperatures in juniper tetrads, measured between 1990 and 2016, varied from 2°C in mountainous regions of Scotland to 11°C in the south of England. This range of geographical variation was mirrored in the minimum daily temperature values (Figure M3). The number of optimal temperature periods 1990-2016, with five consecutive days of mean daily temperatures in the 10-15°C range, varied from 0 to 500 days. The greatest number of optimal periods were concentrated on the west coast of Scotland whereas the lowest number of periods were found on mountainous parts of north-central Scotland and parts of south-east England (Figure M3). The climate suitability predictor was then calculated, based on laboratory observations (Frederickson-Matika, D., unpublished data) of optimal conditions for sporangial production and zoospore dispersal, as the number of periods of five consecutive days that had both ≥1mm rain per day and optimal mean daily temperatures (10-15°C), intersected by at least one day with a mean minimum temperature of ≤5°C per tetrad. These conditions occurred infrequently in only 351 (6.4%) tetrads, and in only 42 (0.8%) tetrads on more than one occasion (Figure M3).

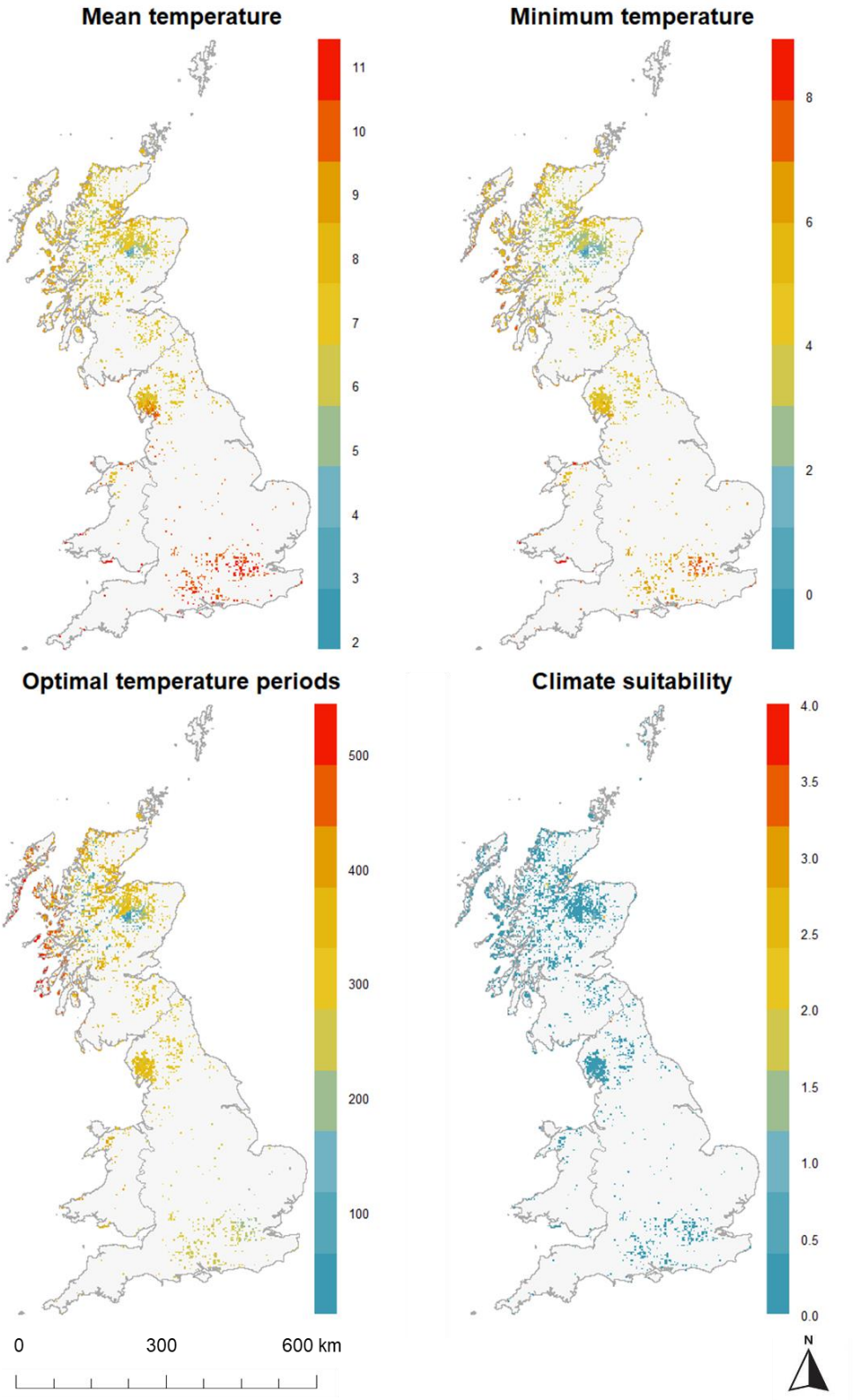

Figure M3. Temperature predictors included in BRTs to produce a 2kmx2km resolution risk map of *P.austrocedri* infection in British juniper in tetrads. Mean and minimum temperature were calculated as daily averages for the period 1990-2016 (°C), optimal temperature as the number of periods with five consecutive days of mean temperatures 10-15°C and climate suitability as optimal temperature periods with >1mm rain per day intersected by at least one day with a minimum temperature < 5°C. See Table 26 in the main text for a description of data sources.

A predictive model of the average, daily rate of radial *P. austrocedri* mycelial growth in response to temperatures was fit to experimental data measuring mycelial growth of ten British isolates in response to constant temperatures between 5°C and 30°C (Henricot *et al*., 2017) over a two week period. The predictive function applied was a modified version of the Magarey generic infection model developed for foliar fungal pathogens (Magarey et al., 2005) fixed *P. austrocedri* growth to only occur above 0°C and fit growth rates via a flexible form parameterised using the maximum, minimum and optimal temperatures for infection derived from the experimental data (see section M.3). Temperature data in the juniper tetrads were only available as daily minimum, mean and maximum values, and so fluctuations within a single day were not accounted for. An interpolation procedure was, therefore, designed to produce a set of 101 temperatures matching a given daily minimum, mean and maximum value across an entire 24-hour period. The results of this interpolation were used as input to the growth model, allowing the growth model to be driven by the data to which we had access. We tested our methodology using a separate data set for which hourly temperature values were available, but for which we inputted only the minimum, mean and maximum values into our interpolation procedure. Tests were performed on thirteen tetrads with positive qPCR results obtained from four juniper populations situated in Sites of Special Scientific Interest (SSSI) in the Cairngorms (North Rothiemurchus Pinewood SSSI), Central Lowlands (Glenartney SSSI), Lake District (Birk Fell SSSI) and Salisbury Plain (Salisbury Plain SSSI) to represent a breadth of different environments. The results showed that interpolation led to only a very small degree of inaccuracy (Figure M5, Figure M6) compared to using the full data set (see section M.3). This allowed us to confidently use the interpolated temperature values in our national scale model. The sum of the mycelial growth extracted at each interpolated temperature from the modified Magarey growth curve was calculated per tetrad per day then averaged across all days from 1st January 1990 to the 31st December 2016 to produce the estimated daily average mycelial growth (mm/day).

The following rasters were extracted to the juniper tetrads using raster::*extract* (Hijmans, 2019) in R at 1km resolution and then the values were averaged for each tetrad. Slope (°) was calculated using the raster::*terrain* function applied with eight neighbours (Hijmans, 2019); the conversion was performed using a raster of altitude (m above sea level) derived from the SRTM 1 arc-second global elevation data (National Aeronautics and Space Administration, 2014) pre-processed to 1km resolution to the extent of GB, from which mean altitude per tetrad was also calculated. Estimates of pH were obtained from rasterised predictions of pH for the top 0-15cm soil depth generated by Thomas et al. (2020) using a Generalised Additive Mixed Model from data collected in 2007 by the Countryside Survey.

Rasters of estimated deer density were obtained from ensemble modelling used to predict an index of presence for roe (*Capreolus capreolus*) (Alexander et al., 2014) and red (*Cervus elaphus*) (Wint et al., 2014) deer across their European range. The datasets were chosen following Pearson's r^2 correlation tests between the red deer raster and counts of red deer conducted in parts of Scotland 2005-2006 provided by the James Hutton Institute (see section M.4). Finally, the pressure potentially exerted by recreational visitors to juniper tetrads was calculated by extracting the residential population density from the "UK gridded population 2011 based on Census 2011 and Land Cover Map 2015" raster (Reis et al., 2017). Instead of extracting values to the juniper tetrads, buffers with a radius of 3.2km or 10.9km were first applied to the juniper tetrad centroids using rgeos::*gDistance* (Bivand, Roger; Rundel, 2019). These distances were calculated as the median and 3rd interquartile distance ranges that walkers travelled to a recreational location containing juniper in England as reported to the Monitor of Engagement with the Natural Environment (MENE) survey undertaken between 2009 and 2019 (Natural England, 2019b). Further details of how these distances were identified are given in section M.5.

Soil properties were extracted from the British Geological Society soil parent material dataset that contained a range of descriptive measurements, including depth and texture, that could be resolved to a small number of informative categories (Lawley, 2012). The "soil texture" classification produced a detailed classification of soil textures derived from measured samples of soils overlying different parent materials, then generalised into a smaller descriptive list of "soil groups" (Lawley, 2012). When the 1km soil parent material raster was extracted to the juniper tetrads using the *intersect* tool in the ARC GIS analysis toolbox, the "soil group" description comprised 23 indicative categories formed from combinations of "heavy", "medium" and/or "light" with the addition of "sandy" to three categories or "silty" to ten categories. Categories describing "sandy" textures accounted for 58% of the area of juniper and were found in 75% of the tetrads, while "silty" textures only accounted for 19% of the area and were present in just 30% of tetrads. Therefore, the area (m^2) of each tetrad found in categories described as "sandy" was calculated as sufficiently informative to test the hypothesis that *P. austrocedri* presence decreases with increasing areas of sandy soils where water availability for sporangial production and zoospore dispersal is reduced. Descriptions of "soil depth" extracted to the juniper tetrads were distributed between five categories ranging from "shallow" to "deep", that were developed using borehole records and expert judgement of engineering strength characteristics of the underlying parent materials (Lawley, 2012). The intermediate soil depth covered a smaller percentage (4%) of the extracted area compared to deep (53%) and shallow (30%) soils, so

categories described as “deep-intermediate” and “intermediate-shallow” were added to the calculation of “intermediate” soil depths (16%). The distribution of soil texture between the soil depth categories was checked to ensure the two risk factors captured different characteristics of the data, and indeed sandy soils were measured in all depth categories accounting for 27% of the area of deep, 24% of shallow and 7% of intermediate soils.

The river length and juniper planting risk factors required that a buffer was created around each juniper tetrad with a 2km radius using *buffer* in the ARC GIS analysis toolbox, resulting in a 6kmx6km grid cell with the juniper tetrad placed in the centre. Vectored maps of the road (15-30m resolution, Ordnance Survey, 2021) and river (50m resolution, Moore et al., 2000) networks across GB were displayed in ARC GIS and clipped to the juniper tetrads (rivers and roads) and the buffered juniper tetrads (rivers only) using *clip* in the analysis toolbox. The lengths (m) of rivers and roads intersecting each tetrad or buffered tetrad were then calculated to produce the river length tetrad, roads, and river length buffer risk factors respectively. Euclidean distance (m) from the centroid of each juniper tetrad to the nearest river was then calculated using the *gDistance* function in R (Bivand, Roger; Rundel, 2019).

The presence of juniper planting in the 6kmx6km buffered juniper tetrads was calculated for different time periods, ending with the most recent *P. austrocedri* detection in 2016 and extending back for the previous ten years at each calculation resulting in five different periods: 2007-2016, 1997-2016, 1987-2016, 1977-2016 and 1967-2016. The juniper planting distribution map comprised of 1027 planting events conducted across the UK at tetrad resolution, generated from citizen science records shared by the Botanical Society of Britain and Ireland (BSBI) and responses to information requests returned by public agencies, utility companies, conservation charities, wildlife trusts and other non-governmental organisations that conducted supplementary juniper planting (Donald et al. 2021). Planting events were defined as an occurrence of juniper planting in a specific tetrad in a specific year. If a range of years was provided with the record of a planting event, the most recent year in the range was used as the year of the event. BSBI recorders were often unable to record the year of original planting, so the year of observation was instead used as the event year. Therefore, the same planting event may be duplicated where records were obtained from multiple sources with different approaches to recording year. To minimise the effect of this, planting events were coded as binary presence/absence during the time period considered. Buffered tetrads were used because both the native and planted juniper maps were produced at 2km resolution, so only exploring the overlap of planting events in a tetrad would miss events conducted immediately adjacent to a native population that fell in a different 2kmx2km grid

cell. It was considered appropriate to use the 2km buffer because a study of *P. austrocedri* infection through time conducted at a juniper population in northern England found colonisation occurred frequently within 500m and infrequently beyond 3km of the nearest symptomatic juniper (Chapter 3). The data were extracted by first converting the map of planting events to polygons in R using BRCmap::*gr2sp_poly* (Harrower, 2016), then identifying buffered tetrads intersected by planting events using sp::*over* (Bivand et al., 2013) and coding planting as present where the year of the intersecting event fell within the range of each planting period.

Finally, the number of sheep recorded in each juniper tetrad by the 2010 return of the AgCensus (EDINA, 2010) was extracted by intersection using sp::*over* (Bivand et al., 2013), following location conversions to polygons of national grid references performed using the functions *gr_num2let* and *gr2sp_poly* in the BRCmap R package (Harrower, 2016). Livestock records were collected by each devolved nation using the same definition i.e. the sum of all breeding and non-breeding sheep. However, the most recent dataset available for England was collected in 2010 at 5km resolution compared to 2km resolution datasets available until 2014 from Wales and 2015 from Scotland. For consistency, and as a year when *P. austrocedri* was likely well established throughout its current range (Green et al., 2015), all data were downloaded for 2010 only. To extract the number of sheep at 2km from the 5km resolution English records, a 5kmx5km grid was created from the 5km sheep grid references in ARC GIS using *create fishnet* in the data management toolbox. The number of sheep were assumed to be evenly distributed across each 5kmx5km grid cell so the number of sheep per tetrad was calculated proportionately to the area of the fishnet grid cell(s) intersected by each tetrad.

M.3 Calculating average *P. austrocedri* mycelial growth rate

This section describes how an average daily rate of mycelial growth was predicted for each juniper tetrad by interpolating diurnal temperature changes from daily predictions of minimum, maximum and mean temperature calculated from 1990 to 2016 and estimating mycelial growth rate from a temperature response model calibrated using experimental measurements collected from seven constant temperature intervals. Radial mycelial growth (mm) of ten British *P. austrocedri* isolates in response to different constant temperatures was measured under experimental conditions described by Henricot et al. (2017) at temperatures of 5, 10, 15, 20, 22.5, 25 and 30°C. Four plates of each isolate were tested at each temperature and the experiment was run twice (Henricot et al., 2017). Colony diameter (mm) was measured after 7 days of incubation at 17°C (week 1) and then after a further 14-16

days at the experimental temperature (week 3) (Henricot et al., 2017). Daily, radial, mycelial growth rate was calculated as

$$\frac{(\text{week3 diameter} - \text{week1 diameter})/2}{\text{number of days between measurements}}$$

then averaged across all plates and replicates for each isolate (Henricot et al., 2017). To predict mycelial growth rates at all intervening temperatures, the experimental data were fit to two different models used to estimate growth curves in response to temperature: the Magarey generic infection model developed for foliar fungal pathogens (Magarey et al., 2005) and the more general *loess* (local polynomial regression fitting) smoothing function available in the R stats package (R Core Team, 2019) (Figure M4).

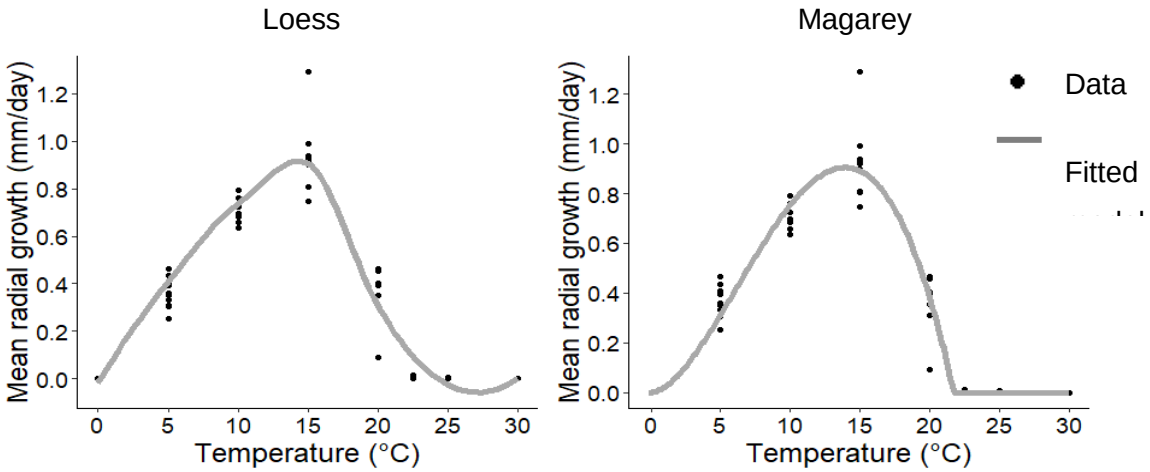

Figure M4. Comparison of loess (L) and Magarey (R) models fit to mean, radial mycelial growth rate data (mm/day) obtained for ten British *P. austrocedri* isolates exposed to constant temperatures for 14-16 days (Henricot et al., 2017).

The Magarey model fits a temperature response function of the form

$$f(T) = \left(\frac{T_{max} - T}{T_{max} - T_{opt}}\right)\left(\frac{T}{T_{opt}}\right)^{(T_{opt} - T_{min})/(T_{max} - T_{opt})}$$

to relate the relative rate of a physiological process, f, to the temperature, T, in which T_{min} is the minimum, T_{max} is the maximum and T_{opt} is the optimal, temperature for that physiological process (here, infection). Where $T < T_{min}$ or $T > T_{max}$ then the rate f is simply

set to 0. Convinced by visually assessing the plotted response curves that the Magarey model provided the best fit to the experimental data (Figure M4), the formula was modified to

$$f(T) = T_{scale}\left(\frac{T_{max} - T}{T_{max} - T_{opt}}\right)\left(\frac{T}{T_{opt}}\right)^{\left(\frac{T_{opt}}{T_{max} - T_{opt}}\right)}$$

by setting T_{min} to zero, below which *P. austrocedri* is extremely unlikely to grow (Green, S., personal communication, 5th October 2020), and to fit absolute growth rates based on the experimental data.

Temperature data with which to estimate the daily average rate of mycelial growth (mm/day) in every juniper tetrad from the predicted growth curve were only available for the period of interest (1990-2016) as daily measurements. While growth rates could be estimated for juniper tetrads using the mean daily temperature value, an improved prediction would incorporate diurnal temperature fluctuations. Since the available data provided minimum and maximum values in addition to the mean, the challenge was to develop a plausible interpolation function that could be based only on these values. A very simple function, based on $g(x)=x^{\alpha}$ was used to build a series of temperature values ($n=101$) across the day that fit the correct minimum (θ_{min}), maximum (θ_{max}), and mean (θ_{av}) values obtained per juniper tetrad per day (integration was performed using pracma::*trapz* in R (Borchers, 2021)). For the total length *d* of a day, the function

$$H(t) = \theta_{min} + (\theta_{max} - \theta_{min})(t/d)^{\alpha}$$

produces the correct minimum and maximum temperature values and recapitulates the correct mean value if α is set according to

$$\frac{1}{1+\alpha} = \frac{\theta_{av} - \theta_{min}}{\theta_{max} - \theta_{min}}.$$

The function did not produce realistic diurnal temperature curves but fulfilled the aim of producing a series of 101 values between the three reference datapoints from which to estimate mycelial growth rates more accurately than using a single mean value. The validity of the function was checked by comparing mycelial growth rates (mm/day) predicted from the daily mean temperature series and the interpolated temperature series created by the function with rates predicted using a series of hourly temperature data for selected tetrads (Figures M5-M7). The hourly data were obtained from 1st January 2017 to the 31st December

2019 from the Met Office (Met Office, 2021) for four test locations situated in different parts of Great Britain where juniper is infected with *P. austrocedri* (northern and central Scotland, northern and southern England). Growth rates predicted using the daily average temperature value alone performed poorly compared to the rates predicted using the hourly series, tending towards under prediction in all areas apart from southern England where growth rates were both under and over predicted (Figure M5). By comparison, the growth rates predicted from the interpolated temperature data matched those predicted using the actual data with almost perfect Pearson's r^2 correlations (r^2 >0.99 in all four examples) and only a slight tendency towards over-prediction at higher growth rates, demonstrating the improvement achieved by interpolating diurnal temperatures from mean, minimum and maximum values (Figure M6). The interpolated temperature series generally produced very similar average mycelial growth rates compared to the actual data across the year, with no strong seasonal bias (Donald, F., unpublished data), exemplified by southern England (Figure M7) that showed the highest discrepancy in predictive rates of the four test locations (Figure M6). Diurnal temperature series were, therefore, fit to the minimum, mean and maximum daily temperature values calculated for all juniper tetrads between 1990 and 2016 using the interpolation function, the result of which was then used to calculate daily mycelial growth rate as described in the main text.

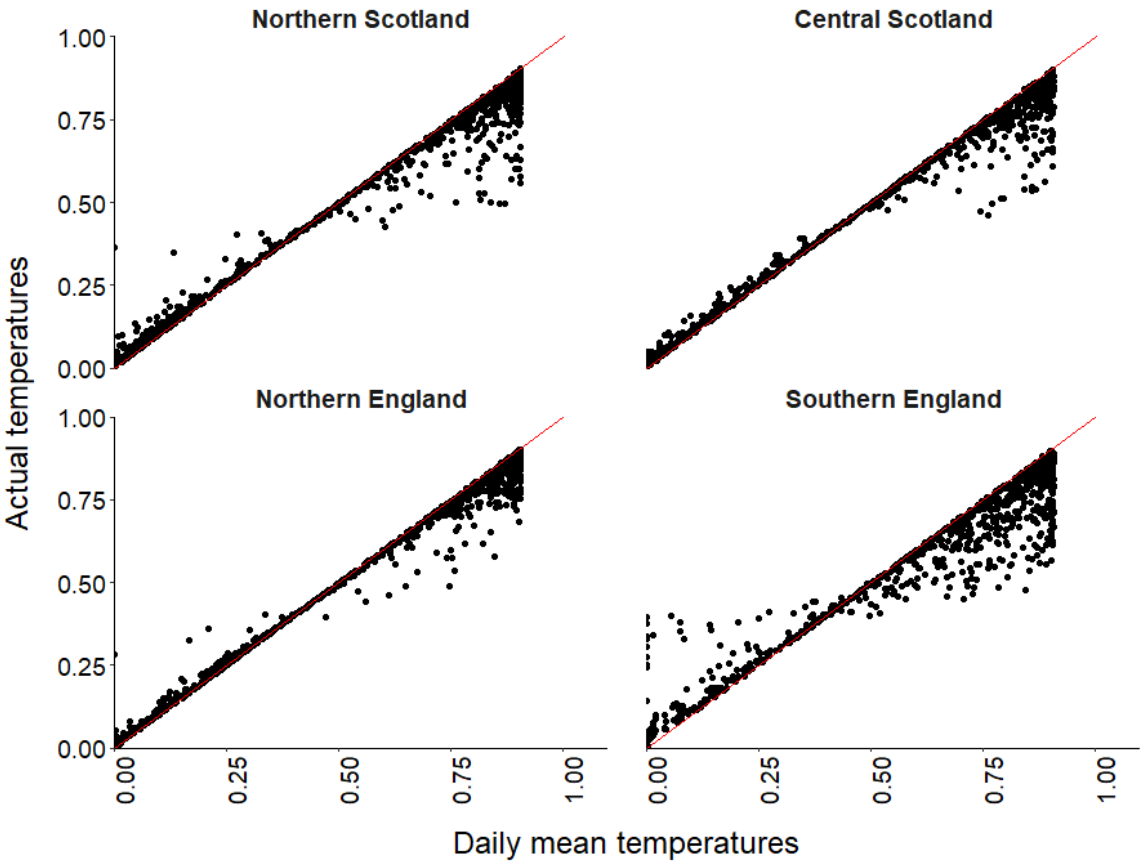

Figure M5. Average mycelial growth rates (mm/day) predicted by the adjusted Magarey function using hourly temperature data compared to daily mean temperature values for four juniper tetrads in Scotland and England infected with *P. austrocedri*. The temperature series used ran from 1st January 2017 to 31st December 2019. The red line shows what the relationship y=x would look like if the growth rates calculated from the hourly temperature series were to match those estimated from the daily mean.

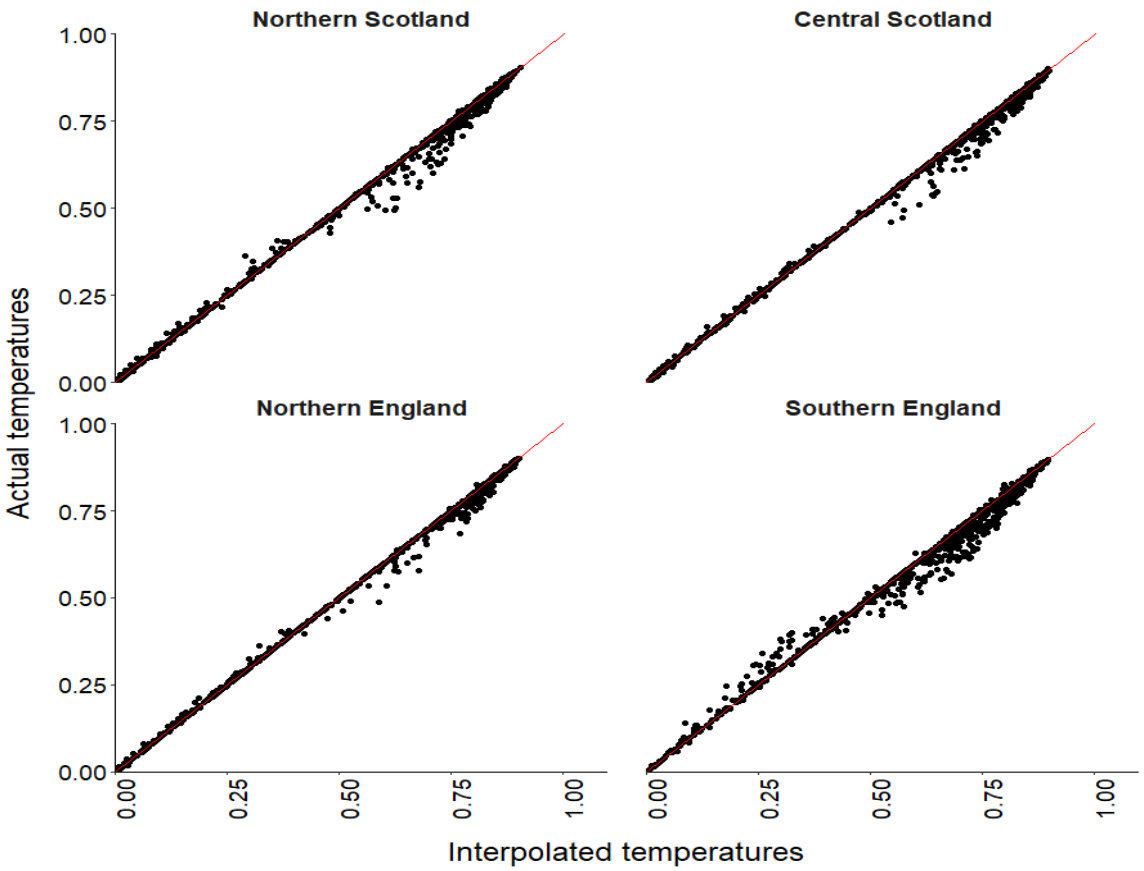

Figure M6. Average mycelial growth rates (mm/day) predicted by the adjusted Magarey function using hourly temperature data compared to temperature interpolated from the daily minimum, maximum and mean values for four juniper tetrads in Scotland and England infected with *P. austrocedri*. The temperature series used ran from 1st January 2017 to 31st December 2019. The red line shows what the relationship y=x would look like if the growth rate predicted using the actual temperatures were to exactly match those interpolated.

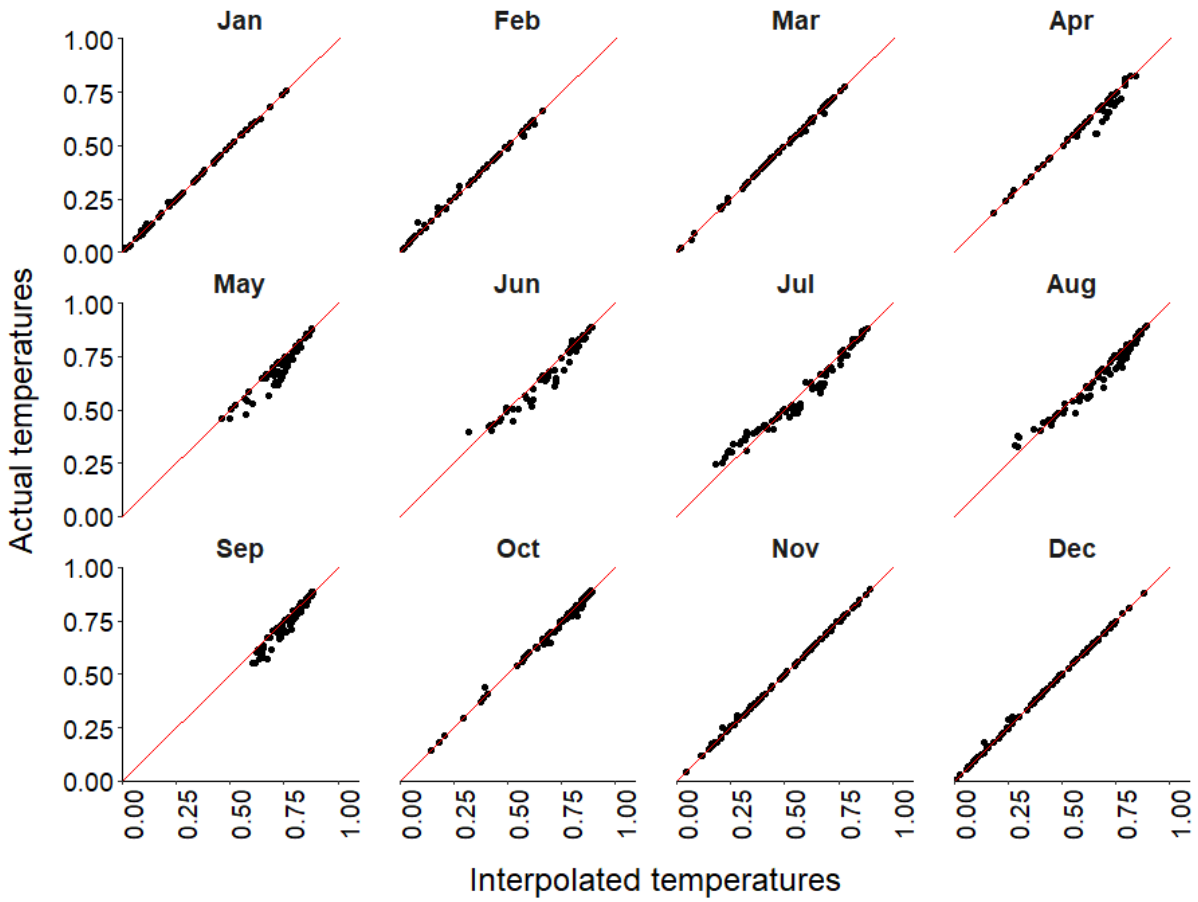

Figure M7. Monthly average mycelial growth rates (mm/day) 2017-2019 predicted by the adjusted Magarey function using hourly temperature data compared to temperature interpolated from the daily minimum, maximum and mean values for the juniper tetrad in southern England (also shown on Figure M6) against the line of perfect correlation (shown in red).

M.4 Exploration of data sources estimating variation in deer density across GB

Obtaining accurate, nationwide estimates of deer density is notoriously difficult (The Scottish Government, 2014) and only two datasets could be found meeting the requisite extent for both roe and red deer. The first dataset considered was published by Croft et al. (2019) who modelled the probability of roe and red deer presence across Great Britain. Species occurrence data were downloaded for the period 2012-2016 from the Mammal Atlas project and the British Trust for Ornithology and 24 variables including rainfall, topography, human disturbance and habitat structure were selected as habitat factors likely to influence deer distributions (Croft et al., 2019). The probability of species presence was predicted using hierarchical, Bayesian, Species Distribution Models that integrated Bernoulli distributed species presence/absence based on habitat suitability and a binomially distributed observation process to account for imperfect species detection (Croft et al., 2019). Alternative datasets were derived using species distribution modelling methods for roe (Alexander et al., 2014) and red (Wint et al., 2014) deer to predict species presence across the whole of Europe. These predictions used species occurrence data from five deer datasets across Europe including 10km records from the UK National Biodiversity Network modelled in relation to habitat factors including temperature and vegetation indices derived from 2001-2008 MODIS satellite imagery, the United Nations Food and Agriculture Organisation (FAO) length of growing periods, travel times to major towns and a weighted human population index to represent the likelihood of human visits based on the population size within the surrounding 30km (Alexander et al., 2014; Wint et al., 2014). Three different models were run with the same input data: Generalised Linear Models fit with multivariate or random forest regressions and the FAO FARMS regression tool created for the purpose of livestock modelling (Alexander et al., 2014; Wint et al., 2014). Each model was run at least 25 times for 50 eco-climate zones before the resulting estimates were averaged across all models to produce a consensus map of predicted presence per species (Alexander et al., 2014; Wint et al., 2014).

To choose the best index of predicted deer presence to integrate into the BRT models, a 3km resolution dataset of red deer counts conducted by six deer management groups in the Cairngorms and NW Scotland during 2005-2006 was obtained from the James Hutton Institute (JHI) (Figure M8). No population counts of roe deer were available to perform an equivalent test. Red deer probability of presence was extracted from Croft et al. (2019) and Wint et al. (2014) to the JHI count centroids with a 1.5km radius buffer using *extract* in the raster R package (Hijmans, 2019). Predictions from both models correlated poorly with the

observed counts but Wint et al. (2014) marginally outperformed the Croft et al. (2019) predictions with a Pearson's r^2 of 0.19 compared to -0.08. The Wint et al. (2014) predictions were, therefore, used in the BRTs as predictions of deer density.

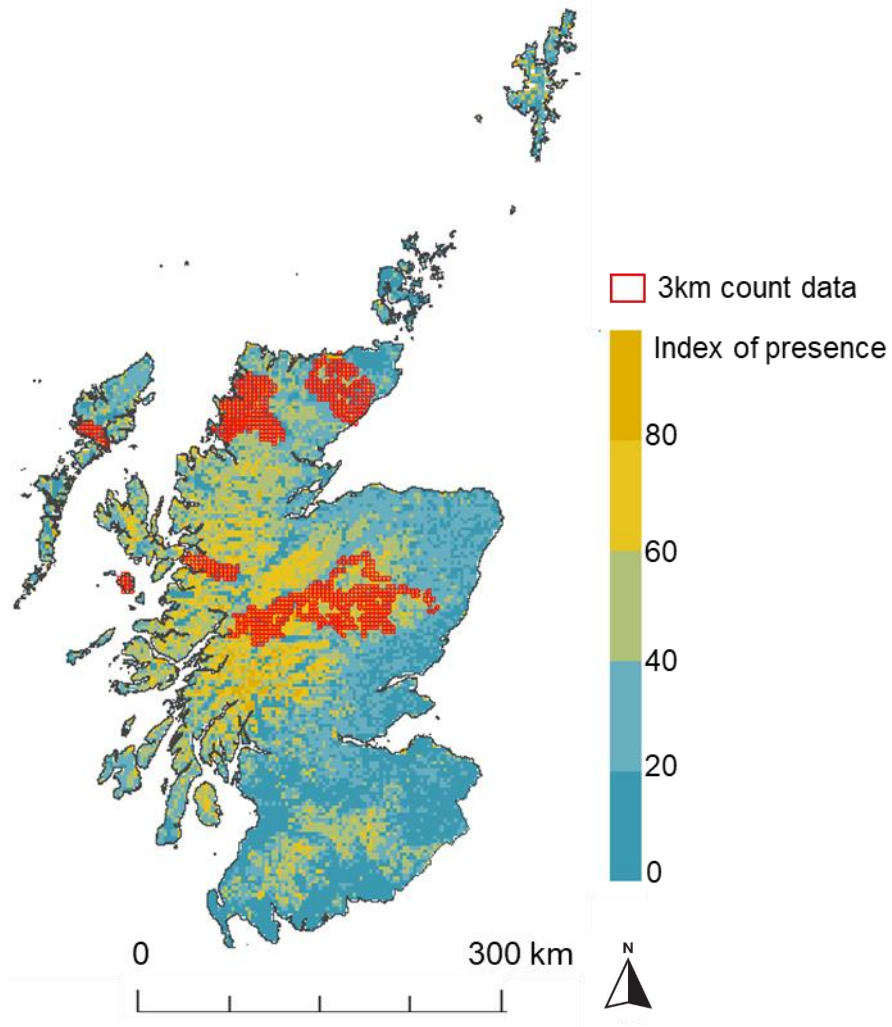

Figure M8. Locations of 3km resolution red deer count data (shown in red) plotted against 1km resolution index of red deer presence cropped to the extent of Scotland (Wint et al., 2014).

M.5 Estimating the intensity of recreational habitat use in juniper tetrads

Between 2009 and 2019, Natural England commissioned a survey called the Monitor of Engagement with the Natural Environment (MENE) that aimed to provide estimates of the number of visited to the natural environment (defined as away from home and private gardens) by the English adult population, their characteristics, patterns of use and participation within key groups at a range of spatial scales (Natural England, 2019c). The surveys were conducted Friday-Tuesday for 51 weeks per year across a minimum of 100

sample locations (postcodes) per week (Natural England, 2019c). Responses were collected from all English regions defined as the North East (5% interviews), North West (13%), Yorkshire and Humber (10%), East Midlands (8%), West Midlands (10%), South West (9%), East England (10%), London (15%) and the South East (15%) (Natural England, 2019c). Question four of the survey asked all visitors to the natural environment which activity from a list they undertook for up to ten visits they could recall in the past year (Natural England, 2019c). The list was presented in a randomised order for each participant with the activities as follows:

- Eating or drinking out
- Fieldsports (for example, shooting and hunting)
- Fishing
- Horse riding
- Off-road cycling or mountain biking
- Off-road driving or motorcycling
- Picnicking
- Playing with children
- Road cycling
- Running
- Appreciating scenery from your car (for example, at a viewpoint)
- Swimming outdoors
- Visits to a beach, sunbathing or paddling in the sea
- Visiting an attraction
- Walking, not with a dog (including short walks, rambling, hill walking)
- Walking, with a dog (including short walks, rambling, hill walking)
- Watersports
- Wildlife watching
- Informal games and sport (for example, Frisbee or golf) SPECIFY
- Any other outdoor activities (for example, climbing) SPECIFY

For each visit, participants also gave the postcode of their original location (i.e. where they travelled from) and grid references (identified from place names or street addresses) of their destination (i.e. where they travelled to) (Natural England, 2019b) (Figure M9). No comparable survey was conducted in Wales. The equivalent survey in Scotland – the People and Nature Survey – was only conducted for the periods 2013/14, 2017/18 and 2019/20 and only asked participants to describe the general type of location visited e.g. “woodlands managed by the Forestry Commission” or “mountain/hill/moorland” rather than specific locations and as such could not be used to estimate distances travelled to juniper populations.

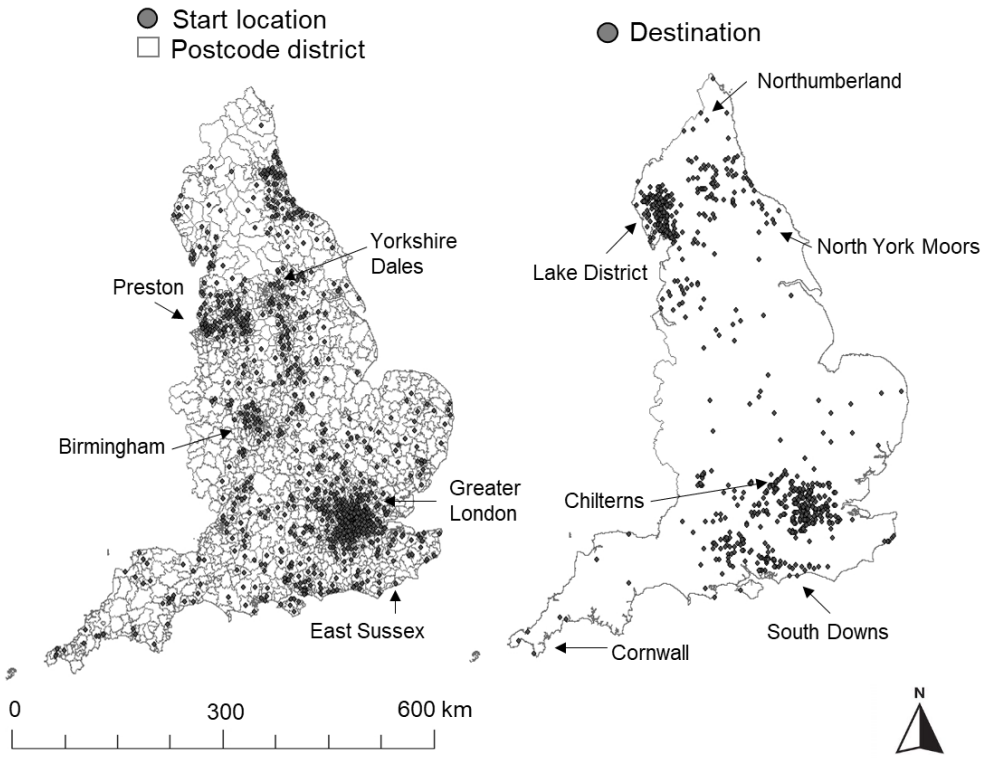

Figure M9. Visits to juniper tetrads in England conducted between 2009 and 2019 for walking reported in the Monitor of Engagement with the Natural Environment surveys (n=5090) (Natural England, 2019c). Start locations were estimated as the centroid of a postcode boundary (L) whereas destinations were provided as ten figure grid references (R). Contains Royal Mail data © Royal Mail copyright and database rights [2015].

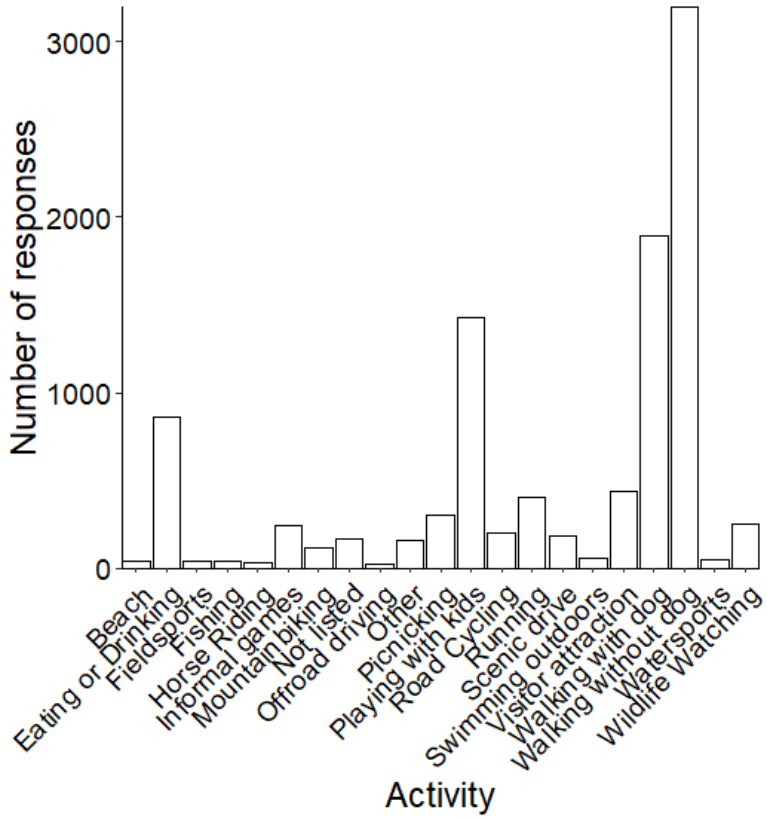

Figure M10. Activities carried out by visitors accessing the natural environment in juniper tetrads in England (n=1393) shown as the number of responses where each activity was specified.

The first step was to identify recreational activities most associated with visits to juniper populations. Of 1393 juniper tetrads present in England, 708 (51%) contained at least one record of a visit from the 198169 provided (Natural England, 2019b) (Figure M9). Activities carried out in tetrads containing juniper were dominated by “walking without dog” (32% records), “walking with dog” (19%), “playing with children” (14%) and “eating and drinking out” (9%) while the remaining activities each accounted for ≤4% of records (Figure M10). As walking activities were the most likely to specifically relate to locations with juniper and accounted for 51% of all visits to juniper tetrads, distance buffers for recreational visits were applied according to the distances travelled by walkers (with and without dogs). Visits ending in a juniper tetrad where walking was specified as the main activity were filtered from the dataset (5090 records). Detailed spatial coordinates for full postcodes were not freely available so the start locations of relevant visits were instead specified as the centroid of one of 2880 possible postcode districts determined by the first 4 postcode digits (OpenDoorLogistics, 2015) (Figure M9). Euclidean distance (m) between the start and end locations was measured using raster::*pointDistance* (Hijmans, 2019) in R. The mean distance travelled was 31km but this value was likely skewed by the small number of visits over 200km, three of which exceeded 500km with visits from the Yorkshire Dales to the southernmost juniper population in Cornwall and from East Sussex to Northumberland (Figure M9, Figure M11). By comparison the median distance of 3.2km was likely to be more robust to the input data resolutions and long-distance outliers (Figure M11). To test the hypothesis that the probability of *P. austrocedri* presence increases with increasing numbers of recreational users, both the median distance of 3.2km, and the 3rd interquartile range distance of 10.9km, were selected (Figure M11).

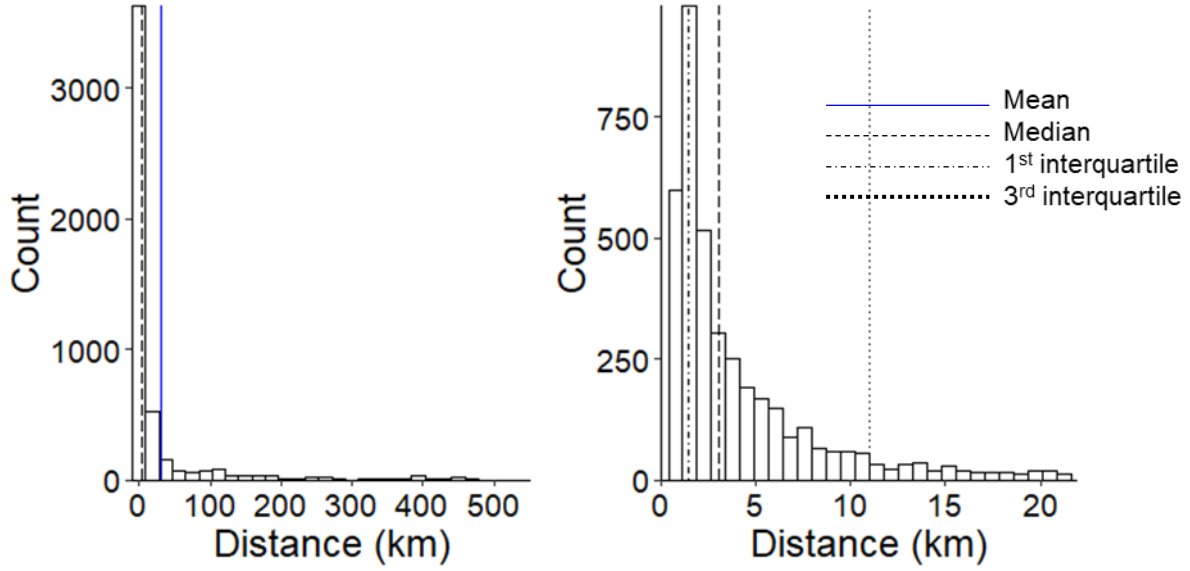

Figure M11. Distribution of distances (km) travelled for walking visits conducted between 2009 and 2019 between postcode centroid start locations and end locations situated in English juniper tetrads reported in the Monitor of Engagement with the Natural Environment surveys (Natural England, 2019c). The mean (blue line) and median (dashed lines) are plotted against the full range of distances travelled (543km) (L) to compare with the first 20km of the distance distribution, the median and interquartile distances (1st=dotdash line, 3rd=dotted) travelled (R).

M.6 Correlations between environmental predictors

Correlations between all environmental predictors were tested using Pearson's r^2 correlation coefficient (Figure M12). Very strong correlations (positive or negative $r^2 > 0.8$) were found between average mean and minimum daily temperatures and cold days (number of days with minimum temperature ≤5°C), mean rainfall and rainy periods (number of periods with 5 consecutive days of rainfall > 1mm), sandy and not sandy (area classified in "soil group" categories not described as "sandy") soils, median and quartile population densities and all pairs of different supplementary planting periods except with plantings conducted from 2007 to 2016 (Figure M12). To account for collinearity, mean and minimum temperature predictors were used in separate models that all contained one rainfall (mean rainfall) and one soil texture (sandy soils) predictor. Alternative predictors describing planting periods, population densities and river lengths were tested separately in models to identify the best predictor for each group.

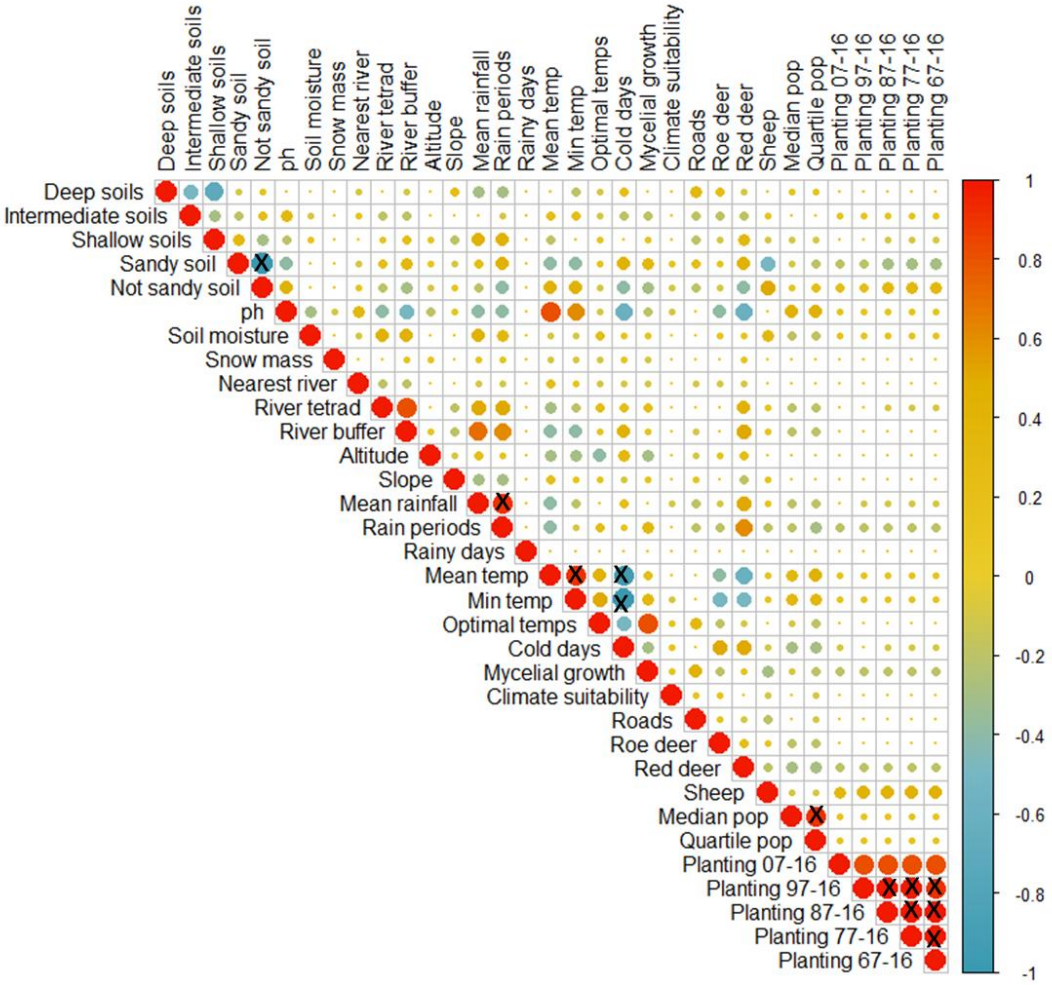

Figure M12. Pearson's r^2 correlation between environmental risk factors used as predictors in BRTs modelling the distribution of *P. austrocedri* in juniper tetrads across Great Britain. The strength and direction of the correlations is shown according to the colour bar and correlation strength by the circle size. Pairs of predictors with r^2 >0.8 are marked with a black x and were either not used in any models (not sandy soils, rainy days, minimum temperature, cold days) or were not included in the same model (population densities "median pop" and "quartile pop", plantings 07-16, 97-16, 87-16, 77-16, 67-16).

M.7 Correction of environmental predictors with positive skew

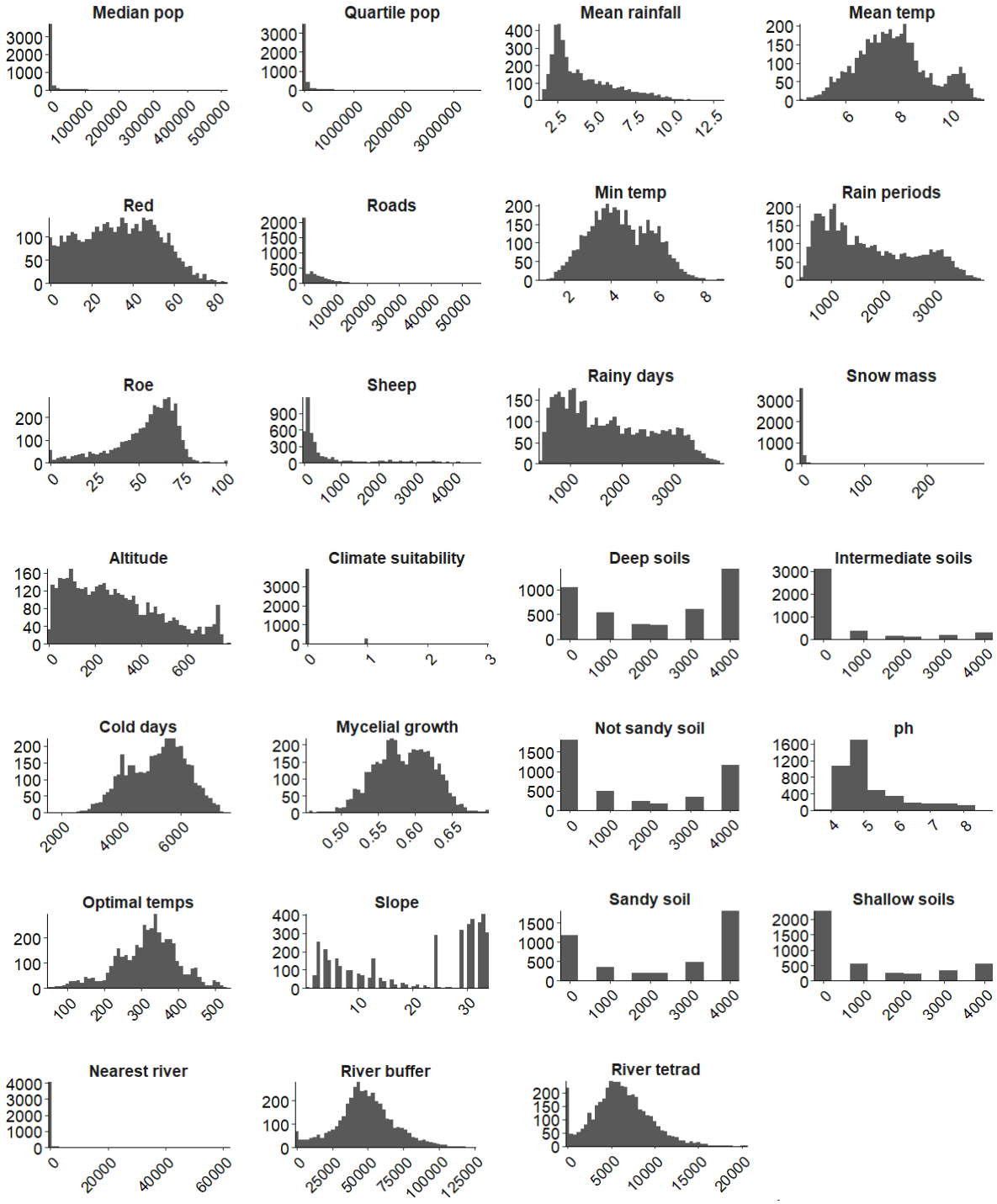

Figure M13. Distributions of all predictors considered for use in the BRTs showing the frequency of juniper tetrads present at each predictor value.

Histograms of all predictors considered for use in the BRTs revealed nine predictors with strong positive skews that were transformed using log10 or square-root transformations prior to modelling (Figure M13, Figure M14). All the transformed versions of the predictors were used in the BRT models.

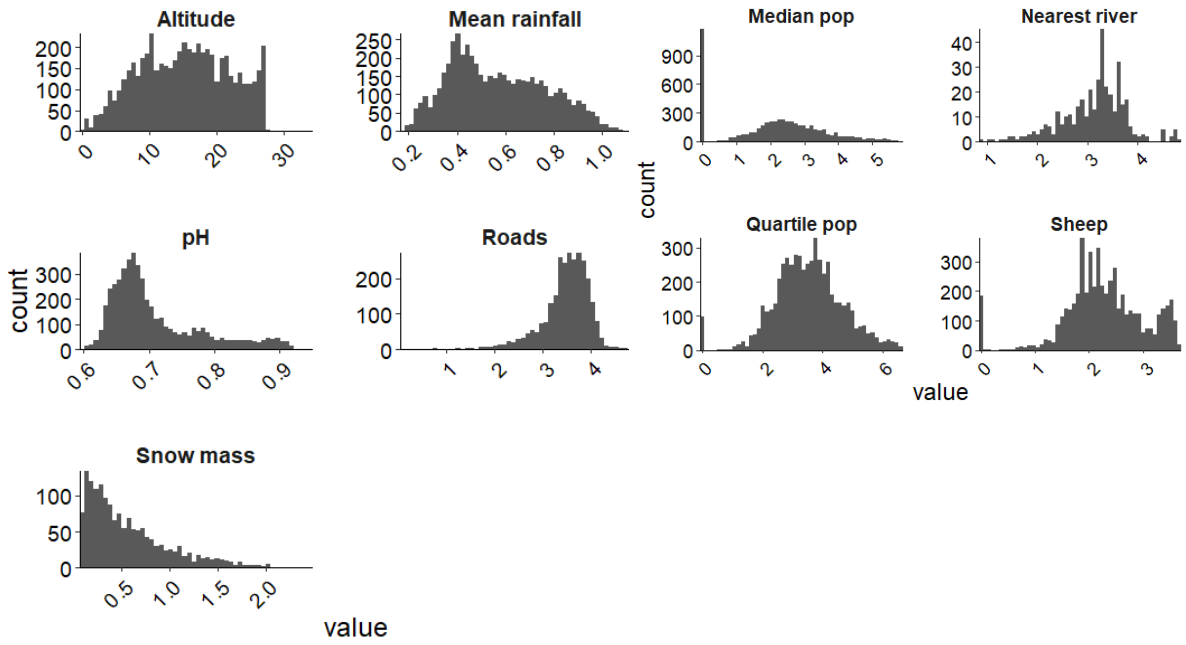

Figure M14. Transformed distributions of nine predictor variables used in BRTs showing the frequency of juniper tetrads present at each predictor value. All predictors had a strong, positive skew so were transformed using a log10 function apart from altitude that was transformed using a square-root transformation.

Appendix N. Supplementary Boosted Regression Trees results

N.1 Accuracy metrics for BRTs with different predictor combinations and absence data

For internal validation, model accuracy metrics were reported for each BRT as measures of cross-validation performance for the simplified models as part of the model fitting process conducted by the dismo::*gbm.step* function. To measure out-of-fit model performance, reflecting the model's ability to predict to new areas, the Boyce index was measured on an independent test dataset. The Boyce Index calculates the correlation between the predicted to expected ratio and the predicted probability of pathogen presence. Here we report all metrics for the model with the highest Boyce index – the best model presented in the main text – and the model with the highest cross-validation AUC that included minimum temperature as the temperature predictor and visited absences (Table N1).

Table N1. Comparison of accuracy metrics returned by models predicting the presence of *P. austrocedri* in British juniper tetrads with the highest Boyce index and highest cross-validation AUC (shown in bold).

Metric	Mean temperature Random absences		Minimum temperature Visited absences	
	mean	s.d.	mean	s.d.
Number of trees	3975.00	1458.54	4351.5	1995.9
Total deviance	1.39	0.00	1.39	0
Residual deviance	0.65	0.15	0.56	0.14
Cross-validation deviance (mean)	1.13	0.09	1.02	0.06
Cross-validation deviance (standard error)	0.08	0.02	0.09	0.02
Training set correlation	0.85	0.05	0.86	0.05
Cross-validation correlation	0.50	0.08	0.58	0.04
Cross- validation correlation (standard error)	0.06	0.01	0.06	0.01
Training set AUC	0.98	0.02	0.98	0.02
Cross-validation AUC	0.78	0.05	**0.83**	0.03
Cross-validation AUC (standard error)	0.04	0.01	0.03	0.01
Cross-validation threshold	0.56	0.02	0.47	0.02
Boyce Index	**0.88**	-	0.42	-

N.2 Accounting for spatial autocorrelation in model residuals

Correlations in the residuals of the best BRT model were calculated using Moran's I statistic summarised across the 100 iterations. Positive, low magnitude spatial autocorrelation was only significant at for the first 25km of the inter-tetrad distances (Figure N1).

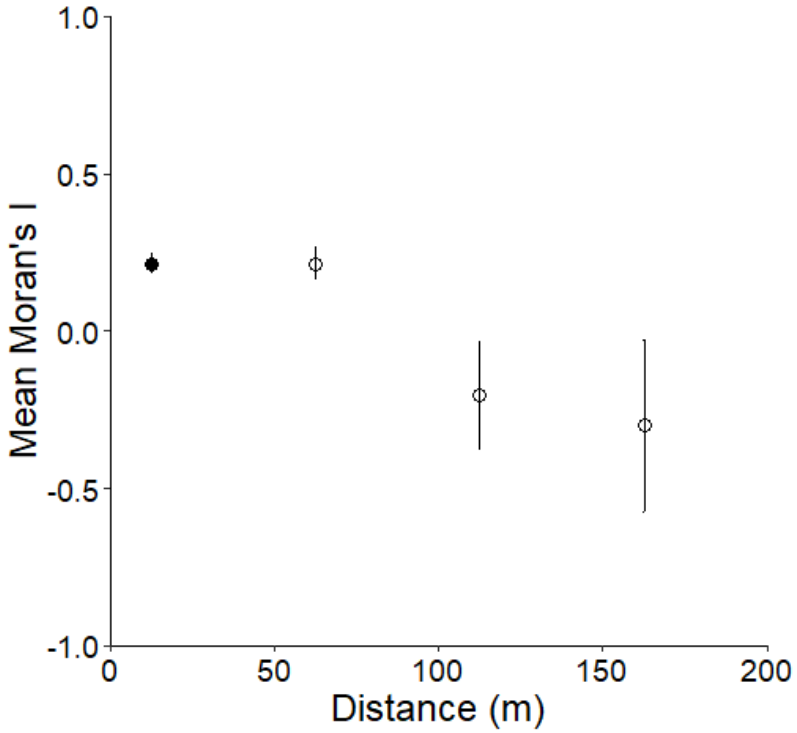

Figure N1. Moran's I values calculated from the residuals of the best performing BRT (Boyce index=0.88), averaged across 100 model iterations, plotted against inter-tetrad distances (km), truncated after 200m. Values with significant p-values (95 % confidence interval, p=0.01) are shown in black.

N.3 Full range of predictions generated from the best BRT

Predictions of *P. austrocedri* presence from the simplified, random absence BRT with the highest Boyce index (0.88) are shown in the main text with increasing probability of presence at intervals of 0.25 (Figure N2). Juniper tetrads with the highest mean probability of *P. austrocedri* presence were also predicted to contain the pathogen in a high percentage of model iterations and were concentrated in central Scotland and northern England, where the pathogen is known to be present (Figure N2). Predicted probability of presence per tetrad varied little with different random absence selections as indicated by small standard deviation values <0.2 (Figure N2).

Interactions were frequently observed in the best model between red deer and roe deer density and predictors that are potentially confounded with the estimation of deer presence, including mean rainfall that interacted with both species in >50 models (Table N2). Roe deer density interacted with river length and sheep density in many more model iterations than red deer, which might reflect genuine habitat overlaps or could also be confounded with environmental covariates used to estimate the roe deer predictor (Table N2). Further investigation of the relationships between roe deer density and *P. austrocedri* presence is advisable, and models could be repeated if new deer density metrics or counts become available.

Table N2. Interactions detected between predictor pairs in the best model, averaged across the number of model iterations (out of 100) where the interaction was present. Interactions with mean values >10 are presented in order of mean interaction size.

Predictor pair	Mean interaction	Number of iterations
Red deer density, soil pH	21.13	1
Red deer density, soil moisture	19.36	1
Mean rainfall, roe deer density	18.09	76
River length tetrad, red deer density	17.75	17
Mean rainfall, red deer density	16.13	63
River length tetrad, roe deer density	15.27	59
Sheep density, roe deer density	14.04	76
Roe deer density, sandy soils	11.57	3
Mean temperature, red deer density	10.33	2
Red deer density roe deer density	10.08	5

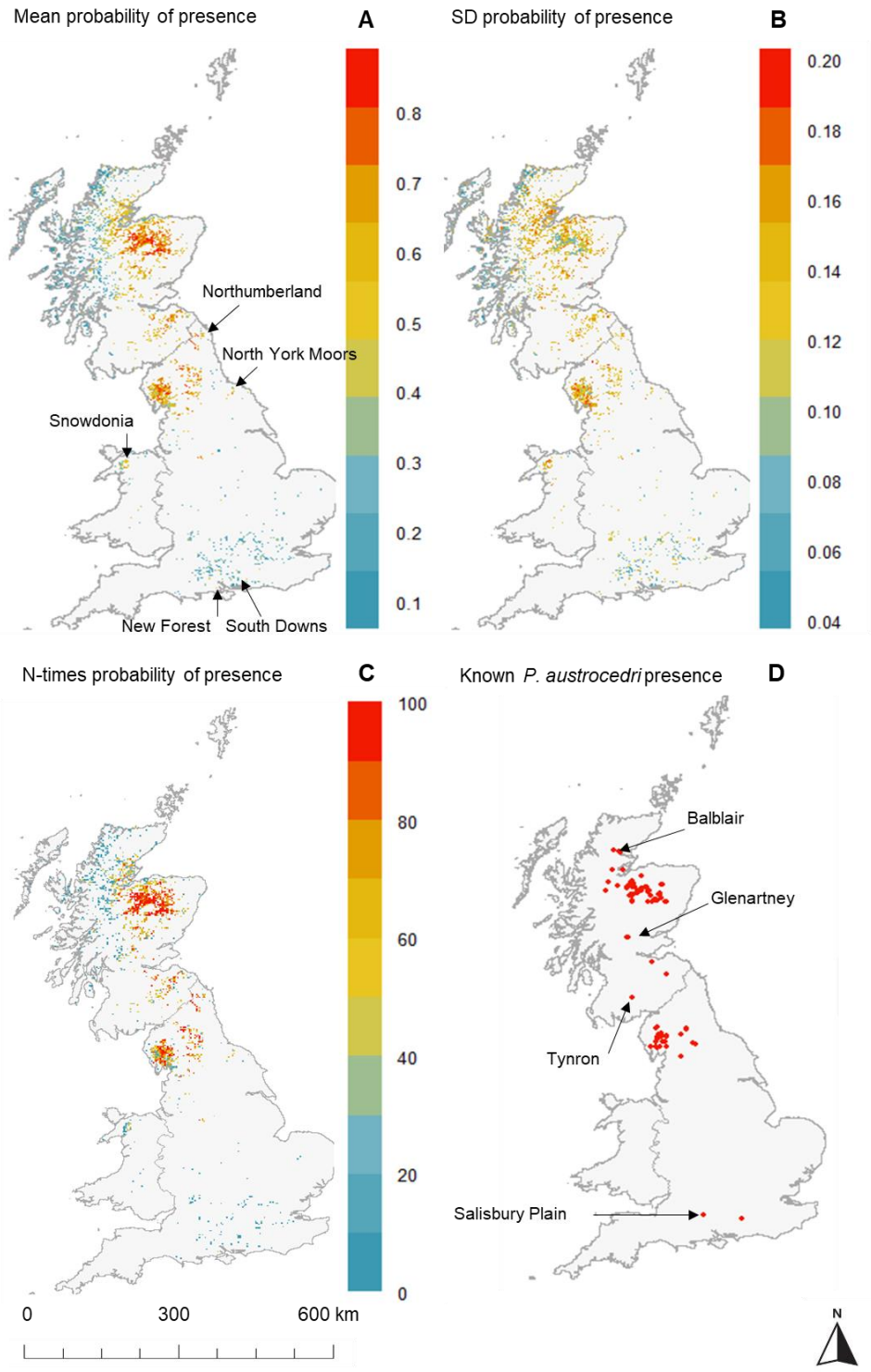

Figure N2. Predictions of *P. austrocedri* presence from the simplified, random absence BRT with the highest Boyce index (0.88). Maps compare the mean (A) and standard deviation (B) of the relative probability of *P. austrocedri* presence per juniper tetrad (2x2km grid cell), and the number of times the pathogen was predicted per grid cell (C), calculated across the 100 iterations of the model with different absence selections. The distribution of all 97 tetrads with positive *P. austrocedri* detections are shown in red (D), as are tetrads with predicted high mean relative probability of infection (A), tetrads with more variable predictions of probability (B) and tetrads where the pathogen was predicted to be present in >80 model iterations (C). Pathogen presence could only be predicted in tetrads containing juniper (A-C); those with <30 presence predictions are shown in blue (C).

N.4 Predictions generated from the best BRT with visited "absence" selections

The BRT using visited "absence" selections that yielded the highest Boyce index (0.66) included the mean daily temperature predictor, population density within 3.2km (median distance travelled walkers visiting juniper tetrads travelled) and length of rivers within a 2km buffer surrounding each juniper tetrad. Probability of *P. austrocedri* presence was highly probable (>0.75) only in central and northern Scotland where pathogen outbreaks have occurred (see Figure 28 in the main text) while occurrences in the southern uplands, the Lake District and the Penines were somewhat probable (>0.50) and were not predicted in southern England (Figure N3).

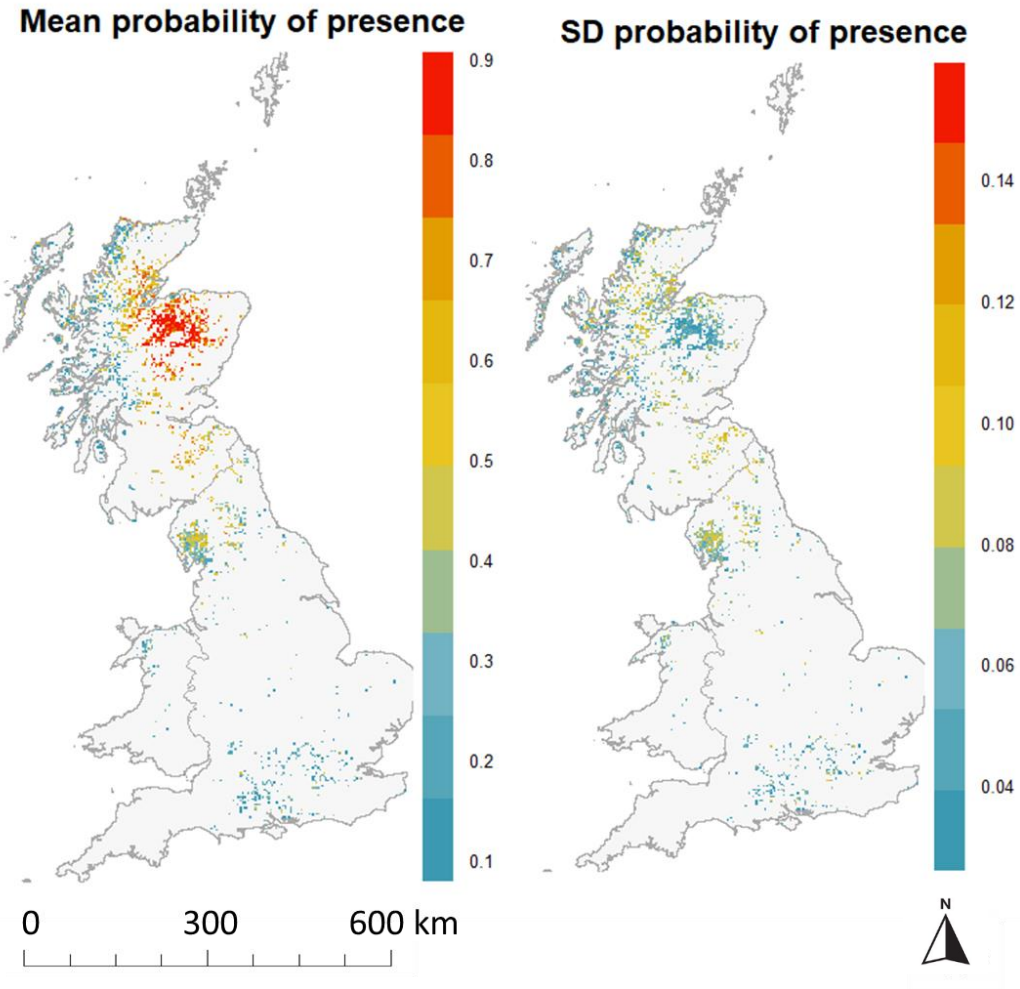

Figure N3. Mean (L) and standard deviation (R) probability of *P. austrocedri* presence in British juniper tetrads predicted by the BRT with the highest Boyce index (0.66) using visited "absences". The predictions shown are averaged across 100 iterations of the model with different selections of visited tetrads. Tetrads with higher predicted mean pathogen presence are shown in red (L) as are tetrads with more variable probability of presence (R).

Appendix O. Stakeholder feedback obtained for the national risk map

O.1 Stakeholder feedback about the predictive *P. austrocedri* risk map

The map of *P. austrocedri* mean predicted probability of presence generated for all juniper tetrads (2kmx2km cells) present across GB was displayed within a Shiny app (available here: https://floradonald-juniper-planting-2020.shinyapps.io/National_map/ and reproduced in Appendix O.2), overlaid with the distribution of confirmed *P. austrocedri* detections in the wider environment. The app was circulated to all 41 stakeholders who participated in the previous survey (Chapter 5, Appendix J). The app allows users to zoom to tetrads of interest and hovering the mouse over a tetrad produces an information box reporting predicted probability of *P. austrocedri* presence. Maps of the top six most informative risk factors found by the best model were presented in the same format. The list of predictors tested in the model and the stakeholder risk ranking was also presented (reproducing Table 26) (Appendix O.2).

A five-question, self-completion survey requesting feedback about stakeholder confidence in, and potential use for, the national risk map was presented as a link to a separate google form within the app, reproduced in Appendix O.3. Before completing the survey, participants were asked to consent to the reproduction of their responses in connection with the presented risk map and informed of their right to withdraw from the survey and request removal of their responses at any time. Stakeholders could participate in the survey from the 14th June 2021 until the 14th August 2021. The first two questions invited stakeholders to choose their level of confidence in the accuracy of the predicted *P. austrocedri* risk map as one of “very confident, “confident”, “unsure”, “not confident” or “not at all confident”, and to outline the reasons for their selection (Appendix O.3). The third and fourth questions asked stakeholders to describe potential uses and limitations of the risk map when applied to their work, and the fifth question invited any further comments as free text (Appendix O.3).

Eight responses were received in total, seven via the survey form and one via email. The naming convention used in Chapter 5 (stakeholder type and number) was extended to the responses obtained from this survey to understand the distribution of results across stakeholder types (see Chapter 5 for a full description). The responses were then analysed to identify phrases relating to two themes: i) the participant’s confidence in the risk map, classified as indicating “confidence” or “uncertainty” (Table O1), and ii) how the results might influence work conducted by the participant, categorised as “uses” and “limitations” (Table O2). All participants addressed both themes. Four participants (50%) detailed

sources of both confidence and uncertainty when interpreting the risk map, compared to two participants (25%) who expressed only confidence and two (25%) who expressed only uncertainty (Table O1). Seven (87.5%) participants described potential uses of the risk map, one of whom identified no limitations, while one participant (12.5%) identified no uses and only limitations (Table O2).

Table O1. Responses obtained from stakeholders describing sources of confidence or uncertainty in using the predicted risk map of *P. austrocedri* presence in British juniper tetrads. Participants are identified using the same combination of stakeholder type and numeral used for their responses received in Chapter 5. The confidence rating selected from the list of five options is presented for survey participants and left blank for the participant who responded by email.

Participant	Confidence rating	Comments discussing sources of:	
		confidence	uncertainty
Assessor 6	Confident	"My actual answer is probably half-way between unsure and confident! I think that the map does look like to correspond very well with what we know in the Lake District, and the lack of symptoms despite confirmed findings in Salisbury Plain"	"I would really want to have a look at high-risk areas distant from known outbreaks to prove it right"
Agent 6	Unsure	"I think that the map does look like to correspond very well with what we know"	"It's difficult at the scale provided to assess the accuracy of the environmental risk factor"
Manager 15	Confident	"Confidence based on the use of empirical data in model development […]. Confident that this is a better predictor than what we just think is."	"Unclear however what assumptions have been made."
Manager 7	Unsure		"Unsure why roe deer are specified, when sika and red deer are in much higher densities"
Grower 2	Confident	"It seems to account well for the identified factors influencing *P. austrocedri* infection. A developing situation with multiple factors at play will always be difficult to model. No specific weaknesses are apparent to me."	
Agent 1	Unsure		"It is difficult to predict (modelling is limited to input)"
Assessor 8	Unsure	"It looks as if the areas predicted as high probability of presence include the majority of areas where it's been found, which is really promising."	"But there are also quite large areas with high probability, but where it hasn't been recorded, and I'd like to know more about this side of things. It may be that it actually is more widely present, but under-recorded, or that these are areas that are very suitable but that it simply hasn't reach - or it might exaggerate risk. Hard to know. I wonder if eDNA work on soil samples might be useful to increase our knowledge of its distribution."
Agent 3	No score	"This looks good."	

Table O2. Responses obtained from stakeholders describing the uses and limitations of the predictive risk map for their work. See Table O1 for further details.

Participant	Comments discussing the risk map:	
	uses	**limitations**
Assessor 6	"Could prove very useful for targeted surveillance (both aerial and ground based)"	"Limitations may be associated with where populations of subsp. *nana* are. I would like to be able to overlay the risk layer with known populations of recently planted juniper to further help targeting."
Agent 6		"There are so many microsites which could override analysis and factors presented at a large scale"
Manager 15	"…probably we may think twice about planting juniper due to any risk of introducing *Phytophthora* and also if we decided to plant being extremely careful about minimising the risks of potentially bringing *Phytophthora* in."	"I am not sure how much this will change action on the ground. We are relying primarily on natural regeneration of juniper and it is a key species for us. Not sure we will act if *P. austrocedri* discovered."
Manager 7	"I think it underlines that we are at quite high risk of *P. austrocedri* infection. So useful to plan ahead…"	"… though not sure what I can do about it."
Grower 2	"Useful but as I'm operating in a very restricted area, where no evidence of infection has been found it is currently of academic interest for my day to day activities."	
Agent 1	"It will be an indicator as with the FC climate change predictions"	"Not convinced about the sheep stocking rate being reduced."
Assessor 8	"I think it's useful on a very broad scale e.g. it suggests that the risk is high throughout the central Highlands, including the whole of the CNPA, and up the north-east coast. Which confirms that biosecurity is vital in this area and should inform any plans for enhancing work on juniper conservation. It might also be useful in informing decisions about where it is appropriate to plant juniper at all, and where this is lower risk."	"I'm not sure how useful it would be to use on a local scale, beyond being aware that there is a significant risk throughout the east and central Highlands. I'd be interested to see how willing people would be to accept where the risk is predicted to be low... especially since much of the west is higher risk for other *Phytophthora*, and so we might feel that high levels of biosecurity are increasingly necessary throughout the country as a matter of course, rather than in response to individual diseases. It might be interesting to look at how predicted risk for juniper phytophthora compares to predicted risks of other *Phytophthora* and other diseases."
Agent 3	"One risk factor that I hadn't really factored for in our management is deer […]. Intriguing if the model is suggesting that there is a difference risk between deer species…"	"I will be advising fencing important juniper sites. Creating bare ground for regeneration could be done by hand but of course there are biosecurity risks involved with that. I have to be honest; I hadn't really considered weed development. It's so tricky! There's no correct answer, we just have to do the best we can…"

O.2 Reproduction of the Shiny App visualising the predictive risk of *Phytophthora austrocedri* infection of juniper in Great Britain

Risk map predicting infection of *Juniperus communis* s.l. populations in the wider environment

Risk predictions were generated at tetrad (2x2km) resolution for all cells known to host juniper 1990-2020 using a Boosted Regression Trees model. The model was trained and tested using an 80:20 ratio of tetrads with known *P. austrocedri* infection diagnosed from positive qPCR results collated by Forest Research, Forestry Commission and FERA 2011-2016, 100 random selections of tetrads where no pathogen symptoms have been reported, and 22 environmental risk factors for disease.

Tetrads (cells with grey outlines) are coloured and labelled according to the mean probability of pathogen presence predicted by the model (low = blue, high = orange/red, missing data = transparent) and tetrads with confirmed *P. austrocedri* presence are overlaid with purple circles. We suggest tetrads at high risk of infection are those identified with probability of presence >0.70. Use the + and - buttons or your mouse to zoom in and out to your region of interest. Please note that the maps may take several minutes to load.

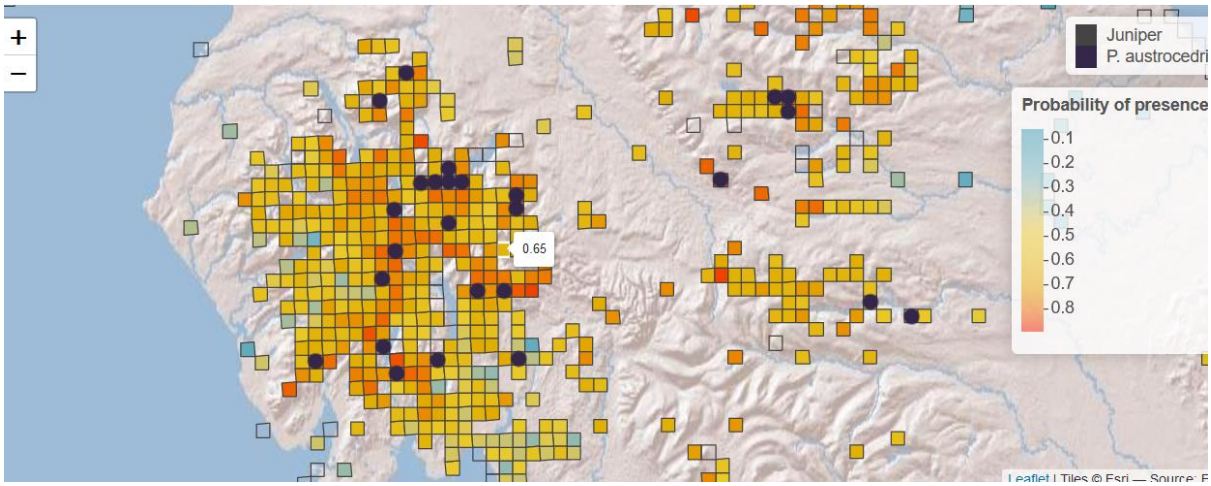

Environmental factors predicting infection risk

The most important risk factors identified by the model were:

- weakly acidic soil pH (c. 5.5);
- increasing density of roe deer;
- 2.5-3mm mean daily rainfall 1990-2016;
- increasing sheep density;
- decreasing mean daily mycelial growth rate (predicted as a function of temperature);
- increasing altitude up to 400m.

The maps below display the data used in the model:

Mycelial growth

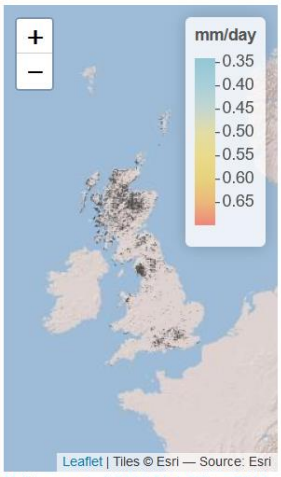

Robinson et al 2020 Met Office 2018

Sheep density

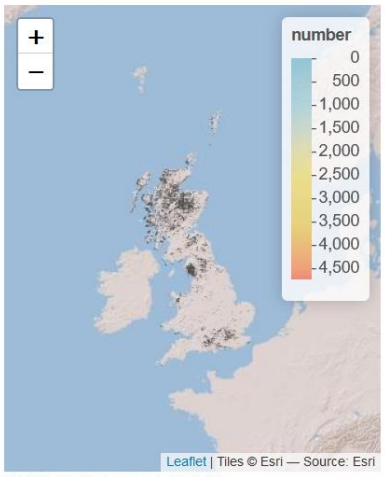

EDINA 2010 Crown Copyright.

Altitude

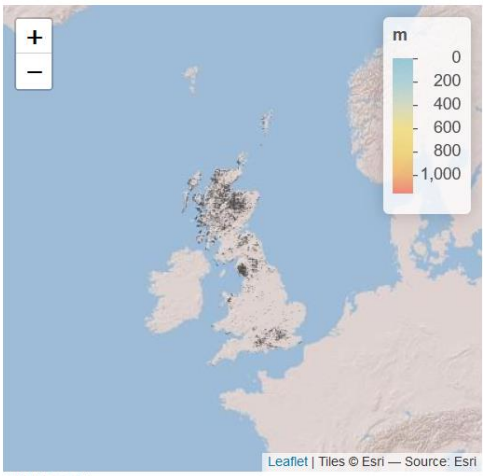

STRM 2014

Soil pH

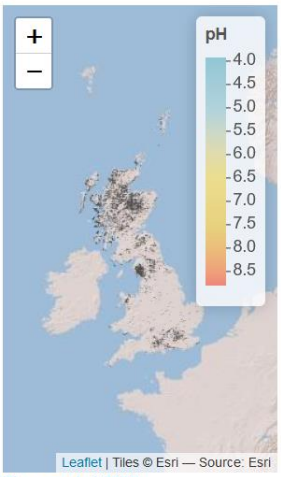

Thomas et al 2020

Roe deer density

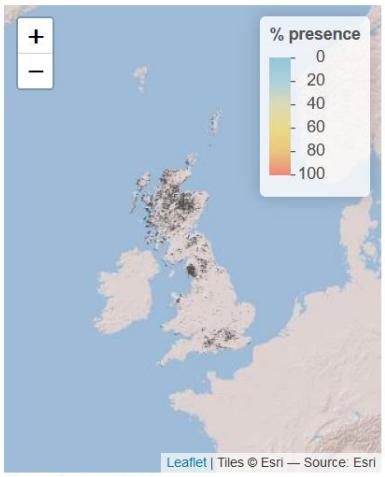

Alexander et al 2014

Mean rainfall

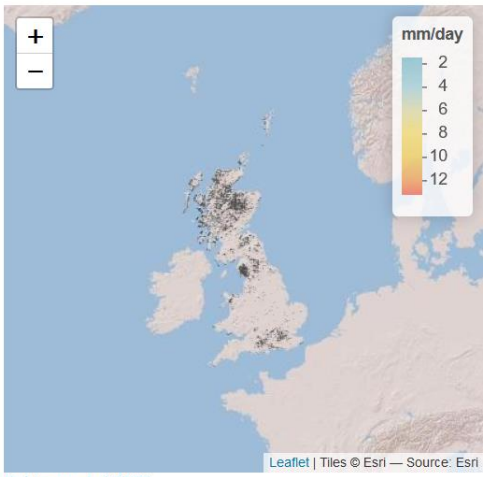

Robinson et al 2020

In the previous survey, I asked you to rank environmental risk factors in order of expected importance in predicting *P. austrocedri* presence, which I then tried to include in the risk

model. A few predictors had to be left out and a few were described using multiple predictors. The table below shows the risk factors I asked you to rank, the weighted importance afforded to all abiotic and biotic risk factors predicted by survey respondents and the corresponding factors used in the risk model.

Risk type		Survey weight	Predictor name	Risk factor description
Abiotic risks	Rainfall	9	Mean rainfall (mm/day)	mean daily rainfall
			Rainy days (n)	number of days rainfall > 1mm
	Soil moisture	7	Soil moisture (mm water/m soil)	mean soil moisture calculated from simulated monthly data
			Snow mass (kg m^2)	mean snow mass calculated from simulated monthly data
	Temperature	5	Mean temperature (°C)	mean daily temperature
			Optimal temperature periods (n)	n periods with 5 consecutive days mean temperature 10-15°C
			Minimum temperature (°C)	minimum daily temperature
	Climate suitability	4	Climate suitability (n)	n periods of 5 consecutive days rain >1mm, mean temp 10-15°C with a min temp < 5°C at some point during that window
	Slope	3	Slope (°)	slope angle
	Altitude	3	Altitude (m)	metres above sea level
	Soil pH	2	pH	pH prediction from 2446 samples of top 0-15cm soil
	Proximity to watercourses	2	Nearest river (m)	distance from tetrad centroid to nearest river
			River length buffer (m)	length of rivers within 2km buffer
			River length tetrad (m)	… within tetrad
	Soil depth	1	Deep soils (m^2)	area of tetrad categorised as "deep"
			Intermediate soils (m^2)	… "intermediate"
			Shallow soils (m^2)	… "shallow"
	Soil texture	1	Sandy soils (m^2)	area of tetrad described as "sandy"
Biotic risks	Juniper planting	9	Planting 2007-2016	presence/absence of planting events within 2km radius (6x6km)
			Planting 1997-2016	
			Planting 1987-2016	
			Planting 1977-2016	
			Planting 1967-2016	
	Recreation	7	Median population (n)	Residential population size within 3.2km radius
			Quartile population (n)	… within 10.9km radius
	Livestock density	6	Sheep (n)	Total number of sheep and lambs (i.e. all breeding and non-breeding sheep
	Deer density	4	Roe deer (index of presence)	Predicted habitat suitability for roe deer
			Red deer (index of presence)	… red deer
	Not included in survey	NA	Roads (m)	Length of roads within tetrad
			Average mycelial growth (mm/day)	Predicted average daily mycelial growth in response to temperature series fit to minimum, mean, and maximum temperatures

Feedback about the national risk map

Risk factors that were mostly highly ranked by stakeholders weren't identified by the model as the best predictors of *P. austrocedri* presence at 2km resolution. There might be many reasons for this, including the resolution or the quality of the spatial risk factors used and the degree to which they represent field level conditions. However, the model has a high accuracy in validation being able to predict 15/19 independent data on *P. austrocedri* infections as >0.70 probability of presence. Therefore, I'd like to know how much confidence you have in the model results and if they may aid your decision-making about juniper.

I would really appreciate your feedback - positive and negative - about the risk map and invite you to complete this short survey (only 6 questions!) >> Risk Map Survey

Thank you for taking the time to review this information.

O.3 Questionnaire to obtain feedback about the national risk map

Predicting risk of *Phytophthora austrocedri* infection of juniper in Great Britain – model feedback

*Required field

Before proceeding to the complete this survey, please take time to read the following information carefully:

1. All responses will be anonymised and may be quoted in my thesis chapter / subsequent publication discussing feedback about the risk model. Your name will only be used to match your stakeholder category based on your previous survey response.

2. Your participation in this research is entirely voluntary and you are free to withdraw at any time.

3. Should you decide to withdraw from the survey, you have the right to request that information already provided be removed and excluded from the research and not used for any other purposes. You can exercise this right at any time and for any reason.

4. Your personal information and other information collected will not be passed onto any person and/or organisation. Your information is confidential and will be treated with utmost privacy.

5. You are free to contact Flora Donald at the UK Centre for Ecology and Hydrology with any queries using her email address flodon@ceh.ac.uk

Are you willing to proceed with this survey. Tick here to confirm consent: *

- ☐ Yes
- ☐ No

Name *

Q1. How confident are you that the model accurately predicts the level of *P. austrocedri* infection risk? *

- ☐ Very confident
- ☐ Confident
- ☐ Unsure
- ☐ Not confident
- ☐ Not at all confident

Q2. Please may you explain your response?

Q3. Will this risk map be useful in your work? Please explain why / why not

Q4. What do you think the limitations of the risk map are? Are there instances when you would not use it?

Q5. Do you have any other comments about the predicted risk map?

Thanks for sharing your feedback. I'll be in touch if any of this material is published further.